Stem Cells International

Tissue-Derived Stem Cell Research

Guest Editors: Ming Li, Kequan Guo, Dong Hyun Kim, and Luca Vanella

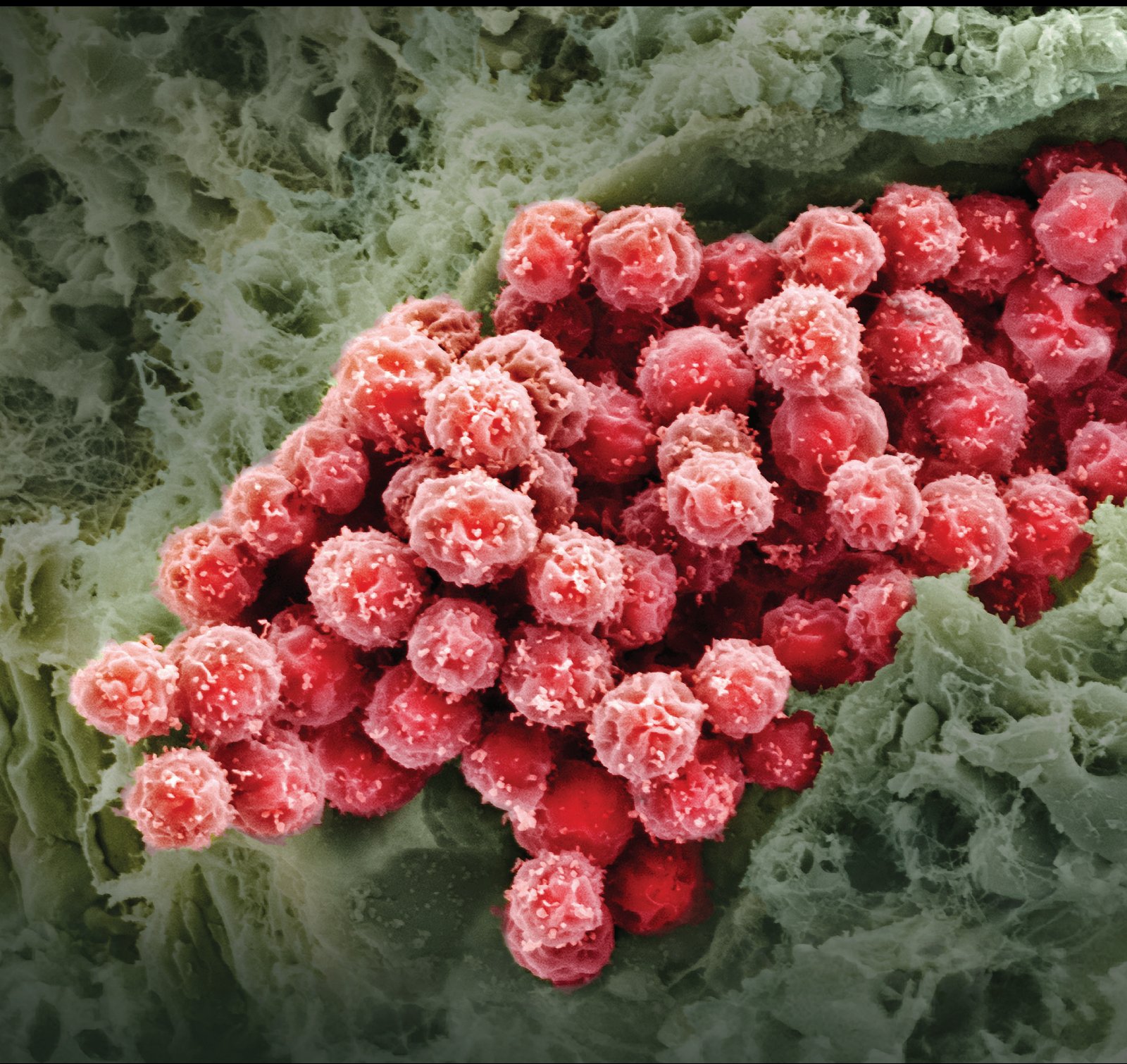

Tissue-Derived Stem Cell Research

Stem Cells International

Tissue-Derived Stem Cell Research

Guest Editors: Ming Li, Kequan Guo, Dong Hyun Kim, and Luca Vanella

Editorial Board

Contents

Tissue-Derived Stem Cell Research
Ming Li, Kequan Guo, Dong Hyun Kim, and Luca Vanella
Volume 2016, Article ID 4801953, 1 page

Dexamethasone Regulates EphA5, a Potential Inhibitory Factor with Osteogenic Capability of Human Bone Marrow Stromal Cells
Tsuyoshi Yamada, Toshitaka Yoshii, Hiroaki Yasuda, Atsushi Okawa, and Shinichi Sotome
Volume 2016, Article ID 1301608, 20 pages

Tissue-Related Hypoxia Attenuates Proinflammatory Effects of Allogeneic PBMCs on Adipose-Derived Stromal Cells *In Vitro*
Polina I. Bobyleva, Elena R. Andreeva, Aleksandra N. Gornostaeva, and Ludmila B. Buravkova
Volume 2016, Article ID 4726267, 13 pages

Pharmacological Therapy in the Heart as an Alternative to Cellular Therapy: A Place for the Brain Natriuretic Peptide?
Nathalie Rosenblatt-Velin, Suzanne Badoux, and Lucas Liaudet
Volume 2016, Article ID 5961342, 18 pages

Effect of Fibroblast Growth Factor 2 on Equine Synovial Fluid Chondroprogenitor Expansion and Chondrogenesis
Marta Bianchessi, Yuwen Chen, Sushmitha Durgam, Holly Pondenis, and Matthew Stewart
Volume 2016, Article ID 9364974, 11 pages

Peripheral Blood Monocytes as Adult Stem Cells: Molecular Characterization and Improvements in Culture Conditions to Enhance Stem Cell Features and Proliferative Potential
Hendrik Ungefroren, Ayman Hyder, Maren Schulze, Karim M. Fawzy El-Sayed, Evelin Grage-Griebenow, Andreas K. Nussler, and Fred Fändrich
Volume 2016, Article ID 7132751, 7 pages

Limbal Stem Cell Deficiency: Current Treatment Options and Emerging Therapies
Michel Haagdorens, Sara Ilse Van Acker, Veerle Van Gerwen, Sorcha Ní Dhubhghaill, Carina Koppen, Marie-José Tassignon, and Nadia Zakaria
Volume 2016, Article ID 9798374, 22 pages

Gene Transfection of Human Turbinate Mesenchymal Stromal Cells Derived from Human Inferior Turbinate Tissues
Jin Seon Kwon, Seung Hun Park, Ji Hye Baek, Truong Minh Dung, Sung Won Kim, Byoung Hyun Min, Jae Ho Kim, and Moon Suk Kim
Volume 2016, Article ID 4735264, 10 pages

Functional Overload Enhances Satellite Cell Properties in Skeletal Muscle
Shin Fujimaki, Masanao Machida, Tamami Wakabayashi, Makoto Asashima, Tohru Takemasa, and Tomoko Kuwabara
Volume 2016, Article ID 7619418, 11 pages

Mesenchymal Stem/Stromal Cells from Discarded Neonatal Sternal Tissue: In Vitro Characterization and Angiogenic Properties
Shuyun Wang, Lakshmi Mundada, Eric Colomb, Richard G. Ohye, and Ming-Sing Si
Volume 2016, Article ID 5098747, 10 pages

Potential Role of Activating Transcription Factor 5 during Osteogenesis
Luisa Vicari, Giovanna Calabrese, Stefano Forte, Raffaella Giuffrida, Cristina Colarossi, Nunziatina Laura Parrinello, and Lorenzo Memeo
Volume 2016, Article ID 5282185, 8 pages

How to Improve the Survival of Transplanted Mesenchymal Stem Cell in Ischemic Heart?
Liangpeng Li, Xiongwen Chen, Wei Eric Wang, and Chunyu Zeng
Volume 2016, Article ID 9682757, 14 pages

Uric Acid-Induced Adipocyte Dysfunction Is Attenuated by HO-1 Upregulation: Potential Role of Antioxidant Therapy to Target Obesity
Komal Sodhi, Jordan Hilgefort, George Banks, Chelsea Gilliam, Sarah Stevens, Hayden A. Ansinelli, Morghan Getty, Nader G. Abraham, Joseph I. Shapiro, and Zeid Khitan
Volume 2016, Article ID 8197325, 11 pages

Effects on Proliferation and Differentiation of Human Umbilical Cord-Derived Mesenchymal Stem Cells Engineered to Express Neurotrophic Factors
Yi Wang, Youguo Ying, and Xiaoyan Cui
Volume 2016, Article ID 1801340, 11 pages

Hindawi Publishing Corporation
Stem Cells International
Volume 2016, Article ID 4801953, 1 page
http://dx.doi.org/10.1155/2016/4801953

Editorial
Tissue-Derived Stem Cell Research

Ming Li,[1] Kequan Guo,[2] Dong Hyun Kim,[3] and Luca Vanella[4]

[1]*Department of Stem Cell Disorders, Kansai Medical University, Hirakata, Osaka 5731010, Japan*
[2]*Department of Cardiac Surgery, Beijing Institute of Heart, Lung & Blood Vessel Disease, Beijing Anzhen Hospital, Capital Medical University, Beijing 100029, China*
[3]*Northwest Ohio Orthopedics and Sports Medicine Inc., NWO Stem Cure, LLC, 7595 County Road 236, Findlay, OH, USA*
[4]*Department of Drug Science, Section of Biochemistry, University of Catania, 95125 Catania, Italy*

Correspondence should be addressed to Ming Li; liming@hirakata.kmu.ac.jp

Received 9 December 2015; Accepted 13 December 2015

Tissue-derived stem cells (TDSCs) are undifferentiated cells, presented in tissues such as bone marrow, blood vessels, and adipose tissues and with the ability to repair damaged areas by generation of new cells and tissues. TDSCs have proven to be a feasible source of cells for tissue regeneration medicine in recent experimental and clinical studies. Mesenchymal stem cells revealed potential benefits in atherosclerosis [1] and endothelial progenitor cells reduced lung damage and improved lung function [2]. Moreover, there were some reports that suggested that adipose derived stem cells may improve injured lung function [3], infracted heart function [4], and injured kidney and its function [5]. Regulation of the process to successfully trigger proper differentiation into the desired cell types is important. Moreover, it is more important to confirm safety of transplantation when stem cells are used to treat diseases.

In the present special issue, the significance and possible clinical applications of TDSCs were presented. Some manuscripts described important biochemical cascade underlying the processes of osteogenesis, adipogenesis, angiogenesis, and their possible applications in new therapy development. All findings and experiences of TDSCs research will open up new possibilities for the treatment of various diseases and extend the human life span.

Ming Li
Kequan Guo
Dong Hyun Kim
Luca Vanella

References

[1] S. H. Abdel-Kawi and K. S. Hashem, "Possible therapeutic effect of stem cell in atherosclerosis in albino rats. A histological and immunohistochemical study," *International Journal of Stem Cells*, vol. 8, no. 2, pp. 200–208, 2015.

[2] A. Güldner, T. Maron-Gutierrez, S. C. Abreu et al., "Expanded endothelial progenitor cells mitigate lung injury in septic mice," *Stem Cell Research & Therapy*, vol. 6, article 230, 2015.

[3] G. I. Aboul-Fotouh, M. B. Zickri, H. G. Metwally, I. R. Ibrahim, S. S. Kamar, and W. Sakr, "Therapeutic effect of adipose derived stem cells versus atorvastatin on amiodarone induced lung injury in male rat," *International Journal of Stem Cells*, vol. 8, no. 2, pp. 170–180, 2015.

[4] L. L. Bagno, D. Carvalho, F. Mesquita et al., "Sustained IGF-1 secretion by adipose-derived stem cell improves infarcted heart function," *Cell Transplantation*, 2015.

[5] W. Yao, Q. Hu, Y. Ma et al., "Human adipose-derived mesenchymal stem cells repair cisplatin-induced acute kidney injury through antiapoptotic pathways," *Experimental and Therapeutic Medicine*, vol. 10, no. 2, pp. 468–476, 2015.

Hindawi Publishing Corporation
Stem Cells International
Volume 2016, Article ID 1301608, 20 pages
http://dx.doi.org/10.1155/2016/1301608

Research Article

Dexamethasone Regulates EphA5, a Potential Inhibitory Factor with Osteogenic Capability of Human Bone Marrow Stromal Cells

Tsuyoshi Yamada,[1,2] Toshitaka Yoshii,[1] Hiroaki Yasuda,[1] Atsushi Okawa,[1,2] and Shinichi Sotome[3]

[1]*Department of Orthopaedic and Spinal Surgery, Graduate School, Tokyo Medical and Dental University, Tokyo 113-8510, Japan*
[2]*Global Center of Excellence (GCOE) Program, International Research Center for Molecular Science in Tooth and Bone Diseases, Tokyo Medical and Dental University, Tokyo 113-8510, Japan*
[3]*Section of Regenerative Therapeutics for Spine and Spinal Cord, Tokyo Medical and Dental University, Tokyo 113-8510, Japan*

Correspondence should be addressed to Shinichi Sotome; sotome.orth@tmd.ac.jp

Received 13 June 2015; Revised 30 November 2015; Accepted 3 December 2015

Academic Editor: Luca Vanella

We previously demonstrated the importance of quality management procedures for the handling of human bone marrow stromal cells (hBMSCs) and provided evidence for the existence of osteogenic inhibitor molecules in BMSCs. One candidate inhibitor is the ephrin type-A receptor 5 (EphA5), which is expressed in hBMSCs and upregulated during long-term culture. In this study, forced expression of EphA5 diminished the expression of osteoblast phenotypic markers. Downregulation of endogenous EphA5 by dexamethasone treatment promoted osteoblast marker expression. EphA5 could be involved in the normal growth regulation of BMSCs and could be a potential marker for replicative senescence. Although Eph forward signaling stimulated by ephrin-B-Fc promoted the expression of ALP mRNA in BMSCs, exogenous addition of EphA5-Fc did not affect the ALP level. The mechanism underlying the silencing of EphA5 in early cultures remains unclear. EphA5 promoter was barely methylated in hBMSCs while histone deacetylation could partially suppress EphA5 expression in early-passage cultures. In repeatedly passaged cultures, the upregulation of EphA5 independent of methylation could competitively inhibit osteogenic signal transduction pathways such as EphB forward signaling. Elucidation of the potential inhibitory function of EphA5 in hBMSCs may provide an alternative approach for lineage differentiation in cell therapy strategies and regenerative medicine.

1. Introduction

Human bone marrow stromal cells (hBMSCs) are an attractive source for bone tissue engineering applications because of their proliferative capacity and multipotency [1, 2]. However, their differentiation potential deteriorates over multiple cell divisions [3–5], and it may thus be difficult to obtain a sufficient number of effective cells for clinical applications through ex vivo expansion. Thus, the clinical application of BMSCs requires a more complete understanding of the mechanisms that lead to the senescence of these cells.

Our previous study revealed that long-term passaged BMSCs are capable of forming bone but can also inhibit bone formation. In particular, we demonstrated the importance of quality management procedures for the handling of hBMSCs and provided evidence for the existence of osteogenic inhibitor molecules in BMSCs. One candidate inhibitor is the ephrin type-A receptor 5 (EphA5), which is expressed at low levels at early passages of hBMSC primary culture and upregulated during long-term culture [5]. EphA5 is a member of the ephrin receptor tyrosine kinase subfamily and can bind ephrins A1, A2, A3, A4, and A5. The ephrin receptors are divided into 2 groups based on the similarity of their extracellular domain sequences and their affinities for binding ephrin-A and ephrin-B ligands. The ephrin receptors have the ability to induce both forward and reverse (bidirectional) signaling between adjacent interacting cells. Recently, ephrins and their receptors were reported to be involved in

bone metabolism. Zhao et al. demonstrated that signaling between the extracellular domains of ephrin-B2 expressed on osteoclasts and EphB4 in osteoblasts suppresses osteoclast differentiation and stimulates osteogenic differentiation [6]. In addition to osteoclast-osteoblast interactions, osteoblast–osteoblast interactions through ephrin A2 and either EphA2 or EphA4 have also been shown to occur [7, 8]. We found that downregulation of endogenous EphA5 using specific siRNAs or dexamethasone (DEX) treatment promoted osteoblast marker expression, suggesting that EphA5 is a potential inhibitor of bone formation [5]. However, there have been no reports on the role of EphA5 in bone metabolism, and the mechanism underlying the inhibitory effect of EphA5 on the osteogenic differentiation of BMSCs remains unclear.

BMSCs are heterogeneous and contain subpopulations of osteoprogenitors and undifferentiated cells, and it is difficult to assess the overall expression profile of each batch of cells in a clinical setting [9]. DEX, which has been used to differentiate BMSCs into adipogenic [1], chondrogenic [10–12], and osteogenic lineages [10, 13], affects not only the proliferation rate but also the subpopulation composition of BMSCs. However, the precise mechanism of how DEX induces differentiation is still unclear. Previously, we hypothesized that DEX does not directly induce BMSCs into specific lineages but rather augments the responsiveness of BMSCs to other differentiation reagents applied together with DEX. We reported that DEX induced selective proliferation of cells with higher differentiation capability not only during the initial proliferation culture but also during subsequent osteogenic induction [14] and that cells that had higher responsiveness to BMP stimulation selectively proliferated under continuous DEX treatment [15]. Moreover, DEX treatment selectively suppressed EphA5 expression [5]. Therefore, EphA5 may be a potential negative prognostic indicator of the responsiveness of BMSCs to differentiation reagents, and it may be involved in the senescence or reduced differentiation potency of BMSCs.

The goals of our research were to determine the effects of EphA5 on BMSC quality and to clarify the inhibitory mechanism involved in the reduction of differentiation potential after repeated cell division. Here, we demonstrated the inhibitory effects of EphA5 on osteogenic differentiation in hBMSCs and investigated its function and mechanism of action, together with the association between EphA5 and DEX treatment. Our findings suggest that EphA5 may be a new therapeutic target and quality control marker for the osteogenic differentiation capability of hBMSCs.

2. Material and Method

All of the experiments in this study were specifically approved by the Review Board of the Tokyo Medical and Dental University and were performed in accordance with the Declaration of Helsinki and university guidelines for the care and use of human subjects. Participants provided their written informed consent to participate in this study.

2.1. Primary Culture of hBMSCs. After informed consent was obtained, BMSCs were cultured from bone marrow aspirates of 34 patients who had received hip surgery at Tokyo Medical and Dental University under a protocol that was approved by the institutional review board. The donors ranged in age from 30 to 87 years. Approximately 2 mL of bone marrow aspirate was obtained from the medullary cavity of the femoral shaft of each patient using a bone marrow biopsy needle (Cardinal Health, Dublin, OH, USA). The aspirate was added to 20 mL of growth medium [Dulbecco's modified Eagle medium (DMEM), Sigma-Aldrich Co., St. Louis, MO, USA] containing 10% fetal bovine serum (Life Technologies Co., Carlsbad, CA, USA) and 1% antibiotic-antimycotic (10,000 U/mL penicillin G sodium, 10,000 μg/mL streptomycin sulfate, and 25 μg/mL amphotericin B; Life Technologies) that contained 200 IU of sodium heparin (Mochida Pharmaceutical Co. Ltd., Tokyo, Japan) and then centrifuged to remove the fat layer. Bone marrow cells were then resuspended in growth medium, and aliquots of the cell suspensions were used to count nucleated cells after hemolysis. Subsequently, 1×10^8 nucleated bone marrow cells were plated into two 225 cm^2 flasks (Becton, Dickinson and Company, Franklin Lakes, NJ, USA). The cells were then cultured in each medium at 37°C in a humidified atmosphere containing 95% air and 5% CO_2, and the medium was replaced every three days. When primary cultures became nearly confluent, the cells were detached with 0.25% trypsin containing 1 mM EDTA (Life Technologies) and subsequently replated for each assay. Cells were passaged at a density of 2×10^3 cells/cm^2, and hBMSCs at passages 1 (P1), P5, and P10 were stored in liquid nitrogen until further use. The collected hBMSCs were either cultured or preserved separately; the cells from individual donors were assayed independently to prevent cross contamination of hBMSCs from different donors.

2.2. Osteogenic Differentiation. BMSCs were replated at 2×10^3 cells/cm^2 in a six-well culture plate. When the culture plates became 80% confluent, the culture media of each group were changed to osteogenic media containing 10 mM β-glycerophosphate (β-GP, Sigma-Aldrich Co.) and 50 μg/mL ascorbic acid phosphate (AA, Wako, Osaka, Japan) [13] with or without 100 nM dexamethasone (DEX, Life Technologies) and/or BMP-2. After zero and seven days of osteogenic culture, the cells were used in each assay.

2.3. RNA Isolation, Real-Time RT-PCR. Total RNA was isolated from the culture dishes using RNeasy Mini Kits (Qiagen, GmbH, Hilden, Germany), and first-strand cDNA was prepared using the PrimeScript RT Reagent Kit with gDNA Eraser (Takara Bio Inc., Shiga, Japan) according to the manufacturer's instructions. Gene expression was quantified by real-time polymerase chain reaction (PCR) using the Mx3000P QPCR System (Agilent Technologies, Inc., Santa Clara, CA, USA) and GoTaq qPCR Master Mix (Promega Co., Fitchburg, WI, USA). Primer sets were predesigned and purchased from Takara Bio Inc. (Table 1). Standards were generated from one specific sample, and every PCR reaction in this study was run with a standard curve to quantify the relative Ct values of the samples. β-actin was used to normalize the amount of template that was present in each sample.

Table 1: RT-PCR primers used in this study.

Genes	Forward	Reverse
β-act	TGGCACCCAGCACAATGAA	CTAAGTCATAGTCCGCCTAGAAGCA
ALP	GGACCATTCCCACGTCT	CCTTGTAGCCAGGCCCATTG
Runx2	CACTGGCGCTGCAACAAGA	CATTCCGGAGCTCAGCAGAATA
ephrin-A1	TGATCGCCACACCGTCTTC	CAGCGTCTGCCACAGAGTGA
ephrin-A2	CTGCCTGCGACTGAAGGTGTA	ACACGAGTTATTGCTGGTGAAGATG
ephrin-A3	TCTGAGGATGAAGGTGTTCGTCTG	TTCTCAAGCTTGGGCACCTG
ephrin-A4	TCGGCTTTGAGTTCTTACCTGGA	AGACACCTGGAGCCTCAAGCA
ephrin-A5	TGCTGGCATGTCGGAGGTTA	ACTGCAAAGCAGGGCAGTACAAG
ephrin-B1	CCAAGAACCTGGAGCCCGTA	AGATGATGTCCAGCTTGTCTCCAAT
ephrin-B2	CTGCTGGATCAACCAGGAATAAAGA	TCCTGAAGCAATCCCTGCAAATA
ephrin-B3	CTGTCTACTGGAACTCGGCGAATAA	CCGATCTGAGGGTACAGCACATAA
EphA1	CCTGTGCTGCAAGGTGTCTGA	GTGAAGATCCGATGGGCAATG
EphA2	GAGCTTTGGCATTGTCATGTGG	GCACTGCATCATGAGCTGGTAGA
EphA3	TTTGTCCTGGCAAGAACCTGAAC	TTCGGGCTCGGATTTGGA
EphA4	GCCGAGTGAGCTCCAATGCTA	GCCTGCATACACAAGGTGAAGCTA
EphA5	GCCCGGCAGTATGTGTCTGTAA	TCCATTGGGACGATCTGGTTC
EphA7	AGAACACTGTCCTCACACTTGACC	TGACAAGCATAAACCACCAGTTCTA
EphA8	CCTATGGAAGTCGGAAACATGGTC	AGAGCCCAGAAATTGGGTAAGAGTG
EphB1	GCCCAATGGCATCATCCTG	ATCAATCCTTGCTGTGTTGGTCTG
EphB2	GACCAAGAGCACACCTGTGATGA	CCACCAGCTGGATGACTGTGA
EphB3	AGACTCGGACTCTGCGGACA	GCTCACTCCACTCGAGGATCA
EphB4	ATGCCTGGAGTTACGGGATTG	TCCAGCATGAGCTGGTGGAG
EphB6	GACCAATGGGAACATCCTGGAC	CCCGCACCTGGAAACCATAG

2.4. Lentivirus Production and Transduction. Lentivirus production was performed using the GeneCopoeia HIV-Based Lentiviral Expression System (GeneCopoeia, Inc., MD, USA): 1.3×10^6 GeneCopoeia 293Ta lentiviral packaging cells were plated in a 10 cm cell culture dish (Greiner Bio-One, Frickenhausen, Germany, Cat. number 664-960) in 10 mL of DMEM supplemented with 10% heat-inactivated fetal bovine serum and incubated at 37°C with 5% CO_2 for 24 hours before transfection.

In a sterile polypropylene tube, we diluted 2.5 μg of lentiviral ORF expression vector plasmid (GeneCopoeia) (Figure 1(a)), 1.25 μg of packaging plasmid, pCAG-HIVgp (a gift from Dr. Miyoshi, RIKEN), and 1.25 μg of VSV-G, Rev plasmid, and pCMV-VSV-G-RSV-Rev (a gift from Dr. Miyoshi, RIKEN) into 200 μL of Opti-MEM l (Invitrogen). In a separate tube, we diluted 15 μL of FuGENE HD Transfection Reagent (Promega, WI, USA) into Opti-MEM l. We added the diluted FuGENE dropwise to the DNA solution and incubated the mixture for 15 minutes at room temperature. We added the DNA-FuGENE complex directly to each dish and incubated the cells in a CO_2 incubator at 37°C overnight. The overnight culture medium was replaced with fresh DMEM medium supplemented with 4% heat-inactivated fetal bovine serum, penicillin-streptomycin, and 1/500 volume of Titer-Boost reagent (GeneCopoeia). Supernatants were collected 48 h after transfection, filtrated through 0.45 μm polyethersulfone (PES) low-protein-binding filters (Whatman, NJ, USA), and concentrated 40 times by Lenti-X Concentrator (Clontech) according to the manufacturer's protocols. The concentrated supernatant containing lentiviral particles was used directly to determine the titer and to transduce target cells in vitro. Lentiviral stocks were aliquoted and stored at −80°C. The titer of each batch of lentiviral vectors was assessed using the Lenti-X qRT-PCR titration kit (Clontech).

We plated 2×10^4 of the target P1 hBMSCs per well in a 24-well plate 24 h prior to viral infection. For each well, 0.5 mL of virus suspension was diluted in growth medium with polybrene at a final concentration of 4 μg/mL. We infected BMSCs by replacing the growth medium over the cells with the diluted viral supernatant [multiplicity of infection: 250 (MOI = 250)] and incubating the cells for 2 h at 4°C, followed by transfer to a 37°C incubator with 5% CO_2 and incubation overnight. The viral supernatant medium was then removed and lentivirus- (LV-) transduced BMSCs were replated at a density of 80 cells/cm^2 (clonal density) or 2×10^3 cells/cm^2 onto a 6-well plate and used for further assays.

2.5. Adhesion Assays. Culture plates for adhesion assays were coated with 7 μg/mL collagen I for 1 h at 37°C and then blocked with 1% BSA in DMEM. LV-transduced BMSCs were replated at a density of 2×10^3 cells/cm^2 onto a 6-well plate precoated with collagen I incubated for 24 h at 37°C. At 2 days after transduction, the nonadherent cells were removed by extensive, aggressive washing with PBS. The remaining adherent cells were then trypsinized and counted in a hemocytometer. Nontreated cells were used as a control. To calculate relative cell attachment, the number of attached cells was normalized to the number of control attached cells.

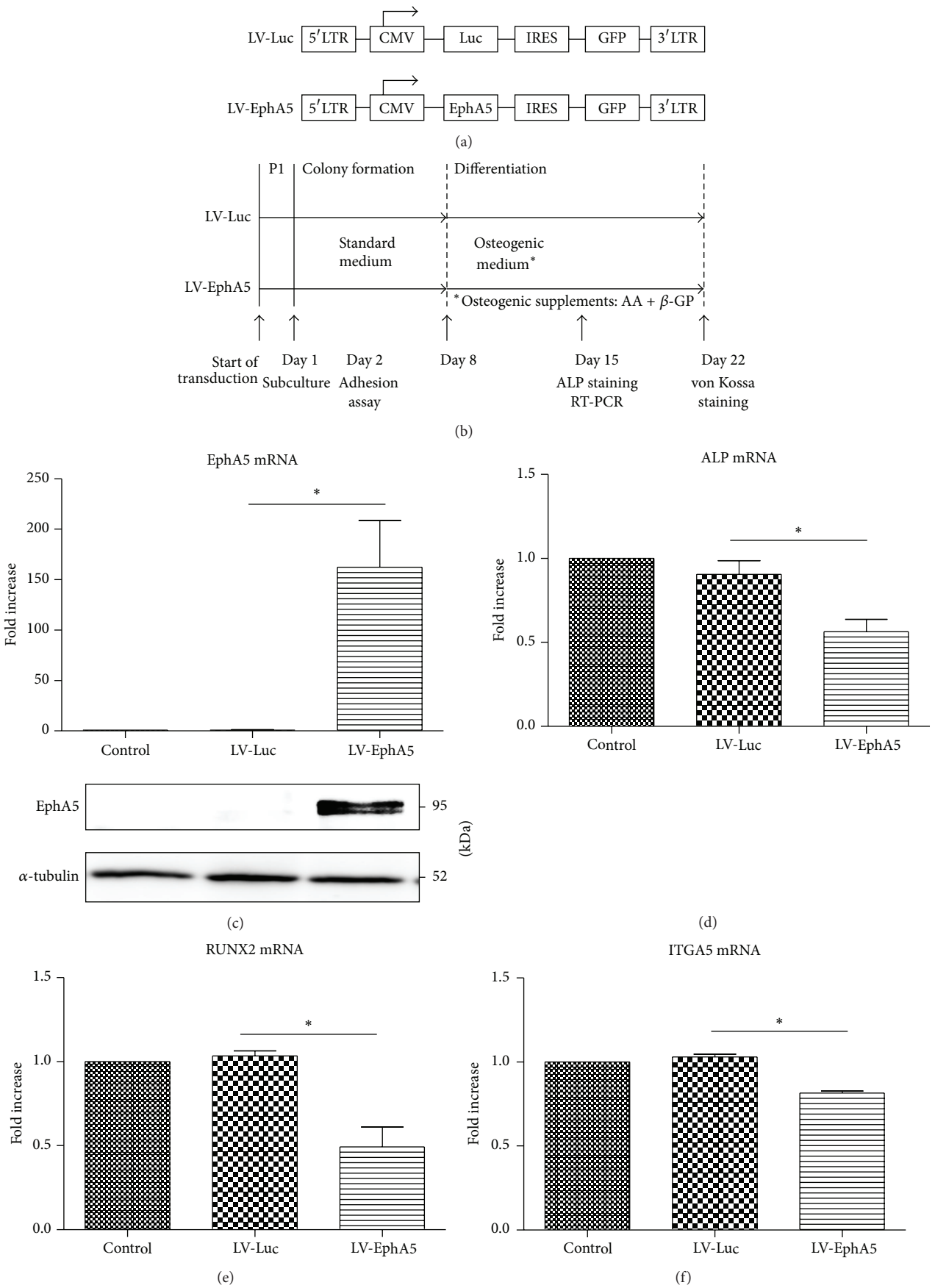

Figure 1: Continued.

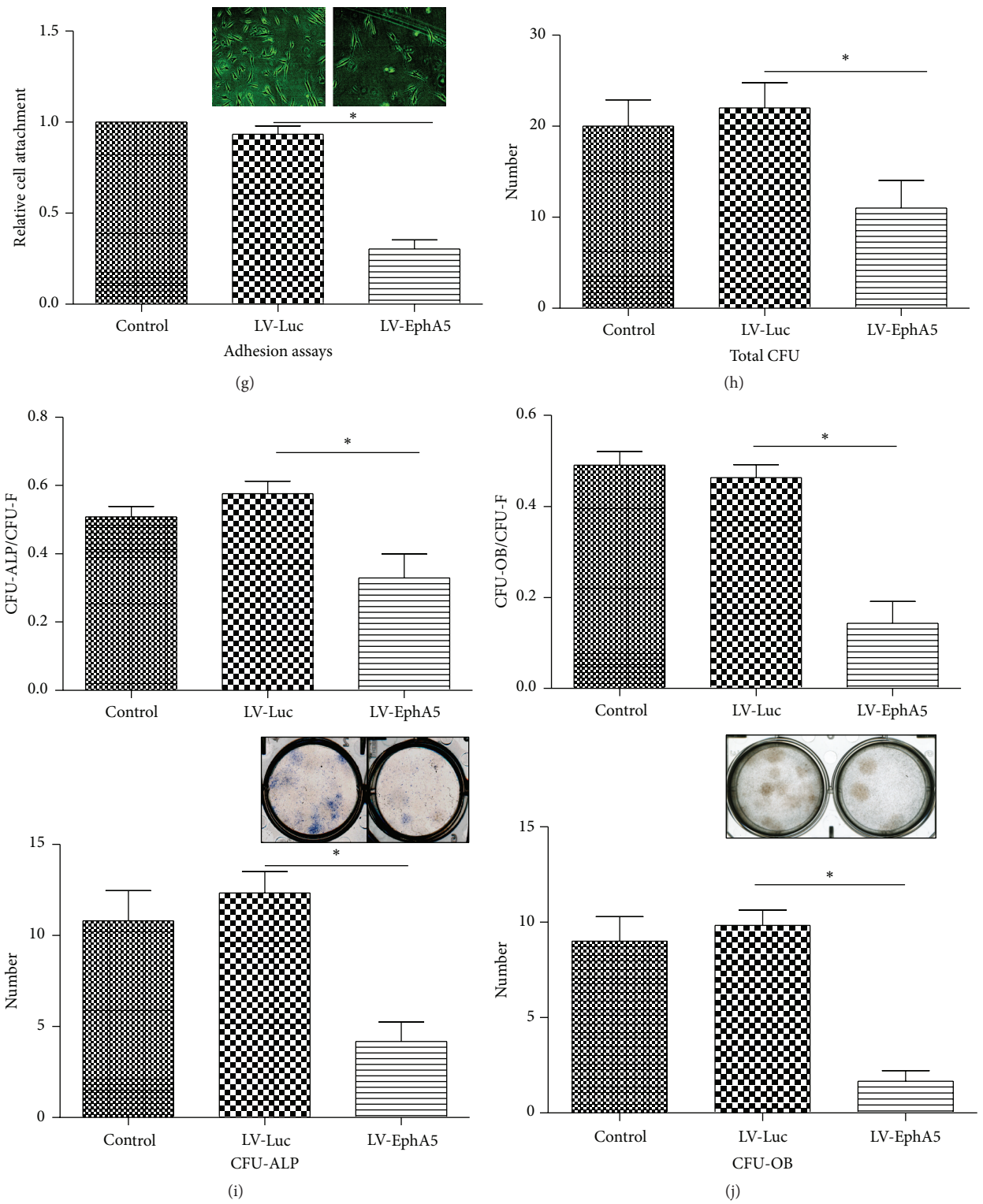

Figure 1: Forced expression of EphA5 inhibits osteoblast differentiation in hBMSCs. (a) Lentiviral constructs for transducing Luc and EphA5. (b) Schematic representation of the cell culture protocol. Adult hBMSCs were transduced with LV-Luc or LV-EphA5. ((c)–(f)) Quantitative analysis of mRNA expression of osteogenic markers at 7 days of osteogenic culture: (c) EphA5, (d) ALP, (e) Runx-2, and (f) ITGA5 ($n = 4$). The fold change of gene expression was normalized against the expression in cell cultures without LV transduction. ((c), lower) EphA5 protein levels were determined by western blot analysis. (g) Adhesion assays ($n = 4$). Images of cell attachment (upper). ((h)–(j)) CFU assays ($n = 4$). (h) Number of total colonies. (i) CFU-ALP positive rate (upper) and number of ALP-positive colonies (lower). Images of wells after ALP staining (middle). (j) CFU-OB positive rate (upper) and number of OB-positive colonies (lower). Images of wells after von Kossa staining (middle).

2.6. CFU Assay. For clonal analysis, colony-forming unit (CFU) assays were performed. BMSCs were plated at 800 cells/well in 6-well culture plates and maintained in each medium for 7 days to form single cell-derived colonies, respectively. Then, the medium was changed to an osteogenic medium (CFU-ALP and CFU-OB).

2.7. CFU-ALP. Dishes were stained for ALP at 7 days of osteogenic induction. Dishes fixed with 10% neutral buffered formalin were washed with PBS and then incubated with a filtered mixture of naphthol AS-MX phosphate (0.1 mg/mL, Sigma-Aldrich Co.), N,N-dimethylformamide (0.5%, Wako), $MgCl_2$ (2 mM), and Fast Blue BB salt (0.6 mg/mL, Sigma-Aldrich) in 0.1 M Tris-Cl (pH 8.5) for 30 min at room temperature.

2.8. CFU-OB. Mineralized colonies were identified by von Kossa staining and designated as colony-forming unit-osteoblasts (CFU-OB). At 14 days of osteogenic induction, cells were washed twice with Gey's balanced salt solution, fixed with 10% formalin, rinsed with 0.1 mol/L cacodylic buffer, and covered with 1.0 mL of 5% silver nitrate (Wako). The cells were then exposed to UV light for 1 h. Finally, the dishes were rinsed with distilled water and air-dried.

After positive colonies were counted in each assay, the dishes were stained with crystal violet to visualize all colonies present on the dishes, and the total number of colonies was determined. Colonies with a diameter < 2 mm and faintly stained colonies were ignored.

2.9. von Kossa Staining for Calcium Deposits. Cells were fixed with 10% formalin for 10 min at 4°C and washed with water three times, after which the cells were incubated with 3% silver nitrate for 60 min and exposed to light from a 40 W lamp. After rinsing with water, the cells were incubated with 5% sodium thiosulfate for 2 min followed by washing with water.

2.10. Western Blot Analysis. Proteins were extracted from hBMSCs. Total cellular protein was prepared by lysing cells in RIPA buffer at various time points. The protein concentration was determined using the BCA Protein Reagent Kit (Pierce, Rockford, IL). A primary antibody for EphA5 (AP7610d, ABGENT) and α-tubulin (11H10) rabbit mAb (#2125S, Cell Signaling Technology, Inc., Tokyo, Japan) were obtained. Protein (15 μg) was separated by 10% SDS-PAGE and then transferred to a polyvinylidene difluoride (PVDF) membrane. After blocking with PVDF Blocking Reagent for *Can Get Signal* (TOYOBO Life Science, Tokyo, Japan), membranes were hybridized with the primary antibody overnight at 4°C and then hybridized with HRP-linked anti-rabbit immunoglobulin G secondary antibody (#7074, Cell Signaling Technology, Inc., Tokyo, Japan) for 1 h at room temperature. We then added Lumigen TMA-6 (Lumigen Inc., Southfield, MI, USA) onto the membrane and let it stand for 2 minutes. The signals were detected using an enhanced chemiluminescence method on an ImageQuant LAS4000 Series system (GE Healthcare UK Ltd., England).

2.11. Microarray Analysis. The total RNA from subconfluent nontreated BMSCs and BMSCs treated with DEX for 6 h at P5 was isolated and then treated with DNase1 for microarray analysis. Total RNA (1 μg) was amplified and labeled with Cy3 or Cy5 using the Ambion Amino Allyl MessageAmp II aRNA Amplification Kit (Life Technologies, Cat. Number 1753) according to the manufacturer's instructions. An Agilent Whole Human Genome Microarray 4 × 44 K (G4110F) was hybridized with 825 ng of amplified RNA at 65°C for 16 h and washed using a Fluidics Station 450 system (Affymetrix, Inc., Santa Clara, CA, USA). The microarray slides were scanned using a GenePix 4000B scanner from Axon Instruments (Union City, CA, USA), and each microarray image was first analyzed using GenePix Pro 6.1 image analysis software (Molecular Devices, LLC, Sunnyvale, CA, USA) to determine the Cy3 and Cy5 fluorescence intensity and background noise for all spots on the array. The microarray data were normalized to the median value, and $\log_2$ ratios were calculated versus the values for the nontreated groups of the corresponding donor sample ($n = 9$). Genes that were up- or downregulated by more than threefold relative to the median value for all donor samples were further classified according to their protein types using the SOSUI program (http://bp.nuap.nagoya-u.ac.jp/sosui/).

2.12. Flow Cytometry Analysis. BMSCs cultured on a 100 mm culture dish with or without DEX treatment (100 nM, 14 days) were harvested by trypsinization. To identify ALP-positive cells, the collected cells were incubated for 30 min at 4°C with mouse monoclonal anti-human ALP antibody (R&D systems, Inc., Minneapolis, MN, USA) and washed and incubated with FITC-conjugated secondary antibody (rat anti-mouse IgG1 monoclonal antibody; Becton, Dickinson and Company) for 30 min at 4°C. Flow cytometric analyses were performed using a FACS Calibur system.

2.13. Ephrin-Fc and EphA5-Fc Treatment. Subconfluent monolayers of cells in 6-well plates were incubated with 0, 0.4, or 4 μg/mL Fc (6-001-A, R&D Systems, Inc., MN, USA), ephrin-Fc (SMPK3, R&D Systems, Inc.), or recombinant rat EphA5-Fc chimera (541-A5, R&D Systems, Inc.) in DMEM containing 10% fetal bovine serum, 50 μg/mL ascorbic acid (Sigma-Aldrich Co.), and 10 mM β-glycerophosphate (Wako) for the indicated times. The mRNA expression level of ALP at day 7 was measured in P1 and P5 cells ($n = 4$).

2.14. 5-Azacytidine and VPA Treatment. Valproic acid (VPA, P4543, Sigma, St. Louis, MO, USA) was dissolved in H_2O at a concentration of 1 M and added to the culture medium at a final concentration of 1 mM. BMSCs were cultured in media supplemented with 10 μM 5-azacytidine (A2385, Sigma) or 5-aza-2′-deoxycytidine (A3656, Sigma) for 4 days or 1 mM valproic acid for 24 h.

2.15. Genomic DNA Extraction and Sodium Bisulfate DNA Modification. Genomic DNA was isolated from cells and tissues using the DNeasy Kit (Qiagen) and stored at −20°C before use. Genomic DNA (1 μg) from P1 cells or P5 cells

was treated with sodium bisulfite according to the manufacturer's recommendations (EZ DNA Methylation-Gold Kit, Zymo Research, Orange, CA). Enzymatically methylated DNA (Universal Methylated Human DNA Standard, Zymo Research) was used as a positive control.

2.16. MSRE Digestion. Each reaction mixture for the OneStep qMethyl procedure was optimized for 20 ng of input DNA according to the manufacturer's recommendations (OneStep qMethyl Kit, Zymo Research, Orange, CA). The designed primers were 5′-AGGAGGCTCGGAGAAGATGC-3′ (forward) and 5′-CATCTCCCTACCTTCGTTGCTG-3′ (reverse), which amplify a DNA locus (region) that contains two methylation-sensitive restriction enzyme (MSRE) sites. The thermocycling conditions used were 37°C for 2 h during MSRE digestion; 1 cycle of 95°C for 10 minutes; 35 cycles of 95°C for 30 seconds, 63°C for 30 seconds, and 72°C for 30 seconds; and a final extension at 72°C for 7 minutes. The methylation level for amplified loci (regions) was determined using the following equation. Percent methylation = $100 \times 2^{-\Delta Ct}$, where ΔCt is the average Ct value from the test reaction minus the average Ct value from the reference reaction.

2.17. Statistical Analysis. The values were expressed as the arithmetic mean ± standard error of the mean (SEM) and analyzed using one-way analysis of variance (ANOVA). Then, Student's t-test was used for between-group comparisons. After the p values were corrected using the Bonferroni correction, statistical significance was determined. Statistical significance is indicated by "$*$" in the graphs.

3. Results

3.1. Forced Expression of EphA5 Suppresses Osteogenic Differentiation in hBMSCs. To overexpress EphA5 in BMSCs and determine the role of EphA5 in osteogenic differentiation, hBMSCs were transduced with a lentiviral vector encoding EphA5 and GFP (Figures 1(a) and 1(b)). The LV-EphA5-transduced cells showed increased GFP expression and increased EphA5 mRNA levels at 7 days of osteogenic culture (Figure 1(c)). EphA5 overexpression in hBMSCs decreased ALP mRNA, Runx2 mRNA, and ITGA5 mRNA expression levels (Figures 1(d), 1(e), and 1(f)) and did not affect EphA2 and EphA4 mRNA expression levels (S1 Figure, in Supplementary Material available online at http://dx.doi.org/10.1155/2016/1301608). LV-EphA5-transduced BMSCs demonstrated decreased adhesion to 6-well plates compared with LV-Luc-transduced BMSCs or control untreated BMSCs at 1 day after seeding. There were no marked differences in the cell morphology between LV-Luc- and LV-EphA5-transduced BMCSs (Figure 1(g)).

Consistent with this effect, LV-EphA5 transduction in hBMSCs decreased the osteogenic capacity of the hBMSCs as indicated by negative ALP staining and selectively inhibited their colony formation. BMSCs transduced with the lentiviral vector at passage 1 were plated at clonal density and cultured in growth medium for 7 days through the colony formation period. Each well was then incubated in osteogenic medium for an additional 7 or 14 days. Colonies were stained and ALP-positive and OB-positive colonies were counted. The total colony number and ratio of ALP- and OB-positive colonies in the LV-EphA5-treated wells were lower than those in the LV-Luc-treated wells (Figures 1(h)–1(j)). These results demonstrate that forced expression of EphA5 is sufficient to decrease not only the expression of osteoblast markers and osteogenic capacity of primary hBMSCs but also cell attachment on culture wells.

3.2. EphA5 is Upregulated in Late Culture and Downregulated during Osteogenic Induction with DEX. We analyzed the expression of all known members of the ephrin and Eph families in the hBMSC cultures after osteogenic induction with DEX and BMP-2 (Figure 2(a)). When DEX treatment was continued for 72 h, the mRNA expression of ephrin-B1, EphA2, EphA5, EphB1, EphB2, and EphB3 among the ephrin receptor tyrosine kinase subfamily was decreased, whereas that of ephrin-B2 and EphB6 was increased. In contrast, BMP-2 treatment increased the expression of ephrin-A4, ephrin-A5, EphA2, EphA3, EphA4, and EphA5. The expression pattern of ephrins and Eph receptors during osteogenic induction using BMP-2 thus differed from that during osteogenic induction using DEX. A synergetic effect of DEX and BMP-2 was observed, as demonstrated by increased ALP mRNA expression. Among the ephrin and Eph families, the expression pattern of EphA5 was closely related to that of EphA2 when hBMSCs were treated with DEX and/or BMP. For example, the fall in EphA5 and EphA2 levels by DEX treatment was matched by rises in EphA3 and EphA4 levels in most samples.

We investigated the effect of continuous DEX treatment throughout the proliferation stage of BMSCs on differentiation capability by comparing DEX-treated cells with untreated cells. DEX treatment throughout the culture period led to dramatic changes in cell morphology (Figure 2(b)). Larger ALP-positive subpopulations were observed after continuous DEX treatment, which indicates that selection of osteogenic cell populations occurred (Figure 2(b)). Furthermore, we evaluated the effect of intercellular contact on the osteogenic capability of BMSCs under different induction protocols (Figure 2(c)). Augmentation of ALP mRNA expression with DEX induction was observed irrespective of cell density, whereas DEX-excluded osteogenic induction exerted a stronger effect at a high cell density than at a low cell density (Figure 2(d)), possibly because of the effect of osteogenic factors requiring cell-cell contact, such as those expressed by aligned osteoblasts, or osteogenic humoral factors released from BMSCs at high density. In contrast, EphA5 mRNA expression was minimally affected by the cell density when the cells were subjected to DEX-excluded osteogenic induction (Figure 2(e), S2 Figures A and B).

To investigate DEX-mediated osteogenesis, BMSCs at P5 were stimulated with 10^{-7} M DEX for various durations. Although the decrease in EphA5 mRNA levels showed biphasic changes, DEX treatment inhibited EphA5 mRNA expression for up to 6 hours in most samples, followed by increased expression of ALP (Figure 2(f)). On the other hand, BMP-2 treatment showed the increase in EphA5 mRNA

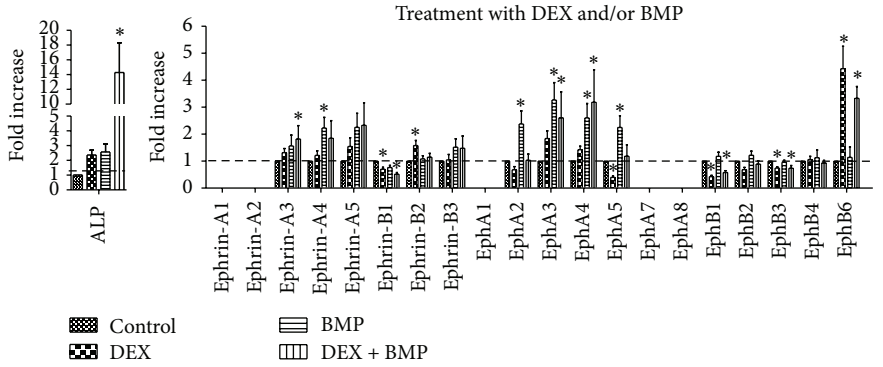

(a)

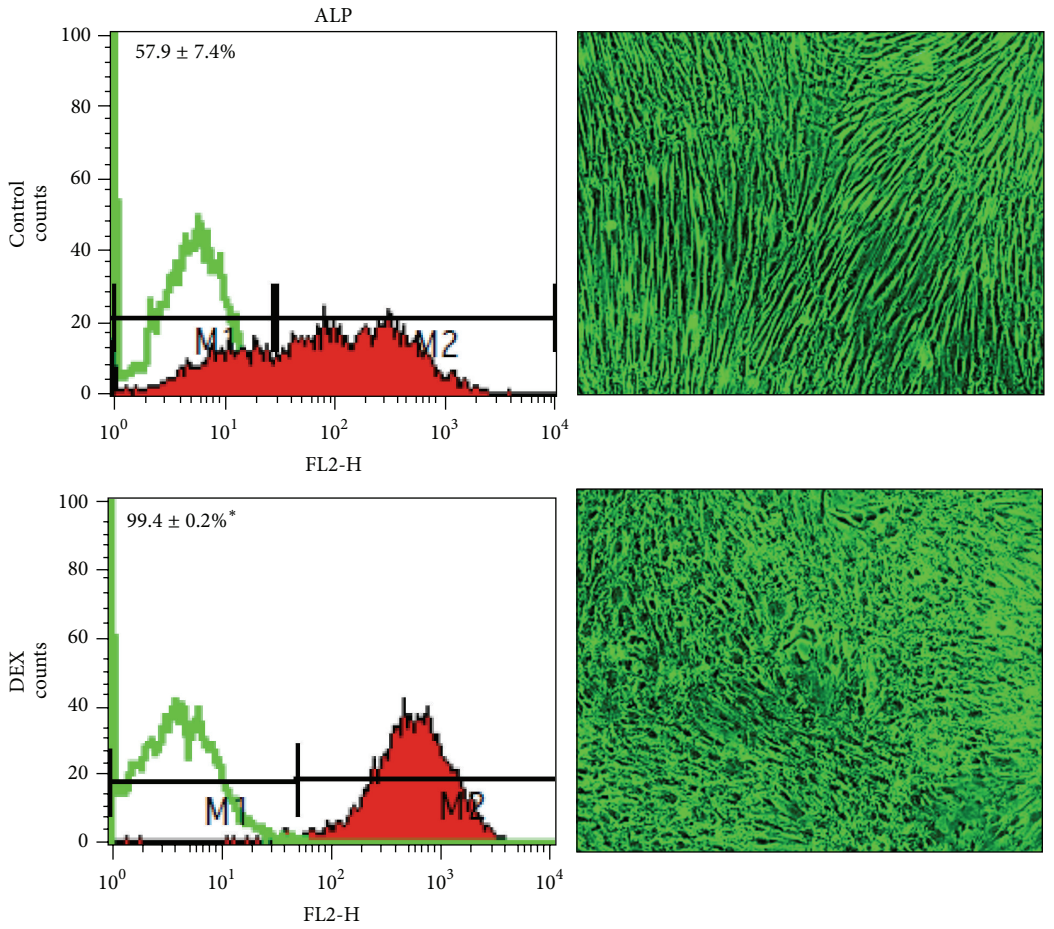

(b)

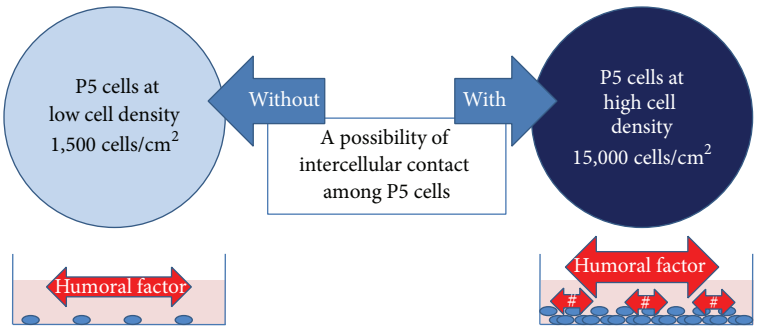

(c)

Figure 2: Continued.

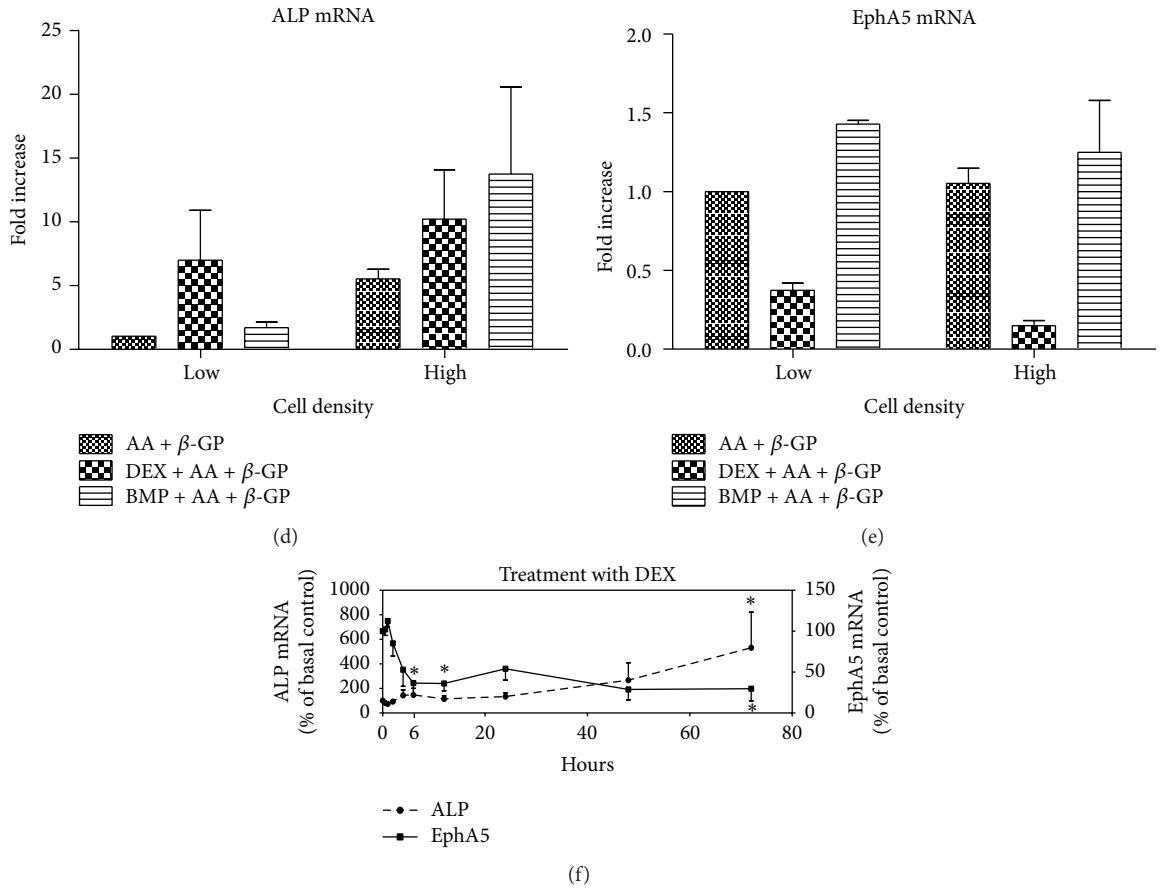

Figure 2: EphA5 is upregulated after repeated passaging and downregulated during osteogenic induction with DEX. (a) Expression of members of the ephrin and Eph receptor families in hBMSCs. P5 BMSCs were differentiated into osteogenic lineages using AA + β-GP + DEX or BMP-2, and quantitative PCR to determine the mRNA expression of ephrin and Eph receptor family members was performed at day 3 of osteogenic induction ($n = 8$). The fold change of gene expression was normalized against the expression level in the nontreated culture. DEX treatment suppressed and BMP treatment increased the mRNA expression of both EphA2 and EphA5, respectively. (b) Cell surface alkaline phosphatase (ALP) expression in hBMSCs at passage 5 was analyzed using flow cytometry (left, $n = 4$). Positive expression was defined as a level of fluorescence higher than 97% of the fluorescence obtained with the corresponding isotype-matched control antibody. Positive expression rates are displayed as the mean ± SEM (green line, isotype control). DEX-treated cells showed a higher positive rate for ALP expression than untreated cells ($^*p < 0.05$). Cell bodies became smaller and showed morphological changes at day 14 of DEX treatment (right, magnification ×40). ((c)–(e)) Effect of cell density on ALP and EphA5 mRNA levels under different osteogenic induction protocols. (c) hBMSCs at P5 were seeded at low cell density, without intercellular contact, or at high cell density, that is, almost at confluency. # shows intracellular contact between P1 and P5 cells. ((d), (e)) Quantitative analyses of (d) ALP and (e) EphA5 mRNA expression. The fold change of gene expression was normalized against the expression in cultures at low density with AA and β-GP treatment ($n = 4$). (f) Quantitative analyses of ALP and EphA5 mRNA expression in BMSCs at passage 5 when treated with DEX. The change in the expression of each gene expression was normalized against the expression in cell cultures prior to DEX addition ($n = 9$). EphA5 expression was transiently reduced after 2 hours of DEX induction and reached a minimum value after 6 h of induction. ALP expression was induced after 24 h of DEX induction, after which EphA5 expression gradually decreased again.

levels, leading to different results compared to DEX treatment (S2 Figure C).

To clarify the mechanism through which DEX promotes hBMSC osteogenesis, the differential gene expression of DEX-untreated BMSCs versus BMSCs treated with DEX for 6 h at P5 was analyzed by Affymetrix GeneChip technology for 9 independent BMSC preparations. The microarray analysis revealed that DEX treatment upregulated ITGA5 (Table 2) and its downstream target PIK3R1, in addition to FKBP5, the Src kinase family (SGEF, SHC4, SLA, and DIRAS3), FoxO1, and BMP-6. As expected, this treatment downregulated not only EphA5 but also downstream targets of EphA such as Rho/RAS-related genes (e.g., RASD1, ARHGAP, and RGNEF). Of note, DEX treatment altered the expression of various interleukins, tumor necrosis factors, and chemokine receptors (Tables 2 and 3). These dramatic changes caused by DEX induction may be a key to understanding the mechanism of osteogenic differentiation. ITGA5 upregulation induced by DEX has been reported to promote osteoblast differentiation of hBMSCs [16] and, in the present study, RT-PCR also revealed that osteogenic induction using DEX promoted ITGA5 expression at 7 days (S3 Figure).

Table 2: Genes upregulated in hBMSCs by DEX treatment. Human genes upregulated by at least threefold in hBMSCs treated with DEX for 6 h at P5 compared with nontreated cells.

Genes		Gene bank	Log_2 ratio
FKBP5	FK506 binding protein 5	NM_004117	3.932
CYP19A1	Cytochrome P450, family 19, subfamily A, polypeptide 1, transcript variant 2	NM_031226	3.880
HEYL	Hairy/enhancer-of-split related to YRPW motif-like	NM_014571	3.162
BMP6	Bone morphogenetic protein 6	NM_001718	3.006
DKK1	Dickkopf homolog 1 (*Xenopus laevis*)	NM_012242	2.889
TNFAIP8L3	Tumor necrosis factor, alpha-induced protein 8-like 3	NM_207381	2.685
INHBB	Inhibin, beta B	NM_002193	2.653
MYPN	Myopalladin	NM_032578	2.594
CPM	Carboxypeptidase M, transcript variant 1	NM_001874	2.590
XIRP1	Xin actin-binding repeat containing 1	NM_194293	2.543
FOXO1	Forkhead box O1	NM_002015	2.413
CDH15	Cadherin 15, type 1, M-cadherin (myotubule)	NM_004933	2.377
GAL	Galanin prepropeptide	NM_015973	2.345
SNCAIP	Synuclein, alpha interacting protein	NM_005460	2.338
RNF128	Ring finger protein 128, transcript variant 1	NM_194463	2.293
PRICKLE2	Prickle homolog 2 (*Drosophila*)	NM_198859	2.289
ADRA1B	Adrenergic, alpha-1B-, receptor	NM_000679	2.267
PTGER2	Prostaglandin E receptor 2 (subtype EP2), 53 kDa	NM_000956	2.254
PPP1R14C	Protein phosphatase 1, regulatory (inhibitor) subunit 14C	NM_030949	2.234
WISP1	WNT1 inducible signaling pathway protein 1, transcript variant 2	NM_080838	2.220
ANGPTL4	Angiopoietin-like 4, transcript variant 1	NM_139314	2.201
DIRAS3	DIRAS family, GTP-binding RAS-like 3	NM_004675	2.173
ZNF469	Zinc finger protein 469	NM_001127464	2.145
CRYGS	Crystallin, gamma S	NM_017541	2.140
MT1M	Metallothionein 1M	NM_176870	2.121
SHC4	SHC (Src homology 2 domain containing) family, member 4	NM_203349	2.070
SGEF	Src homology 3 domain-containing guanine nucleotide exchange factor	NM_015595	2.046
TET3	Tet oncogene family member 3	NM_144993	2.019
PAG1	Phosphoprotein associated with glycosphingolipid microdomains 1	NM_018440	1.986
EEPD1	Endonuclease/exonuclease/phosphatase family domain containing 1	NM_030636	1.980
SLC20A1	Solute carrier family 20 (phosphate transporter), member 1	NM_005415	1.971
CMKLR1	Chemokine-like receptor 1, transcript variant 1	NM_001142343	1.970
FABP5	Fatty acid binding protein 5 (psoriasis-associated)	NM_001444	1.948
ABLIM3	Actin binding LIM protein family, member 3	NM_014945	1.944
SEC14L2	SEC14-like 2 (S. cerevisiae), transcript variant 1	NM_012429	1.942
CAMK2N1	Calcium/calmodulin-dependent protein kinase II inhibitor 1	NM_018584	1.906
HS3ST3B1	Heparan sulfate (glucosamine) 3-O-sulfotransferase 3B1	NM_006041	1.839
KBTBD11	Kelch repeat and BTB (POZ) domain containing 11	NM_014867	1.829
WNT5B	Wingless-type MMTV integration site family, member 5B, transcript variant 2	NM_030775	1.817
SLA	Src-like adaptor, transcript variant 1	NM_001045556	1.788
MT1G	Metallothionein 1G	NM_005950	1.781
MT1A	Metallothionein 1A	NM_005946	1.780
TOP1	Topoisomerase (DNA) I	NM_003286	1.771
MTSS1	Metastasis suppressor 1	NM_014751	1.765
BAIAP2	BAI1-associated protein 2, transcript variant 3	NM_006340	1.750
IRAK3	Interleukin-1 receptor-associated kinase 3, transcript variant 1	NM_007199	1.740
MT1B	Metallothionein 1B	NM_005947	1.734
FADS1	Fatty acid desaturase 1	NM_013402	1.725
ABTB2	Ankyrin repeat and BTB (POZ) domain containing 2	NM_145804	1.715

Table 2: Continued.

Genes		Gene bank	Log_2 ratio
JARID2	Jumonji, AT rich interactive domain 2	NM_004973	1.686
ITGA5	Integrin, alpha 5 (fibronectin receptor, alpha polypeptide)	NM_002205	1.652
MT1X	Metallothionein 1X	NM_005952	1.647
GJB3	Gap junction protein, beta 3, 31 kDa, transcript variant 1	NM_024009	1.645
MT1H	Metallothionein 1H	NM_005951	1.639
HIVEP3	Human immunodeficiency virus type I enhancer binding protein 3	NM_024503	1.619
TCF7	Transcription factor 7 (T-cell specific, HMG-box), transcript variant 1	NM_003202	1.617
NR2F1	Nuclear receptor subfamily 2, group F, member 1	NM_005654	1.613

A total of 28,780 human genes consistent with the quality criteria, genes upregulated threefold or higher are listed.

EphA5 and ITGA5 may therefore be involved in this DEX-mediated osteogenic pathway.

3.3. hBMSCs Treated with EphA5-Fc and Untreated hBMSCs Express ALP mRNA at Similar Levels. In many cell types, Eph forward signaling and ephrin reverse signaling mediate opposite effects. It is therefore important to determine which signal contributes to the deterioration of the differentiation capability of hBMSCs. To clarify the opposite effects of Eph forward signaling and ephrin reverse signaling on the differentiation capability of hBMSCs, we first used various ephrin-Fc constructs to stimulate Eph forward signaling. Treatment with ephrin-A-Fc, which mainly activates various EphA forward signaling pathways, did not affect ALP mRNA levels, while treatment with ephrin-B-Fc significantly increased ALP mRNA expression (Figure 3(a)).

We performed q-PCR assays of cells cultured in the presence of a soluble form of the EphA5 extracellular domain fused to Fc (EphA5-Fc), based on the hypothesis that the EphA5-Fc soluble receptor, upon binding to ephrin ligands, would activate ephrin reverse signaling and inhibit Eph forward signaling by competing with the endogenous EphA5 receptor to bind to the ephrin ligand in hBMSCs. However, we found that exogenous addition of soluble EphA5-Fc did not affect ALP mRNA expression levels in either P1 cells or P5 cells (Figure 3(b)).

3.4. Silencing of EphA5 in Early-Passage hBMSCs Is Not Associated with Aberrant Hypermethylation of Its Promoter. EphA5 was prominently upregulated over the course of hBMSC proliferation. This mechanism may be associated with active suppression at lower passage numbers. To further elucidate the mechanism underlying the silencing of EphA5 in early-passage P1 cells, we analyzed the 5′ regulatory region of the EphA5 gene. In particular, we analyzed a 406 bp segment of a CpG island encompassing the TSS (transcription start site) (−103 to +303 bp; TSS, +1) that contains 38 CpG dinucleotides; this segment spans the core promoter exon and part of intron 1. The methylation level for the EphA5 promoter, which contains two methylation-sensitive restriction enzyme (MSRE) sites, was determined. The methylation level for the EphA5 promoter in hBMSCs at P1 or P5 was similar to that in human nonmethylated DNA as a negative control. EphA5 promoter was barely methylated in P1 and P5 cells, even under DEX treatment (Figure 4(a)).

Treatment of hBMSCs with the DNA methylation inhibitors 5-azacytidine and 5-aza-2′-deoxycytidine did not alter EphA5 mRNA expression, indicating a lack of sensitivity of EphA5 expression to genomic DNA methylation status. However, treatment with the histone deacetylase 1 (HDAC1) inhibitor valproic acid (VPA) for 24 hours significantly increased EphA5 mRNA expression in P1 and P5 cells (Figure 4(b)). We then evaluated whether passage-dependent changes in histone deacetylation affected EphA5 expression by treating BMSCs at each passage with VPA. VPA treatment at 1 mM only slightly increased EphA expression in late-passage cells (Figure 4(c)), which suggests that histone deacetylation suppresses EphA5 expression in early-passage cultures and that chromatin remodeling through histone deacetylation is a potential mechanism for silencing of the EphA5 gene.

4. Discussion

Eph and Eph-related receptors have been implicated in developmental events, particularly in the nervous system [17–22]. The role of Eph receptors and ephrin ligands in cell adhesion and migration [23–25], formation of tissue compartment borders [26–28], and regulation of cell proliferation in various tumors [29–35] is also well documented; however, their potential role in bone biology is only now beginning to emerge. Among the ephrin and Eph family members expressed in hBMSCs, only EphA5 was upregulated in late-passage cultures [5]. In this study, we focused on the effects of EphA5 on BMSC osteogenic differentiation and provided data showing that EphA5 is important for regulating the osteogenic differentiation capability of hBMSCs. Gain-of-function studies showed that EphA5 diminishes the expression of osteoblast phenotypic markers. Downregulation of endogenous EphA5 by specific siRNAs or DEX treatment promoted osteoblast marker expression and osteogenic differentiation [5]. Therefore, considering that prolonged culture periods reduce the osteogenic differentiation potential of hBMSCs and EphA5 is gradually upregulated during long-term culture [5] (S2 Figure B), EphA5 could be involved in both the dormancy process and normal growth regulation of BMSCs and could be a potential

Table 3: Genes downregulated in hBMSCs by DEX treatment. Human genes downregulated by at least threefold in hBMSCs treated with DEX for 6 h at P5 compared with nontreated cells.

Genes		Genebank	Log_2 ratio
EGR2	Early growth response 2 (Krox-20 homolog, *Drosophila*), transcript variant 1	NM_000399	−4.446
CXCL1	Chemokine (C-X-C motif) ligand 1 (melanoma growth stimulating activity, alpha)	NM_001511	−4.060
EGR1	Early growth response 1	NM_001964	−3.989
CXCL2	Chemokine (C-X-C motif) ligand 2	NM_002089	−3.925
ATF3	Activating transcription factor 3, transcript variant 4	NM_001040619	−3.847
EGR3	Early growth response 3	NM_004430	−3.382
NR4A1	Nuclear receptor subfamily 4, group A, member 1, transcript variant 1	NM_002135	−3.312
IER3	Immediate early response 3	NM_003897	−3.294
SERTAD4	SERTA domain containing 4	NM_019605	−3.142
FOS	v-fos FBJ murine osteosarcoma viral oncogene homolog	NM_005252	−3.050
FOSB	FBJ murine osteosarcoma viral oncogene homolog B, transcript variant 1	NM_006732	−3.042
CXCL3	Chemokine (C-X-C motif) ligand 3	NM_002090	−2.950
ZC3H12A	Zinc finger CCCH-type containing 12A	NM_025079	−2.949
IL-8	Interleukin-8	NM_000584	−2.917
GDF15	Growth differentiation factor 15	NM_004864	−2.887
IL-6	Interleukin-6 (interferon, beta 2)	NM_000600	−2.886
MAP3K8	Mitogen-activated protein kinase kinase kinase 8	NM_005204	−2.837
BTG2	BTG family, member 2	NM_006763	−2.669
SEMA6D	Sema domain, transmembrane domain (TM), and cytoplasmic domain, (semaphorin) 6D, transcript variant 6	NM_024966	−2.659
PTGS2	Prostaglandin-endoperoxide synthase 2 (prostaglandin G/H synthase and cyclooxygenase)	NM_000963	−2.586
HES1	Hairy and enhancer of split 1, (*Drosophila*)	NM_005524	−2.520
HAS3	Hyaluronan synthase 3, transcript variant 2	NM_138612	−2.502
NCOA7	Nuclear receptor coactivator 7, transcript variant 1	NM_181782	−2.390
EYA1	Eyes absent homolog 1 (*Drosophila*), transcript variant 3	NM_000503	−2.376
JUNB	Jun B proto-oncogene	NM_002229	−2.356
C10orf10	Chromosome 10 open reading frame 10 (C10orf10)	NM_007021	−2.347
PIM1	Pim-1 oncogene	NM_002648	−2.316
ST8SIA1	ST8 alpha-N-acetyl-neuraminidase alpha-2,8-sialyltransferase 1	NM_003034	−2.256
C5orf41	Chromosome 5 open reading frame 41 (C5orf41)	NM_153607	−2.251
KLHL24	Kelch-like 24 (Drosophila)	NM_017644	−2.248
JUN	Jun oncogene	NM_002228	−2.247
BCL2L11	BCL2-like 11 (apoptosis facilitator), transcript variant 1	NM_138621	−2.227
EBF3	Early B-cell factor 3	NM_001005463	−2.195
NFκBIZ	Nuclear factor of kappa light polypeptide gene enhancer in B-cells inhibitor, zeta, transcript variant 1	NM_031419	−2.188
AMOTL2	Angiomotin like 2	NM_016201	−2.160
TOX	Thymocyte selection-associated high mobility group box	NM_014729	−2.149
NUAK2	NUAK family, SNF1-like kinase, 2	NM_030952	−2.112
SASH1	SAM and SH3 domain containing 1	NM_015278	−2.112
SLC40A1	Solute carrier family 40 (iron-regulated transporter), member 1	NM_014585	−2.102
CCL2	Chemokine (C-C motif) ligand 2	NM_002982	−2.089
ID4	Inhibitor of DNA binding 4, dominant negative helix-loop-helix protein	NM_001546	−2.034

Table 3: Continued.

Genes		Genebank	Log_2 ratio
FAM110B	Family with sequence similarity 110, member B	NM_147189	−2.030
AXUD1	AXIN1 upregulated 1	NM_033027	−2.014
BCL3	B-cell CLL/lymphoma 3	NM_005178	−2.011
ARL4C	ADP-ribosylation factor-like 4C	NM_005737	−2.011
IER2	Immediate early response 2	NM_004907	−2.009
RASD1	RAS, dexamethasone-induced 1	NM_016084	−2.007
OSR2	Odd-skipped related 2 (*Drosophila*), transcript variant 2	NM_053001	−1.985
GAB1	GRB2-associated binding protein 1, transcript variant 1	NM_207123	−1.977
TNFAIP3	Tumor necrosis factor, alpha-induced protein 3	NM_006290	−1.954
PDK4	Pyruvate dehydrogenase kinase, isozyme 4	NM_002612	−1.930
BMP4	Bone morphogenetic protein 4, transcript variant 1	NM_001202	−1.867
BDKRB1	Bradykinin receptor B1	NM_000710	−1.849
IRF1	Interferon regulatory factor 1	NM_002198	−1.840
N4BP2L1	NEDD4 binding protein 2-like 1, transcript variant 1	NM_052818	−1.814
ARHGAP20	Rho GTPase activating protein 20	NM_020809	−1.802
NFκBIA	Nuclear factor of kappa light polypeptide gene enhancer in B-cells inhibitor, alpha	NM_020529	−1.801
CXCR7	Chemokine (C-X-C motif) receptor 7	NM_020311	−1.789
RFTN2	Raftlin family member 2	NM_144629	−1.774
PRICKLE1	Prickle homolog 1 (*Drosophila*)	NM_153026	−1.768
TIAM2	T-cell lymphoma invasion and metastasis 2, transcript variant 1	NM_012454	−1.753
BIRC3	Baculoviral IAP repeat-containing 3, transcript variant 1	NM_001165	−1.751
C5orf4	Chromosome 5 open reading frame 4, transcript variant 2	NM_032385	−1.731
GATA6	GATA binding protein 6	NM_005257	−1.729
CLDN23	Claudin 23	NM_194284	−1.719
TNFRSF11B	Tumor necrosis factor receptor superfamily, member 11b	NM_002546	−1.700
C2orf67	*Homo sapiens* chromosome 2 open reading frame 67 (C2orf67), mRNA [NM_152519]	NM_152519	−1.693
TRIB3	Tribbles homolog 3 (*Drosophila*)	NM_021158	−1.693
EBF1	Early B-cell factor 1	NM_024007	−1.684
PRAGMIN	Homolog of rat pragma of Rnd2	NM_001080826	−1.683
MAFB	v-maf musculoaponeurotic fibrosarcoma oncogene homolog B (avian)	NM_005461	−1.680
ZFP36	Zinc finger protein 36, C3H type, homolog (mouse)	NM_003407	−1.673
IL-7	Interleukin-7	NM_000880	−1.642
RUNX1T1	Runt-related transcription factor 1; translocated to, 1 (cyclin D-related), transcript variant 1	NM_004349	−1.628
HK2	Hexokinase 2	NM_000189	−1.623
EPHA5	EPH receptor A5, transcript variant 1	NM_004439	−1.186

A total of 28,780 human genes consistent with the quality criteria, genes downregulated twofold or higher are listed.

candidate marker for replicative senescence. Previous reports suggested that EphA5 is involved in regulation of tumor dormancy [36, 37]. Furthermore, several studies previously indicated that cell senescence-related genes are localized on human chromosome 4, as introduction of normal human chromosome 4 into three immortal cell lines resulted in a loss of proliferation and reversal of the immortal phenotype [4, 38]. In contrast to EphA2, which resides on chromosome 1; EphA3, EphB1, EphB2, and EphB3 on chromosome 3; EphA4 on chromosome 2; and EphB4 and EphB6 on chromosome 7, EphA5 is located on chromosome 4q13, which might further support its involvement in senescence.

In many cell types, Eph forward signaling and ephrin reverse signaling mediate opposite effects [39–41]. Emerging evidence suggests that cells coexpressing Eph receptors and ephrins exist in many tissues and the coexpression of EphAs and ephrin-A results in *trans*- (between adjacent cells) or *cis*- (in the same cell) interactions [42, 43]. Coclustering

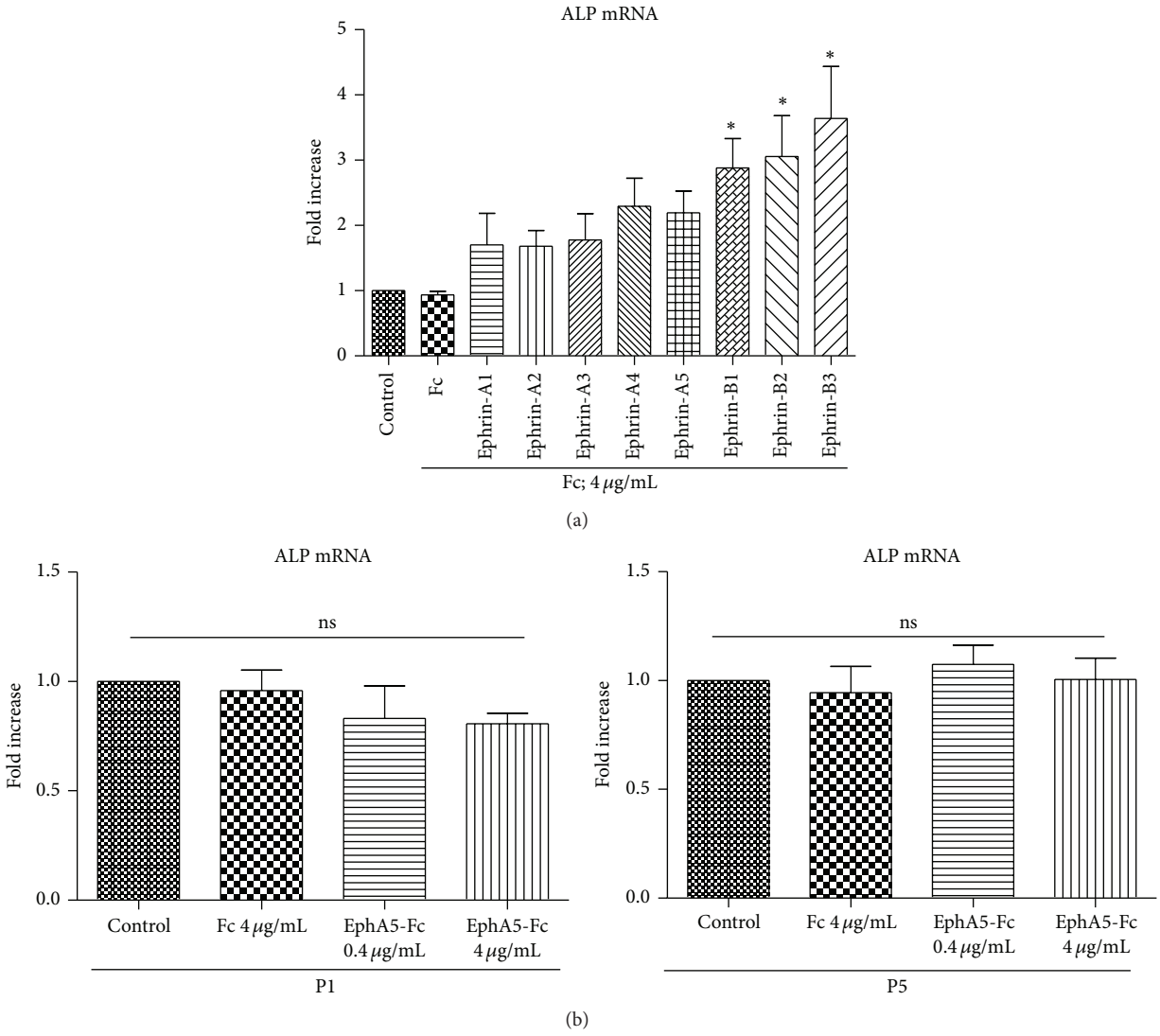

Figure 3: hBMSCs treated with EphA5-Fc express ALP mRNA at levels similar to those of nontreated hBMSCs. (a) hBMSCs at P5 were left untreated (control) or treated for 7 days with 4 μg/mL Fc or ephrin-Fc. Quantitative analysis of ALP mRNA expression ($n = 4$). The fold change of gene expression was normalized against the expression in cell cultures without Fc treatment. (b) hBMSCs at P1 (left) or P5 (right) were left untreated (control) or treated for 7 days with 0 or 4 μg/mL Fc and EphA5-Fc. Quantitative analysis of ALP mRNA expression ($n = 4$). The fold change of gene expression was normalized against the expression in cell cultures without Fc treatment. Images of wells after ALP staining (upper).

occurs also between EphA and EphB receptors, resulting in activation of both receptor types that does not require the presence of both ligands, with outcomes depending on the relative receptor expression [44]. We previously found that various endogenous EphA and EphB receptors are expressed in hBMSC like tumor cells [5]. We now propose that coexpression of Eph receptors and ephrins regulates the osteogenic differentiation of hBMSCs. At early passages of hBMSC primary culture, EphA5 is expressed at low levels, independent of methylation. Under normal conditions, EphA5 and ephrin-As/ephrin-Bs are properly expressed and engaged with each other. The signaling triggered by EphA activation counteracts growth factor signaling by promoting activation of Ras/ERK and PI3K/Akt [45], which contributes to the maintenance of cell homeostasis. Repeated passaging results in selective upregulation of EphA5 but not ephrins [5] thereby leading to an excess of nonligated EphA5.

In the present study, although Eph forward signaling stimulated by ephrin-B-Fc promoted the expression of ALP mRNA in BMSCs as previously reported [6, 46, 47] (Figure 3(a)), treatment with ephrin-A-Fc did not significantly affect osteogenic differentiation in vitro. In particular, exogenous addition of EphA5-Fc, which could activate ephrin reverse signaling or inhibit EphA5 forward signaling by competitive bindings, did not affect the ALP expression level. Moreover, although the expression of EphA5 at low cell density, where there is no possibility of intercellular contact among BMSCs, is nearly identical to that observed

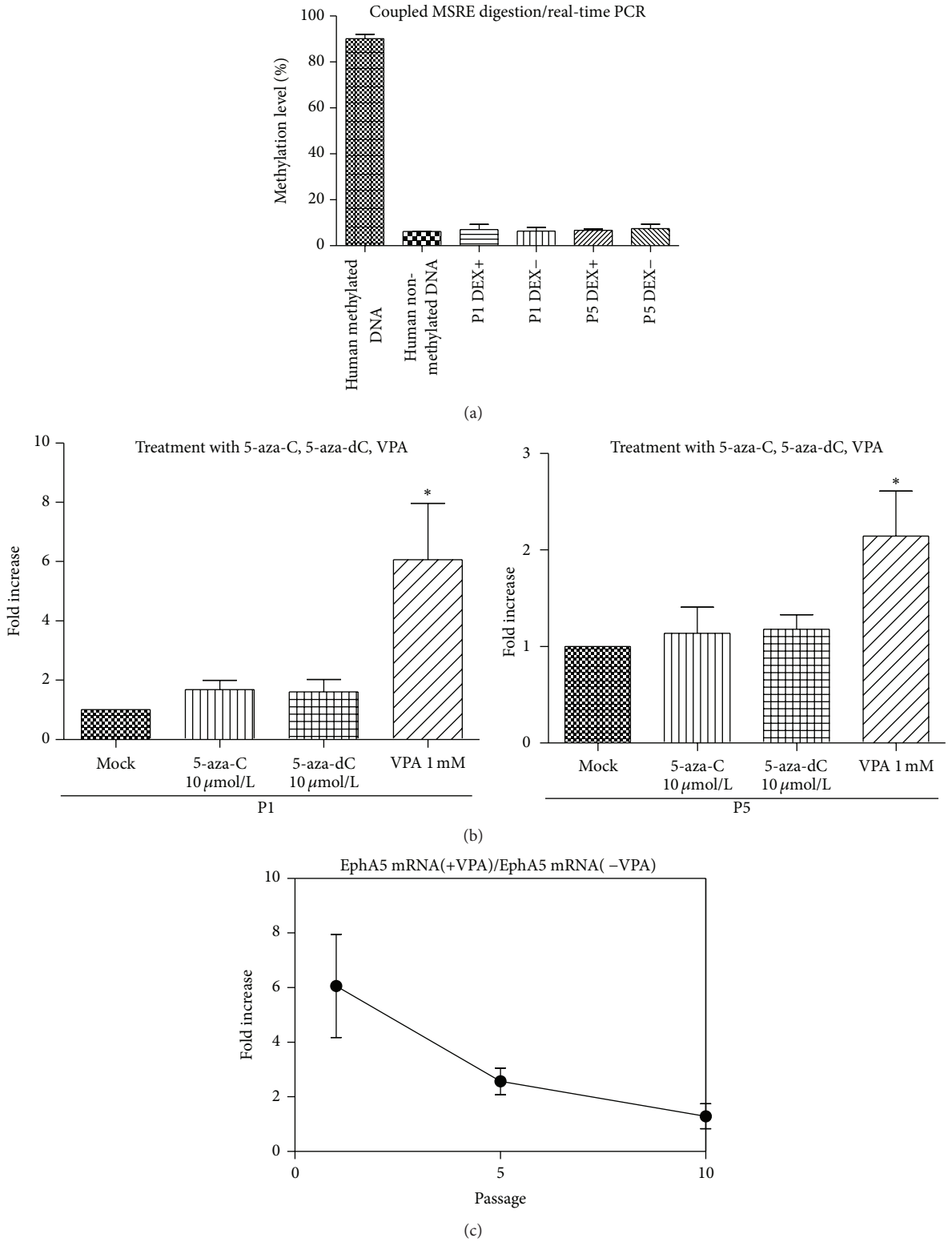

Figure 4: Silencing of EphA5 in early-passage hBMSCs is not associated with aberrant hypermethylation of the EphA5 promoter. (a) The methylation level for the EphA5 promoter that contains two Methylation-Sensitive Restriction Enzymes (MSRE) sites was determined ($n = 4$). The methylation level for the EphA5 promoter in hBMSCs at P1 and P5 was much lower than that in human methylated DNA used as a positive control (PC) and similar to that in human nonmethylated DNA used as a negative control (NC). (b) EphA5 mRNA expression analysis by quantitative RT-PCR in hBMSCs treated with 5-azacytidine (5-aza-C) or 5-aza-2′-deoxycytidine (5-aza-dC) for 4 days, or valproic acid (VPA) for 24 hours ($n = 7$). The fold change of gene expression was normalized to the expression in mock-treated cell cultures. (c) The fold change of in the EphA5 mRNA level caused by VPA treatment at the indicated culture passage numbers was measured ($n = 5$).

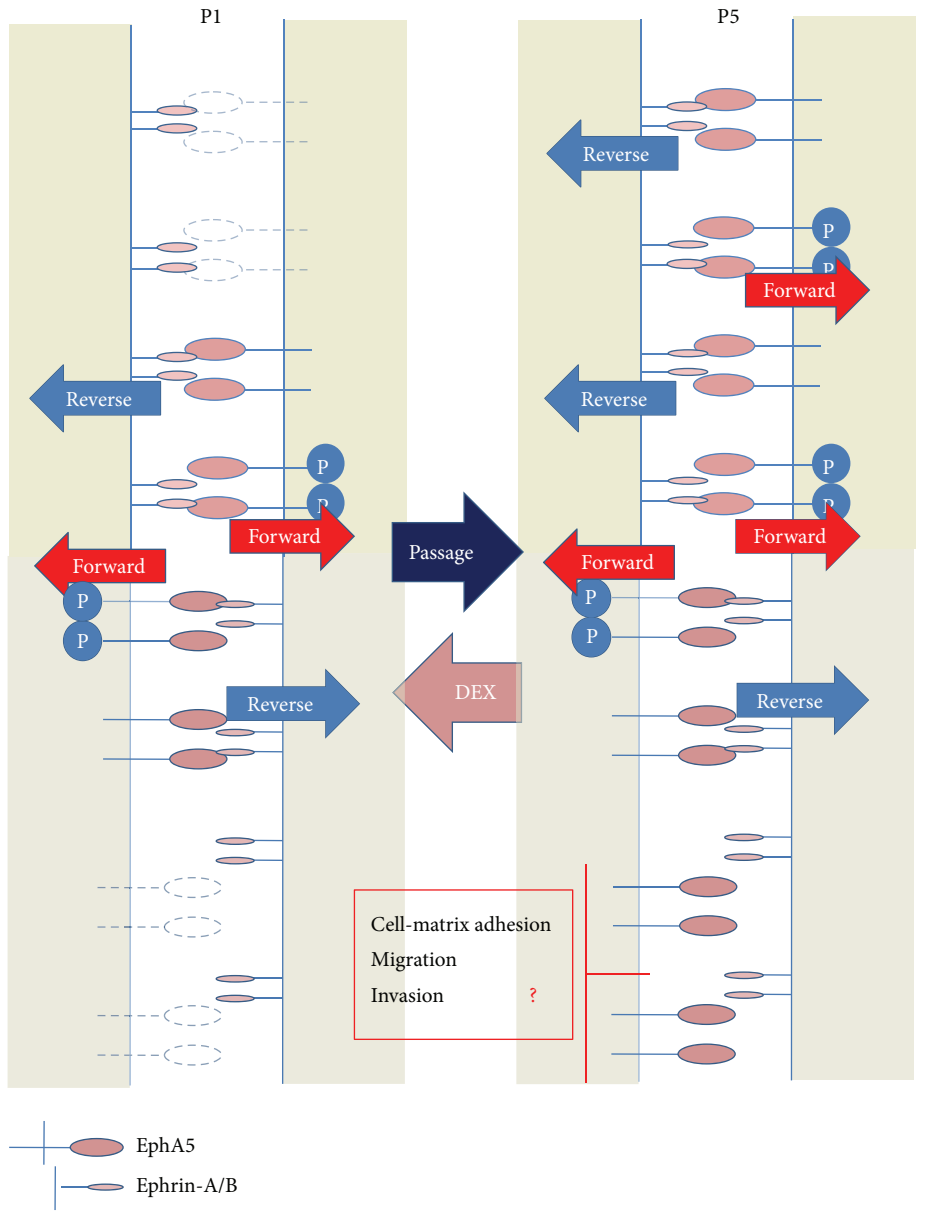

Figure 5: Proposed mechanisms by which EphA5 inhibits hBMSC osteogenesis. Coexpression of EphA5 and ephrins regulates hBMSC osteogenesis. Repeating passaging upregulates EphA5 but not ephrins, which results in an excess of nonligated EphA5. An imbalance between receptor and ligand expression may compromise other Eph ligand-dependent differentiation processes and promote ligand-independent suppression in hBMSCs.

at high cell density with cell-cell contact, the ALP mRNA level is lower at low cell density. Cell-cell contact such as osteoclast-osteoblast [6], osteoblast-osteoblast [7, 8], and BMSCs-BMSCs is generally supposed to be essential for the osteogenic differentiation. In the case that there is no cell-cell contact, the essential signaling for osteogenic differentiation may not be transmitted, leading to the fall in ALP levels. It is becoming increasingly clear that at least some Eph kinases can function without ligand engagement [48]. The increased expression of EphA5 could competitively prevent various ephrins from binding to other Eph receptors and thus inhibit osteogenic signal transduction pathways such as EphB forward signaling. Besides this mechanism, there is a possibility that a large excess of nonligated EphA5 during long-term culture, under physiologically abnormal conditions, may thus have some negligible effect on maintaining the undifferentiated state of BMSCs, independently of ligand binding (Figure 5(a)). Another possibility is that the canonical EphA5 forward signaling stimulated by ephrins or the ephrin reverse signaling stimulated by EphA5 itself does not transmit osteogenic signals. Rather, EphA5 may function to attenuate the signaling of coclustered catalytically incompetent receptors such as EphA10 and EphB6, which may mediate kinase-independent forward signals similarly to

kinase-inactive variant forms of other Eph receptors [49–51]. The present results are difficult to interpret because of the complexity and lack of specificity of ephrin/Eph binding; for example, each ephrin can bind to more than one Eph receptor and vice versa, even between classes A and B. Moreover, the ephrin/Eph signals are transmitted bidirectionally. In general, Fc-clustered ligands are capable of activating the receptor in vitro. Although many authors use the ephrin-Fc as the ligands which can activate Eph forward signals [6, 23, 47, 48, 52], it also remains unclear whether the ephrin-Fc actually induced receptor activation; these ligands often act as inhibitors or blocking reagents rather than activators if not added after cross-linking. The downstream signaling of EphA5 is not supposed to be only one signaling but to be multiple and complicated. EphA5 may mediate the below-mentioned various different pathways and may lead to affect both the downstream signaling which promotes ALP expression and that which suppresses simultaneously, although the overexpression of EphA5 suppressed ALP expression as a result. Alternative EphA or EphB signaling involved in osteogenic induction, and not just EphA5 signaling alone, may participate in this process. Given the variability of Eph expression in hBMSCs, the present results alone could not fully represent the specific mechanism of EphA5 signaling. More global approach is needed to define the exact role of EphA5 beyond this limitation.

Eph receptors are also known to signal through various different pathways and molecules, including small GTPases of the Rho and Ras family, focal adhesion kinase (FAK), the Jak/Stat pathway, and the PI3K pathway. In the present study, DEX treatment downregulated not only EphA5 but also downstream targets of EphA such as Rho/RAS-related genes (e.g., RASD1, ARHGAP, and RGNEF); this is significant findings. Activation of these proteins in various cell lines and carcinoma cells regulates cell-cell interactions through modulation of integrin activity and cell survival pathways [52–54], suggesting that they may perform a similar function in hBMSCs. Regulation of integrin activity has been demonstrated to be a key mechanism underpinning the effects of the ephrin and Eph system on cell-matrix adhesion and migration. For example, ephrin-A signaling activates the integrin pathway, thereby increasing cell adhesion or changing cell morphology and motility [55–57]. EphA-ephrin-A binding also induces integrin clustering for cell segregation during development [58]. Therefore, the EphA5 downregulation induced by DEX may be associated with ITGA5 upregulation [16] to increase osteoblast differentiation and osteogenesis in vitro. In the present study, EphA5 overexpression in hBMSCs decreased not only ITGA5 mRNA levels but also cell attachment to collagen I. This unclear mechanism for the adhesive effects should be fully explored; however, it might be partially involved in the ITGA5 level, which is supposed to be associated with cell adhesion and apoptosis according to the previous report [16]. We previously confirmed that population-selective effects of DEX enhanced the differentiation of BMSCs [14]. However, we did not characterize the selected cells or the mechanism of how they were selected in detail. Notably, we have also confirmed the osteogenic differentiation effects of DEX using immortalized human BMSCs, which are considered to be a single-cell-derived and homogenous population because they have been passaged numerous times (data not published). Studies using homogenous cell populations may depict a process different from our proposed mechanism of cell subpopulation selection by competitive proliferation.

As an alternative to subpopulation selection, we also observed that DEX augmented the responsiveness of hBMSCs to osteogenic stimulation by BMP in the previous study. In particular, DEX treatment promptly augmented BMP-induced phosphorylation of SMAD1/5/8 within 24 h but only scarcely affected the cell subpopulation distribution in the same time period [15]. DEX treatment also inhibited EphA5 mRNA expression by 6 hours, which was associated with increased levels of ALP in the present study. This rapid decrease in EphA5 levels suggests that DEX mediates a phenotypic switch from senescence to rapid growth in hBMSCs through targeting of this dormancy-associated marker EphA5, in addition to the previously observed subpopulation redistribution effect. The decrease in EphA5 levels may contribute to amelioration of cell senescence and to higher cell responsiveness to differentiation-inducing factors. Considering that not only repeating passages but also BMP-2 treatment induced EphA5 expression to some degree, this result seems to indicate that EphA5 is also a differentiation marker rather than a senescence-related marker. But first, there were times when BMP-2 treatment did not increase ALP expression on hBMSCs under certain conditions such as at low density (Figure 2(d)) or in some samples due to the individual responsiveness. Secondly, we have demonstrated that BMP-2 treatment could promote osteogenic differentiations of hBMSCs in a different manner, maintaining or promoting the overall expression profile of ephrins and Eph receptors whereas DEX treatment could have selective effects on ephrin/Eph subfamilies in hBMSCs. We speculate that BMP could upregulate other ephrin/Eph subfamilies or accelerate other ways of signaling which could have stronger effects than those of EphA5, leading to osteogenic differentiation despite increased EphA5 levels. Due to these strong and global effects of BMP-2 with an overall upregulation of many molecules, we think that EphA5 should not be regarded as a differentiation marker even if it could be increased by BMP-2. We observed that DEX treatment selectively inhibited not only mRNA expression of EphA5 but also EphA2, which was also known as an osteogenic inhibitor [7, 23], while DEX increased the levels of osteogenic stimulators such as ephrin-B2 [6] and EphA4 [8]. Apart from the effect of one of well-established osteogenic induction reagents, BMP-2, we have focused on the unclear and selective effect of DEX which could suppress osteogenic inhibitors in this paper. Further experiments must be needed to investigate the association between BMP signaling and ephrin/Eph subfamilies, and the mechanism of a synergetic effect of DEX and BMP-2.

Several studies have provided evidence that EphA5 is frequently downregulated in various cancer cell lines and tumor tissues via aberrant hypermethylation of its promoter [32, 34]. However, the nature of the stimulus that upregulates EphA5 over repeated passaging in BMSCs remains unclear. We indicated that histone deacetylation might be associated with

the observed upregulation of EphA5. As one of limitations to our study, this VPA experiment is a global stimulus and the effect cannot be assigned to EphA5. Histone H3 acetylation at Lys9 and Lys14 (H3K9K14ac) or trimethylation at Lys9 and Lys27 (H3K9me3 and H3K27me3) in general correlates with open or closed chromatin state [59, 60]. We need to investigate posttranslational modification of histone H3 bound to the EphA5 promoters using chromatin immunoprecipitation (ChIP). Recently, miR-34a was reported to negatively modulate chondrogenesis by targeting EphA5 in chick limb mesenchymal cells [61], whereas antiangiogenic and dormancy-promoting molecules including EphA5 were reported to be upregulated by expression of dormancy-associated miR-580, miR-588, and miR-190 [37]. Further studies are thus required to determine the particular stimulus leading to upregulation of EphA5 over repeated passaging, including the potential role of miRNA.

In summary, in repeatedly passaged cultures, the upregulation of dormancy-associated EphA5 independent of methylation may inhibit signaling by other EphA or EphB family members through direct interactions, although competition for ligand binding may also occur. An imbalance between EphA5 and ligand expression may compromise Eph ligand-dependent differentiation processes (Figure 5) and may mediate ligand-independent processes in hBMSCs. Elucidation of the potential inhibitory function of EphA5 expressed in hBMSCs may provide an alternative approach for manipulating the fate of hBMSCs and for lineage differentiation in cell therapy strategies and regenerative medicine.

Conflict of Interests

The authors declare that there is no conflict of interests regarding the publication of this paper.

Acknowledgments

The authors gratefully thank Tetsuya Jinno, MD, and Daisuke Koga, MD, for the collection of bone marrow aspirates during the operation procedure; Ryuta Sakuma, Ph.D., for help with lentivirus production; and Yusuke Hirabayashi, Ph.D., for valuable suggestions. This work was supported by a Grant-in-Aid for Scientific Research from the Japan Society for the Promotion of Science.

References

[1] M. F. Pittenger, A. M. Mackay, S. C. Beck et al., "Multilineage potential of adult human mesenchymal stem cells," *Science*, vol. 284, no. 5411, pp. 143–147, 1999.

[2] D. J. Prockop, "Marrow stromal cells as stem cells for non-hematopoietic tissues," *Science*, vol. 276, no. 5309, pp. 71–74, 1997.

[3] V. Vacanti, E. Kong, G. Suzuki, K. Sato, J. M. Canty, and T. Lee, "Phenotypic changes of adult porcine mesenchymal stem cells induced by prolonged passaging in culture," *Journal of Cellular Physiology*, vol. 205, no. 2, pp. 194–201, 2005.

[4] W. Wagner, P. Horn, M. Castoldi et al., "Replicative senescence of mesenchymal stem cells: a continuous and organized process," *PLoS ONE*, vol. 3, no. 5, Article ID e2213, 2008.

[5] T. Yamada, M. Yuasa, T. Masaoka et al., "After repeated division, bone marrow stromal cells express inhibitory factors with osteogenic capabilities, and EphA5 is a primary candidate," *Bone*, vol. 57, no. 2, pp. 343–354, 2013.

[6] C. Zhao, N. Irie, Y. Takada et al., "Bidirectional ephrinB2-EphB4 signaling controls bone homeostasis," *Cell Metabolism*, vol. 4, no. 2, pp. 111–121, 2006.

[7] N. Irie, Y. Takada, Y. Watanabe et al., "Bidirectional signaling through EphrinA2-EphA2 enhances osteoclastogenesis and suppresses osteoblastogenesis," *The Journal of Biological Chemistry*, vol. 284, no. 21, pp. 14637–14644, 2009.

[8] V. Stiffel, M. Amoui, M. H.-C. Sheng, S. Mohan, and K.-H. W. Lau, "EphA4 receptor is a novel negative regulator of osteoclast activity," *Journal of Bone and Mineral Research*, vol. 29, no. 4, pp. 804–819, 2014.

[9] S. Tanabe, Y. Sato, T. Suzuki, K. Suzuki, T. Nagao, and T. Yamaguchi, "Gene expression profiling of human mesenchymal stem cells for identification of novel markers in early- and late-stage cell culture," *Journal of Biochemistry*, vol. 144, no. 3, pp. 399–408, 2008.

[10] A. Derfoul, G. L. Perkins, D. J. Hall, and R. S. Tuan, "Glucocorticoids promote chondrogenic differentiation of adult human mesenchymal stem cells by enhancing expression of cartilage extracellular matrix genes," *Stem Cells*, vol. 24, no. 6, pp. 1487–1495, 2006.

[11] N. Indrawattana, G. Chen, M. Tadokoro et al., "Growth factor combination for chondrogenic induction from human mesenchymal stem cell," *Biochemical and Biophysical Research Communications*, vol. 320, no. 3, pp. 914–919, 2004.

[12] I. Sekiya, D. C. Colter, and D. J. Prockop, "BMP-6 enhances chondrogenesis in a subpopulation of human marrow stromal cells," *Biochemical and Biophysical Research Communications*, vol. 284, no. 2, pp. 411–418, 2001.

[13] N. Jaiswal, S. E. Haynesworth, A. I. Caplan, and S. P. Bruder, "Osteogenic differentiation of purified, culture-expanded human mesenchymal stem cells in vitro," *Journal of Cellular Biochemistry*, vol. 64, no. 2, pp. 295–312, 1997.

[14] H. Oshina, S. Sotome, T. Yoshii et al., "Effects of continuous dexamethasone treatment on differentiation capabilities of bone marrow-derived mesenchymal cells," *Bone*, vol. 41, no. 4, pp. 575–583, 2007.

[15] M. Yuasa, T. Yamada, T. Taniyama et al., "Dexamethasone enhances osteogenic differentiation of bone marrow-and muscle-derived stromal cells and augments ectopic bone formation induced by bone morphogenetic protein-2," *PLoS ONE*, vol. 10, no. 2, Article ID 0116462, 2015.

[16] Z. Hamidouche, O. Fromigué, J. Ringe et al., "Priming integrin α5 promotes human mesenchymal stromal cell osteoblast differentiation and osteogenesis," *Proceedings of the National Academy of Sciences of the United States of America*, vol. 106, no. 44, pp. 18587–18591, 2009.

[17] Y. Akaneya, K. Sohya, A. Kitamura et al., "Ephrin-A5 and EphA5 interaction induces synaptogenesis during early hippocampal development," *PLoS ONE*, vol. 5, no. 8, Article ID e12486, 2010.

[18] N. M. Abdul-Aziz, M. Turmaine, N. D. E. Greene, and A. J. Copp, "EphrinA-EphA receptor interactions in mouse spinal neurulation: implications for neural fold fusion," *International Journal of Developmental Biology*, vol. 53, no. 4, pp. 559–568, 2009.

[19] Y. Hara, T. Nomura, K. Yoshizaki, J. Frisén, and N. Osumi, "Impaired hippocampal neurogenesis and vascular formation in Ephrin-A5-deficient mice," *Stem Cells*, vol. 28, no. 6, pp. 974–983, 2010.

[20] J. Holmberg, A. Armulik, K.-A. Senti et al., "Ephrin-A2 reverse signaling negatively regulates neural progenitor proliferation and neurogenesis," *Genes and Development*, vol. 19, no. 4, pp. 462–471, 2005.

[21] M. R. Hornberger, D. Dütting, T. Ciossek et al., "Modulation of EphA receptor function by coexpressed ephrinA ligands on retinal ganglion cell axons," *Neuron*, vol. 22, no. 4, pp. 731–742, 1999.

[22] G. Zimmer, B. Kästner, F. Weth, and J. Bolz, "Multiple effects of ephrin-A5 on cortical neurons are mediated by Src family kinases," *The Journal of Neuroscience*, vol. 27, no. 21, pp. 5643–5653, 2007.

[23] H. Miao, E. Burnett, M. Kinch, E. Simon, and B. Wang, "Activation of EphA2 kinase suppresses integrin function and causes focal-adhesion-kinase dephosphorylation," *Nature Cell Biology*, vol. 2, no. 2, pp. 62–69, 2000.

[24] M. J. Ting, B. W. Day, M. D. Spanevello, and A. W. Boyd, "Activation of ephrin A proteins influences hematopoietic stem cell adhesion and trafficking patterns," *Experimental Hematology*, vol. 38, no. 11, pp. 1087–1098, 2010.

[25] M. Tanaka, R. Kamata, and R. Sakai, "EphA2 phosphorylates the cytoplasmic tail of claudin-4 and mediates paracellular permeability," *Journal of Biological Chemistry*, vol. 280, no. 51, pp. 42375–42382, 2005.

[26] N. W. Gale, S. J. Holland, D. M. Valenzuela et al., "Eph receptors and ligands comprise two major specificity subclasses and are reciprocally compartmentalized during embryogenesis," *Neuron*, vol. 17, no. 1, pp. 9–19, 1996.

[27] A. M. Flenniken, N. W. Gale, G. D. Yancopoulos, and D. G. Wilkinson, "Distinct and overlapping expression patterns of ligands for eph-related receptor tyrosine kinases during mouse embryogenesis," *Developmental Biology*, vol. 179, no. 2, pp. 382–401, 1996.

[28] H. U. Wang, Z.-F. Chen, and D. J. Anderson, "Molecular distinction and angiogenic interaction between embryonic arteries and veins revealed by ephrin-B2 and its receptor Eph-B4," *Cell*, vol. 93, no. 5, pp. 741–753, 1998.

[29] S. M. Alam, J. Fujimoto, I. Jahan, E. Sato, and T. Tamaya, "Coexpression of EphB4 and ephrinB2 in tumour advancement of ovarian cancers," *British Journal of Cancer*, vol. 98, no. 4, pp. 845–851, 2008.

[30] J. W. Astin, J. Batson, S. Kadir et al., "Competition amongst Eph receptors regulates contact inhibition of locomotion and invasiveness in prostate cancer cells," *Nature Cell Biology*, vol. 12, no. 12, pp. 1194–1204, 2010.

[31] Y. Dong, J. Wang, Z. Sheng et al., "Downregulation of EphA1 in colorectal carcinomas correlates with invasion and metastasis," *Modern Pathology*, vol. 22, no. 1, pp. 151–160, 2009.

[32] D.-Y. Fu, Z.-M. Wang, B.-L. Wang et al., "Frequent epigenetic inactivation of the receptor tyrosine kinase EphA5 by promoter methylation in human breast cancer," *Human Pathology*, vol. 41, no. 1, pp. 48–58, 2010.

[33] N. I. Herath and A. W. Boyd, "The role of Eph receptors and ephrin ligands in colorectal cancer," *International Journal of Cancer*, vol. 126, no. 9, pp. 2003–2011, 2010.

[34] S. Li, Y. Zhu, C. Ma et al., "Downregulation of EphA5 by promoter methylation in human prostate cancer," *BMC Cancer*, vol. 15, no. 1, article 18, 2015.

[35] B. Wang, "Cancer cells exploit the eph-ephrin system to promote invasion and metastasis: tales of unwitting partners," *Science Signaling*, vol. 4, article pe28, 2011.

[36] N. Almog, L. Ma, R. Raychowdhury et al., "Transcriptional switch of dormant tumors to fast-growing angiogenic phenotype," *Cancer Research*, vol. 69, no. 3, pp. 836–844, 2009.

[37] N. Almog, L. Ma, C. Schwager et al., "Consensus micro RNAs governing the switch of dormant tumors to the fast-growing angiogenic phenotype," *PLoS ONE*, vol. 7, no. 8, Article ID e44001, 2012.

[38] Y. Ning, J. L. Weber, A. M. Killary, D. H. Ledbetter, J. R. Smith, and O. M. Pereira-Smith, "Genetic analysis of indefinite division in human cells: evidence for a cell senescence-related gene(s) on human chromosome 4," *Proceedings of the National Academy of Sciences of the United States of America*, vol. 88, no. 13, pp. 5635–5639, 1991.

[39] E. B. Pasquale, "Eph receptor signalling casts a wide net on cell behaviour," *Nature Reviews Molecular Cell Biology*, vol. 6, no. 6, pp. 462–475, 2005.

[40] E. B. Pasquale, "Eph receptors and ephrins in cancer: bidirectional signalling and beyond," *Nature Reviews Cancer*, vol. 10, no. 3, pp. 165–180, 2010.

[41] D. Schmucker and S. L. Zipursky, "Signaling downstream of Eph receptors and ephrin ligands," *Cell*, vol. 105, no. 6, pp. 701–704, 2001.

[42] R. F. Carvalho, M. Beutler, K. J. M. Marler et al., "Silencing of EphA3 through a cis interaction with ephrinA5," *Nature Neuroscience*, vol. 9, no. 3, pp. 322–330, 2006.

[43] T. Marquardt, R. Shirasaki, S. Ghosh et al., "Coexpressed EphA receptors and ephrin-A ligands mediate opposing actions on growth cone navigation from distinct membrane domains," *Cell*, vol. 121, no. 1, pp. 127–139, 2005.

[44] E. Nievergall, M. Lackmann, and P. W. Janes, "Eph-dependent cell-cell adhesion and segregation in development and cancer," *Cellular and Molecular Life Sciences*, vol. 69, no. 11, pp. 1813–1842, 2012.

[45] H. Miao and B. Wang, "EphA receptor signaling-complexity and emerging themes," *Seminars in Cell & Developmental Biology*, vol. 23, no. 1, pp. 16–25, 2012.

[46] G. R. Mundy and F. Elefteriou, "Boning up on ephrin signaling," *Cell*, vol. 126, no. 3, pp. 441–443, 2006.

[47] A. Arthur, A. Zannettino, R. Panagopoulos et al., "EphB/ephrin-B interactions mediate human MSC attachment, migration and osteochondral differentiation," *Bone*, vol. 48, no. 3, pp. 533–542, 2011.

[48] N. K. Noren, N.-Y. Yang, M. Silldorf, R. Mutyala, and E. B. Pasquale, "Ephrin-independent regulation of cell substrate adhesion by the EphB4 receptor," *Biochemical Journal*, vol. 422, no. 3, pp. 433–442, 2009.

[49] A. Freywald, N. Sharfe, and C. M. Roifman, "The kinase-null EphB6 receptor undergoes transphosphorylation in a complex with EphB1," *The Journal of Biological Chemistry*, vol. 277, no. 6, pp. 3823–3828, 2002.

[50] C. Gu and S. Park, "The EphA8 receptor regulates integrin activity through p110γ phosphatidylinositol-3 kinase in a tyrosine kinase activity-independent manner," *Molecular and Cellular Biology*, vol. 21, no. 14, pp. 4579–4597, 2001.

[51] H. Miao, K. Strebhardt, E. B. Pasquale, T.-L. Shen, J.-L. Guan, and B. Wang, "Inhibition of integrin-mediated cell adhesion but not directional cell migration requires catalytic activity of EphB3 receptor tyrosine kinase. Role of RHO family small

GTPases," *The Journal of Biological Chemistry*, vol. 280, no. 2, pp. 923–932, 2005.

[52] H. L. Holen, M. Shadidi, K. Narvhus, O. Kjøsnes, A. Tierens, and H.-C. Aasheim, "Signaling through ephrin-A ligand leads to activation of Src-family kinases, Akt phosphorylation, and inhibition of antigen receptor-induced apoptosis," *Journal of Leukocyte Biology*, vol. 84, no. 4, pp. 1183–1191, 2008.

[53] M. Aoki, T. Yamashita, and M. Tohyama, "EphA receptors direct the differentiation of mammalian neural precursor cells through a mitogen-activated protein kinase-dependent pathway," *The Journal of Biological Chemistry*, vol. 279, no. 31, pp. 32643–32650, 2004.

[54] K. K. Murai and E. B. Pasquale, "'Eph'ective signaling: forward, reverse and crosstalk," *Journal of Cell Science*, vol. 116, no. 14, pp. 2823–2832, 2003.

[55] J. Huai and U. Drescher, "An ephrin-A-dependent signaling pathway controls integrin function and is linked to the tyrosine phosphorylation of a 120-kDa protein," *The Journal of Biological Chemistry*, vol. 276, no. 9, pp. 6689–6694, 2001.

[56] N. Sharfe, M. Nikolic, L. Cimpeon, A. Van De Kratts, A. Freywald, and C. M. Roifman, "EphA and ephrin-A proteins regulate integrin-mediated T lymphocyte interactions," *Molecular Immunology*, vol. 45, no. 5, pp. 1208–1220, 2008.

[57] T. Yamazaki, J. Masuda, T. Omori, R. Usui, H. Akiyama, and Y. Maru, "EphA1 interacts with integrin-linked kinase and regulates cell morphology and motility," *Journal of Cell Science*, vol. 122, no. 2, pp. 243–255, 2009.

[58] D. Jülich, A. P. Mould, E. Koper, and S. A. Holley, "Control of extracellular matrix assembly along tissue boundaries via integrin and Eph/Ephrin signaling," *Development*, vol. 136, no. 17, pp. 2913–2921, 2009.

[59] S. L. Berger, "Histone modifications in transcriptional regulation," *Current Opinion in Genetics and Development*, vol. 12, no. 2, pp. 142–148, 2002.

[60] R. Cao and Y. Zhang, "The functions of E(Z)/EZH2-mediated methylation of lysine 27 in histone H3," *Current Opinion in Genetics & Development*, vol. 14, no. 2, pp. 155–164, 2004.

[61] D. Kim, J. Song, S. Kim, C. H. Chun, and E. J. Jin, "MicroRNA-34a regulates migration of chondroblast and IL-1β-induced degeneration of chondrocytes by targeting EphA5," *Biochemical and Biophysical Research Communications*, vol. 415, no. 4, pp. 551–557, 2011.

Hindawi Publishing Corporation
Stem Cells International
Volume 2016, Article ID 4726267, 13 pages
http://dx.doi.org/10.1155/2016/4726267

Research Article

Tissue-Related Hypoxia Attenuates Proinflammatory Effects of Allogeneic PBMCs on Adipose-Derived Stromal Cells *In Vitro*

Polina I. Bobyleva, Elena R. Andreeva, Aleksandra N. Gornostaeva, and Ludmila B. Buravkova

Institute of Biomedical Problems, Russian Academy of Sciences, Khoroshevskoye Shosse 76a, Moscow 123007, Russia

Correspondence should be addressed to Elena R. Andreeva; andreeva_er@mail.ru

Received 19 June 2015; Accepted 3 December 2015

Academic Editor: Luca Vanella

Human adipose tissue-stromal derived cells (ASCs) are considered a perspective tool for regenerative medicine. Depending on the application mode ASC/allogeneic immune cell interaction can occur in the systemic circulation under plenty high concentrations of O_2 and in target tissues at lower O_2 levels. Here we examined the effects of allogeneic PHA-stimulated peripheral blood mononuclear cells (PBMCs) on ASCs under ambient (20%) oxygen and "physiological" hypoxia (5% O_2). As revealed with microarray analysis ASCs under 20% O_2 were more affected by activated PBMCs, which was manifested in differential expression of more than 300 genes, whereas under 5% O_2 only 140 genes were changed. Altered gene pattern was only partly overlapped at different O_2 conditions. Under O_2 ASCs retained their proliferative and differentiative capacities, mesenchymal phenotype, and intracellular organelle' state. ASCs were proinflammatory activated on transcription level that was confirmed by their ability to suppress activation and proliferation of mitogen-stimulated PBMCs. ASC/PBMCs interaction resulted in anti-inflammatory shift of paracrine mediators in conditioning medium with significant increase of immunosuppressive LIF level. Our data indicated that under both ambient and tissue-related O_2 ASCs possessed immunosuppressive potential and maintained functional activity. Under "physiological" hypoxia ASCs were less susceptible to "priming" by allogeneic mitogen-activated PBMCs.

1. Introduction

The capacity of multipotent mesenchymal stromal cells (MSCs) to produce biologically active molecules, proliferate rapidly, and differentiate in several mesenchymal lineages as well as their immunosuppressive activity makes them very attractive tool for cell therapy and regenerative medicine [1]. Moreover, MSCs can be applied in an allogeneic setting due the absence/low expression of main histocompatibility molecules class II (MHC-II) and costimulatory molecules on the cell surface [2–4]. The molecular and cellular mechanisms underlying the MSC immunomodulation are currently being actively studied [5–9]. For the manifestation of immunosuppression, MSCs have to be activated (primed) [10–13]. This priming can be carried out by cytokines from activated lymphocytes, primarily, TNF-α, IFN-γ, and IL-1β [11]. After activation MSCs become visible to the immune system cells, such as the NK [14–16]. Thus, they are now MSCs considered more to be immune evasive than immunotolerant, which may affect their functions in allogeneic applications [17]. Most recent studies have focused on the immunomodulatory properties of MSCs, while their functions that are not directly related to immunosuppression are poorly explored. To date, the stability of the MSC mesenchymal phenotype (SSEA4, CD73, CD90, CD105, CD29, and CD44) after priming with proinflammatory cytokines [12, 18] and the retention of multilineage mesenchymal differentiation have been demonstrated [12]. These cytokines differentially modulate proliferative activity [12], the cytokine profile, and the migration of primed MSCs [11]. However, allogeneic MSCs being applied *in vivo* will be exposed not to certain cytokines but to a cocktail of proinflammatory mediators from immune cells. Besides, as shown previously, MSC/immune cells interaction is governed by the factors of local tissue microenvironment, where O_2 level is the most important one [19]. Depending on the application mode, MSC/allogeneic immune cell

interactions can occur in the systemic circulation under plenty high concentrations of O_2 and in target tissues at much lower O_2 levels. Therefore, here, we examined the paracrine effects of allogeneic activated peripheral blood mononuclear cells (PBMCs) under different O_2 levels in the microenvironment on functional state and regeneration-related features of human adipose tissue-derived stromal cells (ASCs).

2. Materials and Methods

2.1. Isolation and Culture of Adipose Tissue-Derived Mesenchymal Stromal Cells (ASCs). Adipose tissue samples were obtained in the frame of Scientific Agreement from multidisciplinary clinic "Souz" (Moscow, Russia) after elective liposuction procedures under local anesthesia from healthy patients with written informed consent. Adipose tissue was processed using guidelines specifically approved by Biomedicine Ethics Committee of Institute of Biomedical Problems, Russian Academy of Sciences (Physiology Section of the Russian Bioethics Committee, Russian Federation National Commission for UNESCO, Permit #314/MCK/09/03/13). Adipose stromal cells (ASCs) were isolated using standard method described by Zuk et al. with modifications by Buravkova et al. [20, 21]. Cells were expanded in α-MEM (22561-021, Gibco, Invitrogen, UK) with 50 U/mL penicillin-streptomycin (PanEco, Russia) and 10% fetal bovine serum (FBS) (sv30160.03, HyClone, USA) at either ambient O_2 tension (20% CO_2, CO_2-incubator (Sanyo, Japan)) or under low O_2 (5% O_2) using a multigas incubator (Sanyo). Cells on the 2nd and 3rd passages were used in the experiments. ASCs expanded under different O_2 were characterised [22] before use.

2.2. Isolation of Peripheral Blood Mononuclear Cells (PBMCs). PBMCs were isolated by density gradient centrifugation (Histopaque 1077, Sigma-Aldrich, USA) of whole blood obtained from healthy volunteers after informed consent according to a standard protocol. Isolated cells were resuspended in RPMI-1640 (31870-025, Gibco) with penicillin-streptomycin and 5% heat-inactivated FBS. PBMCs were activated with 10 μg/mL phytohaemagglutinin (PHA) (L8754-5MG, Sigma-Aldrich, USA).

2.3. Coculture of ASCs with PBMCs. ASCs were plated into the lower chamber of 6-well transwell plates (3412, Corning, USA, 0.4 μm pore size). As ASCs reached a 70–80% monolayer, the medium was changed to RPMI-1640, 5% FBS, and 10 μg/mL PHA. Activated PBMCs (10^6/mL) were added to the upper chamber of the transwell. Cells were cocultured for 72 h at 20% and 5% O_2.

2.4. ASC Viability. ASCs were trypsinised and the suspension was stained with Annexin V, FITC kit (PN IM3546, Beckman Coulter, USA). Live (Ann^-/PI^-), apoptotic (Ann^+), and necrotic (Ann^-PI^+) cells were detected using flow cytometer (Epics XL, Beckman Coulter).

2.5. ASC Proliferation. To determine proliferation activity ASCs were counted in 5 fixed randomly selected view fields before experiment and in the same points after the coculture. Image acquisition was performed using Leica DMIL (Germany) and Nikon Eclipse TiU (Japan) microscopes equipped with digital cameras, and cells were counted using SigmaScan Pro 5.0 Image Analysis Software (SPSS Inc., USA). The proliferation activity was characterised as fold change of ASC number after experiment compared to Day 0.

2.6. Osteodifferentiation. After the experiment ASCs were cultured in complete α-MEM with osteoinductive supplement (100 nM dexamethasone, 10 mM sodium-b-glycerophosphate, and 0.05 mM ascorbic acid-2-phosphate) (Millipore, USA) for 3 weeks. Cells were fixed with 4% paraformaldehyde and stained with 40 mM alizarin red S solution (Sigma-Aldrich). Then matrix-bound dye was dissolved in 10% cetylpyridinium chloride (in 10 mM sodium phosphate buffer, pH7, w/v) and the OD was measured spectrometrically at 562 nm.

2.7. Mitochondria, Lysosomes, Endoplasmic Reticulum (ER), and Reactive Oxygen Species (ROS) Evaluation. Mitochondria, lysosomes, endoplasmic reticulum, and ROS were labeled with MitoTracker Red FM, LysoTracker Green, ERTracker, and H_2DCFDA (Molecular probes, Invitrogen, USA), respectively, according to the manufacturer's protocol. ASCs then were detached with trypsin-EDTA and analyzed by flow cytometry (Epics XL).

2.8. Immunophenotypic Analysis. The immunophenotypic characterisation of ASCs was performed by flow cytometry (Epics XL) using the following monoclonal antibodies: CD45-phycoerythrin (PE), CD73-fluorescein isothiocyanate (FITC), CD90-FITC, CD105-PE, and CD54-PE (IO Test, Beckman Coulter). Trypsinised cells were incubated with the antibodies following the manufacturer's instructions.

2.9. Activation of PBMCs. To characterise the activation, PBMCs were stained with antibody against HLA-DR (PE) (IO Test, Beckman Coulter) following manufacturer's instructions and the share of HLA-DR-positive cells was estimated by flow cytometry.

2.10. Proliferation of PBMCs. Prior to experiment PBMCs were stained with carboxyfluorescein succinimidyl ester (CFSE, Invitrogen) according to standard protocol [23]. Proliferation rate was evaluated after flow cytometry by the proportional decrease of CFSE fluorescence in divided PBMCs.

2.11. Detection of Cytokines in Conditioned Medium. The conditioned medium (CM) was collected after coculture, centrifuged to remove cell debris, and stored at −80°C (low temperature freezer Sanyo). Cytokines were detected in CM using Human th1/th2 11plex FlowCytomix Multiplex Kit (BMS810FF, eBioscience, Bender MedSystems). FlowCytomix probes were analyzed using FaxCalibur cytometer

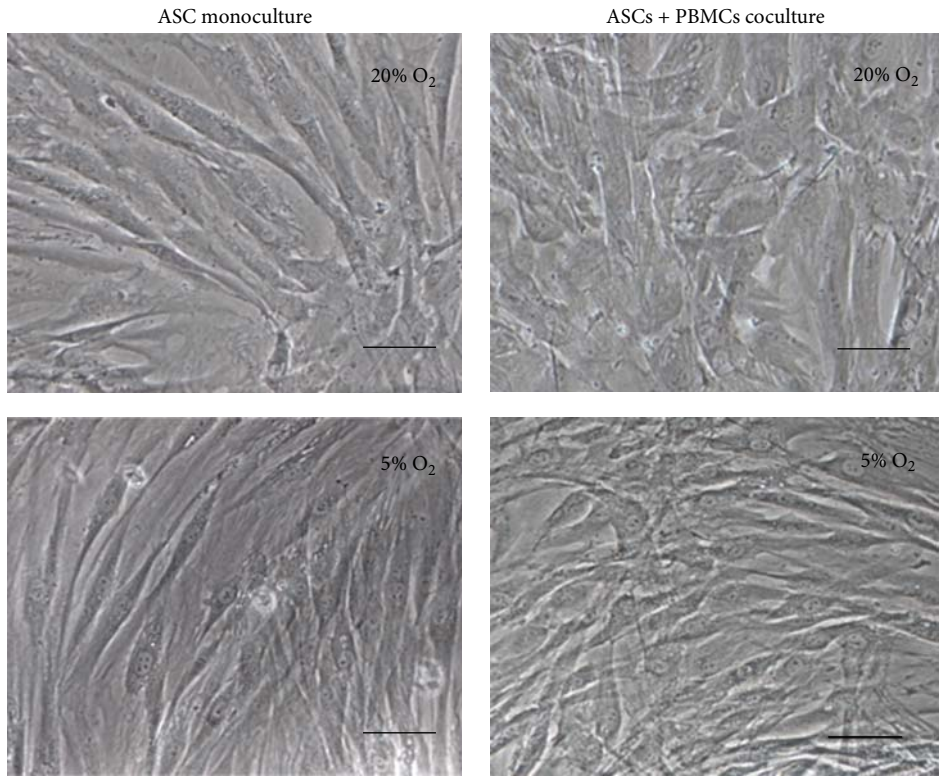

Figure 1: ASC morphology in monoculture and after transwell coculture with PHA-stimulated PBMCs under 20% and 5% O_2. Phase contrast: bar 100 μm.

(Becton Dickinson, USA) and FlowCytomix Pro software. LIF concentration in CM was estimated with Human ELISA Kit (ab100582, Abcam, USA).

2.12. RNA Isolation and Microarray Analysis. To perform gene expression profiling total RNA was isolated from ASCs monoculture and after 72 hrs of coculture with PBMCs at 20% and 5% O_2. Cultured ASCs were detached with 0.05% trypsin-EDTA, washed with PBS, and preserved in RNAlater (Qiagen, USA) at −30°C. Before analysis, ASCs were washed off from the stabilizing agent and the standard procedure for RNA isolation using TRIZOL was applied (according to the manufacturer's protocol). RNA concentration was determined using a Nanodrop; then, 200 ng of RNA was amplified with Illumina TotalPrepTM RNA Amplification Kit (Ambion, USA). The amplified RNA was subsequently used for microarray hybridisation using Human-Ref-12 expression chip (Illumina, USA). The arrays were scanned and analysed using the Illumina Genome Studio v2009.2 software (Gene Expression Module v1.5.4, Illumina). The false discovery rate was controlled by adjusting p values by means of the Benjamini-Hochberg algorithm, followed by the performance of a Gene Set Enrichment Analysis and a one-tailed Fisher's exact test. The microarray data for 22184 genes were filtered by applying two criteria for significance: $p < 0.05$ and fold change (FC) > 2. To further analyse the data EASE v2.0 was used for the distribution of genes to Gene Ontology groups (biological function).

2.13. Statistical Analysis. Statistical analysis was performed using "Microsoft Excel 2010" and "Statistica 7.0" software packages. Differences were assessed by Mann-Whitney nonparametric test. All experiments were replicated, at least thrice, data are presented as mean ± SEM and $p < 0.05$ was considered to be statistically significant.

3. Results

3.1. Effects of PHA-Stimulated PBMCs on ASCs in Cell-Contact Independent Setting. Paracrine interaction with activated PBMCs during 72 hrs did not affect ASC morphology compared to ASC monoculture (Figures 1(a) and 1(b)).

Phenotyping of cocultured ASCs demonstrated that practically all of these cells were positive for CD73 (95.4 ÷ 98.7%), CD90 (95.4 ÷ 99.2%), and CD105 (94.0 ÷ 99.8%), which identified these ASCs as mesenchymal stem/stromal cells according to the recommendations of International Society of Cytotherapy [24] (Figure 2(a)). The mean fluorescence intensity (MFI), which characterised the number of antigen molecules on the ASC surface, did not change for CD73 or CD105. However, CD90 MFI of cocultured ASCs was significantly decreased under 5% O_2 (Figure 2(b)).

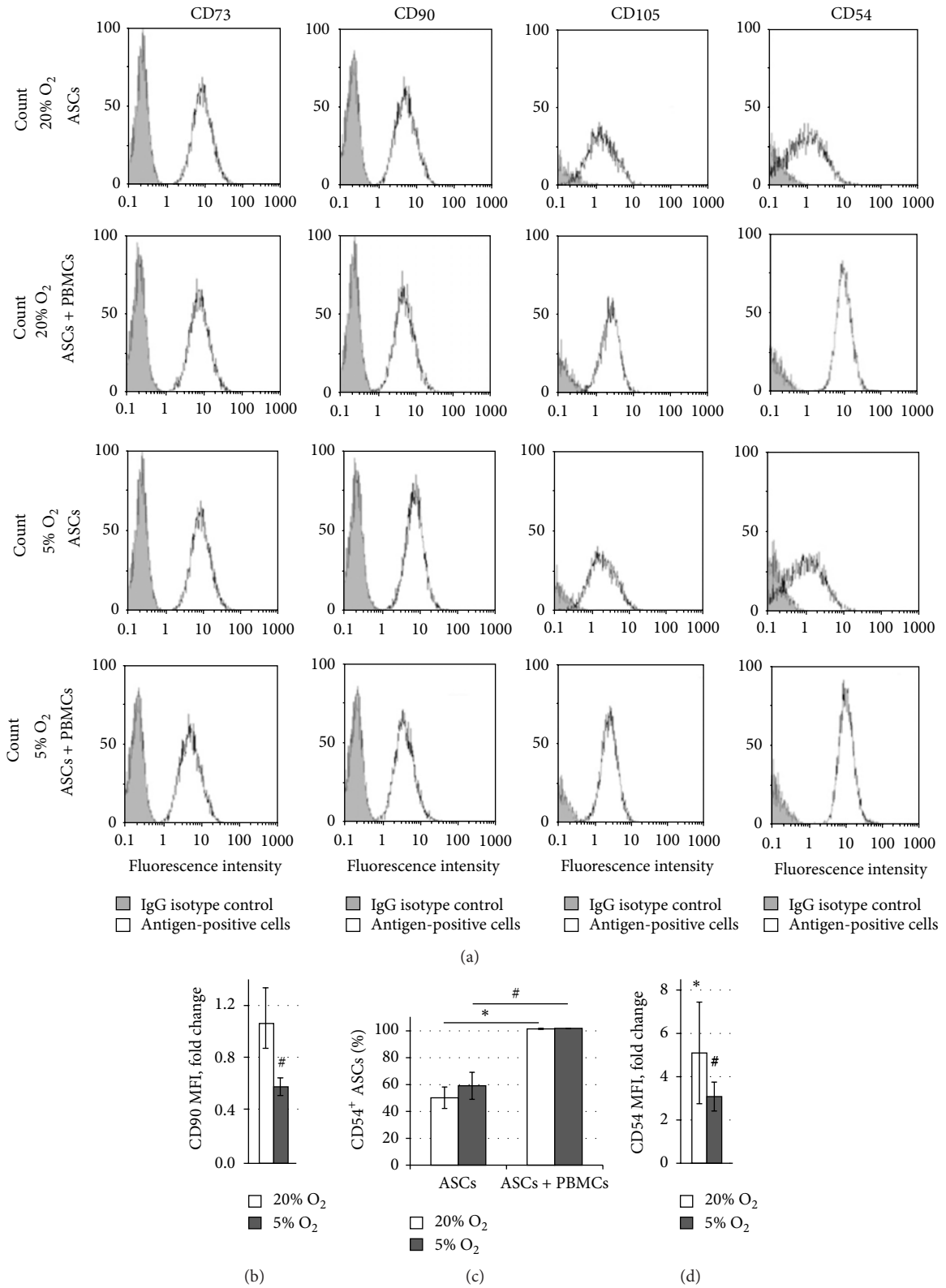

Figure 2: ASC immunophenotype after monoculture and transwell coculture with PHA-stimulated PBMCs under 20% and 5% O_2. (a) Representative histograms of ASC surface marker expression. The white filled histograms indicate the positively stained cells while the grey filled histograms indicate the isotype-matched antibody controls. (b) CD90 mean fluorescence intensity (MFI) on cocultured ASCs versus ASCs in monoculture. (c) The proportion of CD54-positive ASCs in monoculture and transwell coculture with PBMCs. (d) CD54 MFI on cocultured ASCs versus ASCs in monoculture. *Significant difference between monoculture and coculture at 20% O_2 ($p < 0.01$). #Significant difference between monoculture and coculture at 5% O_2 ($p < 0.01$).

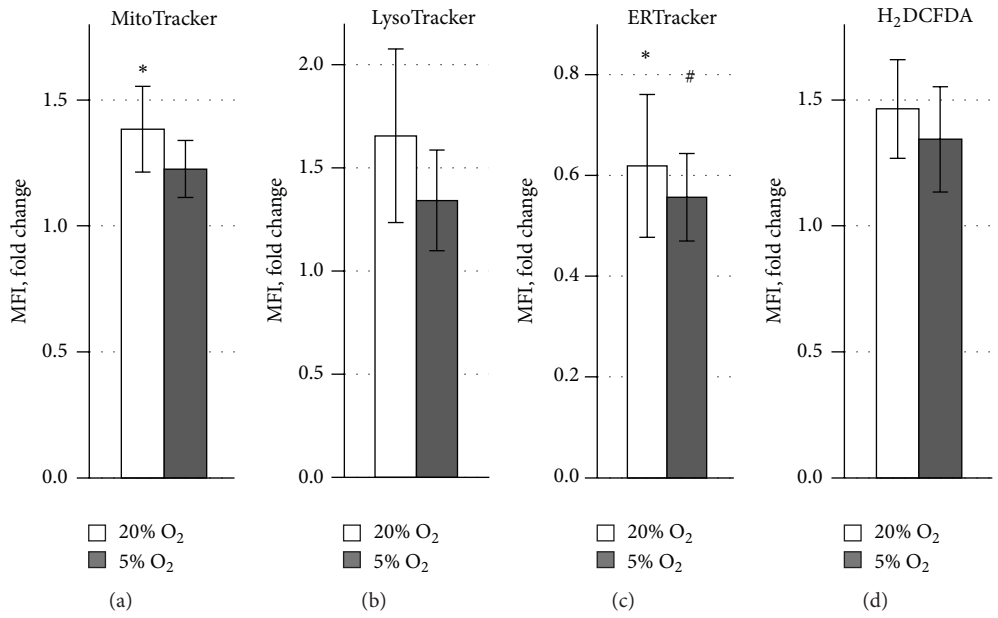

Figure 3: Cellular organelle state and ROS level in ASCs after coculture with PHA-stimulated PBMCs versus ASCs in monoculture. Transmembrane mitochondrial potential (a), lysosome activity (b), endoplasmic reticulum activity (c), and ROS production (d). *Significant difference between monocultured and cocultured ASCs at 20% O_2 ($p < 0.01$). #Significant difference between monocultured and cocultured ASCs at 5% O_2 ($p < 0.01$).

Cellular organelles and ROS level were characterised in cocultured ASCs after staining with an appropriate fluorescent tracker (Figure 3). Under 20% O_2 a significant increase of MitoTracker Red FM MFI was detected, displaying the elevated mitochondrial transmembrane potential (Figure 3(a)). No significant change in the MFI of LysoTracker Green was observed indicating the unaltered lysosome activity of ASCs after interaction with PBMCs (Figure 3(b)). Analysis of the ER compartment showed a significant decline of ER Green staining in cocultured ASCs both under 20% and 5% O_2 (Figure 3(c)). The ROS level was not changed in ASCs after interaction with PBMCs regardless of O_2 concentration (Figure 3(d)).

After paracrine interaction with allogeneic activated PBMCs, the viability of cocultured ASCs was high and did not differ from ASCs in monoculture (Figure 4(a)). Proliferative activity of ASCs was slightly increased during coculture with PBMCs (Figure 4(b)). ASC osteogenic capacity revealed by mineralised matrix production was not affected by interaction with PBMCs and was less marked under 5% O_2 both in monoculture and after coculture with PBMCs (Figures 4(c) and 4(d)), confirming our recent findings [25].

After coculture, ASCs retained the immunomodulatory activity revealed in the suppression of T-cell activation (decrease in the share of HLA-DR-positive PBMCs) and proliferation (Table 1).

After interaction with PBMCs, practically all ASCs were CD54-positive, whereas, in monoculture, only half of ASCs expressed this antigen (Figure 2(c)). Moreover, the CD54 MFI was 5 times higher after coculture under 20% O_2 and 2 times higher at 5% O_2 ($p < 0.05$), indicating an increase in the number of ICAM-1 molecules per ASC (Figure 2(d)).

Table 1: Activation and proliferation rate of PBMCs after coculture with ASCs.

	20% O_2	5% O_2
Activation ($CD3^+/HLA\text{-}DR^+$)	$40.6 \pm 6.5^*\downarrow$	$48.6 \pm 5.3^*\downarrow$
Proliferation rate	$22 \pm 5^*\downarrow$	$15 \pm 2^*\downarrow$

Data are presented as a percentage of changes, when effects in PHA-stimulated PBMC monoculture were considered as 100%. Mean ± SD of 5 independent experiments. *Significant difference from PBMC monoculture ($p < 0.05$).

Paracrine mediators in conditioning medium (CM) of ASC and PBMC monocultures and after coculture were detected (Figure 5). IL-10, TNF-α, and IFN-γ were secreted only by activated PBMCs, whereas IL-6, IL-8, and LIF were detected in both monocultures. The level of cytokine secretion by ASCs and PBMCs did not depend on O_2 concentration except of TNF-α, where the PBMCs synthesized significantly less of this chemokine under 5% O_2. Cell-to-cell interactions affected paracrine profile. Besides membrane-bound ICAM1, soluble form of this adhesion molecule was detected after coculture (Figure 5). The reduction in the concentration of proinflammatory IL-6 and TNF-α was revealed (Figure 5). There were no significant changes in the level of IL-8, IL-10, and IFN-γ (Figure 5). Meanwhile, the level of LIF, which is known to be involved in ASC immunosuppression, was significantly increased after coculture (Figure 5). No effect of oxygen concentration on the production of soluble mediators was noted after coculture.

Thus, 72 hrs of indirect interaction with mitogen-stimulated allogeneic PBMCs did not lead to any alteration of

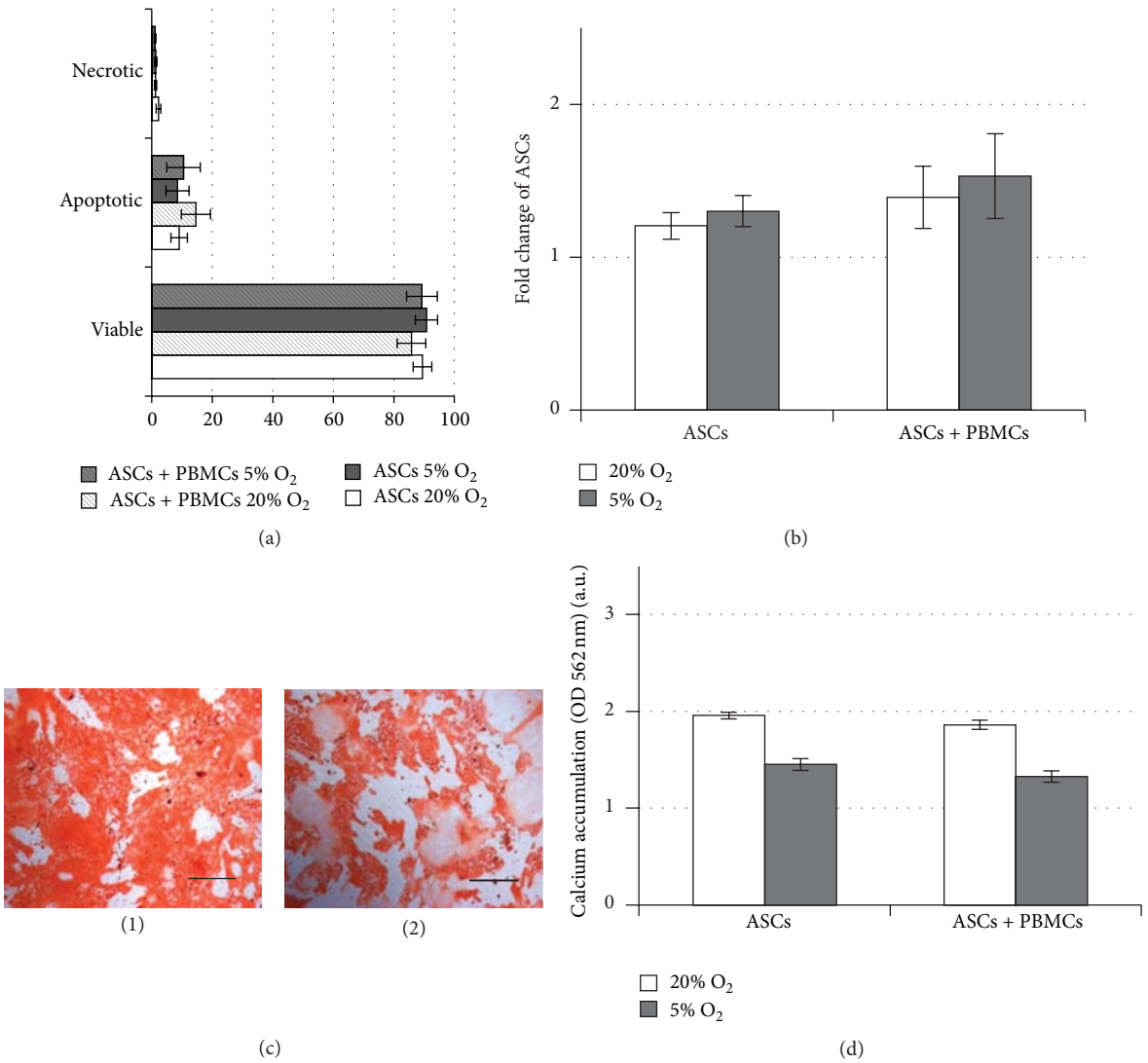

Figure 4: ASC functions after paracrine interaction with PHA-stimulated PBMCs. (a) ASC viability: percentage of viable, apoptotic, and necrotic cells in monoculture and after coculture during 72 h at 20% and 5% O_2. (b) ASC proliferation: the change in cell number in monoculture and after coculture during 72 h at 20% and 5% O_2. (c) Matrix mineralization of ASCs at 20% (1) and 5% O_2 (2), alizarin red staining: bar 200 μm. (d) Osteodifferentiation: matrix mineralization in monocultured and cocultured ASCs. *Significant difference between ASC under 20% and 5% O_2 in monoculture. #Significant difference between ASC under 20% and 5% O_2 in coculture.

ASC functions but provoked a significant shift in the profile of soluble mediators. It was of interest to assess how PBMCs affected the ASC transcriptional activity.

3.2. Effects of PHA-Stimulated PBMCs on ASC Gene Expression: Microarray Analysis. In this study, we identified genes that were differentially expressed in ASCs after interaction with activated PBMCs under different O_2 conditions. Microarray analysis revealed significant change of ASC transcriptome profile: 304 genes at 20% O_2 and 142 at 5% O_2 were differentially expressed. In total, 104 genes were jointly changed both under 20% and 5% O_2 (Figure 6(a)). Ranking according to Gene Ontology (GO) demonstrated that in groups of signal transduction, proliferation, immune response, cell adhesion, stress response, intracellular signal transduction, and cell motility 20 or more genes were differentially expressed under 20% O_2. At 5% O_2 the number of genes with altered expression in the same groups was lower. In some GO groups, the differentially expressed genes were detected only at 20% O_2 (cell homeostasis, protein biosynthesis, and intracellular transport) (Figure 6(b)).

The alteration in the expression of certain most important ASC genes in different functional groups is summarized in Table 2. ASC proinflammatory activation-involved genes demonstrated the significant upregulation confirming "priming" of ASCs by PHA-stimulated PBMCs. The degree of this "priming" practically did not depend on O_2 level in the milieu except for *TRAF3IP2* and *COLEC12*, whose upregulation was higher under 5% O_2. Among the paracrine regulation-entailed molecules the significant upregulation was detected

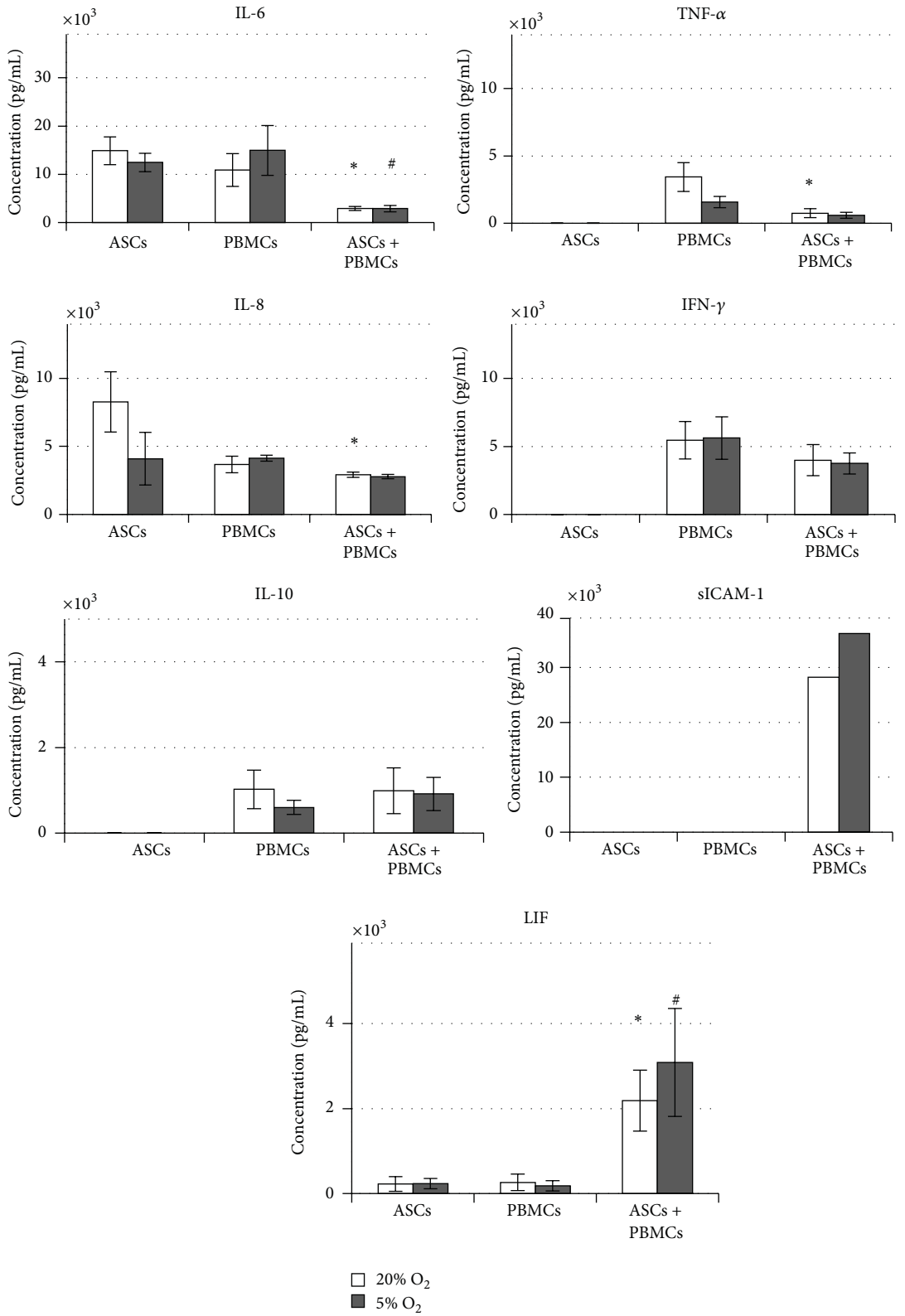

Figure 5: Concentration of soluble mediators in conditioned medium after 72 hrs of culture. *Significant difference between ASC under 20% and 5% O_2 in monoculture. #Significant difference between ASC under 20% and 5% O_2 in coculture.

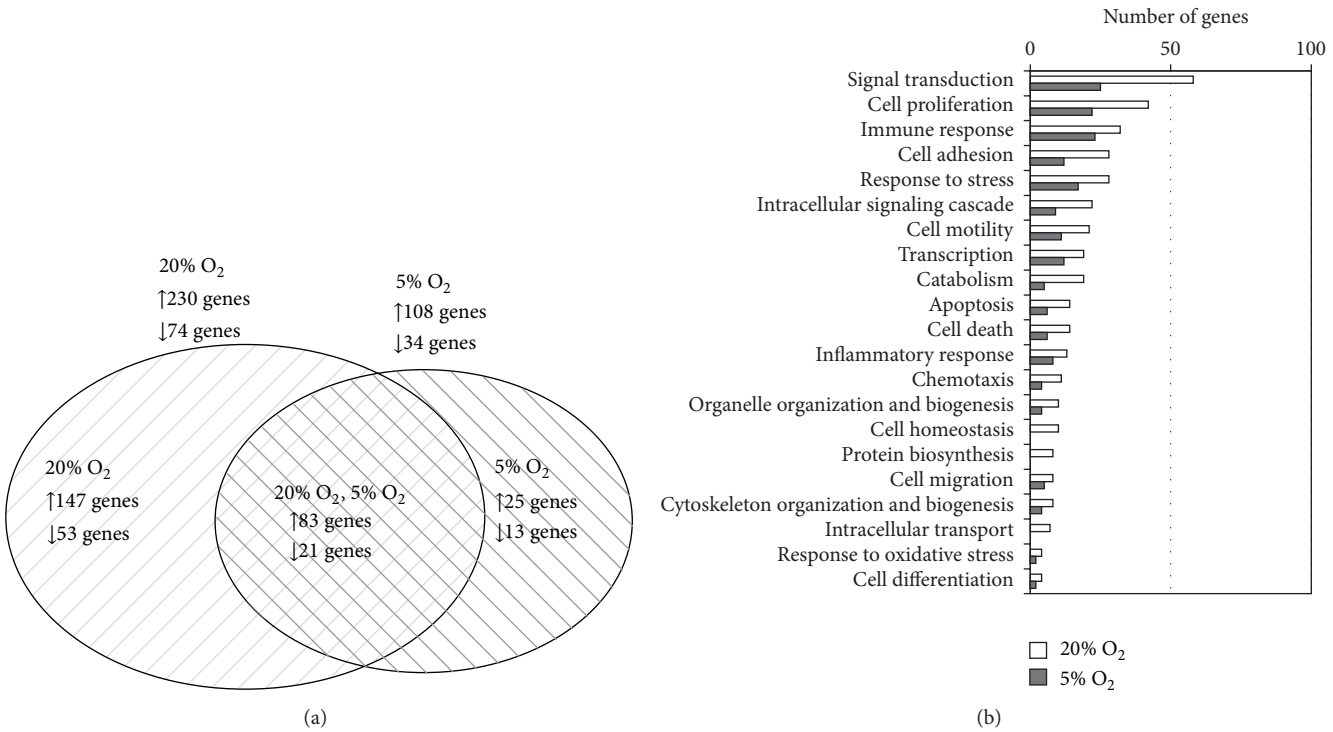

Figure 6: Characterisation of differential gene expression in ASCs after paracrine interaction with PHA-stimulated allogeneic PBMCs. (a) Venn diagram, showing the number of ASC genes commonly or differentially expressed at 20% and 5% O_2. (b) The number of differentially expressed genes in Gene Ontology (GO) groups (biological function).

in CC-, CXC-, and IL-families: *CXCL1*, *CXCL12*, *CXCL5*, *CXCL6*, *CCL2 (MCP-1)*, *CCL5*, *IL11*, *IL1B*, and *IL8*. It is important that, except *MCP-1* and *IL-1β*, the overexpression was more evident under ambient 20% O_2. Moreover, *CXCL1*, *CXCL5*, and *CXCL6*, whose expression increased more than ten- or hundred-fold under 20% O_2, did not changed under 5% O_2. Immunosuppression-associated genes displayed both up- and downregulation in different O_2 conditions. So, *PTGIS* and *TGFBI* were negatively regulated under 20% O_2, while displaying positive regulation under 5% O_2. The data on *LIF* expression supported ELISA data presented above on enhanced production of this mediator under 5% O_2. The group of genes, linked with extracellular matrix remodeling, showed significant increase of matrix metalloproteinase (*MMP1*, *MMP3*) gene transcription simultaneously with collagen upregulation (*COL7A1*). Expression of genes, encoding cell-matrix interaction-mediating molecules (*ITGA11*, *ITGB5*, *PODXL*, and *MFGE8*), was significantly downregulated after ASC/PBMCs interaction under 20% O_2 and had no changes at 5% O_2. Only *PDPN* was upregulated under both O_2 concentrations. Migration-associated genes (*HAS1*, *SLIT2*) displayed enhanced transcription at 20% and 5% O_2. Expression of proliferation-regulated genes (*CDKN3*, *CCNB2*) increased only under ambient O_2, while *CDC20* and *MCM4* were upregulated at both O_2 conditions.

In summary, the data on differential expression of ASC genes after interaction with activated allogeneic PBMCs demonstrated the significant shift in expression pattern that varied depending on O_2 conditions.

4. Discussion

Cell-to-cell interaction is a dynamic process governed by local milieu. When responding to the microenvironmental challenges, cells not only modulate themselves but also regulate the properties of other cells in accordance with their new state. In the present study, we examined the effect of paracrine interaction of allogeneic activated PBMCs and ASCs on functions and the transcriptome of the latter under "physiological" hypoxia (at tissue-related O_2). These effects have been addressed in two aspects: firstly, how does proinflammatory activation by allogeneic PBMCs affect the features (internal state) of ASCs themselves and, secondly, how do ASC functions change after interaction with activated immune cells?

Proinflammatory activation is considered one of the prerequisite for induction the immunomodulatory potential of MSCs [26]. It was shown that this effect is provided in the presence of activated immune cells, as well as certain inflammatory mediators (TNF-α, IFN-γ, IL-1β, and IL- 6). The effects of certain cytokines and of cocktail produced by activated PBMCs can differ significantly [11–13, 27]. So far, global differential gene expression analysis showed only a partial match for genes with altered expression in MSCs exposed to certain cytokines, combinations thereof, or a cocktail from the activated PBMCs. Wherein these certain cytokines stimulated IDO-mediated immunosuppression by MSCs, a cocktail from activated immune cells caused PGE_2-immunosupression [27].

Table 2: Summary of most important differentially expressed ASC genes after paracrine interaction with PHA-stimulated PBMCs under different O_2 concentrations, as determined by microarray analysis.

Gene	Product	ASC + PBMCs versus ASCs, fold change	
		20% O_2	5% O_2
	Proinflammatory activation		
TRAF3IP2	TRAF3 interacting protein 2	4.6	9.3
IRAK3	Interleukin-1 receptor-associated kinase 3	6.3	6.2
IRAK2	Interleukin-1 receptor-associated kinase 2	5.7	6.5
TNFAIP3	Tumor necrosis factor, alpha-induced protein 3	5.1	5.2
IFI44	Interferon-induced protein 44	5.8	6.8
IFI6	Interferon, alpha-inducible protein 6, transcript variant 2	11.1	10.6
IFI6	Interferon, alpha-inducible protein 6, transcript variant 3	4.4	6.3
ISG15	ISG15 ubiquitin-like modifier	4.3	4.6
GBP2	Guanylate binding protein 2, interferon-inducible	3.7	5.2
IFI27	Interferon, alpha-inducible protein 27	4.3	5.4
HLA-H	Major histocompatibility complex, class I, H	2.9	3.8
COLEC12	Collectin subfamily member 12	5.4	7.3
	Paracrine regulation		
CXCL1	Chemokine (C-X-C motif) ligand 1 (melanoma growth stimulating activity, alpha)	46.3	1
CXCL12	Chemokine (C-X-C motif) ligand 12 (stromal cell-derived factor 1)	3.0	3.8
CXCL5	Chemokine (C-X-C motif) ligand 5 (CXCL5)	328.3	1
CXCL6	Chemokine (C-X-C motif) ligand 6 (granulocyte chemotactic protein 2)	200.7	1
CCL2	Chemokine (C-C motif) ligand 2 (monocyte chemotactic protein 1)	11.6	52.4
CCL5	Chemokine (C-C motif) ligand 5 (RANTES)	5.6	7.4
IL11	Interleukin 11	14.2	16.8
IL1B	Interleukin 1, beta	28.7	95.5
IL8	Interleukin 8	81.4	28.0
	Immunosuppression		
HLA-B	Major histocompatibility complex, class I, B	4.6	5.1
HLA-E	Major histocompatibility complex, class I, F	2.7	1
HLA-H	Major histocompatibility complex, class I, H	2.9	3.8
PTGIS	Prostaglandin I2 (prostacyclin) synthase	0.13	2.0
TGFBI	Transforming growth factor, beta-induced	0.33	33.2
LIF	Leukemia inhibitory factor (cholinergic differentiation factor)	3.0	7.4
PTGS2	Prostaglandin-endoperoxide synthase 2 (prostaglandin G/H synthase and cyclooxygenase)	5.3	3.7
	Extracellular matrix		
COL12A1	Collagen, type XII, alpha 1	0.2	1
COL6A2	Collagen, type VI, alpha 2	3.2	1
COL7A1	Collagen, type VII, alpha 1	6.5	7.3
MMP1	Metallopeptidase 1 (interstitial collagenase)	18.9	9.2
MMP3	Matrix metallopeptidase 3 (stromelysin 1, progelatinase)	266.6	317.6
	Migration		
PODN	Podocan	0.1	0.1
HAS1	Hyaluronan synthase 2	12.8	8.1
SLIT2	Slit homolog 2	4.8	3.9
SPHK1	Sphingosine kinase 1	2.5	1
	Cell-matrix interaction		
ITGA11	Integrin, alpha 11	0.2	1
ITGB3	Integrin, beta 3 (platelet glycoprotein IIIa, antigen CD61)	4.9	1
ITGB5	Integrin, beta 5	0.3	1
PODXL	Podocalyxin-like protein	0.1	1
PDPN	Podoplanin	4.6	4.2
MFGE8	Milk fat globule-EGF factor 8 protein (lactadherin)	0.2	1

Table 2: Continued.

Gene	Product	ASC + PBMCs versus ASCs, fold change	
		20% O_2	5% O_2
	Proliferation		
CDKN3	Cyclin-dependent kinase inhibitor 3	9.6	1
CCNB2	Cyclin B2	8.1	1
CDC20	Cell division cycle 20 homolog	6.0	17.5
MCM4	Minichromosome maintenance complex component 4	14.4	7.2
CDKN2B	Cyclin-dependent kinase inhibitor 2B	0.1	0.1

Fold changes are for comparison between ASCs in monoculture and coculture. Positive values indicate higher and negative values indicate lower expression in cocultured ASCs. $p < 0.05$.

In this paper, gene microarray analysis showed that after 72 hours of ASC/PHA-activated allogeneic PBMC paracrine interaction the number of ASC genes with altered expression was more than twice of that under 20% O_2 compared to 5% O_2, and only half of them jointly changed under both O_2 conditions. The upregulation of genes directly involved in "regenerative" ASC functions was detected in this "joint" group. There were genes regulating the cell cycle: *CDKN3* (cyclin-dependent kinase inhibitor), *CCNB2* (cyclin B), *CDC20* (cell cycle 20 homolog), and *MCM4*, the activity of which is related to the initiation of DNA replication. In addition, a negative regulator of cell proliferation, *CDKN2B*, was downregulated, which may also be associated with the increased proliferative activity of ASCs. Besides, the transcription of several other important molecules was upregulated in ASCs after interaction: *HAS1*, hyaluronan synthase, an enzyme that is responsible for the production of hyaluronic acid, which is produced in an active reparative processes allowing migration of stromal cells and vascular growth; *SLIT2*, a protein that positively regulates the production of other important membrane-bound proteoglycans, glypican, that provide adhesion and migration of cells; and *SPHK1*, sphingosine kinase, which phosphorylates sphingosine to sphingosine-1-phosphate, an important regulatory molecule for interaction, cell migration, and proliferation.

Our data demonstrated that ASC "priming" occurred upon interaction with activated PBMCs. Therefore, we detected the upregulation of TNF-α and INF-inducible protein genes (*TNFAIP3*, *IF44*, *GBP2*, etc.) that reflects ASC "pro-inflammatory" activation which is needed to stimulate the production of immunosuppressive factors. Indeed, ASCs upregulated the activity of *HLA-I*, which is consistent with previously described increase of the corresponding protein [28]. We also revealed the elevated transcription of *PTGS2*, prostaglandin G/H synthase and cyclooxygenase, which is known to activate the production of PGE_2, one of the main factors inhibiting the proliferation of T-cells.

ASC/PBMC interaction significantly stimulated transcription of CC, CXC, and IL cytokine families' genes in ASCs. The most significant upregulation was demonstrated for pleiotropic chemokines (*CXCL5*, *CXCL1*, *IL8*, *IL1B*, *IL11*, and *LIF*). These molecules provide chemotaxis, intercellular and intracellular signaling, and regulation of cell proliferation including the autocrine path, participate in the immune response and inflammation, and are responsible for the regulation of blood leukocytes, such as monocytes (MCP-1), lymphocytes (CXCL12), granulocytes (CXCL6), and neutrophils (CXCL5, IL-8, and CXCL1). Furthermore, the participation of CXCL1 and CXCL5 in the stimulation of angiogenesis was shown, which is also very important for regeneration. Cytokine gene activity in some cases did not depend on the concentration of O_2 (*CCL5*, *IL11*); for a number of genes (*CXCL5*, *CXCL6*, and *IL8*) there was significant upregulation at 20% O_2, while for others this was detected at 5% O_2 (CCL2, *IL1B*, and *LIF*).

Transcription of genes, associated with extracellular matrix remodeling, the most important function of MSCs, such as collagen (*COL7A1*) and matrix metalloproteinases (*MMP1*, *MMP3*), was upregulated after ASC/PBMC interaction. The expression of *MMP3* was increased by almost 300 times. Increased matrix-remodeling activity of ASCs was apparently associated with the differential expression of integrins (*ITGA11*, *ITGB3*, and *ITGB5*), which mediated cell-matrix interactions and decreased the expression of a negative regulator of migration, podokan (*PODN*).

Thereby, microarray analysis showed the upregulation of genes, where protein products provide increased proliferative activity of ASCs, and their ability to migrate due to the enhanced extracellular matrix remodeling. Under ambient O_2 (20%) significantly more genes changed their expression after interaction with activated PBMCs compared to tissue-related O_2 (5%). While the transcriptome changes were revealed at both O_2 concentrations, the effect was less marked under 5% O_2. It should be noted that some key genes as *IL-1b*, *LIF*, and *HAS1* were more significantly upregulated under 5% O_2 compared to 20% O_2.

Thus, it can be concluded that interaction with allogeneic activated PBMCs can awaken the "regenerative" potential of ASCs at least at the transcription level. Also, the significant shift in cytokine levels in coculture conditioned medium was detected compared to PBMC and ASC monocultures. It is known that MSC/ASCs in a proinflammatory microenvironment synthesize a variety of soluble mediators, which are of high importance for the implementation of regenerative processes such as EGF, FGF, PDGF, TGF-β, VEGF, HGF, IGF-1, Ang-1, KGF, and SDF-1 [26]. The production of immunosuppressive molecules by MSCs was observed after priming by cytokines from activated leukocytes, in particular, IFN-γ in combination with TNF-α, IL-1α, or IL-1β [26].

Here we compared the cytokine levels in ASC and PBMC monocultures with the cytokine profile after contact-independent coculture. For mediators secreted by PBMCs only, after cocultivation, a marked decrease in the concentration of TNF-α was demonstrated, whereas the level of IFN-γ and IL-10 was the same as in a monoculture. Both ASCs and PBMCs in monoculture synthesized IL-8. The concentration of IL-8 in the coculture was the same as in monocultures, which indicates a decrease in the production of this cytokine in at least one type of interacting cells. Based on the significant upregulation of *IL8* transcription that we found in ASCs after coculture with PBMCs, a substantial inhibition of IL-8 production by PBMCs should be supposed. In ASC and PBMC monocultures we detected two IL-6 superfamily mediators, IL-6 itself and LIF. The concentration of IL-6 was significantly lower after cocultivation compared to monocultures, which may indicate a decrease in IL-6 synthesis in ASCs as well as in PBMCs. Given the absence of transcriptional changes of IL-6 in ASCs, it is reasonable to assume that there is a significant inhibition of this interleukin production in PBMCs. In contrast, after coculture LIF increased significantly compared to monocultures. In addition, we noted upregulation of *LIF* expression in cocultured ASCs. Thus, taking into account the decreased concentration of proinflammatory mediators like TNF-α and IL-6 and the increased production of LIF, which is known to be one of the ASC immunosuppressive mediators [9, 26] the cytokine profile after ASC/PBMC interaction can be characterised as anti-inflammatory one.

In the present paper we have demonstrated that ASC/PBMC paracrine interaction was accompanied by an increase in the number of ICAM-1-expressing ASCs as well as ICAM-1 molecules per cell. Moreover, we also detected soluble sICAM-1 in conditioning medium after coculture. It is known that ICAM-1 plays an important role in leukocyte adhesion and migration in inflammation. Majumdar et al. [29] attributed such an increase in ICAM-1 expression to MSC activation by TNF-α and/or IFN-γ, produced by activated PBMCs. However, while Faßlrinner et al. [30] also found an increase in ICAM-1 expression after interaction of PBMCs and bone marrow MSCs, they demonstrated that blocking IFN-γ, TNF-α did not completely prevent the ICAM-1 elevation suggesting the existence of additional stimuli of ICAM-1 expression. Therefore, Ren et al. [31] revealed that IL-1 also induced ICAM-1 expression. The authors attributed the elevation in ICAM-1 with enhanced immunosuppressive activity of MSC due to the "concentration" of immune cells around MSCs. Our data on increased ICAM-1 MFI on ASCs after coculture with PBMCs support Ren et al.'s [31] findings. It is necessary to point out that under tissue-related O_2 per cell increase of ICAM-1 was less marked. Besides ICAM-1 we also analysed the expression of another adhesion molecule Thy-1 (CD90), a counterreceptor for the leukocyte integrin Mac-1, which usually is considered as mesenchymal cell marker. Though practically all ASCs in mono- and coculture were CD90-positive, the per cell expression of Thy-1 was significantly decreased under tissue-related O_2. As it was shown previously a decline in CD90 expression on MSCs can lead to the loss of immunosuppressive activity [32]. Although we did not detect the attenuation of ASC immunosuppression at "physiologic" hypoxia, the reported decrease of adhesive ICAM-1 and Thy-1 per cell expression may support the abovementioned assumption of weaker proinflammatory activation of ASCs under tissue O_2.

ASC viability and intracellular compartment functions were not hampered after 72 hours of paracrine interaction with activated allogeneic PBMCs. ASCs retained their mesenchymal phenotype ($CD73^+$, $CD90^+$, $CD105^+$, and $CD45^-$) and the capacity to proliferate and osteodifferentiate, which indicates the preservation of ASC functions regardless of O_2 concentration. Earlier, Crop et al., in 2010, showed no effect of proinflammatory activation on ASC osteo- and adipodifferentiation and even found an increase in ASC proliferation rate after 7 days of coculturing [27]. Increase of MSC proliferation after 6–8 days of stimulation with the activated lymphocyte paracrine cocktail was also demonstrated [30]. In this case, the key role apparently belonged not only to IFN-γ, whose action is usually associated with proinflammatory "priming" of MSCs, but by other cytokines as well [30, 33]. Preservation of ASC functions, regardless of the concentration of O_2 in the microenvironment, has an important applied aspect in terms of realisation of allogeneic ASC regenerative potential *in vivo*.

"Physiological" hypoxia is one of the key parameters of the microenvironment, which can modulate the properties of the cells and their interaction. In several papers it has been convincingly shown that the expansion of MSCs under tissue-related O_2 switched them to glycolytic energy metabolism, which was accompanied by an increase of proliferation and reduction of differentiation [22]. Furthermore, the upregulation of "stemness" genes was demonstrated [34–38]. These data suggest that at tissue-related O_2 MSCs can possess properties of uncommitted progenitor cells. Accordingly, such changes may also affect the proinflammatory priming of MSCs. Thus, we demonstrated that under "physiological" hypoxia (tissue-related O_2) ASCs were activated in a proinflammatory manner and retained their functions under ambient and tissue-related O_2, though ASCs exhibited lesser proinflammatory activation at 5% O_2. These data show that the net effect of ASC interactions with other cell types, considered in terms of the *in vivo* situation, depends on a complex set of factors, including the specific issues of tissue microenvironment.

5. Conclusions

Our data demonstrated that paracrine interaction of allogeneic mitogen-stimulated PBMCs and ASCs under ambient O_2 as well as at "physiologic" hypoxia resulted in "priming" of ASCs with significant upregulation of genes involved in proinflammatory activation, immunosuppression, cell proliferation, cytokine regulation, and extracellular matrix remodeling. Under tissue-related O_2 notably less genes were differentially expressed in ASCs compared to 20% O_2. Meanwhile, under both O_2 conditions ASCs retained their functions, immunosuppressive potential and provided the anti-inflammatory cytokine shift. These data are important in terms of allogeneic ASC implementation in cell therapy and regenerative medicine.

Conflict of Interests

The authors declare that there is no conflict of interests regarding the publication of this paper.

Acknowledgments

This work was supported by Grant from Russian Science Foundation no. 14-15-00693. Microarray analysis was funded by Grant from Program no. 7 of Presidium of Russian Academy of Sciences.

References

[1] C. Nombela-Arrieta, J. Ritz, and L. E. Silberstein, "The elusive nature and function of mesenchymal stem cells," *Nature Reviews Molecular Cell Biology*, vol. 12, no. 2, pp. 126–131, 2011.

[2] M. Di Nicola, C. Carlo-Stella, M. Magni et al., "Human bone marrow stromal cells suppress T-lymphocyte proliferation induced by cellular or nonspecific mitogenic stimuli," *Blood*, vol. 99, no. 10, pp. 3838–3843, 2002.

[3] M. Krampera, S. Glennie, J. Dyson et al., "Bone marrow mesenchymal stem cells inhibit the response of naive and memory antigen-specific T cells to their cognate peptide," *Blood*, vol. 101, no. 9, pp. 3722–3729, 2003.

[4] J. M. Ryan, F. P. Barry, J. M. Murphy, and B. P. Mahon, "Mesenchymal stem cells avoid allogeneic rejection," *Journal of Inflammation*, vol. 2, article 8, 2005.

[5] L. B. Buravkova and E. R. Andreeva, "Interaction of human mesenhymal stromal with immune cells," *Human Physiology*, vol. 36, no. 5, pp. 590–598, 2010.

[6] D. I. Ivanyuk, V. V. Turchin, A. G. Popandonulo, and V. K. Grin, "Mechanisms of immunomodulatory effects of mesenchymal stem cells," *Genes and Cells*, vol. 6, no. 2, pp. 27–31, 2011 (Russian).

[7] Y. P. Rubtsov, Y. G. Suzdaltseva, K. V. Goryunov, N. I. Kalinina, V. Y. Sysoeva, and V. A. Tkachuk, "Regulation of immunity via multipotent mesenchymal stromal cells," *Acta Naturae*, vol. 3, no. 4, p. 11, 2011.

[8] K. English and B. P. Mahon, "Allogeneic mesenchymal stem cells: agents of immune modulation," *Journal of Cellular Biochemistry*, vol. 112, no. 8, pp. 1963–1968, 2011.

[9] A. Gebler, O. Zabel, and B. Seliger, "The immunomodulatory capacity of mesenchymal stem cells," *Trends in Molecular Medicine*, vol. 18, no. 2, pp. 128–134, 2012.

[10] W. K. Chan, A. Sik-Yin Lau, J. Chun-Bong Li, H. Ka-Wai Law, Y. L. Lau, and G. Chi-Fung Chan, "MHC expression kinetics and immunogenicity of mesenchymal stromal cells after short-term IFN-gamma challenge," *Experimental Hematology*, vol. 36, no. 11, pp. 1545–1555, 2008.

[11] H. Hemeda, M. Jakob, A.-K. Ludwig, B. Giebel, S. Lang, and S. Brandau, "Interferon-γ and tumor necrosis factor-α differentially affect cytokine expression and migration properties of mesenchymal stem cells," *Stem Cells and Development*, vol. 19, no. 5, pp. 693–706, 2010.

[12] S. J. Prasanna, D. Gopalakrishnan, S. R. Shankar, and A. B. Vasandan, "Pro-inflammatory cytokines, IFNγ and TNFα, influence immune properties of human bone marrow and Wharton jelly mesenchymal stem cells differentially," *PLoS ONE*, vol. 5, no. 2, Article ID e9016, 2010.

[13] J. M. Ryan, F. Barry, J. M. Murphy, and B. P. Mahon, "Interferon-gamma does not break, but promotes the immunosuppressive capacity of adult human mesenchymal stem cells," *Clinical and Experimental Immunology*, vol. 149, no. 2, pp. 353–363, 2007.

[14] M. J. Crop, S. S. Korevaar, R. de Kuiper et al., "Human mesenchymal stem cells are susceptible to lysis by $CD8^+$ T cells and NK cells," *Cell Transplantation*, vol. 20, no. 10, pp. 1547–1559, 2011.

[15] I. Prigione, F. Benvenuto, P. Bocca, L. Battistini, A. Uccelli, and V. Pistoia, "Reciprocal interactions between human mesenchymal stem cells and $\gamma\delta$ T cells or invariant natural killer T cells," *Stem Cells*, vol. 27, no. 3, pp. 693–702, 2009.

[16] S. Schu, M. Nosov, L. O'Flynn et al., "Immunogenicity of allogeneic mesenchymal stem cells," *Journal of Cellular and Molecular Medicine*, vol. 16, no. 9, pp. 2094–2103, 2012.

[17] J. A. Ankrum, J. F. Ong, and J. M. Karp, "Mesenchymal stem cells: immune evasive, not immune privileged," *Nature Biotechnology*, vol. 32, no. 3, pp. 252–260, 2014.

[18] B. Kronsteiner, S. Wolbank, A. Peterbauer et al., "Human mesenchymal stem cells from adipose tissue and amnion influence T-cells depending on stimulation method and presence of other immune cells," *Stem Cells and Development*, vol. 20, no. 12, pp. 2115–2126, 2011.

[19] A. N. Gornostaeva, E. R. Andreeva, and L. B. Buravkova, "Human MMSC immunosuppressive activity at low oxygen tension: direct cell-to-cell contacts and paracrine regulation," *Human Physiology*, vol. 39, no. 2, pp. 136–146, 2013.

[20] P. A. Zuk, M. Zhu, H. Mizuno et al., "Multilineage cells from human adipose tissue: implications for cell-based therapies," *Tissue Engineering*, vol. 7, no. 2, pp. 211–228, 2001.

[21] L. B. Buravkova, O. S. Grinakovskaya, E. R. Andreeva, A. P. Zhambalova, and M. P. Kozionova, "Characteristics of human lipoaspirate-isolated mesenchymal stromal cells cultivated under lower oxygen tension," *Cell and Tissue Biology*, vol. 3, no. 1, pp. 23–28, 2009.

[22] L. B. Buravkova, Y. V. Rylova, E. R. Andreeva et al., "Low ATP level is sufficient to maintain the uncommitted state of multipotent mesenchymal stem cells," *Biochimica et Biophysica Acta*, vol. 1830, no. 10, pp. 4418–4425, 2013.

[23] D. Suva, J. Passweg, S. Arnaudeau, P. Hoffmeyer, and V. Kindler, "In vitro activated human T lymphocytes very efficiently attach to allogenic multipotent mesenchymal stromal cells and transmigrate under them," *Journal of Cellular Physiology*, vol. 214, no. 3, pp. 588–594, 2008.

[24] M. Dominici, K. Le Blanc, I. Mueller et al., "Minimal criteria for defining multipotent mesenchymal stromal cells. The International Society for Cellular Therapy position statement," *Cytotherapy*, vol. 8, no. 4, pp. 315–317, 2006.

[25] O. S. Grinakovskaya, E. R. Andreeva, L. B. Buravkova, Y. V. Rylova, and G. Y. Kosovsky, "Low level of O_2 inhibits commitment of cultured mesenchymal stromal precursor cells from the adipose tissue in response to osteogenic stimuli," *Bulletin of Experimental Biology and Medicine*, vol. 147, no. 6, pp. 760–763, 2009.

[26] S. Ma, N. Xie, W. Li, B. Yuan, Y. Shi, and Y. Wang, "Immunobiology of mesenchymal stem cells," *Cell Death and Differentiation*, vol. 21, no. 2, pp. 216–225, 2014.

[27] M. J. Crop, C. C. Baan, S. S. Korevaar et al., "Inflammatory conditions affect gene expression and function of human adipose tissue-derived mesenchymal stem cells," *Clinical and Experimental Immunology*, vol. 162, no. 3, pp. 474–486, 2010.

[28] K. Le Blanc, I. Rasmusson, C. Götherström et al., "Mesenchymal stem cells inhibit the expression of CD25 (interleukin-2 receptor) and CD38 on phytohaemagglutinin-activated lymphocytes," *Scandinavian Journal of Immunology*, vol. 60, no. 3, pp. 307–315, 2004.

[29] M. K. Majumdar, M. Keane-Moore, D. Buyaner et al., "Characterization and functionality of cell surface molecules on human mesenchymal stem cells," *Journal of Biomedical Science*, vol. 10, no. 2, pp. 228–241, 2003.

[30] F. Faßlrinner, M. Wobus, R. Duryagina et al., "Differential effects of mixed lymphocyte reaction supernatant on human mesenchymal stromal cells," *Experimental Hematology*, vol. 40, no. 11, pp. 934–944, 2012.

[31] G. Ren, X. Zhao, L. Zhang et al., "Inflammatory cytokine-induced intercellular adhesion molecule-1 and vascular cell adhesion molecule-1 in mesenchymal stem cells are critical for immunosuppression," *Journal of Immunology*, vol. 184, no. 5, pp. 2321–2328, 2010.

[32] D. Campioni, R. Rizzo, M. Stignani et al., "A decreased positivity for CD90 on human mesenchymal stromal cells (MSCs) is associated with a loss of immunosuppressive activity by MSCs," *Cytometry Part B: Clinical Cytometry*, vol. 76, no. 3, pp. 225–230, 2009.

[33] S. Ghannam, C. Bouffi, F. Djouad, C. Jorgensen, and D. Noël, "Immunosuppression by mesenchymal stem cells: mechanisms and clinical applications," *Stem Cell Research and Therapy*, vol. 1, article 2, 2010.

[34] G. D'Ippolito, S. Diabira, G. A. Howard, B. A. Roos, and P. C. Schiller, "Low oxygen tension inhibits osteogenic differentiation and enhances stemness of human MIAMI cells," *Bone*, vol. 39, no. 3, pp. 513–522, 2006.

[35] C. Fehrer, R. Brunauer, G. Laschober et al., "Reduced oxygen tension attenuates differentiation capacity of human mesenchymal stem cells and prolongs their lifespan," *Aging Cell*, vol. 6, no. 6, pp. 745–757, 2007.

[36] K. Iida, T. Takeda-Kawaguchi, Y. Tezuka, T. Kunisada, T. Shibata, and K.-I. Tezuka, "Hypoxia enhances colony formation and proliferation but inhibits differentiation of human dental pulp cells," *Archives of Oral Biology*, vol. 55, no. 9, pp. 648–654, 2010.

[37] M. G. Valorani, A. Germani, W. R. Otto et al., "Hypoxia increases Sca-1/CD44 co-expression in murine mesenchymal stem cells and enhances their adipogenic differentiation potential," *Cell and Tissue Research*, vol. 341, no. 1, pp. 111–120, 2010.

[38] L. Basciano, C. Nemos, B. Foliguet et al., "Long term culture of mesenchymal stem cells in hypoxia promotes a genetic program maintaining their undifferentiated and multipotent status," *BMC Cell Biology*, vol. 12, no. 1, pp. 12–24, 2011.

Hindawi Publishing Corporation
Stem Cells International
Volume 2016, Article ID 5961342, 18 pages
http://dx.doi.org/10.1155/2016/5961342

Review Article

Pharmacological Therapy in the Heart as an Alternative to Cellular Therapy: A Place for the Brain Natriuretic Peptide?

Nathalie Rosenblatt-Velin,[1] Suzanne Badoux,[1] and Lucas Liaudet[2]

[1] *Division de Physiopathologie Clinique, Centre Hospitalier Universitaire Vaudois and University of Lausanne, 1005 Lausanne, Switzerland*
[2] *Service de Médecine Intensive Adulte, Centre Hospitalier Universitaire Vaudois and University of Lausanne, 1005 Lausanne, Switzerland*

Correspondence should be addressed to Nathalie Rosenblatt-Velin; nathalie.rosenblatt@chuv.ch

Received 18 June 2015; Revised 8 September 2015; Accepted 8 October 2015

Academic Editor: Kequan Guo

The discovery that stem cells isolated from different organs have the ability to differentiate into mature beating cardiomyocytes has fostered considerable interest in developing cellular regenerative therapies to treat cardiac diseases associated with the loss of viable myocardium. Clinical studies evaluating the potential of stem cells (from heart, blood, bone marrow, skeletal muscle, and fat) to regenerate the myocardium and improve its functional status indicated that although the method appeared generally safe, its overall efficacy has remained modest. Several issues raised by these studies were notably related to the nature and number of injected cells, as well as the route and timing of their administration, to cite only a few. Besides the direct administration of cardiac precursor cells, a distinct approach to cardiac regeneration could be based upon the stimulation of the heart's natural ability to regenerate, using pharmacological approaches. Indeed, differentiation and/or proliferation of cardiac precursor cells is controlled by various endogenous mediators, such as growth factors and cytokines, which could thus be used as pharmacological agents to promote regeneration. To illustrate such approach, we present recent results showing that the exogenous administration of the natriuretic peptide BNP triggers "endogenous" cardiac regeneration, following experimental myocardial infarction.

1. Introduction

Cardiovascular diseases (CVDs) account for 30% of all deaths worldwide, which represented 17.3 million fatalities in 2008 (World Health Organization, Fact sheet number 317), among which 13.5 million (80%) were related to the consequences of coronary heart diseases (CHDs). This number is expected to rise steadily, with an estimated 23.3 million deaths in 2030. The identified causes of this "epidemics" involve a sedentary life of style, an unhealthy diet, as well as the use of tobacco and/or alcohol consumption [1, 2]. All favor the emergence of obesity, diabetes, and/or hypertension which are risk factors for CHDs.

Many efficient therapies have been developed to treat CVDs over the past 30 years, including various reperfusion strategies of occluded coronary vessels, antiplatelet and anticoagulant agents to prevent/treat coronary thrombosis, beta-blocking drugs, or angiotensin-converting enzyme inhibitors, to name only a few [3]. However, despite the identification of risk factors and the improvements in therapy, the morbidity and mortality associated with CHDs remain unacceptably high. A major reason for it is that CHDs induce the loss of a given amount of contractile myocardium, with unavoidable consequences on the functional activity of the heart. Indeed, the mammalian heart has long been considered a postmitotic organ with no capacity to regenerate [4], which is in striking contrast with certain lower vertebrates (zebrafish, urodeles), which have a high cardiac regeneration rate. The various treatments aimed to delay the onset of heart failure or to limit the consequences of CVDs, do not have the ability to replace the damaged cardiac cells, especially the necrotic and/or apoptotic cardiomyocytes [5], and thus

cannot properly "heal" the injured heart. This view has begun to change dramatically with the discovery that the adult heart displays some capacity to regenerate after damage and, hence, that manipulating such regenerative capacity might have therapeutic potential. These emerging concepts will be here concisely reviewed.

2. Regenerative Capacities of the Adult Mammalian Heart

In the last decade, intensive research in the cardiovascular field has allowed a more precise understanding of the cellular and molecular mechanisms governing cardiomyocyte differentiation and proliferation during physiological growth, ageing, and pathophysiological conditions. A milestone observation was the demonstration that cardiac regeneration represents a physiological process occurring during ageing in normal conditions [6]. Although the proportion of newly formed cardiomyocytes is currently debated, the fact that new cardiomyocytes are generated in human hearts during physiological ageing and after heart injuries is now well admitted [6–8]. Different mechanisms have been identified to account for the *de novo* generation of cardiomyocytes in the adult heart. These mechanisms, detailed below, include the proliferation of the preexisting mature cardiomyocytes with or without dedifferentiation, the differentiation of endogenous precursor cells, and the differentiation of exogenous infiltrating cells (for review see [9]).

2.1. Proliferation of Mature Cardiomyocytes. Although cardiomyocytes in mammals demonstrate proliferative capacities during fetal development, it has been commonly admitted that after birth, cardiomyocytes cannot reenter the cell cycle, as DNA replication occurs without cytokinesis or karyokinesis [10]. This assumption was first challenged by the Sadek laboratory, who demonstrated that mouse cardiomyocytes can proliferate after partial surgical resection of the heart at birth [11]. In this mouse model, cardiomyocyte proliferation led to the replacement of the resected tissue and the inhibition of fibrosis. Notwithstanding this obvious regenerative process, the capacity of murine cardiomyocytes to proliferate was lost after 7 days of age. Further evidence of cardiomyocyte ability to proliferate came from the Lee laboratory, who recently proposed that preexisting cardiomyocytes represent the main source of newly formed cardiomyocytes during ageing, as well as following myocardial infarction (MI) [12]. However, although cardiomyocyte proliferation occurs life-long, this process is seldom in the mouse heart after the first month of life [13].

The mechanisms by which cardiomyocytes are able to proliferate are not well established. In zebrafish hearts, mature cardiomyocytes have to dedifferentiate before proliferating [14]. During this dedifferentiation, cardiomyocytes reduce their sarcomere structure (they become smaller and round) and reexpress the alpha skeletal actin (α-ska) protein as well as cardiac progenitor cell markers, such as Nkx2.5 and c-kit. They downregulate the expression of prototypical markers of mature cardiomyocytes, such as Troponin I and α-myosin heavy chain (α-MHC). Their new structure and phenotype facilitate their reentry into the cell cycle. This process has also been observed *in vitro* in cardiomyocyte isolated from rat hearts [15]. However, whether this process occurs *in vivo* in mammal hearts is under debate. Dedifferentiated cardiomyocytes have been detected in the hearts of infarcted sheep hearts or in pressure-and-volume overloaded rabbit hearts [16, 17]. In human hearts after idiopathic dilated cardiomyopathy, infarction or atrial fibrillation dedifferentiated cardiomyocytes were also detected [18, 19]. The presence of these cells has been shown to be dependant at least in part by Oncostatin M [20]. However the results published until now did not demonstrate a direct link between the cardiomyocyte dedifferentiation and the proliferation. In other words, the results demonstrating that dedifferentiated cardiomyocytes proliferate *in vivo* are lacking.

However, stimulation of the cardiomyocyte proliferation appears as a new therapeutical strategy to increase cardiac regeneration especially in pathophysiological conditions. Several factors have been identified to be able to induce cardiomyocytes to reenter the cell cycle: Neuregulin 1 and its ERBB2 receptor [21–24], Periostin [25], the fibroblast growth factor-1 [26, 27], or also the stromal cell-derived factor 1α [28]. The use of miRNAs is also investigated and demonstrated that hsa-miR-590 and hsa-miR-199a were able to stimulate cardiomyocyte proliferation [29]. Interestingly, new results published by Sadek laboratory demonstrated that hypoxia is a crucial factor able to stimulate cardiomyocyte proliferation [30]. The authors identified in adult mouse hearts a small population of proliferating cardiomyocytes expressing Hif-1α and able to give rise to new cardiomyocytes (at a rate of 0.3–1% per year) during physiological ageing. Thus, these results could explain why in neonatal hearts (relatively more hypoxic than adult hearts) cardiomyocytes proliferate. Thus, the oxygen postnatal environment which has been shown to lead to DNA damage response [31], appears as a major regulator of cardiomyocyte proliferation. However, the regulation of other genes such as p21 or the transcription factor Meis1 [32, 33] or the mechanical loading of the hearts [34] could also contribute to the arrest of cardiomyocyte proliferation in postnatal hearts.

2.2. Differentiation of Endogenous Precursor Cells. Cardiac precursor cells (CPCs), which have the capacity to differentiate into mature functional cardiomyocytes, exist in the heart itself. The characterization of these cells remains a difficult task, due to the lack of a defined, highly specific marker. Thus the association of several markers is required to identify cardiovascular progenitor and cardiac precursor cells [35, 36] (Figure 1). Early cardiogenic precursors originate from mesoderm and are identified as expressing the c-kit protein [37–39] (a cellular cytokine receptor initially found at the surface of hematopoietic progenitor cells), the vascular endothelial growth factor (VEGF) receptor 2 protein (Flk-1) [40], and the nuclear transcription factor islet-1 [35, 41, 42]. These relative undifferentiated cells give rise to multipotent cardiovascular progenitors which express the nuclear transcription factor Nkx2.5 [43, 44] together with the islet-1, Flk-1, and c-kit proteins. These progenitors differentiate

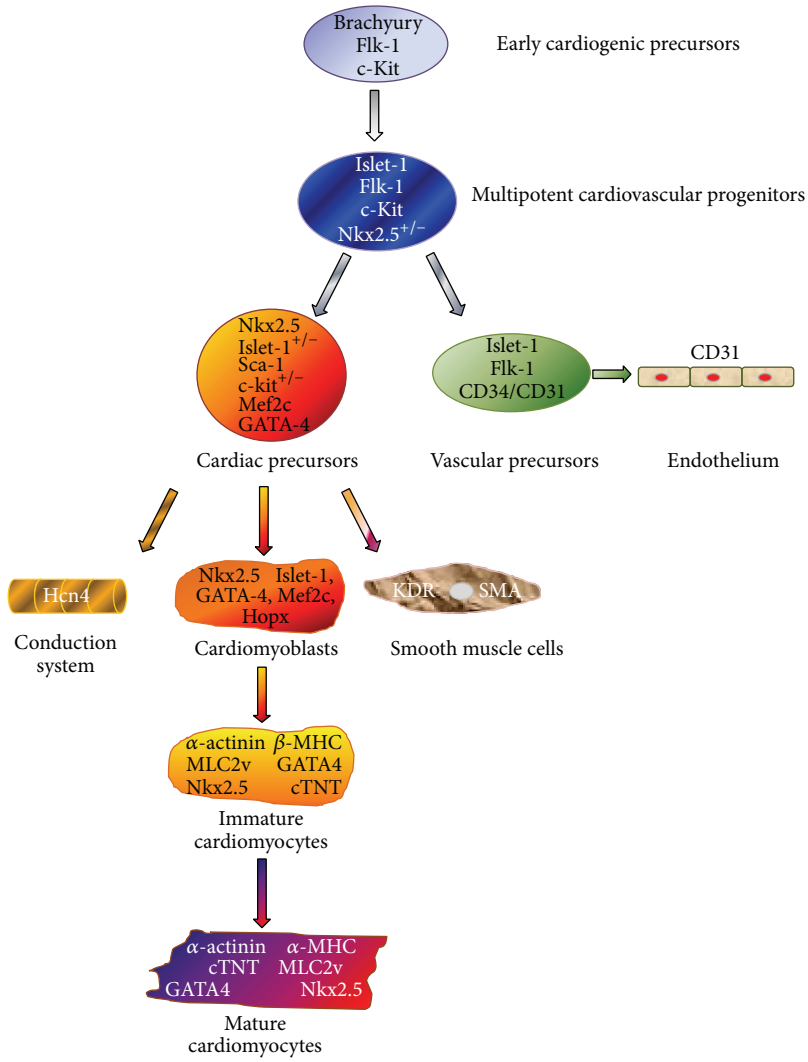

Figure 1: Cardiovascular cell lineage. Schematic representation depicting the origin of cardiomyocytes and endothelial and smooth muscle cells, as well as the conduction system. Several proteins are associated with the different stage of differentiation of the cardiac cells: islet-1, Flk-1, and c-kit are expressed at an undifferentiated stage, whereas the expression of Nkx2.5 and Sca-1 identifies more differentiated cardiac precursor cells.

into vascular precursors expressing the endothelial markers CD34 and CD31 or into cardiac precursor cells expressing notably Nkx2.5, GATA-4, Mef2c, and the stem cell antigen-1 (Sca-1) proteins [42, 45–47]. CPCs can differentiate into cells of the conduction system, into smooth muscle cells, and into cardiomyoblasts expressing Hopx [48]. $Hopx^+$ cells give only rise to cardiac myocytes (immature and mature cardiomyocytes).

The participation of the endogenous CPCs to heart regeneration in physiological conditions is controversial [8, 12]. Under pathological conditions, it is now well established that CPCs can differentiate into cardiomyocytes when they were activated with different stimuli, such as FGF-2, thymosin $\beta 4$, prostaglandin E2, human stem cell factor, or also stromal-cell derived factor 1 (SDF1) [8, 49–53]. However, such involvement seems to be limited in time, as indicated by Hsueh and coworkers who reported that CPC differentiation into cardiomyocytes started at day 7 after MI but saturated on day 10 [51]. Interestingly, in senescent heart, CPCs are quiescent because of lack of stimulation but they can be re-activated by stem cell factor [39]. This suggests that, even in old hearts, activation of endogenous CPCs could be used as a therapeutical way to increase cardiac regeneration.

Among the "direct" activation of CPCs with several factors, the microenvironment of the CPCs can also be modified to increase their potency to participate into heart regeneration. Thus, their migration capacity which is dependent on the SDF1 secreted by the damaged myocardium and its CXCR 4 receptor (expressed by CPCs) can be modulated [54]. The group of Wang induced overexpression of SDF1 by the cardiomyocytes, which led to increased mobilization of

CPCs [55]. SDF1 has also been shown to activate the endogenous cardioblasts in adult hearts after myocardial infarction [53].

2.3. Role of Infiltrating Cells from Extracardiac Origin. Although the role of infiltrating cells is not yet well defined, inhibition of certain aspects of inflammation is detrimental to cardiac repair after myocardial infarction [56–58], pointing to some role of infiltrating cells in the regenerative process. In this respect, evidence has accumulated that monocytes/macrophages are key players in this scenario [57], a concept notably supported by the increased mortality of MI in mice following transient macrophage depletion [58]. Two different subsets of monocytes originating from the bone marrow, with different, yet complementary functions, are mobilized in the heart after MI: the $CD11b^{high}/Ly6C^{high}$ subset infiltrates the heart 1–3 days after MI, exhibits phagocytic, proteolytic, and inflammatory functions, and represents 75% of the monocytes in the infarcted hearts at this stage (of note, $Ly6C^{high}$ monocytes originating from the spleen have also be detected in the MI site [59]); the $CD11b^{high}/Ly\text{-}6C^{low}$ subset colonizes the heart from day 4 to day 7 and produces less inflammatory mediators but expresses vascular-endothelial growth factor (VEGF), thus promoting angiogenesis [56].

Thus whether a paracrine effect of these cells is now evident (for review see [60]), their ability to differentiate into mature cardiomyocytes remains controversial. Indeed, the differentiation into cardiomyocytes of cells isolated from the bone marrow (BMCs) or the blood was first demonstrated [61–65] and then challenged, with the suggestion that these cells might rather fuse with the native cells instead of differentiating [64, 66, 67]. Finally, now several reports demonstrated that both processes, actual differentiation and fusion, coexist [68, 69]. This was, for example, demonstrated for human circulating $CD14^+$ monocytes infiltrating the infarcted myocardium [70] and recently for hematopoietic cells which are able to "fuse" with cardiomyocytes and/or "transdifferentiate" into cardiomyocytes. Whatever the fate of the circulating cells in the heart, numerous factors secreted by these cells have been identified, such as vascular endothelial growth factor (VEGF), insulin growth factor (IGF-1), growth hormone (GH), or hepatocyte growth factor (HGF). These factors promote angiogenesis and atherogenesis but can also stimulate endogenous CPC proliferation and differentiation [71].

3. Therapeutic Issues in Cardiac Regeneration

3.1. Cardiac Cell Therapies. The idea leading to the development of cellular therapy in damaged heart is to replace the large amount of cardiomyocytes which died after heart injuries. Thus, cellular therapies, consisting in injecting "cardiomyocyte precursor cells" from various sources into the injured hearts, have been evaluated as the first option in this novel therapeutic paradigm.

Three categories of stem cells could be used: embryonic, adult, and induced pluripotent stem cells (iPSCs). It is important to mention here that, due primarily to ethical issues, only one clinical trial performed so far has used cardiac progenitors derived from human embryonic cells (hESCs) [72]. However, the use of these cells is promising as they regenerate nonhuman primate hearts [73]. In the same way, iPSCs [74] were not yet tested in patients. Furthermore, the discussion is open concerning the use of stem cells from umbilical cord stroma [75].

Thus almost all clinical trials were performed with adult stem cells (Figure 2). The choice of the type of adult precursor cells to inject must be based on 3 main criteria. (1) They should be easily isolated from patients ("autologous cells") or from healthy donors ("allogeneic cells"). (2) They should be expandable in large number (>100 millions in the case of bone marrow cells), implying that the cells should be kept in an undifferentiated state *in vitro*, to allow high proliferative capacity. (3) They should have the ability to differentiate into mature cardiomyocytes.

Two types of cells fulfilling these criteria have been used in clinical trials: cells isolated from the bone marrow, blood, skeletal muscle, or fat, referred to as "exogenous" precursor cells, and cells isolated from the heart itself (from atrial biopsies) referred to as "endogenous" precursor cells.

3.1.1. The "Exogenous" Precursor Cells. The easiest precursor cells to isolate are obtained from the blood or the bone marrow (BMCs). Thus, a vast majority of clinical trials performed so far used BMCs, either unselected, or sorted according to some markers of undifferentiated BMCs ($CD133^+$ or $CD34^+$ enriched BMCs). Mesenchymal stem cells (MSCs), obtained by specific culture processing of the BMCs, have been frequently used as well and indeed are generally presented as the "most effective cells" which can be injected [76].

The results obtained using BMC injection (usually via an intracoronary or a percutaneous transendocardial injection) have been generally disappointing, as summarized in recent extensive reviews [76, 77]. A meta-analysis of 13 randomized trials of unsorted BMC injection in patients with acute MI concluded that BMCs did not prevent the remodeling process [78]. The REPAIR-AMI trial, which is a multicenter double-blind trial of the intracoronary injection of BMCs after acute MI, reported a 5.5% increase of left ventricular ejection fraction in post-MI patients at 6 months [79]. However, 18 months after cell injection, no significant difference in left ventricular ejection fraction was detected between cell and placebo injected patients included in the REPAIR-AMI trial. Similarly, BMC injection in patients after ST-elevation myocardial infarction (BOOST trial) led to 6% increase of the left ventricular ejection fraction 6 months after cell injection ($P = 0.003$) but only to 2.8% at 18 months ($P = 0.27$) [80]. Recently a meta-analysis using the individual data of the patients involved in 12 randomized trials concluded that intracoronary injection of bone marrow cells after MI provides no benefit for the patients [81].

However, with respect to $CD133^+$ enriched BMCs and MSCs, their administration after acute MI did result in moderate improvements of cardiac parameters when compared to control patients with in some cases a small reduction of the absolute scar size [82–84]. Furthermore, patients injected

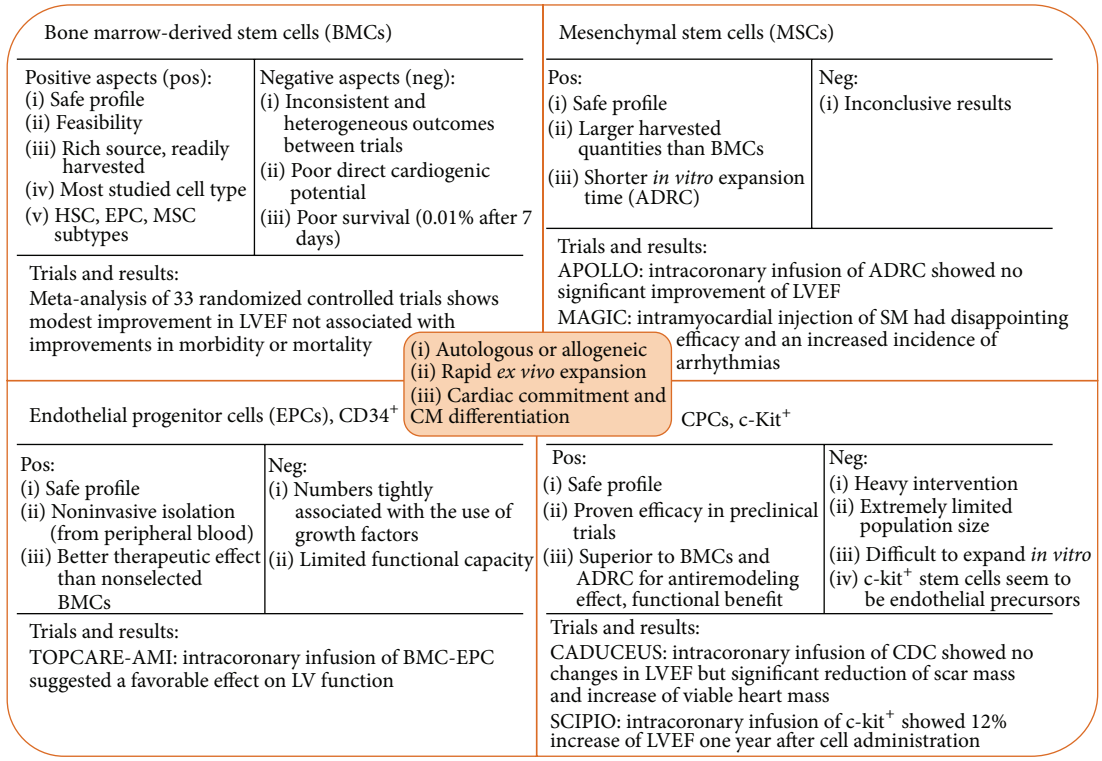

Figure 2: Current state of stem cell therapy for acute myocardial infarction in clinical trials. The optimal cell population for cardiac regenerative cell therapies requires autologous or allogeneic origin, rapid *ex vivo* expansion, and cardiac commitment including differentiation to cardiomyocytes. Numerous clinical trials have been undertaken with moderate results (for reviews see [8, 77, 172–174]). ADRC: adipose-derived stem cells; BMC: bone marrow cells; CDC: cardiosphere-derived cells; CM: cardiomyocytes; EPC: endothelial progenitor cells; HSC: hematopoietic stem cells; LVEF: left ventricular ejection fraction; MSC: mesenchymal stem cells; SC: stem cells.

with a larger percentage of $CD31^+$ cells among their BMCs, demonstrated a greater reduction of infarct size than patients injected with smaller percentage of $CD31^+$ [85]. This clearly demonstrates that the nature of the cells which are injected is crucial for the outcome of the therapy.

Cells other than BMCs have been used in some clinical trials. In the MAGIC trial, patients undergoing coronary bypass surgery for previous MI and severe left ventricular dysfunction were injected with skeletal myoblasts (cultured from a muscle biopsy) within the myocardial scar. Myoblast transfer did not improve LV function in comparison to control patients and was associated with early postoperative arrhythmias [86]. Finally, two recent clinical studies used adipose tissue-derived regenerative cells (ADRCs, isolated from liposuction aspirates), administered to patients with acute MI [87] or severe chronic ischemic cardiomyopathy [88]. Results of these studies are encouraging, as ADRCs were associated with a 50% reduction of myocardial scar formation post-MI and a preserved ventricular function in patients with ischemic cardiomyopathy. Additional studies are needed to confirm these preliminary results.

3.1.2. The "Endogenous" Precursor Cells. Precursor cells do exist within the heart, but their identification has been made difficult by the lack of a highly specific marker. Cells expressing the c-kit have been isolated from the heart, induced to proliferate *in vitro* and reinjected into patients as cardiac precursor cells from "autologous cardiac origin." The first clinical trials with autologous CPCs used $c\text{-}kit^+$ cells obtained from atrial biopsies (SCIPIO study) or from cardiospheres (self-assembling multicellular clusters containing various progenitor cells) obtained from right ventricular tissue (CADUCEUS study). The cells have been injected into the coronary circulation of a small number of patients with ischemic cardiomyopathy or acute MI [89, 90]. These trials first indicated the safety of the CPCs administration procedure. Initial results, obtained 6 months after injection, reported a reduction in the myocardial scar mass, although an improvement in cardiac function was only reported in the SCIPIO trial (but concerns regarding scientific integrity of the latter study have been recently raised [91]). At 1-year follow-up, the CADUCEUS study confirmed the early findings, showing decreased scar size, increased viable myocardium, and improved regional function of the infarcted myocardium [92].

3.1.3. Autologous or Allogeneic Cells? The use of "autologous" injected cells (i.e., cells isolated from the patient itself and reinjected) was first recommended to avoid the immunological problems of rejection. However, their use is limited by the

fact that they are not immediately available in high number and that their isolation could be difficult in critically affected patients. Furthermore, their immunogenicity is higher than expected. Indeed, their isolation and reinjection, their long-term culture in several culture media (for the mesenchymal stem cells isolated from the bone marrow, see review [93]), and their genetic modification or their epigenetic reprogramming (for the iPSCs see [94, 95]) can increase the expression on their cell surfaces of the major histocompatibility complex (MHC in animals or HLA in humans) classes I or II antigens. These "autologous" cells could be thus rejected after their reinjection and this could explain why in human hearts the long-term survival of injected BMCs is very low: only 2–5% of the injected autologous BMCs are still present in the heart a few hours after administration [96], and among these surviving cells, only a few actually become correctly integrated cardiomyocytes. Thus, the amount of injected cells which will eventually integrate into the tissue is not sufficient to improve cardiac function. These results highlight the "paracrine" activity of the injected cells which clearly stimulates the "endogenous" cardiac cells, promotes their proliferation and differentiation, or stimulates other repair mechanisms, such as angiogenesis [97, 98].

Thus, if the injected cells can survive long enough to secrete factors able to stimulate the "endogenous" capacity of the heart to regenerate, allogeneic cell therapy can also be considered as a valid option to induce cardiac regeneration. Therefore, injection of allogeneic MSCs in infarcted rat hearts [99, 100], dog hearts [101], or pig hearts [102] is safe and improves heart function as well as injection of "autologous" MSCs. Interestingly, human cardioblasts originating from the differentiation of allogeneic MSCs were transplanted into a patient developing a cardiomyopathy and demonstrated positive therapeutical effect for more than 2 years [103]. This is also true for cardiosphere-derived cells (CDCs). Indeed, the efficiency of "allogeneic" CDC injection in patients after myocardial infarction is being evaluated in the ALLSTAR trial and will be compared to this obtained by injection of "autologous" CDCs (evaluated in the CADUCEUS trial [90, 104]). Preclinical results obtained in rats and pigs suggested that injection of allogeneic CDCs was safe, induced no immunological reaction, and acted via the same mechanisms than the autologous CDC injection [105].

The injection of allogeneic cells presents several advantages: these cells could be isolated from "healthy" donors, stocked in "biobanks" in large number, thus immediately available in high numbers for patients. However, the immunogenicity of these cells remains a major hurdle to their use in regenerative medicine. Indeed, if the human precursor cells (especially the MSCs) and the human embryonic stem cells express constitutively the HLA proteins at low levels, when stimulated with interferon gamma or fibroblast growth factor 2 (FGF-2), both cell types increased HLA protein expressions, which render these cells able to be rejected rapidly on transplantation [106–110]. That is why currently many researches are aimed at understanding how blunting host immune responses to injected cells. This concerns the development of strategies limiting, for example, the host immune response (by immunosuppressive drugs, by tolerogenic cell therapies, or also by injection of monoclonal antibodies neutralizing the host immune cells). The immunogenicity of the injected cells can also be modified by modulating the site of injection or the way of cell delivering (some biomaterials can escape from host immune reactivity) (for review see [111, 112]).

3.1.4. Important Conclusions Drawn from Cellular Therapies. To sum up, clinical trials evaluating cellular therapies based on "cardiomyocyte precursor cells" from various sources have not been as successful as expected to repair the injured heart. As a matter of fact, all stem cells used in cell therapies, such as BMCs, mesenchymal or adipose tissue-derived stem cells, display important cytokine secretion. This "paracrine" activity of the injected cells seems to be responsible for the positive effects observed in injured hearts after cell injections. Indeed, secreted factors stimulate the "endogenous" cardiac cells and thus promote their proliferation, differentiation, or other repair mechanisms, such as angiogenesis [97, 98]. Thus, the differentiation of the injected cells into functional cardiomyocytes integrated to the injured hearts seems to contribute only minimally to heart regeneration.

Improving the yield of incorporation/differentiation of injected cells and stimulating growth of endogenous cardiac cells to promote heart regeneration open the way to a new therapeutic paradigm based on a pharmacological standpoint. The fact that spontaneous differentiation (although at very low rate) of endogenous CPCs occurs during life demonstrates that these cells are functional but need to be stimulated [6, 7]. Future regenerative therapies should therefore capitalize on this feature and propose novel pharmacological strategies to stimulate the proliferation and differentiation of endogenous precursor cells.

3.2. Pharmacological Therapies to Promote Cell Regeneration

3.2.1. The Complex Micorenvironment of Niches Containing CPCs. CPCs have been shown to be more abundant in the atria, in the heart's apex, and in the epicardium [113, 114], where they are located within specialized microdomains termed niches. The niches also contain differentiated cells, such as cardiomyocytes, fibroblasts, or telocytes, which control the activation state of the CPCs via physical interactions (through cell surface receptor and adhesion molecules such as Notch-1 and integrins) or via chemical, paracrine activity (such as the secretion of cytokines and growth factors) [115].

Whereas at the resting state, CPCs in the niches are kept undifferentiated and quiescent, they become activated to proliferate and differentiate into vascular cells or cardiomyocytes following myocardial injury, especially myocardial infarction. In such conditions, the hypoxic microenvironment, as well as molecules released by dying cardiomyocytes, for example, HMGB-1, plays key roles in the activation of CPCs [39, 116, 117]. Furthermore, growing evidence also indicates that infiltrating inflammatory cells recruited within the infarcted hearts promote CPC activation within the niches by releasing

a wealth of factors, including growth factors (e.g., FGF-2, VEGF), prostaglandins, and cytokines (e.g., IL-10) [49, 51, 71, 76, 118] (see also Section 2.3).

3.2.2. Paracrine Activation of CPCs after Myocardial Infarction: A Role for the Brain Natriuretic Peptide? Thus, it appears evident for us that the identification of a factor able to increase the proliferation and differentiation of the "endogenous" cardiac precursor cells could be a key point in the development of cellular therapies aimed to regenerate injured hearts. That is why we are interested in the brain natriuretic peptide (BNP).

BNP is a cardiac hormone which belongs to the natriuretic peptide family, the other members of which include the atrial natriuretic peptide (ANP) secreted by the cardiac atria and the C-type related natriuretic peptide (CNP) secreted by the brain, bone, and vascular endothelial cells. BNP was first discovered in the bovine brain but it is now well established that the main source of BNP in the body is the heart, especially the ventricles [119]. BNP binds to two distinct guanylyl cyclase receptors, denoted NPR-A and NPR-B, promoting the intracellular generation of cyclic GMP (cGMP) [120]. The accumulation of cGMP in the cytoplasm activates protein kinase G (PKG) and the phosphodiesterases 2, 3, and 5 to elicit downstream signaling [120].

3.2.3. BNP Biosynthesis and Secretion. BNP is a polypeptide of 32 amino acids (32 aa) in humans and pigs and 45 aa in mice and rats. It is processed from a preprohormone of 132-aa, posttranslationally modified into a 108-aa prohormone termed proBNP. The latter is enzymatically cleaved by two convertases, namely, corin and/or furin, resulting in an inactive 76-residue amino-terminal fragment (NT-proBNP) and an active 32-aa C-terminal fragment (BNP). Plasma BNP and NT-proBNP can be detected in healthy people, as well as uncleaved proBNP and O-glycosylated proBNP, which are both biologically inactive [121]. Plasma BNP levels increase in patients with various forms of heart failure and are therefore used as a helpful clinical biomarker for the diagnosis and follow-up of cardiac dysfunction [122]. It is here important to mention that recent studies indicated that plasma BNP measured during chronic heart failure rather consists of the biologically inactive forms proBNP and O-glycosylated proBNP [121, 123, 124]. These results have raised the interesting question that heart failure might be in fact associated with a deficit of biologically active BNP [124].

BNP is primarily secreted by ventricular cardiomyocytes upon excessive stretch, increased transmural pressure, or direct injury (see also Figure 3(b) in neonatal hearts). Cardiac fibroblasts and endothelial cells can also secrete BNP, and, following MI, infiltrating immune cells (including neutrophils, T cells, and macrophages) may represent an additional source of BNP [125]. Interestingly, immature cells such as embryonic stem cells or also satellite cells are also able to secrete BNP [126, 127].

3.2.4. Role of BNP in the Heart. Whereas the effects of BNP on the regulation of natriuresis, diuresis, and vascular tone are well documented, there remains an important gap of knowledge regarding the proper actions of BNP on the heart itself [119, 128]. In the adult, the rapid release of BNP by the heart might represent an important compensatory protective mechanism in various cardiac pathologies. In support of this assumption, it has been reported that treatment with exogenous BNP facilitated the recovery of cardiac function and improved preservation of cardiac tissue in animal models of MI. Possible mechanisms included the inhibition of cardiomyocyte apoptosis, as well as reduction of hypertrophy and fibrosis [129–134]. BNP may also modulate the immune response to cardiac injury and thereby serve to avert excessive or deregulated inflammation in this setting. Several studies performed *in vitro* indicated that BNP can inhibit monocyte chemotaxis [135], deplete the number of monocytes, B lymphocytes, and NK cells in cultured human peripheral blood mononuclear cells [136], and regulate the production of a wealth of inflammatory molecules by human macrophages [137, 138]. *In vivo*, a study using transgenic mice overexpressing BNP reported increased cardiac neutrophil infiltration and MMP-9 expression after MI in transgenic animals, pointing to a key role of BNP in the processes of matrix remodeling and wound healing in this setting [138].

Several studies also pointed out a role of BNP in cardiac embryogenesis. High levels of BNP are measured during midgestation in embryonic hearts, and peaks of BNP secretion correlate with several important steps of cardiac development [139, 140]. In addition, recent findings have indicated that cardiomyocyte proliferation can be modulated during development by ANP or BNP [141]. Furthermore, it is noticeable that plasma BNP in humans is high at birth, progressively declining thereafter, to stabilize at around ten years of age to the levels found in adults [142, 143]. Taken together, these observations suggest that BNP may play important functions as a regulator of cardiomyocyte differentiation and proliferation in the developing embryo. In line with this hypothesis, it has been reported that embryonic stem cells express high levels of BNP which are essential for their proliferation and differentiation [126].

These results raise the possibility that BNP might also be involved in the process of cellular regeneration in the adult. A role of BNP was indeed reported by Kuhn et al. in the process of angiogenesis following skeletal muscle ischemia [127]. In this study, secretion of BNP by vascular satellite cells was found to activate, in a paracrine manner, the regeneration of the adjacent endothelium. So, what about cardiac regeneration?

3.2.5. Role of BNP in Cardiac Regeneration. We addressed the role of BNP in cardiac regeneration in our laboratory by performing a series of experiments evaluating the relationships between CPCs and BNP both *in vitro* and *in vivo*. The first clue for an involvement of BNP in CPC proliferation and differentiation comes from our data indicating the age-dependence of BNP expression in the heart. As shown in Figure 3(a) and already published [117], more cardiac cells stained positive for BNP in mouse neonatal compared to adult hearts: in the neonatal hearts $65 \pm 4\%$ of the cardiac cells were positive for the BNP's staining compared to the adult hearts ($41 \pm 1\%$ of the cells) (Figure 3(a)). BNP staining is

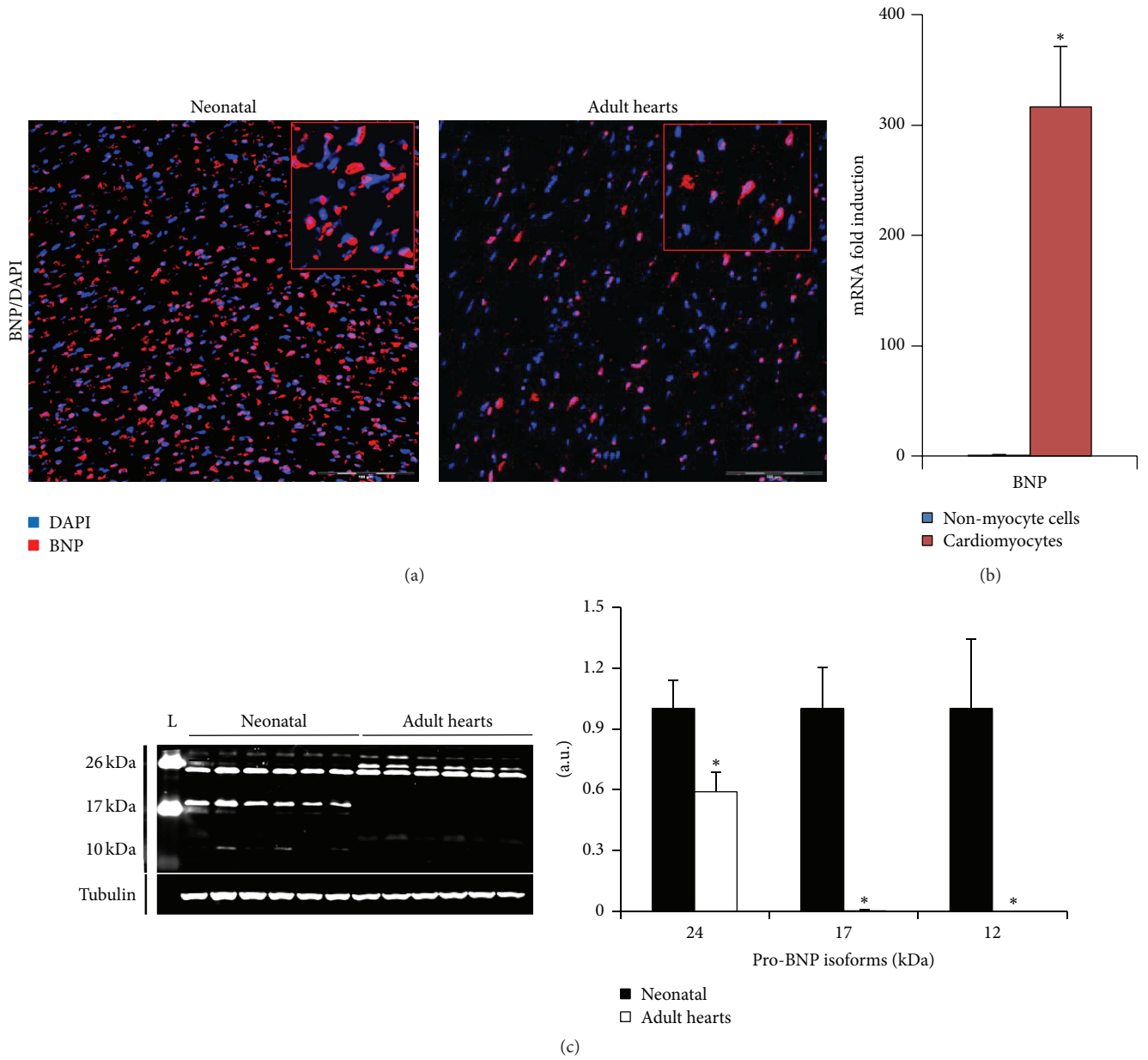

FIGURE 3: Heart expression of BNP is age-dependent and cell specific. (a) Representative microscopy pictures of neonatal and adult hearts stained for BNP (in red) and DAPI (nuclei in blue). High magnification of positive cells in top right inserts. The scale bars represent 100 μm. (b) mRNA expression of BNP using quantitative PCR, in non-myocyte cells (NMCs) (blue) and cardiomyocytes (red). Results expressed as fold-increase above the levels in NMCs. $n = 7$ cardiomyocyte samples compared to 9 NMC samples. Data are means ± SEM, $^*P < 0.05$. (c) Determination of BNP protein levels in neonatal and adult hearts by western blot analysis. BNP protein expression with representative western blot and quantification relative to tubulin, expressed as fold changes relative to the average level of neonatal hearts. Data are means ± SEM, $^*P < 0.05$. a.u.: arbitrary unit.

localized around the nucleus in neonatal and adult cardiac cells (inserts Figure 3(a)). By western blot analysis, several isoforms were detected as our antibody is able to recognize all proBNP isoforms as well as the active form of the BNP (C-terminal peptide). The high molecular weight forms (24 and 17 kDa) correspond to the glycosylated proBNP isoform (Figure 3(c)) as previously described [144, 145], whereas the proBNP (12-13 kDa) was only detected in the neonatal hearts. According to previous reports, the active BNP form (10 kDa) is not detectable in neonatal or adult hearts by western blot analysis [121, 144]. All proBNP isoforms were more abundant in neonatal than in adult hearts (see quantification in Figure 3(c)).

In the neonatal hearts, BNP mRNA is 300-fold more abundant in the cardiomyocytes than in the non-myocyte cells (NMCs), suggesting that the mean source of BNP in the neonatal hearts is the cardiomyocytes (Figure 3(b)). This is also true in the adult hearts: BNP mRNA expressed by the

NMCs represented less than 0.05% of the mRNA coding for BNP detected in the adult hearts (data not shown).

Further indications for a role of BNP in cardiac growth and/or regeneration come from our finding that CPCs identified *in vivo* in neonatal and adult hearts express the BNP receptors, NPR-A, and/or NPR-B [117]. Although BNP can share these receptors with other members of the natriuretic peptide family (NPR-A can also bind the atrial natriuretic peptide and NPR-B the C-type related natriuretic peptide) [120], these data strongly support that CPCs are able to respond to BNP. We then found that treatment with exogenous BNP increased the number of newly formed cardiomyocytes and of proliferating CPCs in neonatal and adult unmanipulated mice. Our next finding was that BNP injection in mice exposed to MI resulted in an increased number of CPCs and of cardiomyocytes expressing Nkx2.5, and this was associated with reduced cardiac remodeling and improved contractile function after MI [117]. Overall, our findings provided strong evidence in support of a crucial role for BNP in controlling proliferation and differentiation of CPCs after birth, therefore suggesting that the administration of BNP might be a useful therapeutic approach to promoting regeneration of the infarcted heart [117].

Furthermore, we observed also that CPCs (identified as being small laminin positive cells expressing Nkx2.5 ($Nkx2.5^+$ cells) or $Sca\text{-}1^+/Nkx2.5^+$ cells or $c\text{-}kit^+/Nkx2.5^+$ cells) stained also positive for BNP, suggesting that CPCs are also able to synthesize BNP (Figure 4). CPCs could thus secrete BNP in an autocrine manner to control their proliferation and differentiation into cardiomyocytes.

3.2.6. Mechanisms of BNP Actions in the Heart: Studies in NPR-A KO and NPR-B Deficient Mice. The demonstration that BNP has potent effects on CPCs prompted us to search for the cellular BNP receptor implicated in such actions. It is known that BNP can bind to two receptors, namely, NPR-A and NPR-B, and we therefore undertook a series of experiments using mice deficient for one or the other of these receptors [120]. We first noticed that the percentage of NPR-A KO mice at birth was lower than expected from the Mendelian frequency (19% instead of 25%), suggesting that NPR-A KO embryos die during embryogenesis, as already reported by others [146]. Furthermore, a high rate of mortality occurs in NPR-A KO pups between day 1 and day 10 (at day 10, only 8% of the surviving pups are NPR-A KO mice, instead of the expected 25%, Figure 5). In contrast, NPR-B-deficient pups are born at the expected Mendelian frequency but die within 3 days after birth (Figure 5). These observations implicate BNP receptors in biological processes critical to survival during embryogenesis and early after natal life. This assumption would be consistent with previously reported roles of BNP and BNP receptors in embryonic stem (ES) cells, as reported by Abdelalim and Tooyama [126, 147]. These authors proposed that NPR-A contributed to the self-renewal and maintenance of pluripotency of ES cells, whereas NPR-B was instead involved in their proliferation [126, 147].

Cardiac defects could be the cause of the premature death of NPR-A KO pups. Indeed, at 15.5 days of gestation, NPR-A KO embryos display a cardiomegaly without fibrosis, as well as dysregulated expression of the Cx43 protein, which could affect cardiac contractility [146]. At adulthood, NPR-A KO mice develop salt-resistant hypertension together with cardiac hypertrophy, which is out of proportion with respect to the increase in blood pressure, implying direct antihypertrophic actions of NPR-A in the heart [146, 148–150]. Concerning the NPR-B system, previous reports indicated impaired endochondral ossification, gastrointestinal tract disorders, and defects of the reproductive organs in NPR-B-deficient mice [151–155], but there is no result on their cardiac phenotype. Some information has been obtained by the use of transgenic rats expressing a dominant-negative mutant of NPR-B, which display a progressive, blood pressure-independent cardiac hypertrophy, which is further enhanced following the induction of congestive heart failure by volume overload [156]. Therefore, these results support that NPR-B is also involved in the control of cardiac growth.

In our own studies, we recently demonstrated that both receptors control the fate of the cardiac precursor cells *in vitro* [117]. First, we demonstrated that CPCs exist in neonatal hearts of NPR-A KO and NPR-B-deficient mice. Secondly, we showed that BNP stimulates CPC proliferation *in vitro* via its binding to NPR-A (Figure 6). Thirdly, we established that BNP stimulates CPC differentiation into cardiomyocytes via binding to NPR-B in cell culture. Whether a defect in the proliferation and/or differentiation of CPCs contributes to cardiac defects and premature death in NPR-A KO and NPR-B-deficient mice remains now to be explored.

3.2.7. The Use of BNP in the Clinic. The first clinical trials with recombinant human BNP (Nesiritide) in patients with acute heart failure reported positive hemodynamic and clinical effects, leading to the common use of this drug in the therapeutic arsenal of both acute and chronic heart failure. Later studies, however, raised several safety concerns about Nesiritide, the drug being possibly associated with greater risk of renal failure and higher mortality, which resulted in significant reduction in its clinical use [157, 158]. Nevertheless, more recent clinical studies reported that low doses of Nesiritide, in particular when administered via subcutaneous route, induced hemodynamic and clinical improvements without increasing nephrotoxicity or the rate of death, thus reopening the debate about the usefulness of BNP therapy in patients with heart failure [157, 159–162]. In addition, a recent meta-analysis on the use of natriuretic peptides (ANP/BNP) in patients with acute MI suggested that this treatment might protect left ventricular function [163] and a large-scale randomized clinical trial (BELIEVE II) has been recently initiated to evaluate such cardioprotective effects of low dose BNP during AMI [164].

Finally, it is particularly noteworthy that an inhibitor of neprilysin has been very recently shown to promote significant benefits in patients with chronic heart failure,

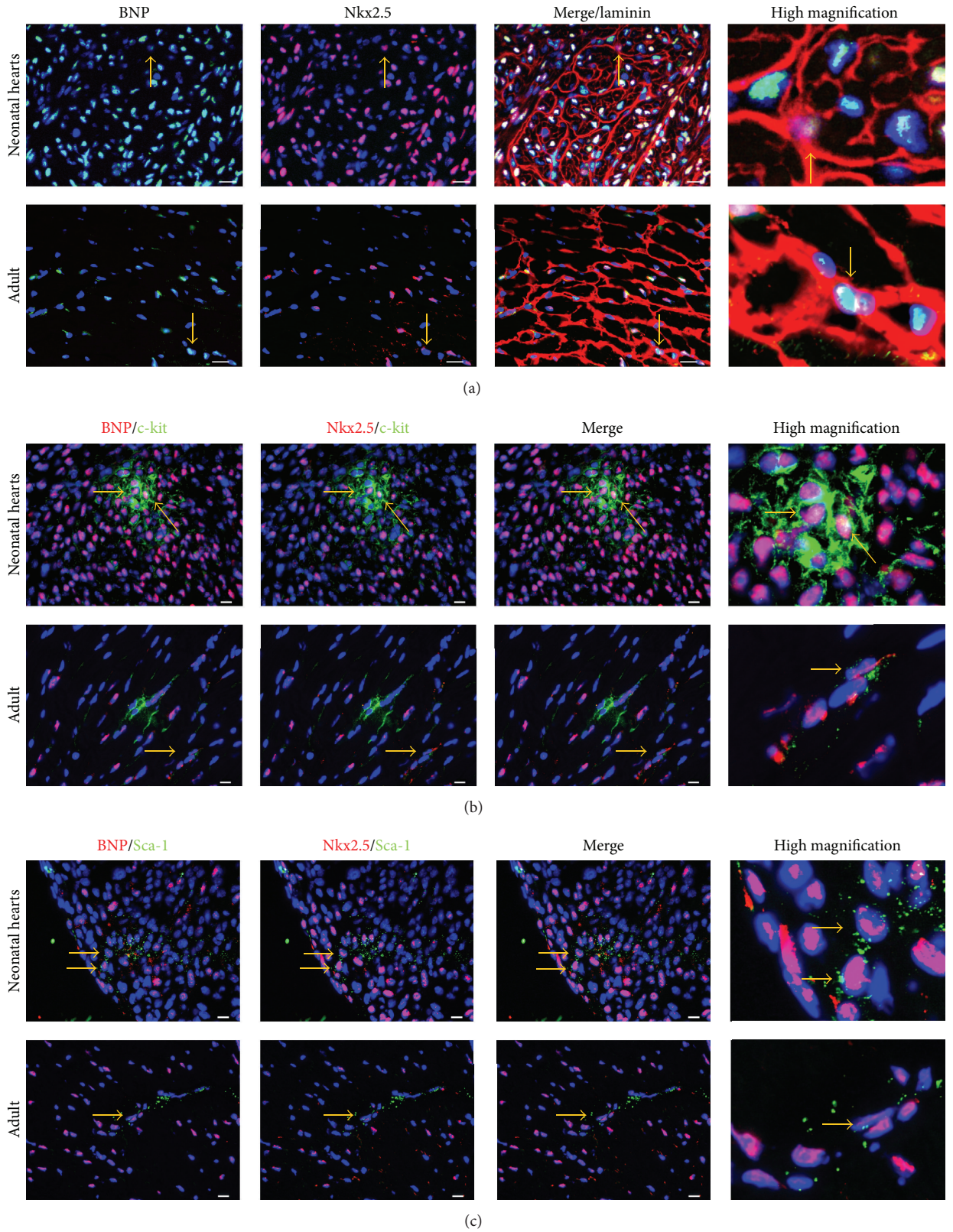

Figure 4: Cardiac precursor cells express BNP in neonatal and adult murine hearts. Cardiac precursor cells were defined as small Nkx2.5$^+$ cells or c-kit$^+$/Nkx2.5$^+$ cells or Sca-1$^+$/Nkx2.5$^+$ cells. Photomicrographs of neonatal or adult heart sections stained for BNP and DAPI (Nuclei) associated with staining for either Nkx2.5 and laminin (a), Nkx2.5 and c-kit (b), or Nkx2.5 and Sca-1 (c). Scale bars represent 80 μm for the pictures in (a) and 10 μm for the pictures in (b) and (c). Yellow arrows depict cells which are considered as being CPCs expressing BNP.

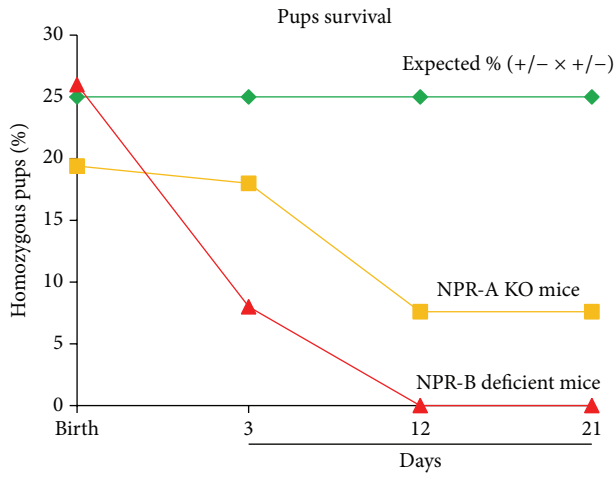

Figure 5: Survival curves of NPR-A KO and NPR-B deficient pups. The results are represented as percentages of the total number of pups (n = 66 for NPR-A KO and 96 for NPR-B deficient mice) obtained in heterozygous breeding (+/− × +/−) and compared to the expected percentages (25%).

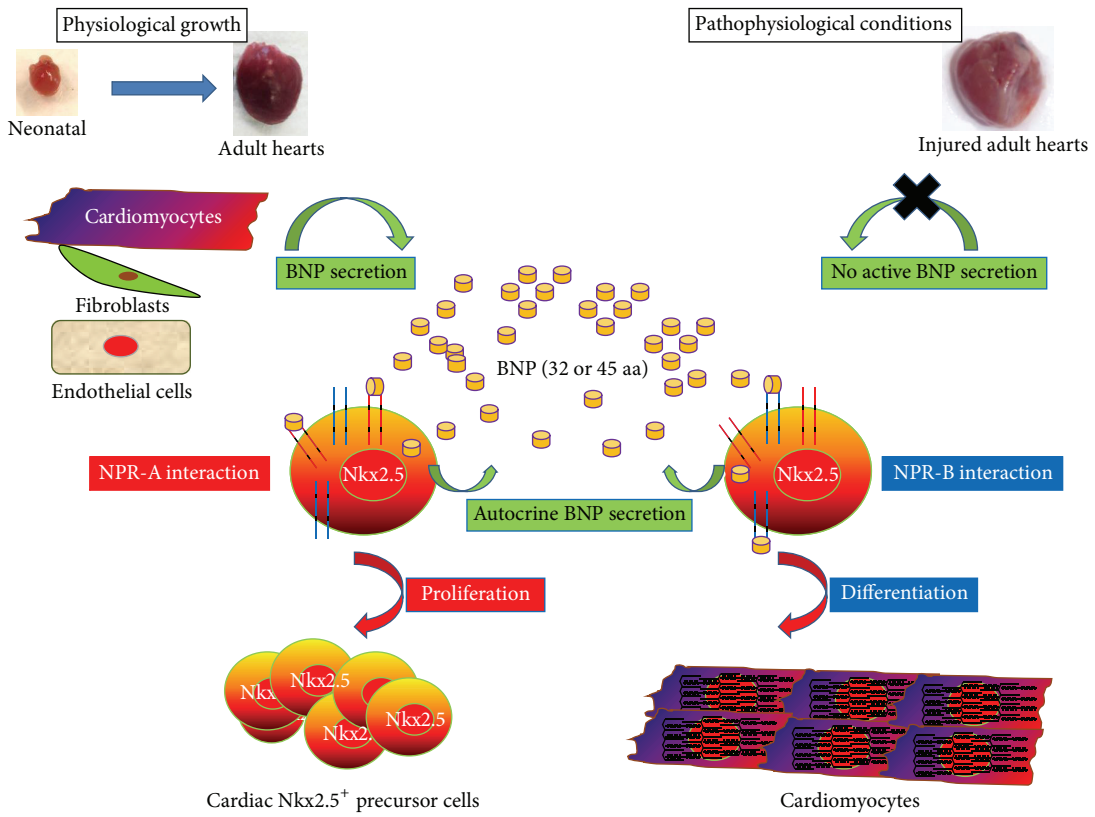

Figure 6: BNP modulation of cardiac precursor cell (CPC) proliferation and differentiation. BNP is secreted during physiological growth by cardiomyocytes, fibroblasts, and endothelial cells. CPCs can also secrete BNP. BNP stimulates via NPR-A CPC proliferation and via NPR-B CPC differentiation into cardiomyocytes. In pathophysiological conditions, it seems that the secreted BNP is devoid of biological activity, suggesting that BNP can be injected to stimulate the CPC proliferation and differentiation. This representation is based on the results previously published [117].

when compared to angiotensin-converting enzyme inhibition (PARADIGM-HF trial) [165, 166]. Neprilysin (NEP) is an endopeptidase able to degrade several factors such as the natriuretic peptides (ANP, CNP, and BNP), but also angiotensin II, bradykinin, or endothelin-1. In the heart, NEP is expressed on the membrane of endothelial cells, vascular smooth muscle cells, fibroblasts, and cardiomyocytes and treatments of rats or rabbits with NEP inhibitors increase the blood level of BNP [167, 168]. However, NEP treatment in animal and humans has also shown to increase the blood level of angiotensin II. That is why NEP inhibitors are used with inhibitors of angiotensin-converting enzyme (ACE) such as the omapatrilat or with blocker of the angiotensin receptor, such as the LCZ696. Omapatrilat has been shown in infarcted mice to increase cardiac function and to decrease the fibrosis and the cardiomyocyte hypertrophy when compared to untreated infarcted mice [169]. However, in humans, omapatrilat was associated with development of angioedema and was not approved by the Food and Drug Administration. Thus great hope focuses now on LCZ696. In infarcted rats, LCZ696 treatment decreases the myocardial fibrosis and the cardiomyocyte hypertrophy and thus increases the ejection fraction of the treated rats compared to untreated one [170].

In patients, the mechanisms of LCZ696 leading to reduced death and rehospitalization are not yet elucidated [171]. However, increasing BNP signaling appears therefore as a meaningful and helpful strategy in patients with myocardial infarction and/or heart failure. Although it is likely that systemic vasodilation and natriuresis are key mechanisms underlying the beneficial effects of natriuretic peptides in the aforementioned studies, the positive effects of BNP on cardiac regenerative processes, as highlighted in our recent work, could also play an important role, an issue which should be critically addressed in ongoing clinical and experimental studies.

4. Conclusion-Future Perspectives

Therapy of cardiovascular diseases represents a major public health challenge. Primary prevention, including lifestyle modification and treatment of traditional cardiovascular risk factors, together with secondary and tertiary prevention by multidrug treatment, has been the mainstay of such therapy for decades. In recent years, novel approaches based upon the regeneration of the injured heart have been developed, holding the promise not only to relieve, but also to directly repair the damaged heart. The observation that stem cells isolated from different organs retain the ability to differentiate into mature adult beating cardiomyocytes promoted strong impetus to launch a series of clinical trials evaluating the therapeutic potential of cellular regenerative therapies in cardiac diseases. Lessons learned from these studies indicated that although such approaches appeared generally safe, their efficacy remained globally limited. Factors such as the nature of the injected cells, their number, and the route and timing of their administration emerged as critical issues which will need to be addressed in future studies to improve such efficacy. Furthermore, it has become obvious that cardiac regeneration involves complex interplays between different cell subsets of both cardiac and extracardiac (blood or bone marrow) origin, which cannot be mimicked by the one and only administration of cardiac precursor cells. A potential strategy to circumvent, at least partly, the limitations of cellular regenerative therapies could rely on the stimulation of the heart's natural ability to induce its own regeneration by pharmacological approaches. Indeed, pharmacological compounds could target not only the cellular precursors but also other cells involved in the regenerative and healing process, for instance, the fibroblasts, the endothelial cells, and the infiltrating cells, such as the different monocyte subsets. Treatment with exogenous brain natriuretic peptide is an example of such strategy, as demonstrated experimentally by its ability to induce "endogenous" cardiac regeneration. Future studies should endeavor to discover novel molecules able to stimulate such genuine capacity of the heart to regenerate, which would represent an indisputable breakthrough in the fight against cardiovascular diseases.

Conflict of Interests

No author has any conflict of interests to disclose with respect to this paper.

Acknowledgments

This work is supported by a grant from the Swiss National Science Foundation (PMPDB-310030_132491) and by the Swiss Cardiology Foundation.

References

[1] R. Kelishadi and P. Poursafa, "A review on the genetic, environmental, and lifestyle aspects of the early-life origins of cardiovascular disease," *Current Problems in Pediatric and Adolescent Health Care*, vol. 44, no. 3, pp. 54–72, 2014.

[2] N. D. Wong, "Epidemiological studies of CHD and the evolution of preventive cardiology," *Nature Reviews Cardiology*, vol. 11, no. 5, pp. 276–289, 2014.

[3] J. J. V. McMurray, S. Adamopoulos, S. D. Anker et al., "ESC Guidelines for the diagnosis and treatment of acute and chronic heart failure 2012: the Task Force for the Diagnosis and Treatment of Acute and Chronic Heart Failure 2012 of the European Society of Cardiology. Developed in collaboration with the Heart Failure Association (HFA) of the ESC," *European heart journal*, vol. 33, no. 14, pp. 1787–1847, 2012.

[4] S. Ausoni and S. Sartore, "From fish to amphibians to mammals: in search of novel strategies to optimize cardiac regeneration," *Journal of Cell Biology*, vol. 184, no. 3, pp. 357–364, 2009.

[5] S. Ausoni and S. Sartore, "The cardiovascular unit as a dynamic player in disease and regeneration," *Trends in Molecular Medicine*, vol. 15, no. 12, pp. 543–552, 2009.

[6] O. Bergmann, R. D. Bhardwaj, S. Bernard et al., "Evidence for cardiomyocyte renewal in humans," *Science*, vol. 324, no. 5923, pp. 98–102, 2009.

[7] J. Kajstura, N. Gurusamy, B. Ogórek et al., "Myocyte turnover in the aging human heart," *Circulation Research*, vol. 107, no. 11, pp. 1374–1386, 2010.

[8] P. C. H. Hsieh, V. F. M. Segers, M. E. Davis et al., "Evidence from a genetic fate-mapping study that stem cells refresh adult mammalian cardiomyocytes after injury," *Nature Medicine*, vol. 13, no. 8, pp. 970–974, 2007.

[9] A. Leri, M. Rota, F. S. Pasqualini, P. Goichberg, and P. Anversa, "Origin of cardiomyocytes in the adult heart," *Circulation Research*, vol. 116, no. 1, pp. 150–166, 2015.

[10] M. A. Laflamme and C. E. Murry, "Heart regeneration," *Nature*, vol. 473, no. 7347, pp. 326–335, 2011.

[11] E. R. Porrello, A. I. Mahmoud, E. Simpson et al., "Transient regenerative potential of the neonatal mouse heart," *Science*, vol. 331, no. 6020, pp. 1078–1080, 2011.

[12] S. E. Senyo, M. L. Steinhauser, C. L. Pizzimenti et al., "Mammalian heart renewal by pre-existing cardiomyocytes," *Nature*, vol. 493, no. 7432, pp. 433–436, 2013.

[13] S. R. Ali, S. Hippenmeyer, L. V. Saadat, L. Luo, I. L. Weissman, and R. Ardehali, "Existing cardiomyocytes generate cardiomyocytes at a low rate after birth in mice," *Proceedings of the National Academy of Sciences of the United States of America*, vol. 111, no. 24, pp. 8850–8855, 2014.

[14] C. Jopling, E. Sleep, M. Raya, M. Martí, A. Raya, and J. C. Izpisua Belmonte, "Zebrafish heart regeneration occurs by cardiomyocyte dedifferentiation and proliferation," *Nature*, vol. 464, no. 7288, pp. 606–609, 2010.

[15] Y. Zhang, T.-S. Li, S.-T. Lee et al., "Dedifferentiation and proliferation of mammalian cardiomyocytes," *PLoS ONE*, vol. 5, no. 9, Article ID e12559, 2010.

[16] G. D. Dispersyn, L. Mesotten, B. Meuris et al., "Dissociation of cardiomyocyte apoptosis and dedifferentiation in infarct border zones," *European Heart Journal*, vol. 23, no. 11, pp. 849–857, 2002.

[17] R. B. Driesen, F. K. Verheyen, W. Debie et al., "Re-expression of alpha skeletal actin as a marker for dedifferentiation in cardiac pathologies," *Journal of Cellular and Molecular Medicine*, vol. 13, no. 5, pp. 896–908, 2009.

[18] T. Kubin, J. Pöling, S. Kostin et al., "Oncostatin M is a major mediator of cardiomyocyte dedifferentiation and remodeling," *Cell Stem Cell*, vol. 9, no. 5, pp. 420–432, 2011.

[19] C. Rücker-Martin, F. Pecker, D. Godreau, and S. N. Hatem, "Dedifferentiation of atrial myocytes during atrial fibrillation: role of fibroblast proliferation in vitro," *Cardiovascular Research*, vol. 55, no. 1, pp. 38–52, 2002.

[20] J. Pöling, P. Gajawada, H. Lörchner et al., "The Janus face of OSM-mediated cardiomyocyte dedifferentiation during cardiac repair and disease," *Cell Cycle*, vol. 11, no. 3, pp. 439–445, 2012.

[21] K. Bersell, S. Arab, B. Haring, and B. Kühn, "Neuregulin1/ErbB4 signaling induces cardiomyocyte proliferation and repair of heart injury," *Cell*, vol. 138, no. 2, pp. 257–270, 2009.

[22] T. Braun and S. Dimmeler, "Breaking the silence: stimulating proliferation of adult cardiomyocytes," *Developmental Cell*, vol. 17, no. 2, pp. 151–153, 2009.

[23] G. D'Uva, A. Aharonov, M. Lauriola et al., "ERBB2 triggers mammalian heart regeneration by promoting cardiomyocyte dedifferentiation and proliferation," *Nature Cell Biology*, vol. 17, no. 5, pp. 627–638, 2015.

[24] C. E. Rupert and K. L. Coulombe, "The roles of neuregulin-1 in cardiac development, homeostasis, and disease," *Biomarker Insights*, vol. 10, pp. 1–9, 2015.

[25] B. Kühn, F. del Monte, R. J. Hajjar et al., "Periostin induces proliferation of differentiated cardiomyocytes and promotes cardiac repair," *Nature Medicine*, vol. 13, no. 8, pp. 962–969, 2007.

[26] F. R. Formiga, B. Pelacho, E. Garbayo et al., "Controlled delivery of fibroblast growth factor-1 and neuregulin-1 from biodegradable microparticles promotes cardiac repair in a rat myocardial infarction model through activation of endogenous regeneration," *Journal of Controlled Release*, vol. 173, no. 1, pp. 132–139, 2014.

[27] T. Novoyatleva, A. Sajjad, D. Pogoryelov, C. Patra, R. T. Schermuly, and F. B. Engel, "FGF1-mediated cardiomyocyte cell cycle reentry depends on the interaction of FGFR-1 and Fn14," *FASEB Journal*, vol. 28, no. 6, pp. 2492–2503, 2014.

[28] C. J. Hou, Y. M. Qi, D. Z. Zhang et al., "The proliferative and migratory effects of physical injury and stromal cell-derived factor-1α on rat cardiomyocytes and fibroblasts," *European Review for Medical and Pharmacological Sciences*, vol. 19, no. 7, pp. 1252–1257, 2015.

[29] A. Eulalio, M. Mano, M. Dal Ferro et al., "Functional screening identifies miRNAs inducing cardiac regeneration," *Nature*, vol. 492, no. 7429, pp. 376–381, 2012.

[30] W. Kimura, F. Xiao, D. C. Canseco et al., "Hypoxia fate mapping identifies cycling cardiomyocytes in the adult heart," *Nature*, vol. 523, no. 7559, pp. 226–230, 2015.

[31] B. N. Puente, W. Kimura, S. A. Muralidhar et al., "The oxygen-rich postnatal environment induces cardiomyocyte cell-cycle arrest through DNA damage response," *Cell*, vol. 157, no. 3, pp. 565–579, 2014.

[32] H. M. Kaija, T. Särkioja, M.-L. Kortelainen, J. T. Vuoristo, H. V. Huikuri, and K. S. Porvari, "Stress-specific responses of p21 expression: implication of transcript variant p21 alt-a in long-term hypoxia," *Journal of Cellular Biochemistry*, vol. 113, no. 2, pp. 544–552, 2012.

[33] A. I. Mahmoud, F. Kocabas, S. A. Muralidhar et al., "Meis1 regulates postnatal cardiomyocyte cell cycle arrest," *Nature*, vol. 497, no. 7448, pp. 249–253, 2013.

[34] D. C. Canseco, W. Kimura, S. Garg et al., "Human ventricular unloading induces cardiomyocyte proliferation," *Journal of the American College of Cardiology*, vol. 65, no. 9, pp. 892–900, 2015.

[35] K.-L. Laugwitz, A. Moretti, L. Caron, A. Nakano, and K. R. Chien, "Islet1 cardiovascular progenitors: a single source for heart lineages?" *Development*, vol. 135, no. 2, pp. 193–205, 2008.

[36] T. Brade, L. S. Pane, A. Moretti, K. R. Chien, and K.-L. Laugwitz, "Embryonic heart progenitors and cardiogenesis," *Cold Spring Harbor Perspectives in Medicine*, vol. 3, no. 10, Article ID a013847, 2013.

[37] J. Ferreira-Martins, B. Ogórek, D. Cappetta et al., "Cardiomyogenesis in the developing heart is regulated by c-kit-positive cardiac stem cells," *Circulation Research*, vol. 110, no. 5, pp. 701–715, 2012.

[38] G. M. Ellison, C. Vicinanza, A. J. Smith et al., "Adult c-kit(pos) cardiac stem cells are necessary and sufficient for functional cardiac regeneration and repair," *Cell*, vol. 154, no. 4, pp. 827–842, 2013.

[39] F. Sanada, J. Kim, A. Czarna et al., "c-Kit-positive cardiac stem cells nested in hypoxic niches are activated by stem cell factor reversing the aging myopathy," *Circulation Research*, vol. 114, no. 1, pp. 41–55, 2014.

[40] S. J. Kattman, T. L. Huber, and G. M. Keller, "Multipotent Flk-1$^+$ cardiovascular progenitor cells give rise to the cardiomyocyte, endothelial, and vascular smooth muscle lineages," *Developmental Cell*, vol. 11, no. 5, pp. 723–732, 2006.

[41] V. Di Felice and G. Zummo, "Stem cell populations in the heart and the role of Isl1 positive cells," *European Journal of Histochemistry*, vol. 57, article e14, 2013.

[42] L. Bu, X. Jiang, S. Martin-Puig et al., "Human ISL1 heart progenitors generate diverse multipotent cardiovascular cell lineages," *Nature*, vol. 460, no. 7251, pp. 113–117, 2009.

[43] K. Hidaka, J.-K. Lee, H. S. Kim et al., "Chamber-specific differentiation of Nkx2.5-positive cardiac precursor cells from murine embryonic stem cells," *The FASEB Journal*, vol. 17, no. 6, pp. 740–742, 2003.

[44] A. Armiñán, C. Gandía, M. Bartual et al., "Cardiac differentiation is driven by NKX2.5 and GATA4 nuclear translocation in tissue-specific mesenchymal stem cells," *Stem Cells and Development*, vol. 18, no. 6, pp. 907–918, 2009.

[45] M. Takamiya, K. H. Haider, and M. Ashraf, "Identification and characterization of a novel multipotent sub-population of Sca-1(+) cardiac progenitor cells for myocardial regeneration," *PLoS ONE*, vol. 6, no. 9, Article ID e25265, 2011.

[46] A. Moretti, M. Bellin, C. B. Jung et al., "Mouse and human induced pluripotent stem cells as a source for multipotent Isl1+ cardiovascular progenitors," *The FASEB Journal*, vol. 24, no. 3, pp. 700–711, 2010.

[47] T. I. Fuentes, N. Appleby, E. Tsay et al., "Human neonatal cardiovascular progenitors: unlocking the secret to regenerative ability," *PLoS ONE*, vol. 8, no. 10, Article ID e77464, 2013.

[48] R. Jain, D. Li, M. Gupta et al., "Integration of BMP and WNT signaling by Hopx specifies commitment of cardiomyoblasts," *Science*, vol. 348, no. 6242, Article ID aaa6071, 2015.

[49] N. Rosenblatt-Velin, M. G. Lepore, C. Cartoni, F. Beermann, and T. Pedrazzini, "FGF-2 controls the differentiation of resident cardiac precursors into functional cardiomyocytes," *Journal of Clinical Investigation*, vol. 115, no. 7, pp. 1724–1733, 2005.

[50] N. Smart, S. Bollini, K. N. Dubé et al., "De novo cardiomyocytes from within the activated adult heart after injury," *Nature*, vol. 474, no. 7353, pp. 640–644, 2011.

[51] Y.-C. Hsueh, J. M. F. Wu, C.-K. Yu, K. K. Wu, and P. C. H. Hsieh, "Prostaglandin E_2 promotes post-infarction cardiomyocyte replenishment by endogenous stem cells," *EMBO Molecular Medicine*, vol. 6, no. 4, pp. 496–503, 2014.

[52] F. L. Xiang, Y. Liu, X. Lu, D. L. Jones, and Q. Feng, "Cardiac-specific overexpression of human stem cell factor promotes epicardial activation and arteriogenesis after myocardial infarction," *Circulation: Heart Failure*, vol. 7, no. 5, pp. 831–842, 2014.

[53] K. Malliaras, A. Ibrahim, E. Tseliou et al., "Stimulation of endogenous cardioblasts by exogenous cell therapy after myocardial infarction," *EMBO Molecular Medicine*, vol. 6, no. 6, pp. 760–777, 2014.

[54] V. F. M. Segers, T. Tokunou, L. J. Higgins, C. MacGillivray, J. Gannon, and R. T. Lee, "Local delivery of protease-resistant stromal cell derived factor-1 for stem cell recruitment after myocardial infarction," *Circulation*, vol. 116, no. 15, pp. 1683–1692, 2007.

[55] K. Wang, X. Zhao, C. Kuang et al., "Overexpression of SDF-1α enhanced migration and engraftment of cardiac stem cells and reduced infarcted size via CXCR4/PI3K pathway," *PLoS ONE*, vol. 7, no. 9, Article ID e43922, 2012.

[56] M. Nahrendorf, F. K. Swirski, E. Aikawa et al., "The healing myocardium sequentially mobilizes two monocyte subsets with divergent and complementary functions," *The Journal of Experimental Medicine*, vol. 204, no. 12, pp. 3037–3047, 2007.

[57] M. P. Santini and N. Rosenthal, "Myocardial regenerative properties of macrophage populations and stem cells," *Journal of Cardiovascular Translational Research*, vol. 5, no. 5, pp. 700–712, 2012.

[58] T. Ben-Mordechai, R. Holbova, N. Landa-Rouben et al., "Macrophage subpopulations are essential for infarct repair with and without stem cell therapy," *Journal of the American College of Cardiology*, vol. 62, no. 20, pp. 1890–1901, 2013.

[59] F. K. Swirski, M. Nahrendorf, M. Etzrodt et al., "Identification of splenic reservoir monocytes and their deployment to inflammatory sites," *Science*, vol. 325, no. 5940, pp. 612–616, 2009.

[60] Y. M. Klyachkin, A. V. Karapetyan, M. Z. Ratajczak, and A. Abdel-Latif, "The role of bioactive lipids in stem cell mobilization and homing: novel therapeutics for myocardial ischemia," *BioMed Research International*, vol. 2014, Article ID 653543, 12 pages, 2014.

[61] J. Kajstura, M. Rota, B. Whang et al., "Bone marrow cells differentiate in cardiac cell lineages after infarction independently of cell fusion," *Circulation Research*, vol. 96, no. 1, pp. 127–137, 2005.

[62] D. Orlic, "Adult bone marrow stem cells regenerate myocardium in ischemic heart disease," *Annals of the New York Academy of Sciences*, vol. 996, pp. 152–157, 2003.

[63] C. Badorff, R. P. Brandes, R. Popp et al., "Transdifferentiation of blood-derived human adult endothelial progenitor cells into functionally active cardiomyocytes," *Circulation*, vol. 107, no. 7, pp. 1024–1032, 2003.

[64] N. Terada, T. Hamazaki, M. Oka et al., "Bone marrow cells adopt the phenotype of other cells by spontaneous cell fusion," *Nature*, vol. 416, no. 6880, pp. 542–545, 2002.

[65] D. Orlic, J. Kajstura, S. Chimenti et al., "Mobilized bone marrow cells repair the infarcted heart, improving function and survival," *Proceedings of the National Academy of Sciences of the United States of America*, vol. 98, no. 18, pp. 10344–10349, 2001.

[66] C. E. Murry, M. H. Soonpaa, H. Reinecke et al., "Haematopoietic stem cells do not transdifferentiate into cardiac myocytes in myocardial infarcts," *Nature*, vol. 428, no. 6983, pp. 664–668, 2004.

[67] J. M. Nygren, S. Jovinge, M. Breitbach et al., "Bone marrow-derived hematopoietic cells generate cardiomyocytes at a low frequency through cell fusion, but not transdifferentiation," *Nature Medicine*, vol. 10, no. 5, pp. 494–501, 2004.

[68] M. Rota, J. Kajstura, T. Hosoda et al., "Bone marrow cells adopt the cardiomyogenic fate *in vivo*," *Proceedings of the National Academy of Sciences of the United States of America*, vol. 104, no. 45, pp. 17783–17788, 2007.

[69] J. Yoon, S.-C. Choi, C.-Y. Park et al., "Bone marrow-derived side population cells are capable of functional cardiomyogenic differentiation," *Molecules and Cells*, vol. 25, no. 2, pp. 216–223, 2008.

[70] H. Kodama, T. Inoue, R. Watanabe et al., "Cardiomyogenic potential of mesenchymal progenitors derived from human circulating $CD14^+$ monocytes," *Stem Cells and Development*, vol. 14, no. 6, pp. 676–686, 2005.

[71] F. S. Loffredo, M. L. Steinhauser, J. Gannon, and R. T. Lee, "Bone marrow-derived cell therapy stimulates endogenous cardiomyocyte progenitors and promotes cardiac repair," *Cell Stem Cell*, vol. 8, no. 4, pp. 389–398, 2011.

[72] P. Menasché, V. Vanneaux, J. R. Fabreguettes et al., "Towards a clinical use of human embryonic stem cell-derived cardiac progenitors: a translational experience," *European Heart Journal*, vol. 36, no. 12, pp. 743–750, 2014.

[73] J. J. H. Chong, X. Yang, C. W. Don et al., "Human embryonic-stem-cell-derived cardiomyocytes regenerate non-human primate hearts," *Nature*, vol. 510, no. 7504, pp. 273–277, 2014.

[74] M. Malecki, E. Putzer, C. Sabo et al., "Directed cardiomyogenesis of autologous human induced pluripotent stem cells recruited to infarcted myocardium with bioengineered antibodies," *Molecular and Cellular Therapies*, vol. 2, article 13, 2014.

[75] Z. Ding, S. Burghoff, A. Buchheiser, G. Kögler, and J. Schrader, "Survival, integration, and differentiation of unrestricted somatic stem cells in the heart," *Cell Transplantation*, vol. 22, no. 1, pp. 15–27, 2013.

[76] P. Menasche, "Cardiac cell therapy: lessons from clinical trials," *Journal of Molecular and Cellular Cardiology*, vol. 50, no. 2, pp. 258–265, 2011.

[77] P. P. Young and R. Schäfer, "Cell-based therapies for cardiac disease: a cellular therapist's perspective," *Transfusion*, vol. 55, no. 2, pp. 441–451, 2015.

[78] E. Martin-Rendon, S. Brunskill, C. Dorée et al., "Stem cell treatment for acute myocardial infarction," *Cochrane Database of Systematic Reviews*, vol. 4, Article ID CD006536, 2008.

[79] V. Schächinger, S. Erbs, A. Elsässer et al., "Intracoronary bone marrow-derived progenitor cells in acute myocardial infarction," *The New England Journal of Medicine*, vol. 355, no. 12, pp. 1210–1221, 2006.

[80] G. P. Meyer, K. C. Wollert, J. Lotz et al., "Intracoronary bone marrow cell transfer after myocardial infarction: 5-year follow-up from the randomized-controlled BOOST trial," *European Heart Journal*, vol. 30, no. 24, pp. 2978–2984, 2009.

[81] M. Gyöngyösi, W. Wojakowski, P. Lemarchand et al., "Meta-analysis of cell-based cardiac studies (ACCRUE) in patients with acute myocardial infarction based on individual patient data," *Circulation Research*, vol. 116, no. 8, pp. 1346–1360, 2015.

[82] S. Golpanian, J. El-Khorazaty, A. Mendizabal et al., "Effect of aging on human mesenchymal stem cell therapy in ischemic cardiomyopathy patients," *Journal of the American College of Cardiology*, vol. 65, no. 2, pp. 125–132, 2015.

[83] B. A. Nasseri, W. Ebell, M. Dandel et al., "Autologous CD133+ bone marrow cells and bypass grafting for regeneration of ischaemic myocardium: the Cardio133 trial," *European Heart Journal*, vol. 35, no. 19, pp. 1263–1274, 2014.

[84] J. M. Hare, J. H. Traverse, T. D. Henry et al., "A randomized, double-blind, placebo-controlled, dose-escalation study of intravenous adult human mesenchymal stem cells (prochymal) after acute myocardial infarction," *Journal of the American College of Cardiology*, vol. 54, no. 24, pp. 2277–2286, 2009.

[85] R. C. Schutt, B. H. Trachtenberg, J. P. Cooke et al., "Bone marrow characteristics associated with changes in infarct size after STEMI: a biorepository evaluation from the CCTRN TIME trial," *Circulation Research*, vol. 116, no. 1, pp. 99–107, 2015.

[86] P. Menasché, O. Alfieri, S. Janssens et al., "The myoblast autologous grafting in ischemic cardiomyopathy (MAGIC) trial: first randomized placebo-controlled study of myoblast transplantation," *Circulation*, vol. 117, no. 9, pp. 1189–1200, 2008.

[87] J. H. Houtgraaf, W. K. den Dekker, B. M. van Dalen et al., "First experience in humans using adipose tissue-derived regenerative cells in the treatment of patients with ST-segment elevation myocardial infarction," *Journal of the American College of Cardiology*, vol. 59, no. 5, pp. 539–540, 2012.

[88] E. C. Perin, R. Sanz-Ruiz, P. L. Sánchez et al., "Adipose-derived regenerative cells in patients with ischemic cardiomyopathy: the PRECISE Trial," *American Heart Journal*, vol. 168, no. 1, pp. 88–95.e2, 2014.

[89] R. Bolli, A. R. Chugh, D. D'Amario et al., "Cardiac stem cells in patients with ischaemic cardiomyopathy (SCIPIO): initial results of a randomised phase 1 trial," *The Lancet*, vol. 378, no. 9806, pp. 1847–1857, 2011.

[90] R. R. Makkar, R. R. Smith, K. Cheng et al., "Intracoronary cardiosphere-derived cells for heart regeneration after myocardial infarction (CADUCEUS): a prospective, randomised phase 1 trial," *The Lancet*, vol. 379, no. 9819, pp. 895–904, 2012.

[91] The Lancet Editors, "Expression of concern: the SCIPIO trial," *The Lancet*, vol. 383, no. 9925, p. 1279, 2014.

[92] K. Malliaras, R. R. Makkar, R. R. Smith et al., "Intracoronary cardiosphere-derived cells after myocardial infarction: evidence of therapeutic regeneration in the final 1-year results of the CADUCEUS trial (cardiosphere-derived autologous stem cells to reverse ventricular dysfunction)," *Journal of the American College of Cardiology*, vol. 63, no. 2, pp. 110–122, 2014.

[93] N. Haque, N. H. Abu Kasim, and M. T. Rahman, "Optimization of pre-transplantation conditions to enhance the efficacy of mesenchymal stem cells," *International Journal of Biological Sciences*, vol. 11, no. 3, pp. 324–334, 2015.

[94] J. M. Polo, S. Liu, M. E. Figueroa et al., "Cell type of origin influences the molecular and functional properties of mouse induced pluripotent stem cells," *Nature Biotechnology*, vol. 28, no. 8, pp. 848–855, 2010.

[95] G. Liang and Y. Zhang, "Genetic and epigenetic variations in iPSCs: potential causes and implications for application," *Cell Stem Cell*, vol. 13, no. 2, pp. 149–159, 2013.

[96] M. Hofmann, K. C. Wollert, G. P. Meyer et al., "Monitoring of bone marrow cell homing into the infarcted human myocardium," *Circulation*, vol. 111, no. 17, pp. 2198–2202, 2005.

[97] M. Z. Ratajczak, M. Kucia, T. Jadczyk et al., "Pivotal role of paracrine effects in stem cell therapies in regenerative medicine: can we translate stem cell-secreted paracrine factors and microvesicles into better therapeutic strategies," *Leukemia*, vol. 26, no. 6, pp. 1166–1173, 2012.

[98] G. Maguire, "Stem cell therapy without the cells," *Communicative & Integrative Biology*, vol. 6, no. 6, Article ID e26631, 2013.

[99] S. M. Chacko, M. Khan, M. L. Kuppusamy et al., "Myocardial oxygenation and functional recovery in infarct rat hearts transplanted with mesenchymal stem cells," *The American Journal of Physiology—Heart and Circulatory Physiology*, vol. 296, no. 5, pp. H1263–H1273, 2009.

[100] Y. Imanishi, A. Saito, H. Komoda et al., "Allogenic mesenchymal stem cell transplantation has a therapeutic effect in acute myocardial infarction in rats," *Journal of Molecular and Cellular Cardiology*, vol. 44, no. 4, pp. 662–671, 2008.

[101] D. C. Vela, G. V. Silva, J. A. R. Assad et al., "Histopathological study of healing after allogenic mesenchymal stem cell delivery in myocardial infarction in dogs," *Journal of Histochemistry and Cytochemistry*, vol. 57, no. 2, pp. 167–176, 2009.

[102] R. R. Makkar, M. J. Price, M. Lill et al., "Intramyocardial injection of allogenic bone marrow-derived mesenchymal stem cells without immunosuppression preserves cardiac function in a porcine model of myocardial infarction," *Journal of Cardiovascular Pharmacology and Therapeutics*, vol. 10, no. 4, pp. 225–233, 2005.

[103] L. V. Kursova, A. G. Konoplyannikov, S. S. Kal'sina, and S. B. Baboyan, "Allogenic cardiomyoblasts raised from human mesenchymal stem cells in the therapy of radiation cardiomyopathy and pericarditis: case report," *Bulletin of Experimental Biology and Medicine*, vol. 157, no. 1, pp. 143–145, 2014.

[104] R. R. U. Smith, E. Marban, and L. Marban, "Enhancing retention and efficacy of cardiosphere-derived cells administered after

myocardial infarction using a hyaluronan-gelatin hydrogel," *Biomatter*, vol. 3, no. 1, Article ID e24490, 2013.

[105] K. Malliaras, T.-S. Li, D. Luthringer et al., "Safety and efficacy of allogeneic cell therapy in infarcted rats transplanted with mismatched cardiosphere-derived cells," *Circulation*, vol. 125, no. 1, pp. 100–112, 2012.

[106] M. Drukker, H. Katchman, G. Katz et al., "Human embryonic stem cells and their differentiated derivatives are less susceptible to immune rejection than adult cells," *Stem Cells*, vol. 24, no. 2, pp. 221–229, 2006.

[107] M. Drukker, G. Katz, A. Urbach et al., "Characterization of the expression of MHC proteins in human embryonic stem cells," *Proceedings of the National Academy of Sciences of the United States of America*, vol. 99, no. 15, pp. 9864–9869, 2002.

[108] C. Bocelli-Tyndall, E. Trella, A. Frachet et al., "FGF2 induces RANKL gene expression as well as IL1β regulated MHC class II in human bone marrow-derived mesenchymal progenitor stromal cells," *Annals of the Rheumatic Diseases*, vol. 74, no. 1, pp. 260–266, 2015.

[109] C. Bocelli-Tyndall, P. Zajac, N. Di Maggio et al., "Fibroblast growth factor 2 and platelet-derived growth factor, but not platelet lysate, induce proliferation-dependent, functional class II major histocompatibility complex antigen in human mesenchymal stem cells," *Arthritis and Rheumatism*, vol. 62, no. 12, pp. 3815–3825, 2010.

[110] P. Lohan, C. M. Coleman, J. M. Murphy, M. D. Griffin, T. Ritter, and A. E. Ryan, "Changes in immunological profile of allogeneic mesenchymal stem cells after differentiation: should we be concerned?" *Stem Cell Research & Therapy*, vol. 5, article 99, 2014.

[111] J. L. Zakrzewski, M. R. M. van den Brink, and J. A. Hubbell, "Overcoming immunological barriers in regenerative medicine," *Nature Biotechnology*, vol. 32, no. 8, pp. 786–794, 2014.

[112] R. Al-Daccak and D. Charron, "Allogenic benefit in stem cell therapy: cardiac repair and regeneration," *Tissue Antigens*, vol. 86, no. 3, pp. 155–162, 2015.

[113] B. Zhou, Q. Ma, S. Rajagopal et al., "Epicardial progenitors contribute to the cardiomyocyte lineage in the developing heart," *Nature*, vol. 454, no. 7200, pp. 109–113, 2008.

[114] A. Leri, J. Kajstura, and P. Anversa, "Cardiac stem cells and mechanisms of myocardial regeneration," *Physiological Reviews*, vol. 85, no. 4, pp. 1373–1416, 2005.

[115] K. Urbanek, D. Cesselli, M. Rota et al., "Stem cell niches in the adult mouse heart," *Proceedings of the National Academy of Sciences of the United States of America*, vol. 103, no. 24, pp. 9226–9231, 2006.

[116] F. Limana, A. Germani, A. Zacheo et al., "Exogenous high-mobility group box 1 protein induces myocardial regeneration after infarction via enhanced cardiac C-kit$^+$ cell proliferation and differentiation," *Circulation research*, vol. 97, no. 8, pp. e73–e83, 2005.

[117] C. Bielmann, S. Rignault-Clerc, L. Liaudet et al., "Brain natriuretic peptide is able to stimulate cardiac progenitor cell proliferation and differentiation in murine hearts after birth," *Basic Research in Cardiology*, vol. 110, article 455, 2015.

[118] V. Dayan, G. Yannarelli, F. Billia et al., "Mesenchymal stromal cells mediate a switch to alternatively activated monocytes/macrophages after acute myocardial infarction," *Basic Research in Cardiology*, vol. 106, no. 6, pp. 1299–1310, 2011.

[119] T. Nishikimi, K. Kuwahara, and K. Nakao, "Current biochemistry, molecular biology, and clinical relevance of natriuretic peptides," *Journal of Cardiology*, vol. 57, no. 2, pp. 131–140, 2011.

[120] L. R. Potter, A. R. Yoder, D. R. Flora, L. K. Antos, and D. M. Dickey, "Natriuretic peptides: their structures, receptors, physiologic functions and therapeutic applications," in *cGMP: Generators, Effectors and Therapeutic Implications*, vol. 191 of *Handbook of Experimental Pharmacology*, pp. 341–366, Springer, Berlin, Germany, 2009.

[121] A. Clerico, S. Vittorini, and C. Passino, "Circulating forms of the b-type natriuretic peptide prohormone: pathophysiologic and clinical considerations," *Advances in Clinical Chemistry*, vol. 58, pp. 31–44, 2012.

[122] E. Morita, H. Yasue, M. Yoshimura et al., "Increased plasma levels of brain natriuretic peptide in patients with acute myocardial infarction," *Circulation*, vol. 88, no. 1, pp. 82–91, 1993.

[123] F. Liang, J. O'Rear, U. Schellenberger et al., "Evidence for functional heterogeneity of circulating B-type natriuretic peptide," *Journal of the American College of Cardiology*, vol. 49, no. 10, pp. 1071–1078, 2007.

[124] H. H. Chen, "Heart failure: a state of brain natriuretic peptide deficiency or resistance or both!," *Journal of the American College of Cardiology*, vol. 49, no. 10, pp. 1089–1091, 2007.

[125] A. H. Bruggink, N. de Jonge, M. F. M. van Oosterhout et al., "Brain natriuretic peptide is produced both by cardiomyocytes and cells infiltrating the heart in patients with severe heart failure supported by a left ventricular assist device," *Journal of Heart and Lung Transplantation*, vol. 25, no. 2, pp. 174–180, 2006.

[126] E. M. Abdelalim and I. Tooyama, "BNP signaling is crucial for embryonic stem cell proliferation," *PLoS ONE*, vol. 4, no. 4, Article ID e5341, 2009.

[127] M. Kuhn, K. Völker, K. Schwarz et al., "The natriuretic peptide/guanylyl cyclase—a system functions as a stress-responsive regulator of angiogenesis in mice," *Journal of Clinical Investigation*, vol. 119, no. 7, pp. 2019–2030, 2009.

[128] K. Kuwahara and K. Nakao, "Regulation and significance of atrial and brain natriuretic peptides as cardiac hormones," *Endocrine Journal*, vol. 57, no. 7, pp. 555–565, 2010.

[129] S. P. D'Souza and G. F. Baxter, "B type natriuretic peptide: a good omen in myocardial ischaemia?" *Heart*, vol. 89, no. 7, pp. 707–709, 2003.

[130] B. Ren, Y. Shen, H. Shao, J. Qian, H. Wu, and H. Jing, "Brain natriuretic peptide limits myocardial infarct size dependent of nitric oxide synthase in rats," *Clinica Chimica Acta*, vol. 377, no. 1-2, pp. 83–87, 2007.

[131] D. S. Burley and G. F. Baxter, "B-type natriuretic peptide at early reperfusion limits infarct size in the rat isolated heart," *Basic Research in Cardiology*, vol. 102, no. 6, pp. 529–541, 2007.

[132] B. Wu, H. Jiang, R. Lin, B. Cui, H. Wen, and Z. Lu, "Pretreatment with B-type natriuretic peptide protects the heart from ischemia-reperfusion injury by inhibiting myocardial apoptosis," *Tohoku Journal of Experimental Medicine*, vol. 219, no. 2, pp. 107–114, 2009.

[133] A.-M. Moilanen, J. Rysä, E. Mustonen et al., "Intramyocardial BNP gene delivery improves cardiac function through distinct context-dependent mechanisms," *Circulation: Heart Failure*, vol. 4, no. 4, pp. 483–495, 2011.

[134] A. Cataliotti, J. M. Tonne, D. Bellavia et al., "Long-term cardiac pro-B-type natriuretic peptide gene delivery prevents the development of hypertensive heart disease in spontaneously hypertensive rats," *Circulation*, vol. 123, no. 12, pp. 1297–1305, 2011.

[135] N. Glezeva, P. Collier, V. Voon et al., "Attenuation of monocyte chemotaxis—a novel anti-inflammatory mechanism of action for the cardio-protective hormone B-type natriuretic peptide," *Journal of Cardiovascular Translational Research*, vol. 6, no. 4, pp. 545–557, 2013.

[136] S. M. Shaw, J. E. Fildes, C. M. Puchałka, M. Basith, N. Yonan, and S. G. Williams, "BNP directly immunoregulates the innate immune system of cardiac transplant recipients in vitro," *Transplant Immunology*, vol. 20, no. 3, pp. 199–202, 2009.

[137] V. Chiurchiù, V. Izzi, F. D'Aquilio, F. Carotenuto, P. Di Nardo, and P. M. Baldini, "Brain Natriuretic Peptide (BNP) regulates the production of inflammatory mediators in human THP-1 macrophages," *Regulatory Peptides*, vol. 148, no. 1–3, pp. 26–32, 2008.

[138] R. Kawakami, Y. Saito, I. Kishimoto et al., "Overexpression of brain natriuretic peptide facilitates neutrophil infiltration and cardiac matrix metalloproteinase-9 expression after acute myocardial infarction," *Circulation*, vol. 110, no. 21, pp. 3306–3312, 2004.

[139] B. B. Das, S. Raj, and R. Solinger, "Natriuretic peptides in cardiovascular diseases of fetus, infants and children," *Cardiovascular & Hematological Agents in Medicinal Chemistry*, vol. 7, no. 1, pp. 43–51, 2009.

[140] V. A. Cameron and L. J. Ellmers, "Minireview: natriuretic peptides during development of the fetal heart and circulation," *Endocrinology*, vol. 144, no. 6, pp. 2191–2194, 2003.

[141] J. R. Becker, S. Chatterjee, T. Y. Robinson et al., "Differential activation of natriuretic peptide receptors modulates cardiomyocyte proliferation during development," *Development*, vol. 141, no. 2, pp. 335–345, 2014.

[142] V. A. Cameron, G. D. Aitken, L. J. Ellmers, M. A. Kennedy, and E. A. Espiner, "The sites of gene expression of atrial, brain, and C-type natriuretic peptides in mouse fetal development: temporal changes in embryos and placenta," *Endocrinology*, vol. 137, no. 3, pp. 817–824, 1996.

[143] L. Schwachtgen, M. Herrmann, T. Georg, P. Schwarz, N. Marx, and A. Lindinger, "Reference values of NT-proBNP serum concentrations in the umbilical cord blood and in healthy neonates and children," *Zeitschrift für Kardiologie*, vol. 94, no. 6, pp. 399–404, 2005.

[144] J. M. Tonne, J. M. Campbell, A. Cataliotti et al., "Secretion of glycosylated pro-B-type natriuretic peptide from normal cardiomyocytes," *Clinical Chemistry*, vol. 57, no. 6, pp. 864–873, 2011.

[145] J. Peng, J. Jiang, W. Wang, X. Qi, X.-L. Sun, and Q. Wu, "Glycosylation and processing of pro-B-type natriuretic peptide in cardiomyocytes," *Biochemical and Biophysical Research Communications*, vol. 411, no. 3, pp. 593–598, 2011.

[146] N. J. A. Scott, L. J. Ellmers, J. G. Lainchbury et al., "Influence of natriuretic peptide receptor-1 on survival and cardiac hypertrophy during development," *Biochimica et Biophysica Acta—Molecular Basis of Disease*, vol. 1792, no. 12, pp. 1175–1184, 2009.

[147] E. M. Abdelalim and I. Tooyama, "NPR-A regulates self-renewal and pluripotency of embryonic stem cells," *Cell Death & Disease*, vol. 2, no. 3, article e127, 2011.

[148] L. J. Ellmers, N. J. A. Scott, J. Piuhola et al., "Npr1-regulated gene pathways contributing to cardiac hypertrophy and fibrosis," *Journal of Molecular Endocrinology*, vol. 38, no. 1-2, pp. 245–257, 2007.

[149] J. W. Knowles, G. Esposito, L. Mao et al., "Pressure-independent enhancement of cardiac hypertrophy in natriuretic peptide receptor A-deficient mice," *The Journal of Clinical Investigation*, vol. 107, no. 8, pp. 975–984, 2001.

[150] I. Kishimoto, T. Tokudome, T. Horio, D. L. Garbers, K. Nakao, and K. Kangawa, "Natriuretic peptide signaling via guanylyl cyclase (GC)-A: an endogenous protective mechanism of the heart," *Current Cardiology Reviews*, vol. 5, no. 1, pp. 45–51, 2009.

[151] C. Sogawa, A. Abe, T. Tsuji, M. Koizumi, T. Saga, and T. Kunieda, "Gastrointestinal tract disorder in natriuretic peptide receptor B gene mutant mice," *The American Journal of Pathology*, vol. 177, no. 2, pp. 822–828, 2010.

[152] C. Sogawa, T. Tsuji, Y. Shinkai, K. Katayama, and T. Kunieda, "Short-limbed dwarfism: slw is a new allele of Npr2 causing chondrodysplasia," *The Journal of Heredity*, vol. 98, no. 6, pp. 575–580, 2007.

[153] N. Tamura, L. K. Doolittle, R. E. Hammer, J. M. Shelton, J. A. Richardson, and D. L. Garbers, "Critical roles of the guanylyl cyclase B receptor in endochondral ossification and development of female reproductive organs," *Proceedings of the National Academy of Sciences of the United States of America*, vol. 101, no. 49, pp. 17300–17305, 2004.

[154] C. Sogawa, Y. Fujiwara, S. Tsukamoto et al., "Mutant phenotype analysis suggests potential roles for C-type natriuretic peptide receptor (NPR-B) in male mouse fertility," *Reproductive Biology and Endocrinology*, vol. 12, article 64, 2014.

[155] K. A. Geister, M. L. Brinkmeier, M. Hsieh et al., "A novel loss-of-function mutation in Npr2 clarifies primary role in female reproduction and reveals a potential therapy for acromesomelic dysplasia, Maroteaux type," *Human Molecular Genetics*, vol. 22, no. 2, pp. 345–357, 2013.

[156] T. H. Langenickel, J. Buttgereit, I. Pagel-Langenickel et al., "Cardiac hypertrophy in transgenic rats expressing a dominant-negative mutant of the natriuretic peptide receptor B," *Proceedings of the National Academy of Sciences of the United States of America*, vol. 103, no. 12, pp. 4735–4740, 2006.

[157] T. Ahmad and G. M. Felker, "Subcutaneous B-type natriuretic peptide for treatment of heart failure: a dying therapy reborn?" *Journal of the American College of Cardiology*, vol. 60, no. 22, pp. 2313–2315, 2012.

[158] C. Partovian, S.-X. Li, X. Xu et al., "Patterns of change in nesiritide use in patients with heart failure: how hospitals react to new information," *JACC: Heart Failure*, vol. 1, no. 4, pp. 318–324, 2013.

[159] S. S. Gottlieb, A. Stebbins, A. A. Voors et al., "Effects of nesiritide and predictors of urine output in acute decompensated heart failure: results from ASCEND-HF (acute study of clinical effectiveness of nesiritide and decompensated heart failure)," *Journal of the American College of Cardiology*, vol. 62, no. 13, pp. 1177–1183, 2013.

[160] C. M. O'Connor, R. C. Starling, A. F. Hernandez et al., "Effect of nesiritide in patients with acute decompensated heart failure," *The New England Journal of Medicine*, vol. 365, no. 1, pp. 32–43, 2011.

[161] H. H. Chen, F. L. Martin, R. J. Gibbons et al., "Low-dose nesiritide in human anterior myocardial infarction suppresses aldosterone and preserves ventricular function and structure: a proof of concept study," *Heart*, vol. 95, no. 16, pp. 1315–1319, 2009.

[162] H. H. Chen, J. F. Glockner, J. A. Schirger, A. Cataliotti, M. M. Redfield, and J. C. Burnett Jr., "Novel protein therapeutics for systolic heart failure: chronic subcutaneous B-type natriuretic peptide," *Journal of the American College of Cardiology*, vol. 60, no. 22, pp. 2305–2312, 2012.

[163] T. Lyu, Y. Zhao, T. Zhang et al., "Natriuretic peptides as an adjunctive treatment for acute myocardial infarction," *International Heart Journal*, vol. 55, no. 1, pp. 8–16, 2014.

[164] S. J. Sangaralingham, J. C. Burnett Jr., P. M. McKie, J. A. Schirger, and H. H. Chen, "Rationale and design of a randomized, double-blind, placebo-controlled clinical trial to evaluate the efficacy of B-type natriuretic peptide for the preservation of left ventricular function after anterior myocardial infarction," *Journal of Cardiac Failure*, vol. 19, no. 8, pp. 533–539, 2013.

[165] J. J. V. McMurray, M. Packer, A. S. Desai et al., "Angiotensin-neprilysin inhibition versus enalapril in heart failure," *The New England Journal of Medicine*, vol. 371, no. 11, pp. 993–1004, 2014.

[166] M. Packer, J. J. McMurray, A. S. Desai et al., "Angiotensin receptor neprilysin inhibition compared with enalapril on the risk of clinical progression in surviving patients with heart failure," *Circulation*, vol. 131, no. 1, pp. 54–61, 2015.

[167] W. Jiang, D.-Y. Cai, C.-S. Pan et al., "Changes in production and metabolism of brain natriuretic peptide in rats with myocardial necrosis," *European Journal of Pharmacology*, vol. 507, no. 1–3, pp. 153–162, 2005.

[168] Y. Hirata, H. Hayakawa, E. Suzuki, and M. Omata, "Does endothelin work as an intrarenal mechanism to alter pressure natriuresis in spontaneously hypertensive rats?" *Journal of Hypertension*, vol. 12, no. 3, pp. 251–257, 1994.

[169] J. Xu, O. A. Carretero, Y.-H. Liu et al., "Dual inhibition of ACE and NEP provides greater cardioprotection in mice with heart failure," *Journal of Cardiac Failure*, vol. 10, no. 1, pp. 83–89, 2004.

[170] T. G. von Lueder, B. H. Wang, A. R. Kompa et al., "Angiotensin receptor neprilysin inhibitor LCZ696 attenuates cardiac remodeling and dysfunction after myocardial infarction by reducing cardiac fibrosis and hypertrophy," *Circulation: Heart Failure*, vol. 8, no. 1, pp. 71–78, 2015.

[171] A. S. Jaffe, "Unwinding the interaction of natriuretic peptides and neprilysin," *Journal of the American College of Cardiology*, vol. 65, no. 7, pp. 666–667, 2015.

[172] J. C. Garbern and R. T. Lee, "Cardiac stem cell therapy and the promise of heart regeneration," *Cell Stem Cell*, vol. 12, no. 6, pp. 689–698, 2013.

[173] S. A. Doppler, M.-A. Deutsch, R. Lange, and M. Krane, "Cardiac regeneration: current therapies-future concepts," *Journal of Thoracic Disease*, vol. 5, no. 5, pp. 683–697, 2013.

[174] S.-Y. Liao and H.-F. Tse, "Multipotent (adult) and pluripotent stem cells for heart regeneration: what are the pros and cons?" *Stem Cell Research & Therapy*, vol. 4, article 151, 2013.

Hindawi Publishing Corporation
Stem Cells International
Volume 2016, Article ID 9364974, 11 pages
http://dx.doi.org/10.1155/2016/9364974

Research Article

Effect of Fibroblast Growth Factor 2 on Equine Synovial Fluid Chondroprogenitor Expansion and Chondrogenesis

Marta Bianchessi,[1] Yuwen Chen,[2] Sushmitha Durgam,[1] Holly Pondenis,[1] and Matthew Stewart[1]

[1]*Department of Veterinary Clinical Medicine, University of Illinois, Urbana, IL 61802, USA*
[2]*QPS Taiwan, Center of Toxicology and Preclinical Sciences, No. 103, Lane 169, Kangning Street, Xizhi District, New Taipei City 221, Taiwan*

Correspondence should be addressed to Matthew Stewart; matt1@illinois.edu

Received 14 June 2015; Revised 29 September 2015; Accepted 30 September 2015

Academic Editor: Luca Vanella

Mesenchymal stem cells have been identified in the synovial fluid of several species. This study was conducted to characterize chondroprogenitor (CP) cells in equine synovial fluid (SF) and to determine the effect of fibroblast growth factor 2 (FGF-2) on SF-CP monolayer proliferation and subsequent chondrogenesis. We hypothesized that FGF-2 would stimulate SF-CP proliferation and postexpansion chondrogenesis. SF aspirates were collected from adult equine joints. Colony-forming unit (CFU) assays were performed during primary cultures. At first passage, SF-cells were seeded at low density, with or without FGF-2. Following monolayer expansion and serial immunophenotyping, cells were transferred to chondrogenic pellet cultures. Pellets were analyzed for chondrogenic mRNA expression and cartilage matrix secretion. There was a mean of 59.2 CFU/mL of SF. FGF-2 increased the number of population doublings during two monolayer passages and halved the population doubling times. FGF-2 did not alter the immunophenotype of SF-CPs during monolayer expansion, nor did FGF-2 compromise chondrogenesis. Hypertrophic phenotypic markers were not expressed in control or FGF-2 groups. FGF-2 did prevent the development of a "fibroblastic" cell layer around pellet periphery. FGF-2 significantly accelerates in vitro SF-CP expansion, the major hurdle to clinical application of this cell population, without detrimentally affecting subsequent chondrogenic capacity.

1. Introduction

Articular cartilage is a highly specialized connective tissue, responsible for equilibrating loads across joint surfaces and minimizing friction during joint motion. Cartilage is an alymphatic, avascular, and aneural tissue, with a comparatively low cellular density. These characteristics limit the intrinsic reparative capacity of articular cartilage [1]. Current surgical treatments for articular cartilage injuries [2–4] do not reliably restore a functional and phenotypically stable cartilage matrix. Further, in vitro expansion of chondrocytes, prior to reimplantation into cartilage lesions, compromises the specialized phenotype of these cells [5, 6].

Mesenchymal stem cells (MSCs) represent a promising alternative resource for cartilage repair, given their chondrogenic potential, capacity for considerable proliferative expansion, ease of access, and immunogenic properties. The majority of initial research on stem cell chondrogenesis has been carried out using bone marrow-derived stem cells [7, 8], but it is now well recognized that progenitor cells exist in most tissues and body fluids, albeit in very low numbers, and that the chondrogenic capacities of these progenitor cell populations vary considerably [9–14]. The majority of MSC populations undergo chondrogenesis that culminates in a hypertrophic phenotype [8, 10, 15–17], not optimal for articular cartilage repair.

Several recent studies, utilizing synovial fluid aspirates from a range of species, have demonstrated that progenitor cells can be isolated from synovial fluid (SF-CP), expanded in vitro [18–22] and, under appropriate culture conditions, induced to express a nonhypertrophic chondrogenic phenotype that is more consistent with articular chondrocyte

characteristics [19, 23–26]. Consistently, SF-CP concentrations are increased in arthritic conditions [18–22], suggesting a role for these cells in host responses to joint trauma and/or degeneration. Accepting their phenotypic suitability, the very low numbers of these cells in synovial fluid [19, 22, 23, 26] and intrinsic limits to proliferation [20, 27] represent major obstacles to potential clinical applications of SF-CPs [20, 28, 29].

Fibroblast growth factor 2 (FGF-2), also known as basic fibroblast growth factor, is a potent mitogen in many cell types and also increases chondrogenesis and cartilage matrix formation in some progenitor populations [30–32]. The purpose of this study was to determine the effect of FGF-2 on equine SF-CP monolayer expansion and subsequent chondrogenic differentiation. We hypothesized that FGF-2 will stimulate SF-CP proliferation and improve postexpansion chondrogenesis.

2. Materials and Methods

2.1. Collections. This study was conducted with the approval of the University of Illinois' IACUC. Synovial fluid samples were collected aseptically from the tibiotarsal or metacarpotarsophalangeal joints of young adult horses (18 Standardbreds, two Thoroughbreds, and seven Quarter horses). There were 15 fillies/mares, four colts/stallions, and 8 geldings, with an age range of 2–4 years. The synovial aspirates were collected immediately prior to arthroscopy for removal of osteochondral lesions. The joints had minimal clinical or arthroscopic evidence of osteoarthritis.

2.2. Cell Culture. Two mL of synovial fluid was plated in 10 mL of low-glucose Dulbecco modified Eagle medium (DMEM) supplemented with 10% fetal bovine serum, 100 U of sodium penicillin/mL, and 100 μg of streptomycin sulfate/mL. The primary cultures were incubated at 37°C in 5% CO_2 with 90% humidity. Colony-forming units (CFU), defined as focal clusters of 25 or more cells (reflecting four or more cell divisions), were monitored in each dish during the first seven days in culture and were counted on day 7.

2.3. Cell Expansion. The primary monolayers were trypsinized at approximately 80% confluence, counted, and replated at 1×10^4 cells/cm^2. Cell viability was determined by trypan blue exclusion. First passage cells were maintained in growth medium (as above) or in medium supplemented with 100 ng of FGF-2/mL. In a previous study, this FGF-2 dose was found to optimally stimulate chondrogenesis of equine bone marrow-derived MSCs [32]. The medium was changed every 2 to 3 days, until 80% confluence. Replating was continued for two passages, to generate sufficient cell numbers for subsequent chondrogenesis experiments. The population doublings during each passage were calculated using the following formula: Log_2 (harvested cell number/seeded cell number). The population doubling times during each passage were calculated dividing the time of each passage by the population doubling value.

2.4. Immunophenotypic Analysis. Flow cytometry was used to evaluate the SF-CP immunophenotype (CD29, CD44, and CD90) during monolayer expansion, following previously published recommendations [33, 34]. CD45 was included as a negative control for hematopoietic progenitors. At each passage, 2×10^6 SF-CPs were resuspended in DMEM media with 1% BSA [34]. The following antibodies were used according to the manufacturers' recommendations: anti-human conjugated anti-CD29-Alexa 488 (BioLegend, San Diego, CA); anti-horse conjugated anti-CD44-RPE (AbD Serotec, BioRad, Hercules, CA); anti-horse nonconjugated anti-CD90-Alexa 647 (Accurate Chemical and Scientific Corporation, Westbury, NY); and anti-human conjugated anti-CD45-Alexa 488 (AbD Serotec, BioRad, Hercules, CA) [34]. Bone marrow-derived MSCs and chondrocytes were used as biological controls. The following filters were used in a flow cytometry analyzer (Accuri C6, BD Biosciences, CA) to isolate the emission wavelength of the conjugated fluorochromes: FL-1 (510 nm and 545 nm wavelengths of light) for CD29 (519 nm emission) and CD45 (519 nm emission), FL-2 (560–580 nm wavelength) for CD44 (578 nm emission), and FL-4 (665–695 nm wavelength) for CD90 (668 nm emission). After the emission analysis on "FCS Express (Flow Research Edition)," data were expressed as "percentage of deviation from the control antibody groups."

2.5. In Vitro Chondrogenesis. After monolayer expansion through two passages in the absence or presence of FGF-2, the cells were trypsinized and resuspended at 5×10^5 cells/mL in chondrogenic medium (high-glucose, glutamine-sodium pyruvate-DMEM containing 5 ng of TGF-β1/mL, 37.5 μg of ascorbic acid/mL, 10^{-7} M dexamethasone, 6.25 μg of insulin/mL, 6.25 μg of transferrin/mL, 6.25 ng of selenite/mL, 300 μg of L-glutamine/mL, 100 U of sodium penicillin/mL, and 100 μg of streptomycin sulfate/mL). Five hundred microliters of medium, containing 2.5×10^5 cells, was centrifuged at 390 rfu for 5 min in 1.5 mL microcentrifuge tubes. The caps of the microcentrifuge tubes were punctured with an 18G needle after pelleting to allow gas exchange. After 3 days in the centrifuge tubes, the pellets were gently aspirated from the tubes and transferred to 6- or 24-well ultralow attachment culture plates (Corning Inc., Corning, NY). Pellets were maintained in chondrogenic medium, with changes every 48–72 hours. On days 10 and 20, a single representative pellet in each group was fixed in 4% paraformaldehyde for histologic processing. The remaining pellets were snap-frozen in liquid nitrogen and stored at −80 degrees Celsius for further analyses.

2.6. Pellet DNA Content. The Hoechst fluorescence assay [35] was used to measure DNA content of the pellets. Three pellets were digested in 250 μL of papain digest (0.15 mg/mL; SIGMA Chemical MPC, St. Louis, MO) for 16 hours at 65°C. Serial dilutions of calf thymus DNA were used to generate a standard curve. Duplicate 10 μL aliquots of each sample and standard were pipetted into black 96-well microplates. Hoechst 33258 fluorescent dye was added in each well and the optical density was measured at 485 nm wavelength

Table 1: Primers used in the qPCR reactions.

Gene (amplicon size)		Primers	Annealing temperature
EF1-alpha (328 bp)	S	5′ CCCGGACACAGAGACTTCAT	62.1°C
	A	5′ AGCATGTTGTCACCATTCCA	
Col II (223 bp)	S	5′ AGCAGGAATTTGGTGTGGAC	62.1°C
	A	5′ TCTGCCCAGTTCAGGTCTCT	
Col X (244 bp)	S	5′ TGCCAACCAGGGTGTAACAG	62.1°C
	A	5′ ACATTACTGGGGTGCCGTTC	
ALP (260 bp)	S	5′ CCACGTCTTCACATTTGGTG	54.2°C
	A	5′ AGACTGCGCCTGGTAGTT	
Aggrecan (202 bp)	S	5′ GACGCCGAGAGCAGGTGT	62.1°C
	A	5′ AAGAAGTTGTCGGGCTGGTT	
Sox9 (304 bp)	S	5′ GAACGCACATCAAGACGGAG	56.2°C
	A	5′ CTGGTGGTCTGTGTAGTCGT	
Mef2c (55 bp)	S	5′ CCCAACTTTGAGTGCCAGT	55.3°C
	A	5′ ATGTGAGGTCTCCACCCATC	
Runx2 (115 bp)	S	5′ CAGACCAGCAGCACTCCATA	56.8°C
	A	5′ GAGCGTCAACACCATTC	

(FLUOstar Optima Microplate Reader, BMG LABTECH, Durham, NC). The values were adjusted to "μg of DNA per pellet."

2.7. Pellet Collagen Type II Content. Three pellets from each treatment group/time point were digested in 50 μL of pepsin-acetic acid (0.5 mg/mL) at 4°C overnight, with continuous mixing on a rotator. The day after, the pellets were transferred to an elastase digestion solution (1 mg/mL pancreatic elastase in 1x TBS) for 24 h. A commercial ELISA assay was used to measure collagen type II protein in each sample, following the manufacturer's recommended protocol (Chondrex Inc., Redmond, WA). Briefly, 100 μL of capture antibody solution was pipetted in each well of 96-well plates and incubated at 4°C overnight. The next day, the wells were washed before adding 50 μL of the sample digests and type II collagen standards. After 2 hours of incubation at room temperature, the detection antibody solution (50 μL) was added to each well, followed by a second incubation. Streptavidin peroxidase solution (100 μL) was then added, followed by a one-hour incubation. Lastly, 100 μL of chromatin dilution buffer solution was added to each well. After 30 min of incubation, 50 μL of stop solution (2N sulfuric acid) was added to each well and the optical densities were measured spectrometrically at 405 nm using a FLUOstar Optima Microplate Reader (BMG LABTECH, Durham, NC). The collagen type II values were converted to "μg/pellet."

2.8. Pellet Sulfated Glycosaminoglycan Content. The dimethyl methylene blue dye-binding (DMMB) assay was used to measure sulfated glycosaminoglycans (sGAG) in the pellets [36]. Three pellets from each treatment/time group were digested in 250 μL of 0.15 mg/mL papain digestion buffer (SIGMA Chemical MPC, St. Louis, MO) for 16 hours at 65°C overnight. The next day, the samples were digested with DNAse at 37°C for 20 minutes. Two hundred microliters of DMMB reagent was added to 50 μL of the digested samples and optical densities were measured at 530 nm (FLUOstar Optima Microplate Reader, BMG LABTECH, Durham, NC), along with serial dilutions of chondroitin sulfate standards. The "sGAG" values were expressed as "μg sGAG/pellet."

2.9. RNA Isolation, Reverse Transcription, and PCR Amplification. Total RNA was extracted using a commercial guanidinium thiocyanate-phenol reagent (Trizol, Invitrogen Corp., Life Technologies, Grand Island, NY), following the manufacturer's instructions. The isolates were purified over silica columns (RNeasy, Qiagen Inc., Hilden, Germany). One microgram of total RNA from each sample was reverse-transcribed (Superscript II, Invitrogen Corp., Life Technologies, Grand Island, NY), using standard protocols and oligo-dT primers.

Gene-specific primers for collagen type II, aggrecan, alkaline phosphatase (ALP), collagen type X, Sox9, Mef2C, and Runx2 (Table 1) were designed from available published sequences in Genbank and using ClustalW multiple sequence alignment (available at http://www.ebi.ac.uk/) and Primer 3 software (http://bioinfo.ut.ee/primer3-0.4.0/). Primer specificity was confirmed by melt curve specificities and by cloning and sequencing the amplicons during optimization experiments. PCR amplifications were catalyzed by Taq DNA polymerase (BioRad iCycler, BioRad Laboratories, Hercules, CA) in the presence of Sybr green. Relative gene expression was quantified using the $2^{-\Delta\Delta CT}$ method [37], corrected for amplification efficiencies, and normalized to expression of the reference gene, elongation factor-1α (EF1α).

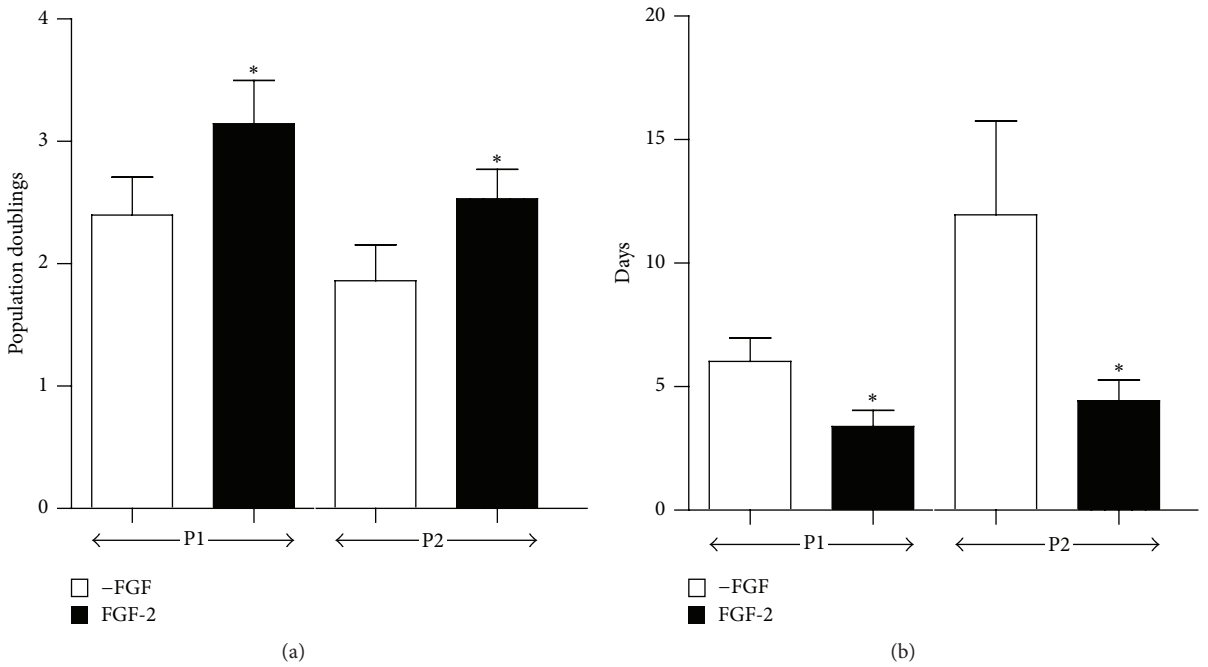

Figure 1: Effect of FGF-2 supplementation on SF-CP proliferation. (a) Population doublings and (b) population doubling (PD) times, during the first (P1) and second (P2) passages, in the absence (white bars) or presence (black bars) of FGF-2 (mean ± SD; $n = 15$). In both figures, asterisks indicate significant differences between the control and FGF-treated cultures at each passage.

2.10. Histologic Examination. One representative pellet from each treatment/time group was fixed in 4% paraformaldehyde for 24 hours. The pellets were then immobilized in cassettes using HistoGel (Richard-Allan Scientific, Radnor, PA), transferred to PBS solution, and stored at 4°C. The pellets were dehydrated in alcohol, embedded in paraffin, sectioned at 8 μm, and stained with Toluidine Blue. Histological images were acquired using 20x and 40x objectives, utilizing the Nanozoomer 2.0 HT Digital Pathology System machine (Hamamatsu Photonics K.K., Hamamatsu, Japan).

2.11. Statistical Analyses. The normality of distribution of the quantitative data (monolayer proliferation, pellet DNA content, pellet sGAG content, pellet collagen type II content, and relative mRNA expression) was confirmed using the Shapiro-Wilk test, the Bell histogram, and Normal Q-Q plot (IBM SPSS Statistics). The data were expressed as "mean ± standard deviation." Paired Student's t-tests were used to assess the effects of FGF-2 on population doubling and population doubling times. Two-way repeated measures ANOVA was used to assess the effect of FGF-2 across time on cell proliferation, pellet DNA content, pellet sGAG content, pellet collagen type II content, and relative mRNA expression. A p value of ≤ 0.05 was considered significant.

3. Results and Discussion

3.1. Results

3.1.1. Cell Expansion. There were, on average, 59.2 CFUs/mL of synovial fluid (range 25.2–178.7 CFUs/mL; $n = 11$) in primary cultures of aspirates. The time between initial seeding of the aspirates and near-confluence of the primary cultures was 17.1 ± 5.2 days. Supplementing media with FGF-2 significantly increased population doubling during both the first (2.59 ± 1.29 in control cultures versus 3.34 ± 1.43 in FGF-2 cultures; $p = 0.013$, $n = 15$) and second (1.86 ± 1.13 in control cultures versus 2.53 ± 0.93 in FGF-2 cultures; $p = 0.063$, $n = 15$; Figure 1(a)) passages. Accepting the variation in responses, this represents an approximate 1.6-fold increase in cell numbers in response to FGF-2 during both passages. FGF-2 also significantly reduced the population doubling times (Figure 1(b)). During the first passage, control cultures required 5.6 ± 3.60 days for each population doubling, while cultures treated with FGF-2 required approximately half this time (2.88 ± 1.93 days; $p = 0.02$, $n = 15$). During the second passage, the mean population doubling time in control cultures increased to 10.25 + 9.25 days. Again, FGF-2 administration reduced the doubling time by approximately 50% (4.48 ± 3.42 days) in the second passage cultures.

3.1.2. Immunophenotypic Analysis. SF-CPs were immunopositive for the three surface cell markers CD29, CD44, and CD90 that characterize equine MSCs [33, 34] and negative for the hematopoietic marker, CD45. FGF-2 administration did not affect the immunophenotype of SF-CPs during monolayer expansion (Figure 2). Further, the immunophenotype of SF-CPs did not change significantly across passages in either group.

3.1.3. Pellet DNA Content. Monolayer expansion of SF-CPs in the presence of FGF-2 had no significant "carry over" effect

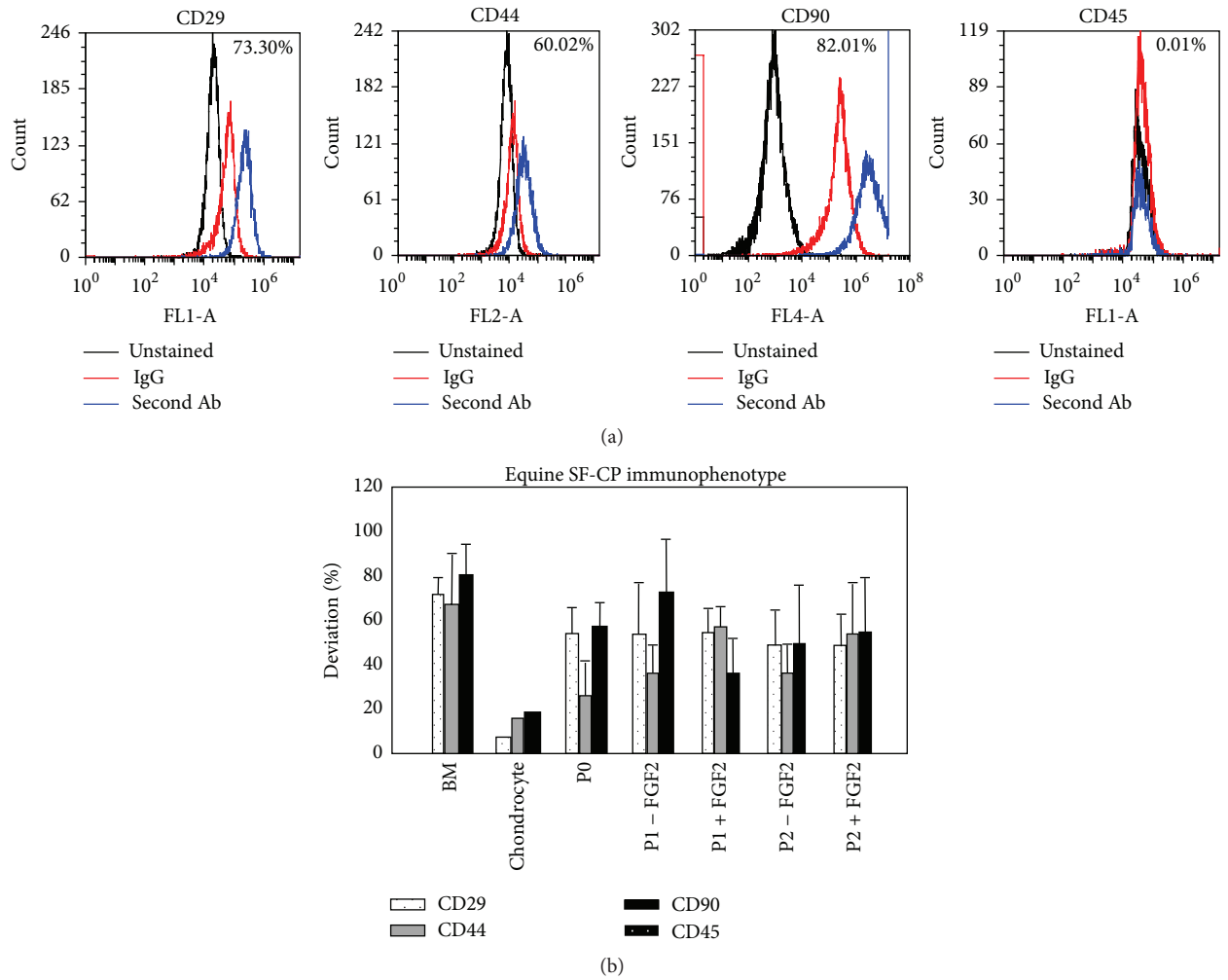

FIGURE 2: SF-CP immunophenotype characterization. (a) Representative immune-phenotypic profile of passage 1 SF-CPs (horse 2), supplemented with FGF-2. (b) Immunophenotypic characterization (mean ± SD) of SF-CPs at passages 0, 1, and 2, along bone marrow (BM) MSCs and chondrocyte control populations ($n = 8$).

on the DNA content of chondrogenic pellets at either time point (Figure 3; $p = 0.913$; $n = 6$). In both the control and FGF-2 pellets, DNA contents were stable at approximately 3 μg/pellet throughout the time course of the experiments.

3.1.4. Chondrogenic Gene Expression. FGF-2 significantly increased Sox9 mRNA levels expression on day 20 (1.5 ± 0.6-fold increase in control pellets versus 3.5 ± 1.05-fold increase in FGF-2 pellets, $p = 0.02$; Figure 4(a)) but had no effect on expression of the transcription factors Runx2 and Mef2c (Figures 4(b) and 4(c)), both required for hypertrophic differentiation [38–41]. FGF-2 increased collagen type II mRNA levels 2-3-fold on day 10 (10.8 ± 13-fold increase in control pellets versus 31.3 ± 39-fold increase in FGF-2 pellets) and day 20 (18.9 ± 20.7-fold increase in control pellets versus 36.6 ± 40.7-fold increase in FGF-2 pellets); however these differences were not statistically significant, due to high interdonor variability (Figure 5(a)). Steady state aggrecan mRNA levels increased approximately 500-fold by day 10 in both the control (458 ± 765-fold increase) and FGF-2 (473 ± 726-fold increase) groups, in comparison to undifferentiated SF-CPs, and this upregulation was sustained on day 20. FGF-2 had no significant effect on aggrecan expression (Figure 5(b)).

Collagen type X and ALP transcript levels were extremely low in all the pellet experiments (threshold cycles were routinely 8–10 higher than in cell populations capable of hypertrophic differentiation; Figures 6(a) and 6(b)). In control pellets, collagen type X transcript levels fell throughout the 20-day culture period (0.63 ± 0.81-fold on day 10 and 0.37 ± 0.36-fold on day 20), while ALP mRNA levels increased only slightly (25.3 ± 42.67 on day 10 and 29.3 ± 38.33 on day 20). FGF-2 did not significantly alter expression of collagen type X (0.33 ± 0.43-fold on day 10 and 0.25 ± 0.20-fold on day 20) or ALP (28.0 ± 42.67-fold on day 10 and 39.33 ± 66.67-fold on day 20), consistent with the Mef2c and Runx2 results.

3.1.5. Pellet Matrix Content. FGF-2 administration did not affect collagen type II protein (on day 10: 0.20 ± 0.04 μg/pellet in control pellets versus 0.19 ± 0.06 μg/pellet in FGF-2 pellets;

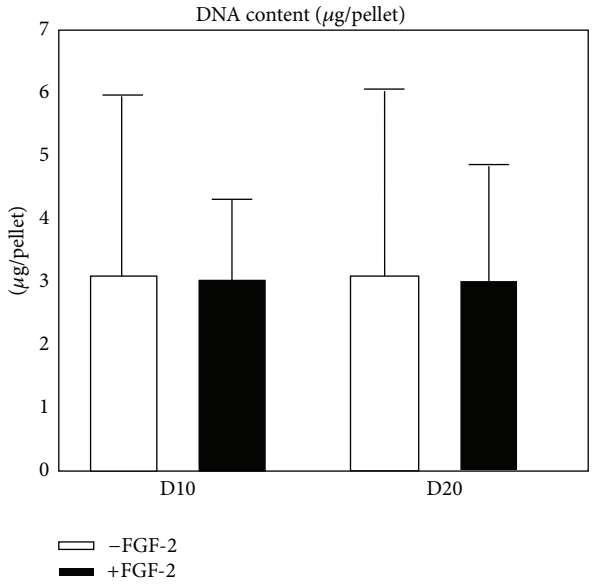

Figure 3: DNA content (μg/pellet) on days 10 and 20 of chondrogenic culture, with (white) or without (black) FGF-2 supplementation ($n = 6$).

on day 20: 0.22 ± 0.02 μg/pellet in control pellets versus 0.23 ± 0.01 μg/pellet in FGF-2 pellets) or sGAG (on day 10: 12.8 ± 4.5 μg/pellet in control pellets versus 10.9 ± 1.8 μg/pellet in FGF-2 pellets; on day 20: 14.5 ± 5.7 μg/pellet in control pellets versus 12.65 ± 4.7 in FGF-2 pellets) contents in the pellets at either time point (Figures 7(a) and 7(b)), consistent with the qPCR results.

3.1.6. Pellet Histology. Toluidine Blue staining intensity, reflecting sGAG content, was not affected by FGF-2 administration during monolayer expansion. Overall pellet size was also unaltered. It was notable, however, that FGF-2 supplementation prevented the development of a flattened "fibroblastic" cell layer that occupied the peripheral 100 μm of control pellets (Figure 8). There were no indications of central hypertrophic differentiation in either group, consistent with the qPCR data.

3.2. Discussion. Consistent with our previous studies [26] and the reports from several other groups [18–25], equine SF-CPs were capable of considerable in vitro proliferation (Figure 1) and subsequent chondrogenic differentiation (Figures 7 and 8). There was considerable variation in the number of CFUs per mL of synovial fluid and the time required for establishing primary SF-CP cultures. These results are consistent with other reports [19, 20, 22] and are likely influenced by the initial uneven distribution of clonal cell groups across the plate surfaces and consequent variation in local cell densities. In light of this, the "80% confluence" designation for primary culture passages should be considered a nominal value.

Monolayer expansion in medium supplemented with FGF-2 significantly increased population doubling and halved the population doubling times during both passages. In this respect, the hypothesis addressing FGF-2's effect on SF-CP proliferation is accepted. This potent mitogenic effect has also been reported in several previous studies in human bone marrow-derived stem cells [30, 42–45] with 2-3-fold increases in proliferation rates being reported. FGF-2 exerts its mitogenic effects via the MAPK signaling pathway [30, 42, 46], accelerating transit through the G1 phase of the cell cycle [47]. The proliferative activity of the control cultures during passage 2 was noticeably less than during passage 1, reflected by reduced population doublings and a twofold increase in the PD time (Figure 1). Although all control cultures did reach confluence during P2, these outcomes suggest that control cultures were approaching senescence. Proliferative failure was reported by Kurose et al., 2010, in six of 25 synovial fluid samples from human knee OA patients [20]. FGF-2 supplementation slows the development of senescence in proliferating bone marrow-derived stem cell populations [48–50], and it is highly likely that FGF-2 influences progenitor cells from synovial fluid similarly. Collectively, the increased population doublings during passage and reduced population doubling times stimulated by FGF-2 mitigate a major obstacle to using of SF-CPs for potential clinical applications, such as intrinsic cartilage repair, tissue engineered cartilage, and the immune-modulation of inflammatory arthritis [20, 28, 29].

Accepting species differences in progenitor cell immunoprofiles, the cell surface marker profiles from equine SF-CPs were consistent with results from other studies [20, 27–29] and were characteristic of equine MSCs (CD29+, CD44+, CD90+, and CD45−; [33, 34]). The impact of FGF-2 on SF-CP proliferation did not negatively influence the immunophenotype of the expanded cell populations. Of particular interest, the relative expression of these stem cell markers did not change significantly during multiple passages, suggesting that there was no "enrichment" process occurring through selective stem cell proliferation. Rather, the immunophenotypic consistency across passages suggests that SF-CPs were the predominant cell type engaged in population expansion in the primary cultures and subsequent passages.

FGF-2 administration during monolayer expansion did not negatively impact subsequent SF-CP chondrogenesis, despite the reported detrimental effects of prolonged expansion on MSC chondrogenic capacity [42] and the more general "dedifferentiating" effects prolonged monolayer expansion exerts on the chondrocytic phenotype [5, 6]. FGF-2 increased steady state mRNA levels of the chondrogenic transcription factor, Sox9, on day 20, and both collagen type II and aggrecan transcripts were also increased by FGF-2, although not to a statistically significant degree. Despite these effects, FGF administration did not alter collagen type II protein or sGAG deposition within the pellet matrices. In light of these outcomes, the hypothesis addressing FGF-2's effect on SF-CP chondrogenesis is rejected. This "disconnection" between transcriptional and translational productivity is a common observation in stem cell/tissue engineering biology and indicates that the biosynthetic capacities of newly in vitro differentiated MSCs do not match those of fully differentiated cell populations [42, 51]. This limitation will need to be

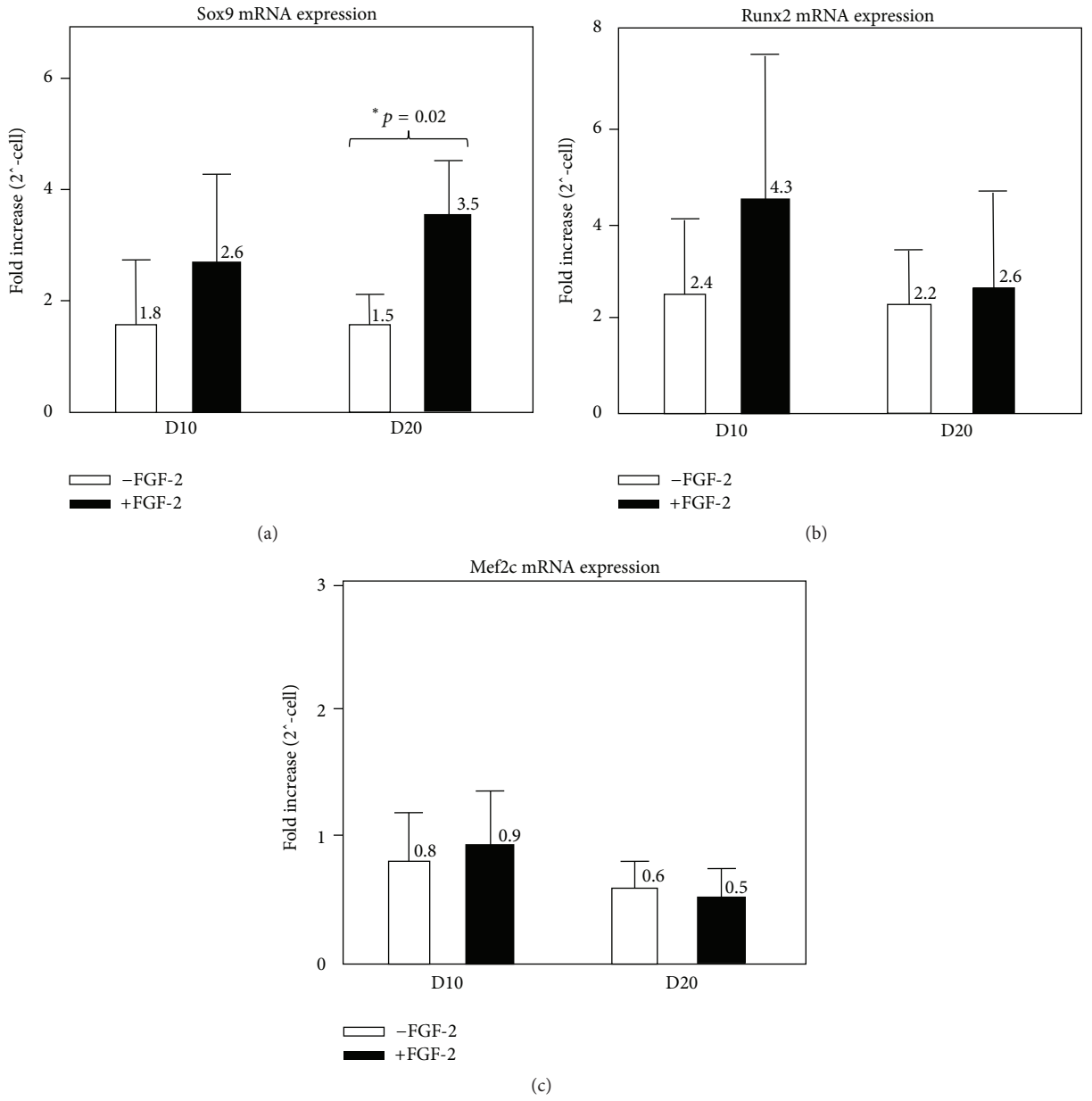

Figure 4: Sox9 (a), Runx2 (b), and Mef2c (c) mRNA expression (fold increase) on days 10 and 20 of chondrogenic culture with (white) or without (black) FGF-2 supplementation ($n = 3; 3; 3$).

resolved for stem cell applications to be successful in tissue engineering applications.

Although there was no quantitative effect on cartilage matrix production, FGF-2 clearly improved the histological characteristics and cytomorphology of the chondrogenic pellets, preventing the development of a zone of flattened cells around the pellet surface, approximately 100 μm deep (Figure 8). This peripheral zone of flattened "dedifferentiated" or "perichondral" cells is a consistent feature of MSC and chondrocytic pellet culture models [6, 29, 30, 32, 42, 52] and is considerably more substantial than the flattened superficial zone of mature articular cartilage [53]. The absence of this feature in pellets from FGF-treated SF-CPs suggests that expansion in the presence of FGF-2 generates a phenotypic homogeneity in the expanded population that is not present in populations expanded in FBS alone.

Chondrogenic equine SF-CPs do not express hypertrophic chondrocytic markers (collagen type X or ALP) under control culture conditions, and FGF-supplementation did not affect this. The threshold cycles for these genes in the SF-CP samples were routinely between 8 and 10 cycles (2-3 logs) higher than thresholds in cell populations (such as growth plate chondrocytes and bone marrow-derived MSCs) undergoing robust hypertrophy (data not shown).

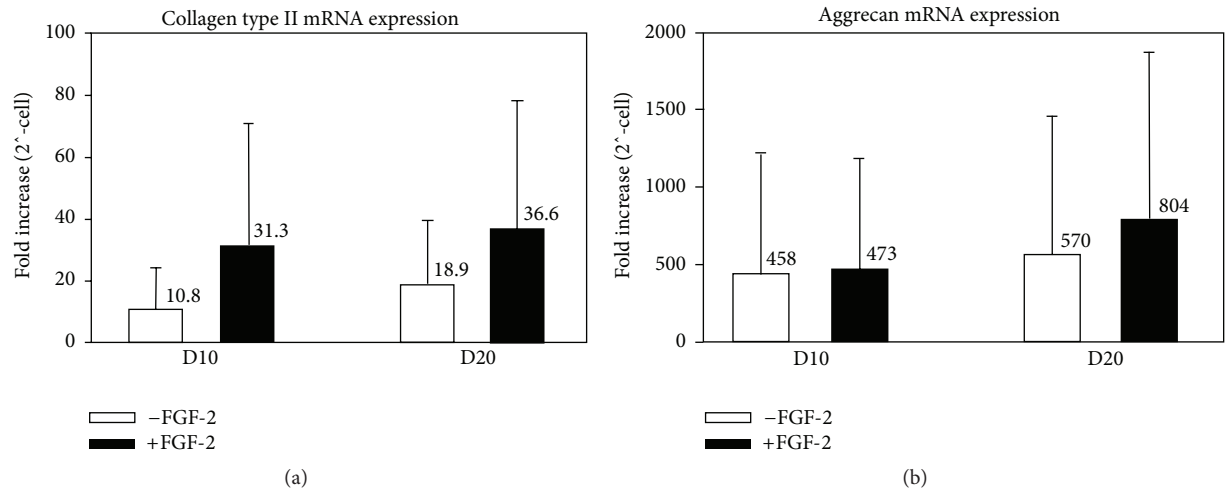

Figure 5: Collagen type II (a) and aggrecan (b) mRNA expression (fold increase) on days 10 and 20 of chondrogenic culture with (white) or without (black) FGF-2 supplementation (n = 5; 5).

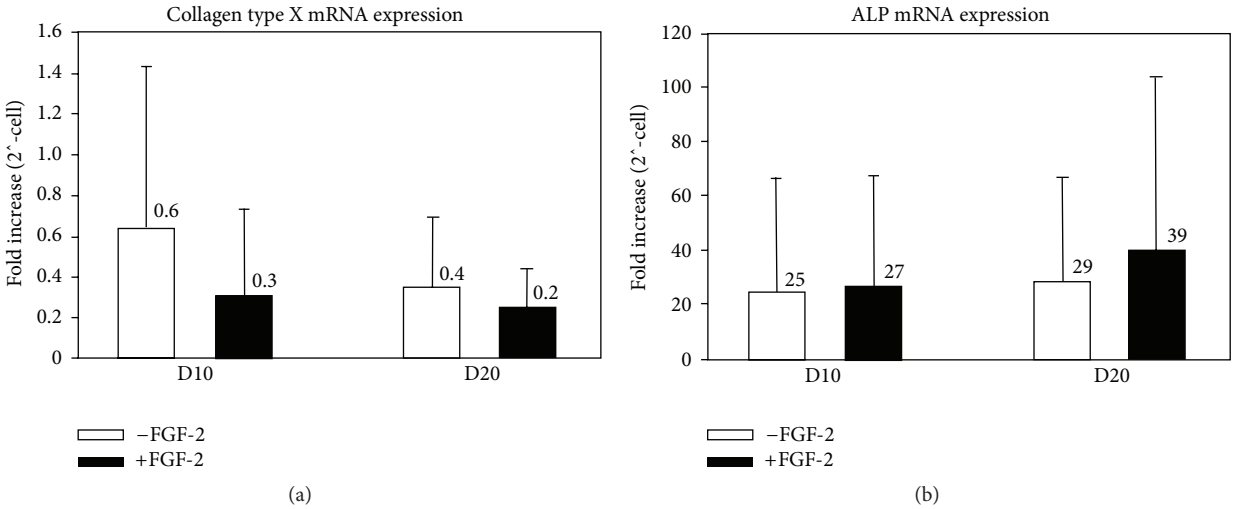

Figure 6: Collagen type X (a) and ALP (b) mRNA expression (fold increase) on days 10 and 20 of chondrogenic culture with (white) or without (black) FGF-2 supplementation (n = 3; 5).

This "nonhypertrophic" phenotype lends credence to the use of SF-CPs for articular cartilage repair applications, since the phenotypic match is far closer than with other MSC sources.

The source(s) of SF-CPs has not yet been definitively determined. Chondroprogenitors are present in the subchondral bone marrow compartment and, under appropriate pathological conditions [54], migrate into fibrillated cartilage and the joint space. However, there were no overt arthritic changes in the joints of the horses used in this study, and increased numbers of SF-CPs were found in the synovial fluids of early arthritic disease cases in people [18], prior to the development of overt cartilage fibrillation or penetration into the subchondral bone space. Comparative gene expression profiling by Morito et al., 2008 [21], and by Sekiya et al., 2012 [22], strongly suggested that SF-CPs are derived from the synovium, rather than the bone marrow compartment, and this possibility is also supported by the findings of Jones et al., 2008 [18], in that the number of synovial fluid CFUs correlated with the prevalence of microscopic synovial tissue fragments in the fluid aspirates, and of Zhang et al., 2004, who demonstrated that synovial fluid contains chemotactic factors that recruit stem cells from osteoarthritic synovium [55]. In severely pathological joints, it is possible that progenitors in synovial fluid originate from several intra- and periarticular tissue sources, the synovium [21, 22, 57], subchondral bone space [54], and the articular cartilage itself [55, 56]. Future research should focus on identifying the sources of SF-CPs and developing strategies to utilize these cells to support articular cartilage homeostasis and repair.

4. Conclusions

FGF-2 significantly increased SF-CPs in vitro expansion, significantly increasing population doublings and reducing

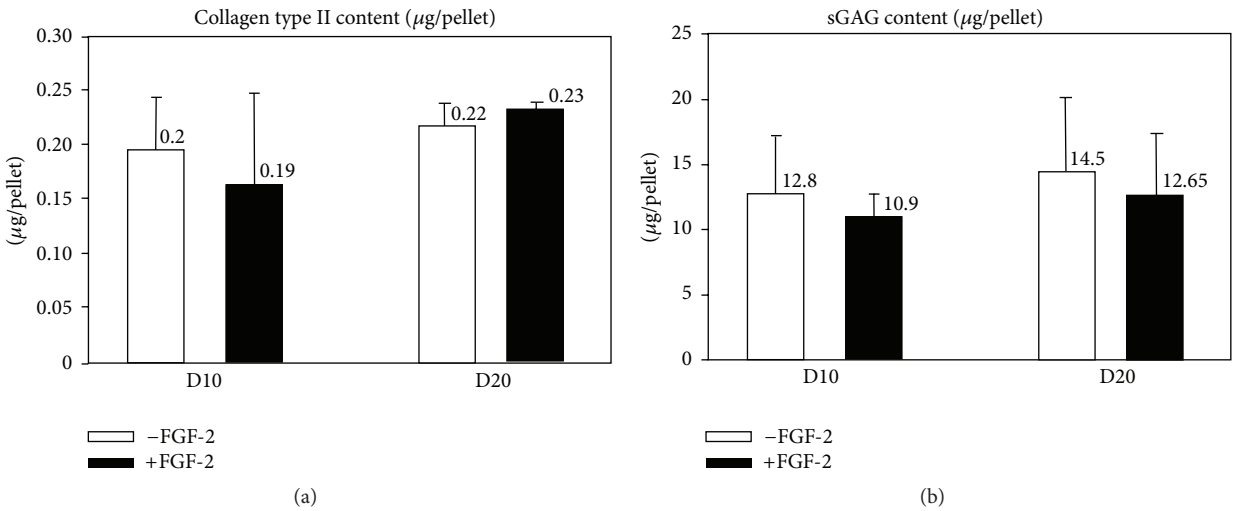

Figure 7: Collagen type II (a) and sGAG (b) proteins content (μg/pellet) on days 10 and 20 of chondrogenic culture with (white) or without (black) FGF-2 supplementation ($n = 5$).

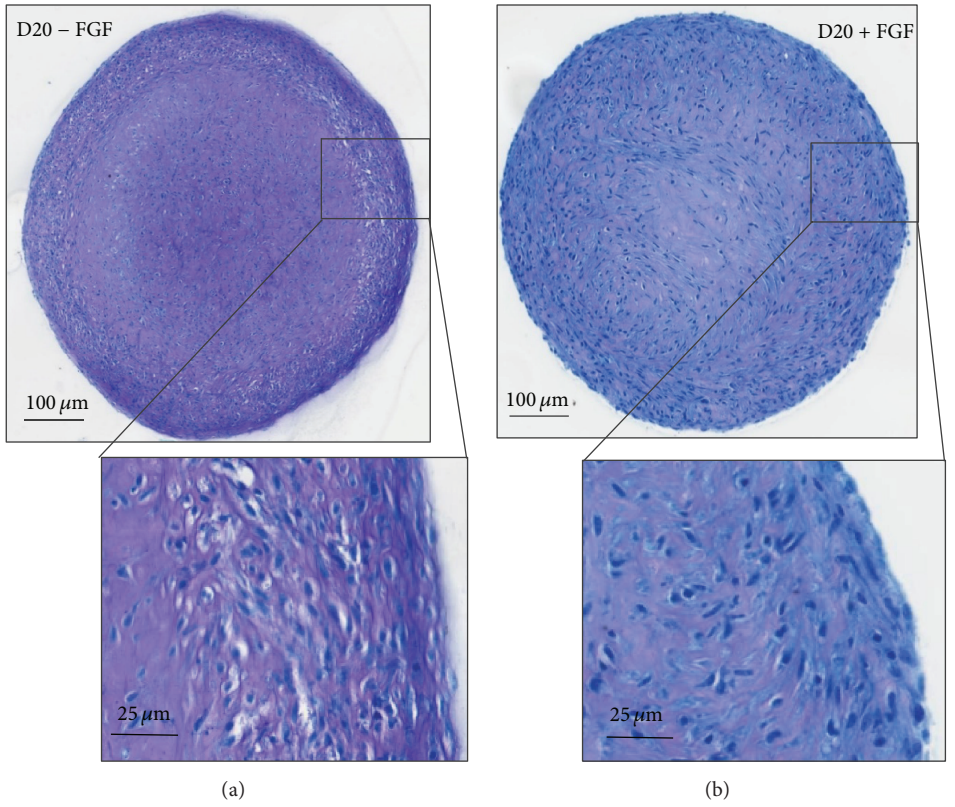

Figure 8: Histological sections of chondrogenic pellets on day 20. Pellets from cells expanded in control medium (a) or medium supplemented with FGF-2 (b) were stained with Toluidine Blue.

population doubling times. FGF-2 did not affect the immunophenotype of SF-CPs during expansion or compromise subsequent SF-CP chondrogenesis. FGF-2 did prevent the development of a flattened "fibroblastic" cell layer around the periphery of the pellets indicating a phenotypic homogeneity in the expanded cell populations. FGF-2 supplementation of SF-CP monolayer cultures significantly accelerates population expansion prior to subsequent clinical applications for articular cartilage repair.

Conflict of Interests

The authors declare that there is no conflict of interests regarding the publication of this paper.

Acknowledgment

This study was funded by the United States Department of Agriculture's Section 1433 Animal Health and Diseases program.

References

[1] T. Aigner and L. McKenna, "Molecular pathology and pathobiology of osteoarthritic cartilage," *Cellular and Molecular Life Sciences*, vol. 59, no. 1, pp. 5–18, 2002.

[2] O. F. W. Gardner, C. W. Archer, M. Alini, and M. J. Stoddart, "Chondrogenesis of mesenchymal stem cells for cartilage tissue engineering," *Histology and Histopathology*, vol. 28, no. 1, pp. 23–42, 2013.

[3] A. Mobasheri, G. Kalamegam, G. Musumeci, and M. E. Batt, "Chondrocyte and mesenchymal stem cell-based therapies for cartilage repair in osteoarthritis and related orthopaedic conditions," *Maturitas*, vol. 78, no. 3, pp. 188–198, 2014.

[4] E. A. Makris, A. H. Gomoll, K. N. Malizos, J. C. Hu, and K. A. Athanasiou, "Repair and tissue engineering techniques for articular cartilage," *Nature Reviews Rheumatology*, vol. 11, no. 1, pp. 21–34, 2015.

[5] S.-W. Kang, S. P. Yoo, and B.-S. Kim, "Effect of chondrocyte passage number on histological aspects of tissue-engineered cartilage," *Bio-Medical Materials and Engineering*, vol. 17, no. 5, pp. 269–276, 2007.

[6] M. C. Stewart, K. M. Saunders, N. Burton-Wurster, and J. N. Macleod, "Phenotypic stability of articular chondrocytes in vitro: effects of culture models, bone morphogenetic protein 2, and serum supplementation," *Journal of Bone and Mineral Research*, vol. 15, no. 1, pp. 166–174, 2000.

[7] A. M. Mackay, S. C. Beck, J. M. Murphy, F. P. Barry, C. O. Chichester, and M. F. Pittenger, "Chondrogenic differentiation of cultured human mesenchymal stem cells from marrow," *Tissue Engineering*, vol. 4, no. 4, pp. 415–428, 1998.

[8] J. U. Yoo, T. S. Barthel, K. Nishimura et al., "The chondrogenic potential of human bone-marrow-derived mesenchymal progenitor cells," *The Journal of Bone and Joint Surgery—American Volume*, vol. 80, no. 12, pp. 1745–1757, 1998.

[9] M. Al-Nbaheen, R. vishnubalaji, D. Ali et al., "Human stromal (mesenchymal) stem cells from bone marrow, adipose tissue and skin exhibit differences in molecular phenotype and differentiation potential," *Stem Cell Reviews and Reports*, vol. 9, no. 1, pp. 32–43, 2013.

[10] Y. Sakaguchi, I. Sekiya, K. Yagishita, and T. Muneta, "Comparison of human stem cells derived from various mesenchymal tissues: superiority of synovium as a cell source," *Arthritis and Rheumatism*, vol. 52, no. 8, pp. 2521–2529, 2005.

[11] M. A. Vidal, S. O. Robinson, M. J. Lopez et al., "Comparison of chondrogenic potential in equine mesenchymal stromal cells derived from adipose tissue and bone marrow," *Veterinary Surgery*, vol. 37, no. 8, pp. 713–724, 2008.

[12] H. Wegmeyer, A.-M. Bröske, M. Leddin et al., "Mesenchymal stromal cell characteristics vary depending on their origin," *Stem Cells & Development*, vol. 22, no. 19, pp. 2606–2618, 2013.

[13] M. Q. Wickham, G. R. Erickson, J. M. Gimble, T. P. Vail, and F. Guilak, "Multipotent stromal cells derived from the infrapatellar fat pad of the knee," *Clinical Orthopaedics and Related Research*, vol. 412, pp. 196–212, 2003.

[14] H. Yoshimura, T. Muneta, A. Nimura, A. Yokoyama, H. Koga, and I. Sekiya, "Comparison of rat mesenchymal stem cells derived from bone marrow, synovium, periosteum, adipose tissue, and muscle," *Cell and Tissue Research*, vol. 327, no. 3, pp. 449–462, 2007.

[15] F. Barry, R. E. Boynton, B. Liu, and J. M. Murphy, "Chondrogenic differentiation of mesenchymal stem cells from bone marrow: differentiation-dependent gene expression of matrix components," *Experimental Cell Research*, vol. 268, no. 2, pp. 189–200, 2001.

[16] D. A. De Ugarte, K. Morizono, A. Elbarbary et al., "Comparison of multi-lineage cells from human adipose tissue and bone marrow," *Cells Tissues Organs*, vol. 174, no. 3, pp. 101–109, 2003.

[17] K. Pelttari, A. Winter, E. Steck et al., "Premature induction of hypertrophy during in vitro chondrogenesis of human mesenchymal stem cells correlates with calcification and vascular invasion after ectopic transplantation in SCID mice," *Arthritis & Rheumatism*, vol. 54, no. 10, pp. 3254–3266, 2006.

[18] E. A. Jones, A. English, K. Henshaw et al., "Enumeration and phenotypic characterization of synovial fluid multipotential mesenchymal progenitor cells in inflammatory and degenerative arthritis," *Arthritis and Rheumatism*, vol. 50, no. 3, pp. 817–827, 2004.

[19] E. A. Jones, A. Crawford, A. English et al., "Synovial fluid mesenchymal stem cells in health and early osteoarthritis: detection and functional evaluation at the single-cell level," *Arthritis and Rheumatism*, vol. 58, no. 6, pp. 1731–1740, 2008.

[20] R. Kurose, S. Ichinohe, G. Tajima et al., "Characterization of human synovial fluid cells of 26 patients with osteoarthritis knee for cartilage repair therapy," *International Journal of Rheumatic Diseases*, vol. 13, no. 1, pp. 68–74, 2010.

[21] T. Morito, T. Muneta, K. Hara et al., "Synovial fluid-derived mesenchymal stem cells increase after intra-articular ligament injury in humans," *Rheumatology*, vol. 47, no. 8, pp. 1137–1143, 2008.

[22] I. Sekiya, M. Ojima, S. Suzuki et al., "Human mesenchymal stem cells in synovial fluid increase in the knee with degenerated cartilage and osteoarthritis," *Journal of Orthopaedic Research*, vol. 30, no. 6, pp. 943–949, 2012.

[23] W. Ando, J. J. Kutcher, R. Krawetz et al., "Clonal analysis of synovial fluid stem cells to characterize and identify stable mesenchymal stromal cell/mesenchymal progenitor cell phenotypes in a porcine model: a cell source with enhanced commitment to the chondrogenic lineage," *Cytotherapy*, vol. 16, no. 6, pp. 776–788, 2014.

[24] B. A. Jones and M. Pei, "Synovium-derived stem cells: A tissue-specific stem cell for cartilage engineering and regeneration," *Tissue Engineering—Part B: Reviews*, vol. 18, no. 4, pp. 301–311, 2012.

[25] R. J. Krawetz, Y. E. Wu, L. Martin, J. B. Rattner, J. R. Matyas, and D. A. Hart, "Synovial fluid progenitors expressing CD90+ from normal but not osteoarthritic joints undergo chondrogenic differentiation without micro-mass culture," *PLoS ONE*, vol. 7, no. 8, Article ID e43616, 2012.

[26] M. Stewart, Y. Chen, E. Caporali, and A. Stewart, "Isolation and chondrogenic differentiation of cells isolated from synovial fluid," *Regenerative Medicine*, vol. 4, no. 6, pp. S27–S28, 2009.

[27] E. Alegre-Aguarn, P. Desportes, F. Garca-Lvarez, T. Castiella, L. Larrad, and M. J. Martnez-Lorenzo, "Differences in surface marker expression and chondrogenic potential among various tissue-derived mesenchymal cells from elderly patients with osteoarthritis," *Cells Tissues Organs*, vol. 196, no. 3, pp. 231–240, 2012.

[28] W. J. Lee, Y. S. Hah, S. A. Ock et al., "Cell source-dependent in vivo immunosuppressive properties of mesenchymal stem cells derived from the bone marrow and synovial fluid of minipigs," *Experimental Cell Research*, vol. 333, no. 2, pp. 273–288, 2015.

[29] H. Tang, W. Chen, C. Chiang, L. Chen, Y. Chang, and C. Chen, "Differentiation effects of platelet-rich plasma concentrations on synovial fluid mesenchymal stem cells from pigs cultivated in alginate complex hydrogel," *International Journal of Molecular Sciences*, vol. 16, no. 8, pp. 18507–18521, 2015.

[30] L. A. Solchaga, K. Penick, J. D. Porter, V. M. Goldberg, A. I. Caplan, and J. F. Welter, "FGF-2 enhances the mitotic and chondrogenic potentials of human adult bone marrow-derived mesenchymal stem cells," *Journal of Cellular Physiology*, vol. 203, no. 2, pp. 398–409, 2005.

[31] Y. Hiraki, C. Shukunami, K. Iyama, and H. Mizuta, "Differentiation of chondrogenic precursor cells during the regeneration of articular cartilage," *Osteoarthritis and Cartilage*, vol. 9, pp. S102–S108, 2001.

[32] A. A. Stewart, C. R. Byron, H. Pondenis, and M. C. Stewart, "Effect of fibroblast growth factor-2 on equine mesenchymal stem cell monolayer expansion and chondrogenesis," *American Journal of Veterinary Research*, vol. 68, no. 9, pp. 941–945, 2007.

[33] C. De Schauwer, G. R. Van de Walle, S. Piepers et al., "Successful isolation of equine mesenchymal stromal cells from cryopreserved umbilical cord blood-derived mononuclear cell fractions," *Equine Veterinary Journal*, vol. 45, no. 4, pp. 518–522, 2013.

[34] C. De Schauwer, S. Piepers, G. R. Van de Walle et al., "In search for cross-reactivity to immunophenotype equine mesenchymal stromal cells by multicolor flow cytometry," *Cytometry Part A*, vol. 81, no. 4, pp. 312–323, 2012.

[35] Y.-J. Kim, R. L. Y. Sah, J.-Y. H. Doong, and A. J. Grodzinsky, "Fluorometric assay of DNA in cartilage explants using Hoechst 33258," *Analytical Biochemistry*, vol. 174, no. 1, pp. 168–176, 1988.

[36] R. W. Farndale, C. A. Sayers, and A. J. Barrett, "A direct spectrophotometric microassay for sulfated glycosaminoglycans in cartilage cultures," *Connective Tissue Research*, vol. 9, no. 4, pp. 247–248, 1982.

[37] K. J. Livak and T. D. Schmittgen, "Analysis of relative gene expression data using real-time quantitative PCR and the $2^{-\Delta\Delta C_T}$ method," *Methods*, vol. 25, no. 4, pp. 402–408, 2001.

[38] M. Inada, T. Yasui, S. Nomura et al., "Maturational disturbance of chondrocytes in Cbfa1-deficient mice," *Developmental Dynamics*, vol. 214, no. 4, pp. 279–290, 1999.

[39] I. S. Kim, F. Otto, B. Zabel, and S. Mundlos, "Regulation of chondrocyte differentiation by Cbfa1," *Mechanisms of Development*, vol. 80, no. 2, pp. 159–170, 1999.

[40] H. Enomoto, M. Enomoto-Iwamoto, M. Iwamoto et al., "Cbfa1 is a positive regulatory factor in chondrocyte maturation," *The Journal of Biological Chemistry*, vol. 275, no. 12, pp. 8695–8702, 2000.

[41] M. A. Arnold, Y. Kim, M. P. Czubryt et al., "MEF2C transcription factor controls chondrocyte hypertrophy and bone development," *Developmental Cell*, vol. 12, no. 3, pp. 377–389, 2007.

[42] L. A. Solchaga, K. Penick, V. M. Goldberg, A. I. Caplan, and J. F. Welter, "Fibroblast growth factor-2 enhances proliferation and delays loss of chondrogenic potential in human adult bone-marrow-derived mesenchymal stem cells," *Tissue Engineering Part A*, vol. 16, no. 3, pp. 1009–1019, 2010.

[43] A. M. Handorf and W.-J. Li, "Fibroblast growth Factor-2 primes human mesenchymal stem cells for enhanced chondrogenesis," *PLoS ONE*, vol. 6, no. 7, Article ID e22887, 2011.

[44] R. B. Jakobsen, E. Østrup, X. Zhang, T. S. Mikkelsen, and J. E. Brinchmann, "Analysis of the effects of five factors relevant to in vitro chondrogenesis of human mesenchymal stem cells using factorial design and high throughput mRNA-profiling," *PLoS ONE*, vol. 9, no. 5, Article ID e96615, 2014.

[45] D. Correa, R. Somoza, P. Lin et al., "Sequential exposure to fibroblast growth factors (FGF) 2, 9 and 18 enhances hMSC chondrogenic differentiation," *Osteoarthritis and Cartilage*, vol. 23, no. 3, pp. 443–453, 2015.

[46] R. Goetz and M. Mohammadi, "Exploring mechanisms of FGF signalling through the lens of structural biology," *Nature Reviews Molecular Cell Biology*, vol. 14, no. 3, pp. 166–180, 2013.

[47] D. Gospodarowicz, I. Vlodavsky, and N. Savion, "The extracellular matrix and the control of proliferation of vascular endothelial and vascular smooth muscle cells," *Journal of Supramolecular Structure*, vol. 13, no. 3, pp. 339–372, 1980.

[48] G. Bianchi, A. Banfi, M. Mastrogiacomo et al., "Ex vivo enrichment of mesenchymal cell progenitors by fibroblast growth factor 2," *Experimental Cell Research*, vol. 287, no. 1, pp. 98–105, 2003.

[49] B. Gharibi and F. J. Hughes, "Effects of medium supplements on proliferation, differentiation potential, and in vitro expansion of mesenchymal stem cells," *Stem Cells Translational Medicine*, vol. 1, no. 11, pp. 771–782, 2012.

[50] S. Tsutsumi, A. Shimazu, K. Miyazaki et al., "Retention of multilineage differentiation potential of mesenchymal cells during proliferation in response to FGF," *Biochemical and Biophysical Research Communications*, vol. 288, no. 2, pp. 413–419, 2001.

[51] T. B. Kurth, F. Dell'Accio, V. Crouch, A. Augello, P. T. Sharpe, and C. De Bari, "Functional mesenchymal stem cell niches in adult mouse knee joint synovium in vivo," *Arthritis and Rheumatism*, vol. 63, no. 5, pp. 1289–1300, 2011.

[52] A. A. Stewart, C. R. Byron, H. C. Pondenis, and M. C. Stewart, "Effect of dexamethasone supplementation on chondrogenesis of equine mesenchymal stem cells," *American Journal of Veterinary Research*, vol. 69, no. 8, pp. 1013–1021, 2008.

[53] R. Fujioka, T. Aoyama, and T. Takakuwa, "The layered structure of the articular surface," *Osteoarthritis and Cartilage*, vol. 21, no. 8, pp. 1092–1098, 2013.

[54] S. Koelling, J. Kruegel, M. Irmer et al., "Migratory chondrogenic progenitor cells from repair tissue during the later stages of human osteoarthritis," *Cell Stem Cell*, vol. 4, no. 4, pp. 324–335, 2009.

[55] S. Zhang, T. Muneta, T. Morito, T. Mochizuki, and I. Sekiya, "Autologous synovial fluid enhances migration of mesenchymal stem cells from synovium of osteoarthritis patients in tissue culture system," *Journal of Orthopaedic Research*, vol. 26, no. 10, pp. 1413–1418, 2008.

[56] R. Williams, I. M. Khan, K. Richardson et al., "Identification and clonal characterisation of a progenitor cell sub-population in normal human articular cartilage," *PLoS ONE*, vol. 5, no. 10, Article ID e13246, 2010.

[57] D. Harvanová, T. Tóthová, M. Šarišský, J. Amrichová, and J. Rosocha, "Isolation and characterization of synovial mesenchymal stem cells," *Folia Biologica*, vol. 57, no. 3, pp. 119–124, 2011.

Hindawi Publishing Corporation
Stem Cells International
Volume 2016, Article ID 7132751, 7 pages
http://dx.doi.org/10.1155/2016/7132751

Review Article

Peripheral Blood Monocytes as Adult Stem Cells: Molecular Characterization and Improvements in Culture Conditions to Enhance Stem Cell Features and Proliferative Potential

Hendrik Ungefroren,[1] Ayman Hyder,[2,3] Maren Schulze,[4] Karim M. Fawzy El-Sayed,[5,6] Evelin Grage-Griebenow,[1] Andreas K. Nussler,[7] and Fred Fändrich[2]

[1]*First Department of Medicine, UKSH, Campus Lübeck, Ratzeburger Allee 160, 23538 Lübeck, Germany*
[2]*Clinic for Applied Cellular Medicine, UKSH, Campus Kiel, Arnold-Heller Strasse 3, Haus 18, 24105 Kiel, Germany*
[3]*Faculty of Science, Damietta University, Damietta 34517, Egypt*
[4]*Department of General, Visceral and Transplantation Surgery, University Hospital Essen, Hufelandstrasse 55, 45147 Essen, Germany*
[5]*Clinic for Conservative Dentistry and Periodontology, School of Dental Medicine, UKSH, Campus Kiel, Arnold-Heller Strasse 3, Haus 26, 24105 Kiel, Germany*
[6]*Oral Medicine and Periodontology Department, Faculty of Oral and Dental Medicine, Cairo University, 1 Mathaf El Manial Street, Giza, Egypt*
[7]*BG Unfallklinik Tübingen, Eberhard Karls Universität Tübingen, Schnarrenbergstraße 95, 72076 Tübingen, Germany*

Correspondence should be addressed to Hendrik Ungefroren; hendrik.ungefroren@uksh.de

Received 19 June 2015; Accepted 26 August 2015

Academic Editor: Ming Li

Adult stem or programmable cells hold great promise in diseases in which damaged or nonfunctional cells need to be replaced. We have recently demonstrated that peripheral blood monocytes can be differentiated *in vitro* into cells resembling specialized cell types like hepatocytes and pancreatic beta cells. During phenotypic conversion, the monocytes downregulate monocyte/macrophage differentiation markers, being indicative of partial dedifferentiation, and are partially reprogrammed to acquire a state of plasticity along with expression of various markers of pluripotency and resumption of mitosis. Upregulation of stem cell markers and mitotic activity in the cultures was shown to be controlled by autocrine production/secretion of activin A and transforming growth factor-beta (TGF-β). These reprogrammed monocyte derivatives were termed "programmable cells of monocytic origin" (PCMO). Current efforts focus on establishing culture conditions that increase both the plasticity and proliferation potential of PCMO in order to be able to generate large amounts of blood-derived cells suitable for both autologous and allogeneic therapies.

1. Introduction

Adult stem or programmable cells represent a promising alternative to embryonic stem cells in regenerative medicine and in tissue engineering [1]. Although not considered a classical adult stem cell, monocytes have been shown to be capable of acquiring stem cell-like properties [2–5]. Peripheral blood monocytes have some practical advantages over other types of adult stem/progenitor cells when they are used for clinical purposes: (1) they can be retrieved from a readily accessible body compartment by a low-invasive procedure or are incurred as waste products in blood donations; (2) they can be readily maintained in culture; (3) they have a low risk of tumorigenicity due to their limited proliferative capacity and the lack of *telomerase reverse transcriptase* (hTERT) [6]; (4) they can be applied to patients in both an autologous and an allogeneic setting, obviating the need for immunosuppression. Autologous cell material for transplantation may otherwise only be derived from adult stem cell populations such as bone marrow-derived stem cells or from human embryonic stem cells generated by somatic cell nuclear transfer or from cells with induced pluripotency (iPS). However, all these potential cell sources suffer from biological, economic, and/or ethical drawbacks [7].

Serious disadvantages of using monocytes are their limited number in the blood circulation and their low proliferation potential *in vitro*. For transplantation purposes, it is necessary to increase cell yields by *in vitro* expansion. Another obstacle is the monocytes' varying differentiation potential into specialized cell types which is largely donor-dependent. To be clinically relevant, conditions should be optimized towards the production of large amounts of cells from one single donor. Therefore, the main goal is to enhance the cells' proliferation potential during culture while at the same time maintaining or even improving their differentiation potential towards the desired cell type. In the course of this paper, we provide an overview on the molecular events during the dedifferentiation phase, for example, when the cells acquire their stem cell-like characteristics, and subsequently discuss various strategies that have been showing promise to increase cell numbers during *in vitro* culture.

2. Macrophage Phenotypic and Functional Heterogeneity and Monocyte Plasticity

The circulating monocyte is a very versatile progenitor cell that gives rise to diverse cell types. It is generated from hematopoietic stem cells via the common myeloid progenitor (CMP) and the granulocyte/monocyte progenitor which represents the precursor populations for monoblasts. Monoblasts are the earliest form committed to becoming monocytes and their progeny emigrates from the bone marrow into the peripheral blood. When not recruited to inflammatory lesions, peripheral blood monocytes are capable of undergoing maturation into several types of tissue-resident macrophages (reviewed in [8]) such as resting tissue macrophages, Kupffer cells, Langerhans cells of the skin, dendritic cells, microglia, osteoclasts, and endothelial cells. When appropriately stimulated, monocytes will migrate to sites of inflammation and extravasate from the circulation into the tissues, acquiring the characteristics of an activated macrophage with an inflammatory phenotype. In an acute inflammatory response, this usually entails production of inflammatory cytokines, antimicrobial oxidative radicals, tissue-debriding proteinases, and an elevated phagocytic activity. Once the wound is cleared of inflammatory debris, macrophages contribute to the process of wound resolution, promoting angiogenesis, matrix production, and cell proliferation. This functional switch to an alternatively activated, anti-inflammatory, and regeneration-promoting phenotype appears to be initiated by phagocytosis of apoptotic cells and to be regulated by a variety of tissue-derived cytokines, hormones, and metabolites [9]. In certain carcinomas, macrophages can be recruited into this tissue to adopt a specific phenotype that eventually promotes tumor progression. These tumor-associated macrophages (TAMs) are chronically polarized to exhibit activities that support tumor growth and metastasis, suppress adaptive immune responses, and hence resemble an alternatively activated type [9]. How the functional plasticity of monocytes/macrophages is generated is currently a matter of debate [9].

Functional heterogeneity of macrophages may depend on the differentiation of functional sublineages, or alternatively macrophages are functionally plastic cells which are capable of altering their functional activities progressively in response to changing signals generated in their microenvironment (functional plasticity hypothesis). The functional plasticity and regenerative potential of monocytes/macrophages may be much greater than what is previously thought. Several cultured human cell populations that originate from circulating monocytes have the capacity to differentiate into nonphagocytic pluripotent stem cell-like cells such as pluripotent stem cells (PSCs) [2], MOMC [3, 5], CD14+CD34^{low}KDR+ subset [10], and PCMO [4, 11, 12].

3. Differentiation Potential of PCMO and Molecular Evidence for Monocytes as Potential Stem Cells

Recently, we have developed a protocol to induce from monocytes by *in vitro* culture an apparently more plastic derivative, which we named "programmable cells of monocytic origin" (PCMO). These cells following a 4–6-day treatment with macrophage colony-stimulating factor (M-CSF), interleukin-3 (IL-3), and human serum were susceptible following exposure to appropriate induction media to differentiate into cells with endothelial characteristics, chondrocytes, and osteoblasts/osteocytes (manuscript in preparation). A study by Yang and coworkers suggested *in situ* osteogenic differentiation of and bone formation by transplanted human PBMNCs [13]. We have also shown earlier that PCMO generated from human peripheral blood or from either blood or spleen of a nonhuman primate can be converted to insulin-producing cells [4]. However, our focus was on PCMO-derived hepatocyte-like cells (so-called NeoHepatocytes), which express various hepatocyte markers and exhibit hepatocyte-specific metabolic functions *in vitro* and *in vivo* [4, 11]. Intriguingly, NeoHepatocytes were able to improve survival in a rat model of acute liver failure [14] and monocyte-derived hepatocyte-like cells even showed promise in the treatment of HBV-related decompensated liver cirrhosis [15]. A more general loss of the monocyte/macrophage phenotype would thus be in favor of a dedifferentiation process and would lend support to our contention that PCMO represent cells which have reverted to a more primitive progenitor with less restricted differentiation potential. In line with this, it was found that in response to the specific culture conditions monocytes silence the monopoietic marker genes *PRDMI* and *ICSBP* while maintaining expression of the lineage-specific transcription factors *PU.1* [4]. Even more informative was the pattern of Krüppel-like factor 4 (Klf4), a nuclear factor of monocyte → macrophage differentiation which is expressed in a monocyte-restricted and stage-specific pattern during myelopoiesis and promotes inflammatory monocyte differentiation [16]. *Klf4* was rapidly silenced following exposure of monocytes to PCMO culture conditions and transcript levels remained low until day 6 after which they became undetectable. Other markers associated with specialized functions, for example, those involved in sensing and killing of invading microorganisms such as CD14, toll-like receptors (TLRs 2, 4, 7, and 9),

Table 1: List of specific genes and their mode of regulation during the monocyte → PCMO conversion.

Downregulated genes	Upregulated genes
PRDMI	OCT4 (A isoform)
ICSBP	NANOG
KLF4	Myc
CD14	
TLRs (2, 4, 7, 9)	
Nox4	
$p47^{phox}$	

and two subunits of the reactive oxygen producing enzyme NAD(P)H oxidase (Nox4 and $p47^{phox}$), respectively, were downregulated although with different kinetics [6]. Expression of TLRs and Nox4 was dramatically decreased at the transcriptional level on day 6 of culture, while expression of $p47^{phox}$ remained unaltered at the mRNA level but appeared to be downregulated at the protein level starting from day 2 in PCMO medium [6]. A list of markers that are downregulated during the monocyte → PCMO conversion is provided in Table 1.

3.1. Expression and Reactivation of Pluripotency Markers during PCMO Generation. Despite the well-documented broad differentiation potential of monocytes, surprisingly little is known about the mechanisms which allow them to maintain an uncommitted precursor state. We therefore wondered whether the mechanisms underlying the phenotypic plasticity of ESCs also operate in PCMO. In this respect, we provided evidence at the mRNA and protein level that PCMO share in common several markers of ESCs such as OCT4 (also termed POU5f, including OCT4A, the isoform associated with pluripotency) and NANOG [6]. Both proteins can function as activators of self-renewal and pluripotency genes and as repressors of lineage commitment genes. Interestingly, the endogenous *OCT4* and *NANOG* genes appear to be reactivated and the kinetics corresponded well with the time-dependent pattern of sensitivity towards hepatocytic differentiation [6]. Other genes implicated in maintenance of self-renewal and pluripotency and expressed in PCMO include *growth and differentiation factor 3* (*GDF3*), *DPPA3*/*STELLA*/*PGC7*, *ABCG2*, *Connexin-43*, *NCAM*, *DNMT3b*, *UTF*, *BMP2*, *CRIPTO*/*TDGF1*, *E-CADHERIN*, and *CD105*. Other genes like *SOX2*, *GABRB3*, *NODAL*, *LEFTY B*, and *hTERT* were negative in PCMO. The data indicate that critical pluripotency regulators (e.g., OCT4 and NANOG) and possibly other factors of the pluripotency network, such as Myc (see Table 1), are reactivated in PCMO and likely control their plastic behavior. Indeed, PCMO appear to resemble in some aspects partially reprogrammed cell lines [17] in that they reactivate genes related to stem cell renewal and maintenance (e.g., *MYC*) and pluripotency (*OCT4*, *NANOG*). These results show that in appropriate growth factor environment circulating monocytes can, at least partially, be reprogrammed without exogenous introduction of pluripotency factors.

3.2. TGF-β/Activin Signaling and Enhancement of Pluripotency Marker Expression. In ES cells, maintenance of and exit from the undifferentiated stage are primarily controlled by members of the TGF-β/activin family of growth factors through regulation of the pluripotency-associated transcription factors OCT4 and NANOG [18, 19]. There is also evidence for a role of TGF-β/activin-related factors in regulating stemness of monocytes/PCMO. We have shown recently that TGF-β and its receptors, TGF-β type II receptor and activin receptor-like kinase 5 (ALK5), are expressed in PCMO. Moreover, we found that TGF-β is secreted by PCMO into the culture supernatant as determined by ELISA, with levels of TGF-β1 declining during monocyte conversion to PCMO. In contrast, levels of activin A (the β_A-β_A homodimer) in the culture supernatants *increased* until day 4 of culture. Interestingly, PCMO express not only the activin A ligand but also the receptors ActRIIA and ALK4, both of which were upregulated until day 4 of culture, suggesting enhanced responsiveness of the cells to (autocrine) activin stimulation. Reciprocal autocrine signaling by TGF-β and activin in the cultures was confirmed by the demonstration that C-terminal phosphorylation/activation of Smad3, the primary target of ALK5, declined until day 4 of culture, while activation of Smad2, the primary target of ALK4, rose over the same time period. We confirmed sensitivity of PCMO to activin signaling by showing that recombinant activins (A, B, and AB) induced C-terminal phosphorylation of Smad2 but not Smad3.

3.3. Epigenetic Changes during PCMO Generation. The methylation of histones plays a crucial role in epigenetic regulation of gene expression during mammalian development. In general, transcribed genes are associated with trimethylation at Lys-4 of histone H3 (me-H3(K4)) [20], whereas many silenced genes are associated with H3(K27) trimethylation [21]. Interestingly, the induction of both *NANOG* and *OCT4* coincided with transient changes in histone modifications indicative of transcriptional (re)activation [6]. In undifferentiated cells, the *OCT4* promoter is packaged with nucleosomes that contain markers of active chromatin, namely, histone H3 highly acetylated at Lys-9 and Lys-14, and me-H3(K4) [22]. We noted a transient rise in global me-H3(K4) in PCMO cultures that closely mirrored the time course of *OCT4* transcriptional activity. The methylation of the *OCT4* promoter remained high during various stages of PCMO generation, as revealed by bisulfite conversion and pyrosequencing at specific CpG islands in the *OCT4* distal enhancer [6], suggesting that promoter demethylation was not the underlying mechanism of *OCT4* induction. Preliminary data indicate that treatment of PCMO with 5-azacytidine can increase their plasticity. We are currently studying whether this is reflected also in the upregulation of pluripotency-determining genes.

4. Culture Conditions Favoring Stem Cell Features of Monocyte

We are currently pursuing three strategies to enhance the stem cell character of PCMO under the assumption that a

more stem cell-like progenitor will impact the phenotype of the desired differentiated cell type: (1) avoidance of activating/differentiation stimuli (proinflammatory agents and bacterial components) which might prevent proper dedifferentiation of monocytes, (2) comparison of PCMO plasticity and proliferative activity of PCMO under suspended and adherent growth conditions, and (3) enhancement of PCMO plasticity/pluripotency marker expression by modulation of activin and TGF-β signaling.

4.1. Avoidance of Activating/Differentiation Stimuli Which Might Prevent Proper Dedifferentiation of Monocytes. In order to prevent activation to proinflammatory macrophages, it seems mandatory to deplete the medium of the cells of any potential proinflammatory agents, bacterial components, or foreign antigens that cause activation of monocytes in the course of an immune reaction. Our data clearly demonstrate that the use of autologous serum reduced initial macrophage activation in PCMO cultures and subsequently improved both yield and function of differentiated NeoHepatocytes. An autologous approach might also be useful in other stem cell preparation processes where cell activation during generation shall be kept to a minimum.

4.2. Comparison of PCMO Plasticity of PCMO under Suspended and Adherent Growth Conditions. Adherence of primary peripheral blood monocytes is essential for the differentiation into macrophages. On the other side, PCMO development must be accompanied by keeping a state of *de*differentiation. To keep cells in *de*differentiated state, it is theoretically logic to culture them in suspension to prevent differentiation into macrophages from occurring. The switch from suspended to adherent growth which was associated with changes in cell morphology [4] also affected proteins involved in cell adhesion and cytoskeletal regulation such as $p60^{Src}$ in β-actin and E-cadherin (which all increased) over the 4–6-day culture period [6]. Together, these data suggest that monocytes during their conversion to PCMO undergo partial *de*differentiation. The expressions of the stem cell marker genes *OCT4* and *NANOG* were higher in adherent than in suspended cells.

The comparison of the resulting differentiated NeoHepatocytes, which originated from adherent and suspended PCMO, showed mixed results. Cells in suspension resulted in NeoHepatocytes with higher levels of CYP1A1/2, CYP2D6, and UDPG and higher urea metabolism, while adherent PCMO resulted in NeoHepatocytes with higher SRB-1 and glucose metabolism. These hepatocyte-specific assays may indicate an independent regulation of PCMO plasticity and proliferation.

4.3. Enhancement of PCMO Plasticity/Pluripotency Marker Expression by Modulation of Activin and TGF-β Signaling. We have recently shown that during PCMO generation pluripotency marker expression is controlled positively by activin/Smad2 and negatively by TGF-β/Smad3 signaling. Specifically, inhibition of autocrine activin signaling by the activin-binding protein follistatin reduced both Smad2 activation and OCT4A/NANOG upregulation. It can be concluded that treatment of PCMO with activin(s) would enhance OCT4A/NANOG expression and pluripotency. Conversely, inhibition of autocrine TGF-β signaling by anti-TGF-β antibody reduced Smad3 activation and moderately enhanced OCT4A/NANOG expression arguing for TGF-β inhibition as an additional or complementary strategy to increase stemness in PCMO. Several TGF-β pathway inhibitors (that should not cross-inhibit activin signaling such as the commonly used ALK4/5 small molecule inhibitor SB431542) are available for this purpose [23].

5. Strategies to Enhance the Proliferation Potential of PCMO

As mentioned above, expansion and differentiation conditions must be optimized towards the production of large amounts of PCMO from one single donor. We have previously shown that monocytes resume proliferation under PCMO culture conditions [6]; however, the percentage of cells that reentered mitosis was still low. Apart from the use of autologous serum which improved the yield of differentiated NeoHepatocytes by increasing cell numbers during the PCMO stage [24], we are currently pursuing three other strategies to achieve this: (1) enhancement of proliferation following adhesion culture, (2) coculture of PCMO with lymphocytes, and (3) addition of mitogenic growth factors.

5.1. Comparison of PCMO Proliferation under Suspended and Adherent Growth Conditions. We have compared the proliferative activities of PCMO cultured in suspension *versus* adherence. Proliferation was studied by immunofluorescence for Ki67 that marks the development from G1- to S-phase in the cell cycle. In contrast to our expectations, the data showed that proliferation of PCMO was *higher* in adherently growing than in suspended cultures as revealed by the appearance of a subset of Ki67-positive monocytes and downregulation of $p21^{WAF1}$ [25].

5.2. Enhancement of Proliferation following Coculture of PCMO with Autologous Lymphocytes. The ultimate goal is to enhance the cells' proliferation potential during PCMO culture without impairing their differentiation potential and to further enhance the differentiation potential without compromising their proliferative activity. We observed that PCMO proliferation was much higher in mixed cultures (PBMC "contaminated" with autologous lymphocytes) than in pure cultures of monocytes purified by elutriation, indicating that direct cell-cell interactions or factors secreted by lymphocytes are interacting with PCMO to increase their proliferation. In order to clarify the role of autologous lymphocytes in PCMO proliferation, elutriated monocytes were cocultured with increasing numbers of lymphocytes from the same donor in separated inserts with a pore size of 0.4 μm that allow for the transfer of micromolecules but not of cells (Figure 1(a), top). Our results showed an increase in the fraction of Ki67-positive monocytes that was proportional to the number of cocultured lymphocytes (expressed by the lymphocyte : monocyte ratio, Figure 1).

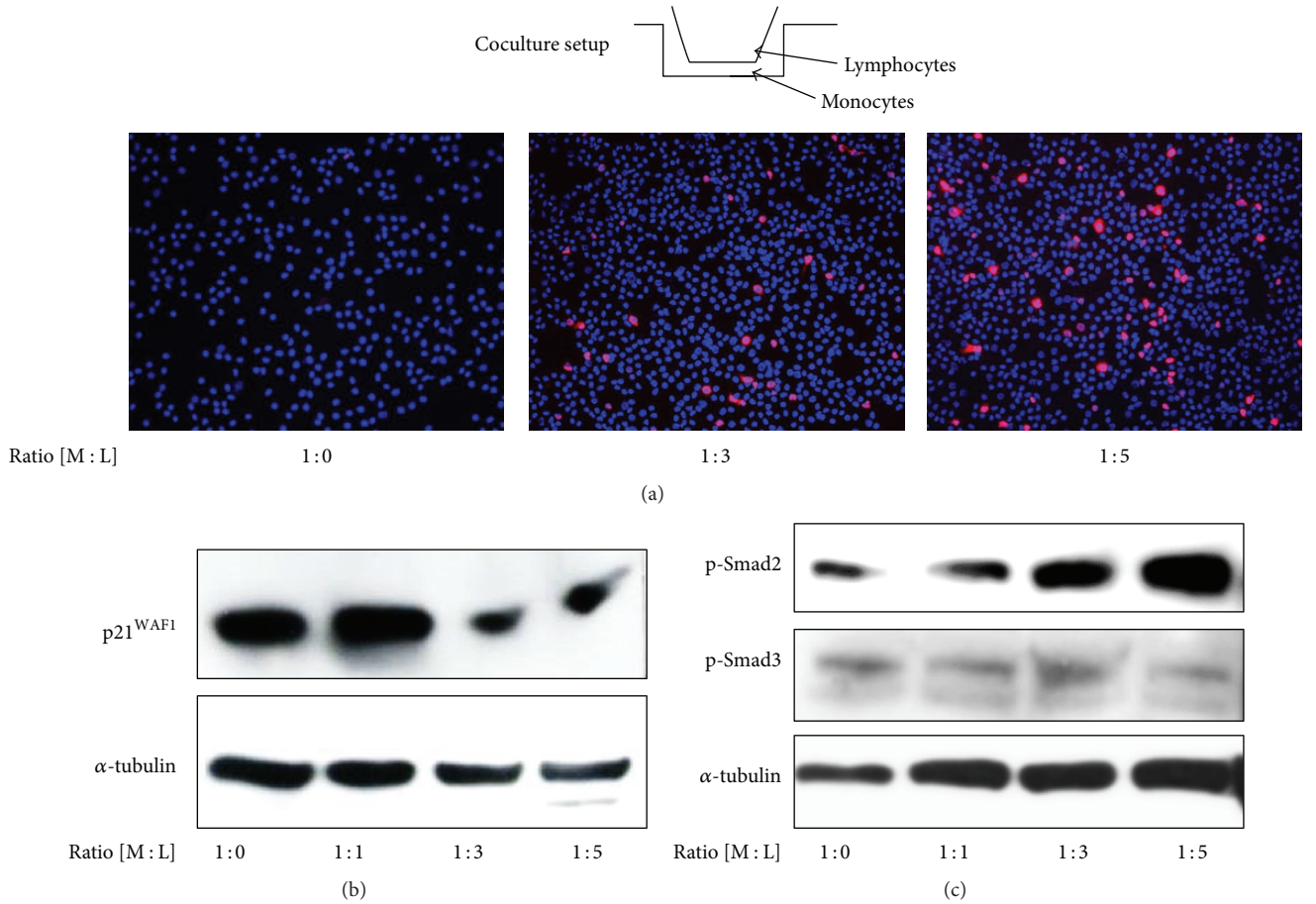

FIGURE 1: Coculture with lymphocytes increases the fraction of mitotically active PCMO. (a) Adherently growing peripheral blood monocytes isolated by elutriation were indirectly cocultured with increasing numbers of autologous lymphocytes in transwell inserts (top, pore size 0.4 μm). Ratios of monocytes (M) : lymphocytes (L) are indicated below the images. After 4 days, cultured cells were fixed and double-stained with an antibody to Ki67 (magenta) and DAPI (blue) as control. The procedure of elutriation was described previously [25]. (b) Detection of $p21^{WAF1}$ expression in elutriated monocytes cocultured with lymphocytes at different ratios. After coculture, monocytes were lysed and analyzed for expression of $p21^{WAF1}$ by immunoblotting. The housekeeping protein α-tubulin served as a loading control. (c) As in (b), except that the immunoblots were probed with antibodies to phospho-Smad2 (p-Smad2) and phospho-Smad3 (p-Smad3). Signal strengths of Smad3 and Smad2 should be assessed relative to those for α-tubulin.

The increase in mitotically active monocytes was accompanied by a downregulation of the cell cycle inhibitor $p21^{WAF1}$ at monocyte : lymphocyte ratios greater than 1 : 1 (Figure 1(b)) and likely reflects a derepression from growth arrest. Since $p21^{WAF1}$ is induced by TGF-β/Smad3 signaling and TGF-β1 is present in supernatants of PCMO cultures [25], we addressed the question as to whether lymphocytes may inhibit TGF-β signaling activity by monitoring the activation status of Smad3 (and Smad2 as control) by phosphoimmunoblotting. In cocultured monocytes, a decrease in phosphorylation of Smad3 was observed relative to monocultured monocytes, while activation of Smad2 was only marginally affected when assessed relative to the levels of the housekeeping protein α-tubulin (Figure 1(c)). These results suggest that autologous lymphocytes enhance the proliferation of monocytes by suppressing the growth-inhibitory TGF-β/Smad3/$p21^{WAF1}$ axis.

5.3. Enhancement of Proliferation following Addition of Mitogenic Growth Factors

5.3.1. EGF/HB-EGF. During earlier studies we observed activation of extracellular signal-regulated kinase (ERK)1 in monocytes with its activity peaking on days 3-4 of PCMO culture [4]. Since the MEK/ERK pathway is activated prominently by epidermal growth factor (EGF), which is known to induce proliferation in many types of cells and its receptor is overexpressed in proliferative cells [26], we evaluated possible direct effects of EGF on PCMO proliferation. Heparin-binding epidermal growth factor (HB-EGF), 20–22 kDa glycoprotein from the EGF family, was also reported to have proliferative effects and to be a potent mitogen for many cell types [27]. Human peripheral blood monocytes were reported to express a functional EGF receptor (EGFR) [28, 29], while the EGF receptors c-erbB2, c-erbB3,

and c-erbB4 have not been studied. However, a link between EGF or HB-EGF and proliferation in monocytes has not yet been reported.

EGF and HB-EGF enhanced cell proliferation of PCMO as demonstrated by increased expression of cycle control genes (ABL, ANAPC2, CDC2, CDK4, and CDK6), an increase in phosphorylation of the retinoblastoma protein (Rb → pRb → ppRb), and increased PCMO cell numbers after stimulation with EGF or HB-EGF [30]. EGF also raised the number of monocytes expressing the proliferation marker Ki67. PCMO expressed the EGF receptors EGFR (ERBB1) and ERBB3, and expression of both increased during PCMO generation. Phosphoimmunoblotting of PCMO indicated that both EGF and HB-EGF activated MEK-1/2 and ERK1/2 in a concentration-dependent fashion with the effect of EGF being more prominent [30]. EGF treatment further decreased expression of $p47^{phox}$ and increased that of NANOG indicating enhanced *de*differentiation and pluripotency, respectively. Treatment with both EGF and HB-EGF resulted in NeoHepatocytes with improved functional parameters [30]. The results suggested that the addition of EGF or HB-EGF to PCMO differentiation medium superactivates MEK/ERK signaling which then increases proliferation of PCMO and functional differentiation of PCMO-derived NeoHepatocytes.

5.3.2. TGF-β/Activin. A screening for agents that stimulate PCMO proliferation resulted in the identification of the ALK4/5/7 inhibitor SB431542 [31] as an agent that increased the total number of PCMO, probably by preventing the cytostatic function of TGF-β on PCMO. Inhibition of autocrine TGF-β signaling by either SB431542 or anti-TGF-β antibody reduced Smad3 activation and strongly increased the number of Ki67-positive cells. Relief from growth inhibition is primarily the result of reduced TGF-β/Smad3 and, to a lesser extent, activin/Smad2 signaling [25]. Inhibition of TGF-β receptors during PCMO culture seems to be a suitable tool to further expand PCMO in order to maximize cell yield for future transplantation purposes. However, since SB431542 also inhibits ALK4 and ALK7 and thus activin signaling, care must be taken that this function is not at the expense of a decrease in pluripotency. More specific inhibitors of TGF-β signaling need to be employed to avoid this problem [23].

6. Concluding Remarks

Within the last decade, we and others have contributed to the realization that monocytes are extremely versatile and plastic cells and that this feature might be exploited *in vitro* to utilize these cells as stem cell-like cells in regenerative medicine. Various cell preparations derived from peripheral blood monocytes have been shown to express markers of pluripotency/ESCs such as OCT4 and NANOG, although their stem cell function has not been demonstrated unequivocally. On a larger scale, similarities were found between transcriptomic profiles of macrophages and murine undifferentiated ESCs but not differentiated stem cells [32]. Moreover, the similarity of monocytes with adult stem cells is also evident from the observation that efficient reprogramming of adult (neural) stem cells to monocytes can be achieved by ectopic expression of only a single gene, namely, PU.1 [33]. PCMO display several features of partially reprogrammed cell lines such as partial reactivation of genes related to stem cell renewal and maintenance (such as *MYC*) and some pluripotency genes (*OCT4* and *NANOG*) and incomplete repression of lineage-specifying transcription factors (such as PU.1). Another feature of stable partially reprogrammed cell lines is DNA hypermethylation at pluripotency-related loci. Based on these observations, it may be possible to further enhance the stem cell character of PCMO and eventually induce a pluripotent state through genetic complementation of *SOX2*, silencing of *PU.1*, and/or treatment of PCMO with small-molecule compounds that modify chromatin or enhance the action of pluripotency factors. It should be mentioned, however, that there is the possibility that the reexpression of *OCT4* in monocytes/PCMO in response to MCSF/IL-3/serum exposure does not reflect a physiological mechanism; nevertheless, it may result in a therapeutically relevant cell type. Interestingly, we observed some similarities in marker expression between PCMO and alternatively activated macrophages such as AMAC-1, FoxP3, and IDO (HU, unpublished). Since M2-polarized macrophages are known to fulfill regenerative functions following tissue damage in the course of an inflammatory process, they not only may contribute to the healing process by secretion of cytokines but also may themselves act as stem cell cells to restore tissue-specific cells. In this respect and in light of our data that autologous serum reduced initial macrophage activation in PCMO and improved both yield and function of differentiated NeoHepatocytes (see above), it would be interesting to compare PCMO with classically activated, alternatively activated, or deactivated macrophages for their expression of pluripotency-determining genes and their multipotency. We believe that both phenotype and metabolic function of PCMO-derived specialized cell types, for example, NeoHepatocytes, can be improved not only by optimizing the conditions for cell-type specific differentiation but also by enhancing even more effectively the PCMO plasticity through the above mentioned strategies.

Conflict of Interests

The authors declare that there is no conflict of interests regarding the publication of this paper.

References

[1] M. Schulze, F. Fändrich, H. Ungefroren, and B. Kremer, "Adult stem cells—perspectives in treatment of metabolic diseases," *Acta Gastro-Enterologica Belgica*, vol. 68, no. 4, pp. 461–465, 2005.

[2] Y. Zhao, D. Glesne, and E. Huberman, "A human peripheral blood monocyte-derived subset acts as pluripotent stem cells," *Proceedings of the National Academy of Sciences of the United States of America*, vol. 100, no. 5, pp. 2426–2431, 2003.

[3] M. Kuwana, Y. Okazaki, H. Kodama et al., "Human circulating $CD14^+$ monocytes as a source of progenitors that exhibit mesenchymal cell differentiation," *Journal of Leukocyte Biology*, vol. 74, no. 5, pp. 833–845, 2003.

[4] M. Ruhnke, H. Ungefroren, A. Nussler et al., "Differentiation of in vitro-modified human peripheral blood monocytes into hepatocyte-like and pancreatic islet-like cells," *Gastroenterology*, vol. 128, no. 7, pp. 1774–1786, 2005.

[5] N. Seta and M. Kuwana, "Derivation of multipotent progenitors from human circulating $CD14^+$ monocytes," *Experimental Hematology*, vol. 38, no. 7, pp. 557–563, 2010.

[6] H. Ungefroren, S. Groth, A. Hyder et al., "The generation of programmable cells of monocytic origin involves partial repression of monocyte/macrophage markers and reactivation of pluripotency genes," *Stem Cells and Development*, vol. 19, no. 11, pp. 1769–1780, 2010.

[7] N. M. P. King and J. Perrin, "Ethical issues in stem cell research and therapy," *Stem Cell Research and Therapy*, vol. 5, no. 4, article 85, 2014.

[8] S. Gordon and P. R. Taylor, "Monocyte and macrophage heterogeneity," *Nature Reviews Immunology*, vol. 5, no. 12, pp. 953–964, 2005.

[9] R. D. Stout, S. K. Watkins, and J. Suttles, "Functional plasticity of macrophages: In situ reprogramming of tumor-associated macrophages," *Journal of Leukocyte Biology*, vol. 86, no. 5, pp. 1105–1109, 2009.

[10] P. Romagnani, F. Annunziato, F. Liotta et al., "CD14+$CD34^{low}$ cells with stem cell phenotypic and functional features are the major source of circulating endothelial progenitors," *Circulation Research*, vol. 97, no. 4, pp. 314–322, 2005.

[11] M. Ruhnke, A. K. Nussler, H. Ungefroren et al., "Human monocyte-derived neohepatocytes: a promising alternative to primary human hepatocytes for autologous cell therapy," *Transplantation*, vol. 79, no. 9, pp. 1097–1103, 2005.

[12] F. Fändrich and H. Ungefroren, "The programmable cell of monocytic origin (PCMO): a potential adult stem/progenitor cell source for the generation of islet cells," *Advances in Experimental Medicine and Biology*, vol. 654, pp. 667–682, 2010.

[13] H. S. Yang, G. H. Kim, W.-G. La et al., "Enhancement of human peripheral blood mononuclear cell transplantation-mediated bone formation," *Cell Transplantation*, vol. 20, no. 9, pp. 1445–1452, 2011.

[14] M. Glanemann, G. Gaebelein, N. Nussler et al., "Transplantation of monocyte-derived hepatocyte-like cells (NeoHeps) improves survival in a model of acute liver failure," *Annals of Surgery*, vol. 249, no. 1, pp. 149–154, 2009.

[15] L. Yan, Y. Han, J. Wang, J. Liu, L. Hong, and D. Fan, "Peripheral blood monocytes from patients with HBV related decompensated liver cirrhosis can differentiate into functional hepatocytes," *American Journal of Hematology*, vol. 82, no. 11, pp. 949–954, 2007.

[16] J. K. Alder, R. W. Georgantas III, R. L. Hildreth et al., "Kruppel-like factor 4 is essential for inflammatory monocyte differentiation in vivo," *Journal of Immunology*, vol. 180, no. 8, pp. 5645–5652, 2008.

[17] T. S. Mikkelsen, J. Hanna, X. Zhang et al., "Dissecting direct reprogramming through integrative genomic analysis," *Nature*, vol. 454, no. 7200, pp. 49–55, 2008.

[18] K.-S. Park, "TGF-beta family signaling in embryonic stem cells," *International Journal of Stem Cells*, vol. 4, no. 1, pp. 18–23, 2011.

[19] D. James, A. J. Levine, D. Besser, and A. Hemmati-Brivanlou, "TGFβ/activin/nodal signaling is necessary for the maintenance of pluripotency in human embryonic stem cells," *Development*, vol. 132, no. 6, pp. 1273–1282, 2005.

[20] H. Santos-Rosa, R. Schneider, A. J. Bannister et al., "Active genes are tri-methylated at K4 of histone H3," *Nature*, vol. 419, no. 6905, pp. 407–411, 2002.

[21] L. A. Boyer, K. Plath, J. Zeitlinger et al., "Polycomb complexes repress developmental regulators in murine embryonic stem cells," *Nature*, vol. 441, no. 7091, pp. 349–353, 2006.

[22] N. Feldman, A. Gerson, J. Fang et al., "G9a-mediated irreversible epigenetic inactivation of Oct-3/4 during early embryogenesis," *Nature Cell Biology*, vol. 8, no. 2, pp. 188–194, 2006.

[23] I. Calone and S. Souchelnytskyi, "Inhibition of TGFβ signaling and its implications in anticancer treatments," *Experimental Oncology*, vol. 34, no. 1, pp. 9–16, 2012.

[24] S. Ehnert, C. Seeliger, H. Vester et al., "Autologous serum improves yield and metabolic capacity of monocyte-derived hepatocyte-like cells: possible implication for cell transplantation," *Cell Transplantation*, vol. 20, no. 9, pp. 1465–1477, 2011.

[25] H. Ungefroren, A. Hyder, H. Hinz et al., "Pluripotency gene expression and growth control in cultures of peripheral blood monocytes during their conversion into programmable cells of monocytic origin (PCMO): evidence for a regulatory role of autocrine activin and TGF-β," *PLOS ONE*, vol. 10, no. 2, Article ID e0118097, 2015.

[26] B. A. Schiff, A. B. McMurphy, S. A. Jasser et al., "Epidermal growth factor receptor (EGFR) is overexpressed in anaplastic thyroid cancer, and the EGFR inhibitor gefitinib inhibits the growth of anaplastic thyroid cancer," *Clinical Cancer Research*, vol. 10, no. 24, pp. 8594–8602, 2004.

[27] T. M. Nolan, N. Di Girolamo, M. T. Coroneo, and D. Wakefield, "Proliferative effects of heparin-binding epidermal growth factor-like growth factor on pterygium epithelial cells and fibroblasts," *Investigative Ophthalmology and Visual Science*, vol. 45, no. 1, pp. 110–113, 2004.

[28] D. J. Lamb, H. Modjtahedi, N. J. Plant, and G. A. A. Ferns, "EGF mediates monocyte chemotaxis and macrophage proliferation and EGF receptor is expressed in atherosclerotic plaques," *Atherosclerosis*, vol. 176, no. 1, pp. 21–26, 2004.

[29] G. Chan, M. T. Nogalski, and A. D. Yurochko, "Activation of EGFR on monocytes is required for human cytomegalovirus entry and mediates cellular motility," *Proceedings of the National Academy of Sciences of the United States of America*, vol. 106, no. 52, pp. 22369–22374, 2009.

[30] A. Hyder, S. Ehnert, H. Hinz, A. K. Nüssler, F. Fändrich, and H. Ungefroren, "EGF and HB-EGF enhance the proliferation of programmable cells of monocytic origin (PCMO) through activation of MEK/ERK signaling and improve differentiation of PCMO-derived hepatocyte-like cells," *Cell Communication and Signaling*, vol. 10, no. 1, article 23, 2012.

[31] G. J. Inman, F. J. Nicolas, J. F. Callahan et al., "SB-431542 is a potent and specific inhibitor of transforming growth factor-β superfamily type I receptor-like kinase (ALK) receptors ALK4, ALK5, and ALK7," *Molecular Pharmacology*, vol. 62, pp. 65–74, 2002.

[32] G. M. Charrière, B. Cousin, E. Arnaud et al., "Macrophage characteristics of stem cells revealed by transcriptome profiling," *Experimental Cell Research*, vol. 312, no. 17, pp. 3205–3214, 2006.

[33] M. Forsberg, M. Carlén, K. Meletis et al., "Efficient reprogramming of adult neural stem cells to monocytes by ectopic expression of a single gene," *Proceedings of the National Academy of Sciences of the United States of America*, vol. 107, no. 33, pp. 14657–14661, 2010.

Hindawi Publishing Corporation
Stem Cells International
Volume 2016, Article ID 9798374, 22 pages
http://dx.doi.org/10.1155/2016/9798374

Review Article

Limbal Stem Cell Deficiency: Current Treatment Options and Emerging Therapies

Michel Haagdorens,[1,2,3] Sara Ilse Van Acker,[1] Veerle Van Gerwen,[1] Sorcha Ní Dhubhghaill,[1,2] Carina Koppen,[1,2] Marie-José Tassignon,[1,2] and Nadia Zakaria[1,2,4]

[1] *Faculty of Medicine and Health Sciences, Department of Ophthalmology, Visual Optics and Visual Rehabilitation, University of Antwerp, Campus Drie Eiken, T building, T4-Ophthalmology, Universiteitsplein 1, 2610 Antwerp, Belgium*
[2] *Department of Ophthalmology, Antwerp University Hospital, Dienst Oogheelkunde, Wilrijkstraat 10, 2650 Edegem, Belgium*
[3] *Research Foundation-Flanders, Egmontstraat 5, 1000 Brussels, Belgium*
[4] *Center for Cell Therapy and Regenerative Medicine, Antwerp University Hospital, CCRG-Oogheelkunde, Wilrijkstraat 10, 2650 Edegem, Belgium*

Correspondence should be addressed to Michel Haagdorens; michelhaagdorens@gmail.com

Received 19 June 2015; Accepted 18 August 2015

Academic Editor: Kequan Guo

Severe ocular surface disease can result in limbal stem cell deficiency (LSCD), a condition leading to decreased visual acuity, photophobia, and ocular pain. To restore the ocular surface in advanced stem cell deficient corneas, an autologous or allogenic limbal stem cell transplantation is performed. In recent years, the risk of secondary LSCD due to removal of large limbal grafts has been significantly reduced by the optimization of cultivated limbal epithelial transplantation (CLET). Despite the great successes of CLET, there still is room for improvement as overall success rate is 70% and visual acuity often remains suboptimal after successful transplantation. Simple limbal epithelial transplantation reports higher success rates but has not been performed in as many patients yet. This review focuses on limbal epithelial stem cells and the pathophysiology of LSCD. State-of-the-art therapeutic management of LSCD is described, and new and evolving techniques in ocular surface regeneration are being discussed, in particular, advantages and disadvantages of alternative cell scaffolds and cell sources for cell based ocular surface reconstruction.

1. Introduction

Located at the anterior segment of the eye, the cornea is highly organised transparent tissue consisting of multiple cellular and noncellular layers [1]. The corneal epithelium covers the corneal surface and plays a major role in protection and transparency [2, 3]. Epithelial cells are shed regularly and replaced by stem cell sources located at the limbus, a rim of tissue located at the junction of the cornea and sclera (Figures 1(A) and 1(B)). The limbal epithelial stem cells (LESCs) reside in specific regions at the limbus known as the limbal stem cell niches [4]. Damage to the stem cells or disruption of the niches may lead to Limbal Stem Cell Deficiency (LSCD). In the absence of a healthy corneal epithelium, the conjunctiva proliferates over the cornea resulting in opacification and vascularization, which in turn may lead to reduced vision, pain, and photophobia [5, 6]. LSCD can be caused by a wide variety of primary and secondary causes (Table 1) but is most frequently seen associated with severe chemical or thermal burns.

Diagnosis of LSCD is often on the bases of history and clinical findings, which include loss of limbal anatomy, corneal conjunctivalization, persistent epithelial defects, and scar formation [7, 8]. In partial LSCD clinical signs are present but limited to specific regions, which may be quantified by the number of limbal clock hours involved. The diagnosis is confirmed by impression cytology [9], illustrating the presence of goblet cells, increased cytokeratin

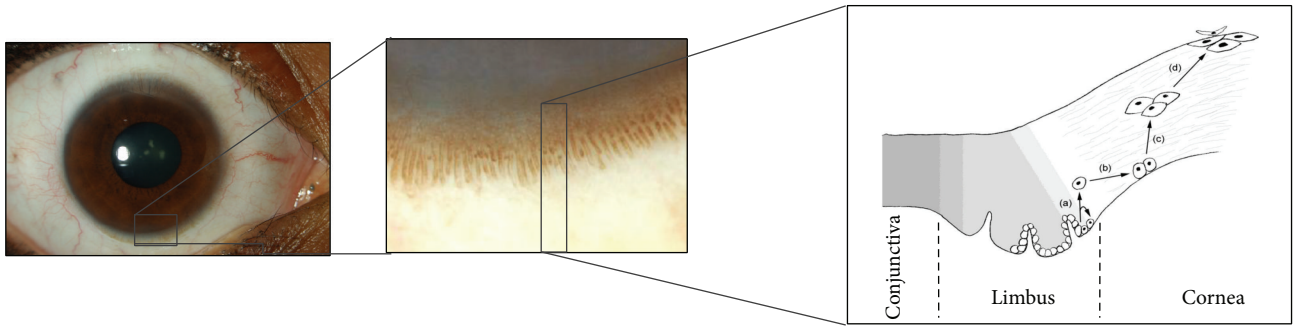

Figure 1: (A) Overview of the anterior surface of the human eye, in which the sclera (with overlying conjunctiva) and cornea can easily be discriminated. (B) The limbus is highly pigmented in some individuals, and allows clear visualization of the limbal palisades of Vogt. The cornea (and underlying dark iris) is pictured above, and conjunctiva (and underlying sclera) below. (C) Diagram of a cross section through the conjunctival, limbal and corneal epithelium. Limbal progenitor cells (a) differentiate into transient amplifying cells (b), post-mitotic cells (c) and finally terminally differentiated cells (d). Movement of cells in X, Y, Z direction is presented by proliferation of stem cells(a), differentiation and centripetal migration (b, c), and desquamation (d) respectively.

Table 1: Aetiology of LSCD.

Primary causes	Reference
Aniridia	[67, 71, 72]
Multiple endocrine deficiency	[9, 67]
Epidermal dysplasia	
Ectrodactyly-ectodermal-dysplasia-clefting syndrome	[73]
Congenital erythrokeratodermia	[74]
Dyskeratosis congenita	[75, 76]
Secondary causes	
Thermal or chemical burns	[67, 77]
Contact lens wear	[67, 78]
Inflammatory eye disease:	
Stevens-Johnson syndrome, toxic epidermal necrolysis	[67]
Ocular cicatricial pemphigoid	[79]
Chronic limbitis: autoimmune disease, extensive microbiological infection, atopic conjunctivitis	[80]
Neurotrophic keratitis	[80]
Extensive limbal cryotherapy, radiation, or surgery	[81]
Bullous keratopathy	[82]
Topical antimetabolites (5-FU, Mitomycin C)	[83, 84]
Systemic chemotherapy (Hydroxyurea)	[85]

5-FU: 5-fluorouracil.

19 (CK19) expression, and reduced CK3/12 expression [10]. More recently CK7, mucin1, and mucin5AC have been reported as more specific than CK19 for diagnostic purposes [11–14].

In vivo confocal microscopy (IVCM) and anterior optical coherence tomography (OCT) are promising techniques that may assist in diagnosing and quantifying LSCD and guiding therapeutic management. IVCM provides high-resolution images of anatomical structures at the cellular level [15, 16]. A number of practical factors limit its use; firstly there is no consensus on the definitive morphological appearance of LESCs, surrounding niche cells or goblet cells on IVCM [17, 18]. Secondly, in the presence of a hazy cornea, the technique is less effective in defining structures due to high degree of backscatter, and finally it requires the prolonged cooperation of the patient [19]. Anterior OCT, and in particular Fourier Domain OCT (FD-OCT), is a more rapid and convenient method of imaging limbal, scleral, and conjunctival structures, though, with significantly lower resolution than IVCM [20]. 3D guided reconstructions of the limbus can be made and may assist guided limbal biopsy [20]. Furthermore, FD-OCT can be applied in imaging hazy corneas and facilitates intraoperative dissection of fibrovascular pannus.

2. Treatment of LSCD

Therapeutic options for LSCD range from conservative to invasive and depend on the severity of the pathology

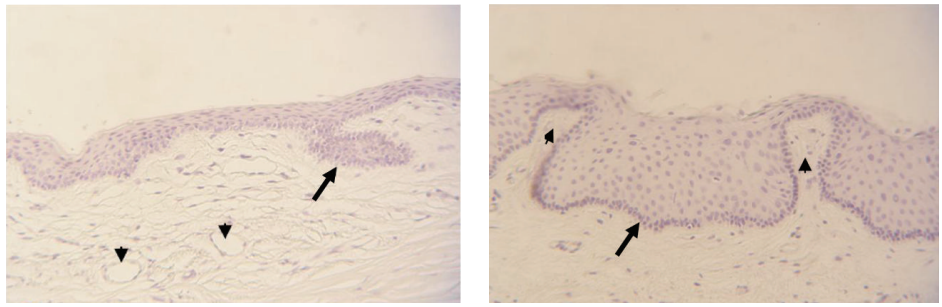

(a) (b)

Figure 2: Haematoxylin staining of cross section through normal limbal region. Arrow in (a) indicates a LESC containing limbal epithelial crypt; arrowheads indicate blood vessels. Arrow in (b) indicates a limbal crypt, flanked by two focal stromal projections (arrowhead).

(Table 2). Conservative therapeutic options include supportive management, corneal scraping, and amniotic membrane patching. In these cases, recovery depends on the presence of some remaining LESCs that can be rehabilitated to restore the epithelium. If there are no remaining stem cell reserves, the cornea must be reseeded with new LESCs [7, 21]. Over the past 18 years, optimizing reseeding techniques has been a major focus of corneal tissue engineering. The earliest techniques required large sections of donor tissue either from the patient's fellow eye (autograft) or from a healthy donor or cadaver (allograft). Taking such large biopsies places the donor eye at risk of developing LSCD. In 1997, Pellegrini et al. reported the first application of *ex vivo* expansion of a very small stem cell biopsy in the treatment of LSCD [22]. The *ex vivo* technique significantly reduced the risk to the donor eye. Since the original report, numerous clinical trials have reported outcomes of tissue engineered corneal surface reconstruction [22–60]. This review will focus on the nature of LESCs and the evolution and optimization of cultivated limbal epithelial stem cell transplantation (CLET) as well as possible future directions.

3. Limbal Epithelial Stem Cell Niches and Markers

A stem cell niche is the unique microenvironment that surrounds stem cells and modulates their function and fate through internal and external factors. LESCs reside in a such well-protected microenvironment, the limbal stem cell niche. The niches are protected from UV-radiation by (i) melanocytes that reside in the basal layers of the limbal epithelium and (ii) the upper and lower eyelid that offer cover to the superior and inferior limbus [8, 61, 62]. The niche's undulated basement membrane protects LESCs from shear force, whereas limbal stromal blood vessels and mesenchymal cells supply it with oxygen, cytokines, growth factors (e.g., the keratinocyte growth factor), and other nutrients [16, 63–65]. The niche also regulates the LESC cell cycle to keep them in an undifferentiated resting state [16, 66]. Proliferation of a LESC gives rise to two daughter cells, where one remains an oligopotent LESC and the other differentiates into a transient amplifying cell (TAC). After a high but limited number of mitoses, TACs differentiate into "postmitotic cells" and subsequently "terminally differentiated cells" [67–69] (Figure 1(C)). During this differentiation process, cells migrate centripetally from the niche to the corneal surface [4] according to the XYZ-hypothesis [70], that is, proliferation of basal epithelial cells (x), differentiation and centripetal migration (y), and isolation/desquamation (z).

Recently, Molvaer et al. localized and described the three different limbal stem cell niches, (i) the limbal epithelial crypts (LECs), (ii) the limbal crypts (LCs), and (iii) the focal stromal projections (FSPs) (Figure 2) [98]. LECs were first described in 2005 as projections extending from the undersurface of the limbal epithelium into the stroma. These projections extend radially into the conjunctival stroma parallel to the palisade or circumferentially along the limbus at right angles to the palisade (Figure 2(a)) [99]. In 2007, LCs and FSPs were described as additional stem cell niches. LCs are projections of the limbal epithelium into the stroma, which are laterally enclosed by the palisades of Vogt [16]. The defined area corresponds in part to the previously described interpalisades (Figure 2(b)). FSPs are finger-shaped projections of stroma containing a central blood vessel, which extend upward into the limbal epithelium [16]. More recently, a further subdivision was made between basal and superficial LCs, the former containing LESCs with melanocytes, the latter containing TACs [100]. It has been proven that all three limbal stem cell niches are mainly present at the superior, and to lesser extent, the inferior limbus. There is no consensus, however, about the exact number and location of niches in the limbus [98].

Stemness and differentiation of LESCs have been investigated through the analysis of various cell markers. Though no specific marker for LESCs has been identified [101, 102], ABCG2 (also known as BRCP1) [103], p63α [104], and ΔNp63 [105] isoforms are the leading markers used in putative LESC identification. Additional stem cell markers have been described, with integrins $\alpha v\beta 3/5$ and the ABCB5 gene most recently [106, 107]. Ordonez et al. identified integrin $\alpha v\beta 3/5$ in less than 4% of cells present in the limbal epithelial niche. However, these cells had phenotypic and functional LESC properties [106].

Table 2: Treatment options for limbal stem cell deficiency.

Procedure	Mechanism of action and remarks	References
	Conservative nonsurgical options	
Autologous serum drops	Serum drops promote migration and proliferation of healthy epithelium while lubricating the ocular surface, preventing epithelial adhesion to the tarsal conjunctiva, and reducing shear stress.	[86–88]
Therapeutic soft contact lens	Therapeutic lenses promote healing of persistent epithelial defects (PED) and prevent the formation of new defects.	[89]
Therapeutic scleral lens	Scleral lenses promote healing of PED while improving vision (optical effect) and reducing pain and photophobia (therapeutic effect). They also prevent formation of new epithelial defects.	[90]
Eye lubrication	Ocular surface lubrication prevents epithelial adhesion to the tarsal conjunctiva and reduces shear stress. Unlike autologous serum drops, residual stem cell migration and proliferation is not enhanced.	[89]
	Conservative surgical options	
Corneal scraping	During scraping the overgrown conjunctiva is removed, enabling reepithelialisation by islands of functioning corneal epithelial stem cells. However, because the conjunctival epithelium migrates more rapidly than the corneal epithelium, it may be necessary to repeat the procedure two to three times.	[91]
Amniotic membrane transplantation (AMT)	AMT promotes proliferation and migration of residual LESCs, contributing to the recovery of the corneal surface, improved visual acuity, and alleviation of pain and photophobia. Low immunogenicity, and anti-inflammatory, antiangiogenic, antifibrotic, antimicrobial, and antiapoptotic properties of the amniotic membrane assist in its therapeutic effect. An AMT is performed immediately after corneal scraping as the overgrown conjunctiva is removed and the amnion membrane is patched over the epithelial defect. Variable clinical outcome may be attributed to inter- and intradonor variation of the biologically sourced membrane.	[88, 92]
	Limbal epithelial stem cell transplantation	
Conjunctival limbal autograft (CLAU)	Autologous graft derived from the patient's healthy eye, using the conjunctiva as carrier tissue. As this procedure involves dissecting 2 clock hours each of limbal tissue superiorly and inferiorly, CLAU holds the risk of inducing LSCD in the healthy donor eye.	[6, 21, 50, 89]
Conjunctival limbal allograft (CLAL)	Allogenic graft derived from a living related (lr-CLAL) or deceased donor (c-CLAL), using the conjunctiva as carrier tissue. CLAL comes with an increased risk of transmitting infectious disease and promoting neoplasia due to the long-term use of immunosuppressants. The surgical procedure and number of clock hours to be dissected are similar to that for CLAU. Lr-CLAL may induce LSCD in the healthy donor eye.	[6, 21, 50, 89]
Keratolimbal allograft (KLAL)	Allogenic graft derived from a deceased donor, using the cornea as carrier tissue. As in CLAL, there is an increased risk of disease transmission and formation of neoplasia. KLAL requires approximately 6 clock hours of tissue to be removed from the donor limbus and transplanted onto the stem cell deficient eye.	[6, 21, 50, 89]
Ex vivo cultivated limbal epithelial stem cells (CLET)	Autologous or allogenic transplantation of cultivated stem cells, most commonly using the human amniotic membrane or fibrin as a carrier for the composite graft. The major advantage of this technique is the reduced risk of inducing LSCD in the healthy donor eye, and the decreased incidence of immunological rejection as Langerhans cells are not cultured in the composite graft. However, the use of HAM or the transplantation of allogenic LESCs bears the risk of disease transmission. Furthermore, the use of immunosuppressants may be necessary in allogenic transplantation with limited HLA-compatibility. Finally, some culture protocols use animal-derived products, which pose the theoretical risk of zoonosis and/or elicit an immune response in the acceptor.	[21, 22, 59, 93]
Simple limbal epithelial transplantation (SLET)	Autologous transplantation of tiny limbal grafts that are distributed and glued evenly over a HAM. Circumventing difficulties of *ex vivo* culture techniques, epithelialisation is achieved *in vivo*. As seen in CLET, there is limited risk of immunological rejection or induction of LSCD in the healthy donor eye. Furthermore difficulties of *ex vivo* culturing are avoided, promoting cost-effectiveness. However, the rate of LESC expansion *in vivo* must be greater than that of the rapidly proliferative conjunctiva to attain successful engraftment.	[94]

4. Cultured Limbal Epithelial Stem Cell Transplantation

As a technique, cultured limbal epithelial stem cells transplantation (CLET) is in its infancy. The overall success rate is estimated to be 76% [21], though direct comparison of clinical trials is difficult due to the wide diversity of pathologies treated, culture protocols, surgical approach, and subjective and objective outcome parameters. When recently published clinical reports are taken into account, success rate decreases slightly to 70%. Details on culture methods and clinical results of published reports are described (Table 3). No significant differences were found in the clinical outcomes based on initial cause of LSCD, source of donor tissue (autologous or allogenic), or culture technique (explants or suspension) [21, 93]. Some culture protocols require the use of lethally irradiated or Mitomycin C-treated 3T3 feeder cells, either in direct contact or in coculture with the LESCs [25, 29, 31, 35, 37, 41–45, 47, 50–52, 55, 58–60]. The feeder layers are involved in promoting niche regulation and stemness of cultivated cells. Though no adverse reactions have been reported in the use of 3T3 feeder layers in large case series [108, 109], avoiding xenogenic material may help reduce the risk of animal-derived infection and graft rejection. The search for alternatives to bovine and other animal products in cultivation protocols, for example, fetal bovine serum and animal-derived growth factors, has led to recent clinical studies cultivating LESCs under nonxenogenic conditions [52, 54, 55, 57–59]. Other advances in the field that may also translate to a higher success rate in future trials include feeder layers of human fibroblasts or Mesenchymal Stem Cells (MSCs) [110–114], standardized GMP (Good Manufacturing Practice) protocols [115] for HAM preparation and *ex vivo* culture, use of autologous serum drops postoperatively, and minimal manipulation of the graft during transplantation [116–118].

In 2012, simple limbal epithelial transplantation (SLET) was described as a novel surgical technique for the treatment of unilateral LSCD [94]. During SLET surgery, a small strip of donor limbal tissue (e.g., 2×2 mm) is divided into several smaller pieces, which are then distributed evenly over a HAM placed on the cornea [94]. The surgery obviates the need for a culture protocol entirely. Although each clinical study reported a success rate of 100% in a small case series (Table 4) [94–97, 119, 120], the long-term effectiveness of the technique is yet to be proven.

5. Alternative Cell Carriers

In clinical trials, HAM is the most commonly used cell carrier for ocular surface reconstruction [23–27, 29–33, 35–42, 44, 45, 47, 48, 50–60]. However, there are risks associated with the use of HAM including possible transfer of infectious agents, variable tissue quality, and limited transparency, which is why alternative seeding scaffolds have been proposed [42, 121].

5.1. Modified HAM. Chemical crosslinking of HAM may enhance mechanical and thermal stability, optical transparency, and resistance to collagenase digestion [122–126]. The crosslinking agents that have been investigated are Glutaraldehyde, (L-Lysine-modulated) Carbodiimide, and $Al_2(SO_4)_3$ [122–126]. *In vitro* experiments showed that Glutaraldehyde conferred a higher degree of cytotoxicity than Carbodiimide [123], whereas the addition of L-lysine to the Carbodiimide crosslinking enhanced mechanical and thermal strength, the ability to support LESCs, and resistance to enzymatic digestion, though higher concentrations could compromise transparency and biocompatibility [126].

5.2. Collagen. Collagen is the main extracellular matrix protein of the cornea and has been widely investigated in the development of biomimetic carrier materials. It is naturally biocompatible and relatively inexpensive to isolate [127, 128]. LESCs can be successfully cultivated on collagen carriers, while maintaining normal phenotype and achieving multilayered stratification when transplanted *in vivo* [127, 129, 130]. Cell attachment and proliferation can be further improved, by coating scaffolds with extracellular matrix proteins (e.g., laminin, type IV collagen, and fibronectin) or derivative adhesion peptides (e.g., YIGSR, IKVAV, and RGC) [131–137]. Most experimental studies have been performed using animal-derived collagen (e.g., porcine collagen type I, rat tail collagen type I, bovine dermal collagen, and fish scale) [127, 138–144]. This collagen may transmit diseases or induce immune reactions, and therefore the more expensive recombinant human collagen (RHC) type I and type III are being investigated further for clinical translation [145–151]. Despite the advantages associated with their use, collagen hydrogels are inherently weak due to the high water content [152]. Several methods have been proposed to improve the mechanical properties of collagen hydrogels.

5.2.1. Chemically Crosslinked Collagen. Griffith et al. have reported the construction of biosynthetic collagen scaffolds consisting of concentrated type I and type III RHC solutions, crosslinked with 1-ethyl-3-(3-dimethyl aminopropyl) Carbodiimide (EDC) and N-hydroxysuccinimide (NHS) [153–155]. When LESCs were cultivated *in vitro* on the optically transparent constructs, a stratified epithelium formed and covered the surface within three weeks. The constructs were sufficiently robust to provide adequate mechanical stability and elasticity for surgical manipulation. Type III collagen hydrogels tended to be mechanically superior. *In vivo* verification and validation showed that the acellular scaffolds stayed optically clear and promoted regeneration of corneal cells, nerves, and tear film, without the need for long-term immunosuppression [149]. However, the mechanical properties of the constructs were significantly lower than human corneas and the long-term stability still needs to be ascertained.

To improve the mechanical properties of the constructs, Griffith et al. have investigated reinforced membranes fabricated from EDC/NHS crosslinked type III RHC and PEG-diacrylate crosslinked 2-methacryloyloxyethyl phosphorylcholine (MPC) [151, 156–158]. These hydrogels showed increased mechanical strength and stability against enzymatic digestion and UV degradation and promoted corneal cell and nerve regeneration while optical properties were

Table 3: Culture methods and clinical results of published CLET reports.

	Patients	Type of graft	Substrate	3T3s used	Animal Free culturing conditions	GMP	Success rate	2-line visual improvement	Subsequent surgery	Complications	Follow-up (months) Mean	Follow-up (months) Range
Ang et al. [38]	1	Allograft	HAM (denuded)	+	+	–	100% (1/1)	0% (0/1)	—	—	48	—
Baradaran-Rafii et al. [45]	8	Autograft	HAM (denuded)	–	–	–	88% (7/8)	63% (7/8)	KP (4)	Perforation (1)	34	6–48
Basu et al. [55]	50	Autograft	HAM	–	+	–	66% (33/50)	76% (38/50)	KP (8)	Bleeding (23), bacterial keratitis (1)	28	12–90
Daya et al. [34]	10	Allograft	3T3s	+	–	–	70% (7/10)	33% (3/9)	KP (5), cataract (1), KLAL (5)	Infective keratitis (1)	28	12–50
Di Girolamo et al. [43]	2	Autograft	Siloxane Hydrogel CL	–	–	–	100% (2/2)	50% (1/2)	—	—	10.5	8–13
Di Iorio et al. [48]	166	Autograft	Fibrin	+	–	–	80% (133/166)	—	KP (33)	—	—	>6
Fatima et al. [41]	1	Autograft	HAM	–	–	–	100% (1/1)	100% (1/1)	KP (1)	—	37	—
Gisoldi et al. [46]	6	Autograft	Fibrin	+	–	+	83% (5/6)	83% (5/6)	KP (4), cataract (1)	—	24	11–34
Grueterich et al. [29]	1	Autograft	HAM	–	–	–	100% (1/1)	100% (1/1)	KP (1), cataract (1)	—	21	—
Kawashima et al. [40]	6	Autograft (2), allograft (4)	HAM (denuded)	+	+	–	100% (6/6)	67% (4/6)	KP (6), cataract (5)	CRVO (1)	32	20–44
Koizumi et al. [26]	13	Allograft	HAM (denuded)	+	+	–	77% (10/13)	38% (5/13)	—	Rejection (3), infection (1), conjunctival invasion (2), conjunctival fibrosis (1)	11	6–13
Koizumi et al. [27]	3	Allograft	HAM (denuded)	+	+	–	100% (3/3)	0% (0/2)	—	—	6	—
Kolli et al. [50]	8	Autograft	HAM	–	–	+	100% (8/8)	63% (5/8)	KP (1), graft redo (1)	—	19	12–30
Meller et al. [44]	1	Allograft	HAM	–	–	–	100% (1/1)	100% (1/1)	—	Perforation (1)	31	—
Nakamura et al. [32]	3	Allograft	HAM (denuded)	+	+	–	100% (3/3)	33% (1/3)	—	—	13	12–14
Nakamura et al. [33]	1	Autograft	HAM (denuded)	+	+	–	100% (1/1)	100% (1/1)	—	—	19	—
Nakamura et al. [36]	9	Autograft (2), allograft (7)	HAM (denuded)	+	+	–	100% (9/9)	67% (6/9)	—	Infective keratitis (1)	14.6	6–20
Pathak et al. [58]	9	Autograft	HAM	–	+	–	56% (5/9)	33% (3/9)	KP (1), graft redo (1), AMT (1)	—	18.5	11–24

Table 3: Continued.

	Patients	Type of graft	Substrate	3T3s used	Animal Free culturing conditions	GMP	Success rate	2-line visual improvement	Subsequent surgery	Complications	Follow-up (months) Mean	Follow-up (months) Range
Pauklin et al. [51]	44	Autograft (30), allograft (14)	HAM	−	−	−	68% (30/44)	73% (32/44)	KP (8), cataract (5)	Bleeding (1), perforation (2)	28.5	9–72
Pellegrini et al. [22]	2	Autograft	3T3s	+	−	−	100% (2/2)	50% (1/2)	KP (1)	—	—	>24
Prabhasawat et al. [54]	19	Autograft (12), allograft (7)	Ham (denuded)	−	+	−	73.7% (14/19)	68.4% (13/19)	KP (6), lid correction (3), cataract (3), tarsorrhaphy (1)	Infection (3), PED (3), symblepharon (1)	26.1	6–47
Rama et al. [28]	18	Autograft	Fibrin	+	−	−	78% (14/18)	33% (6/18)	KP (3)	Persistent inflammation with bleeding (4)	17.5	12–72
Rama et al. [49]	107	Autograft	Fibrin	+	−	+	68% (73/107)	54% (61/107)	KP (62), PTK (2)	Bleeding (12), inflammation (59), herpetic keratitis (3), blephari-tis/epitheliopathy (35), residual fibrin (11)	35	12–120
Sangwan et al. [31]	2	Autograft	HAM	−	−	−	100% (2/2)	50% (1/2)	—	Recurrence (1)	12	—
Sangwan et al. [31]	15	Autograft (11), allograft (4)	HAM	−	−	−	100% (15/15)	87% (13/15)	KP (15)	Rejection (4), glaucoma (1)	15.3	7–24
Sangwan et al. [37]	78	Autograft	HAM	−	−	−	73% (57/78)	37% (18/49)	KP (19)	Phthisis (2), keratitis (2), glaucoma (2)	18.3	3–40
Sangwan et al. [52]	200	Autograft	Ham (denuded)	−	+	−	71% (142/200)	60.5% (121/200)	—	Bleeding (56), PED (13), corneal melting (5), bacterial keratitis (3)	36	12–91
Schwab [23]	19	Autograft (17), allograft (2)	HAM	+	−	−	74% (14/19)	16% (3/19)	Graft redo (1)	—	10.5	2–24
Schwab et al. [24]	14	Autograft (10), allograft (4)	HAM (denuded)	+	+	−	71% (10/14)	36% (5/14)	KP (1)	Epithelial loss (1), cyclosporine-related (2), infectious keratitis (1), pyogenic granuloma (1)	13	6–19
Sejpal et al. [57]	107	Autograft	HAM (denuded)	−	+	−	49.5% (53/107)	54.2% (58/107)	KP (19), lid or fornix correction (16)	Infection (7), inflammatory granuloma (4), glaucoma (1), corneal thinning (1), bleeding (1), panophthalmitis (1)	41.2	12–118

Table 3: Continued.

	Patients	Type of graft	Substrate	3T3s used	Animal Free culturing conditions	GMP	Success rate	2-line visual improvement	Subsequent surgery	Complications	Follow-up (months) Mean	Follow-up (months) Range
Sharma et al. [53]	50	Autograft (34), allograft (16)	HAM (denuded)	−	−	−	74% (37/50)	68% (34/50)	KP (4)	—	11	1.5–25
Shimazaki et al. [30]	13	Allograft	HAM (denuded)	−	−	−	38.5% (5/13)	76.9% (10/13)	—	Perforation (4), infection (2)	—	—
Shimazaki et al. [39]	27	Autograft (7), allograft (20)	HAM (denuded)	+	−	−	59% (16/27)	48% (13/27)	KP (8), limbal transplant (3)	Infection (1), ulceration (4), perforation (4)	29.3	6–85
Shortt et al. [42]	16	Autograft (9), allograft (7)	HAM (denuded)	−	−	+	75% (12/16)	22% (2/9)	Graft redo (1)	Infection (1), cyclosporin related (1), graft detachment (1)	9.3	6–13
Subramaniam et al. [56]	40	Autograft	HAM (denuded)	−	−	−	45% (18/40)	—	KP (10)	—	33.4	1–87
Thanos et al. [47]	1	Autologous	HAM	−	−	−	100% (1/1)	100% (1/1)	—	—	24	—
Tsai et al. [25]	6	Autograft (3), allograft (3)	HAM (denuded)	−	−	−	100% (6/6)	50% (3/6)	—	—	15	12–18
Vazirani et al. [60]	70	Autograft	HAM (denuded)	−	−	−	71% (49/70)	—	—	—	17.5	—
Zakaria et al. [59]	18	Autograft (15), allograft (3)	HAM (denuded)	−	+	+	67% (12/18)	28% (5/18)	KP (7)	—	24	4–48
Overall	1164	Autograft (1029), allograft (135)					70.26%	54.92%			25.4	1–120

GMP: good manufacturing practice; HAM: human amniotic membrane; CL: contact lens; KP: keratoplasty; AMT: amnion membrane transplantation; PTK: phototherapeutic keratectomy; CRVO: central retinal vein occlusion; PED: persistent epithelial defect.

Table 4: Published clinical outcomes of SLET.

	Patients	Type of graft	Substrate	Success rate	2-line visual improvement	Subsequent surgery	Complications	Follow-up (months)	
								Mean	Range
Amescua et al. [95]	4	Autograft	HAM	100% (4/4)	100% (4/4)	—	—	7.5	6–9
Bhalekar et al. [96]	1	Allograft	HAM	100% (1/1)	100% (1/1)	—	Rejection	6	—
Bhalekar et al. [119]	1	Autograft	HAM	100% (1/1)	100% (1/1)	—	—	>1	—
Bhalekar et al. [120]	1	Autograft	HAM	100% (1/1	100% (1/1)	—	Epithelial plaque hyperplasia	14	—
Vazirani et al. [97]	1	Autograft	HAM	100% (1/1)	100% (1/1)	Graft redo, conjunctival autografting	—	6	—
Sangwan et al. [94]	6	Autograft	HAM	100% (6/6)	100% (6/6)	—	—	9.2	4–48
Overall	14			100%	100%			8	4–48

HAM: human amniotic membrane.

comparable to a normal cornea [156]. Cell-free RHC-MPC implants have been grafted in 7 eyes, in which patients showed stable epithelia 12 months postoperatively and the best corrected vision improved by 1-2 lines [151, 158]. Another form of collagen hydrogel, genipin-crosslinked chitosan-collagen and PEG-Carbodiimide chitosan-collagen hydrogel, has also been examined for ocular surface reconstruction [139, 159]. *In vitro* experiments with these constructs show maintenance of regular stratified multilayered epithelium [159], while initial animal testing shows good biocompatibility [139]. Use in human corneal regeneration has not yet been reported.

5.2.2. Plastic Compression Collagen. In 2010, Mi et al. improved the mechanical strength of collagen hydrogels by compressing and blotting the constructs between paper sheets and a nylon mesh thereby reducing the water content of the gels [160]. LESCs cultivated on this construct displayed a smooth and homogenous morphology, whereas cells cultured on conventional hydrogels were distributed more heterogeneously. Subsequent studies confirmed that plastically compressed collagen gels are optically transparent and easy to handle, had improved mechanical strength, and support LESC adhesion, proliferation, and stratification [160–163]. Mechanical strength could further be improved by photochemical crosslinking [164]. Kits that enable the production of 3D plastic compressed cultures have recently become commercially available (RAFT, TAP Biosystems, Hertfordshire, UK).

5.3. Fibrin. Fibrin is the biodegradable product formed during coagulation. Fibrin membranes can be fabricated by combining fibrinogen and thrombin, both harvested from human plasma. Fibrin derivates have been used extensively in ophthalmology, typically as a glues or membranes [165–168].

Four clinical studies have reported the use of fibrin as a substrate in CLET surgery [28, 46, 48, 49]. In animal studies, fibrin gels were found to degrade completely after 3 days [169]. After gel degradation, the transplanted cells adhered directly to the host corneal stroma. In early 2015, Holoclar (Chiesi, Italy) has been conditionally approved to be released in Italy as the first commercially available stem cell therapy for LSCD treatment. Existing data on Holoclar have been obtained by retrospective patient follow-up, and annual renewal of approval will be guided by results of a current multicenter, prospective phase IV clinical trial. Nevertheless, practical use of this fibrin-based Advanced Therapeutic Medicinal Product (ATMP) is limited to autologous stem cell transplantation in unilateral cases after chemical or thermal burn. Notably, the technique still utilizes lethally irradiated murine 3T3-J2 fibroblast feeder cells and bovine serum during graft generation, which brings into question the safety of the xeno-based cell product [49].

5.4. Siloxane Hydrogel Contact Lenses. In the initial CLET clinical trial by Lu et al., a 3T3 cocultured human epithelial sheet was mounted on a soft contact lens, prior to transplantation as a carrier [170]. In a subsequent study by Di Girolamo et al., the LESCs were cultivated directly on the contact lens [171]. Gore et al. investigated cultivation of LESCs on contact lenses that were coated with a 3T3 feeder layer [172]. In this study, *in vitro* cultivated LESCs formed a multilayered corneal epithelium, while some basal cells maintained their stemness. Plasma polymer-coated contact lenses also promoted *in vitro* LESC adhesion and proliferation [173]. Transplantation of these LESCs in a LSCD rabbit model gave rise to patches of stratified epithelium; however, recipient corneas showed only partial reconstruction, possibly due to short-term follow-up (26 days).

5.5. Poly(ε-caprolactone). Poly(ε-caprolactone) is a highly flexible and strong material that has already been used as a scaffold for skin, bone, and MSC applications. The biocompatibility and optical transparency of poly(ε-caprolactone) may be improved by electrospinning and surface modification, and such modified sheets can support LESC cultivation [174]. The *in vivo* use of the material has not yet been reported.

5.6. Chitosan-Gelatin. Chitosan is a stiff crystalline polysaccharide that is extracted from chitin from arthropod exoskeletons. Membranes of pure chitosan are too stiff for ocular purposes but the addition of gelatine and crosslinkers can improve the material handling [175]. Chitosan-gelatine membranes have extensively been investigated for regeneration of bone, cartilage, and skin [176–178]. Chitosan-gelatin membranes with a 20 : 80 ratio supported the growth of LESCs that expressed CK3/12, CK15, and ABCG2 [179]. Again, the *in vivo* use of this material has not been reported.

5.7. Silk Fibroin. Silk fibroin (SF), obtained from *Bombyx mori* (domesticated silkworm), can be processed into thin transparent membranes. It is nonimmunogenic, degradable, mechanically strong, and optically transparent and has been used as suture material and in bone and cartilage regeneration [180–182]. Cultivation of LESCs on nonporous SF films gives rise to a stratified corneal-like epithelium [183–187]. Porous SF membranes can be developed by mixing SF and poly(ethylene glycol) (PEG) and have supported LESC growth [183] although results have varied [186]. It may be possible to coculture MSCs within pores to recreate the stromal microenvironment [186]. SF may also be combined with chitosan (SF-CS) and the constructed scaffolds have been investigated with some success [188, 189]. LESCs that were seeded on such lamellar corneas were comparable to native tissue, as outgrown cells had physiological morphology and high levels of CK3/12 expression [189]. Furthermore, biocompatibility of SF and SF-CS films has been observed in rabbit corneas for up to six months [183, 188]. However, membranes constructed from SF derived from *Antheraea pernyi* (wild silkworm) proved to be more prone to becoming opaque, displayed lower permeability, and were more brittle than conventional nonporous SF films [187].

5.8. Human Anterior Lens Capsule. The Human Anterior Lens Capsule (HaLC) is a dense membrane consisting of Collagen IV, laminin, and heparin sulphate proteoglycans. HaLC is characterized by a gradually increasing thickness

(±0.35 μm per year) and simultaneous loss of mechanical strength (±1% each year) [190, 191]. LESCs have been successfully cultivated on HaLCs, with *in vitro* viability of >95%; cell density and cell morphology were similar to LESCs cultivated on plastic [192]. LESCs, cultured under nonxenogenic conditions maintained their oligopotency, while some cells showed directional differentiation into corneal epithelium [193]. This promising alternative scaffold needs further *in vivo* verification. Concern has been raised, however, that the diameter of extracted HaLC may not be large enough for corneal treatments [192].

5.9. Keratin. Reichl et al. succeeded in fabricating a transparent membrane from keratin extracted from human hair [194]. LESC behavior on the films was similar to that on HAM and was not affected by prior plasma treatment sterilization of the material [195]. Unfortunately, suturing is impaired by a high rate of suture tear-out [195].

5.10. Poly(lactide-co-glycolide). Poly(lactide-co-glycolide) (PLGA) is an FDA-approved, biodegradable, and noncytotoxic material that has been used in products such as dissolvable sutures [196]. Transparent electrospun PLGA scaffolds are easy to handle, store, and suture [197]; however when LESCs were cultivated on these carriers, the scaffolds began to disintegrate *in vitro* and were fragile to handle. Additional research has shown that PLGA can be chemically altered to achieve predictable and slower breakdown, both *in vitro* and *in vivo* [198, 199]. Disintegration was now evident by two weeks after initiation of LESC cultivation, with complete breakdown occurring by six weeks *in vitro* [199].

5.11. Polymethacrylate. Polymethacrylate has been used in ophthalmology to produce rigid intraocular lenses and contact lenses. It can be fabricated into transparent biocompatible hydrogels, which can support LESC proliferation [200, 201]. Augmenting the polymethacrylate with 1,4-diaminobutane has been shown to improve LESC adherence and proliferation [202].

5.12. Hydroxyethylmethacrylate. Hydroxyethylmethacrylate and poly-2-hydroxyethylmethacrylate have been used to manufacture soft contact lenses, the Chirila Kpro and the AlphaCor (Addition Technology Inc., Des Plaines, IL) [203, 204]. One study has investigated hydroxyethylmethacrylate in ocular surface reconstruction and concluded that LESCs and fibroblasts could adhere and proliferate to hydroxyethylmethacrylate hydrogels that were surface modified with type I collagen and arginine-glycine-aspartic acid ligand [205].

5.13. Poly(ethylene glycol). PEG is a biocompatible polymer used in pharmaceutical products (e.g., capsules, tablet binders, ointments, and slow release medications). Transparent hydrogels based on PEG-diacrylate and PEG-diacrylamide have been used *in vivo* and showed favourable results for the latter as PEG-diacrylate implants showed inflammation, corneal haze, and corneal ulceration. Rabbits with PEG-diacrylamide implants, on the other hand, remained healthy and had clear corneas and noninflamed eyes for up to 6 months after transplantation [206, 207]. *In vitro* experiments showed that photolithographical surface coating with collagen type I was necessary to allow LESC adhesion and proliferation [208]. PEG-diacrylate and PEG-diacrylamide hydrogels were intended for full thickness corneal regeneration; however, thinner gels intended for anterior corneal regeneration are yet to be investigated. PEG has also been combined with chitosan and silk fibroin to make even stronger and more transparent biomaterials [209].

5.14. Platelet Poor Plasma. Platelet-Poor Plasma (PPP) is blood plasma with very low numbers of thrombocytes ($< 10 \times 10^3/\mu$L), which are removed by centrifugation. Biodegradable, transparent PPP membranes can be manufactured to function as a seeding scaffold in autologous and allogenic CLET. LESC allografts mounted on autologous PPP sheets in LSCD rabbits improved corneal transparency and resulted in a multilayered CK3/12+ epithelium [210, 211].

5.15. Poly(vinyl alcohol). Poly(vinyl alcohol) is a transparent hydrogel with good mechanical strength. Poly(vinyl alcohol) shows low cell affinity, but when incorporated with collagen type I it can support a fully stratified corneal epithelium *in vitro* [212], but to support *in vivo* epithelialization poly(vinyl alcohol)-collagen requires the assistance of HAM [213].

6. Carrier-Free Transplantation

Nishida et al. reported a temperature-responsive polymer, that is, poly(*N*-isopropylacrylamide) (PIPAAm), that could release intact, transplantable epithelial sheets that retain stem cells and epithelial cells [214]. The copolymer PIPAAm-PEG is at present commercialized as Mebiol gel and is hydrophilic at temperatures below 20°C and hydrophobic at temperatures above. Experiments have shown that Mebiol supports LESC cultivation *in vitro* and that autologous CLET in Mebiol restores the ocular epithelial surface in a LSCD rabbit model. The particular properties of Mebiol gel allow for easy graft transplantation. Drops of cooled Mebiol gel containing cultured LESCs can be applied to the ocular surface and a contact lens placed over it to keep it in place [215].

Furthermore, *in vitro* fibrin degradation, biodegradable type I collagen, and centrifugation proved to be effective techniques in fabricating carrier-free epithelial sheets. Cultured cells did proliferate and differentiate under the respective conditions, and cell-survival in the subsequent carrier-free state was preserved [216–218].

7. Alternative Cell Populations

LSCD frequently manifests as a bilateral condition where no residual stem cells are available for *ex vivo* culture. Allograft material from living related donors or cadavers may be used, but this is associated with an increased risk of disease transmission, rejection, and neoplasia (associated with immunosuppressive agents). Alternative cell populations could potentially replace the use of allogenic material

and within the last decade a number of approaches have been explored with varying success [219].

7.1. Oral Mucosal Epithelial Cells. In 2003, Nakamura et al. described Cultivated Oral Mucosal Epithelial Transplantation (COMET) in a rabbit animal model [220]. Oral Mucosal Epithelial Cells (OMECs) are cultured on a HAM until a stratified epithelium is attained and then transplanted. The construct mimics the corneal epithelium as transplanted stem cells maintain their stemness at the ectopic site, and OMECs acquire corneal epithelial-like markers such as CK3, CK19, Ki-67, p63, p75, and cornea-specific PAX6 and CK12 [221–223]. COMET has been successful (i.e., regenerating a totally epithelized, stable, and avascular corneal surface) in patients with severe total LSCD [221, 223–232]. However, transplanted cultivated sheets are not completely identical to *in vivo* corneal epithelium, which leads to a variable degree of *in vivo* keratinization and stratification (up to 12 cell layers) [221, 228]. Small case series favour CLET, as COMET is associated with higher rates of peripheral corneal neovascularisation, inferior best corrected visual improvement, and increased risk of dry eye conditions postoperatively [221, 228].

7.2. Conjunctival Epithelial Cells. Human conjunctival epithelial cells grown on HAM have been used to reconstruct the ocular surface in rabbits with LSCD [233]. The transplanted conjunctival call sheets formed a five- to six-layer epithelium that remained transparent, smooth, avascular, and without epithelial defects [234]. Transplanted cells keep expressing both conjunctival (CK4) and corneal epithelial markers (CK3/12). Human conjunctival epithelial cell transplantation has been used clinically [235] and in one study in conjunction with a contact lens, which was removed at day 22 [43]. Almost 2 years after successful transplantation, a well-formed epithelium with 5 to 6 layers was present with rare PAS-positive cells, and positivity for CK3, CK19, P63, connexin 43, and MUC5AC [235]. Best corrected visual acuity significantly improved postoperatively, yet the effect was rather modest compared to CLET. Pain and photophobia were not being evaluated.

7.3. Hair Follicle Bulge-Derived Epithelial Stem Cells. Unlike OMECs, epithelial stem cells derived from the bulge region of the hair follicle are able to terminally differentiate into a corneal epithelial phenotype when transplanted onto the ocular surface [236]. The concept was proven in an animal study, in which hair follicle stem cells were cultured on a 3T3 feeder layer and transplanted into a LSCD mouse model [237]. The grafts were able to reconstruct the ocular surface in 80% of transplanted animals [237].

7.4. Amniotic Epithelial Cells. Human amniotic epithelial cells are characterized by their stem cell properties, low immunogenicity, production of growth factors that promote epithelialization, and their ability of controlled transdifferentiation into other cell types [238–241]. Amniotic epithelial cells can differentiate into corneal epithelial cells when seeded on the superficial corneal stroma in rabbit LSCD models [238–240, 242]. The differentiated cells had a similar structure, morphology, and physiology as that of normal stratified corneal epithelium. However, one study indicated that the stratified epithelial cells had no polarity with regard to defined superficial corneal epithelial cells, wing cells, or basal cells [238].

7.5. Human Embryonic Stem Cells. Human embryonic stem cells are pluripotent cells derived from the inner cell mass of the human embryo and can successfully differentiate into corneal epithelial-like cell [243, 244]. In a study from Zhu et al., human embryonic stem cells were induced to form LESC-like cells and were seeded on an acellular porcine corneal matrix [245]. Seeded cells formed stratified and closely arranged epithelioid cell sheets consisting of a basal layer of cuboid-shaped cells (p63a and ABCG2 positive) and suprabasal layers of elongated cells (CK3 positive). In rabbit LSCD models, the tissue engineered graft had the potential to reconstruct the ocular surface [245]. Embryonic stem cells also differentiate into corneal epithelial cells when in direct contact with the corneal stroma [246]. A major drawback to the use of human embryonic stem cells is the immune response they elicit, and the ethical controversy surrounding the origin of the stem cells [244, 247].

7.6. Induced Pluripotent Stem Cells. Induced Pluripotent Stem Cells (iPSCs) are a type of stem cells generated by manipulation of differentiated adult cells. In 2006, the iPSC technique was first described by Takahashi and Yamanaka and used four specific transcription factors to dedifferentiate adult cells into PSCs [248]. Hayashi et al.described a strategy to differentiate LESCs from human iPSCs that were derived from human adult corneal limbal epithelial cells or human dermal fibroblasts [249]. The iPSCs derived from adult corneal limbal epithelial cells gave rise to more corneal epithelial colonies and exhibited higher expression of specific corneal epithelial differentiation markers than iPSCs derived from fibroblasts [249, 250]. This may be due to the maintenance of epigenetic characteristics of the original adult cell during iPSC formation and subsequent differentiation [250, 251]. A significant drawback of the iPSC technique is that not all limbal epithelial cells preferentially differentiate into corneal epithelial cells [249]. Recently, a two-step differentiation method was developed to differentiate human iPSCs into a homogenous population of p63-positive epithelial cells with the ability to differentiate into corneal epithelial-like cells [252].

7.7. Umbilical Cord Lining Epithelial Stem Cells and Wharton's Jelly Mesenchymal Stem Cells. In 2011, Reza et al. described umbilical mucin-expressing cord lining epithelial stem cells as an alternative cell population in anterior corneal reconstruction [253]. These cells are nontumorigenic, highly proliferative, and ethically acceptable. The cells' low immunogenicity may obviate the postoperative use of immunosuppressants. *In vivo* verification in a rabbit model showed clear corneal surface regeneration with phenotypical CK3/CK12 expression [253]. Wharton's Jelly Mesenchymal Stem Cells have also been proposed for anterior corneal tissue engineering. Garzón et al. demonstrated that these MSCs could

transdifferentiate *in vitro* into corneal epithelial-like cells, with the expression of epithelial cell markers (CK3/CK12, PKG, ZO1, and Cnx43) [254].

7.8. Mesenchymal Stem Cells. In 2006, Ma et al. were the first to expand MSCs on HAM and subsequently transplant the construct onto the ocular surface of LSCD rats [255]. Although bone marrow-derived human MSCs did not differentiate into epithelial-like cells, the transplanted MSCs successfully reconstructed the damaged corneal surface as a smooth and continuous epithelium, and avascular and transparent cornea were being observed [255]. The therapeutic effect may be due to the MSCs' anti-inflammatory and antiangiogenic properties, rather than direct epithelial differentiation. Gu et al. subsequently succeeded in differentiating rabbit-derived bone marrow MSCs into corneal epithelial-like cells [256]. *In vitro,* differentiation was modulated by either (i) coculturing rabbit LESCs with MSCs or (ii) adding a LESC-derived supernatant to the MSCs [256]. Several other methods of inducing MSC differentiation have since been described [257–259]. In a LSCD rat model, corneal epithelial-like differentiation was modulated by cytokines, produced by rat Corneal Stromal Cells [257]. In 2011, Reinshagen et al. injected enriched MSCs under an AMT in LSCD rabbits [258]. Data indicated that injected MSCs may maintain their stem cell character or may differentiate into epithelial progenitor cells. More recently, it has been discovered that bone marrow-derived MSCs are capable of differentiating into corneal epithelial-like cells, when cultured in specialized DMEM-medium [259]. Adipose tissue-derived MSCs and limbal MSCs also can differentiate into corneal epithelial-like cells when exposed to (i) secreted factors of differentiated human corneal epithelial cells or (ii) DMEM-medium, respectively [260–263].

7.9. Human Immature Dental Pulp Stem Cells. Human immature dental pulp stem cells express both MSC and embryonic stem cell markers and have the capacity to differentiate into derivatives of the three germinal layers *in vitro*. In a LSCD rabbit experiment, transplanted human immature dental pulp stem cells were capable of reconstructing the ocular surface with a well-formed corneal epithelium that expresses LESC markers in the basal cell layer and EC markers in suprabasal cell layers [74, 264].

8. Conclusion

Over the past few years, great advances in LESC identification and characterization and ocular surface reconstruction have been made. With the introduction of CLET and SLET, a safe and successful treatment option for LSCD has been introduced [22–60, 94–97, 119, 120]. In particular, the tendency towards (i) standardized nonxenogenic GMP protocols in scaffold manufacturing and cell cultivation and (ii) "no touch graft surgery" is expected to improve success rates in future CLET trials [52, 55, 58, 59]. SLET seems to be very promising [94–97, 119, 120]; however, large cohort inclusion, allogenic transplantation, and long-term follow-up have yet to be performed. Further elaboration of "tear sampling" as a tool to identify factors that may be involved in the development and/or maintenance of corneal neovascularization in humans has been described [265]. This technique may assist in monitoring the inflammatory state of the LSCD eye and further improve preoperative management and postoperative outcome of patients. However, specific identification of the LESCs remains a hurdle and characterization is still based on a combination of phenotypic expression patterns [266]. Despite the successes and evolving techniques in LESC transplantation, detailed interaction and signaling pathways between LESCs, niche cells, and surrounding extracellular matrix are not fully understood. Research and knowledge within these domains will help understand (i) physiological LESC maintenance, (ii) *in vitro* and *in vivo* microenvironment simulation, and (iii) long-term effectiveness of LESC transplantation. Such knowledge may potentiate the development of new pharmacological solutions (e.g., eye drops that contain LESC growth factors) that stimulate remaining dormant LESCs of the diseased eye. These alternatives would be of great value in cases of extensive ocular inflammation, as these patients are not good candidates for surgical intervention.

Better *in vitro* and *in vivo* replication of the niche may also lead to more efficient cultivation and transplantation of LESCs and alternative cell populations. Of the investigated alternative seeding membranes, only HAM, fibrin, Siloxane Hydrogen contact lens, and collagen membranes have been used in patients [22–60, 94–97, 119, 120, 149, 151]. In particular, the conditional approval of Holoclar (Chiesi, Italy) is a huge step forward in the accessibility of LSCD treatment in daily practice. Furthermore, RHC membranes seem to be very promising for tissue engineering, the collagen being of nonxenogenic origin and the addition of MPC addressing many shortcomings of conventional collagen hydrogels. Other alternative scaffolds are still in an experimental phase and have yet to be validated in humans. COMET and human conjunctival epithelial cell transplantation have both been successfully performed in selected patients [43, 221, 223–232, 235]. However, as iPSCs get widespread attention in many medical disciplines, it is believed that this autologous cell population will play a prominent role in LSCD treatment in the coming years.

In conclusion, it can be certain that better and more convenient treatment options for LSCD patients will emerge in the near future. New treatment options will target optical transparency, biocompatibility, intraoperative handling, physicochemical strength, and cost-effectiveness. The important focus on sterility, reproducibility, and minimal mutagenicity and cytotoxicity is further stimulated by the widespread introduction of GMP guidelines.

Conflict of Interests

The authors declare that there are no competing financial interests for any of them.

Acknowledgments

This research was funded by "The Research Foundation-Flanders" (FWO) and EuroNanoMed2.

References

[1] J. W. McTigue, "The human cornea: a light and electron microscopic study of the normal cornea and its alterations in various dystrophies," *Transactions of the American Ophthalmological Society*, vol. 65, pp. 591–660, 1967.

[2] G. Cotsarelis, S.-Z. Cheng, G. Dong, T.-T. Sun, and R. M. Lavker, "Existence of slow-cycling limbal epithelial basal cells that can be preferentially stimulated to proliferate: implications on epithelial stem cells," *Cell*, vol. 57, no. 2, pp. 201–209, 1989.

[3] P. A. Hall and F. M. Watt, "Stem cells: the generation and maintenance of cellular diversity," *Development*, vol. 106, no. 4, pp. 619–633, 1989.

[4] A. Schermer, S. Galvin, and T. T. Sun, "Differentiation-related expression of a major 64K corneal keratin in vivo and in culture suggests limbal location of corneal epithelial stem cells," *The Journal of Cell Biology*, vol. 103, no. 1, pp. 49–62, 1986.

[5] M. S. Shapiro, J. Friend, and R. A. Thoft, "Corneal re-epithelialization from the conjunctiva," *Investigative Ophthalmology & Visual Science*, vol. 21, no. 1, part 1, pp. 135–142, 1981.

[6] E. J. Holland, "Epithelial transplantation for the management of severe ocular surface disease," *Transactions of the American Ophthalmological Society*, vol. 94, pp. 677–743, 1996.

[7] H. S. Dua and A. Azuara-Blanco, "Limbal stem cells of the corneal epithelium," *Survey of Ophthalmology*, vol. 44, no. 5, pp. 415–425, 2000.

[8] K. Higa, S. Shimmura, H. Miyashita, J. Shimazaki, and K. Tsubota, "Melanocytes in the corneal limbus interact with K19-positive basal epithelial cells," *Experimental Eye Research*, vol. 81, no. 2, pp. 218–223, 2005.

[9] V. Puangsricharern and S. C. Tseng, "Cytologlogic evidence of corneal diseases with limbal stem cell deficiency," *Ophthalmology*, vol. 102, no. 10, pp. 1476–1485, 1995.

[10] M. Sacchetti, A. Lambiase, M. Cortes et al., "Clinical and cytological findings in limbal stem cell deficiency," *Graefe's Archive for Clinical and Experimental Ophthalmology*, vol. 243, no. 9, pp. 870–876, 2005.

[11] V. Barbaro, S. Ferrari, A. Fasolo et al., "Evaluation of ocular surface disorders: a new diagnostic tool based on impression cytology and confocal laser scanning microscopy," *British Journal of Ophthalmology*, vol. 94, no. 7, pp. 926–932, 2010.

[12] K. Jirsova, L. Dudakova, S. Kalasova, V. Vesela, and S. Merjava, "The OV-TL 12/30 clone of anti-cytokeratin 7 antibody as a new marker of corneal conjunctivalization in patients with limbal stem cell deficiency," *Investigative Ophthalmology and Visual Science*, vol. 52, no. 8, pp. 5892–5898, 2011.

[13] A. Ramirez-Miranda, M. N. Nakatsu, S. Zarei-Ghanavati, C. V. Nguyen, and S. X. Deng, "Keratin 13 is a more specific marker of conjunctival epithelium than keratin 19," *Molecular Vision*, vol. 17, pp. 1652–1661, 2011.

[14] I. Garcia, J. Etxebarria, A. Boto-De-Los-Bueis et al., "Comparative study of limbal stem cell deficiency diagnosis methods: detection of MUC5AC mRNA and goblet cells in corneal epithelium," *Ophthalmology*, vol. 119, no. 5, pp. 923–929, 2012.

[15] I. Jalbert, F. Stapleton, E. Papas, D. F. Sweeney, and M. Coroneo, "In vivo confocal microscopy of the human cornea," *British Journal of Ophthalmology*, vol. 87, no. 2, pp. 225–236, 2003.

[16] A. J. Shortt, G. A. Secker, P. M. Munro, P. T. Khaw, S. J. Tuft, and J. T. Daniels, "Characterization of the limbal epithelial stem cell niche: Novel imaging techniques permit in vivo observation and targeted biopsy of limbal epithelial stem cells," *Stem Cells*, vol. 25, no. 6, pp. 1402–1409, 2007.

[17] N. Efron, M. Al-Dossari, and N. Pritchard, "*In vivo* confocal microscopy of the bulbar conjunctiva," *Clinical & Experimental Ophthalmology*, vol. 37, no. 4, pp. 335–344, 2009.

[18] J. Hong, W. Zhu, H. Zhuang et al., "In vivo confocal microscopy of conjunctival goblet cells in patients with Sjogren's syndrome dry eye," *British Journal of Ophthalmology*, vol. 94, no. 11, pp. 1454–1458, 2010.

[19] A. Miri, T. Alomar, M. Nubile et al., "In vivo confocal microscopic findings in patients with limbal stem cell deficiency," *British Journal of Ophthalmology*, vol. 96, no. 4, pp. 523–529, 2012.

[20] K. L. Lathrop, D. Gupta, L. Kagemann, J. S. Schuman, and N. SundarRaj, "Optical coherence tomography as a rapid, accurate, noncontact method of visualizing the palisades of Vogt," *Investigative Opthalmology & Visual Science*, vol. 53, no. 3, pp. 1381–1387, 2012.

[21] O. Baylis, F. Figueiredo, C. Henein, M. Lako, and S. Ahmad, "13 Years of cultured limbal epithelial cell therapy: a review of the outcomes," *Journal of Cellular Biochemistry*, vol. 112, no. 4, pp. 993–1002, 2011.

[22] G. Pellegrini, C. E. Traverso, A. T. Franzi, M. Zingirian, R. Cancedda, and M. De Luca, "Long-term restoration of damaged corneal surfaces with autologous cultivated corneal epithelium," *The Lancet*, vol. 349, no. 9057, pp. 990–993, 1997.

[23] I. R. Schwab, "Cultured corneal epithelia for ocular surface disease," *Transactions of the American Ophthalmological Society*, vol. 97, pp. 891–986, 1999.

[24] I. R. Schwab, M. Reyes, and R. R. Isseroff, "Successful transplantation of bioengineered tissue replacements in patients with ocular surface disease," *Cornea*, vol. 19, no. 4, pp. 421–426, 2000.

[25] R. J. Tsai, L. M. Li, and J. K. Chen, "Reconstruction of damaged corneas by transplantation of autologous limbal epithelial cells," *The New England Journal of Medicine*, vol. 343, no. 2, pp. 86–93, 2000.

[26] N. Koizumi, T. Inatomi, T. Suzuki, C. Sotozono, and S. Kinoshita, "Cultivated corneal epithelial transplantation for ocular surface reconstruction in acute phase of Stevens-Johnson syndrome," *Archives of Ophthalmology*, vol. 119, no. 2, Article ID 11176998, pp. 298–300, 2001.

[27] N. Koizumi, T. Inatomi, T. Suzuki, C. Sotozono, and S. Kinoshita, "Cultivated corneal epithelial stem cell transplantation in ocular surface disorders11The authors have no financial interest in this work.," *Ophthalmology*, vol. 108, no. 9, pp. 1569–1574, 2001.

[28] P. Rama, S. Bonini, A. Lambiase et al., "Autologous fibrin-cultured limbal stem cells permanently restore the corneal surface of patients with total limbal stem cell deficiency," *Transplantation*, vol. 72, no. 9, pp. 1478–1485, 2001.

[29] M. Grueterich, E. M. Espana, A. Touhami, S.-E. Ti, and S. C. G. Tseng, "Phenotypic study of a case with successful transplantation of ex vivo expanded human limbal epithelium for unilateral total limbal stem cell deficiency," *Ophthalmology*, vol. 109, no. 8, pp. 1547–1552, 2002.

[30] J. Shimazaki, M. Aiba, E. Goto, N. Kato, S. Shimmura, and K. Tsubota, "Transplantation of human limbal epithelium cultivated on amniotic membrane for the treatment of severe ocular surface disorders," *Ophthalmology*, vol. 109, no. 7, pp. 1285–1290, 2002.

[31] V. S. Sangwan, G. K. Vemuganti, G. Iftekhar, A. K. Bansal, and G. N. Rao, "Use of autologous cultured limbal and conjunctival

epithelium in a patient with severe bilateral ocular surface disease induced by acid injury: a case report of unique application," *Cornea*, vol. 22, no. 5, pp. 478–481, 2003.

[32] T. Nakamura, N. Koizumi, M. Tsuzuki et al., "Successful regrafting of cultivated corneal epithelium using amniotic membrane as a carrier in severe ocular surface disease," *Cornea*, vol. 22, no. 1, pp. 70–71, 2003.

[33] T. Nakamura, T. Inatomi, C. Sotozono, N. Koizumi, and S. Kinoshita, "Successful primary culture and autologous transplantation of corneal limbal epithelial cells from minimal biopsy for unilateral severe ocular surface disease," *Acta Ophthalmologica Scandinavica*, vol. 82, no. 4, pp. 468–471, 2004.

[34] S. M. Daya, A. Watson, J. R. Sharpe et al., "Outcomes and DNA analysis of ex vivo expanded stem cell allograft for ocular surface reconstruction," *Ophthalmology*, vol. 112, no. 3, pp. 470–477, 2005.

[35] V. S. Sangwan, H. P. Matalia, G. K. Vemuganti et al., "Early results of penetrating keratoplasty after cultivated limbal epithelium transplantation," *Archives of Ophthalmology*, vol. 123, no. 3, pp. 334–340, 1960.

[36] T. Nakamura, T. Inatomi, C. Sotozono et al., "Transplantation of autologous serum-derived cultivated corneal epithelial equivalents for the treatment of severe ocular surface disease," *Ophthalmology*, vol. 113, no. 10, pp. 1765–1772, 2006.

[37] V. S. Sangwan, H. P. Matalia, G. K. Vemuganti et al., "Clinical outcome of autologous cultivated limbal epithelium transplantation," *Indian Journal of Ophthalmology*, vol. 54, no. 1, pp. 29–34, 2006.

[38] L. P. K. Ang, C. Sotozono, N. Koizumi, T. Suzuki, T. Inatomi, and S. Kinoshita, "A comparison between cultivated and conventional limbal stem cell transplantation for Stevens-Johnson syndrome," *American Journal of Ophthalmology*, vol. 143, no. 1, pp. 178–180, 2007.

[39] J. Shimazaki, K. Higa, F. Morito et al., "Factors influencing outcomes in cultivated limbal epithelial transplantation for chronic cicatricial ocular surface disorders," *The American Journal of Ophthalmology*, vol. 143, no. 6, pp. 945–953, 2007.

[40] M. Kawashima, T. Kawakita, Y. Satake, K. Higa, and J. Shimazaki, "Phenotypic study after cultivated limbal epithelial transplantation for limbal stem cell deficiency," *Archives of Ophthalmology*, vol. 125, no. 10, pp. 1337–1344, 2007.

[41] A. Fatima, G. K. Vemuganti, G. Iftekhar, G. N. Rao, and V. S. Sangwan, "In vivo survival and stratification of cultured limbal epithelium," *Clinical and Experimental Ophthalmology*, vol. 35, no. 1, pp. 96–98, 2007.

[42] A. J. Shortt, G. A. Secker, M. S. Rajan et al., "Ex vivo expansion and transplantation of limbal epithelial stem cells," *Ophthalmology*, vol. 115, no. 11, pp. 1989–1997, 2008.

[43] N. Di Girolamo, M. Bosch, K. Zamora, M. T. Coroneo, D. Wakefield, and S. L. Watson, "A contact lens-based technique for expansion and transplantation of autologous epithelial progenitors for ocular surface reconstruction," *Transplantation*, vol. 87, no. 10, pp. 1571–1578, 2009.

[44] D. Meller, T. Fuchsluger, M. Pauklin, and K.-P. Steuhl, "Ocular surface reconstruction in graft-versus-host disease with HLA-identical living-related allogeneic cultivated limbal epithelium after hematopoietic stem cell transplantation from the same donor," *Cornea*, vol. 28, no. 2, pp. 233–236, 2009.

[45] A. Baradaran-Rafii, M. Ebrahimi, M. R. Kanavi et al., "Midterm outcomes of autologous cultivated limbal stem cell transplantation with or without penetrating keratoplasty," *Cornea*, vol. 29, no. 5, pp. 502–509, 2010.

[46] R. A. M. C. Gisoldi, A. Pocobelli, C. M. Villani, D. Amato, and G. Pellegrini, "Evaluation of molecular markers in corneal regeneration by means of autologous cultures of limbal cells and keratoplasty," *Cornea*, vol. 29, no. 7, pp. 715–722, 2010.

[47] M. Thanos, M. Pauklin, K.-P. Steuhl, and D. Meller, "Ocular surface reconstruction with cultivated limbal epithelium in a patient with unilateral stem cell deficiency caused by epidermolysis bullosa dystrophica hallopeau-siemens," *Cornea*, vol. 29, no. 4, pp. 462–464, 2010.

[48] E. Di Iorio, S. Ferrari, A. Fasolo, E. Böhm, D. Ponzin, and V. Barbaro, "Techniques for culture and assessment of limbal stem cell grafts," *Ocular Surface*, vol. 8, no. 3, pp. 146–153, 2010.

[49] P. Rama, S. Matuska, G. Paganoni, A. Spinelli, M. De Luca, and G. Pellegrini, "Limbal stem-cell therapy and long-term corneal regeneration," *The New England Journal of Medicine*, vol. 363, no. 2, pp. 147–155, 2010.

[50] S. A. I. Kolli, S. Ahmad, M. Lako, and F. Figueiredo, "Successful clinical implementation of corneal epithelial stem cell therapy for treatment of unilateral limbal stem cell deficiency," *Stem Cells*, vol. 28, no. 3, pp. 597–610, 2010.

[51] M. Pauklin, T. A. Fuchsluger, H. Westekemper, K.-P. Steuhl, and D. Meller, "Midterm results of cultivated autologous and allogeneic limbal epithelial transplantation in limbal stem cell deficiency," *Developments in Ophthalmology*, vol. 45, pp. 57–70, 2010.

[52] V. S. Sangwan, S. Basu, G. K. Vemuganti et al., "Clinical outcomes of xeno-free autologous cultivated limbal epithelial transplantation: a 10-year study," *British Journal of Ophthalmology*, vol. 95, no. 11, pp. 1525–1529, 2011.

[53] S. Sharma, R. Tandon, S. Mohanty et al., "Culture of corneal limbal epithelial stem cells: experience from benchtop to bedside in a tertiary care hospital in India," *Cornea*, vol. 30, no. 11, pp. 1223–1232, 2011.

[54] P. Prabhasawat, P. Ekpo, M. Uiprasertkul, S. Chotikavanich, and N. Tesavibul, "Efficacy of cultivated corneal epithelial stem cells for ocular surface reconstruction," *Clinical Ophthalmology*, vol. 6, pp. 1483–1492, 2012.

[55] S. Basu, H. Ali, and V. S. Sangwan, "Clinical outcomes of repeat autologous cultivated limbal epithelial transplantation for ocular surface burns," *The American Journal of Ophthalmology*, vol. 153, no. 4, pp. 643–650.e2, 2012.

[56] S. Subramaniam, K. Sejpal, A. Fatima, S. Gaddipati, G. Vemuganti, and V. Sangwan, "Coculture of autologous limbal and conjunctival epithelial cells to treat severe ocular surface disorders: Long-term survival analysis," *Indian Journal of Ophthalmology*, vol. 61, no. 5, pp. 202–207, 2013.

[57] K. Sejpal, M. H. Ali, S. Maddileti et al., "Cultivated limbal epithelial transplantation in children with ocular surface burns," *JAMA Ophthalmology*, vol. 131, no. 6, pp. 731–736, 2013.

[58] M. Pathak, S. Cholidis, K. Haug et al., "Clinical transplantation of ex vivo expanded autologous limbal epithelial cells using a culture medium with human serum as single supplement: a retrospective case series," *Acta Ophthalmologica*, vol. 91, no. 8, pp. 769–775, 2013.

[59] N. Zakaria, T. Possemiers, S. Dhubhghaill et al., "Results of a phase I/II clinical trial: standardized, non-xenogenic, cultivated limbal stem cell transplantation," *Journal of Translational Medicine*, vol. 12, article 58, 2014.

[60] J. Vazirani, S. Basu, H. Kenia et al., "Unilateral partial limbal stem cell deficiency: contralateral versus ipsilateral autologous cultivated limbal epithelial transplantation," *American Journal of Ophthalmology*, vol. 157, no. 3, pp. 584.e2–590.e2, 2014.

[61] K. Y. H. Chee, A. Kicic, and S. J. Wiffen, "Limbal stem cells: the search for a marker," *Clinical & Experimental Ophthalmology*, vol. 34, no. 1, pp. 64–73, 2006.

[62] M. A. Dziasko, H. E. Armer, H. J. Levis, A. J. Shortt, S. Tuft, and J. T. Daniels, "Localisation of epithelial cells capable of holoclone formation in vitro and direct interaction with stromal cells in the native human limbal crypt," *PLoS ONE*, vol. 9, no. 4, Article ID e94283, 2014.

[63] I. K. Gipson, "The epithelial basement membrane zone of the limbus," *Eye*, vol. 3, part 2, pp. 132–140, 1989.

[64] J. T. Daniels, J. K. G. Dart, S. J. Tuft, and P. T. Khaw, "Corneal stem cells in review," *Wound Repair and Regeneration*, vol. 9, no. 6, pp. 483–494, 2001.

[65] F. E. Kruse and S. C. Tseng, "Growth factors modulate clonal growth and differentiation of cultured rabbit limbal and corneal epithelium," *Investigative Ophthalmology & Visual Science*, vol. 34, no. 6, pp. 1963–1976, 1993.

[66] R. Schofield, "The stem cell system," *Biomedicine & Pharmacotherapy*, vol. 37, no. 8, pp. 375–380, 1983.

[67] S. C. Tseng, "Concept and application of limbal stem cells," *Eye*, vol. 3, part 2, pp. 141–157, 1989.

[68] F. E. Kruse, "Stem cells and corneal epithelial regeneration," *Eye*, vol. 8, part 2, pp. 170–183, 1994.

[69] H. S. Dua, J. S. Saini, A. Azuara-Blanco, and P. Gupta, "Limbal stem cell deficiency: concept, aetiology, clinical presentation, diagnosis and management," *Indian Journal of Ophthalmology*, vol. 48, no. 2, pp. 83–92, 2000.

[70] R. A. Thoft and J. Friend, "The X, Y, Z hypothesis of corneal epithelial maintenance," *Investigative Ophthalmology & Visual Science*, vol. 24, no. 10, pp. 1442–1443, 1983.

[71] K. Nishida, S. Kinoshita, Y. Ohashi, Y. Kuwayama, and S. Yamamoto, "Ocular surface abnormalities in aniridia," *American Journal of Ophthalmology*, vol. 120, no. 3, pp. 368–375, 1995.

[72] K. Ramaesh, T. Ramaesh, G. N. Dutton, and B. Dhillon, "Evolving concepts on the pathogenic mechanisms of aniridia related keratopathy," *The International Journal of Biochemistry & Cell Biology*, vol. 37, no. 3, pp. 547–557, 2005.

[73] A. F. Felipe, A. Abazari, K. M. Hammersmith, C. J. Rapuano, P. K. Nagra, and B. M. Peiro, "Corneal changes in ectrodactyly-ectodermal dysplasia-cleft lip and palate syndrome: case series and literature review," *International Ophthalmology*, vol. 32, no. 5, pp. 475–480, 2012.

[74] J. Á. Gomes, B. Geraldes Monteiro, G. B. Melo et al., "Corneal reconstruction with tissue-engineered cell sheets composed of human immature dental pulp stem cells," *Investigative Opthalmology & Visual Science*, vol. 51, no. 3, pp. 1408–1414, 2010.

[75] D. Aslan and R. F. Akata, "Dyskeratosis congenita and limbal stem cell deficiency," *Experimental Eye Research*, vol. 90, no. 3, pp. 472–473, 2010.

[76] D. Aslan, R. F. Akata, H. Holme, T. Vulliamy, and I. Dokal, "Limbal stem cell deficiency in patients with inherited stem cell disorder of dyskeratosis congenita," *International Ophthalmology*, vol. 32, no. 6, pp. 615–622, 2012.

[77] W. J. Hughes, "Alkali burns of the eye," *Clinical and Pathologic Course*, vol. 36, article 189, 1946.

[78] R. P. Bhatia, R. Srivastava, and A. Ghosh, "Limbal stem cell study in contact lens wearers," *Annals of Ophthalmology*, vol. 41, no. 2, pp. 87–92, 2009.

[79] S. Ahmad, "Concise review: limbal stem cell deficiency, dysfunction, and distress," *Stem Cells Translational Medicine*, vol. 1, no. 2, pp. 110–115, 2012.

[80] S. Deng, K. Sejpal, and P. Bakhtiari, "Presentation, diagnosis and management of limbal stem cell deficiency," *Middle East African Journal of Ophthalmology*, vol. 20, no. 1, pp. 5–10, 2013.

[81] M. S. Sridhar, G. K. Vemuganti, A. K. Bansal, and G. N. Rao, "Impression cytology-proven corneal stem cell deficiency in patients after surgeries involving the limbus," *Cornea*, vol. 20, no. 2, pp. 145–148, 2001.

[82] F. dos Santos Paris, E. D. Gonçalves, J. de Nadai Barros, M. S. de Queiroz Campos, E. H. Sato, and J. A. P. Gomes, "Impression cytology findings in bullous keratopathy," *British Journal of Ophthalmology*, vol. 94, no. 6, pp. 773–776, 2010.

[83] R. T. F. Pires, A. Chokshi, and S. C. G. Tseng, "Amniotic membrane transplantation or conjunctival limbal autograft for limbal stem cell deficiency induced by 5-fluorouracil in glaucoma surgeries," *Cornea*, vol. 19, no. 3, pp. 284–287, 2000.

[84] B. W. Dudney and M. A. Malecha, "Limbal stem cell deficiency following topical mitomycin C treatment of conjunctival-corneal intraepithelial neoplasia," *American Journal of Ophthalmology*, vol. 137, no. 5, pp. 950–951, 2004.

[85] P. Ellies, D. F. Anderson, A. Touhami, and S. C. G. Tseng, "Limbal stem cell deficiency arising from systemic chemotherapy," *British Journal of Ophthalmology*, vol. 85, no. 3, pp. 373–374, 2001.

[86] G. Geerling, J. T. Daniels, J. K. G. Dart, I. A. Cree, and P. T. Khaw, "Toxicity of natural tear substitutes in a fully defined culture model of human corneal epithelial cells," *Investigative Ophthalmology and Visual Science*, vol. 42, no. 5, pp. 948–956, 2001.

[87] F. Mantelli and P. Argüeso, "Functions of ocular surface mucins in health and disease," *Current Opinion in Allergy and Clinical Immunology*, vol. 8, no. 5, pp. 477–483, 2008.

[88] S. Rauz and V. P. Saw, "Serum eye drops, amniotic membrane and limbal epithelial stem cells—tools in the treatment of ocular surface disease," *Cell and Tissue Banking*, vol. 11, no. 1, pp. 13–27, 2010.

[89] M. Fernandes, V. S. Sangwan, S. K. Rao et al., "Limbal stem cell transplantation," *Indian Journal of Ophthalmology*, vol. 52, no. 1, Article ID 15132374, pp. 5–22, 2004.

[90] M. M. Schornack, "Limbal stem cell disease: management with scleral lenses," *Clinical and Experimental Optometry*, vol. 94, no. 6, pp. 592–594, 2011.

[91] H. S. Dua, "The conjunctiva in corneal epithelial wound healing," *British Journal of Ophthalmology*, vol. 82, no. 12, pp. 1407–1411, 1998.

[92] D. F. Anderson, P. Ellies, R. T. F. Pires, and S. C. G. Tseng, "Amniotic membrane transplantation for partial limbal stem cell deficiency," *British Journal of Ophthalmology*, vol. 85, no. 5, pp. 567–575, 2001.

[93] A. J. Shortt, G. A. Secker, M. D. Notara et al., "Transplantation of ex vivo cultured limbal epithelial stem cells: a review of techniques and clinical results," *Survey of Ophthalmology*, vol. 52, no. 5, pp. 483–502, 2007.

[94] V. S. Sangwan, S. Basu, S. MacNeil, and D. Balasubramanian, "Simple limbal epithelial transplantation (SLET): a novel surgical technique for the treatment of unilateral limbal stem cell deficiency," *British Journal of Ophthalmology*, vol. 96, no. 7, pp. 931–934, 2012.

[95] G. Amescua, M. Atallah, N. Nikpoor, A. Galor, and V. L. Perez, "Modified simple limbal epithelial transplantation using cryopreserved amniotic membrane for unilateral limbal stem cell deficiency," *American Journal of Ophthalmology*, vol. 158, no. 3, pp. 469.e2–475.e2, 2014.

[96] S. Bhalekar, S. Basu, and V. S. Sangwan, "Successful management of immunological rejection following allogeneic simple limbal epithelial transplantation (SLET) for bilateral ocular burns," *BMJ Case Reports*, vol. 2013, 2013.

[97] J. Vazirani, S. Basu, and V. Sangwan, "Successful simple limbal epithelial transplantation (SLET) in lime injury-induced limbal stem cell deficiency with ocular surface granuloma," *BMJ Case Reports*, 2013.

[98] R. K. Molvaer, A. Andreasen, S. Heegaard et al., "Interactive 3D computer model of the human corneolimbal region: crypts, projections and stem cells," *Acta Ophthalmologica*, vol. 91, no. 5, pp. 457–462, 2013.

[99] H. S. Dua, V. A. Shanmuganathan, A. O. Powell-Richards, P. J. Tighe, and A. Joseph, "Limbal epithelial crypts: a novel anatomical structure and a putative limbal stem cell niche," *British Journal of Ophthalmology*, vol. 89, no. 5, pp. 529–532, 2005.

[100] C. Bath, D. Muttuvelu, J. Emmersen, H. Vorum, J. Hjortdal, and V. Zachar, "Correction: transcriptional dissection of human limbal niche compartments by massive parallel sequencing," *PLoS ONE*, vol. 8, no. 11, 2013.

[101] A. Joseph, A. O. R. Powell-Richards, V. A. Shanmuganathan, and H. S. Dua, "Epithelial cell characteristics of cultured human limbal explants," *British Journal of Ophthalmology*, vol. 88, no. 3, pp. 393–398, 2004.

[102] U. Schlötzer-Schrehardt and F. E. Kruse, "Identification and characterization of limbal stem cells," *Experimental Eye Research*, vol. 81, no. 3, pp. 247–264, 2005.

[103] K. Watanabe, K. Nishida, M. Yamato et al., "Human limbal epithelium contains side population cells expressing the ATP-binding cassette transporter ABCG2," *FEBS Letters*, vol. 565, no. 1–3, pp. 6–10, 2004.

[104] A. Yang, R. Schweitzer, D. Sun et al., "p63 is essential for regenerative proliferation in limb, craniofacial and epithelial development," *Nature*, vol. 398, no. 6729, pp. 714–718, 1999.

[105] E. Di Iorio, V. Barbaro, A. Ruzza, D. Ponzin, G. Pellegrini, and M. De Luca, "Isoforms of ΔNp63 and the migration of ocular limbal cells in human corneal regeneration," *Proceedings of the National Academy of Sciences of the United States of America*, vol. 102, no. 27, pp. 9523–9528, 2005.

[106] P. Ordonez, S. Chow, D. Wakefield, and N. Di Girolamo, "Human limbal epithelial progenitor cells express $\alpha v\beta 5$-integrin and the interferon-inducible chemokine CXCL10/IP-10," *Stem Cell Research*, vol. 11, no. 2, pp. 888–901, 2013.

[107] B. R. Ksander, P. E. Kolovou, B. J. Wilson et al., "*ABCB5* is a limbal stem cell gene required for corneal development and repair," *Nature*, vol. 511, no. 7509, pp. 353–357, 2014.

[108] M. De Luca, G. Pellegrini, and H. Green, "Regeneration of squamous epithelia from stem cells of cultured grafts," *Regenerative Medicine*, vol. 1, no. 1, pp. 45–57, 2006.

[109] H. Green, "The birth of therapy with cultured cells," *BioEssays*, vol. 30, no. 9, pp. 897–903, 2008.

[110] Y. Oie, R. Hayashi, R. Takagi et al., "A novel method of culturing human oral mucosal epithelial cell sheet using post-mitotic human dermal fibroblast feeder cells and modified keratinocyte culture medium for ocular surface reconstruction," *British Journal of Ophthalmology*, vol. 94, no. 9, pp. 1244–1250, 2010.

[111] M. Omoto, H. Miyashita, S. Shimmura et al., "The use of human mesenchymal stem cell–derived feeder cells for the cultivation of transplantable epithelial sheets," *Investigative Opthalmology & Visual Science*, vol. 50, no. 5, pp. 2109–2115, 2009.

[112] S. M. Sharma, T. Fuchsluger, S. Ahmad et al., "Comparative analysis of human-derived feeder layers with 3T3 fibroblasts for the ex vivo expansion of human limbal and oral epithelium," *Stem Cell Reviews and Reports*, vol. 8, no. 3, pp. 696–705, 2012.

[113] P. Carrier, A. Deschambeault, C. Audet et al., "Impact of cell source on human cornea reconstructed by tissue engineering," *Investigative Opthalmology & Visual Science*, vol. 50, no. 6, pp. 2645–2652, 2009.

[114] M. N. Nakatsu, S. Gonzalez, H. Mei, and S. X. Deng, "uman limbal mesenchymal cells support the growth of human corneal epithelial stem/progenitor cells," *Investigative Ophthalmology & Visual Science*, vol. 55, no. 10, pp. 6953–6959, 2014.

[115] The Commission of the European Communities, "Commission directive 2003/94/EC of 8 October 2003. Laying down the principles and guidelines of good manufacturing practice in respect of medicinal products for human use and investigational medicinal products for human use," *Official Journal of the European Union*, vol. L262, pp. 22–26, 2003.

[116] M. Notara, D. B. Haddow, S. MacNeil, and J. T. Daniels, "A xenobiotic-free culture system for human limbal epithelial stem cells," *Regenerative Medicine*, vol. 2, no. 6, pp. 919–927, 2007.

[117] V. M. Varghese, T. Prasad, and T. V. Kumary, "Optimization of culture conditions for an efficient xeno-feeder free limbal cell culture system towards ocular surface regeneration," *Microscopy Research and Technique*, vol. 73, no. 11, pp. 1045–1052, 2010.

[118] N. Zakaria, C. Koppen, V. Van Tendeloo, Z. Berneman, A. Hopkinson, and M.-J. Tassignon, "Standardized limbal epithelial stem cell graft generation and transplantation," *Tissue Engineering Part C: Methods*, vol. 16, no. 5, pp. 921–927, 2010.

[119] S. Bhalekar, S. Basu, I. Lal, and V. S. Sangwan, "Successful autologous simple limbal epithelial transplantation (SLET) in previously failed paediatric limbal transplantation for ocular surface burns," *BMJ Case Reports*, 2013.

[120] S. Bhalekar, V. S. Sangwan, and S. Basu, "Growth of corneal epithelial cells over in situ therapeutic contact lens after simple limbal epithelial transplantation (SLET)," *BMJ Case Reports*, 2013.

[121] S. Ijiri, A. Kobayashi, K. Sugiyama, and S. C. G. Tseng, "Evaluation of visual acuity and color vision in normal human eyes with a sutureless temporary amniotic membrane patch," *American Journal of Ophthalmology*, vol. 144, no. 6, pp. 938.e1–942.e1, 2007.

[122] D. H.-K. Ma, J.-Y. Lai, H.-Y. Cheng, C.-C. Tsai, and L.-K. Yeh, "Carbodiimide cross-linked amniotic membranes for cultivation of limbal epithelial cells," *Biomaterials*, vol. 31, no. 25, pp. 6647–6658, 2010.

[123] J.-Y. Lai and D. H.-K. Ma, "Glutaraldehyde cross-linking of amniotic membranes affects their nanofibrous structures and limbal epithelial cell culture characteristics," *International Journal of Nanomedicine*, vol. 8, no. 1, pp. 4157–4168, 2013.

[124] J.-Y. Lai, S. J. Lue, H.-Y. Cheng, and D. H. Ma, "Effect of matrix nanostructure on the functionality of carbodiimide cross-linked amniotic membranes as limbal epithelial cell scaffolds," *Journal of Biomedical Nanotechnology*, vol. 9, no. 12, pp. 2048–2062, 2013.

[125] S. Sekar, K. Sasirekha, S. Krishnakumar, and T. P. Sastry, "A novel cross-linked human amniotic membrane for corneal implantations," *Proceedings of the Institution of Mechanical Engineers Part H: Journal of Engineering in Medicine*, vol. 227, no. 3, pp. 221–228, 2013.

[126] J.-Y. Lai, P.-R. Wang, L.-J. Luo, and S.-T. Chen, "Stabilization of collagen nanofibers with l-lysine improves the ability of

carbodiimide cross-linked amniotic membranes to preserve limbal epithelial progenitor cells," *International Journal of Nanomedicine*, vol. 9, no. 1, pp. 5117–5130, 2014.

[127] H. S. Geggel, J. Friend, and R. A. Thoft, "Collagen gel for ocular surface," *Investigative Ophthalmology & Visual Science*, vol. 26, no. 6, pp. 901–905, 1985.

[128] M. Griffith, W. B. Jackson, N. Lagali, K. Merrett, F. Li, and P. Fagerholm, "Artificial corneas: a regenerative medicine approach," *Eye*, vol. 23, no. 10, pp. 1985–1989, 2009.

[129] E. J. Orwin and A. Hubel, "In vitro culture characteristics of corneal epithelial, endothelial, and keratocyte cells in a native collagen matrix," *Tissue Engineering*, vol. 6, no. 4, pp. 307–319, 2000.

[130] W. M. Ambrose, A. Salahuddin, S. So et al., "Collagen Vitrigel membranes for the *in vitro* reconstruction of separate corneal epithelial, stromal, and endothelial cell layers," *Journal of Biomedical Materials Research Part B: Applied Biomaterials*, vol. 90, no. 2, pp. 818–831, 2009.

[131] Y. G. He and J. P. McCulley, "Growing human corneal epithelium on collagen shield and subsequent transfer to denuded cornea in vitro," *Current Eye Research*, vol. 10, no. 9, pp. 851–863, 1991.

[132] H. Kobayashi and Y. Ikada, "Covalent immobilization of proteins on to the surface of poly(vinyl alcohol) hydrogel," *Biomaterials*, vol. 12, no. 8, pp. 747–751, 1991.

[133] K. Merrett, C. M. Griffith, Y. Deslandes, G. Pleizier, and H. Sheardown, "Adhesion of corneal epithelial cells to cell adhesion peptide modified pHEMA surfaces," *Journal of Biomaterials Science, Polymer Edition*, vol. 12, no. 6, pp. 647–671, 2001.

[134] L. Aucoin, C. M. Griffith, G. Pleizier, Y. Deslandes, and H. Sheardown, "Interactions of corneal epithelial cells and surfaces modified with cell adhesion peptide combinations," *Journal of Biomaterials Science, Polymer Edition*, vol. 13, no. 4, pp. 447–462, 2002.

[135] C. Wallace, J. T. Jacob, A. Stoltz, J. Bi, and K. Bundy, "Corneal epithelial adhesion strength to tethered-protein/peptide modified hydrogel surfaces," *Journal of Biomedical Materials Research*, vol. 72, no. 1, pp. 19–24, 2005.

[136] N. Ahmadiankia, M. Ebrahimi, A. Hosseini, and H. Baharvand, "Effects of different extracellular matrices and co-cultures on human limbal stem cell expansion in vitro," *Cell Biology International*, vol. 33, no. 9, pp. 978–987, 2009.

[137] A. Chakraborty, J. Dutta, S. Das, and H. Datta, "Comparison of ex vivo cultivated human limbal epithelial stem cell viability and proliferation on different substrates," *International Ophthalmology*, vol. 33, no. 6, pp. 665–670, 2013.

[138] Y. Liu, M. Griffith, M. A. Watsky et al., "Properties of porcine and recombinant human collagen matrices for optically clear tissue engineering applications," *Biomacromolecules*, vol. 7, no. 6, pp. 1819–1828, 2006.

[139] M. Rafat, F. Li, P. Fagerholm et al., "PEG-stabilized carbodiimide crosslinked collagen-chitosan hydrogels for corneal tissue engineering," *Biomaterials*, vol. 29, no. 29, pp. 3960–3972, 2008.

[140] N. Pasyechnikova, V. Vit, M. Leus et al., "Collagen-based bioengineered substitutes of donor corneal allograft implantation: assessment and hypotheses," *Medical Hypothesis, Discovery & Innovation Ophthalmology Journal*, vol. 1, no. 1, pp. 10–13, 2012.

[141] C. C. Lin, R. Ritch, S. M. Lin et al., "A new fish scale-derived scaffold for corneal regeneration," *European Cells & Materials*, vol. 19, pp. 50–57, 2010.

[142] S. Krishnan, S. Sekar, M. F. Katheem, S. Krishnakumar, and T. P. Sastry, "Fish scale collagen—a novel material for corneal tissue engineering," *Artificial Organs*, vol. 36, no. 9, pp. 829–835, 2012.

[143] T. H. Van Essen, C. C. Lin, A. K. Hussain et al., "A fish scale-derived collagen matrix as artificial cornea in rats: properties and potential," *Investigative Opthalmology & Visual Science*, vol. 54, no. 5, pp. 3224–3233, 2013.

[144] Z. Wu, Q. Zhou, H. Duan et al., "Reconstruction of auto-tissue-engineered lamellar cornea by dynamic culture for transplantation: a rabbit model," *PLoS ONE*, vol. 9, no. 4, Article ID e93012, 2014.

[145] J. Myllyharju, M. Nokelainen, A. Vuorela, and K. I. Kivirikko, "Expression of recombinant human type I-III collagens in the yeast *Pichia pastoris*," *Biochemical Society Transactions*, vol. 28, no. 4, pp. 353–357, 2000.

[146] D. Olsen, C. Yang, M. Bodo et al., "Recombinant collagen and gelatin for drug delivery," *Advanced Drug Delivery Reviews*, vol. 55, no. 12, pp. 1547–1567, 2003.

[147] M. Tomita, H. Munetsuna, T. Sato et al., "Transgenic silkworms produce recombinant human type III procollagen in cocoons," *Nature Biotechnology*, vol. 21, no. 1, pp. 52–56, 2002.

[148] H. Stein, M. Wilensky, Y. Tsafrir et al., "Production of bioactive, post-translationally modified, heterotrimeric, human recombinant type-I collagen in transgenic tobacco," *Biomacromolecules*, vol. 10, no. 9, pp. 2640–2645, 2009.

[149] P. Fagerholm, N. S. Lagali, J. A. Ong et al., "Stable corneal regeneration four years after implantation of a cell-free recombinant human collagen scaffold," *Biomaterials*, vol. 35, no. 8, pp. 2420–2427, 2014.

[150] M. Mirazul Islam, V. Cėpla, C. He et al., "Functional fabrication of recombinant human collagen–phosphorylcholine hydrogels for regenerative medicine applications," *Acta Biomaterialia*, vol. 12, pp. 70–80, 2015.

[151] O. Buznyk, N. Pasyechnikova, M. M. Islam, S. Iakymenko, P. Fagerholm, and M. Griffith, "Bioengineered corneas grafted as alternatives to human donor corneas in three high-risk patients," *Clinical and Translational Science*, 2015.

[152] E. Bell, B. Ivarsson, and C. Merrill, "Production of a tissue-like structure by contraction of collagen lattices by human fibroblasts of different proliferative potential in vitro," *Proceedings of the National Academy of Sciences of the United States of America*, vol. 76, no. 3, pp. 1274–1278, 1979.

[153] N. Lagali, M. Griffith, P. Fagerholm, K. Merrett, M. Huynh, and R. Munger, "Innervation of tissue-engineered recombinant human collagen-based corneal substitutes: a comparative in vivo confocal microscopy study," *Investigative Ophthalmology and Visual Science*, vol. 49, no. 9, pp. 3895–3902, 2008.

[154] K. Merrett, P. Fagerholm, C. R. McLaughlin et al., "Tissue-engineered recombinant human collagen-based corneal substitutes for implantation: performance of type I versus type III collagen," *Investigative Opthalmology & Visual Science*, vol. 49, no. 9, pp. 3887–3894, 2008.

[155] W. Liu, K. Merrett, M. Griffith et al., "Recombinant human collagen for tissue engineered corneal substitutes," *Biomaterials*, vol. 29, no. 9, pp. 1147–1158, 2008.

[156] W. Liu, C. Deng, C. R. McLaughlin et al., "Collagen-phosphorylcholine interpenetrating network hydrogels as corneal substitutes," *Biomaterials*, vol. 30, no. 8, pp. 1551–1559, 2009.

[157] C. R. McLaughlin, M. C. Acosta, C. Luna et al., "Regeneration of functional nerves within full thickness collagen-phosphorylcholine corneal substitute implants in guinea pigs," *Biomaterials*, vol. 31, no. 10, pp. 2770–2778, 2010.

[158] M. Griffith, M. Islam, S. Iakymenko, N. Pasyechnikova, and O. Buznyk, "Next generation corneal implants as alternative to high risk donor transplantation," *Acta Ophthalmologica*, vol. 92, supplement s253, 2014.

[159] M. Grolik, K. Szczubiałka, B. Wowra et al., "Hydrogel membranes based on genipin-cross-linked chitosan blends for corneal epithelium tissue engineering," *Journal of Materials Science: Materials in Medicine*, vol. 23, no. 8, pp. 1991–2000, 2012.

[160] S. Mi, B. Chen, B. Wright, and C. J. Connon, "Plastic compression of a collagen gel forms a much improved scaffold for ocular surface tissue engineering over conventional collagen gels," *Journal of Biomedical Materials Research Part A*, vol. 95, no. 2, pp. 447–453, 2010.

[161] H. J. Levis, R. A. Brown, and J. T. Daniels, "Plastic compressed collagen as a biomimetic substrate for human limbal epithelial cell culture," *Biomaterials*, vol. 31, no. 30, pp. 7726–7737, 2010.

[162] H. J. Levis, G. S. L. Peh, K.-P. Toh et al., "Plastic compressed collagen as a novel carrier for expanded human corneal endothelial cells for transplantation," *PLoS ONE*, vol. 7, no. 11, Article ID e50993, 2012.

[163] H. J. Levis, J. Menzel-Severing, R. A. Drake, and J. T. Daniels, "Plastic compressed collagen constructs for ocular cell culture and transplantation: a new and improved technique of confined fluid loss," *Current Eye Research*, vol. 38, no. 1, pp. 41–52, 2013.

[164] S. Mi, V. V. Khutoryanskiy, R. R. Jones, X. Zhu, I. W. Hamley, and C. J. Connon, "Photochemical cross-linking of plastically compressed collagen gel produces an optimal scaffold for corneal tissue engineering," *Journal of Biomedical Materials Research Part A*, vol. 99, no. 1, pp. 1–8, 2011.

[165] H. I. Atrah, "Fibrin glue," *The British Medical Journal*, vol. 308, no. 6934, pp. 933–934, 1994.

[166] M. Radosevich, H. A. Goubran, and T. Burnouf, "Fibrin sealant: scientific rationale, production methods, properties, and current clinical use," *Vox Sanguinis*, vol. 72, no. 3, pp. 133–143, 1997.

[167] K. H. Siedentop, J. J. Park, A. N. Shah, T. K. Bhattacharyya, and K. M. O'Grady, "Safety and efficacy of currently available fibrin tissue adhesives," *American Journal of Otolaryngology*, vol. 22, no. 4, pp. 230–235, 2001.

[168] C. Buchta, M. Dettke, P. T. Funovics et al., "Impact of manufacturing, irradiation and filtration steps to bacterial contamination of autologous fibrin sealant," *Biologicals*, vol. 32, no. 3, pp. 165–169, 2004.

[169] M. Talbot, P. Carrier, C. J. Giasson et al., "Autologous transplantation of rabbit limbal epithelia cultured on fibrin gels for ocular surface reconstruction," *Molecular Vision*, vol. 12, pp. 65–75, 2006.

[170] L. Lu, P. S. Reinach, and W. W. Kao, "Corneal epithelial wound healing," *Experimental Biology and Medicine*, vol. 226, no. 7, pp. 653–664, 2001.

[171] N. Di Girolamo, J. Chui, D. Wakefield, and M. T. Coroneo, "Cultured human ocular surface epithelium on therapeutic contact lenses," *British Journal of Ophthalmology*, vol. 91, no. 4, pp. 459–464, 2007.

[172] A. Gore, V. Horwitz, H. Gutman et al., "Cultivation and characterization of limbal epithelial stem cells on contact lenses with a feeder layer: toward the treatment of limbal stem cell deficiency," *Cornea*, vol. 33, no. 1, pp. 65–71, 2014.

[173] K. D. Brown, S. Low, I. Mariappan et al., "Plasma polymer-coated contact lenses for the culture and transfer of corneal epithelial cells in the treatment of limbal stem cell deficiency," *Tissue Engineering Part A*, vol. 20, no. 3-4, pp. 646–655, 2014.

[174] S. Sharma, D. Gupta, S. Mohanty, M. Jassal, A. K. Agrawal, and R. Tandon, "Surface-modified electrospun poly(epsilon-caprolactone) scaffold with improved optical transparency and bioactivity for damaged ocular surface reconstruction," *Investigative Ophthalmology & Visual Science*, vol. 55, no. 2, pp. 899–907, 2014.

[175] J. Berger, M. Reist, J. M. Mayer, O. Felt, N. A. Peppas, and R. Gurny, "Structure and interactions in covalently and ionically crosslinked chitosan hydrogels for biomedical applications," *European Journal of Pharmaceutics and Biopharmaceutics*, vol. 57, no. 1, pp. 19–34, 2004.

[176] E. Khor and L. Y. Lim, "Implantable applications of chitin and chitosan," *Biomaterials*, vol. 24, no. 13, pp. 2339–2349, 2003.

[177] S. Bhat, A. Tripathi, and A. Kumar, "Supermacroprous chitosan-agarose-gelatin cryogels: in vitro characterization and in vivo assessment for cartilage tissue engineering," *Journal of The Royal Society Interface*, vol. 8, no. 57, pp. 540–554, 2011.

[178] H. Liu, J. Mao, K. Yao, G. Yang, L. Cui, and Y. Cao, "A study on a chitosan-gelatin-hyaluronic acid scaffold as artificial skin in vitro and its tissue engineering applications," *Journal of Biomaterials Science, Polymer Edition*, vol. 15, no. 1, pp. 25–40, 2004.

[179] A. De la Mata, T. Nieto-Miguel, M. López-Paniagua et al., "Chitosan-gelatin biopolymers as carrier substrata for limbal epithelial stem cells," *Journal of Materials Science: Materials in Medicine*, vol. 24, no. 12, pp. 2819–2829, 2013.

[180] K.-H. Kim, L. Jeong, H.-N. Park et al., "Biological efficacy of silk fibroin nanofiber membranes for guided bone regeneration," *Journal of Biotechnology*, vol. 120, no. 3, pp. 327–339, 2005.

[181] C. Shangkai, T. Naohide, Y. Koji et al., "Transplantation of allogeneic chondrocytes cultured in fibroin sponge and stirring chamber to promote cartilage regeneration," *Tissue Engineering*, vol. 13, no. 3, pp. 483–492, 2007.

[182] K. H. Lee, D. H. Baek, C. S. Ki, and Y. H. Park, "Preparation and characterization of wet spun silk fibroin/poly(vinyl alcohol) blend filaments," *International Journal of Biological Macromolecules*, vol. 41, no. 2, pp. 168–172, 2007.

[183] K. Higa, N. Takeshima, F. Moro et al., "Porous silk fibroin film as a transparent carrier for cultivated corneal epithelial sheets," *Journal of Biomaterials Science, Polymer Edition*, vol. 22, no. 17, pp. 2261–2276, 2011.

[184] L. J. Bray, K. A. George, S. L. Ainscough, D. W. Hutmacher, T. V. Chirila, and D. G. Harkin, "Human corneal epithelial equivalents constructed on *Bombyx mori* silk fibroin membranes," *Biomaterials*, vol. 32, no. 22, pp. 5086–5091, 2011.

[185] J. Liu, B. D. Lawrence, A. Liu, I. R. Schwab, L. A. Oliveira, and M. I. Rosenblatt, "Silk fibroin as a biomaterial substrate for corneal epithelial cell sheet generation," *Investigative Opthalmology & Visual Science*, vol. 53, no. 7, pp. 4130–4130, 2012.

[186] L. J. Bray, K. A. George, D. W. Hutmacher, T. V. Chirila, and D. G. Harkin, "A dual-layer silk fibroin scaffold for reconstructing the human corneal limbus," *Biomaterials*, vol. 33, no. 13, pp. 3529–3538, 2012.

[187] T. A. Hogerheyde, S. Suzuki, S. A. Stephenson et al., "Assessment of freestanding membranes prepared from *Antheraea pernyi* silk fibroin as a potential vehicle for corneal epithelial cell transplantation," *Biomedical Materials*, vol. 9, no. 2, Article ID 025016, 2014.

[188] L. Guan, P. Tian, H. Ge et al., "Chitosan-functionalized silk fibroin 3D scaffold for keratocyte culture," *Journal of Molecular Histology*, vol. 44, no. 5, pp. 609–618, 2013.

[189] L. Guan, H. Ge, X. Tang et al., "Use of a silk fibroin-chitosan scaffold to construct a tissue-engineered corneal stroma," *Cells Tissues Organs*, vol. 198, no. 3, pp. 190–197, 2013.

[190] B. P. Danysh, K. J. Czymmek, P. T. Olurin, J. G. Sivak, and M. K. Duncan, "Contributions of mouse genetic background and age on anterior lens capsule thickness," *The Anatomical Record*, vol. 291, no. 12, pp. 1619–1627, 2008.

[191] S. Krag, T. Olsen, and T. T. Andreassen, "Biomechanical characteristics of the human anterior lens capsule in relation to age," *Investigative Ophthalmology & Visual Science*, vol. 38, no. 2, pp. 357–363, 1997.

[192] A. Galal, J. J. Perez-Santonja, J. L. Rodriguez-Prats, M. Abad, and J. Alio, "Human anterior lens capsule as a biologic substrate for the ex vivo expansion of limbal stem cells in ocular surface reconstruction," *Cornea*, vol. 26, no. 4, pp. 473–478, 2007.

[193] R. Albert, Z. Veréb, K. Csomós et al., "Cultivation and characterization of cornea limbal epithelial stem cells on lens capsule in animal material-free medium," *PLoS ONE*, vol. 7, no. 10, Article ID e47187, 2012.

[194] S. Reichl, M. Borrelli, and G. Geerling, "Keratin films for ocular surface reconstruction," *Biomaterials*, vol. 32, no. 13, pp. 3375–3386, 2011.

[195] M. Borrelli, S. Reichl, Y. Feng, M. Schargus, S. Schrader, and G. Geerling, "In vitro characterization and ex vivo surgical evaluation of human hair keratin films in ocular surface reconstruction after sterilization processing," *Journal of Materials Science: Materials in Medicine*, vol. 24, no. 1, pp. 221–230, 2013.

[196] M. Mohan and S. K. Angra, "Vicryl suture in ophthalmic surgery," *Indian Journal of Ophthalmology*, vol. 27, no. 3, pp. 24–28, 1979.

[197] P. Deshpande, R. McKean, K. A. Blackwood et al., "Using poly(lactide-co-glycolide) electrospun scaffolds to deliver cultured epithelial cells to the cornea," *Regenerative Medicine*, vol. 5, no. 3, pp. 395–401, 2010.

[198] K. A. Blackwood, R. McKean, I. Canton et al., "Development of biodegradable electrospun scaffolds for dermal replacement," *Biomaterials*, vol. 29, no. 21, pp. 3091–3104, 2008.

[199] P. Deshpande, C. Ramachandran, V. S. Sangwan, and S. Macneil, "Cultivation of limbal epithelial cells on electrospun poly (lactide-co-glycolide) scaffolds for delivery to the cornea," *Methods in Molecular Biology*, vol. 1014, pp. 179–185, 2013.

[200] A. Ma, B. Zhao, A. J. Bentley et al., "Corneal epithelialisation on surface-modified hydrogel implants," *Journal of Materials Science: Materials in Medicine*, vol. 22, no. 3, pp. 663–670, 2011.

[201] S. Rimmer, C. Johnson, B. Zhao et al., "Epithelialization of hydrogels achieved by amine functionalization and co-culture with stromal cells," *Biomaterials*, vol. 28, no. 35, pp. 5319–5331, 2007.

[202] E. Hassan, P. Deshpande, F. Claeyssens, S. Rimmer, and S. MacNeil, "Amine functional hydrogels as selective substrates for corneal epithelialization," *Acta Biomaterialia*, vol. 10, no. 7, pp. 3029–3037, 2014.

[203] S. A. Holak, H. M. Holak, and H. Bleckmann, "AlphaCor keratoprosthesis: postoperative development of six patients," *Graefe's Archive for Clinical and Experimental Ophthalmology*, vol. 247, no. 4, pp. 535–539, 2009.

[204] T. V. Chirila, I. J. Constable, G. J. Crawford et al., "Poly(2-hydroxyethyl methacrylate) sponges as implant materials: in vivo and in vitro evaluation of cellular invasion," *Biomaterials*, vol. 14, no. 1, pp. 26–38, 1993.

[205] A. M. Oelker and M. W. Grinstaff, "Synthesis, characterization, and in vitro evaluation of a hydrogel-based corneal onlay," *IEEE Transactions on NanoBioscience*, vol. 11, no. 1, pp. 37–45, 2012.

[206] L. Hartmann, K. Watanabe, L. L. Zheng et al., "Toward the development of an artificial cornea: improved stability of interpenetrating polymer networks," *Journal of Biomedical Materials Research Part B: Applied Biomaterials*, vol. 98, no. 1, pp. 8–17, 2011.

[207] X. W. Tan, L. Hartman, K. P. Tan et al., "In vivo biocompatibility of two PEG/PAA interpenetrating polymer networks as corneal inlays following deep stromal pocket implantation," *Journal of Materials Science: Materials in Medicine*, vol. 24, no. 4, pp. 967–977, 2013.

[208] D. Myung, W. Koh, A. Bakri et al., "Design and fabrication of an artificial cornea based on a photolithographically patterned hydrogel construct," *Biomedical Microdevices*, vol. 9, no. 6, pp. 911–922, 2007.

[209] B. Ozcelik, K. D. Brown, A. Blencowe, M. Daniell, G. W. Stevens, and G. G. Qiao, "Ultrathin chitosan-poly(ethylene glycol) hydrogel films for corneal tissue engineering," *Acta Biomaterialia*, vol. 9, no. 5, pp. 6594–6605, 2013.

[210] F. L. Gimeno, V. Lavigne, S. Gatto, J. O. Croxatto, L. Correa, and J. E. Gallo, "Advances in corneal stem-cell transplantation in rabbits with severe ocular alkali burns," *Journal of Cataract and Refractive Surgery*, vol. 33, no. 11, pp. 1958–1965, 2007.

[211] F. L. Gimeno, V. Lavigne, S. Gatto, J. O. Croxatto, L. Correa, and J. E. Gallo, "One-year follow-up of epithelial corneal cell sheet allografts mounted on platelet poor plasma in rabbits," *Molecular Vision*, vol. 15, pp. 2771–2779, 2009.

[212] H. Miyashita, S. Shimmura, H. Kobayashi et al., "Collagen-immobilized poly (vinyl alcohol) as an artificial cornea scaffold that supports a stratified corneal epithelium," *Journal of Biomedical Materials Research Part B: Applied Biomaterials*, vol. 76B, no. 1, pp. 56–63, 2006.

[213] Y. Uchino, S. Shimmura, H. Miyashita et al., "Amniotic membrane immobilized poly(vinyl alcohol) hybrid polymer as an artificial cornea scaffold that supports a stratified and differentiated corneal epithelium," *Journal of Biomedical Materials Research—Part B: Applied Biomaterials*, vol. 81, no. 1, pp. 201–206, 2007.

[214] K. Nishida, M. Yamato, Y. Hayashida et al., "Functional bioengineered corneal epithelial sheet grafts from corneal stem cells expanded ex vivo on a temperature-responsive cell culture surface," *Transplantation*, vol. 77, no. 3, pp. 379–385, 2004.

[215] G. Sitalakshmi, B. Sudha, H. N. Madhavan et al., "Ex vivo cultivation of corneal limbal epithelial cells in a thermoreversible polymer (Mebiol Gel) and their transplantation in rabbits: an animal model," *Tissue Engineering Part A*, vol. 15, no. 2, pp. 407–415, 2009.

[216] K. Higa, S. Shimmura, N. Kato et al., "Proliferation and differentiation of transplantable rabbit epithelial sheets engineered with or without an amniotic membrane carrier," *Investigative Opthalmology & Visual Science*, vol. 48, no. 2, pp. 597–604, 2007.

[217] Q. Ke, X. Wang, Q. Gao et al., "Carrier-free epithelial cell sheets prepared by enzymatic degradation of collagen gel," *Journal of Tissue Engineering and Regenerative Medicine*, vol. 5, no. 2, pp. 138–145, 2011.

[218] W. Zhang, J. Xiao, C. Li et al., "Rapidly constructed scaffold-free cornea epithelial sheets for ocular surface reconstruction,"

Tissue Engineering Part C: Methods, vol. 17, no. 5, pp. 569–577, 2011.

[219] V. Holan and E. Javorkova, "Mesenchymal stem cells, nanofiber scaffolds and ocular surface reconstruction," *Stem Cell Reviews and Reports*, vol. 9, no. 5, pp. 609–619, 2013.

[220] T. Nakamura, K.-I. Endo, L. J. Cooper et al., "The successful culture and autologous transplantation of rabbit oral mucosal epithelial cells on amniotic membrane," *Investigative Opthalmology & Visual Science*, vol. 44, no. 1, pp. 106–116, 2003.

[221] H.-C. J. Chen, H.-L. Chen, J.-Y. Lai et al., "Persistence of transplanted oral mucosal epithelial cells in human cornea," *Investigative Ophthalmology & Visual Science*, vol. 50, no. 10, pp. 4660–4668, 2009.

[222] S. Krishnan, G. K. Iyer, and S. Krishnakumar, "Culture & characterisation of limbal epithelial cells & oral mucosal cells," *Indian Journal of Medical Research*, vol. 131, no. 3, pp. 422–428, 2010.

[223] S. Gaddipati, R. Muralidhar, V. Sangwan, I. Mariappan, G. Vemuganti, and D. Balasubramanian, "Oral epithelial cells transplanted on to corneal surface tend to adapt to the ocular phenotype," *Indian Journal of Ophthalmology*, vol. 62, no. 5, pp. 644–648, 2014.

[224] K. Nishida, M. Yamato, Y. Hayashida et al., "Corneal reconstruction with tissue-engineered cell sheets composed of autologous oral mucosal epithelium," *The New England Journal of Medicine*, vol. 351, no. 12, pp. 1187–1196, 2004.

[225] L. P. K. Ang, T. Nakamura, T. Inatomi et al., "Autologous serum-derived cultivated oral epithelial transplants for severe ocular surface disease," *Archives of Ophthalmology*, vol. 124, no. 11, pp. 1543–1551, 2006.

[226] T. Inatomi, T. Nakamura, N. Koizumi, C. Sotozono, N. Yokoi, and S. Kinoshita, "Midterm results on ocular surface reconstruction using cultivated autologous oral mucosal epithelial transplantation," *The American Journal of Ophthalmology*, vol. 141, no. 2, pp. 267–275, 2006.

[227] Y. Satake, K. Higa, K. Tsubota, and J. Shimazaki, "Long-term outcome of cultivated oral mucosal epithelial sheet transplantation in treatment of total limbal stem cell deficiency," *Ophthalmology*, vol. 118, no. 8, pp. 1524–1530, 2011.

[228] T. Nakamura, K. Takeda, T. Inatomi, C. Sotozono, and S. Kinoshita, "Long-term results of autologous cultivated oral mucosal epithelial transplantation in the scar phase of severe ocular surface disorders," *British Journal of Ophthalmology*, vol. 95, no. 7, pp. 942–946, 2011.

[229] C. Burillon, L. Huot, V. Justin et al., "Cultured autologous oral mucosal epithelial cell sheet (CAOMECS) transplantation for the treatment of corneal limbal epithelial stem cell deficiency," *Investigative Ophthalmology and Visual Science*, vol. 53, no. 3, pp. 1325–1331, 2012.

[230] C. Sotozono, T. Inatomi, T. Nakamura et al., "Visual improvement after cultivated oral mucosal epithelial transplantation," *Ophthalmology*, vol. 120, no. 1, pp. 193–200, 2013.

[231] C. Sotozono, T. Inatomi, T. Nakamura et al., "Cultivated oral mucosal epithelial transplantation for persistent epithelial defect in severe ocular surface diseases with acute inflammatory activity," *Acta Ophthalmologica*, vol. 92, no. 6, pp. e447–e453, 2014.

[232] S. Kolli, S. Ahmad, H. S. Mudhar, A. Meeny, M. Lako, and F. C. Figueiredo, "Successful application of ex vivo expanded human autologous oral mucosal epithelium for the treatment of total bilateral limbal stem cell deficiency," *Stem Cells*, vol. 32, no. 8, pp. 2135–2146, 2014.

[233] H. Tanioka, S. Kawasaki, K. Yamasaki et al., "Establishment of a cultivated human conjunctival epithelium as an alternative tissue source for autologous corneal epithelial transplantation," *Investigative Opthalmology & Visual Science*, vol. 47, no. 9, pp. 3820–3827, 2006.

[234] L. P. K. Ang, H. Tanioka, S. Kawasaki et al., "Cultivated human conjunctival epithelial transplantation for total limbal stem cell deficiency," *Investigative Opthalmology & Visual Science*, vol. 51, no. 2, p. 758, 2010.

[235] J. R. S. Ricardo, P. C. Cristovam, P. A. N. Filho et al., "Transplantation of conjunctival epithelial cells cultivated ex vivo in patients with total limbal stem cell deficiency," *Cornea*, vol. 32, no. 3, pp. 221–228, 2013.

[236] G. Cotsarelis, T.-T. Sun, and R. M. Lavker, "Label-retaining cells reside in the bulge area of pilosebaceous unit: implications for follicular stem cells, hair cycle, and skin carcinogenesis," *Cell*, vol. 61, no. 7, pp. 1329–1337, 1990.

[237] E. A. Meyer-Blazejewska, M. K. Call, O. Yamanaka et al., "From hair to cornea: toward the therapeutic use of hair follicle-derived stem cells in the treatment of limbal stem cell deficiency," *Stem Cells*, vol. 29, no. 1, pp. 57–66, 2011.

[238] Q. Zhou, X.-Y. Liu, Y.-X. Ruan et al., "Construction of corneal epithelium with human amniotic epithelial cells and repair of limbal deficiency in rabbit models," *Human Cell*, vol. 28, no. 1, pp. 22–36, 2015.

[239] K. Zhou, C. Koike, T. Yoshida et al., "Establishment and characterization of immortalized human amniotic epithelial cells," *Cellular Reprogramming*, vol. 15, no. 1, pp. 55–67, 2013.

[240] G. Pratama, V. Vaghjiani, J. Y. Tee et al., "Changes in culture expanded human amniotic epithelial cells: implications for potential therapeutic applications," *PLoS ONE*, vol. 6, no. 11, Article ID e26136, 2011.

[241] T. Miki, T. Lehmann, H. Cai, D. B. Stolz, and S. C. Strom, "Stem cell characteristics of amniotic epithelial cells," *Stem Cells*, vol. 23, no. 10, pp. 1549–1559, 2005.

[242] S. S. Fatimah, S. L. Ng, K. H. Chua, A. R. Hayati, A. E. Tan, and G. C. Tan, "Value of human amniotic epithelial cells in tissue engineering for cornea," *Human Cell*, vol. 23, no. 4, pp. 141–151, 2010.

[243] J. A. Thomson, J. Itskovitz-Eldor, S. S. Shapiro et al., "Embryonic stem cell lines derived from human blastocysts," *Science*, vol. 282, no. 5391, pp. 1145–1147, 1998.

[244] S. Ahmad, R. Stewart, S. Yung et al., "Differentiation of human embryonic stem cells into corneal epithelial-like cells by in vitro replication of the corneal epithelial stem cell niche," *Stem Cells*, vol. 25, no. 5, pp. 1145–1155, 2007.

[245] J. Zhu, K. Zhang, Y. Sun et al., "Reconstruction of functional ocular surface by acellular porcine cornea matrix scaffold and limbal stem cells derived from human embryonic stem cells," *Tissue Engineering Part A*, vol. 19, no. 21-22, pp. 2412–2425, 2013.

[246] W. Zhang, W. Yang, X. Liu, L. Zhang, W. Huang, and Y. Zhang, "Rapidly constructed scaffold-free embryonic stem cell sheets for ocular surface reconstruction," *Scanning*, vol. 36, no. 3, pp. 286–292, 2014.

[247] E. Kiskinis and K. Eggan, "Progress toward the clinical application of patient-specific pluripotent stem cells," *The Journal of Clinical Investigation*, vol. 120, no. 1, pp. 51–59, 2010.

[248] K. Takahashi and S. Yamanaka, "Induction of pluripotent stem cells from mouse embryonic and adult fibroblast cultures by defined factors," *Cell*, vol. 126, no. 4, pp. 663–676, 2006.

[249] R. Hayashi, Y. Ishikawa, M. Ito et al., "Generation of corneal epithelial cells from induced pluripotent stem cells derived from human dermal fibroblast and corneal limbal epithelium," *PLoS ONE*, vol. 7, no. 9, Article ID e45435, 2012.

[250] D. Sareen, M. Saghizadeh, L. Ornelas et al., "Differentiation of human limbal-derived induced pluripotent stem cells into limbal-like epithelium," *Stem Cells Translational Medicine*, vol. 3, no. 9, pp. 1002–1012, 2014.

[251] K. Kim, A. Doi, B. Wen et al., "Epigenetic memory in induced pluripotent stem cells," *Nature*, vol. 467, no. 7313, pp. 285–290, 2010.

[252] A. Mikhailova, T. Ilmarinen, H. Uusitalo, and H. Skottman, "Small-molecule induction promotes corneal epithelial cell differentiation from human induced pluripotent stem cells," *Stem Cell Reports*, vol. 2, no. 2, pp. 219–231, 2014.

[253] H. M. Reza, B.-Y. Ng, F. L. Gimeno, T. T. Phan, and L. P.-K. Ang, "Umbilical cord lining stem cells as a novel and promising source for ocular surface regeneration," *Stem Cell Reviews and Reports*, vol. 7, no. 4, pp. 935–947, 2011.

[254] I. Garzón, M. A. Martín-Piedra, C. Alfonso-Rodríguez et al., "Generation of a biomimetic human artificial cornea model using Wharton's jelly mesenchymal stem cells," *Investigative Opthalmology & Visual Science*, vol. 55, no. 7, pp. 4073–4083, 2014.

[255] Y. Ma, Y. Xu, Z. Xiao et al., "Reconstruction of chemically burned rat corneal surface by bone marrow-derived human mesenchymal stem cells," *Stem Cells*, vol. 24, no. 2, pp. 315–321, 2006.

[256] S. Gu, C. Xing, J. Han, M. O. M. Tso, and J. Hong, "Differentiation of rabbit bone marrow mesenchymal stem cells into corneal epithelial cells in vivo and ex vivo," *Molecular Vision*, vol. 15, pp. 99–107, 2009.

[257] T.-S. Jiang, L. Cai, W.-Y. Ji et al., "Reconstruction of the corneal epithelium with induced marrow mesenchymal stem cells in rats," *Molecular Vision*, vol. 16, pp. 1304–1316, 2010.

[258] H. Reinshagen, C. Auw-Haedrich, R. V. Sorg et al., "Corneal surface reconstruction using adult mesenchymal stem cells in experimental limbal stem cell deficiency in rabbits," *Acta Ophthalmologica*, vol. 89, no. 8, pp. 741–748, 2011.

[259] C. M. Rohaina, K. Y. Then, A. M. H. Ng et al., "Reconstruction of limbal stem cell deficient corneal surface with induced human bone marrow mesenchymal stem cells on amniotic membrane," *Translational Research*, vol. 163, no. 3, pp. 200–210, 2014.

[260] J. A. West-Mays and D. J. Dwivedi, "The keratocyte: corneal stromal cell with variable repair phenotypes," *The International Journal of Biochemistry & Cell Biology*, vol. 38, no. 10, pp. 1625–1631, 2006.

[261] M. J. Branch, K. Hashmani, P. Dhillon, D. R. Jones, H. S. Dua, and A. Hopkinson, "Mesenchymal stem cells in the human corneal limbal stroma," *Investigative Opthalmology & Visual Science*, vol. 53, no. 9, pp. 5109–5116, 2012.

[262] K. Hashmani, M. J. Branch, L. E. Sidney et al., "Characterization of corneal stromal stem cells with the potential for epithelial transdifferentiation," *Stem Cell Research & Therapy*, vol. 4, no. 3, article 75, 2013.

[263] T. Nieto-Miguel, S. Galindo, R. Reinoso et al., "In vitro simulation of corneal epithelium microenvironment induces a corneal epithelial-like cell phenotype from human adipose tissue mesenchymal stem cells," *Current Eye Research*, vol. 38, no. 9, pp. 933–944, 2013.

[264] B. G. Monteiro, R. C. Serafim, G. B. Melo et al., "Human immature dental pulp stem cells share key characteristic features with limbal stem cells," *Cell Proliferation*, vol. 42, no. 5, pp. 587–594, 2009.

[265] N. Zakaria, S. Van Grasdorff, K. Wouters et al., "Human tears reveal insights into corneal neovascularization," *PLoS ONE*, vol. 7, no. 5, Article ID e36451, 2012.

[266] E. L. Davies and M. T. Fuller, "Regulation of self-renewal and differentiation in adult stem cell lineages: lessons from the *Drosophila* male germ line," *Cold Spring Harbor Symposia on Quantitative Biology*, vol. 73, pp. 137–145, 2008.

Hindawi Publishing Corporation
Stem Cells International
Volume 2016, Article ID 4735264, 10 pages
http://dx.doi.org/10.1155/2016/4735264

Research Article

Gene Transfection of Human Turbinate Mesenchymal Stromal Cells Derived from Human Inferior Turbinate Tissues

Jin Seon Kwon,[1] Seung Hun Park,[1] Ji Hye Baek,[1] Truong Minh Dung,[1] Sung Won Kim,[2] Byoung Hyun Min,[1] Jae Ho Kim,[1] and Moon Suk Kim[1]

[1]*Department of Molecular Science and Technology, Ajou University, Suwon 443-749, Republic of Korea*
[2]*Department of Otolaryngology-Head and Neck Surgery, The Catholic University of Korea, College of Medicine, Seoul 137-701, Republic of Korea*

Correspondence should be addressed to Moon Suk Kim; moonskim@ajou.ac.kr

Received 4 June 2015; Accepted 24 August 2015

Academic Editor: Kequan Guo

Human turbinate mesenchymal stromal cells (hTMSCs) are novel stem cells derived from nasal inferior turbinate tissues. They are easy to isolate from the donated tissue after turbinectomy or conchotomy. In this study, we applied hTMSCs to a nonviral gene delivery system using polyethyleneimine (PEI) as a gene carrier; furthermore, the cytotoxicity and transfection efficiency of hTMSCs were evaluated to confirm their potential as resources in gene therapy. DNA-PEI nanoparticles (NPs) were generated by adding the PEI solution to DNA and were characterized by a gel electrophoresis and by measuring particle size and surface charge of NPs. The hTMSCs were treated with DNA-PEI NPs for 4 h, and toxicity of NPs to hTMSCs and gene transfection efficiency were monitored using MTT assay, fluorescence images, and flow cytometry after 24 h and 48 h. At a high negative-to-positive charge ratio, DNA-PEI NPs treatment led to cytotoxicity of hTMSCs, but the transfection efficiency of DNA was increased due to the electrostatic effect between the NPs and the membranes of hTMSCs. Importantly, the results of this research verified that PEI could deliver DNA into hTMSCs with high efficiency, suggesting that hTMSCs could be considered as untapped resources for applications in gene therapy.

1. Introduction

Stem cells could be categorized into two main types: embryonic stem cells (ESCs) that are derived from the inner cell mass of blastocysts [1] and adult stem cells (ASCs) [2], which are separated from a variety of adult tissues of mammals [3]. ESCs show pluripotency and the ability to differentiate into the endoderm, mesoderm, and ectoderm, but are associated with ethical issues because the embryo must be destroyed in the process of cell harvesting [4, 5]. On the other hand, ASCs can be isolated from adult tissues without any ethical problems and show the self-renewal or differentiation characteristics into other types of stem cells existing in the same germ layer [6, 7]. One suggested disadvantage of ASCs is the limitation of the types of stem cells into which they can differentiate. However, this issue has also been overcome following recent studies demonstrating the potential of stem cell transdifferentiation to extraneous cells with their origin tissues [8–10]. The most commonly used ASCs for regenerative medicine are mesenchymal stem cells (MSCs), especially MSCs derived from bone marrow (BMSCs), because of their characteristics such as ease of isolation and fast proliferation *in vitro*. Furthermore, other types of MSCs have been discovered and separated from various adult tissues such as fat, umbilical cord blood, dental tissues, placenta, and peripheral blood [11–15], for use in the fields of tissue engineering and regenerative medicine.

Human turbinate-derived mesenchymal stromal cells (hTMSCs) are regarded as a type of MSCs that are isolated from the eliminated inferior turbinate tissues in nose. The procedure for obtaining bone marrow for harvesting hBMSCs is associated with a high level of pain, and therefore new approaches are needed. However, hTMSCs can be separated from the tissues discarded following a turbinectomy or septoplasty owing to hypertrophy of the nasal inferior turbinate tissues. The MSC-like characteristics of hTMSCs have been

confirmed using CD markers in previous studies [16]. In addition, hTMSCs can proliferate rapidly *in vitro*, similar to other types of MSCs, and show the ability to differentiate into osteoblast- and chondrocyte-like cells *in vitro* [16–18], as well as bone-like tissues in a hydrogel system *in vivo* [19]. According to these characteristics of hTMSCs, they can also be considered as promising cell sources for tissue engineering and regenerative medicine.

Gene therapy is an attempt used to heal illnesses at the level of DNA, with the potential to cure chronic granulomatous disease, immunodeficiency, cancer, and other complicated diseases [20–22]. Gene therapy involves the intracellular introduction of foreign genes using a virus or nonviral system containing a specific site for physical or chemical attachment to DNA. The information encoded in DNA is transferred to mRNA via transcription; thereafter, the mRNA combines with tRNA and prepares the chain of amino acids for formation of the protein. This is a major advantage of gene therapy, in that specific cells are created with a desired function by controlling protein synthesis using DNA. Moreover, this gene-based therapy could target specific diseases [23]. Thus, desirable and tailorable stem cells can be prepared using gene transfer, and stem cells can be applied for the regeneration of various tissues using a gene delivery system.

Polyethyleneimine (PEI) is most well-known polymeric gene transfer carrier in the field of nonviral gene delivery [24, 25]. It has amine groups in every repeating unit in its molecular structure, which allows it to combine with DNA and form complexes [26]. Furthermore, the protonated amines of PEI in the endosomes promote the inflow of ions and destruction of the endosome membrane. This process could be a possible mechanism for the delivery of DNA into nuclei and the subsequent elimination of PEI [27]. In a previous study, the transfection efficiencies between linear and branched PEI were compared at the same concentration, and the efficiencies were higher when branched PEI was applied [28]. These results verified that the number of primary amines in PEI influences the gene transfection efficiency.

The overall objective of the present research was to transfect enhanced green fluorescence protein (EGFP) genes to hTMSCs using a branched PEI-containing gene carrier. We addressed the following questions in this study. (1) Are hTMSCs appropriate cell sources for gene therapy? (2) Is PEI an effective gene carrier for hTMSCs? (3) Could we apply this gene delivery system for adjusting the expression of specific proteins of hTMSCs in further studies? Resolving these questions would provide evidence of the applicability of hTMSCs in gene therapy and regenerative medicine.

2. Materials and Methods

2.1. Materials. Branched PEI (10 kDa) and rhodamine B isothiocyanate (Rhod B ITC) were purchased from Sigma-Aldrich (St. Louis, MO, USA), and pEGFP-N2 encoding a red-shifted variant of the wild-type green fluorescence protein was purchased from Clontech (BD Biosciences; Palo Alto, CA, USA).

2.2. Isolation and Culture of hTMSCs. Fresh inferior turbinate tissue was obtained from the discarded tissue obtained from a young woman (age 22) who underwent partial turbinectomy at the Catholic University of Korea, St. Mary's Hospital. The protocols of this study were recognized by the Internal Review Board for Human Subjects Research and Ethics Committee (KIRB-00399_18-005), and informed assent was acquired from the patient before enrollment in this experiment. The obtained inferior turbinate tissue was washed 3–5 times using a saline solution with gentamicin (Kukje Pharmaceutical Industries; Sungnam, Korea). The tissue was then washed three more times with Antibiotic-Antimycotic solution (Gibco; Gaithersburg, MD, USA), and twice more with phosphate-buffered saline (PBS), before being cut into pieces (1 mm^3). The washed tissue was placed in a culture dish in Dulbecco's Modified Eagle's Medium (Gibco) containing 10% fetal bovine serum (FBS; Gibco BRL; Grand Island, NY, USA) and incubated at 37°C in an atmosphere of 5% CO_2. The medium was changed to fresh medium every 2-3 days. The cells floating on culture plates were separated from the tissue fragments. The obtained hTMSCs were cultured in cell growth medium with 10% FBS and 1% penicillin-streptomycin (Gibco BRL) in minimal essential medium-alpha (MEM-α) on a tissue culture flask (BD Falcon; San Jose, CA, USA) at 37°C and under 5% CO_2. The hTMSCs were stained with CD34 (hematopoietic-positive marker), CD90 (MSCs marker), and CD166 (MSCs marker) antibodies on the surface of cells and were evaluated using flow cytometry (BD Bioscience) for confirming their stemness properties as MSCs. The viabilities of hTMSCs were assured using trypan blue staining before seeding. The gene transfection was performed at 70% confluence of hTMSCs.

2.3. Extraction of DNA and Preparation of DNA-PEI Nanoparticles (NPs). The plasmid DNA was cultivated in *Escherichia coli* (strain DH5α) and then endotoxin-free cDNA was extracted using PureLink HiPure Plasmid Filter Midiprep Kit (Invitrogen; Löhne, Germany) following the manufacturer's protocol. The purity and concentration of DNA were measured with a nanodrop spectrophotometer (ND-1000 UV/Vis Spectrophotometer; Thermo Scientific; Wilmington, DE, USA). The DNA was diluted to a 1 mg/mL concentration in Tris-EDTA buffer. The PEI solution dissolved in distilled water (DW) was added to 1 μg of DNA at various negative-to-positive (N/P) charge ratios of 1, 2, 4, 8, 12, and 16, respectively. The solution of DNA-PEI was vortexed immediately and incubated for 30 min to form NPs.

2.4. Characterization of DNA-PEI NPs. The formation of DNA-PEI NPs was verified by carrying out gel electrophoresis on 1.2% agarose gels in Tris-acetate-EDTA buffer (AMRESCO; Solon, OH, USA) and visualized using a UV image station (UVP; BioDoc-It Imaging System; Upland, CA, USA) with ethidium bromide (AMRESCO; Solon, OH, USA). The particle size and surface zeta potential of DNA-PEI

NPs were measured by dynamic light scattering (ELSZ-1000; Otsuka Electronics; Osaka, Japan) at room temperature.

2.5. Cytotoxicity Test. The hTMSCs were sown on 24-well plates (Nunc; Roskilde, Denmark) with 2×10^4 cells/well density and incubated for 24 h before being treated with the DNA-PEI NPs. The cells were washed with serum-free MEM-α to remove FBS and replaced in fresh MEM-α. The hTMSCs were treated with each of the DNA-PEI NPs for 4 h and then the medium was replaced by cell growth medium. After 24 h and 48 h of transfection with each N/P charge of DNA-PEI NPs, a cytotoxicity test was performed with the 3-(4,5-dimethylthiazol-2-yl)-2,5-diphenyltetrazolium bromide (MTT) assay, a colorimetric assay used to measure the activity of cellular enzymes that decrease the water-soluble MTT reagents to its insoluble purple-colored formazan. In brief, 100 μL of the MTT solution (5 mg/mL in PBS) was added to each well of hTMSCs and the plates were incubated at 37°C in a 5% CO_2 atmosphere. After 4 h, the entire medium was removed, 500 μL of dimethyl sulfoxide (DMSO) was added, and the plates were incubated for 30 min under 100 rpm shaking to solve the formazan crystals. The optical density at 590 nm was measured using an enzyme-linked immunosorbent assay plate reader (EL808 Ultra Microplate Reader; Bio-Tek Instruments; Winooski, VT, USA). All experiments were accomplished in triplicate.

2.6. Transfection Efficiency. The hTMSCs were plated 5×10^4 cells/well density in a 12-well plate (Nunc) at 24 h before transfection. Two micrograms of DNA was added to each well in the form of DNA-PEI NPs with various N/P charge ratios. The hTMSCs were treated with each ratio of DNA-PEI NPs for 4 h. After 24 h and 48 h of transfection, the treated hTMSCs were monitored to confirm the expression of EGFP using Axio Imager A1 (Carl Zeiss Microimaging GmbH; Göttingen, Germany), analyzed with AxioVision Rel. 4.8 software (Carl Zeiss Microimaging GmbH), and harvested through trypsinization to assess transfection efficiency. Harvested hTMSCs were washed with PBS and fixed with 4% paraformaldehyde (Biosesang Inc.; Gyeonggi, Korea) for 24 h. The hTMSCs were resuspended in 100 μL of iced PBS. The green fluorescence of transfected hTMSCs was detected using a FACSCanto II flow cytometer (BD Biosciences) with 520 nm and 570 nm bandpass filters for EGFP. For all samples, 10,000 events were acquired, and data analysis was performed using BD FACSDiva Software (BD Biosciences).

2.7. Synthesis of Rhod-PEI. To monitor the insertion time of DNA-PEI NPs into hTMSCs, Rhod B ITC, a red fluorescence dye, was used to label the 5% primary amine groups of PEI. PEI was dissolved in 0.1 M sodium carbonate at 2 mg/mL concentration. Fifty microliters of Rhod B ITC solution in dry DMSO (1 mg/mL) was slowly dropwised to the PEI solution and stirred for 24 h at 4°C. After 24 h, ammonium chloride solution in DW was introduced at a final concentration of 50 mM to quench the reaction. Rhod-PEI was dialyzed using a membrane filter (1000 Da, Spectrum Laboratories Inc.; Rancho Dominguez, CA, USA) for elimination of unreacted Rhod B ITC and diluted in DW at the same concentration with normal PEI.

2.8. Acquisition of Time-Dependent Images of Transfected hTMSCs. Real-time images of transfected hTMSCs with DNA-Rhod-PEI were captured and evaluated to assess the insertion time of DNA-Rhod-PEI NPs and intracellular expression of pEGFP. hTMSCs were seeded 3×10^4 cells/well of density on a 2-chamber slide (Thermo Fisher Scientific; Grand Island, NY, USA) and incubated for 24 h. The hTMSCs were treated with 5 μg/mL Hoechst 33342 solution in culture medium in 20 min to stain the nuclei and were then washed with serum-free MEM-α. DNA-Rhod-PEI NPs prepared with N/P 8 were added to the hTMSCs. After 4 h, the NPs were removed and the culture medium was added to the transfected hTMSCS. Expression of Rhod-PEI, pEGFP, and Hoechst 33342 in hTMSCs at different time points was monitored using an OLYMPUS IX51 inverted fluorescence microscope (Olympus; Tokyo, Japan, with a Moticam Pro 285A CCD camera) and analyzed with Motic Images Advanced software (Motic; Xiamen, China).

2.9. Statistical Analysis. All statistical analyses were conducted through one-way ANOVA analysis of variance with Bonferroni's post hoc test using SPSS 12.0 software (SPSS Inc.; Chicago, IL, USA).

3. Results

3.1. Characterization of hTMSCs. The hTMSCs, derived from the inner tissues of the nose, were easily isolated from the donated tissue after turbinectomy or conchotomy. For characterization of the hTMSCs, flow cytometry was conducted to evaluate the expression of the specific markers at the fifth passage: CD34 (blood cell antibody) as a negative marker and CD90 and CD166 (MSCs-related markers) as positive markers. As a result, the CD34-positive rate of hTMSCs was 0.4%, indicating that hTMSCs are not blood-derived cells. By contrast, over 95% of the cells were CD90- and CD166-positive (99.9% and 98.6%, resp.), indicating that hTMSCs have MSC-like features (Figure 1). Moreover, in accordance with previous research, the hTMSCs rapidly proliferated from passages one to five [18]. These properties of hTMSCs suggest their potential in various fields requiring MSCs and their applicability in gene therapy for curing diseases.

3.2. Characterization of DNA-PEI NPs. The cellular uptake mechanisms of gene transfer using PEI are still unidentified, although endocytosis is the most potent mechanism of nonviral gene transfection using nanosized particles (Figure 2(a)). In this study, DNA-PEI NPs were prepared with various N/P ratios ranging from 1 to 16 to assess complex formation and transfection efficiencies to hTMSCs depending on the N/P charge ratio. The complexation of DNA with PEI was evaluated through an agarose gel retardation assay. The results of electrophoresis showed that the DNA migration was completely retarded by complexation with the positively charged PEI at every N/P ratio (Figure 2(b)). The particle

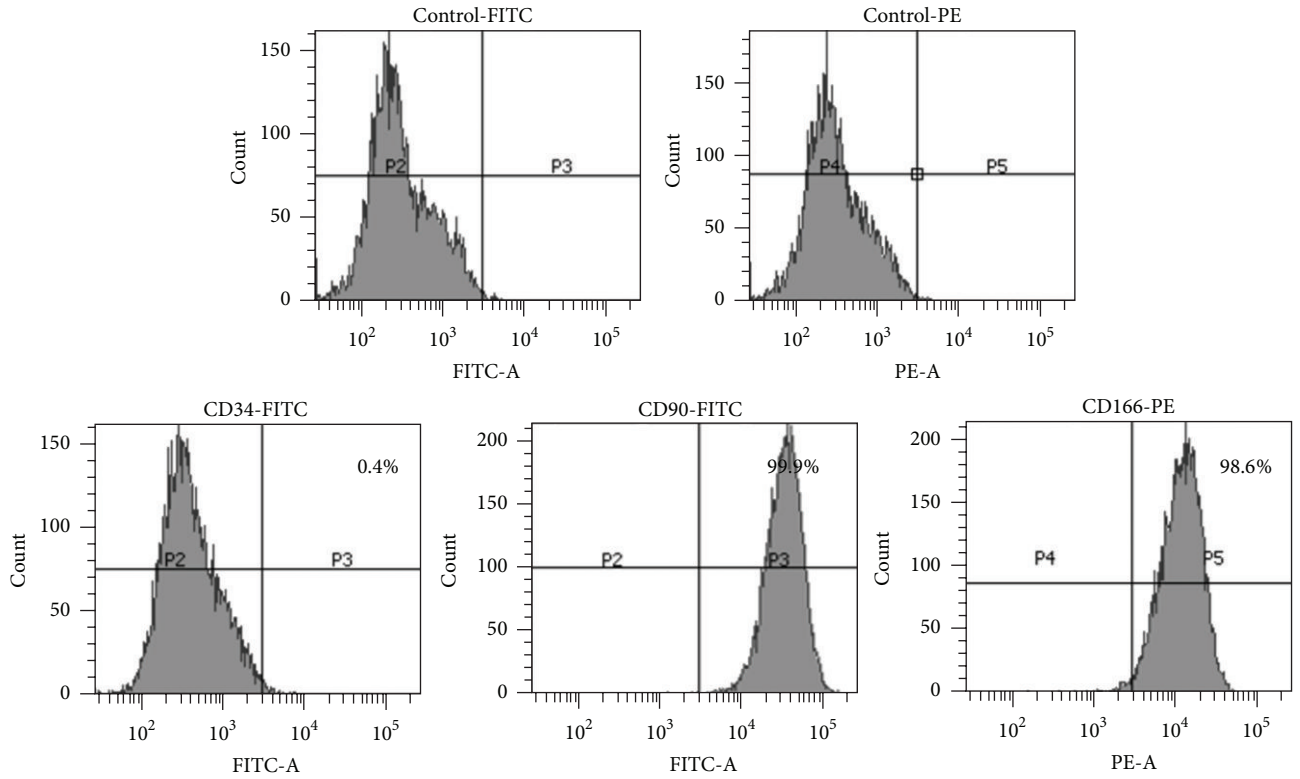

Figure 1: Cell-surface marker expression of hTMSCs using CD34 (negative) and CD90 and CD166 (positive) for confirming their stemness properties as MSCs.

size and zeta potential were measured for characterization of the DNA-PEI NPs. As shown in Figure 2(c), the particle size of DNA was above 1000 nm; however, after addition of PEI, the particle size of the DNA-PEI NPs clearly decreased in a PEI concentration-dependent manner. The zeta potential of DNA was −20 mV because of the phosphate groups in DNA; however, the zeta potentials of the DNA-PEI NPs increased with the addition of more PEI. These results indicate that the DNA-PEI NPs condensed and changed to positively charged particles with the addition of PEI. The nanosized and positively charged particles could enable the insertion of DNA into hTMSCs by endocytosis and attraction.

3.3. Cytotoxicity of DNA-PEI NPs to hTMSCs. The cytotoxicity of DNA-PEI NPs to hTMSCs was measured using an MTT assay at a wavelength of 590 nm. Figure 3 revealed the viabilities of hTMSCs at 24 h and 48 h after treatment with DNA-PEI NPs. The cytotoxicity of DNA-PEI NPs to hTMSCs steadily increased in accordance with increasing N/P charge ratios. From N/P 1 to 8, the hTMSCs showed significant toxicity compared to the control group, but they still proliferated till 48 h after treatment of DNA-PEI NPs. However, the percent viability of hTMSCs was below 50% with treatment of N/P 12 at 24 h and 48 h; at an N/P charge ratio of 16, the optical density of hTMSCs at 48 h was similar to that at 24 h. This result indicated that DNA-PEI NPs with an N/P charge ratio of 16 are the most toxic to hTMSCs and inhibit cell growth.

3.4. Transfection Efficiencies to hTMSCs. After introducing the plasmid with EGFP into cells, green fluorescence protein was synthesized in the membrane of the cells, which allowed for the gene transfection efficiency to be evaluated through measuring the expression level of green fluorescence. To monitor transfection efficiencies, the hTMSCs were treated with DNA-PEI NPs at N/P charge ratios of 1–16, and the green fluorescence was detected with a fluorescence microscope (Figure 4) and flow cytometry (Figure 5). Green fluorescence expression was not observed in the nontreated hTMSCs, whereas the green fluorescence of DNA-PEI-treated hTMSCs was enhanced in accordance with the increment of N/P charge ratios. However, at an N/P charge ratio of 16, the transfection efficiency was similar to that at an N/P charge ratio of 12, and it was difficult to directly compare the cells at other N/P ratios. These results indicate that the transfection efficiency was poor with a high amount of PEI and that DNA-PEI NPs with an N/P charge ratio of 16 were too toxic to the hTMSCs, which reduced the number of cells. These results are in accordance with the cell viability analysis.

3.5. Time-Dependent Images of Transfected hTMSCs. To assess the insertion of DNA-PEI into the hTMSCs, PEI was labeled with the red fluorescence dye rhodamine B ITC,

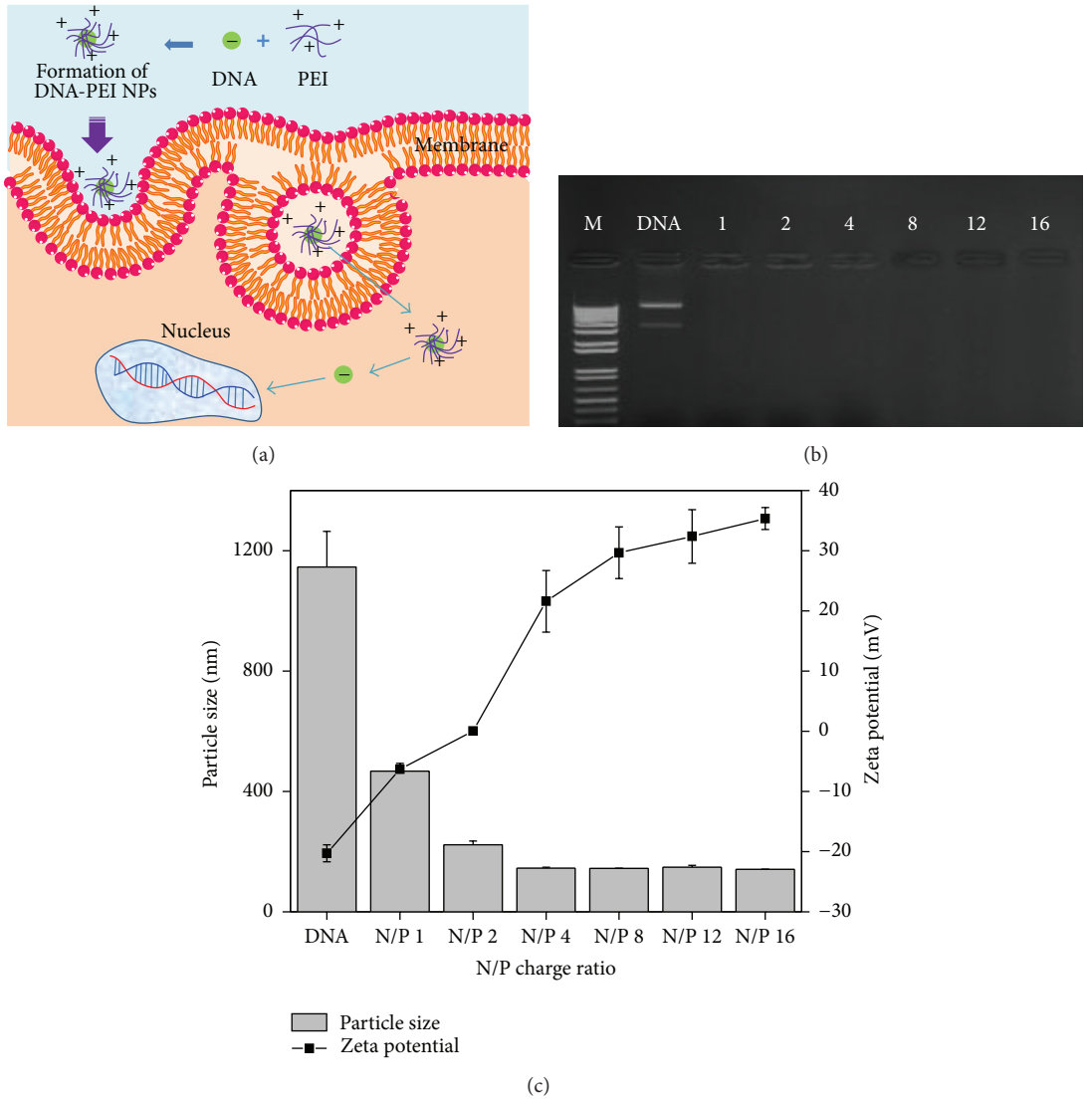

Figure 2: (a) Schematic diagrams of endocytosis using DNA-PEI NPs and the results of (b) electrophoresis on a 1.2% agarose gel and (c) particle sizes and zeta potentials of the DNA-PEI NPs.

and DNA-Rhod-PEI NPs were prepared by adding Rhod-PEI solution to DNA with an N/P charge ratio of 8 (Figure 6). Immediately after treatment, we observed phase and blue fluorescence (nuclei) in the images. At 2 h after adding the DNA-Rhod-PEI NPs, there was no fluorescence expression of pEGFP, but the red fluorescence (Rhod-PEI) was observed near the nuclei. This demonstrated that the DNA-Rhod-PEI NPs had attached to the membrane of hTMSCs within 2 h, and the NPs became closer to the nucleic acids of hTMSCs at 5 h. The red fluorescence of Rhod-PEI was weaker at 7 h compared to that at 5 h. The green fluorescence of plasmid DNA was expressed in the nucleic acids of hTMSCs at 9 h, and as of 11 h, distinct green fluorescence was observed in the membrane of hTMSCs. After 24 h, the red fluorescence had slightly moved away from the nucleus of the cells. These results indicated that DNA-PEI was inserted from 2 h to 7 h, and green fluorescence protein was synthesized from nucleic acids at 9 h after treating the cells with DNA-Rhod-PEI NPs. After 24 h, the Rhod-PEI leaked out of the cells and stayed in the cytoplasm of hTMSCs.

4. Discussion

The stromal cells used in this study, hTMSCs, were isolated from human inferior turbinate tissue and characterized as MSCs. hTMSCs can differentiate into other types of adult cells such as chondrocytes, adipocytes, and osteoblasts [16–19, 29]. Because of these characteristics, hTMSCs have been considered as critical resources in the treatment of disease in the fields of tissue engineering and regenerative medicine. To assess the feasibility of hTMSCs as promising sources for gene therapy, we conducted gene delivery to hTMSCs and

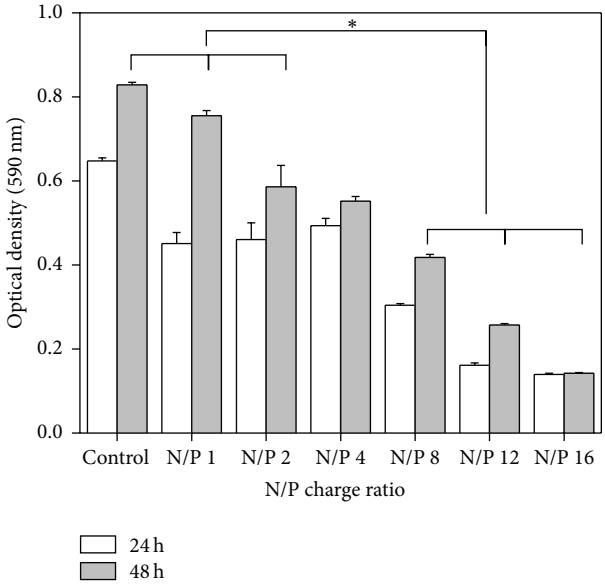

Figure 3: Viability of hTMSCs treated with DNA-PEI NPs at various N/P charge ratios, measured by the MTT assay ($^*P < 0.001$).

evaluated the transfection efficiency using PEI as a nonviral gene carrier.

PEI has been used as a gene carrier because it contains many amine groups in the main chain of its chemical structure, which are positively charged in solution state, making it possible to transfer a gene into the cells and protect the DNA by the proton sponge effect of PEI [27]. In our work, after adding the PEI solution to DNA, the characteristics of the DNA-PEI NPs were evaluated through a variety of methods such as electrophoresis on an agarose gel and measurements of particle size and zeta potential. The particle size of DNA-PEI NPs decreased from 1145 nm to 140 nm in accordance with increasing PEI concentration due to condensation between DNA and PEI [26], and the zeta potential increased from −20 mV to 30 mV by increasing the positively charged amine groups. DNA-PEI NPs are formed by the electrostatic interaction between DNA and nanosized particles [30, 31].

We evaluated the cytotoxicity and transfection efficiency of hTMSCs after 4 h treatment of DNA-PEI NPs. The cytotoxicity of DNA-PEI NPs with higher N/P charge ratios was higher than that of DNA-PEI NPs with low N/P charge ratios; on the other hand, the green fluorescence of hTMSCs was enhanced by introducing DNA into the cells. PEI likely shows cytotoxicity in gene delivery [32–34] because it increases the intracellular pH by disrupting the pH regulation mechanism and depolarizing the cell membrane [35]. Uptake of NPs is considered to be an adhesion process; therefore, in the case of positively charged NPs, the particles could strongly interact with the cell membrane [36]. As observed in previous studies, the DNA-PEI NPs showed greater cytotoxicity to hTMSCs compared to other MSCs. However, the transfection efficiency of hTMSCs was about twice as high as that observed with other MSCs in previous studies under the same experimental conditions [25, 37]. These results demonstrate that hTMSCs are a great cell source for gene transfection. PEI, the most well-known polymeric gene carrier, could also be used as gene carriers for hTMSCs; however, the cytotoxicity of PEI has to be resolved before effective gene transfection can be achieved.

To monitor the uptake time and intracellular green fluorescence expression of transfected hTMSCs over time, hTMSCs were treated with DNA-Rhod-PEI NPs with an N/P charge ratio of 8. At the initial time point, there was no fluorescence observed, but after a couple of hours, the red fluorescence of Rhod-PEI was detected on the cytoplasm surface of hTMSCs. Green fluorescent protein was expressed in the nucleus of hTMSCs at 9 h after treatment of DNA-Rhod-PEI NPs, which was demonstrated by the colocalization of green fluorescence with the Hoechst stain of nucleic acids. At a longer incubation time, EGFP expression was observed in the cytoplasm and nucleic acids of hTMSCs, and the Rhod-PEI dissociated from the nucleus of hTMSCs. In previous studies, the dissociation of DNA-carrier complexes was observed after uptake into the nucleic acids of cells by DNA polymerase during transcription [38]. However, in our study, the DNA was transfected into hTMSCs, and then the red fluorescence of Rhod-PEI was detected in the cytoplasm of hTMSCs by dissociation of DNA-Rhod-PEI NPs.

Few studies have examined the transfection of specific gene using lentiviral vectors and specific differentiation of stem cells [39]. In this work, although, to the best of our knowledge, we provide the first evidence that DNA-PEI NPs induce gene transfection of hTMSCs, further studies are currently underway to exploit BMP-2 gene delivery into hTMSCs using nonviral gene carrier and to investigate osteogenic differentiation of the transfected hTMSCs.

5. Conclusion

We evaluated the introduction of DNA into hTMSCs using a common gene carrier, PEI, to confirm the applicability of hTMSCs in gene therapy. DNA-PEI NPs were formed at various N/P charge ratios by the interaction between DNA and PEI. Greater cytotoxicity of transfected hTMSCs was detected for DNA-PEI NPs with higher N/P charge ratios using the MTT assay. The transfection efficiency of hTMSCs was about 30% using PEI as a gene carrier at N/P 12. Our results demonstrated that PEI, a general nonviral gene carrier, is applicable for gene transfection of hTMSCs and that hTMSCs are a potential resource for gene therapy because their gene transfection efficiencies were higher than those of other MSCs. Through this research, we could verify that hTMSCs are promising cell sources for gene transfection *in vitro*, and this system could be applied for controlling the expression of specific proteins depending on the types of genes transfected. However, the optimized formulation of DNA and PEI that might achieve high transfection efficiency in the low cell toxicity are needed as further studies.

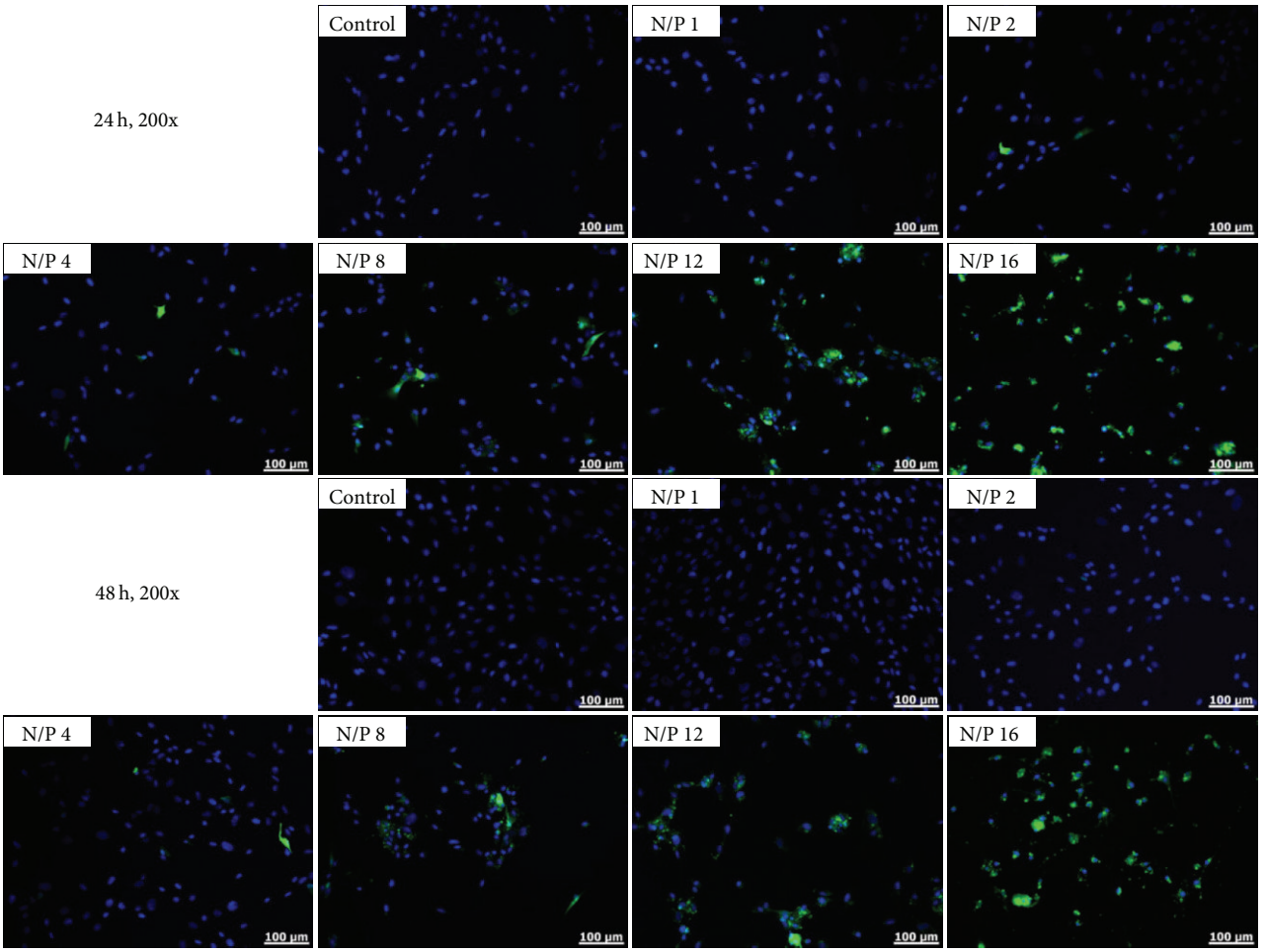

Figure 4: Fluorescence images of hTMSCs after treatment with DNA-PEI NPs. EGFP shows green fluorescence and the DAPI-stained nucleus is indicated as blue fluorescence. Magnification is ×200 and the scale bar represents 100 μm.

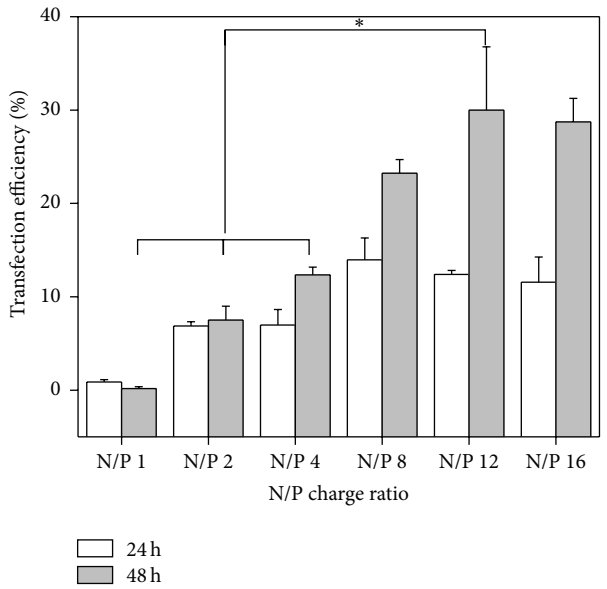

Figure 5: Transfection efficiency of hTMSCs treated with DNA-PEI NPs at N/P charge ratios of 1–16 ($^{*}P < 0.001$).

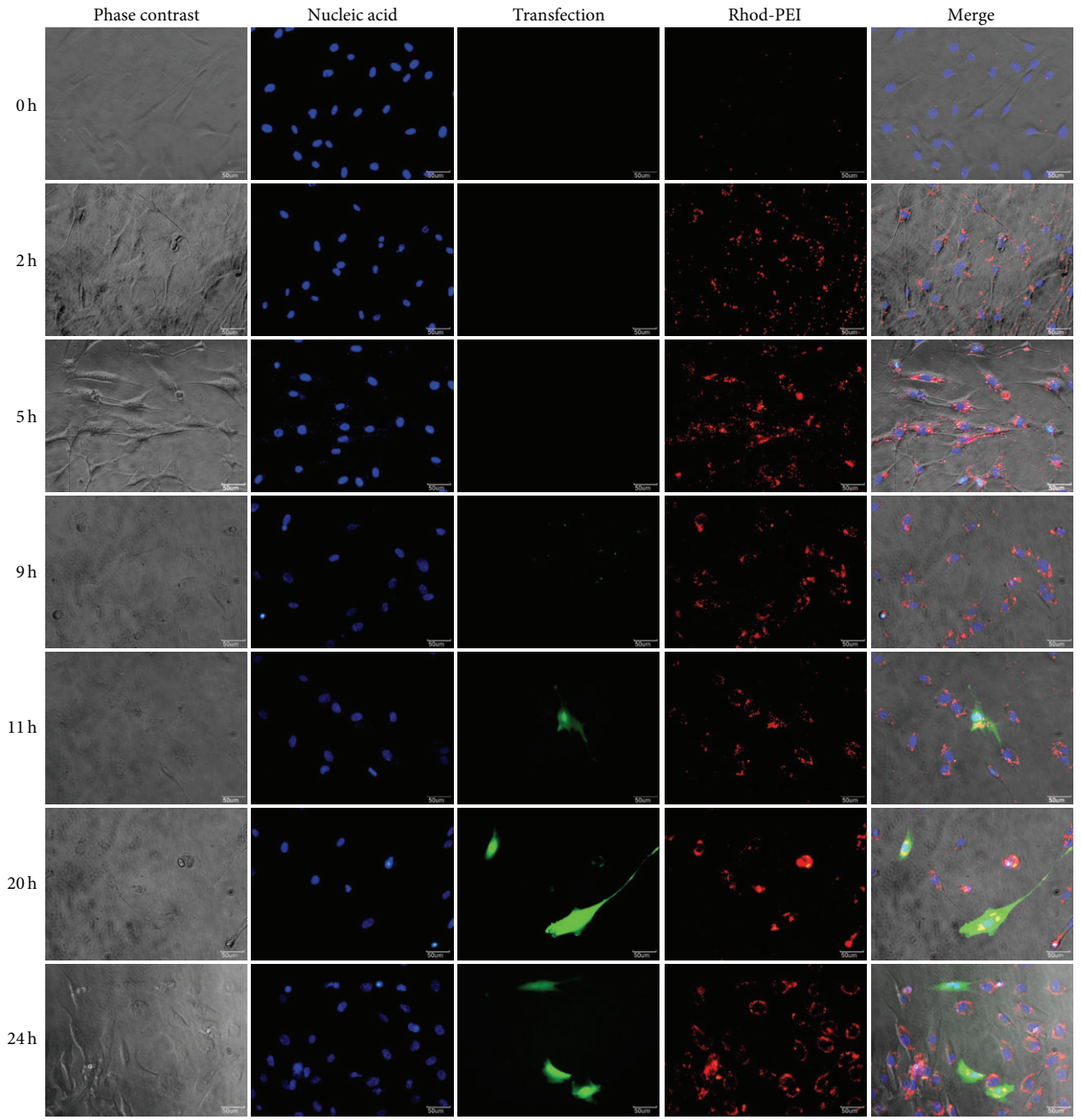

Figure 6: Intracellular expression of EGFP and Rhod-PEI in hTMSCs treated with DNA-PEI NPs at an N/P charge ratio of 8. Time-dependent images of the intracellular expression of EGFP and Rhod-PEI were captured immediately after treating the cells with DNA-PEI NPs. EGFP shows green fluorescence, Hoechst 33342-stained nuclei show blue fluorescence, and Rhod-PEI shows red fluorescence. Magnification is ×400 and the scale bar represents 50 μm.

Conflict of Interests

The authors declare that there are no competing financial interests.

Acknowledgments

This study was supported by a Grant from a Basic Science Research Program (2013R1A2A2A04014200 and 2014M3A9E5073700) and Priority Research Centers Program (2009-0093826) through the National Research Foundation of Korea (NRF) funded by the Ministry of Education.

References

[1] K. Takahashi, K. Tanabe, M. Ohnuki et al., "Induction of pluripotent stem cells from adult human fibroblasts by defined factors," *Cell*, vol. 131, no. 5, pp. 861–872, 2007.

[2] X. L. Xu, F. Yi, H.-Z. Pan et al., "Progress and prospects in stem cell therapy," *Acta Pharmacologica Sinica*, vol. 34, no. 6, pp. 741–746, 2013.

[3] J. Czyz, C. Wiese, A. Rolletschek, P. Blyszczuk, M. Cross, and A. M. Wobus, "Potential of embryonic and adult stem cells in vitro," *Biological Chemistry*, vol. 384, no. 10-11, pp. 1391–1409, 2003.

[4] A. McLaren, "Ethical and social considerations of stem cell research," *Nature*, vol. 414, no. 6859, pp. 129–131, 2001.

[5] D. W. Landry and H. A. Zucker, "Embryonic death and the creation of human embryonic stem cells," *The Journal of Clinical Investigation*, vol. 114, no. 9, pp. 1184–1186, 2004.

[6] D. S. Vieyra, K. A. Jackson, and M. A. Goodell, "Plasticity and tissue regenerative potential of bone marrow-derived cells," *Stem Cell Reviews*, vol. 1, no. 1, pp. 65–69, 2005.

[7] N. E. Sharpless and R. A. DePinho, "How stem cells age and why this makes us grow old," *Nature Reviews Molecular Cell Biology*, vol. 8, no. 9, pp. 703–713, 2007.

[8] D. G. Phinney and D. J. Prockop, "Concise review: mesenchymal stem/multipotent stromal cells: the state of transdifferentiation and modes of tissue repair—current views," *Stem Cells*, vol. 25, no. 11, pp. 2896–2902, 2007.

[9] D. Bhartiya, K. R. Boheler, and P. Rameshwar, "Multipotent to pluripotent properties of adult stem cells," *Stem Cells International*, vol. 2013, Article ID 813780, 2 pages, 2013.

[10] J. S. Kwon, G. H. Kim, D. Y. Kim et al., "Neural differentiation of rat muscle-derived stem cells in the presence of valproic acid: a preliminary study," *Tissue Engineering and Regenerative Medicine*, vol. 9, no. 1, pp. 10–16, 2012.

[11] H. H. Ahn, K. S. Kim, J. H. Lee et al., "In vivo osteogenic differentiation of human adipose-derived stem cells in an injectable in situ-forming gel scaffold," *Tissue Engineering: Part A*, vol. 15, no. 7, pp. 1821–1832, 2009.

[12] I. Rogers and R. F. Casper, "Umbilical cord blood stem cells," *Best Practice & Research: Clinical Obstetrics & Gynaecology*, vol. 18, no. 6, pp. 893–908, 2004.

[13] K. Sakai, A. Yamamoto, K. Matsubara et al., "Human dental pulp-derived stem cells promote locomotor recovery after complete transection of the rat spinal cord by multiple neuroregenerative mechanisms," *The Journal of Clinical Investigation*, vol. 122, no. 1, pp. 80–90, 2012.

[14] R. Cuevas-Diaz Duran, M. T. González-Garza, A. Cardenas-Lopez, L. Chavez-Castilla, D. E. Cruz-Vega, and J. E. Moreno-Cuevas, "Age-related yield of adipose-derived stem cells bearing the low-affinity nerve growth factor receptor," *Stem Cells International*, vol. 2013, Article ID 372164, 9 pages, 2013.

[15] W. L. Fu, C. Y. Zhou, and J. K. Yu, "A new source of mesenchymal stem cells for articular cartilage repair: MSCs derived from mobilized peripheral blood share similar biological characteristics in vitro and chondrogenesis in vivo as MSCs from bone marrow in a rabbit model," *The American Journal of Sports Medicine*, vol. 42, no. 3, pp. 592–601, 2014.

[16] S. H. Hwang, S. W. Kim, S. Y. Kim et al., "Human turbinate mesenchymal stromal cells as a potential option for cartilage tissue engineering," *Tissue Engineering and Regenerative Medicine*, vol. 8, no. 6, pp. 536–543, 2011.

[17] S. W. Kim, J. H. Cho, M. W. Hong, J.-W. Rhie, and H. R. Yoon, "Induction of chondrogenic differentiation in cultured fibroblasts isolated from the inferior turbinate," *Otolaryngology—Head and Neck Surgery*, vol. 139, no. 1, pp. 143–148, 2008.

[18] S. H. Hwang, S. Y. Kim, S. H. Park et al., "Osteogenic differentiation of human turbinate mesenchymal stromal cells," *Tissue Engineering and Regenerative Medicine*, vol. 8, no. 6, pp. 544–553, 2011.

[19] J. S. Kwon, S. W. Kim, D. Y. Kwon et al., "Invivo osteogenic differentiation of human turbinate mesenchymal stem cells in an injectable in situ-forming hydrogel," *Biomaterials*, vol. 35, no. 20, pp. 5337–5346, 2014.

[20] S. Stein, M. G. Ott, S. Schultze-Strasser et al., "Genomic instability and myelodysplasia with monosomy 7 consequent to *EVI1* activation after gene therapy for chronic granulomatous disease," *Nature Medicine*, vol. 16, no. 2, pp. 198–204, 2010.

[21] S. Hacein-Bey-Abina, J. Hauer, A. Lim et al., "Efficacy of gene therapy for X-linked severe combined immunodeficiency," *The New England Journal of Medicine*, vol. 363, no. 4, pp. 355–364, 2010.

[22] Y. Wu, W. Wang, Y. Chen et al., "The investigation of polymer-siRNA nanoparticle for gene therapy of gastric cancer in vitro," *International Journal of Nanomedicine*, vol. 5, no. 1, pp. 129–136, 2010.

[23] A. Mountain, "Gene therapy: the first decade," *Trends in Biotechnology*, vol. 18, no. 3, pp. 119–128, 2000.

[24] W. T. Godbey, K. K. Wu, and A. G. Mikos, "Poly(ethylenimine) and its role in gene delivery," *Journal of Controlled Release*, vol. 60, no. 2-3, pp. 149–160, 1999.

[25] H. H. Ahn, J. H. Lee, K. S. Kim et al., "Polyethyleneimine-mediated gene delivery into human adipose derived stem cells," *Biomaterials*, vol. 29, no. 15, pp. 2415–2422, 2008.

[26] J. P. Clamme, J. Azoulay, and Y. Mély, "Monitoring of the formation and dissociation of polyethylenimine/DNA complexes by two photon fluorescence correlation spectroscopy," *Biophysical Journal*, vol. 84, no. 3, pp. 1960–1968, 2003.

[27] A. K. Varkouhi, M. Scholte, G. Storm, and H. J. Haisma, "Endosomal escape pathways for delivery of biologicals," *Journal of Controlled Release*, vol. 151, no. 3, pp. 220–228, 2011.

[28] L. Wightman, R. Kircheis, V. Rössler et al., "Different behavior of branched and linear polyethylenimine for gene delivery in vitro and in vivo," *The Journal of Gene Medicine*, vol. 3, no. 4, pp. 362–372, 2001.

[29] S. H. Hwang, S. Y. Kim, S. H. Park et al., "Human inferior turbinate: an alternative tissue source of multipotent mesenchymal stromal cells," *Otolaryngology—Head and Neck Surgery*, vol. 147, no. 3, pp. 568–574, 2012.

[30] S. M. Zou, P. Erbacher, J. S. Remy, and J. P. Behr, "Systemic linear polyethylenimine (L-PEI)-mediated gene delivery in the mouse," *The Journal of Gene Medicine*, vol. 2, no. 2, pp. 128–134, 2000.

[31] J. H. Lee, H. H. Ahn, K. S. Kim et al., "Polyethyleneimine-mediated gene delivery into rat pheochromocytoma PC-12 cells," *Journal of Tissue Engineering & Regenerative Medicine*, vol. 2, no. 5, pp. 288–295, 2008.

[32] A. C. Hunter, "Molecular hurdles in polyfectin design and mechanistic background to polycation induced cytotoxicity," *Advanced Drug Delivery Reviews*, vol. 58, no. 14, pp. 1523–1531, 2006.

[33] H. Lv, S. Zhang, B. Wang, S. Cui, and J. Yan, "Toxicity of cationic lipids and cationic polymers in gene delivery," *Journal of Controlled Release*, vol. 114, no. 1, pp. 100–109, 2006.

[34] S. M. Moghimi, P. Symonds, J. C. Murray, A. C. Hunter, G. Debska, and A. Szewczyk, "A two-stage poly(ethylenimine)-mediated cytotoxicity: implications for gene transfer/therapy," *Molecular Therapy*, vol. 11, no. 6, pp. 990–995, 2005.

[35] Ira, Y. Mély, and G. Krishnamoorthy, "DNA vector polyethyleneimine affects cell pH and membrane potential: a time-resolved fluorescence microscopy study," *Journal of Fluorescence*, vol. 13, no. 4, pp. 339–347, 2003.

[36] H. Gao, W. Shi, and L. B. Freund, "Mechanics of receptor-mediated endocytosis," *Proceedings of the National Academy of Sciences of the United States of America*, vol. 102, no. 27, pp. 9469–9474, 2005.

[37] D. Y. Kim, J. S. Kwon, J. H. Lee, L. M. Jin, J. H. Kim, and M. S. Kim, "Effects of the surface charge of stem cell membranes and DNA/Polyethyleneimine nanocomplexes on gene transfection efficiency," *Journal of Biomedical Nanotechnology*, vol. 11, no. 3, pp. 522–530, 2015.

[38] M. Thomas and A. M. Klibanov, "Non-viral gene therapy: polycation-mediated DNA delivery," *Applied Microbiology and Biotechnology*, vol. 62, no. 1, pp. 27–34, 2003.

[39] X. Gao, A. Usas, Y. Tang et al., "A comparison of bone regeneration with human mesenchymal stem cells and muscle-derived stem cells and the critical role of BMP," *Biomaterials*, vol. 35, no. 25, pp. 6859–6870, 2014.

Hindawi Publishing Corporation
Stem Cells International
Volume 2016, Article ID 7619418, 11 pages
http://dx.doi.org/10.1155/2016/7619418

Research Article

Functional Overload Enhances Satellite Cell Properties in Skeletal Muscle

Shin Fujimaki,[1,2] Masanao Machida,[3] Tamami Wakabayashi,[1] Makoto Asashima,[1] Tohru Takemasa,[2] and Tomoko Kuwabara[1]

[1]*Stem Cell Engineering Research Group, Biotechnology Research Institute for Drug Discovery, Department of Life Science and Biotechnology, National Institute of Advanced Industrial Science and Technology (AIST), Central 4, 1-1-4 Higashi, Tsukuba Science City, Ibaraki 305-8562, Japan*
[2]*Physical Education, Health and Sport Sciences, Graduate School of Comprehensive Human Sciences, University of Tsukuba, 1-1-1 Tennodai, Tsukuba Science City, Ibaraki 305-8574, Japan*
[3]*Organization for General Education, Saga University, 1 Honjo-machi, Saga 840-8502, Japan*

Correspondence should be addressed to Tomoko Kuwabara; t.warashina@aist.go.jp

Received 25 May 2015; Accepted 29 July 2015

Academic Editor: Luca Vanella

Skeletal muscle represents a plentiful and accessible source of adult stem cells. Skeletal-muscle-derived stem cells, termed satellite cells, play essential roles in postnatal growth, maintenance, repair, and regeneration of skeletal muscle. Although it is well known that the number of satellite cells increases following physical exercise, functional alterations in satellite cells such as proliferative capacity and differentiation efficiency following exercise and their molecular mechanisms remain unclear. Here, we found that functional overload, which is widely used to model resistance exercise, causes skeletal muscle hypertrophy and converts satellite cells from quiescent state to activated state. Our analysis showed that functional overload induces the expression of MyoD in satellite cells and enhances the proliferative capacity and differentiation potential of these cells. The changes in satellite cell properties coincided with the inactivation of Notch signaling and the activation of Wnt signaling and likely involve modulation by transcription factors of the Sox family. These results indicate the effects of resistance exercise on the regulation of satellite cells and provide insight into the molecular mechanism of satellite cell activation following physical exercise.

1. Introduction

Skeletal-muscle-specific stem cells, termed satellite cells, contribute to the postnatal maintenance, growth, repair, and regeneration of skeletal muscle [1]. These cells are located between the basal lamina and plasma membrane of skeletal muscle fibers in which they represent 2.5%–6% of all nuclei and remain in a quiescent state under normal physiological conditions [2]. In response to muscle injury or exercise, satellite cells are activated and proliferate and differentiate into mature fibers [3]. Exercise positively affects muscle fiber composition via regulation of satellite cells to improve muscle performance. Previous studies have shown that the number of satellite cells is increased by long-term or acute exercise training in humans and animals [4, 5] and decreases during aging in conjunction with a reduction in the muscle quality and functional potential [6]. Loss of skeletal muscle mass, known as sarcopenia, is a serious health issue that affects millions of aging adults. Since exercise can improve muscle strength and endurance capacity, it can serve as a means of preventing muscle atrophy and reducing the risk of sarcopenia.

Satellite cells can be mitotically quiescent or in an activated proliferative state during skeletal muscle turnover. These two states can be distinguished by the expression of specific markers. All satellite cells express the stem-cell-specific transcription factor, paired-box 7 (Pax7). In addition, activated satellite cells express myogenic factor 5 (Myf5) and myogenic differentiation (MyoD) [7]. There have been few studies examining functional alterations in satellite cells such as proliferative capacity and differentiation efficiency following exercise. Furthermore, the molecular mechanisms

by which exercise-stimulating extracellular factors control the satellite cell activation and differentiation remain unclear.

Physical exercise induces changes in extracellular signaling in skeletal muscle that affect satellite cells. For instance, Notch signaling is involved in fate determination and regulates satellite cell proliferation, and previous studies have shown that physical exercise increases the expression of Notch signaling pathway components—including ligands, Notch receptor, and downstream effectors—in myogenic cells [8–10]. On the other hand, Wnt signaling, which contributes to satellite cell activation and lineage specification in skeletal muscle, is activated by exercise [11–13]. The shift from Notch to Wnt signaling controls the transition from proliferation to differentiation in myogenic progenitors during muscle regeneration [14]. Although the effect of exercise on Notch and Wnt signaling has been well studied, detailed knowledge of their relationship to satellite cell function remains elusive.

Functional overload (FO) is experimentally induced by ablating of synergistic muscles in the facies posterior of the lower legs of animals and is widely used to model resistance exercise, leading to a variety of physiological effects such as skeletal muscle hypertrophy and metabolic improvement as well as muscle fiber-type transition [15–18]. Notably, the number of satellite cells in skeletal muscle increases following FO by mechanisms that are as yet unclear [19].

In this study, we investigated the effects of FO on satellite cells, including their proliferation and differentiation. We found that muscle mass and the number of activated but not of quiescent satellite cells increased following FO, which also increased the proliferative capacity and differentiation potential of these cells. Changes in satellite cell properties were accompanied by the inactivation of Notch signaling and the activation of Wnt signaling. These results provide insight into the molecular mechanism of satellite cell activation following physical exercise.

2. Methods

2.1. Animals. Animal experiments were carried out in a humane manner after receiving approval from the Institutional Animal Care and Use Committee of the National Institute of Advanced Industrial Science and Technology. Animals were housed in standard cages in facilities with controlled temperature and humidity under a 12 : 12 h light/dark cycle and had free access to chow and water. Female Fischer344 rats (Japan SLC Inc., Hamamatsu, Japan) 12 weeks of age were used in this study. Rats were randomly divided into control and FO groups. There were no differences in body weight among rats at the start of the experiment.

2.2. FO and Tissue Sampling. The plantaris muscle of rats in the FO group was overloaded by surgically removing the soleus and gastrocnemius muscles as previously described [15]. Rats were sacrificed 2 weeks after the surgery with an overdose of pentobarbital. For RNA or protein extraction, the plantaris muscle was dissected from each rat and frozen in liquid nitrogen after measuring the wet weight and stored at −80°C until homogenization. For immunohistochemistry, rats were subjected to transcardial perfusion with phosphate-buffered saline followed by 4% paraformaldehyde (PFA). The plantaris muscle was dissected and postfixed in 4% PFA until analysis.

2.3. Satellite Cell Isolation and Culture. Primary satellite cells were obtained from plantaris muscles digested with pronase as previously described [20]. To assess proliferation, cells were cultured in growth medium consisting of low-glucose Dulbecco's Modified Eagle's Medium (DMEM) supplemented with 10% fetal bovine serum (FBS), 20 ng/mL basic fibroblast growth factor (FGF), and 1% antibiotic-antimycotic liquid (anti-anti) in laminin-coated 8-well chambers at 37°C and 5% CO_2. The medium was removed 3 days later and cells were fixed with 4% PFA for immunocytochemistry. To evaluate satellite cell differentiation, myogenic differentiation was induced by culturing cells in differentiation medium consisting of low-glucose DMEM supplemented with 10% FBS, 10% horse serum, and 1% anti-anti in laminin-coated 6-well plates or 8-well chambers at 37°C and 5% CO_2. After 1 and 2 days, cells in the 8-well chambers were fixed with 4% PFA for immunocytochemistry and those in the 6-well plates were collected in Isogen reagent (Nippon Gene, Tokyo, Japan) for RNA isolation.

2.4. Immunostaining. Fixed samples were placed in a 30% sucrose solution and stored at 4°C overnight. Cross sections were cut at a thickness of 200 μm on a microtome (ROM-380, Yamato Kohki, Saitama, Japan) and stored in tissue collection medium (25% glycerin, 30% ethylene glycol, and 0.05 M PO_4) at −20°C until analysis. Sections and fixed cells were washed, permeabilized with Tris-buffered saline (TBS) containing 0.25% Triton X, blocked with 5% normal donkey serum in TBS, and incubated with the following primary antibodies: mouse anti-Pax7 (1 : 10; Developmental Studies Hybridoma Bank (DSHB), Iowa City, IA, USA), rabbit anti-MyoD (1 : 200; Santa Cruz Biotechnology, Santa Cruz, CA, USA), rabbit anti-Dystrophin (1 : 200; GeneTex, Irvine, CA, USA), and mouse anti-myosin heavy chain (MyHC) (MF20, 1 : 10; DSHB) for 3 days (sections) or 1 day (cells) at 4°C. Immunoreactivity was detected by incubation with Cy3-conjugated donkey anti-mouse IgG (1 : 500; Jackson ImmunoResearch, West Grove, PA, USA) or Alexa Fluor 488-conjugated donkey anti-rabbit IgG (1 : 500; Life Technologies, Carlsbad, CA, USA) overnight at 4°C. Samples were counterstained with 4′,6-diamidino-2-phenylindole (Wako Pure Chemical Industries, Osaka, Japan). After several washes, sections and cells were mounted on glass slides using Vectashield (Vector Laboratories, Burlingame, CA, USA). Images were acquired using an Olympus FV1000-D confocal microscope (Olympus, Tokyo, Japan).

2.5. RNA Isolation and Quantitative Real Time- (qRT-) PCR Analysis. Total RNA was isolated from frozen muscle tissue and cultured cells using Isogen reagent. RNA samples were treated with Turbo DNase (Life Technologies, Carlsbad, CA, USA) to remove genomic DNA. cDNA was synthesized using

Table 1: Primer sequences for qRT-PCR.

Target gene		Sequence (5′-3′)	Product length
GAPDH	Forward	GTATGTCGTGGAGTCTACTG	157 bp
	Reverse	CTTGAGGGAGTTGTCATATTTC	
RPL32	Forward	AGATTCAAGGGCCAGATCCT	196 bp
	Reverse	CTACGAAGGCTTTTCGGTTC	
Pax7	Forward	AGTGAGTTCGATTAGCCGAG	153 bp
	Reverse	GAGCCTTCATCAAGACGGTT	
MyoD	Forward	GCAAGCGCAAGACCACTAAC	172 bp
	Reverse	TCAATGTAGCGGATGGCGTT	
Myogenin	Forward	TCAACCAGGAGGAGCGCGAT	208 bp
	Reverse	ATGCTGTCCACGATGGACGT	
MyHC3	Forward	TGCTGTGCTGTACAACCTCA	201 bp
	Reverse	AGCATGAACTGGTAGGCGTT	
Hes1	Forward	CAACACGACACCGGACAAAC	159 bp
	Reverse	TTGGAATGCCGGGAGCTATC	
HeyL	Forward	AGCCAGCTTTCGCCATGAAG	179 bp
	Reverse	GCGCCGTTTCTCTATGATCC	
Wnt3	Forward	TTGCGTCTTCCACTGGTGCTGCTA	206 bp
	Reverse	AGCTGGCAATCGTCCTTGCTCCTT	
R-spondin1	Forward	CGCCTGGATACTTTGATGCC	115 bp
	Reverse	AAGCCCTCCTGACACTTGGT	
Sox8	Forward	TATGGAGGCGCTTCCTACTC	141 bp
	Reverse	CAGCTGCTCCGTCTTGATAT	
Sox11	Forward	GCGGTCAGGATAAAGAGGATG	200 bp
	Reverse	AAAGGAAGGGAAGAGTGGGGA	

PrimeScript RT Master Mix (Takara Bio, Otsu, Japan) according to the manufacturer's recommendations. The cDNA was diluted 10-fold with diethylpyrocarbonate-treated water and used as a template for qRT-PCR, which was carried out using Thunderbird SYBR qPCR Mix (Toyobo, Osaka, Japan) on a CFX96 system (Bio-Rad, Hercules, CA, USA). Primers were synthesized by Life Technologies (Tokyo, Japan) (Table 1). The reaction conditions were 40 cycles of 95°C for 15 s and 60°C for 40 s. The dissociation curve for each sample was analyzed to verify the specificity of each reaction. Relative mRNA levels of target genes were determined with the ΔΔCt method and normalized to the expression of *ribosomal protein L32* (*RPL32*) (in vivo analysis) or *glyceraldehyde 3 phosphate dehydrogenase* (*GAPDH*) (in vitro analysis). There were no differences between results determined by the ΔΔCt and the standard curve methods (data not shown).

2.6. Protein Extraction and Western Blot Analysis. Tissue samples were homogenized in lysis buffer (50 mM HEPES, pH 7.4; 150 mM NaCl; 10 mM EDTA; 10 mM NaF; 10 mM $Na_4P_2O_7$; 2 mM Na_3VO_4; 1% sodium deoxycholate; 1% Nonidet P-40; and 0.2% sodium dodecyl sulphate (SDS)) with protease inhibitor mix containing aprotinin, E-64, leupeptin hemisulfate monohydrate, bestatin, and pepstatin A (Nacalai Tesque, Kyoto, Japan) on ice. Homogenates were centrifuged at 1770 ×g and 4°C for 10 min and the supernatant was collected. Protein concentration was measured using a bicinchoninic acid protein assay kit (Thermo Fisher Scientific, Yokohama, Japan) and normalized to 2 μg/μL with SDS-polyacrylamide gel electrophoresis (PAGE) loading buffer (62.5 mM Tris-HCl, pH 6.8; 2% w/v SDS; 10% glycerol; 50 mM dithiothreitol; and 0.01% w/v Bromophenol Blue). Protein samples were resolved by SDS-PAGE (SuperSep Ace; Wako Pure Chemical Industries) and transferred to polyvinylidene difluoride membranes, which were blocked with Blocking One solution (Nacalai Tesque) for 1 h at room temperature. Membranes were probed overnight at 4°C with the following primary antibodies (all from Cell Signaling Technology, Danvers, MA, USA): rabbit anti-Akt (1 : 1,000), rabbit anti-phospho-Akt (Ser473; 1 : 1,000), rabbit anti-p70 S6 kinase (p70S6K) (1 : 1,000), rabbit anti-phospho-p70S6K (Thr389; 1 : 500), rabbit anti-glycogen synthase kinase (GSK) 3β (1 : 2,000), rabbit anti-phospho-GSK3β (Ser9; 1 : 2,000), rabbit anti-β-catenin (1 : 2,000), and anti-GAPDH (1 : 2,000). This was followed by incubation with horseradish peroxidase-conjugated donkey anti-rabbit IgG (1 : 20,000; GE Healthcare, Fairfield, CT, USA) for 1 h at room temperature. After repeated washes in TBS containing 0.05% Tween 20, membranes were incubated in Pierce Thermo Western Blotting Substrate (Thermo Fisher Scientific, Waltham, MA, USA) and protein bands were visualized by chemiluminescence on an LAS-3000 Mini system (Fujifilm, Tokyo, Japan). Images of each membrane were

analyzed using National Institutes of Health ImageJ software (http://rsbweb.nih.gov/ij/) as previously described [21]. Mean intensity and standard deviation (SD) were calculated. β-catenin immunoreactivity was normalized to that of GAPDH.

2.7. Statistical Analysis. Data were analyzed with Student's t-test and are expressed as mean ± SD. P values < 0.05 were considered significant.

3. Results

3.1. FO Induces Skeletal Muscle Hypertrophy. Rats were subjected to FO for 1 week to model resistance exercise. There were no differences in body mass between FO and control rats at the end of the experiment (data not shown). However, the wet weight of the plantaris muscles was significantly higher in FO than control rats (207.28 ± 19.7 mg versus 161.72 ± 19.3 mg) (Figures 1(a) and 1(b)). The cross-sectional area of the plantaris muscle also increased following FO (Figures 1(c) and 1(d)). In previous studies, FO resulted in the activation of Akt/mammalian target of rapamycin/p70S6K signaling, which increased cellular protein synthesis [22, 23]. Accordingly, Akt (Ser473) and S6K (Thr389) phosphorylation levels were higher in FO than in control rats (Figure 1(e)). These results indicate that FO reliably induces plantaris hypertrophy.

3.2. Functional Overload Facilitated Satellite Cell Activation and Proliferation. We examined the effects of FO on proliferation by immunocytochemical analysis of Pax7 and MyoD in a primary culture of satellite cells isolated from the plantaris muscle and cultured in growth medium for 3 days (Figure 2(a)). The number of $Pax7^+MyoD^+$ satellite cells increased >1.3-fold after FO (Figure 2(b)), indicating that proliferative capacity was enhanced.

Activated satellite cells express the myogenic regulatory factors (MRFs) Myf5 and MyoD, two key transcription factors for myogenic lineage progression and differentiation, in addition to the stem-cell-specific transcription factor Pax7 [7]. We investigated changes in the number as well as the character of satellite cells after FO by evaluating the expression of these markers. The number of $Pax7^+$ cells was >2-fold higher in FO than in control rats (Figure 2(c)), consistent with a previous report [19]. Because $Pax7^+$ cells include both quiescent and activated satellite cell populations, immunohistochemical staining for Pax7 and MyoD using plantaris cross sections was performed to determine how the satellite cell population changes after functional overload. Since positive Pax7 immunoreactivity is observed in both quiescent and activated satellite cells, we examined the coexpression of Pax7 and MyoD (a marker of activated satellite cells) in plantaris muscle cross sections to determine the identity of the satellite cell population after FO. $Pax7^+MyoD^+$ activated satellite cells were rarely observed in controls but were prevalent in FO rats; the number of $Pax7^+MyoD^+$ cells increased following FO by about 9-fold (Figure 2(d)). Taken together, these results suggest that resistance exercise induces satellite cell proliferation and activation.

3.3. Functional Overload Increased the Efficiency of Satellite Cell Differentiation. Differentiating myoblasts fuse to generate myotubes. We investigated the effect of FO on the differentiation potential of satellite cells isolated from the plantaris muscle and cultured in differentiation medium for 2 days (Figure 3(a)). An immunocytochemical analysis of MyHC expression, which is indicative of newly generated myotubes, showed that myoblasts derived from FO satellite cells formed larger myotubes as compared to those from control cells; the fusion index (i.e., number of nuclei/myotube) was > 3-fold in the FO as compared to the control group (Figure 3(b)), indicating increased differentiation potential in cells from overloaded muscle.

The expression levels of *Pax7*, *MyoD*, *myogenin* (a differentiation marker), and *MyHC3* in isolated satellite cells were evaluated by qRT-PCR. RNA was collected from cells on days 0, 1, and 2 (before and 1 and 2 days after inducing differentiation, resp.) to detect changes in gene expression. Although *Pax7* expression in control cells increased over time, in FO cells the level increased on day 1 before returning to baseline on day 2 (Figure 3(c), upper left panel), suggesting that satellite cells derived from FO plantaris muscle committed to a myogenic lineage and thus downregulated *Pax7* expression at an earlier time point than control cells. Indeed, *MyoD* level increased over time in all cells but was consistently higher in FO than in control cells (Figure 3(c), upper right panel), suggesting that the majority of satellite cells derived from FO plantaris muscle were already activated when the cells were isolated. *Myogenin* and *MyHC3* were expressed at low levels on days 0 and 1; the levels were upregulated on day 2 in all cells but were significantly higher in FO as compared to control cells (Figure 3(c), lower panels), consistent with the observed increase in *MyoD* expression in the former. These results indicate that satellite cell differentiation and myotube formation were accelerated as a result of FO and that the decrease in *Pax7* expression and relatively high levels of *MyoD*, *myogenin*, and *MyHC3* may be responsible for efficient cell fusion in the generation of myotubes. Additionally, the increase in the mRNA expression of MRFs in FO cells suggests a regulatory link between the extracellular signal arising from FO and the transcriptional control of these myogenic genes (especially *MyoD*).

3.4. Overload-Induced Satellite Cell Activation Involves Notch, Wnt, and Sox. The Notch and Wnt signaling pathways regulate satellite cell self-renewal and myogenesis during embryogenesis [24]. Binding of Notch receptors to their ligands releases the Notch intracellular domain, which is translocated into the nucleus and binds recombinant signal-binding protein for immunoglobulin κ J, thereby activating the transcription of target genes such as those belonging to the Hes and Hey families [25–27]. These basic helix-loop-helix (bHLH) repressors form inactive Hes/MyoD or Hey/MyoD heterodimers to inhibit MyoD expression in quiescent satellite cells, [28, 29], thereby preventing their differentiation into myoblasts. We assessed the expression of *Hes1* and *HeyL* in plantaris muscle by qRT-PCR and found that the transcript levels were significantly lower in FO

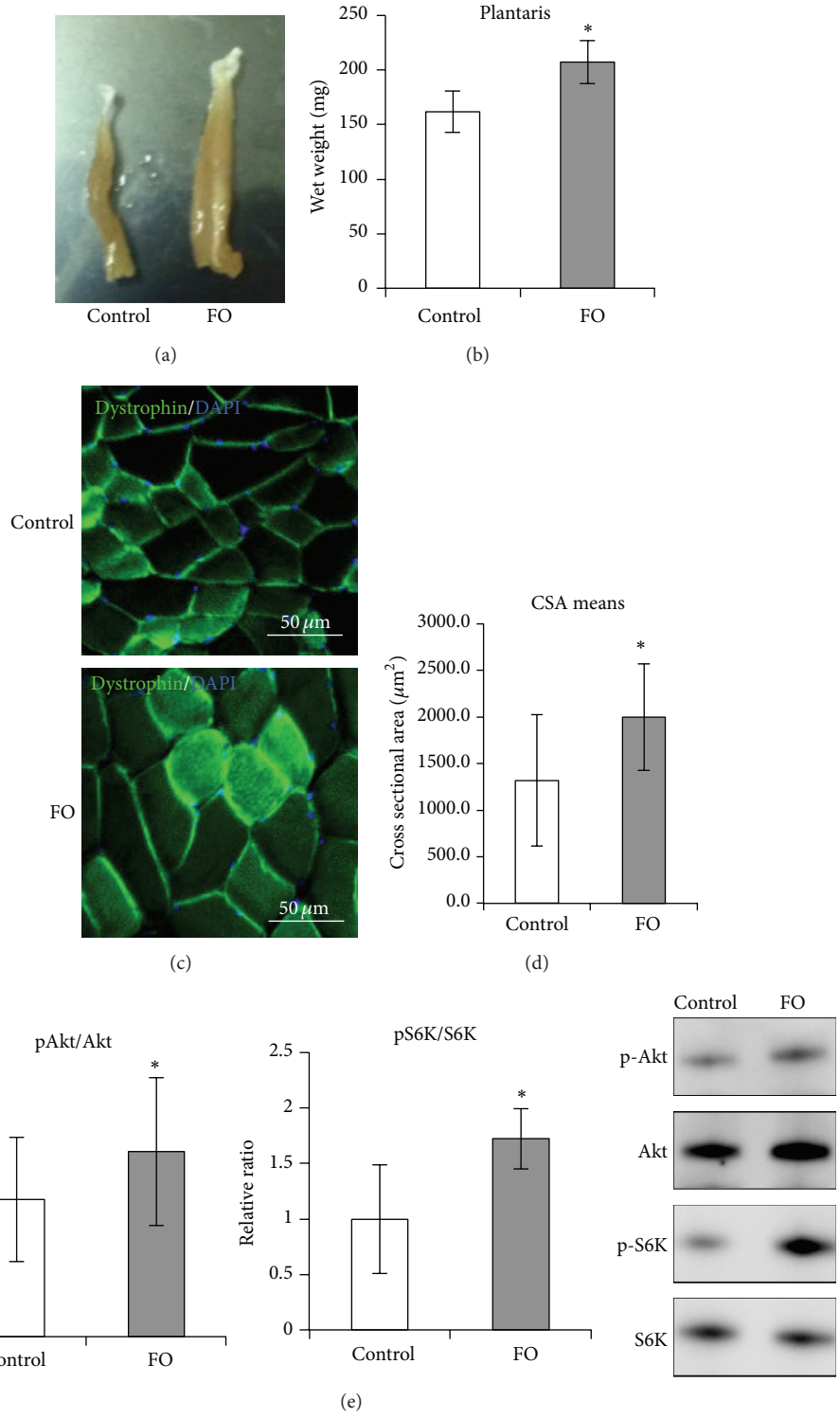

Figure 1: Skeletal muscle hypertrophy following functional overload. (a, b) Change in muscle weight following functional overload. A photograph of plantaris muscles isolated from control and FO groups (a) and a graph representing wet weight of plantaris in each group (b). (c, d) Change in cross-sectional area of plantaris following functional overload. Representative merged images of immunohistochemistry staining for Dystrophin (green) with DAPI from control and FO groups (c) and a graph plotting the means of cross-sectional area in each group (d) are shown. (e) Representations of Akt (Ser473) phosphorylation levels (left) and p70S6K (Thr389) phosphorylation levels (center), as detected by Western blot analysis. The typical blot patterns are described in the right panels. Phosphorylation levels were calculated to divide the signal of the phosphorylated form against the total protein expression for Akt or S6K. The relative ratio, normalized to the signal observed for the control group, is shown. All values are expressed as the mean ± SDM ($n = 5$). Significant differences: ∗compared to control group ($P < 0.05$).

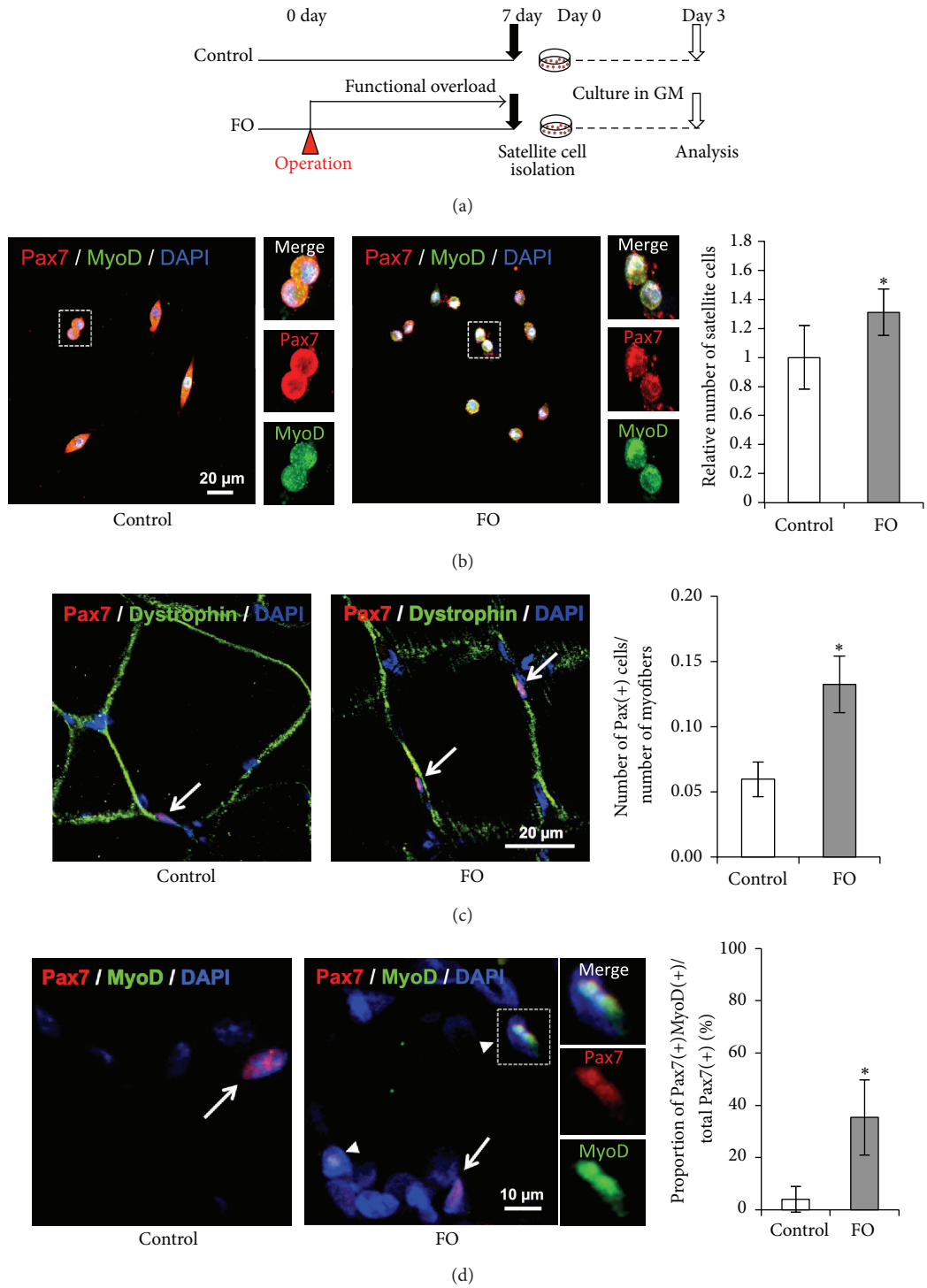

FIGURE 2: Satellite cell activation and proliferation following functional overload. (a) Schematic representation of the experimental design. FO group rats had a surgical operation to ablate synergistic muscles and received functional overload stimulation for 1 week. Satellite cells were isolated from plantaris of each group of rats 7 days after operation and were cultured in growth medium for 3 days. (b) Immunocytochemistry analysis of cultivated-satellite cells. Representative merged images of immunocytochemistry staining for Pax7 (red) and MyoD (green) with DAPI from control group (left panel) and FO group (right panel) are shown. Magnification of the area surrounded by the dotted square is shown in the right panels. Relative number, normalized to the number observed for the control group, of Pax7(+)MyoD(+) cells is shown in the right graph. (c, d) Immunohistochemistry analysis of satellite cells following functional overload. Representative merged images of immunohistochemistry staining for Pax7 (red) and Dystrophin (green) (c) or for Pax7 (red) and MyoD (green) (d) with DAPI from control group (left panel) and FO group (right panel) are shown. Magnification of the area surrounded by the dotted square is shown in the right panels. The proportion of Pax7(+) cells per myofibers (c) or the proportion of Pax7(+)MyoD(+) cells per total Pax7(+) cells (d) is shown in the right graphs. White arrows and arrowheads indicate Pax7(+) cells and Pax7(+)MyoD(+) cells, respectively. All values are expressed as mean ± SDM ($n = 5$). Significant differences: ∗ compared to control group ($P < 0.05$).

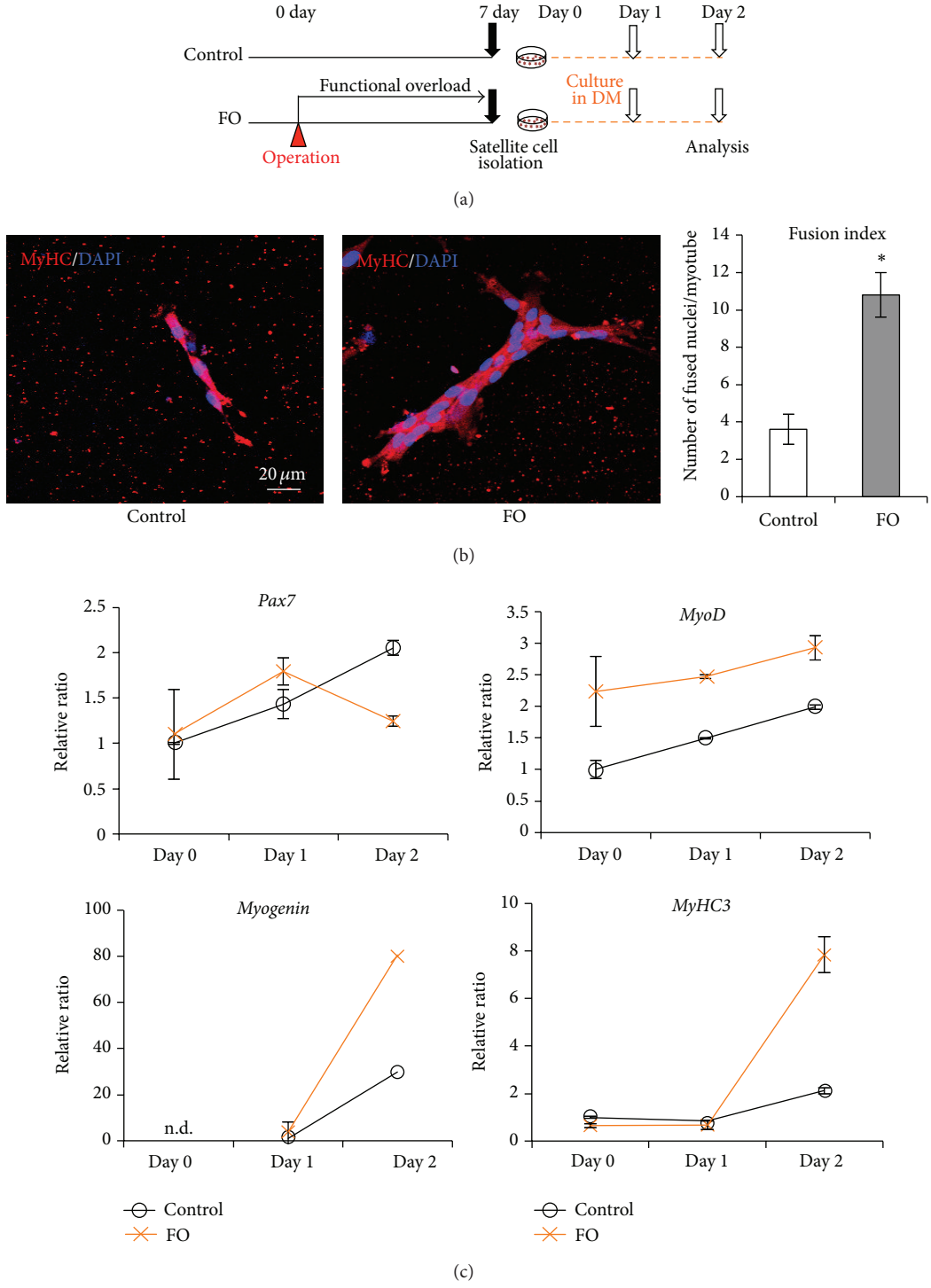

FIGURE 3: Acceleration of satellite cell differentiation following functional overload. (a) Schematic representation of the experimental design. FO group rats had a surgical operation to ablate synergistic muscles and received functional overload stimulation for 1 week. Satellite cells were isolated from plantaris of each group of rats 7 days after operation and were cultured in differentiation medium for 2 days. (b) Immunocytochemistry analysis of cultivated-satellite cells. Representative merged images of immunocytochemistry staining for MyHC (red) with DAPI from control group (left panel) and FO group (right panel) are shown. Fusion index, calculated to average the number of nuclei fused into a myotube, is shown in the right graph. (c) Expression profiles of stem cell markers in differentiation process of satellite cells. mRNA expression levels of *Pax7* (upper left), *MyoD* (upper right), *myogenin* (lower left), and *MyHC3* (lower right) in cultured cells were measured by qRT-PCR analysis on days 0, 1, and 2 (before and 1 and 2 days after inducing differentiation, resp.). In the graphs, black lines and orange lines represent control group and FO group, respectively. Target mRNA expression was normalized to that of *GAPDH* and then plotted as the expression ratio relative to the control group. All values are expressed as mean ± SDM ($n = 5$). Significant differences: ∗ compared to control group ($P < 0.05$). n.d.: not detectable.

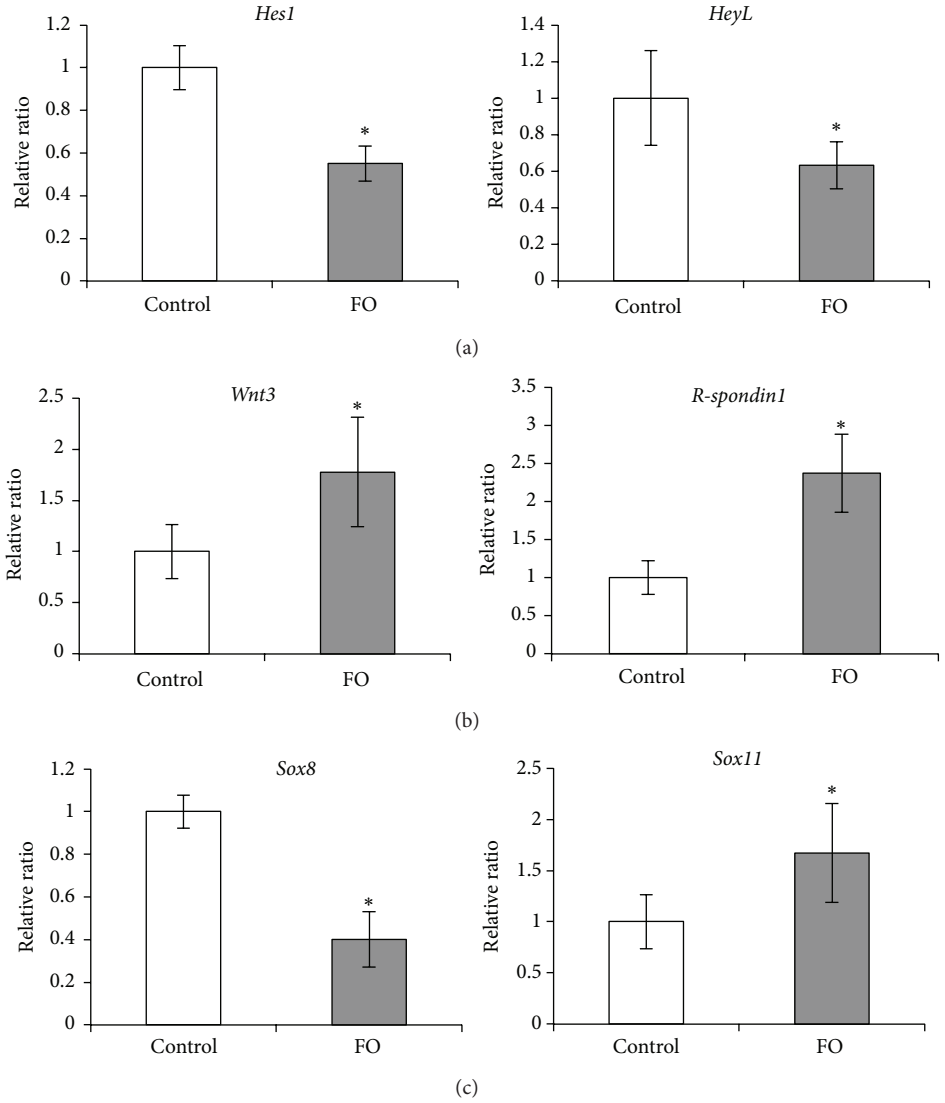

Figure 4: Changes in Notch, Wnt, and Sox expression following functional overload. (a, b, c) Expression levels of Notch signaling-related genes, Wnt signaling-related genes, and Sox genes. Amounts of *Hes1* and *HeyL* (a), *Wnt3* and *R-spondin1* (b), and *Sox8* and *Sox11* (c) mRNAs in the plantaris were measured by qRT-PCR analysis. Target mRNA expressions were normalized to that of *RPL32* and then plotted as the expression ratio relative to control group. All values are expressed as mean ± SDM ($n = 5$). Significant differences: $*$ compared to control group ($P < 0.05$).

than in control rats (Figure 4(a)), suggesting that resistance exercise induces a shift in satellite cells from a quiescent to an activated state by blocking Notch signaling.

Wnts are secreted proteins that bind to Frizzled receptors in the plasma membrane [30]. This stabilizes β-catenin, which forms a complex with T cell factor (TCF)/leukocyte enhancer factor (LEF) that is translocated into the nucleus and activates the transcription of target genes [31, 32]. Wnt signaling regulates myogenesis via modulation of MRF expression [24], and it was recently found that the Wnt activator R-spondin induces myogenic differentiation of satellite cells [33]. We examined whether FO affects Wnt signaling in skeletal muscle by qRT-PCR analysis of plantaris muscle samples. *Wnt3* and *R-spondin1* mRNA levels were increased in FO as compared to control rats (Figure 4(b)), suggesting the activation of Wnt signaling by resistance exercise that caused a shift in satellite cells from a quiescent to an activated state.

The Sox family comprises high mobility group-box transcription factors that are involved in development and differentiation of various tissues. Sox8 and Sox9 are simultaneously downregulated in satellite cells during differentiation, and their overexpression inhibits myotube formation and leads to a reduction in the expression of MyoD and myogenin, suggesting that these factors negatively regulate satellite cell differentiation to maintain a pool of self-renewing progenitors [34]. Additionally, Sox11 is expressed in differentiated myotubes and may positively regulate satellite cell differentiation [34]. We found that *Sox8* transcript was decreased while that of *Sox11* was increased in FO as compared to control rats

(Figure 4(c)), as determined by qRT-PCR. Taken together, our data suggest that resistance exercise induces satellite cell activation and myogenesis via regulation of Notch and Wnt signaling pathways and modulation of *Sox8* and *Sox11* levels.

4. Discussion

The present study investigated changes in satellite cell character induced by resistance exercise and the molecular mechanisms underlying their activation. We found that FO, an experimental model of resistance exercise, enhanced satellite cell proliferation and differentiation, effects that were likely exerted via regulation of Notch and Wnt signaling pathways.

Physical exercise has various physiological effects, including a reduction in body mass, increased maximum oxygen uptake, and metabolic improvements and an increased number of satellite cells in skeletal muscle [35–37], although the mechanistic basis for the enhancement of satellite cell proliferation and differentiation has not been previously reported. We confirmed in our model that satellite cells derived from overloaded muscles had higher proliferative capacity and differentiation potential as compared to those derived from control muscles. On the other hand, one study reported that satellite cells derived from nonloaded mice by hindlimb suspension decreased differentiation potential [38]. These findings suggest that externally applied mechanical stimuli, including physical exercise, can modulate skeletal muscle satellite cell properties. The bHLH transcription factor MyoD induces myogenic differentiation by forming heterodimers at E-box regulatory sequences of muscle-specific genes such as *myogenin*, *actin α1*, *myocyte enhancer factor 2s*, *troponin c2*, *i2*, and *t3* (*Tnnc2*, *Tnni2*, and *Tnnt3)*, among others [39, 40]. We found that satellite cells derived from overloaded muscles expressed high levels of *MyoD*, which was associated with increased proliferation and differentiation. It was recently demonstrated that exercise induces the chromatin remodeling at the *MyoD* promoter and stimulates transcription [13]. Therefore, resistance exercise likely promotes satellite cell proliferation and differentiation by inducing the upregulation of *MyoD*.

Notch and Wnt signaling pathways have been shown to regulate satellite cell fate determination and proliferation. Notch signaling, which is activated by physical exercise [8], suppresses myogenic differentiation via inhibition of *MyoD* expression in satellite cells. However, we found that the expression of the Notch targets *Hes1* and *HeyL* decreased following 1 week of FO. One possible explanation for this is that exercise-induced Notch activation is a transient response that returns to the baseline 18 h later [41]. Another study showed that the levels of *HeyL* and *Delta4*, which is a principal ligand of the Notch signaling pathway, were downregulated in adult mice following 4 weeks of wheel running [13]. Moreover, inhibiting Notch signaling using a pharmacological γ-secretase inhibitor induced myotube hypertrophy [42]. Thus, exercise-induced changes in satellite cell properties are likely modulated by Notch signaling, although the detailed mechanism has yet to be elucidated.

Wnt signaling plays essential roles in embryonic development but also in the maintenance of adult stem cells in various tissues. In adult neurogenesis, astrocyte cells surrounding adult neural stem cells secrete Wnt3, which triggers neurogenesis by inducing the expression of the bHLH transcription factor NeuroD [43–45]. Since Wnt3 expression in the adult brain can be altered by external stimuli such as exercise [46], stem cell niches act as sensors that regulate adult neural stem cell behavior. In adult skeletal muscle, *Wnt3* and *R-spondin1* expression was increased along with satellite cell activation by resistance exercise. We surmised that Wnt-induced *MyoD* expression in satellite cells caused their shift from a quiescent to an activated, proliferative state in rats subjected to FO, consistent with the findings of a previous study [13].

Sox genes are essential for the development and differentiation of various tissues as well as fate determination in satellite cells [34]. We found that the switch in satellite cells from quiescent state to activated state occurred in conjunction with *Sox8* downregulation, suggesting that Sox8 negatively regulates satellite cell activation. During central nervous system development, Sox2 blocks neurogenesis in embryonic stem cells [47]. However, Wnt activation along with the removal of Sox2 triggers *NeuroD* expression and neurogenesis. This regulatory mechanism depends on overlapping Sox2 and TCF/LEF binding sites in the *NeuroD1* promoter [44], implying that neuronal differentiation occurs via crosstalk between Sox2 and Wnt signaling. We propose that the expression of MyoD—another bHLH transcription factor—in satellite cells is regulated by a similar mechanism and that Sox8 regulates myogenic differentiation of these cells via modulation of the Wnt signaling pathway, although a more detailed characterization of this interaction is required.

5. Conclusions

The findings of study revealed the effects of resistance exercise on the regulation of satellite cells properties, including an increase in cell number and enhanced differentiation potential resulting in skeletal muscle hypertrophy. These effects were associated with the downregulation of Notch and upregulation of Wnt signaling and likely involve modulation by transcription factors of the Sox family. Our results suggest that resistance exercise can be effective in preventing the progression of sarcopenia. However, further studies investigating the factors that link Notch and Wnt signaling pathways to satellite cell activation during exercise are needed for a more complete understanding of the functions and intrinsic ability of satellite cells in adult myogenesis.

Conflict of Interests

The authors declare that there is no conflict of interests regarding the publication of this paper.

Authors' Contribution

Tomoko Kuwabara designed the research, contributed to acquisition of data, and helped writing the paper; Shin

Fujimaki performed the research, analyzed data, and wrote the paper; Masanao Machida and Tamami Wakabayashi contributed to acquisition of data; and Makoto Asashima and Tohru Takemasa supported the research and provided resources. All authors read and approved the paper for publication.

Acknowledgments

The authors thank Hideto Takimoto for providing assistance with animal care. Shin Fujimaki, Masanao Machida, Makoto Asashima, and Tomoko Kuwabara were supported by the National Institute of Advanced Industrial Science and Technology. Tomoko Kuwabara and Tohru Takemasa were supported by a Grant-in-Aid for Scientific Research (B). Tomoko Kuwabara was partly supported by a Grant-in-Aid for Scientific Research on Innovative Areas, The Takeda Science Foundation, and the Mitsubishi Foundation.

References

[1] S. Kuang and M. A. Rudnicki, "The emerging biology of satellite cells and their therapeutic potential," *Trends in Molecular Medicine*, vol. 14, no. 2, pp. 82–91, 2008.

[2] H. S. Alameddine, M. Dehaupas, and M. Fardeau, "Regeneration of skeletal muscle fibers from autologous satellite cells multiplied in vitro. An experimental model for testing cultured cell myogenicity," *Muscle & Nerve*, vol. 12, no. 7, pp. 544–555, 1989.

[3] S. B. P. Chargé and M. A. Rudnicki, "Cellular and molecular regulation of muscle regeneration," *Physiological Reviews*, vol. 84, no. 1, pp. 209–238, 2004.

[4] M. M. Umnova and T. P. Seene, "The effect of increased functional load on the activation of satellite cells in the skeletal muscle of adult rats," *International Journal of Sports Medicine*, vol. 12, no. 5, pp. 501–504, 1991.

[5] H. K. Smith, L. Maxwell, C. D. Rodgers, N. H. McKee, and M. J. Plyley, "Exercise-enhanced satellite cell proliferation and new myonuclear accretion in rat skeletal muscle," *Journal of Applied Physiology*, vol. 90, no. 4, pp. 1407–1414, 2001.

[6] V. Renault, L.-E. Thorne, P.-O. Eriksson, G. Butler-Browne, and V. Mouly, "Regenerative potential of human skeletal muscle during aging," *Aging Cell*, vol. 1, no. 2, pp. 132–139, 2002.

[7] P. S. Zammit, F. Relaix, Y. Nagata et al., "Pax7 and myogenic progression in skeletal muscle satellite cells," *Journal of Cell Science*, vol. 119, no. 9, pp. 1824–1832, 2006.

[8] K. A. Carey, M. M. Farnfield, S. D. Tarquinio, and D. Cameron-Smith, "Impaired expression of Notch signaling genes in aged human skeletal muscle," *The Journals of Gerontology, Series A: Biological Sciences and Medical Sciences*, vol. 62, no. 1, pp. 9–17, 2007.

[9] S. K. Tsivitse, M. G. Peters, A. L. Stoy, J. A. Mundy, and R. S. Bowen, "The effect of downhill running on Notch signaling in regenerating skeletal muscle," *European Journal of Applied Physiology*, vol. 106, no. 5, pp. 759–767, 2009.

[10] M. Akiho, H. Nakashima, M. Sakata, Y. Yamasa, A. Yamaguchi, and K. Sakuma, "Expression profile of Notch-1 in mechanically overloaded plantaris muscle of mice," *Life Sciences*, vol. 86, no. 1-2, pp. 59–65, 2010.

[11] K. Sakamoto, D. E. W. Arnolds, I. Ekberg, A. Thorell, and L. J. Goodyear, "Exercise regulates Akt and glycogen synthase kinase-3 activities in human skeletal muscle," *Biochemical and Biophysical Research Communications*, vol. 319, no. 2, pp. 419–425, 2004.

[12] W. G. Aschenbach, R. C. Ho, K. Sakamoto et al., "Regulation of dishevelled and β-catenin in rat skeletal muscle: an alternative exercise-induced GSK-3β signaling pathway," *The American Journal of Physiology—Endocrinology and Metabolism*, vol. 291, no. 1, pp. E152–E158, 2006.

[13] S. Fujimaki, R. Hidaka, M. Asashima, T. Takemasa, and T. Kuwabara, "Wnt protein-mediated satellite cell conversion in adult and aged mice following voluntary wheel running," *The Journal of Biological Chemistry*, vol. 289, no. 11, pp. 7399–7412, 2014.

[14] A. S. Brack, I. M. Conboy, M. J. Conboy, J. Shen, and T. A. Rando, "A temporal switch from notch to Wnt signaling in muscle stem cells is necessary for normal adult myogenesis," *Cell Stem Cell*, vol. 2, no. 1, pp. 50–59, 2008.

[15] M. Miyazaki, Y. Hitomi, T. Kizaki, H. Ohno, S. Haga, and T. Takemasa, "Contribution of the calcineurin signaling pathway to overload-induced skeletal muscle fiber-type transition," *Journal of Physiology and Pharmacology*, vol. 55, no. 4, pp. 751–764, 2004.

[16] H. Choi, P.-J. I. Selpides, M. M. Nowell, and B. C. Rourke, "Functional overload in ground squirrel plantaris muscle fails to induce myosin isoform shifts," *American Journal of Physiology—Regulatory, Integrative and Comparative Physiology*, vol. 297, no. 3, pp. R578–R586, 2009.

[17] D. A. Rivas, E. P. Morris, and R. A. Fielding, "Lipogenic regulators are elevated with age and chronic overload in rat skeletal muscle," *Acta Physiologica*, vol. 202, no. 4, pp. 691–701, 2011.

[18] T. A. Washington, J. M. Healey, R. W. Thompson, L. L. Lowe, and J. A. Carson, "Lactate dehydrogenase regulation in aged skeletal muscle: regulation by anabolic steroids and functional overload," *Experimental Gerontology*, vol. 57, pp. 66–74, 2014.

[19] C. S. Fry, J. D. Lee, J. R. Jackson et al., "Regulation of the muscle fiber microenvironment by activated satellite cells during hypertrophy," *The FASEB Journal*, vol. 28, no. 4, pp. 1654–1665, 2014.

[20] M. E. Danoviz and Z. Yablonka-Reuveni, "Skeletal muscle satellite cells: background and methods for isolation and analysis in a primary culture system," *Methods in Molecular Biology*, vol. 798, pp. 21–52, 2012.

[21] M. D. Chapman, G. Keir, A. Petzold, and E. J. Thompson, "Measurement of high affinity antibodies on antigen-immunoblots," *Journal of Immunological Methods*, vol. 310, no. 1-2, pp. 62–66, 2006.

[22] D. L. Mayhew, J.-S. Kim, J. M. Cross, A. A. Ferrando, and M. M. Bamman, "Translational signaling responses preceding resistance training-mediated myofiber hypertrophy in young and old humans," *Journal of Applied Physiology*, vol. 107, no. 5, pp. 1655–1662, 2009.

[23] M. Miyazaki, J. J. Mccarthy, M. J. Fedele, and K. A. Esser, "Early activation of mTORC1 signalling in response to mechanical overload is independent of phosphoinositide 3-kinase/Akt signalling," *The Journal of Physiology*, vol. 589, no. 7, pp. 1831–1846, 2011.

[24] S. Fujimaki, M. Machida, R. Hidaka, M. Asashima, T. Takemasa, and T. Kuwabara, "Intrinsic ability of adult stem cell in skeletal muscle: an effective and replenishable resource to the establishment of pluripotent stem cells," *Stem Cells International*, vol. 2013, Article ID 420164, 18 pages, 2013.

[25] R. Kopan and M. X. G. Ilagan, "The canonical Notch signaling pathway: unfolding the activation mechanism," *Cell*, vol. 137, no. 2, pp. 216–233, 2009.

[26] S. Jarriault, C. Brou, F. Logeat, E. H. Schroeter, R. Kopan, and A. Israel, "Signalling downstream of activated mammalian notch," *Nature*, vol. 377, no. 6547, pp. 355–358, 1995.

[27] H. Kato, T. Sakai, K. Tamura et al., "Functional conservation of mouse Notch receptor family members," *FEBS Letters*, vol. 395, no. 2-3, pp. 221–224, 1996.

[28] Y. Sasai, R. Kageyama, Y. Tagawa, R. Shigemoto, and S. Nakanishi, "Two mammalian helix-loop-helix factors structurally related to *Drosophila* hairy and Enhancer of split," *Genes & Development*, vol. 6, no. 12, pp. 2620–2634, 1992.

[29] J. Sun, C. N. Kamei, M. D. Layne et al., "Regulation of myogenic terminal differentiation by the hairy-related transcription factor CHF2," *The Journal of Biological Chemistry*, vol. 276, no. 21, pp. 18591–18596, 2001.

[30] H. Clevers and R. Nusse, "Wnt/beta-catenin signaling and disease," *Cell*, vol. 149, no. 6, pp. 1192–1205, 2012.

[31] M. Katoh and M. Katoh, "WNT signaling pathway and stem cell signaling network," *Clinical Cancer Research*, vol. 13, no. 14, pp. 4042–4045, 2007.

[32] M. Abu-Elmagd, L. Robson, D. Sweetman, J. Hadley, P. Francis-West, and A. Münsterberg, "Wnt/Lef1 signaling acts via Pitx2 to regulate somite myogenesis," *Developmental Biology*, vol. 337, no. 2, pp. 211–219, 2010.

[33] X. H. Han, Y.-R. Jin, M. Seto, and J. K. Yoon, "A WNT/beta-catenin signaling activator, R-spondin, plays positive regulatory roles during skeletal myogenesis," *The Journal of Biological Chemistry*, vol. 286, no. 12, pp. 10649–10659, 2011.

[34] K. Schmidt, G. Glaser, A. Wernig, M. Wegner, and O. Rosorius, "Sox8 is a specific marker for muscle satellite cells and inhibits myogenesis," *The Journal of Biological Chemistry*, vol. 278, no. 32, pp. 29769–29775, 2003.

[35] J. G. Swallow, P. Koteja, P. A. Carter, and T. Garland Jr., "Food consumption and body composition in mice selected for high wheel-running activity," *Journal of Comparative Physiology. B Biochemical, Systemic, and Environmental Physiology*, vol. 171, no. 8, pp. 651–659, 2001.

[36] R. L. Schultz, E. L. Kullman, R. P. Waters et al., "Metabolic adaptations of skeletal muscle to voluntary wheel running exercise in hypertensive heart failure rats," *Physiological Research*, vol. 62, no. 4, pp. 361–369, 2013.

[37] H. K. Smith and T. L. Merry, "Voluntary resistance wheel exercise during post-natal growth in rats enhances skeletal muscle satellite cell and myonuclear content at adulthood," *Acta Physiologica*, vol. 204, no. 3, pp. 393–402, 2012.

[38] P. O. Mitchell and G. K. Pavlath, "Skeletal muscle atrophy leads to loss and dysfunction of muscle precursor cells," *The American Journal of Physiology—Cell Physiology*, vol. 287, no. 6, pp. C1753–C1762, 2004.

[39] Y. Cao, R. M. Kumar, B. H. Penn et al., "Global and gene-specific analyses show distinct roles for Myod and Myog at a common set of promoters," *The EMBO Journal*, vol. 25, no. 3, pp. 502–511, 2006.

[40] V. Saccone and P. L. Puri, "Epigenetic regulation of skeletal myogenesis," *Organogenesis*, vol. 6, no. 1, pp. 48–53, 2010.

[41] M. G. MacKenzie, D. L. Hamilton, M. Pepin, A. Patton, and K. Baar, "Inhibition of myostatin signaling through Notch activation following acute resistance exercise," *PLoS ONE*, vol. 8, no. 7, Article ID e68743, 2013.

[42] M. Kitzmann, A. Bonnieu, C. Duret et al., "Inhibition of Notch signaling induces myotube hypertrophy by recruiting a subpopulation of reserve cells," *Journal of Cellular Physiology*, vol. 208, no. 3, pp. 538–548, 2006.

[43] D.-C. Lie, S. A. Colamarino, H.-J. Song et al., "Wnt signalling regulates adult hippocampal neurogenesis," *Nature*, vol. 437, no. 7063, pp. 1370–1375, 2005.

[44] T. Kuwabara, J. Hsieh, A. Muotri et al., "Wnt-mediated activation of NeuroD1 and retro-elements during adult neurogenesis," *Nature Neuroscience*, vol. 12, no. 9, pp. 1097–1105, 2009.

[45] T. Kuwabara, M. N. Kagalwala, Y. Onuma et al., "Insulin biosynthesis in neuronal progenitors derived from adult hippocampus and the olfactory bulb," *EMBO Molecular Medicine*, vol. 3, no. 12, pp. 742–754, 2011.

[46] M. Okamoto, K. Inoue, H. Iwamura et al., "Reduction in paracrine Wnt3 factors during aging causes impaired adult neurogenesis," *The FASEB Journal*, vol. 25, no. 10, pp. 3570–3582, 2011.

[47] M. Bylund, E. Andersson, B. G. Novitch, and J. Muhr, "Vertebrate neurogenesis is counteracted by Sox1-3 activity," *Nature Neuroscience*, vol. 6, no. 11, pp. 1162–1168, 2003.

Hindawi Publishing Corporation
Stem Cells International
Volume 2016, Article ID 5098747, 10 pages
http://dx.doi.org/10.1155/2016/5098747

Research Article

Mesenchymal Stem/Stromal Cells from Discarded Neonatal Sternal Tissue: In Vitro Characterization and Angiogenic Properties

Shuyun Wang, Lakshmi Mundada, Eric Colomb, Richard G. Ohye, and Ming-Sing Si

Section of Pediatric Cardiovascular Surgery, Department of Cardiac Surgery, University of Michigan, Ann Arbor, MI, USA

Correspondence should be addressed to Ming-Sing Si; mingsing@umich.edu

Received 28 February 2015; Accepted 22 July 2015

Academic Editor: Kequan Guo

Autologous and nonautologous bone marrow mesenchymal stem/stromal cells (MSCs) are being evaluated as proangiogenic agents for ischemic and vascular disease in adults but not in children. A significant number of newborns and infants with critical congenital heart disease who undergo cardiac surgery already have or are at risk of developing conditions related to inadequate tissue perfusion. During neonatal cardiac surgery, a small amount of sternal tissue is usually discarded. Here we demonstrate that MSCs can be isolated from human neonatal sternal tissue using a nonenzymatic explant culture method. Neonatal sternal bone MSCs (sbMSCs) were clonogenic, had a surface marker expression profile that was characteristic of bone marrow MSCs, were multipotent, and expressed pluripotency-related genes at low levels. Neonatal sbMSCs also demonstrated in vitro proangiogenic properties. Sternal bone MSCs cooperated with human umbilical vein endothelial cells (HUVECs) to form 3D networks and tubes in vitro. Conditioned media from sbMSCs cultured in hypoxia also promoted HUVEC survival and migration. Given the neonatal source, ease of isolation, and proangiogenic properties, sbMSCs may have relevance to therapeutic applications.

1. Introduction

Mesenchymal stem/stromal cells (MSCs) are known for their proangiogenic qualities and are currently being developed to treat a wide variety of diseases in adults caused or complicated by inadequate tissue perfusion and vascularization [1–5]. Children with congenital heart disease who undergo heart surgery are also affected by diseases of perfusion and vascularization such as congenital coronary anomalies and capillary rarefaction secondary to hypertrophy seen in a multitude of defects [6, 7] or by severe complications of treatment such as stroke [8, 9]. MSC proangiogenic therapy for these pediatric patients would have potential utility but has not been explored. An important consideration for these patients is the tissue source for MSCs, and MSCs from placenta, Wharton's jelly, and umbilical cord have been described, although contamination of maternal cells may complicate isolate from some of these tissues [10–13].

According to the Society of Thoracic Surgeons National Database, severe congenital heart disease requiring surgical correction in the neonatal and infant period occurs in over 10,000 patients each year in the United States. These patients require surgical correction via a median sternotomy. After median sternotomy, fragments of trabecular bone tissue and some marrow are often present on the sternotomy saw blade or are scattered about the operative field. Here we evaluated our hypothesis that sbMSCs could be isolated from this discarded sternal tissue obtained from neonatal heart surgery and that sbMSCs possess proangiogenic qualities.

2. Materials and Methods

2.1. Sternal Bone MSC Isolation. This study was approved by the University of Michigan Institutional Review Board. Under informed consent, six patients (aged 2–7 days) with hypoplastic left heart syndrome, D-transposition of the great arteries, and truncus arteriosus were included in this study.

After sternotomy with a pneumatic-driven sternal saw (Stryker Corporation, Kalamazoo, MI), bone tissue was

Table 1: Quantitative PCR primers used in this study.

Gene	Forward primer	Reverse primer
β-actin	TCCCTGGAGAAGAGCTACGA	AGCACTGTGTTGGCGTACAG
Sox-2	GCGAACCATCTCTGTGGTCT	GGAAAGTTGGGATCGAACAA
Oct-4	CGTGAAGCTGGAGAAGGAGA	CATCGGCCTGTGTATATCCC
Nanog	GATTTGTGGGCCTGAAGAAA	TTGGGACTGGTGGAAGAATC
VEGFA	GCCTTGCTGCTCTACCTCCA	ATGATTCTGCCCTCCTCCTTCT
bFGF	GCTGGTGATGGGAGTTGTATTT	CTGCCGCCTAAAGCCATATT
ANG1	GCTCACCATCATCTCCCTTATC	CTCACAGACTCAATCACCTTCC
HIF-1 α	CAGCAACTTGAGGAAGTACC	CAGGGTCAGCACTACTTCG
HGF	CTCACACCCGCTGGGAGTAC	TCCTTGACCTTGGATGCATTC

rinsed off the blade with saline. Free bony fragments in the operative field were also collected. Sternal tissue was then placed into three 10 cm culture dishes. Approximately 3–5 mL of Dulbecco's Modified Eagle Medium, with high-glucose concentration, GlutaMax I, 10% heat-inactivated fetal bovine serum, 100 U/mL penicillin, and 100 μg/mL streptomycin, and 0.25 μg/mL Fungizone (all from Gibco, Carlsbad, CA) were added to partially cover the tissue without detaching the tissue from the dish and then changed every 5 days. After 14–21 days, tissue was rinsed off and cells were trypsinized and replated. Sternal bone MSCs (sbMSCs) were passaged 1 : 4 when reaching 70% confluency, and all experiments utilized sbMSCs between passages 3–8.

2.2. Colony Forming Unit Efficiency. For colony forming unit efficiency (CFE) determination, sbMSCs ($n = 5$ patient) were diluted in MSC medium in singe cell suspension and plated at 100 cells per 10 cm tissue culture dishes (Corning Life Sciences, Tewksbury, MA). After 14 days of incubation with medium changes every 2-3 days under standard conditions, sbMSCs were washed with PBS, fixed with methanol, and stained with crystal violet. Colonies with >50 cells were counted and recorded.

2.3. Flow Cytometric Characterization. Surface markers of passage 4 sbMSCs ($n = 4$ patients) were characterized by flow cytometry using antibodies against CD29, CD44, CD45, CD90, CD105, CD73, CD166, CD49e, CD56, STRO-1, CD271, SSEA-4, HLA-ABC, HLA-DR, and nestin (all from BD Biosciences, San Jose, CA, except Stro1 which was purchased from BioLegend, San Diego, CA) and a Beckman Coulter MoFlo Astrios flow cytometer using the appropriate isotype-matched and unstained controls.

2.4. Trilineage Differentiation Capacity. The multipotency of sbMSCs ($n = 4$ patients) was investigated using the Human Mesenchymal Stem Cell Functional Identification Kit (R&D Systems Inc., Minneapolis, MN) according to the manufacturer's directions. After incubation in differentiation media for 14–21 days, cells were stained with an anti-osteocalcin antibody, Oil Red O, and anti-FABP-4 antibody, and anti-aggrecan antibody, and imaged using a confocal microscope (Nikon Instruments Inc., Melville, NY). Efficiency of adipogenic differentiation was estimated by the percent area of Oil Red O staining using ImageJ (http://imagej.nih.gov/ij/) and the plugin Threshold Colour (http://www.mecourse.com/landinig/software/software.html). Random 100x images ($n = 5$/sbMSC line) were filtered by hue followed by the application of a saturation filter. The fraction of remaining pixels relative to the initial total was calculated to yield the percent coverage of staining. One-way ANOVA with post hoc Tukey test was used to compare the difference between Oil Red O staining of the different sbMSC lines.

2.5. Pluripotency Gene Expression. Expression of the pluripotency genes *Sox-2*, *Oct-4*, and *Nanog* was determined in passage 4 sbMSCs ($n = 5$ patients) relative to human induced pluripotent stem cells (hiPSCs, generously supplied by Dr. Eric Devaney) using qPCR. Total RNA was extracted using the RNeasy Mini Kit (Qiagen, Valencia, CA). Reverse transcription was carried out using the High Capacity cDNA Reverse Transcription Kit with random primers (Applied Biosystems, Grand Island, NY). Quantitative real-time polymerase chain reaction was performed in StepOne Plus Real-Time PCR system (Applied Biosystems) with a reaction mixture containing cDNA, forward primer, and reverse primer (Table 1), and 1x iTaq Universal SYBR Green Supermix (Bio-Rad Laboratories, Hercules, CA). Fold change in gene expression was calculated based on the $2^{-\Delta\Delta CT}$ method. Three independent experiments were performed.

2.6. Angiogenic Gene Expression. We evaluated expression for *VEGFA*, *bFGF*, *ANG1*, *HIF-1α*, and *HGF* in neonatal sbMSC ($n = 6$ patients) relative to that in human umbilical vein endothelial cells (HUVECs, from Lonza, Basel, Switzerland) using qPCR. Primers for qPCR analysis are listed in Table 1. Cell monolayers were washed with PBS and then trypsinized. Cells were centrifuged and washed with PBS. For experimental details of qPCR and data analysis, please see above for pluripotency gene analysis. Three independent experiments were performed.

2.7. Sprouting and Tubule Formation. We also explored the ability of sbMSCs to promote sprouting and tubule formation in coculture with HUVECs in three dimensions. Cell cultures were dissociated using trypsin/EDTA, centrifuged, and resuspended in EGM-2 media (Lonza) containing 0.275% methylcellulose (Sigma-Aldrich, St. Louis, MO). Cells in

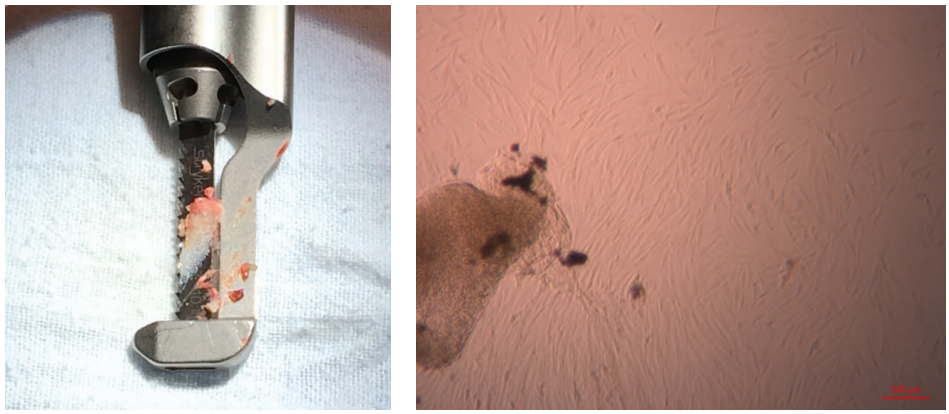

(a) (b)

Figure 1: Discarded neonatal sternal tissue contains MSCs. (a) Sternotomy saw blade with sternal tissue during neonatal cardiac surgery. (b) Plastic-adherent MSCs migrating from sternal tissue after 14 days. Scale bar = 100 μm.

suspension were then seeded on the lid of a nonadhesive petri dish (20 μL per drop) containing a total of 800 cells/spheroid with a 1 : 1 sbMSC to HUVECs composition. Hanging drops were then incubated overnight at 37°C and 5% CO_2 to allow for spheroid formation.

Fibrin hydrogel was generated in each well of a 24-well plate as described above followed by the addition of 75 spheroids/well prior to polymerization to ensure that spheroids were embedded within the hydrogel. After fibrinogen polymerization, basal EGM-2 was added to each well. Spheroids were then incubated for 7 days and imaged at 100x using an inverted phase contrast microscope (n = 20 spheroids/line). Images were digitally acquired. Experiments were performed using sbMSCs isolated from three different patients (lines).

2.8. Hypoxic sbMSC Conditioned Media Generation. Hypoxia is a pathophysiologic consequence of vascular and perfusion deficits [14, 15]. Hypoxia has also been shown to enhance the proangiogenic properties of the MSC secretome [16–19]. Thus, we determined whether sbMSCs conditioned media in the setting of hypoxia could also promote human umbilical vein endothelial cell (HUVEC) survival and migration. To generate hypoxic conditioned media, sbMSCs (n = 4 patients) were cultured in T75 flask with 6 mL of basal EGM-2 media at 1% O_2 using a hypoxic incubator (Eppendorf Inc., Enfield, CT). Conditioned media was then collected at 48 hours and stored at −80°C until used in downstream experiments.

2.9. Endothelial Cell Migration. Promotion of HUVEC migration by hypoxic sbMSC conditioned media was assessed by a scratch assay. To prevent proliferation, HUVECs were treated with 0.01 mg/mL mitomycin C (Sigma-Aldrich) for 2 hours, washed with PBS, and then plated in a 96-well microplate (Essen Biosciences, Ann Arbor, MI) at a density of 2.5×10^4 cells per well (8 wells/group). Cells were incubated under standard conditions for 24 hours to allow for attachment. A wound maker pin tool (Essen Biosciences) was used to create a scratch in the HUVEC monolayer in each well. Cells were then washed twice prior to addition of hypoxic sbMSC conditioned media. Basal EGM-2 media or supplemented EGM-2 media were added to control wells. Cell migration was monitored at 2-hour intervals for 24 hours and analyzed with CellPlayer Cell Migration Software (Essen Biosciences). Average wound density, confluence, and width were determined at each time point. Independent experiments were performed in duplicate.

2.10. Endothelial Cell Proliferation. The ability of hypoxic sbMSC secretome to promote HUVEC proliferation was evaluated. HUVECs 5×10^3 cells were plated in each well in a 96-well microplate (6 wells/group) and allowed to attach for 24 hours under standard conditions followed by 24 hours of serum starvation. After 24-hour incubation hypoxic sbMSC conditioned media, basal EGM-2 media or supplemented EGM-2 media were added. After 48-hour incubation, 20 μL of 5 mg/mL of MTT (dimethylthiazol diphenyltetrazolium bromide) in PBS was added to each well and incubated for 4 h at 37°C and 5% CO_2. The supernatant was removed and 200 μL dimethyl sulfoxide (Sigma-Aldrich) was added to each well to dissolve the formazan crystals for 20 minutes. Absorbance at 570 nm was then determined with a plate reader (Promega, Madison, WI). Independent experiments were performed in duplicate.

2.11. Statistical Analysis. Statistical analyses were performed using Prism 6 (GraphPad Software Inc., San Diego, CA, USA). Where appropriate, one-way or two-way analysis of variance (ANOVA) with post hoc Tukey's honestly significant difference test was used for analyzing differences between groups. Statistical significance was set at $p < 0.05$.

3. Results

Sternal tissue was able to be harvested during neonatal cardiac surgery (Figure 1(a)). After culturing for 14–21 days, MSCs migrated out of adherent trabecular bone fragments

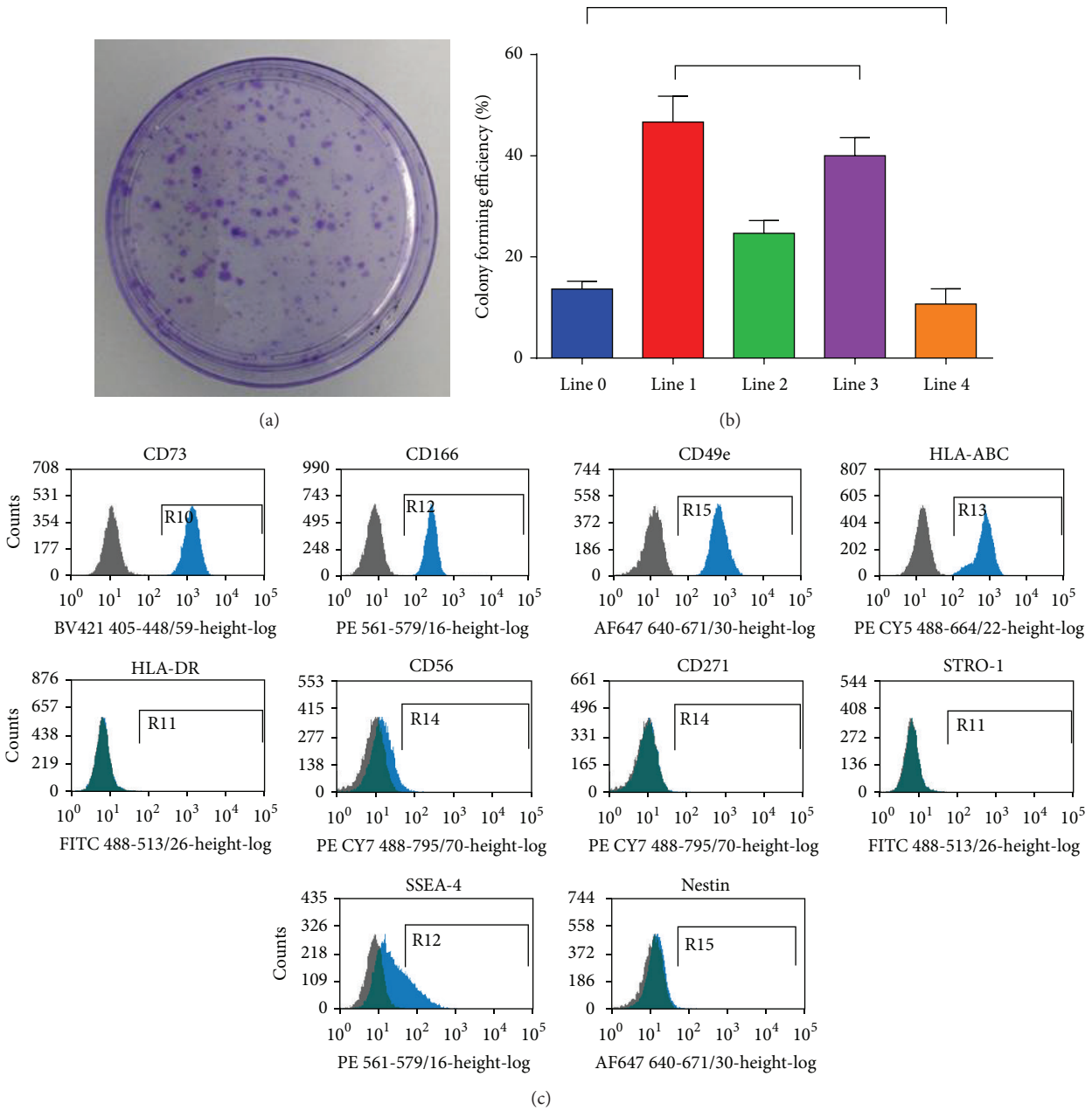

Figure 2: Characteristics of human neonatal sbMSCs. (a and b) Neonatal sbMSCs were clonogenic as demonstrated by colony forming efficiency. (b) Colony forming efficiency was significantly different between the sbMSC lines by one-way ANOVA followed by post hoc Tukey test, except for the bracketed combinations. (c) Neonatal sbMSCs surface marker characterization by flow cytometry. Results are representative of 3 other lines.

(Figure 1(b)). Neonatal sbMSCs were able to be cryopreserved, thawed, and expanded (data not shown).

Neonatal sbMSCs demonstrated many of the characteristics of bone marrow MSCs. Neonatal sbMSCs were clonogenic (Figures 2(a) and 2(b)) with CFE ranging between 11 and 47%. The surface phenotype of sbMSCs was further evaluated by flow cytometry. Neonatal sbMSCs demonstrated characteristic surface marker phenotype with positive expression for CD29, CD44, CD90, CD105, CD73, CD166, CD49e, and HLA-ABC. Neonatal sbMSCs demonstrated negative expression for CD45, HLA-DR, CD56, CD271, STRO-1, and nestin (Figure 2(c)). There was also a substantial fraction of sbMSCs that were positive for SSEA-4 (Figure 2(c)).

Neonatal sbMSCs were multipotent (Figures 3(a)–3(d)) and cells from different patients appeared to have similar efficiency in osteogenic and chondrogenic differentiation (data not shown) but noticeable differences in adipogenic differentiation, which was quantified by digital image analysis

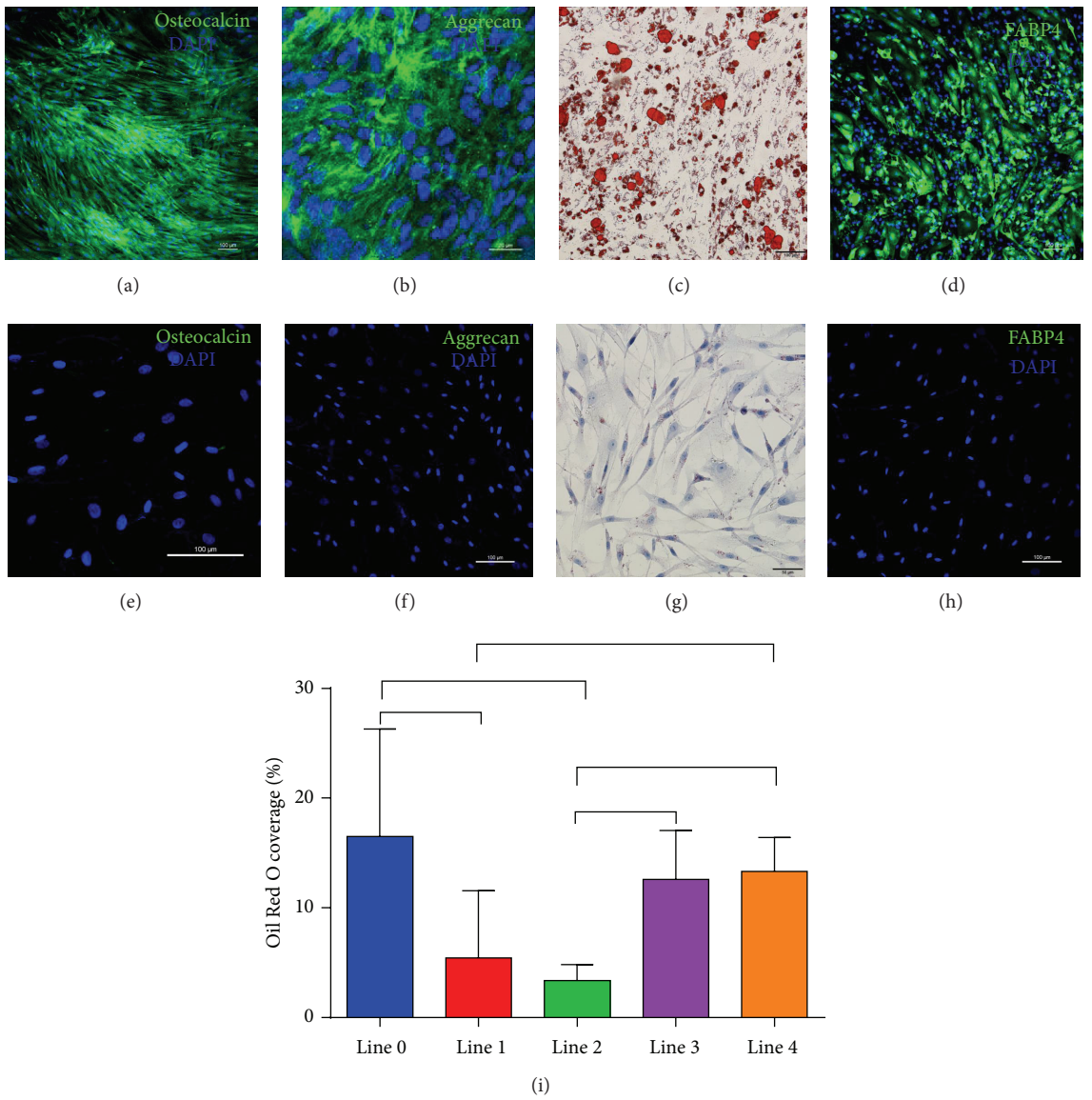

Figure 3: Trilineage differentiation of neonatal sbMSCs. Sternal MSCs ($n = 4$ lines) were incubated with differentiation media for 14–21 days. (a) Osteogenic differentiation was demonstrated by anti-osteocalcin staining. (b) Chondrogenic differentiation by anti-aggrecan staining. (c and d) Adipogenic differentiation was demonstrated by Oil Red O and anti-FABP. (e–h) Neonatal sbMSCs cultured in standard growth media did not demonstrate any spontaneous differentiation. (i) Varying efficiency of adipogenic differentiation of sbMSCs by Oil Red O staining as quantified by image analysis. Data were analyzed by one-way ANOVA with post hoc Tukey test and significant differences ($p < 0.05$) are indicated with brackets.

(Figure 3(e)). Neonatal sbMSCs that were cultured in standard growth media did not manifest any spontaneous trilineage differentiation (Figures 3(f)–3(h)). Neonatal sbMSCs also demonstrated low levels of *Sox-2*, *Oct-4*, and *Nanog* gene expression as compared to hiPSCs, which is consistent with the expression of pluripotency genes in MSCs isolated from other tissues [20–22]. One of the sbMSC lines (line 2) had significantly greater expression of these pluripotency genes as compared to the other lines (Figure 4).

Neonatal sbMSCs also demonstrated proangiogenic properties in vitro. As compared to HUVECs, neonatal sbMSCs demonstrated an increased expression of several angiogenic growth factor genes (Figure 5). *VEGFA* and *ANG1* expressions were significantly increased in all sbMSC lines, whereas *bFGF*, *HIF-1α*, and *HGF* were significantly increased in a subset of the analyzed sbMSC lines. While spheroids containing just HUVECs did not manifest any sprouting at 6 days (Figure 6(a)), those that contained sbMSCs manifested increased sprouting (Figure 6(b)). Spheroids with the combination of HUVECs + sbMSCs yielded the most sprouting (Figure 6(c)), which continued to progress over 6 days (Figures 6(d)–6(f)). A subset of these sprouts appeared tube-like (Figures 6(d) and 6(e)) and sprouts from adjacent spheroids were also able to anastomose to one another (Figure 6(f)).

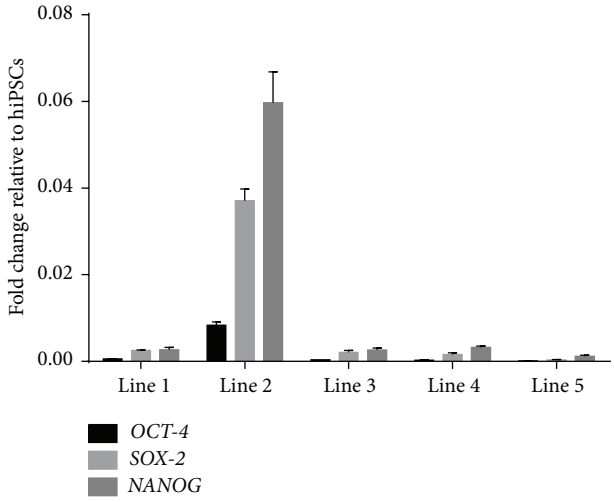

Figure 4: Neonatal sbMSCs express pluripotency-related genes *Oct-4*, *Nanog*, and *Sox-2* as determined by quantitative real-time PCR. Neonatal sbMSC line 2 had significantly upregulated expression of all these genes as compared to the other lines. Data were analyzed by two-way ANOVA and post hoc Tukey test and significant differences ($p < 0.05$).

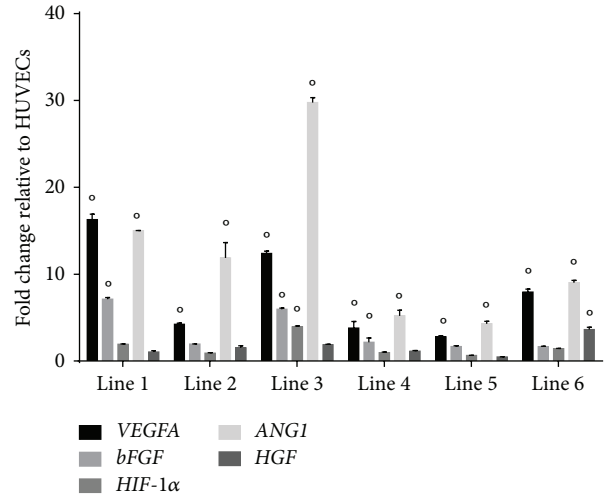

Figure 5: Neonatal sbMSCs express angiogenic genes. All neonatal sbMSC lines expressed *VEGFA* and *ANG1* to a greater degree than HUVECs, whereas half of the sbMSCs lines evaluated also had increased *bFGF* expression. Data were analyzed by two-way ANOVA with post hoc Tukey test (∘ designates $p < 0.05$ versus HUVECs).

Conditioned media from hypoxic neonatal sbMSCs promoted HUVEC migration and survival (Figure 7(a)). Conditioned media from all hypoxic sbMSC lines promoted, to varying degrees, HUVEC migration in a scratch assay, as indicated by a decrease in wound width and an increase in wound density and confluence. Conditioned media from all hypoxic sbMSC lines also induced proliferation of HUVECs, although to a lesser degree than that induced by supplemented EGM-2 media (Figure 7(b)).

4. Discussion

Consistent with the accepted notion that MSCs are present in almost every tissue [23–25], our results indicate that MSCs can be isolated from small amounts of free bone tissue that is present during the conduct of neonatal cardiac surgeries. We confirmed that neonatal sbMSCs share many characteristics of the prototypic bone marrow derived MSCs: sbMSCs are clonogenic, have surface markers consistent with bone marrow derived MSCs, and are multipotent. In general, the CFE of these sbMSCs was higher than reported for bone marrow derived MSCs isolated from adult donors (7–15%) [26].

MSCs are usually isolated from bone marrow aspirates from long bones or iliac crest of older individuals. MSCs have also been isolated from trabecular bone fragments (femur and tibia) although this technique utilized enzymatic digestion [27–29]. Sottile et al. described a similar nonenzymatic

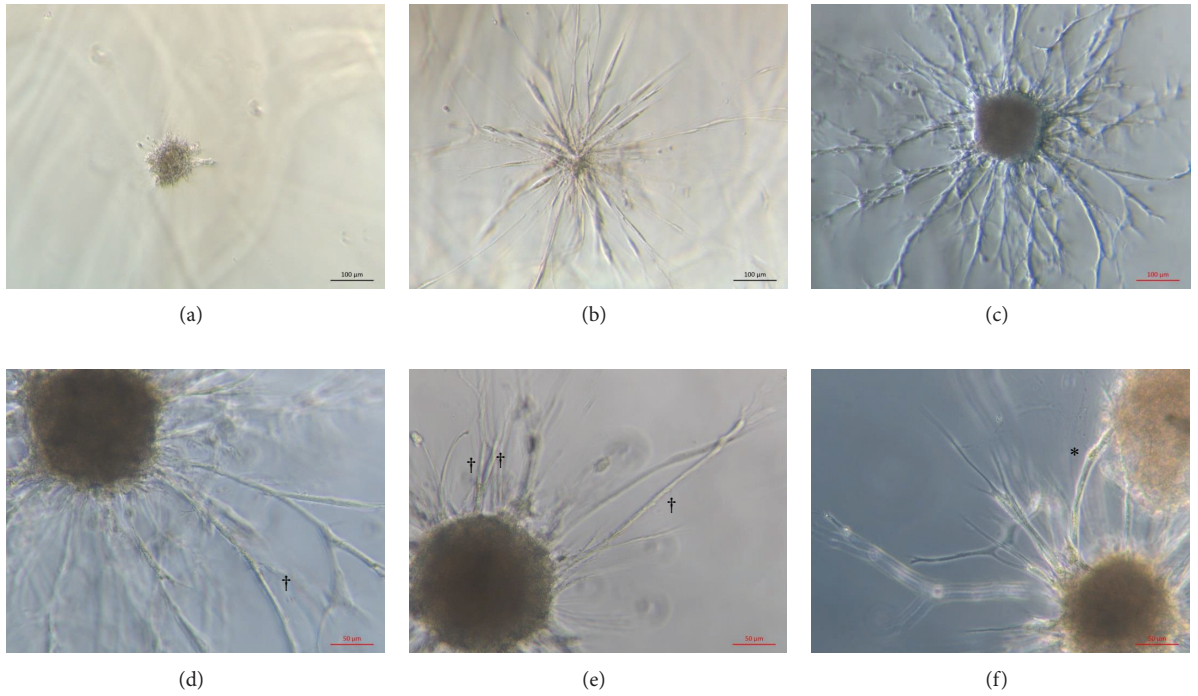

Figure 6: Neonatal sbMSCs cooperate with HUVECs in spheroids to form a complex sprouting network in fibrin gel. (a) Spheroids containing HUVECs (400 cells/spheroid) manifested minimal sprouting at 6 days. (b) Spheroids containing sbMSCs (400 cells/spheroid) had manifested increased sprouting after 6 days. (c) Spheroids containing HUVECs and sbMSCs (800 cells/spheroid with 1 : 1 ratio of each cell type) demonstrated a complex sprouting network at 6 days. Scale bar = 100 μm. (d and e) Tube formation (†) was evident in a subset of sprouts emanating from spheroids. Scale bar = 50 μm. (f) Adjacent spheroids were sometimes connected to each other by anastomosing sprouts (∗). Scale bar = 20 μm.

isolation method of human femur trabecular bone fragments to obtain MSCs [30]. MSCs have also been isolated from adult human sternal marrow [31]. Unique to our study is that we were able to isolate MSCs from normally discarded and overlooked sternal tissue from neonates undergoing cardiac surgery.

The sbMSCs that we have described here may have enhanced therapeutic potential because they come from a neonatal source. It is known that aging abrogates the proliferative and therapeutic potential of bone marrow derived MSCs [26, 32, 33]. While the use of discarded sternal tissue as described in this study required a relatively small amount of tissue from which MSCs can be isolated, larger samples could be harvested without negative effects on the patient. Although these amounts of bone would not be as large as those able to be harvested from an adult, an enhanced proliferative and therapeutic potential of neonatal MSCs may ultimately compensate for this.

We also demonstrated that neonatal sbMSCs possess proangiogenic characteristics in vitro. The tubule formation that we observed when cocultured with HUVECs indicates that sbMSCs functionally promote angiogenesis which is consistent with the behavior of spheroids containing cord blood MSCs and HUVECs as well as adipose MSCs and endothelial progenitor cells [34, 35]. Like MSCs isolated from other tissues, neonatal sbMSCs expressed angiogenic growth factor genes [36, 37]. In conditions of hypoxia (mimicking the in vivo environment in the setting of vascular disease), sbMSCs secreted factors into the conditioned media that were able to promote HUVEC migration as well as surviving from serum starvation. Taken together, these results indicate that neonatal sbMSCs may have potential in promoting angiogenesis in vivo, although this was not examined here directly.

Neonates undergoing heart surgery for complex congenital heart defects have or are at risk of developing diseases of perfusion and vascularization secondary to congenital coronary anomalies and capillary rarefaction secondary to hypertrophy seen in a multitude of defects [6, 7] or caused by severe complications of treatment such as stroke [8, 9]. While others have proposed the potential use of umbilical cord and cord blood derived MSCs to treat neonatal cardiovascular and hypoxic ischemic encephalopathy [38–40], the results of our in vitro studies here suggest that autologous proangiogenic sbMSCs may also have utility in these clinical situations.

5. Conclusions

In conclusion, neonatal sbMSCs share many characteristics with bone marrow derived MSCs and are also proangiogenic. Therefore, discarded neonatal sternal tissue during neonatal cardiac surgery may be a potential source of MSCs for therapeutic use, especially for those pediatric patients with

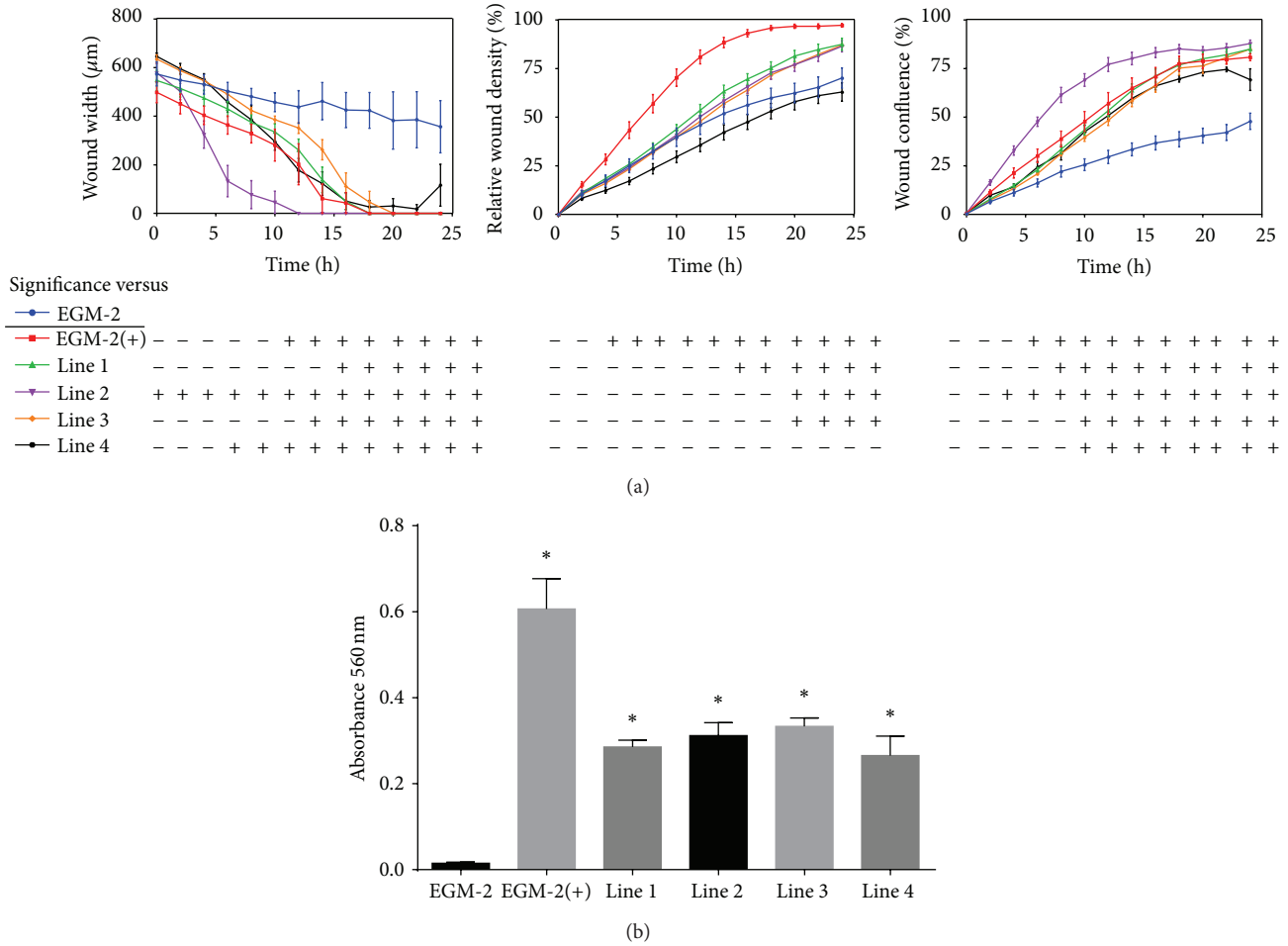

Figure 7: Conditioned media from hypoxic neonatal sbMSCs promote HUVEC migration and proliferation. (a) HUVEC migration was assessed by a scratch assay. Conditioned media from all hypoxic sbMSCs lines enhanced and accelerated scratch healing as assessed by average (error bars = standard deviation) wound width, density, and confluence as compared to basal media, EGM-2. Growth factor supplemented EGM-2(+) was used as a positive control. Data were analyzed by one-way ANOVA with post hoc Tukey test and are representative of two independent experiments. (b) HUVEC proliferation was assessed by the MTT assay. Conditioned media from all hypoxic sbMSCs lines enhanced HUVECs proliferation as compared to basal EGM-2 ($*$, $p < 0.05$). Data were analyzed by one-way ANOVA with post hoc Tukey test and are representative of two independent experiments.

complex heart disease who have or are at significant risk of developing diseases of perfusion and vascularization.

Conflict of Interests

The authors declare that they have no conflict of interests.

Acknowledgment

This study was supported by the Department of Cardiac Surgery at the University of Michigan.

References

[1] G. P. Lasala, J. A. Silva, and J. J. Minguell, "Therapeutic angiogenesis in patients with severe limb ischemia by transplantation of a combination stem cell product," *Journal of Thoracic and Cardiovascular Surgery*, vol. 144, no. 2, pp. 377–382, 2012.

[2] P. K. Gupta, A. Chullikana, R. Parakh et al., "A double blind randomized placebo controlled phase I/II study assessing the safety and efficacy of allogeneic bone marrow derived mesenchymal stem cell in critical limb ischemia," *Journal of Translational Medicine*, vol. 11, no. 1, article 143, 2013.

[3] A. K. Das, B. J. J. B. Abdullah, S. S. Dhillon, A. Vijanari, C. H. Anoop, and P. K. Gupta, "Intra-arterial allogeneic mesenchymal stem cells for critical limb ischemia are safe and efficacious: report of a phase i study," *World Journal of Surgery*, vol. 37, no. 4, pp. 915–922, 2013.

[4] G. P. Lasala, J. A. Silva, B. A. Kusnick, and J. J. Minguell, "Combination stem cell therapy for the treatment of medically refractory coronary ischemia: a Phase I study," *Cardiovascular Revascularization Medicine*, vol. 12, no. 1, pp. 29–34, 2011.

[5] D. Lu, B. Chen, Z. Liang et al., "Comparison of bone marrow mesenchymal stem cells with bone marrow-derived mononuclear cells for treatment of diabetic critical limb ischemia and foot ulcer: a double-blind, randomized, controlled trial,"

Diabetes Research and Clinical Practice, vol. 92, no. 1, pp. 26–36, 2011.

[6] N. Kayalar, H. M. Burkhart, J. A. Dearani, F. Cetta, and H. V. Schaff, "Congenital coronary anomalies and surgical treatment," *Congenital Heart Disease*, vol. 4, no. 4, pp. 239–251, 2009.

[7] B. Johansson, S. Mörner, A. Waldenström, and P. Stål, "Myocardial capillary supply is limited in hypertrophic cardiomyopathy: a morphological analysis," *International Journal of Cardiology*, vol. 126, no. 2, pp. 252–257, 2008.

[8] T. Domi, D. S.Edgell, B. W. McCrindle et al., "Frequency, predictors, and neurologic outcomes of vaso-occlusive strokes associated with cardiac surgery in children," *Pediatrics*, vol. 122, no. 6, pp. 1292–1298, 2008.

[9] G. Trittenwein, A. Nardi, H. Pansi et al., "Early postoperative prediction of cerebral damage after pediatric cardiac surgery," *Annals of Thoracic Surgery*, vol. 76, no. 2, pp. 576–580, 2003.

[10] M. J. Kim, K. S. Shin, J. H. Jeon et al., "Human chorionic-plate-derived mesenchymal stem cells and Wharton's jelly-derived mesenchymal stem cells: a comparative analysis of their potential as placenta-derived stem cells," *Cell and Tissue Research*, vol. 346, no. 1, pp. 53–64, 2011.

[11] R. Anzalone, M. L. Iacono, S. Corrao et al., "New emerging potentials for human wharton's jelly mesenchymal stem cells: immunological features and hepatocyte-like differentiative capacity," *Stem Cells and Development*, vol. 19, no. 4, pp. 423–438, 2010.

[12] M. M. Carvalho, F. G. Teixeira, R. L. Reis, N. Sousa, and A. J. Salgado, "Mesenchymal stem cells in the umbilical cord: phenotypic characterization, secretome and applications in central nervous system regenerative medicine," *Current Stem Cell Research and Therapy*, vol. 6, no. 3, pp. 221–228, 2011.

[13] C. F. Heazlewood, H. Sherrell, J. Ryan, K. Atkinson, C. A. Wells, and N. M. Fisk, "High incidence of contaminating maternal cell overgrowth in human placental mesenchymal stem/stromal cell cultures: a systematic review," *Stem Cells Translational Medicine*, vol. 3, no. 11, pp. 1305–1312, 2014.

[14] Y. A. Dzal, S. E. Jenkin, S. L. Lague, M. N. Reichert, J. M. York, and M. E. Pamenter, "Oxygen in demand: how oxygen has shaped vertebrate physiology," *Comparative Biochemistry and Physiology Part A: Molecular & Integrative Physiology*, vol. 186, pp. 4–26, 2015.

[15] Z. Lokmic, J. Musyoka, T. D. Hewitson, and I. A. Darby, "Hypoxia and hypoxia signaling in tissue repair and fibrosis," *International Review of Cell and Molecular Biology*, vol. 296, pp. 139–185, 2012.

[16] L. Chen, Y. B. Xu, J. L. Zhao et al., "Conditioned medium from hypoxic bone marrow-derived mesenchymal stem cells enhances wound healing in mice," *PLoS ONE*, vol. 9, no. 4, Article ID e96161, 2014.

[17] E. K. Jun, Q. Zhang, B. S. Yoon et al., "Hypoxic conditioned medium from human amniotic fluid-derived mesenchymal stem cells accelerates skin wound healing through TGF-β/SMAD2 and PI3K/AKT pathways," *International Journal of Molecular Sciences*, vol. 15, no. 1, pp. 605–628, 2014.

[18] A. Burlacu, G. Grigorescu, A.-M. Rosca, M. B. Preda, and M. Simionescu, "Factors secreted by mesenchymal stem cells and endothelial progenitor cells have complementary effects on angiogenesis in vitro," *Stem Cells and Development*, vol. 22, no. 4, pp. 643–653, 2013.

[19] J. G. Rasmussen, O. Frøbert, L. Pilgaard et al., "Prolonged hypoxic culture and trypsinization increase the pro-angiogenic potential of human adipose tissue-derived stem cells," *Cytotherapy*, vol. 13, no. 3, pp. 318–328, 2011.

[20] S. Carelli, F. Messaggio, A. Canazza et al., "Characteristics and properties of mesenchymal stem cells derived from microfragmented adipose tissue," *Cell Transplantation*, vol. 24, no. 7, pp. 1233–1252, 2015.

[21] G. Siegel, T. Kluba, U. Hermanutz-Klein, K. Bieback, H. Northoff, and R. Schäfer, "Phenotype, donor age and gender affect function of human bone marrow-derived mesenchymal stromal cells," *BMC Medicine*, vol. 11, article 146, 2013.

[22] C. Tantrawatpan, S. Manochantr, P. Kheolamai, Y. U-pratya, A. Supokawe, and S. Issaragrisil, "Pluripotent gene expression in mesenchymal stem cells from human umbilical cord Wharton's jelly and their differentiation potential to neural-like cells," *Journal of the Medical Association of Thailand*, vol. 96, no. 9, pp. 1208–1217, 2013.

[23] F.-J. Lv, R. S. Tuan, K. M. C. Cheung, and V. Y. L. Leung, "Concise review: the surface markers and identity of human mesenchymal stem cells," *Stem Cells*, vol. 32, no. 6, pp. 1408–1419, 2014.

[24] C. Bluguermann, L. Wu, F. Petrigliano, D. Mcallister, S. Miriuka, and D. A. Evseenko, "Novel aspects of parenchymal-mesenchymal interactions: from cell types to molecules and beyond," *Cell Biochemistry and Function*, vol. 31, no. 4, pp. 271–280, 2013.

[25] S. S. Huang, V. Leung, S. L. Peng et al., "Developmental definition of MSCs: new insights into pending questions," *Cellular Reprogramming*, vol. 13, no. 6, pp. 465–472, 2011.

[26] G. Siegel, T. Kluba, U. Hermanutz-Klein, K. Bieback, H. Northoff, and R. Schäfer, "Phenotype, donor age and gender affect function of human bone marrow-derived mesenchymal stromal cells," *BMC Medicine*, vol. 11, no. 1, article 146, 2013.

[27] Y. Sakaguchi, I. Sekiya, K. Yagishita, S. Ichinose, K. Shinomiya, and T. Muneta, "Suspended cells from trabecular bone by collagenase digestion become virtually identical to mesenchymal stem cells obtained from marrow aspirates," *Blood*, vol. 104, no. 9, pp. 2728–2735, 2004.

[28] R. Tuli, S. Tuli, S. Nandi et al., "Characterization of multipotential mesenchymal progenitor cells derived from human trabecular bone," *Stem Cells*, vol. 21, no. 6, pp. 681–693, 2003.

[29] R. Tuli, M. R. Seghatoleslami, S. Tuli et al., "A simple, high-yield method for obtaining multipotential mesenchymal progenitor cells from trabecular bone," *Molecular Biotechnology*, vol. 23, no. 1, pp. 37–49, 2003.

[30] V. Sottile, C. Halleux, F. Bassilana, H. Keller, and K. Seuwen, "Stem cell characteristics of human trabecular bone-derived cells," *Bone*, vol. 30, no. 5, pp. 699–704, 2002.

[31] V. Paunescu, E. Deak, D. Herman et al., "In vitro differentiation of human mesenchymal stem cells to epithelial lineage," *Journal of Cellular and Molecular Medicine*, vol. 11, no. 3, pp. 502–508, 2007.

[32] F. Z. Asumda, "Age-associated changes in the ecological niche: implications for mesenchymal stem cell aging," *Stem Cell Research & Therapy*, vol. 4, article 47, 2013.

[33] M. S. Choudhery, M. Khan, R. Mahmood, A. Mehmood, S. N. Khan, and S. Riazuddin, "Bone marrow derived mesenchymal stem cells from aged mice have reduced wound healing, angiogenesis, proliferation and anti-apoptosis capabilities," *Cell Biology International*, vol. 36, no. 8, pp. 747–753, 2012.

[34] W.-Y. Lee, H.-W. Tsai, J.-H. Chiang et al., "Core-shell cell bodies composed of human cbMSCs and HUVECs for functional

vasculogenesis," *Biomaterials*, vol. 32, no. 33, pp. 8446–8455, 2011.

[35] S.-H. Hsu, T.-T. Ho, N.-C. Huang, C.-L. Yao, L.-H. Peng, and N.-T. Dai, "Substrate-dependent modulation of 3D spheroid morphology self-assembled in mesenchymal stem cell-endothelial progenitor cell coculture," *Biomaterials*, vol. 35, no. 26, pp. 7295–7307, 2014.

[36] D. G. Phinney, "A Sage view of mesenchymal stem cells," *International Journal of Stem Cells*, vol. 2, no. 1, pp. 1–10, 2009.

[37] A. Bronckaers, P. Hilkens, W. Martens et al., "Mesenchymal stem/stromal cells as a pharmacological and therapeutic approach to accelerate angiogenesis," *Pharmacology & Therapeutics*, vol. 143, no. 2, pp. 181–196, 2014.

[38] C. T. J. van Velthoven, A. Kavelaars, and C. J. Heijnen, "Mesenchymal stem cells as a treatment for neonatal ischemic brain damage," *Pediatric Research*, vol. 71, no. 4, pp. 474–481, 2012.

[39] J. Carroll, "Human cord blood for the hypoxic-ischemic neonate," *Pediatric Research*, vol. 71, no. 4, pp. 459–463, 2012.

[40] S. C. Peral, H. M. Burkhart, S. Oommen et al., "Safety and feasibility for pediatric cardiac regeneration using epicardial delivery of autologous umbilical cord blood-derived mononuclear cells established in a porcine model system," *Stem Cells Translational Medicine*, vol. 4, no. 2, pp. 195–206, 2015.

Hindawi Publishing Corporation
Stem Cells International
Volume 2016, Article ID 5282185, 8 pages
http://dx.doi.org/10.1155/2016/5282185

Research Article

Potential Role of Activating Transcription Factor 5 during Osteogenesis

Luisa Vicari,[1] Giovanna Calabrese,[1] Stefano Forte,[1] Raffaella Giuffrida,[1] Cristina Colarossi,[2] Nunziatina Laura Parrinello,[2] and Lorenzo Memeo[1,2]

[1]*IOM Ricerca Srl, Via Penninazzo 11, 95029 Viagrande, Italy*
[2]*Department of Experimental Oncology, Mediterranean Institute of Oncology, Via Penninazzo 7, 95029 Viagrande, Italy*

Correspondence should be addressed to Lorenzo Memeo; lorenzo.memeo@grupposamed.com

Received 9 June 2015; Revised 30 July 2015; Accepted 2 August 2015

Academic Editor: Ming Li

Human adipose-derived stem cells are an abundant population of stem cells readily isolated from human adipose tissue that can differentiate into connective tissue lineages including bone, cartilage, fat, and muscle. Activating transcription factor 5 is a transcription factor of the ATF/cAMP response element-binding protein (CREB) family. It is transcribed in two types of mRNAs (activating transcription factor 5 isoform 1 and activating transcription factor 5 isoform 2), encoding the same single 30-kDa protein. Although it is well demonstrated that it regulates the proliferation, differentiation, and apoptosis, little is known about its potential role in osteogenic differentiation. The aim of this study was to evaluate the expression levels of the two isoforms and protein during osteogenic differentiation of human adipose-derived stem cells. Our data indicate that activating transcription factor 5 is differentially expressed reaching a peak of expression at the stage of bone mineralization. These findings suggest that activating transcription factor 5 could play an interesting regulatory role during osteogenesis, which would provide a powerful tool to study bone physiology.

1. Introduction

Human adipose-derived stem cells (hADSCs) are an alternative, accessible, and abundant source of stem cells readily isolated from adipose tissue that can differentiate *in vitro* into multiple lineages, including adipocytes, chondrocytes, osteocytes, neural-like cells, endothelial cells, and cardiomyocytes under lineage-specific culture conditions [1–9]. This tissue provides a potential adult stem cell reservoir for each individual representing an interesting resource for regenerative medicine [10–15].

The ability to isolate and expand the culture and differentiate the hADSCs *in vitro* into particular lineages provides the opportunity to study events associated with differentiation.

Activating transcription factor 5 (ATF5) is a member of the ATF/cAMP response element-binding protein (CREB) family, which includes a large group of basic leucine zipper (bZIP) proteins with different transcriptional regulatory functions [16]. ATF5 plays a pivotal role in promoting cell survival, differentiation, proliferation, and apoptosis [17].

Consistent with this, accumulating data have proven that ATF5 downregulation allows for differentiation in mature oligodendrocytes, neurons, and astrocytes [18–21]. Moreover ATF5 promotes proliferation of cerebral cortical neuroprogenitor cells and is required for terminal differentiation and survival of olfactory sensory neurons [22]. In addition several studies have previously demonstrated that ATF5 is highly expressed in a variety of tumors [23, 24].

ATF5 gene generates two transcripts, ATF5 isoform 1 (activating transcription factor 5, transcript variant 1: NM_012068.5) and ATF5 isoform 2 (activating transcription factor 5, transcript variant 2: NM_001193646.1). They differ only in their 5′-untranslated regions (UTRs) designated ATF5-5′ UTRα and ATF5-5′ UTRβ; their coding regions are identical and originate the same 30-kDa protein [25]. The significance of these two transcripts is currently not clarified.

Although ATF5 is previously demonstrated to play a role in osteogenic differentiation [26, 27], it has never been described in detail. Furthermore, these two isoforms have never been investigated in osteogenesis.

In the present study we analysed the two ATF5 mRNA isoforms and protein to evaluate the modulation of their expression during different stages of bone formation. To this end, mRNAs and proteins were collected during the whole period to perform qRT-PCR and immunocytochemical analysis.

Our findings suggest that ATF5 mRNAs and protein present a different expression profile and provide new insights about ATF5 role in osteogenesis.

2. Materials and Methods

2.1. Isolation, Ex Vivo Expansion, and Characterization of Human Adipose-Derived Stem Cells. hADSCs were obtained from adipose tissue biopsies of the Pathology Unit at the Mediterranean Institute of Oncology (Viagrande, Italy) after informed consent. The adipose tissue was mechanically dissociated into smaller pieces and digested at 37°C with a collagenase I solution (Gibco, Thermo Fisher Scientific, Waltham, MA, USA). After two hours, the fragments were centrifuged, the floating fat was removed, and the remaining supernatant was filtered and centrifuged. To select adherent cells, the final pellet was resuspended in growth medium (ADSC basal medium, Lonza Group Ltd., Basel, Switzerland) supplemented with foetal bovine serum (FBS; Invitrogen, Thermo Fisher Scientific, Waltham, MA, USA), L-glutamine and gentamicin-amphotericin B (GA-1000, Lonza) and incubated overnight in 75 cm^2 flasks at 37°C in a humidified atmosphere containing 5% CO_2. The following day, nonadherent cells were removed. Selected hADSCs were maintained in 75 cm^2 flask, and the medium changed every 3-4 days and expanded until 80–90% confluence.

hADSCs were characterized by flow cytometry analysis. 1×10^4 cells/tube were stained with the following antibodies: CD45 FITC (clone J.33), CD34 PE (clone 581), CD73 PE (clone 581), CD90 FITC (clone F15.42.1.5), CD105 PE (clone 1G2), GlyA PE (clone 11E4B7.6), CD31PE (clone 1F11), CD117 PE (clone 104D2D1), CD271 FITC (clone ME20.4-1.H4), and respective isotopic controls according to manufacturer indications. All antibodies were purchased from Beckman Coulter (Milano, Italy), except CD271 that is provided by Miltenyi Biotec (Bologna, Italy).

2.2. In Vitro Osteogenic Differentiation of Human Adipose-Derived Stem Cells. For osteogenic differentiation, hADSCs were seeded at a density of $3{,}1 \times 10^4$ cells/cm^2 on collagen I coated plate in growth medium. After 24 hours, growth medium was replaced with osteogenic induction medium (Lonza) containing osteogenic basal medium (Lonza) supplemented with growth factors, dexamethasone, ascorbate, L-glutamine, penicillin/streptomycin, and β-glycerophosphate (Lonza). The medium was changed every 3-4 days. The osteogenic differentiation was observed during the whole period by microscopy. The osteogenic phenotype was confirmed by immunocytochemical analysis with specific markers and Alizarin Red S staining.

For immunocytochemical analysis the cells were seeded in 8-well BD Falcon culture slides (Corning Inc., Corning, NY, USA) at a density of 5000 cells per cm^2 in ADSC-growth medium. After 48 hours the medium was removed, and the adherent cells were washed and fixed with paraformaldehyde 4% (PFA, Sigma Aldrich, Saint Louis, MO, USA) for 15 minutes. Subsequently, the cells were permeabilized and blocked. The primary incubation was performed, overnight at 4°C, with the following antibodies: rabbit anti-human ATF5 (1 : 500, Novus Biologicals, Littleton, CO, USA), rabbit anti-human osteopontin (1 : 250, Novus Biologicals), and mouse anti-human osteocalcin (1 : 200, Santa Cruz Biotechnology Inc., Dallas, TX, USA). After washing, slides were incubated with the appropriate secondary AlexaFluor 568 antibodies (Life Technologies Italia, Monza, Italy) for 2 hours at room temperature and the nuclei counterstained with DAPI. Afterwards they were mounted with fluorescent mounting medium Permafluor (Thermo Scientific). Digital images were acquired using a Leica DMI4000B fluorescence microscope (Leica Microsystems Srl, Milan, Italy) and cells count was performed by using CellProfiler [28].

For Alizarin Red S staining, cells were fixed with PFA 4% for 15 minutes and incubated with 2% Alizarin Red S solution for 5 minutes. After incubation the staining solution was removed and the culture slides were washed to eliminate excessive colour.

2.3. Total RNA Extraction and Reverse Transcription. Total RNA was extracted from hADSCs during the whole period with the RNeasy Mini Isolation Kit (Qiagen, Valencia, CA, USA). RNA purity was calculated measuring the ratio of the absorbance at 260 and 280 nm and considering 1.8–2.0 as admissible range of ratios for pure RNAs. RNA quality was determined by Agilent 2100 Bioanalyzer RNA assays (Agilent technologies, Santa Clara, CA, USA) and by calculating the ratio of the 28S and 18S ribosomal RNA intensity peaks. Total RNA was stored at −80°C.

RNA samples (1,0 μg) were reverse-transcribed by using the High-Capacity cDNA Reverse Transcription (Applied Biosystems, Thermo Fisher Scientific, Waltham, MA, USA) according to manufacturer's protocol. RT products were stored at −20°C.

2.4. Real-Time RT-PCR. Target mRNAs concentration was assessed by quantitative real-time PCR (qRT-PCR) on Applied Biosystem 7900HT fast real-time PCR system using comparative Ct method with fast SYBR Green chemistry (Applied Biosystem). PCR primers were designed using Primer BLAST [29] to specifically recognize selected transcripts by targeting exon-exon junctions and tested for off-targeting using human RefSeq database [30]. Both human glyceraldehyde-3-phosphate dehydrogenase and tubulin beta were used as endogenous controls. Isoforms specific ATF5 primer pairs were designed to recognize unique regions in 5′ UTRs. Run-related transcription factor 2 (RUNX2), OSTERIX, and alkaline phosphatase (ALPL) primers were used to evaluate osteogenic commitment. Each molecular endpoint was tested in triplicate. Relative quantitation of mRNA expression has been evaluated using the ΔΔct method with the proliferation mRNA level used as reference. Statistical analysis of ATF5 expression levels in temporal groups has been performed using the analysis of variance.

The following primers were used to perform qRT-PCR: ATF5_1 fw: CAGGAAATTCTGCAAGCAAGGAA; ATF5_1 rev: CGGCGACACTCTTCCCTCTG; ATF5_2 fw: TGTCCTCGGATCACAGTCTCT; ATF5_2 rev: AAGTGGAAGACTCCATGGCTG; OSTERIX fw: TGCTTGAGGAGGAAGTTCACTATG; OSTERIX rev: TGCCCAGAGTTGTTGAGTCC; ALPL fw: GACCCTTGACCCCCACAAT; ALPL rev: CGCCTCGTACTGCATGTCCCCT; RUNX2 fw: GGAGTGGACGAGGCAAGAGTTT; RUNX2 rev: AGCTTCTGTCTGTGCCTTCTGG; GAPDH fw: GCTCTCCAGAACATCATCCCTGCC; GAPDH rev: GCGTTGTCATACCAGGAAATGAGCTT; β-TUB fw: GCGCATTCCAACCTTCCAG; β-TUB rev: CCCAGAACTTGGCACCGAT.

2.5. Western Blot. Cell pellets were homogenized with RIPA lysis buffer (1 : 5 w/v). For western blot quantification, 40 μg of protein was separated on a precast 4–20% trisglycine gel (Thermo Scientific, Rockford, IL, USA) and transferred to a nitrocellulose membrane. After overnight blocking at 4°C with 5% nonfat dry milk, membranes were incubated for 4 h with rabbit anti-human ATF5 primary antibody (Novus Biologicals, Catalog number NBP2-15500; dilution 1 : 1000). Then, membranes were washed and incubated for 1 h with peroxidase-conjugate goat anti-rabbit secondary antibody (Thermo Scientific group; Catalog number 1858415; dilution 1 : 6000). Peroxidase activity was developed by enhanced chemiluminescent substrate (Pierce Biotechnology Inc., Thermo Scientific group; Catalog number 34075) and visualized by autoradiography. Then, the protocol was repeated for quantification of actin, using a rabbit anti-actin primary antibody (Santa Cruz, Catalog number SC130657; dilution 1 : 500) followed by a goat anti-rabbit secondary antibody (Pierce Biotechnology Inc., Thermo Fisher Scientific, Waltham, MA, USA; Catalog number 1858413; dilution 1 : 5000). Density values relative to all proteins were normalized to actin levels measured in the same membrane.

3. Results

3.1. hADSCs Differentiate in Osteocytes in Presence of Osteogenic Inductive Factors. hADSCs derived from three different cell lines at passage 3 were cultured for 24 days in the presence of osteogenic medium. Alizarin Red S staining was used to examine the differentiation of hADSCs into osteocytes. After 8, 16, and 24 days of culture, hADSCs produced a densely mineralized extracellular matrix, followed by calcium precipitates within the cytoplasm. In particular Alizarin Red staining showed that cell calcium content increased over time; in fact, greater amount and size of calcium stores within the cytoplasm were observed (Figure 1(a)).

To confirm the osteogenic commitment of hADSCs we performed qRT-PCR analysis after 3, 11, 16, 21, and 24 days of osteogenic induction with the transcription factors RUNX2 and OSTERIX and the bone related gene ALPL (Figure 1(b)). The gene expression was analyzed in at least three different adipose-derived cell lines to compensate for the biological variance. qRT-PCR analysis of RUNX2, the central control gene within the osteoblast phenotype, showed that its expression level increased during osteogenic differentiation reaching a peak at day 21 according to what was previously reported [31]. The ALPL enzyme, an important component of osteogenesis, displayed a typical peak prior to mineralization (day 11), as shown in Figure 1(b).

The expression pattern of the OSTERIX gene was very similar to that of ALPL. OSTERIX, a marker of committed osteoprogenitors, was significantly enhanced after day 3 of osteogenic induction reaching a peak at day 11.

3.2. ATF5_1 and ATF5_2 Expression Levels Show a Peak at the Bone Mineralization Stage. To evaluate the expression levels of the two ATF5 isoforms (ATF5_1 and ATF5_2) during osteogenic differentiation we performed qRT-PCR analysis.

For qRT-PCR analysis we divided the days of osteogenic differentiation into 8 groups (proliferation, D 0–3, D 4–7, D 8–11, D 12–15, D 16–19, D 20–22, and D 23–28). The mean relative expression of ATF5 isoforms in each interval is reported in Figure 2. Proliferation group is used as reference for quantitation.

The results of qRT-PCR showed that the expression of ATF5_1 was unaltered between day 0 and day 7 and gradually increased until day 22 (approximately 3, 5 times), successively showing a threefold decrease at day 28 (Figure 2(a)).

The expression of ATF5_2 decreased during the first 15 days of osteogenic differentiation and reached a peak at days 20–22, decreasing again successively (Figure 2(b)). When both the isoforms were considered together (ATF5_1-2, average of the two ATF5 isoforms mRNAs), our data showed that after an initial decrease from day 0 to day 11 ATF5_1-2 levels increased with a peak at days 20–22 and then decreased approximately about 2 times (Figure 2(c)). Statistical analysis of ATF5 expression levels in temporal groups indicates a significant modulation of both isoforms during differentiation ($p < 0.001$ for both isoforms and for their averaged relative quantitation).

In summary our results showed that while ATF5_1 and ATF5_2 mRNAs expression profile seems to differ in the early stages of osteogenic induction (proliferation, matrix maturation, and early-mineralization stages), they exhibit the same expression peak in the stage of late bone mineralization (D 20–22), as also confirmed by the ATF5 protein expression. After D 23–28 days, both ATF5 mRNA isoforms were downregulated.

The present study provides the first description of the expression levels of the two ATF5 isoforms during osteogenic differentiation.

3.3. ATF5 Protein Is Expressed in the Bone Mineralization Stage during Osteogenic Differentiation. To evaluate ATF5 protein expression, cells growth in osteogenic medium after 3, 11, 16, 21, and 24 days was assessed by immunocytochemical analysis.

In accordance with the data of qRT-PCR, we found that ATF5 protein (Figure 3) had an expression peak (71,9%) during the stage of bone mineralization, day 21, decreasing successively after day 24 (5,9%) as shown in Table 1.

Table 1: Number and percentage of positive cells for ATF5, OP, and OC. Percentages of positive cells were calculated on the total amount of DAPI for each image (Figure 3).

	Prolif.			D 3			D 11			D 16			D 21			D 24		
	D	R	%	D	R	%	D	R	%	D	R	%	D	R	%	D	R	%
ATF5	31	29	93,5	76	53	69,7	309	1	0,3	511	100	19,6	814	585	71,9	589	35	5,9
OP	29	29	100	105	86	81,9	466	234	50,2	128	128	100	834	329	39,4	783	321	41
OC	23	5	21,7	136	2	1,5	356	140	39,3	811	265	32,7	750	248	33	805	331	41,1

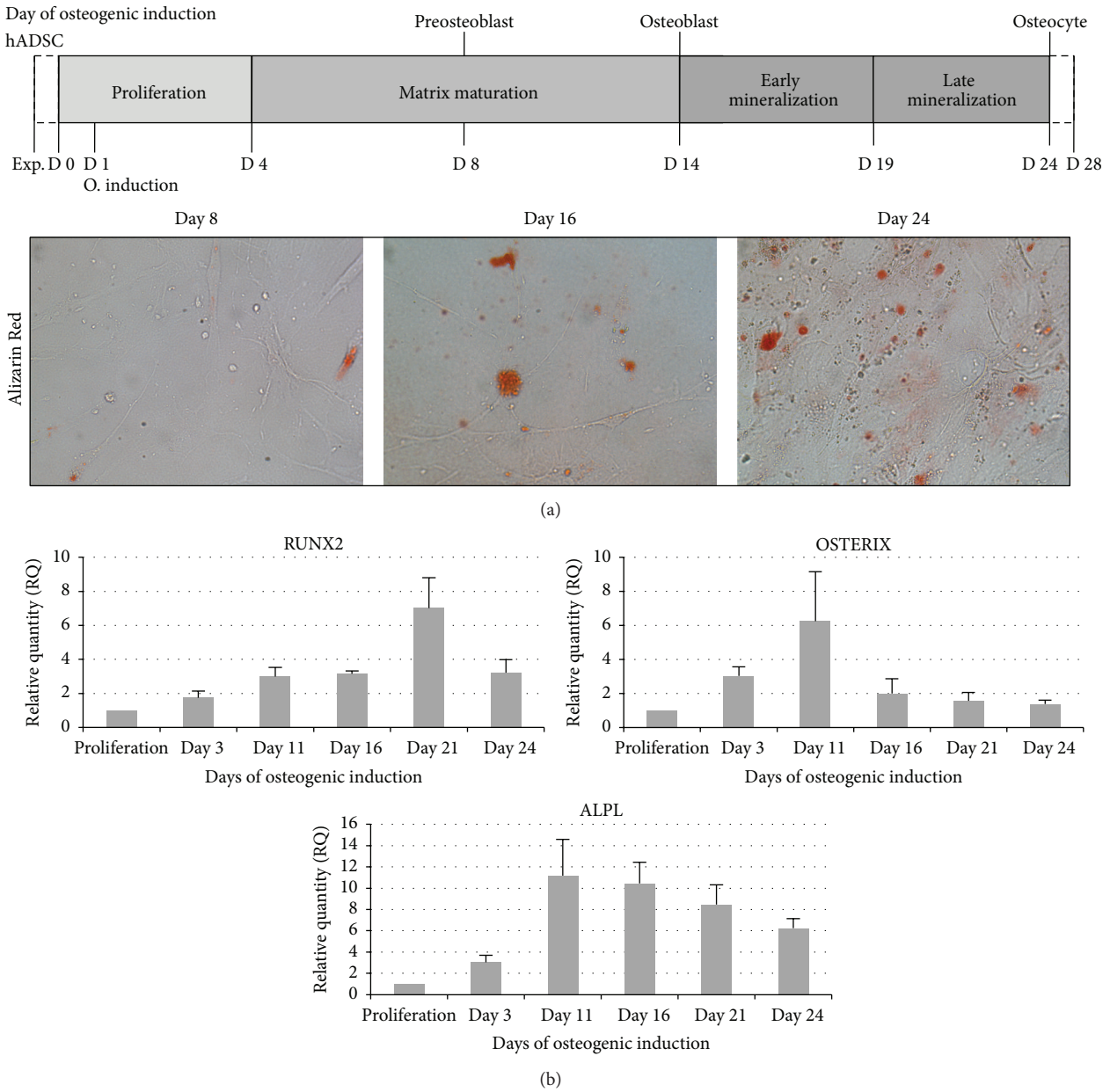

Figure 1: (a) Alizarin Red S staining of hADSCs during osteogenic differentiation. Mineralization of the extracellular matrix with the presence of calcium precipitates was visualized by staining with Alizarin Red S at days 8, 16, and 24. (b) Gene expression levels during osteogenic differentiation of hADSCs. Relative quantification of mRNA level assessed by qRT-PCR for RUNX2, OSTERIX, and ALPL after 3, 11, 16, 21, and 24 days of osteogenic differentiation. Proliferation group is used as reference for quantitation.

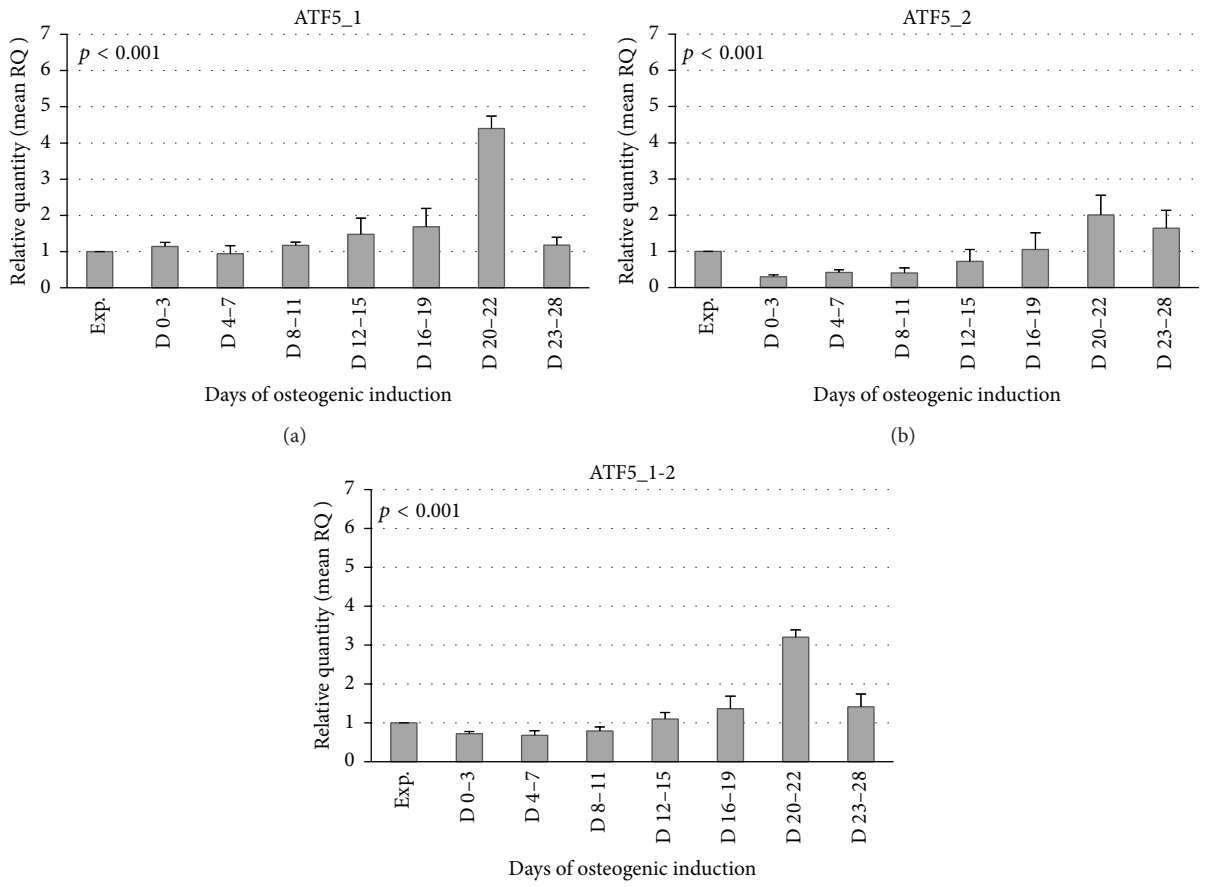

Figure 2: ATF5 expression levels during osteogenic differentiation of hADSCs. (a, b, c) Relative quantification of mRNA levels assessed by real-time PCR for ATF5 isoforms, conducted on RNA from hADSCs, either undifferentiated (proliferation) or differentiated (D 0–D 28). Proliferation group is used as reference for quantitation. The analysis of variance of both ATF5 isoforms relative expression levels indicates a statistically significant modulation during osteogenic differentiation ($p < 0.001$).

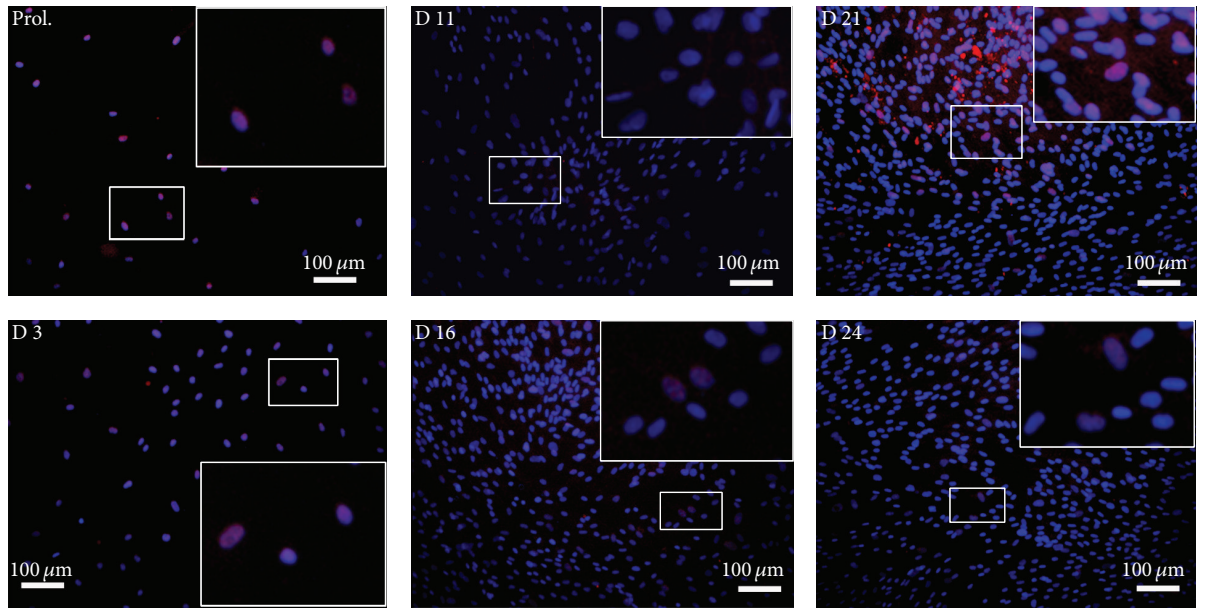

Figure 3: ATF5 during osteogenic differentiation. Immunocytochemical analysis of ATF5 at specific time points (proliferation, days 3, 11, 16, 21, and 24).

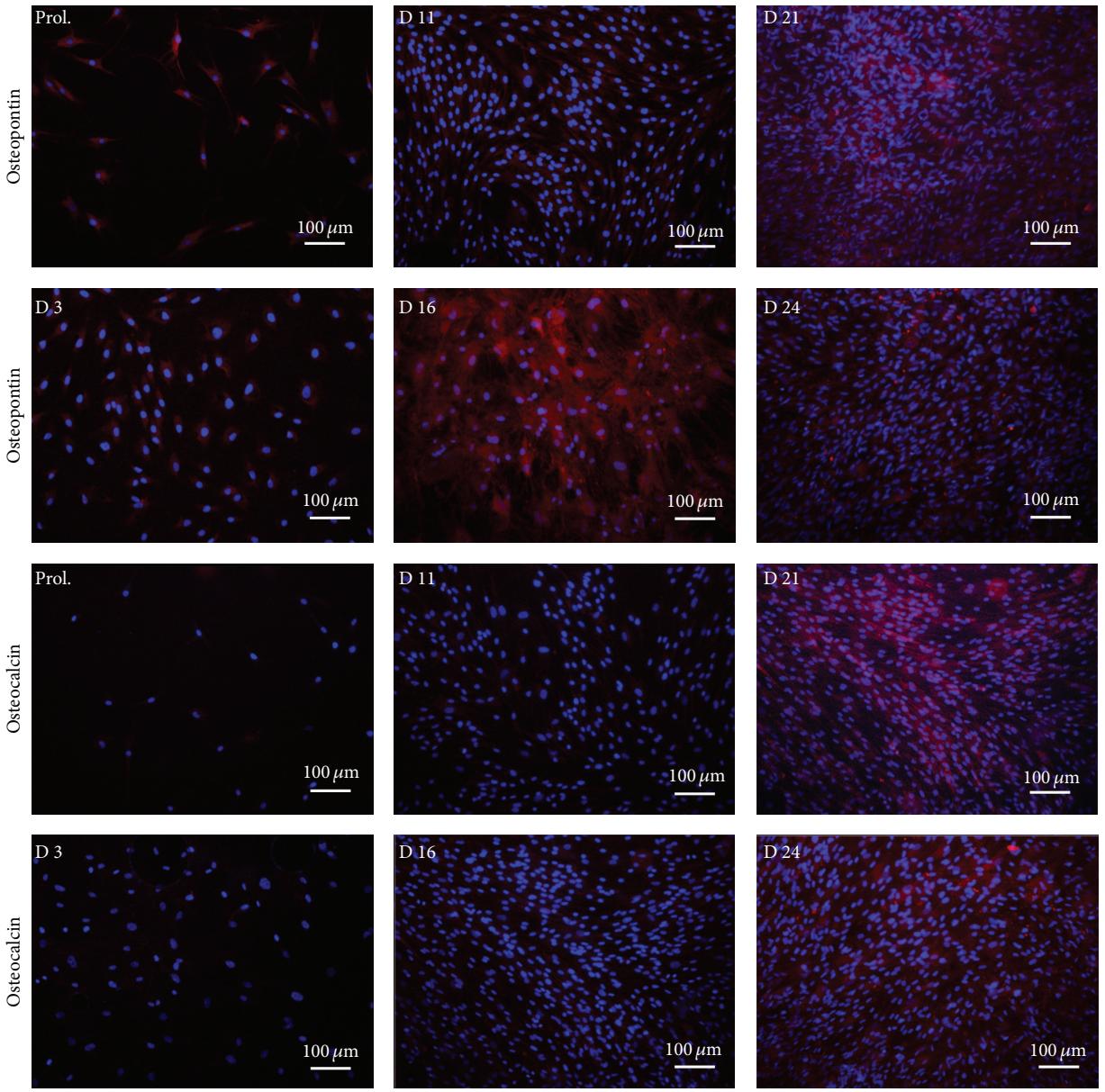

Figure 4: Early and late markers during osteogenic differentiation. Immunocytochemical analysis of OP and OC at specific time points (proliferation, days 3, 11, 16, 21, and 24).

To evaluate a potential relationship between ATF5 and typical early/late bone mineralization markers, we performed an immunocytochemical analysis with osteopontin (OP, early osteogenic marker) and osteocalcin (OC, late osteogenic marker).

Consistent with previous studies we observed that hADSCs had a basal OP expression during proliferation and the intensity increased remarkably at day 16 during bone mineralization; at day 21 a significative number of OP and OC positive cells were present (Figure 4).

3.4. Western Blot. In order to evaluate ATF5 levels during the different stages of osteogenic differentiation, we performed a western blot analysis at different time points: proliferation, days 3, 11, 16, 21, and 24. Our results show a low expression of ATF5 at early stages (proliferation, day 3 and day 11) with protein level increase from day 16 to day 21 and markedly reduced quantity during the later stage of osteogenic differentiation (day 24) (Figure 5). These data are in line with those obtained by cytochemical analysis.

4. Discussion

Osteogenesis is a complex process comprising various stages, including proliferation, condensation, differentiation, and activation of bone cells, which lead to the matrix maturation and successive mineralization. A great variety of molecules and pathways are required to induce the osteogenic process,

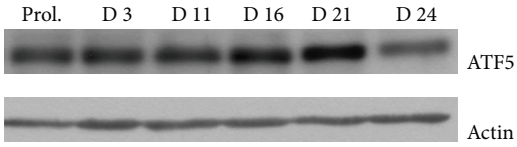

Figure 5: Western blot analysis, using human anti-ATF5 antibody, in hADSCs at specific time points (proliferation, days 3, 11, 16, 21, and 24).

including molecules belonging to the wingless-int (WNT), the bone morphogenetic protein (BMP), the hedgehog (HH), and the fibroblast growth factor (FGF) families [31–33].

During the last decades, the advancements in the use of MSCs in regenerative therapy have driven increasing attention on the molecular networks involved in bone formation process. Among these, Leong et al. [26, 27] reported that ATF5 expression decreased at day 28 of hADSCs osteogenic differentiation. In addition, they showed that knockdown of ATF5 with siRNA presented an increased sensitivity to osteogenic induction.

Our study provides the first description of temporal change of ATF5 isoforms expression during osteogenic differentiation. In particular, we observed that ATF5_1 and ATF5_2 reached a peak of expression at the stage of bone mineralization and subsequently decreased in the final stage (day 24), reaching almost the proliferation levels.

Although we do not have a mechanistic explanation for these findings, the present study could represent a first step elucidating the relationship between ATF5 and typical osteogenic related genes.

These results indicate that ATF5 could play a potential role in bone mineralization. Therefore, it would be reasonable to believe that it could operate together with the osteogenic differentiation genes previously described in our paper as OC and OP, or RUNX2, distal-less homeobox 5 (Dlx5), and bone sialoprotein (BSP) recently reported by Hagh et al. [34] that showed the same ATF5 trend.

Finally, functional studies are necessary to identify the transcriptional targets of this factor and the mechanisms by which its expression is regulated.

5. Conclusions

In conclusion, we have provided evidence that both ATF5_1 and ATF5_2 mRNA isoforms are potentially involved in the osteogenic induction of hADSCs *in vitro*, as demonstrated by the peaks of expression at the stage of bone mineralization. Furthermore, these preliminary data could suggest that ATF5 works together with specific osteogenic genes for the regulation of bone mineralization, providing new information about the two isoforms' involvement in osteogenic development.

Conflict of Interests

The authors declare that they have no conflict of interests.

Authors' Contribution

Luisa Vicari and Giovanna Calabrese contributed equally to this work.

Acknowledgments

The authors thank Gabriele Anastasi and Giovanni Ferlito for their technical assistance. This work was supported by 00829 PON 2007–2013.

References

[1] B. Mailey, A. Hosseini, J. Baker et al., "Adipose-derived stem cells: methods for isolation and applications for clinical use," *Methods in Molecular Biology*, vol. 1210, pp. 161–181, 2014.

[2] P. C. Baer and H. Geiger, "Adipose-derived mesenchymal stromal/stem cells: tissue localization, characterization, and heterogeneity," *Stem Cells International*, vol. 2012, Article ID 812693, 11 pages, 2012.

[3] G. Bassi, L. Pacelli, R. Carusone, J. Zanoncello, and M. Krampera, "Adipose-derived stromal cells (ASCs)," *Transfusion and Apheresis Science*, vol. 47, no. 2, pp. 193–198, 2012.

[4] B. A. Bunnell, M. Flaat, C. Gagliardi, B. Patel, and C. Ripoll, "Adipose-derived stem cells: isolation, expansion and differentiation," *Methods*, vol. 45, no. 2, pp. 115–120, 2008.

[5] M. Locke, J. Windsor, and P. R. Dunbar, "Human adipose-derived stem cells: isolation, characterization and applications in surgery," *ANZ Journal of Surgery*, vol. 79, no. 4, pp. 235–244, 2009.

[6] S. Kern, H. Eichler, J. Stoeve, H. Klüter, and K. Bieback, "Comparative analysis of mesenchymal stem cells from bone marrow, umbilical cord blood, or adipose tissue," *Stem Cells*, vol. 24, no. 5, pp. 1294–1301, 2006.

[7] B. Puissant, C. Barreau, P. Bourin et al., "Immunomodulatory effect of human adipose tissue-derived adult stem cells: comparison with bone marrow mesenchymal stem cells," *British Journal of Haematology*, vol. 129, no. 1, pp. 118–129, 2005.

[8] J. M. Gimble and F. Guilak, "Differentiation potential of adipose derived adult stem (ADAS) cells," *Current Topics in Developmental Biology*, vol. 58, pp. 137–160, 2003.

[9] P. A. Zuk, M. Zhu, P. Ashjian et al., "Human adipose tissue is a source of multipotent stem cells," *Molecular Biology of the Cell*, vol. 13, no. 12, pp. 4279–4295, 2002.

[10] P. A. Zuk, M. Zhu, H. Mizuno et al., "Multilineage cells from human adipose tissue: implications for cell-based therapies," *Tissue Engineering*, vol. 7, no. 2, pp. 211–228, 2001.

[11] W. Tsuji, J. P. Rubin, and K. G. Marra, "Adipose-derived stem cells: implications in tissue regeneration," *World Journal of Stem Cells*, vol. 6, no. 3, pp. 312–321, 2014.

[12] C. Romagnoli and M. L. Brandi, "Adipose mesenchymal stem cells in the field of bone tissue engineering," *World Journal of Stem Cells*, vol. 6, no. 2, p. 144, 2014.

[13] E. H. Kim and C. Y. Heo, "Current applications of adipose-derived stem cells and their future perspectives," *World Journal of Stem Cells*, vol. 6, no. 1, pp. 65–68, 2014.

[14] M. Konno, A. Hamabe, S. Hasegawa et al., "Adipose-derived mesenchymal stem cells and regenerative medicine," *Development Growth and Differentiation*, vol. 55, no. 3, pp. 309–318, 2013.

[15] J. M. Gimble, A. J. Katz, and B. A. Bunnell, "Adipose-derived stem cells for regenerative medicine," *Circulation Research*, vol. 100, no. 9, pp. 1249–1260, 2007.

[16] S. P. Persengiev and M. R. Green, "The role of ATF/CREB family members in cell growth, survival and apoptosis," *Apoptosis*, vol. 8, no. 3, pp. 225–228, 2003.

[17] Y. Wei, Y. Ge, F. Zhou et al., "Identification and characterization of the promoter of human ATF5 gene," *Journal of Biochemistry*, vol. 148, no. 2, pp. 171–178, 2010.

[18] L. A. Greene, H. Y. Lee, and J. M. Angelastro, "The transcription factor ATF5: role in neurodevelopment and neural tumors," *Journal of Neurochemistry*, vol. 108, no. 1, pp. 11–22, 2009.

[19] J. M. Angelastro, T. N. Ignatova, V. G. Kukekov et al., "Regulated expression of ATF5 is required for the progression of neural progenitor cells to neurons," *The Journal of Neuroscience*, vol. 23, no. 11, pp. 4590–4600, 2003.

[20] J. M. Angelastro, J. L. Mason, T. N. Ignatova et al., "Downregulation of activating transcription factor 5 is required for differentiation of neural progenitor cells into astrocytes," *The Journal of Neuroscience*, vol. 25, no. 15, pp. 3889–3899, 2005.

[21] J. L. Mason, J. M. Angelastro, T. N. Ignatova et al., "ATF5 regulates the proliferation and differentiation of oligodendrocytes," *Molecular and Cellular Neuroscience*, vol. 29, no. 3, pp. 372–380, 2005.

[22] S.-Z. Wang, J. Ou, L. J. Zhu, and M. R. Green, "Transcription factor ATF5 is required for terminal differentiation and survival of olfactory sensory neurons," *Proceedings of the National Academy of Sciences of the United States of America*, vol. 109, no. 45, pp. 18589–18594, 2012.

[23] S. E. Monaco, J. M. Angelastro, M. Szabolcs, and L. A. Greene, "The transcription factor ATF5 is widely expressed in carcinomas, and interference with its function selectively kills neoplastic, but not nontransformed, breast cell lines," *International Journal of Cancer*, vol. 120, no. 9, pp. 1883–1890, 2007.

[24] Z. Sheng, L. Ma, J. E. Sun, L. J. Zhu, and M. R. Green, "An activating transcription factor 5-mediated survival pathway as a target for cancer therapy," *Oncotarget*, vol. 6, pp. 457–460, 2010.

[25] M. Hatano, M. Umemura, N. Kimura et al., "The 5′-untranslated region regulates ATF5 mRNA stability via nonsense-mediated mRNA decay in response to environmental stress," *The FEBS Journal*, vol. 280, no. 18, pp. 4693–4707, 2013.

[26] D. T. Leong, M. C. Abraham, A. Gupta, T.-C. Lim, F. T. Chew, and D. W. Hutmacher, "ATF5, a possible regulator of osteogenic differentiation in human adipose-derived stem cells," *Journal of Cellular Biochemistry*, vol. 113, no. 8, pp. 2744–2753, 2012.

[27] D. T. Leong, M. C. Abraham, F. T. Chew, T. C. Lim, and D. W. Hutmacher, "ATF5, a possible regulator of osteogenic differentiation in adult mesenchymal stem cells," *Journal of Stem Cells Regenerative Medicine*, vol. 2, no. 1, pp. 110–112, 2007.

[28] A. E. Carpenter, T. R. Jones, M. R. Lamprecht et al., "CellProfiler: image analysis software for identifying and quantifying cell phenotypes," *Genome Biology*, vol. 7, no. 10, article R100, 2006.

[29] J. Ye, G. Coulouris, I. Zaretskaya, I. Cutcutache, S. Rozen, and T. Madden, "Primer-BLAST: a tool to design target-specific primers for polymerase chain reaction," *BMC Bioinformatics*, vol. 13, article 134, 2012.

[30] K. D. Pruitt, G. R. Brown, S. M. Hiatt et al., "RefSeq: an update on mammalian reference sequences," *Nucleic Acids Research*, vol. 42, no. 1, pp. D756–D763, 2014.

[31] G. R. Kirkhamand and S. H. Cartmell, "Genes and proteins involved in the regulation of osteogenesis," in *Topics in Tissue Engineering*, vol. 3, R.R.E.C., 2007.

[32] F. Milat and K. W. Ng, "Is Wnt signalling the final common pathway leading to bone formation?" *Molecular and Cellular Endocrinology*, vol. 310, no. 1-2, pp. 52–62, 2009.

[33] M. Zaidi, "Skeletal remodeling in health and disease," *Nature Medicine*, vol. 13, no. 7, pp. 791–801, 2007.

[34] M. F. Hagh, M. Noruzinia, Y. Mortazavi et al., "Different methylation patterns of RUNX2, OSX, DLX5 and BSP in osteoblastic differentiation of mesenchymal stem cells," *Cell Journal*, vol. 17, no. 1, pp. 71–82, 2015.

Hindawi Publishing Corporation
Stem Cells International
Volume 2016, Article ID 9682757, 14 pages
http://dx.doi.org/10.1155/2016/9682757

Review Article

How to Improve the Survival of Transplanted Mesenchymal Stem Cell in Ischemic Heart?

Liangpeng Li,[1] Xiongwen Chen,[2] Wei Eric Wang,[1] and Chunyu Zeng[1]

[1]*Department of Cardiology, Daping Hospital, Third Military Medical University, 10 Changjiangzhilu Road, Chongqing 400042, China*
[2]*Cardiovascular Research Center, Temple University School of Medicine, Philadelphia, PA 14190, USA*

Correspondence should be addressed to Wei Eric Wang; weiericwang@163.com and Chunyu Zeng; chunyuzeng100@163.com

Received 17 April 2015; Accepted 18 June 2015

Academic Editor: Luca Vanella

Mesenchymal stem cell (MSC) is an intensely studied stem cell type applied for cardiac repair. For decades, the preclinical researches on animal model and clinical trials have suggested that MSC transplantation exerts therapeutic effect on ischemic heart disease. However, there remain major limitations to be overcome, one of which is the very low survival rate after transplantation in heart tissue. Various strategies have been tried to improve the MSC survival, and many of them showed promising results. In this review, we analyzed the studies in recent years to summarize the methods, effects, and mechanisms of the new strategies to address this question.

1. Introduction

Ischemic heart disease is the leading cause of death worldwide. Severe ischemic heart disease, especially myocardial infarction (MI) and heart failure, causes a significant loss of functional cardiomyocytes [1]. However, heart is an organ with very limited self-renewal capacity because adult cardiomyocytes can hardly regenerate [2]. Over the past decades, there has been tremendous enthusiasm in an attempt to repair cardiac tissue with stem cell transplantation [3]. Mesenchymal stem cell (MSC), with advantages in immunologic privilege, easy to be acquired, and multilineage potential, has been widely studied both in animal model and in clinical trials [4]. Low survival rate after transplantation is one of the crucial reasons accounting for the hampered cardiac repair effect of MSC. The harsh microenvironment with ischemia, inflammation, oxidative stress, and mechanical stress contributes to the great cell loss. Hence, a number of strategies have been used in attempt to overcome this obstacle. In this review, we summarize the advance of these strategies recently reported.

2. Characterization of MSC

MSCs are generally described as nonhematopoietic subpopulation of cells with multilineage potential to differentiate into various tissues of mesodermal origin [5]. MSCs were first identified and isolated from bone marrow (BM) more than 40 years ago [6]. They can also be isolated from other sources, such as adipose [7], synovial tissue [8], lung [9], umbilical cord blood [10], peripheral blood [11], and olfactory bulbs [12], or even in virtually all postnatal organs and tissues [13]. Among these, the most frequently used MSCs in studies for cardiac repair are BM-derived MSC (BM-MSC) and adipose-derived MSC (ADSC).

MSC has been proven to differentiate into osteoblasts, chondrocytes, and adipocytes [14]. It is also reported that MSC can transdifferentiate into mesodermal derived cell types including cardiomyocyte [15, 16], but the cardiogenic potential of MSCs is still controversial [17, 18].

MSCs are fairly heterogeneous cell population but lacks a specific marker to define MSCs [19]. According to minimum criteria that were proposed by The International Society for Cell Therapy in 2006, MSCs are characterized as (1) adherence to plastic in standard culture conditions; (2) expressing surface molecules CD73, CD90, and CD105, but in the absence of f CD34, CD45, HLA-DR, CD14 or CD11b, CD79a, or CD19; (3) a capacity for differentiation to osteoblasts, adipocytes, and chondroblasts *in vitro* [20]. Besides, MSCs possess species-specific characteristics [21], and the characteristics of MSCs may also vary according to the source of

tissue [22]. For example, ADSCs were superior to BMSC with respect to maintenance of proliferating ability [23].

3. MSC Transplantation for Treating Ischemic Heart Disease

The first study exploring the cardiac regenerative effect of MSC was carried out in 1999 on a rat MI model induced by cryoinjury [24]. The autologous MSC was induced into cardiogenic cells by 5-azacytidine *in vitro* and transplanted into the scar of the injured hearts. The transplantation improved cardiac function, prevented remodeling, and promoted angiogenesis. In the following decades, MSCs were transplanted for treating chronic or acute ischemic heart injury in rodent models and large animals. The underlying mechanisms for the therapeutic effect include directly transdifferentiation into functional cardiomyocyte/endothelial cell, secretion of a broad spectrum of cytokine in a paracrine manner, and stimulating local cardiac stem cell proliferation [25]. It was reported that MSC can differentiate into cardiomyocyte phenotype induced by 5-azacytidine [26], coculture [15], and *in vivo* [16] models. Some observed that MSCs transdifferentiate into cardiomyocyte *in vivo*, but the cardiogenic potential of MSCs remains highly controversial. Fazel et al. injected MSCs from β-galactosidase (β-gal) transgenetic mice into the injured ischemic myocardium. As a result, there was no β-gal positive cardiomyocyte observed 28 days after transplantation in recipient hearts, indicating that the transdifferentiate ability of MSCs is lacking [27]. Noiseux et al. found a very few MSC-derived cardiomyocytes after transplantation, but nearly all of which were demonstrated to result from cell fusion [18]. Thus it seems that paracrine function but rather cardiogenic transdifferentiation predominantly accounts for the therapeutic effect of MSC transplantation [28].

Paracrine function of MSCs results from the MSC secretion of antiapoptotic, proangiopoietic factors (growth factors, cytokines, surface molecules, mRNA, miRNA, and exosomes) [29]. Several growth factors which consisted in conditioned medium, such as VEGF [30], FGF [31], IGF, and HGF [32], also showed cardiac regenerative capability when applied to MI model. Exosomes (or microvesicle) secretion by transplanted MSCs was reported by increasing studies [33]. Exosomes are cholesterol-rich, phospholipid vesicles of 30–100 nm enriched with microRNAs (miRNAs). MSCs-derived miRNAs-bearing exosomes are readily internalized into cardiomyocyte or and endothelial cell, resulting in cardioprotective effect via angiogenetic, antiapoptotic, or anti-inflammatory effect. MSC exosomes transferring miR-22 (can target methyl CpG binding protein 2) [34] and miR-221 (can inhibit p53-upregulated modulator of apoptosis) [35] reduce cardiomyocyte apoptosis. MSC exosomes can also reduce neutrophil and macrophage infiltration after myocardium ischemic/reperfusion injury [36].

Mitochondria transferring between MSCs and neighboring somatic cells via a "tunneling nanotube" (TNT), composed of partial membrane fusion and F-actin, was reported. This process rescued aerobic respiration of cells harboring mitochondria damage [37]. MSC also showed capacity to convey functional mitochondria to connected cardiomyocyte via TNT [38]. In a human MSCs-mouse adult cardiomyocyte coculture system, heterogeneous partial cell fusion by "tunneling nanotube" junction formation has been observed. These partial fused cells exhibited a progenitor cell-like phenotype or were described as "reprogramming/dedifferentiation." The mitochondria conveyed through TNT were necessary for the transient partial fusion-dependent cardiomyocyte reprogramming [38]. Although the *in vivo* evidence of TNT formation and mitochondria transfer between MSC and cardiomyocyte were lacking, these findings suggested an alternative mechanism for MSC mediated beneficial effect.

Despite the underlying mechanism which remains to be clarified, the established cardioprotective effect of MSC therapy has been confirmed by most preclinical studies. In 2001, the first clinical trial of BMSCs transplantation on MI patient was conducted [39]. Thereafter, a large number of phase I/II clinical trials were designed to test the safety, feasibility, and efficiency of MSC therapy [40]. A phase II/III trial with 80 patients enrolled was conducted recently [41]. Overall, the safety and feasibility profiles of MSC therapy have been well established by most of the trials followed from 1 month to 2 years, such as POSEIDON [42], C-CURE [43], TAC-HFT [44], and MSC-HF [45]. The efficacy is also suggested, as observed improvement in 6 min walk (POSEIDON, C-CURE, and TAC-HFT), EF (C-CURE, MSC-HF), Minnesota Living with Heart Failure Questionnaire (MLHFQ) (POSEIDON, TAC-HFT), event-free survival in a 2-year follow-up (C-CURE), and reduced LV chamber (POSEIDON, C-CURE, and MSC-HF), and scar size (POSEIDON). Moreover, POSEIDON proved that allogenic MSC is comparable to autologous MSC without significant alloimmune reactions [42], supporting a favorable feasibility for MSC therapy; in addition to improved EF, a reduction in ventricular arrhythmias and improved pulmonary function were also reported in the trial employing MSC to treat patients with acute MI [46]. However, to confirm the efficacy of MSC therapy, especially the long-term outcome in patient, more rigorously designed, multicenter, long-term follow-up, well-interpreted trials with larger sample size are required. Although most of these trials have demonstrated that MSC therapy in clinical trials appears to be safe and effective [47], there are also reported investigations without observed benefits of MSC application [41]. According to the systematic review reported by Lunde et al., the MSC therapy had moderate beneficial effect on improving cardiac function (LVEF increased by 2.99% on average [48]) and limited effects on long-term effect or global end point [49].

4. Poor MSC Survival and Its Mechanisms

4.1. MSC Survival in Animal Model of MI. Among the factors which hurdle the therapeutic effect of MSC treatment, the poor survival after cell transplantation is a crucial one. Positron emission tomography (PET) tracking of MSC delivered by catheter-based transendocardial injection showed retention of approximately 6% of injected cells in porcine ischemic myocardium at 10 days after injection [50]. Toma

et al. reported that less than 0.44% of MSCs survived by day 4 after engraftment in immunodeficient mouse hearts [16]. Accordingly, approximate 1% of MSCs were detected 24 hours after transplantation in rat heart with experimental MI [51].

4.2. MSC Survival in Ischemic Human Heart. Clinical trials have consistently demonstrated that the retention and survival of stem cells are quite low after transplantation into infarcted heart. In a small group of STEMI patients, intracoronary infusion of BMSCs labeled with 18F-FDG showed minimal retention in the infarct region (1.3% to 2.6%) when imaged by PET at 50–75 minutes after cell injection [52]. Intracoronary infusion of cultured peripheral mononuclear cells labeled with ^{111}Inoxine in patients with recent STEMI resulted in activity of 6.3 ± 2.9% in the heart 24 h after injection, but it declined to 2.1% when measured 2 days later [54].

Considering that the acute MI can cause over one billion cardiomyocyte losses, one cannot realistically expect a clinically meaningful benefit from such a tiny number of residual donor cells [55]. This may account for the modest improvement of cardiac function reported in clinical trials.

4.3. Mechanisms for the Poor Survival of Transplanted MSC. The loss of cells number occurs in several ways: (1) a mechanical leakage of cells immediately after injection was due to the continuous compressive mechanical stress; (2) cell death, including both necrosis and apoptosis, was subsequently worsened by a harsh microenvironment of hypoxia, inflammation, and oxidative stress comprising superoxide anions and hydrogen peroxide [56]; (3) gradual loss is also attributed to the limited self-renewing rate of stem cell in ischemic myocardium, due to the lack of oxygen, inadequate nutrients, and the disrupted extracellular cell matrix (ECM).

5. Strategies to Improve MSC Survival

Several strategies have been explored to augment the longevity of engrafted cells in the hostile ischemic environment. The strategies are (1) more effective ways of delivery; (2) tissue engineering strategies involving scaffolds made of natural or synthetic polymers; (3) preconditioning of MSC before transplantation; (4) genetic manipulation of MSCs; (5) combined administration of MSC with another cell type or medicine.

5.1. Delivery Route. Stem cell can be delivered to myocardium through different ways, including peripheral intravenous infusion, direct surgical injection during open heart surgery, catheter-based intracoronary infusion, retrograde coronary venous infusion, and transendocardial injection [57, 58]. Using γ-emission counting of harvested organs 1 hour after cell delivery, it has been demonstrated that intramyocardial injection had the highest retention rate of delivered BMSCs. Significantly more cells were retained after intramyocardial injection (11 ± 3%) compared with intracoronary (2.6 ± 0.3%) and interstitial retrograde coronary venous infusion (3.2 ± 1%). Intramyocardial injection is the most frequently reported route for MSC therapy in animal studies, but most of the clinical trials applied catheter-based intracoronary infusion.

However, there are still some disadvantages along with needle-injection: (1) a washout of cells through channel leakage and the vascular system; (2) an inhomogeneous distribution of cells [59]. To overcome these obstacles, a cell sheet/patch based delivery method has been developed. Confluent, intact cell layers (usually 2 to 3 layers) with abundant ECM and cell-cell interaction can be acquired by culturing MSCs in thermosensitive dishes or fibrin-coated culture plate (confluent cell sheet detached spontaneously at room temperature within 30 minutes), several weeks after MI. The cell sheet was deposited onto the infarcted myocardium, and the MSC can be engrafted into myocardium and the sheet was absorbed gradually [55]. In rat model of MI, two months after the implantation, the three-layer ADSC sheet showed superior effect of cell retention compared with isolated ASDC delivered by intramyocardial injection [60].

5.2. Biomaterials. Due to the disrupted ECM and compressive mechanical stress, the infarcted myocardium is not an environment conducive to cell survival. Therefore, cardiac tissue engineering emerged as a promising strategy, and three-dimensional polymeric scaffolds for stem cells were developed. Scaffolds temporarily provide the biomechanical support for cells until they are able to produce their own extracellular matrix [61–63]. Scaffolds seeded with MSC showed better performance in cardiac repair than injection of MSC alone [64]. There are mainly two types of scaffold.

5.2.1. Thermosensitive Hydrogel. Hydrogel as a biocompatible material was used to prevent the first wave loss of transplanted MSC due to the myocardium contraction. Hydrogels are in situ formation, biodegradable, and cell adhesive. Once delivered together with MSC, it can self-cross-link to form semigrid scaffold which could ameliorate the cell loss.

There are various types of hydrogels applied in MSC therapy for MI: (1) natural hydrogels, such as fibrin glue [65], collagen [66], alginate [67], and cardiogel [68]; cardiogel is a cardiac fibroblast-derived ECM, which was designed to mimic the natural environment suitable for transplanted MSC [68]; (2) synthetic hydrogel, including silanized hydroxypropyl methylcellulose (Si-HPMC) [69] and poly(lactide-co-epsilon-caprolactone) [64]; (3) combination of different materials in a certain ratio, such as poly(N-isopropylacrylamide) (PNIPAAm) plus single-wall carbon nanotubes (SWCNTs) [70], alginate/chitosan [71], poly(glycerol sebacate) combined with collagen [72], and hydrophobic poly(ε-caprolactone)-2-hydroxylethyl methacrylate (PCL-HEMA) plus PNIPAAm [73]. Hydrogel can also serve as a medium to support the diffusion of molecules [74]. Since interleukin-10 (IL-10) is an anti-inflammation cytokine, a combination of MSC, Matrigel, and IL-10 plasmids was designed to improve cell survival [75].

Hydrogel is effective in improving cell survival in stem cell therapy. In a rat MI model, intramyocardial injection of MSCs with Si-HPMC (one of the synthetic hydrogels) showed

better performance in cell retention and cardiac function preservation than MSCs injection alone [76]. In a swine MI model, retention of MSC suspended in 2% alginate (a natural hydrogel) before transplantation was approximately 4-fold compared to that in control MSCs at two weeks after delivery [77]. Similarly, coinjection with fibrin glue increased ADSC survival by about 30% on a rat MI model [78].

The first clinical trial using injectable bioabsorbable scaffold (IK-5001), a solution of 1% sodium alginate plus 0.3% calcium gluconate, combined with MSCs by intracoronary delivery has been carried out (http://www.clinicaltrials.gov.: NCT01226563). This first-in-man pilot study also showed that intracoronary deployment of an IK-5001 scaffold is feasible, effective, and well tolerated in patients with STEMI [79].

5.2.2. Patch/Cell Sheet. To avoid the shortcomings of needle injection, biocompatible patches seeded with MSC emerged as an alternative strategy to circumvent the lack of cell engraftment. Solid form of biomaterials (such as collagen) seeded with cells was sutured onto the surface of infarcted area. The patch can be absorbed gradually while the stem cells engrafted into the myocardium.

ADSC-cellularized sheets were implanted onto the epicardium of on chronic rat MI model [80]. No cell was detected in ADSC alone group, but cell sheet exhibited $25.3 \pm 7.0\%$ and $6.4 \pm 4\%$ engraftment rate at 1 week and 1 month after MI [60, 80]. The same group performed a head-to-head comparison of cell engraftment between the conventional injection, deposition of the bilayer myoblast cell sheet, and deposition of the myoblast cells seeded in collagen sponge in rat MI model. Both cell constructs are superior to conventional needle injection. The myoblast-seeded collagen sponge group produced the best outcome with regard to engraftment cells number and reduced fibrosis [55].

5.3. Hypoxic, Hyperoxic, and Pharmacological Preconditioning of MSCs. Although severe hypoxia can lead to cell death, repeated episodes of short period exposure to hypoxia (hypoxia-preconditioning) have shown conferring cytoprotective benefits [81]. Usually, MSCs were cultured under hypoxia (0.5% oxygen) or normoxic conditions for 24 hours: hypoxia-preconditioning reduced about 25% of cell death at day 1 and 40% of cell death at day 3 after delivery compared with normoxic control [82]. This effect is associated with the increased expression of prosurvival and proangiogenic factors including hypoxia-inducible factor 1 (HIF-1α), angiopoietin-1, vascular endothelial growth factor (VEGF), erythropoietin, Bcl-2, and Bcl-xL [82]. Moreover, hypoxia-preconditioning induced autophagy protected MSC from apoptosis, which may be also accounted for the improvement of MSC survival [83].

On the other hand, preconditioning with hyperoxia (100% oxygen) or/and Z-VAD-FMK pan-caspase inhibitor promoted MSCs viability and proliferation, by decreasing caspases 1, 3, 6, 7, and 9 expression and increasing survival genes such as Akt [84].

Sevoflurane, an inhaled anesthetic widely used in clinical anesthesia, has similar effect of hypoxia-preconditioning. Sevoflurane pretreatment minimized MSC apoptosis and the loss of its mitochondrial membrane potential induced by hypoxia, which may be mediated by HIF and Akt pathways [84].

Study also revealed that MSCs for transplantation could be preconditioned by coculturing with cells. MSC preconditioned with cardiomyocytes in culture exerted enhanced therapeutic effect compared with MSC alone [85]. The hetero-cell-to-cell connection altered the MSC paracrine of cardioprotective soluble factors such as VEGF, HGF, SDF-1α, and MCP-3.

Preconditioning of MSCs with TGF-α enhanced the VEGF secretion of transplanted MSC *in vivo*, thereby enhancing MSCs' ability to protect myocardium from IR injury [86]. Platelet-derived growth factor-BB (PDGF) treatment of MSCs resulted in rapid activation of both Akt and ERK and upregulated VEGF. Thus, MSCs with PDGF preconditioning exhibited a greater capacity of functional recovery compared with naïve MSCs in I/R injured heart [87].

Preconditioning can be operated *in vitro* prior to transplantation, which circumvents the side effect caused by other approaches such as genetic manipulation. Since the forced gene manipulation in stem cells raises concern about the safety in long-term effect, the continuous overexpression of gene in MSCs may be harmful if the microenvironment switches to different stage [88].

5.4. Genetic Modification of MSCs. Genes related to cardiac protection from I/R injuries such as Akt and Integrin-linked kinase [89] and genes involved in apoptosis such as Bcl-2 [90] promoted stem cell survival in ischemic myocardium.

Akt has been well documented among genetic approaches. In both rat and porcine model of MI, transplantation of Akt-engineered MSCs led to improved LVEF and reduced scar size and fibrosis; this is because not only were Akt-engineered MSCs more resistant to apoptosis [18, 91], Akt modification also enhanced MSC secretion of paracrine factors such as VEGF, IGF-1, and FGF-2 [92]. A double overexpression system in MSCs comprising Akt and angiopoietin-1 (an important modulator in angiogenesis) further improved cell survival [93]. Overexpression of heat shock protein 20 (Hsp-20) [94], secreted frizzled related protein 2 (sFRP2), a modulator of the Wnt signaling [95], survivin [96], heme oxygenase (HO-1) [97], GSK-3β [98], ERBB4 [99], CCR-1 [100], and serum derived factor-1 (SDF-1) [101] in MSC had similar beneficial effect on cell survival.

We have demonstrated previously that silencing of prolyl hydroxylase domain protein 2 (PHD2) enhanced ADSC survival after transplantation into murine ischemic myocardium, by maintenance of active HIF-1α [102]. PHD2 silencing can also enhance ADSC paracrine antiapoptotic effect on cardiomyocytes against ischemia via NF-κB signaling. Similarly, GATA-4 overexpression in MSCs increased both MSC survival and angiogenic potential in ischemic myocardium [103].

In addition to coding gene, microRNA (miR) has been explored for stem cell therapy with its multitargets property. Overexpression of miR-1 in MSCs promoted their survival 2-3-fold at 7 days after transplantation, leading to more

conducive repair of infarct injury and improved heart function. miR-1 promoted MSC survival via regulating caspase 9, Bcl-2, and Bax [104]. miR-210 engineering has similar effect in MSCs through antioxidative c-Met pathway [105].

5.5. Cotransplantation of MSCs with Other Cells. CS/PCs, such as c-kit positive residential progenitor cells in heart [106], emerged as another potential cell source for cardiac repair [106]. Clinical trial of CS/PCs reported encouraging results in preserving cardiac function for patients with ischemic cardiomyopathy [107]. Based on the observation that MSC can stimulate endogenous CS/PCs proliferation [25] and regulate CS/PCs niches [108], studies have been performed to explore the effect of using MSCs together with CS/PCs [109, 110]. In a porcine model of MI, a combination of human CS/PCs and MSCs labeled with iron oxide for CMR imaging was delivered into myocardium 14 days after MI. CMR revealed that this combination was 7-fold greater cell engraftment than either cell type alone, thereby further reduced scar size, and improved cardiac function [110].

Inflammatory status in acute stage is another important factor causing the low retention of transplanted MSCs. Previous studies have shown that $CD4^+CD25^{hi}FoxP3^+$ T regulatory (Treg) cells have a potential to suppress inflammation, thus providing a favorable environment for MSC engraftment [53, 111]. The cotransplantation of autologous Treg cells with MSC dramatically increased the MSC survival rate and proliferation in a porcine MI model with no deleterious side effects observed [112].

5.6. Administration of MSCs with Medication. Statins have some cardioprotective function independent of their lipid-lowering ability. They can protect endothelial function, increase nitric oxide bioavailability, and exert antioxidant/anti-inflammatory effects [113–117]. Combination of Simvastatin (0.25 mg/kg/d) and MSC transplantation (3×10^7 cells per animal) showed approximately 4-fold higher MSC survival rate compared with MSC alone. This was due to the fact that oxidative stress and inflammatory response were significantly reduced in the infarcted regions by Simvastatin [118]. Other groups reported that Rosuvastatin improved survival of ADSCs after transplantation into infarcted hearts. Improved cardiac function and reduced fibrosis were observed in Rosuvastatin plus ADSC group. Bioluminescence imaging and histological staining *in vivo* revealed that Rosuvastatin (20 mg/kg per day for 28 days) enhanced the survival of engrafted ADSC approximately 1.3-fold compared to MSC alone. This was associated with the idea that Rosuvastatin increased Akt, ERK phosphorylation, promoted the subsequent FoxO3a phosphorylation and nuclear export, and decreased the proapoptotic proteins in ADSCs [119].

5.7. Another Optimization for MSC Therapy

5.7.1. Time Point. Li and colleagues compared the time points for optimizing MSC efficacy. Among 1 h, 1 week, and 2 weeks delivery after acute MI, time point of 1 week exhibited the most abundant MSC survival. Delivery at a later time point may lead to impeded cell retention, whereas cell administration too early may lead to poor engraftment due to the intensive inflammatory response in the acute stage [120]. According to an analysis of 7 randomized controlled trials with 660 patients with MI undergoing emergent percutaneous coronary intervention and receiving intracoronary BMSC transplantation, the effect of BMSC delivery at 4 to 7 days was superior to that within 24 hours [121].

5.7.2. Intactness. Adhesion is important for cell survival. Disruption of cell-ECM contact by trypsinization prior to cell transplantation may impair cell viability and facilitate apoptosis. Recently, improving MSC survival after transplantation with effective adhesion attracts much attention. MSCs were expanded on microcarrier beads in spin culture and directly transplanted, which avoided trypsinization and detachment of cell-ECM interaction, showing significantly less apoptosis than trypsinized control cells [122].

5.7.3. Extracorporeal Shock Wave. Genetically overexpression of SDF-1 in MSC can improve cell retention in ischemic myocardium [123]. Extracorporeal shock wave, similar to that used to treat nephrolithiasis, has been experimentally demonstrated to increase homing factor such as SDF-1 in target tissue [124]. Whether shock wave treatment can increase MSC retention requires further investigation. However, the phase I/II, double-blind, randomized, placebo-controlled trial CELLWAVE (NCT NCT00326989) conducted among patients reported that patients with chronic heart failure receiving shock wave treatment prior to intracoronary BM-MNC infusion had a modest but significant improvement in LVEF compared to shock wave/placebo infusion [125]. Although the cell retention has not been evaluated in this trial, extracorporeal shock wave remains a strategy of interest in future.

6. Discussion

The poor viability of transplanted MSCs hampers their therapeutic efficacy for cardiac repair. A number of strategies have been conducted to augment the longevity of engraft cell in the hostile environment. We summarized the efficacy of promoting MSC survival with different strategies (Table 1, Figure 1). Myocardium injection has superior cell retention compared with other traditional routes such as catheter-based intracoronary infusion. MSCs seeded biocompatible materials scaffold delivered by injection or suturing to the epicardium hold promising potential. Biomaterials such as hydrogel can prevent the first wave loss of transplanted MSC due to the myocardium contraction. Preconditioning and genetic modification of MSCs can enhance the resistance of MSCs against hypoxia, oxidation, and inflammation. MSC transplantation together with CS/PC or Treg cells showed enhanced cell engraftment. Statin improves MSC survival after transplantation based on its multipotent function. A limitation of this review is that the efficacies of approaches improving cell retention are difficult to be compared with each other. This is

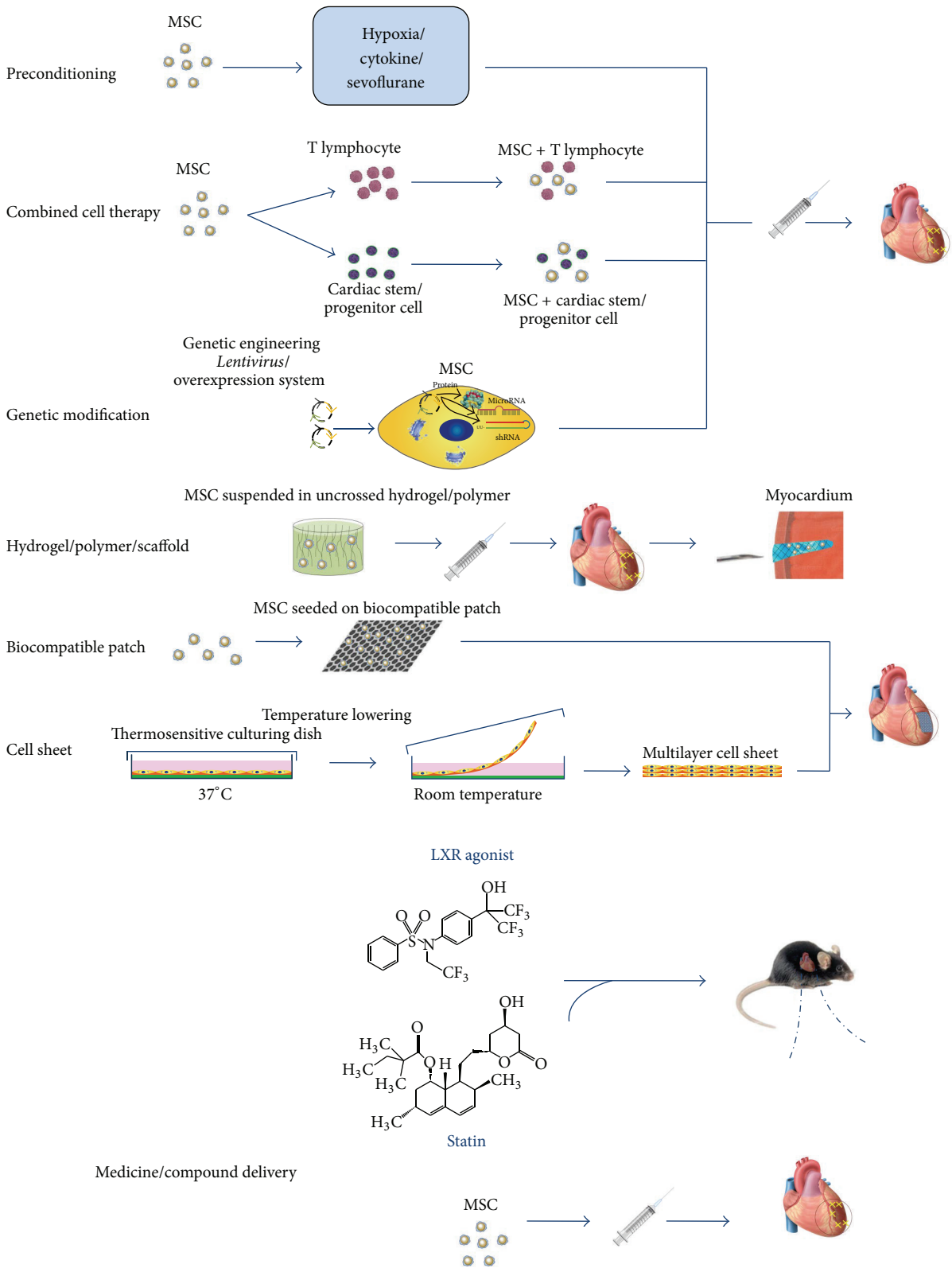

Figure 1: Schematic cartoon to illustrate the strategies to improve survival of MSC in ischemic myocardium. MSC can be either pretreated by hypoxia/cytokine or genetically modified before delivery to myocardium. Hydrogel/polymer with suspended MSC forms a semigrid scaffold when injected into the myocardium, which improves cell retention. MSC can be also seeded on biocompatible patch or form cell layer by culturing in thermosensitive dish; both of them can be deposited or sutured onto the epicardium of the infarcted area. Combined with another cell type (CSC, Treg cell) or medicine/compound (statin), they improve the survival of MSC.

Table 1: Strategies to improve MSC survival in ischemic myocardium.

Treatment	Species	Cell amount	Labeling and measurement	Survival						Unit	Fold changes (approximately)			References
Genetic modification														
Bcl-2 overexpression	Rat	6×10^6	BrdU labeling and immunofluorescence	4 days		3 weeks		6 weeks		Brdu positive per 1000 nuclei	4 days	3 weeks	6 weeks	[90]
				Bcl-2 MSC 325	Vector-MSC 100	Bcl-2 MSC 180	Vector-MSC 57	Bcl-2 MSC 110	Vector-MSC 50		2.2 fold	1.9 fold	1.2 fold	
GATA4 overexpression	Rat	1.5×10^6	SRY gene quantification	4 days						Cells per mg tissue		2.8 fold		[102]
				GATA4-MSC 4				Vector-MSC 1.4						
HSP20 overexpression	Rat	1×10^6	SRY gene quantification	4 days						Fold		2 fold		[94]
				Hsp20-MSC 2				GFP-MSC 1						
Akt overexpression	Mouse	5×10^5	GFP overexpression and immunofluorescence	3 days		7 days		14 days		GFP+ cells	3 days	7 days	14 days	[18]
				Akt-MSC 510	GFP-MSC 220	Akt-MSC 100	GFP-MSC 18	Akt-MSC 7	GFP-MSC 1		>2 fold	>6 fold	>5 fold	
Survivin overexpression	Rat	2×10^6	PCR for GFP	7 days				24 days		Ratio of GFP/GAPDH	7 days		28 days	[96]
				Survivin-MSC 0.62	GFP-MSC 0.25			Survivin-MSC 0.56	GFP-MSC 0.1		2.5 fold		4.3 fold	
HO-1 overexpression	Mouse	1×10^6	SRY gene quantification	4 hours		24 hours		1 week		Implanted cells	4 hours	24 hours	1 week	[97]
				HO-1-MSC 70%	LacZ-MSC 20%	HO-1-MSC 20%	LacZ-MSC 8%	HO-1-MSC 15%	LacZ-MSC 2%		3.5 fold	1.5 fold	7.5 fold	
GSK-3β	Mouse	1.5×10^5	GFP overexpression and immunofluorescence	12 weeks						GFP^{pos} cells/mm^2		—		[98]
				GSK-3β-GFP-MSC 25.8				GFP-MSC 0%						
ERBB4 overexpression	Mouse	3×10^5	GFP overexpression and immunofluorescence	4 weeks						GFP^{pos} cells/mm^2		5.6 fold		[99]
				ERBB4-GFP-MSC 28				GFP-MSC 5						
CCR1 overexpression	Mouse	3×10^5	GFP overexpression and immunofluorescence	72 hours						Cells/mm^2		2.5 fold		[100]
				CCR1-GFP-MSC 100				GFP-MSC 42						
mir-1 overexpression	Mouse	5×10^6	SRY gene quantification	1 week						Cells/mg tissue		2.26 fold		[103]
				mir-1-MSC 3.4×10^3				MSC 1.5×10^3						
PHD2 silencing	Mouse	1×10^5	GFP overexpression and immunofluorescence	4 weeks						% of cell delivered		5.4 fold		[102]
				shPHD2-MSC 0.65 ± 0.09%				MSC 0.12 ± 0.04%						
SDF-1 overexpression	Rat	5×10^5	DAPI labeling	1 week						Cells/mm^2		4 fold		[101]
				SDF-1-MSC 200				EGFP-MSC 55						
sFrp2 overexpression	Mouse	2.5×10^5	GFP counting	30 days						Cells		4 fold		[94]
				sFrp2-MSC 8				GFP-MSC 2						
Hydrogel/polymer/scaffold														
PNIPAAm + SWCNTs + BMSC	Rat	2×10^6	Dil labeling	1 week						Cell numbers/filed		1.5 fold		[70]
				PNIPAAm + SWCNTs + BMSC 33				PBS + BMSC 21						

Table 1: Continued.

Treatment	Species	Cell amount	Labeling and measurement	Survival				Unit	Fold changes (approximately)		References
Fibrin glue + ADSC	Rat	5×10^6	DAPI labeling	24 hours Fibrin + ADSC 19.10 ± 3.13%		ADSC 14.16 ± 2.73%		% of cell delivered	1.4 fold		[78]
				4 weeks (grafted size) Fibrin + ADSC 11.52 ± 2.34%		ADSC 5.85 ± 1.35		Grafted size	1.96 fold		
Alginate + MSC	Swine	2×10^6	Dil labeling	2 weeks Alginate + MSC 12		MSC 3		Area of engraftment%	4 fold		[77]
Fibrin glue + skeletal myoblast	Rat	5×10^6	Dil labeling	5 weeks Fibrin glue + skeletal myoblast 9.7 ± 4.2%		BSA + skeletal myoblast 4.3 ± 1.5%		% of the infarcted area	2.2 fold		[65]
a-Cyclodextrin/(MPEG-PCL-MPEG)	Rabbit	2×10^7	DAPI labeling	4 weeks a-Cyclodextrin/(MPEG-PCL-MPEG) + MSC 2150 ± 235		MSC 845 ± 156		Cells/mm^2	2.5 fold		[127]
Dex-PCL-HEMA/PNIPAAm + BMMNC	Rabbit	1×10^7	DAPI labeling	48 hours Dex-PCL-HEMA/PNIPAAm + BMMNC 21		BMMNC 12		% of cell delivered	1.75 fold		[73]
Patch/cellsSheet											
Collagen scaffold loaded with IL-10 plasmid	Rat	—	Dil labeling	4 weeks Scaffold + IL-10 plasmid + MSC 13	Scaffold + MSC 2.5	Scaffold alone 0		Cells/mm^2	>5 fold		[75]
Collagen patch seeded with ADSC	Rat	3.5×10^5	GFP counting	1 week (engraftment) Collagen patch seeded with ADSC 25.3 ± 7.0%		ADSC alone 0		% of cell delivered	—		[80]
				1 month (engraftment) Collagen patch seeded with ADSC 6.4 ± 4%		ADSC alone 0		% of cell delivered	—		
MSC cell sheet	Rat	4×10^6	SRY gene quantification	3 days MSC cell sheet 56.0 ± 7.2%	MSC injection 5.0 ± 1.0%	28 days MSC cell sheet 9.1 ± 1.9%	MSC injection 0.5 ± 0.2%	Implanted cells	3 days >11 fold	28 days >18 fold	[128]
Triple-layer autologous ADSC sheet	Rat	1×10^7	GFP counting	2 months Triple-layer autologous ADSC sheet 2-3 (moderate or large number of cells)		ADSC 0-1 (no or minimal amount of cells)		Scoring	—		[60]
Collagen sponge seeded with myoblast	Rat	5×10^7	Human gene PCR	4 weeks (engraftment) Collagen sponge seeded with myoblast 6.2 [0.00, 17.40]	Myoblast cell sheet 0 [0.00, 88.00]	Myoblast injection 0 [0.00, 2.60]		DNA ng/μL (mean [min, max])	—		[55]
Combined therapy											
MSC + CS/PC coimplantation	Rat	$2 \times 10^8/1 \times 10^6$	Alu immunofluorescence	4 weeks MSC + CS/PC 7.5	MSC alone 2	CPC alone 0		Cells/cm^3	7 fold		[110]

Table 1: Continued.

Treatment	Species	Cell amount	Labeling and measurement	Survival				Unit	Fold changes (approximately)		References
Rosuvastatin + MSC	Mouse	1×10^6	GFP overexpression and bioluminescence imaging	2 weeks				Photons/s/cm^2/sr	1.75		[119]
				Rosuvastatin + MSC		MSC alone					
				$0.71 \pm 0.02 \times 10^5$		$0.40 \pm 0.05 \times 10^5$					
Atorvastatin + MSC	Rat	5×10^6	SRY gene quantification	4 weeks				Cells/per high power field	4 fold		[129]
				Atorvastatin + MSC		MSC alone					
				22.0 ± 1.7		5.7 ± 1.2					
Simvastatin (SIMV) + MSC	Swine	3×10^7	DAPI labeling	6 weeks				Cells/per 5 sections	4~5 fold		[113]
				SIMV + MSC		MSC					
				310.6 ± 83.8		70.5 ± 22.3					
LXR agonist T0901317	Mouse	1×10^6	GFP overexpression and bioluminescence imaging	4 weeks				Photons/s/cm^2/sr	5.4 fold		[130]
				T0901317 + ADSC		ADSC alone					
				$0.27 \pm 0.05 \times 10^5$		$0.05 \pm 0.03 \times 10^5$					
IP6Ks inhibitor TNP	Mouse	1×10^6	GFP overexpression and immunofluorescence	2 weeks				Cells/mm2	2.5 fold		[131]
				TNP + MSC		MSC alone					
				366 ± 34.2		114 ± 17.8					
Ghrelin pretreatment	Mouse	7×10^5	GFP overexpression and bioluminescence imaging	3 weeks				Photons/s/cm^2/sr	1.75 fold		[132]
				ADSC pretreated with grhelin		ADSC					
				$0.7 \pm 0.02 \times 10^5$		$0.4 \pm 0.03 \times 10^5$					
Ad-HIF-α + MSC	Mouse	1×10^6	SRY gene quantification/bioluminescence imaging	3 weeks				Cell survival rate	2.14 fold		[133]
				Ad-HIF-α combined with MSC		MSC alone					
				1.50%		0.70%					
HGF/VEGF + MSC	Mouse	0.5×10^6	Bioluminescence imaging	3 days		4 days		Fold changes	3 days	4 days	[134]
				HGF + MSC	MSC alone	VEGF + MSC	MSC alone		HGF	VEGF	
				1.67 ± 0.43	1	1.44 ± 0.55	1		1.67 ± 0.43	1.44 ± 0.55	

partially due to the measurements of cell retention in different studies.

As paracrine effects are nowadays considered as predominant therapeutic effect of MSCs [126], there is an attempt to apply functional fraction of conditioned medium (or its components such as exosome) of cultured MSCs instead of direct cell delivery to treat heart disease [33–35]. However, some effects, including mitochondria transfer effect between MSC and cardiomyocytes [38], cannot be mimicked by paracrine factors alone. Further, the strategies acquired from MSC studies to promote cell survival have broader significance. Some stem cell types such as embryonic stem cell and inducible pluripotent stem cell (iPSC) have indisputable capacity to generate new cardiomyocytes, which are conducted in preclinical studies. The optimized methods for MSC transplantation can be tested in iPSC-derived cell treatment in ischemic myocardium, leading to greater efficacy for cardiac regeneration [127–134].

Conflict of Interests

The authors declare that there is no conflict of interests regarding the publication of this paper.

References

[1] S. J. Jansen Of Lorkeers, J. E. C. Eding, H. M. Vesterinen et al., "Similar effect of autologous and allogeneic cell therapy for ischemic heart disease: systematic review and meta-analysis of large animal studies," *Circulation Research*, vol. 116, no. 1, pp. 80–86, 2015.

[2] N. Kawaguchi and T. Nakanishi, "Cardiomyocyte regeneration," *Cells*, vol. 2, no. 1, pp. 67–82, 2013.

[3] M. R. Rosen, R. J. Myerburg, D. P. Francis, G. D. Cole, and E. Marbán, "Translating stem cell research to cardiac disease therapies: pitfalls and prospects for improvement," *Journal of the American College of Cardiology*, vol. 64, no. 9, pp. 922–937, 2014.

[4] I.-K. Ko and B.-S. Kim, "Mesenchymal stem cells for treatment of myocardial infarction," *International Journal of Stem Cells*, vol. 1, no. 1, pp. 49–54, 2008.

[5] A. Farini, C. Sitzia, S. Erratico, M. Meregalli, and Y. Torrente, "Clinical applications of mesenchymal stem cells in chronic diseases," *Stem Cells International*, vol. 2014, Article ID 306573, 11 pages, 2014.

[6] A. J. Friedenstein, R. K. Chailakhjan, and K. S. Lalykina, "The development of fibroblast colonies in monolayer cultures of guinea-pig bone marrow and spleen cells," *Cell and Tissue Kinetics*, vol. 3, no. 4, pp. 393–403, 1970.

[7] P. A. Zuk, M. Zhu, H. Mizuno et al., "Multilineage cells from human adipose tissue: implications for cell-based therapies," *Tissue Engineering*, vol. 7, no. 2, pp. 211–228, 2001.

[8] C. De Bari, F. Dell'Accio, P. Tylzanowski, and F. P. Luyten, "Multipotent mesenchymal stem cells from adult human synovial membrane," *Arthritis and Rheumatism*, vol. 44, no. 8, pp. 1928–1942, 2001.

[9] F. Sabatini, L. Petecchia, M. Tavian, V. J. de Villeroché, G. A. Rossi, and D. Brouty-Boyé, "Human bronchial fibroblasts exhibit a mesenchymal stem cell phenotype and multilineage differentiating potentialities," *Laboratory Investigation*, vol. 85, no. 8, pp. 962–971, 2005.

[10] H. R. Jang, J. H. Park, G. Y. Kwon et al., "Effect of preemptive treatment with human umbilical cord blood-derived mesenchymal stem cells on the development of renal ischemia-reperfusion injury in mice," *American Journal of Physiology. Renal Physiology*, vol. 307, no. 10, pp. F1149–F1161, 2014.

[11] N. J. Zvaifler, L. Marinova-Mutafchieva, G. Adams et al., "Mesenchymal precursor cells in the blood of normal individuals," *Arthritis Research*, vol. 2, no. 6, pp. 477–488, 2000.

[12] Y.-S. Huang, I.-H. Li, S.-H. Chueh et al., "Mesenchymal stem cells from rat olfactory bulbs can differentiate into cells with cardiomyocyte characteristics," *Journal of Tissue Engineering and Regenerative Medicine*, 2013.

[13] L. da Silva Meirelles, P. C. Chagastelles, and N. B. Nardi, "Mesenchymal stem cells reside in virtually all post-natal organs and tissues," *Journal of Cell Science*, vol. 119, no. 11, pp. 2204–2213, 2006.

[14] A. H. Piersma, K. G. M. Brockbank, R. E. Ploemacher, E. van Vliet, K. M. Brakel-van Peer, and P. J. Visser, "Characterization of fibroblastic stromal cells from murine bone marrow," *Experimental Hematology*, vol. 13, no. 4, pp. 237–243, 1985.

[15] E. Y. Plotnikov, T. G. Khryapenkova, A. K. Vasileva et al., "Cell-to-cell cross-talk between mesenchymal stem cells and cardiomyocytes in co-culture," *Journal of Cellular and Molecular Medicine*, vol. 12, no. 5, pp. 1622–1631, 2008.

[16] C. Toma, M. F. Pittenger, K. S. Cahill, B. J. Byrne, and P. D. Kessler, "Human mesenchymal stem cells differentiate to a cardiomyocyte phenotype in the adult murine heart," *Circulation*, vol. 105, no. 1, pp. 93–98, 2002.

[17] S. Fazel, L. Chen, R. D. Weisel et al., "Cell transplantation preserves cardiac function after infarction by infarct stabilization: augmentation by stem cell factor," *The Journal of Thoracic and Cardiovascular Surgery*, vol. 130, no. 5, pp. 1310.e1–1310.e10, 2005.

[18] N. Noiseux, M. Gnecchi, M. Lopez-Ilasaca et al., "Mesenchymal stem cells overexpressing Akt dramatically repair infarcted myocardium and improve cardiac function despite infrequent cellular fusion or differentiation," *Molecular Therapy*, vol. 14, no. 6, pp. 840–850, 2006.

[19] A. Keating, "Mesenchymal stromal cells: new directions," *Cell Stem Cell*, vol. 10, no. 6, pp. 709–716, 2012.

[20] M. Dominici, K. Le Blanc, I. Mueller et al., "Minimal criteria for defining multipotent mesenchymal stromal cells. The International Society for Cellular Therapy position statement," *Cytotherapy*, vol. 8, no. 4, pp. 315–317, 2006.

[21] C. Nombela-Arrieta, J. Ritz, and L. E. Silberstein, "The elusive nature and function of mesenchymal stem cells," *Nature Reviews: Molecular Cell Biology*, vol. 12, no. 2, pp. 126–131, 2011.

[22] R. A. Panepucci, J. L. C. Siufi, W. A. Silva Jr. et al., "Comparison of gene expression of umbilical cord vein and bone marrow-derived mesenchymal stem cells," *Stem Cells*, vol. 22, no. 7, pp. 1263–1278, 2004.

[23] R. H. Lee, B. Kim, I. Choi et al., "Characterization and expression analysis of mesenchymal stem cells from human bone marrow and adipose tissue," *Cellular Physiology and Biochemistry*, vol. 14, no. 4–6, pp. 311–324, 2004.

[24] S. Tomita, R.-K. Li, R. D. Weisel et al., "Autologous transplantation of bone marrow cells improves damaged heart function," *Circulation*, vol. 100, no. 19, pp. II247–II256, 1999.

[25] K. E. Hatzistergos, H. Quevedo, B. N. Oskouei et al., "Bone marrow mesenchymal stem cells stimulate cardiac stem cell

proliferation and differentiation," *Circulation Research*, vol. 107, no. 7, pp. 913–922, 2010.

[26] S. Wakitani, T. Saito, and A. I. Caplan, "Myogenic cells derived from rat bone marrow mesenchymal stem cells exposed to 5-azacytidine," *Muscle & Nerve*, vol. 18, no. 12, pp. 1417–1426, 1995.

[27] S. Fazel, L. Chen, R. D. Weisel et al., "Cell transplantation preserves cardiac function after infarction by infarct stabilization: augmentation by stem cell factor," *Journal of Thoracic and Cardiovascular Surgery*, vol. 130, no. 5, pp. 1310.e1–1310.e10, 2005.

[28] H. Reinecke, E. Minami, W.-Z. Zhu, and M. A. Laflamme, "Cardiogenic differentiation and transdifferentiation of progenitor cells," *Circulation Research*, vol. 103, no. 10, pp. 1058–1071, 2008.

[29] M. Z. Ratajczak, M. Kucia, T. Jadczyk et al., "Pivotal role of paracrine effects in stem cell therapies in regenerative medicine: can we translate stem cell-secreted paracrine factors and microvesicles into better therapeutic strategies," *Leukemia*, vol. 26, no. 6, pp. 1166–1173, 2012.

[30] R. C. Scott, J. M. Rosano, Z. Ivanov et al., "Targeting VEGF-encapsulated immunoliposomes to MI heart improves vascularity and cardiac function," *The FASEB Journal*, vol. 23, no. 10, pp. 3361–3367, 2009.

[31] J. A. I. Virag, M. L. Rolle, J. Reece, S. Hardouin, E. O. Feigl, and C. E. Murry, "Fibroblast growth factor-2 regulates myocardial infarct repair: effects on cell proliferation, scar contraction, and ventricular function," *The American Journal of Pathology*, vol. 171, no. 5, pp. 1431–1440, 2007.

[32] E. Ruvinov, J. Leor, and S. Cohen, "The promotion of myocardial repair by the sequential delivery of IGF-1 and HGF from an injectable alginate biomaterial in a model of acute myocardial infarction," *Biomaterials*, vol. 32, no. 2, pp. 565–578, 2011.

[33] L. Huang, W. Ma, Y. Ma, D. Feng, H. Chen, and B. Cai, "Exosomes in mesenchymal stem cells, a new therapeutic strategy for cardiovascular diseases?" *International Journal of Biological Sciences*, vol. 11, no. 2, pp. 238–245, 2015.

[34] Y. Feng, W. Huang, M. Wani, X. Yu, and M. Ashraf, "Ischemic preconditioning potentiates the protective effect of stem cells through secretion of exosomes by targeting Mecp2 via miR-22," *PLoS ONE*, vol. 9, no. 2, Article ID e88685, 2014.

[35] B. Yu, M. Gong, Y. Wang et al., "Cardiomyocyte protection by gata-4 gene engineered mesenchymal stem cells is partially mediated by translocation of mir-221 in microvesicles," *PLoS ONE*, vol. 8, no. 8, Article ID e73304, 2013.

[36] F. Arslan, R. C. Lai, M. B. Smeets et al., "Mesenchymal stem cell-derived exosomes increase ATP levels, decrease oxidative stress and activate PI3K/Akt pathway to enhance myocardial viability and prevent adverse remodeling after myocardial ischemia/reperfusion injury," *Stem Cell Research*, vol. 10, no. 3, pp. 301–312, 2013.

[37] J. L. Spees, S. D. Olson, M. J. Whitney, and D. J. Prockop, "Mitochondrial transfer between cells can rescue aerobic respiration," *Proceedings of the National Academy of Sciences of the United States of America*, vol. 103, no. 5, pp. 1283–1288, 2006.

[38] A. Acquistapace, T. Bru, P.-F. Lesault et al., "Human mesenchymal stem cells reprogram adult cardiomyocytes toward a progenitor-like state through partial cell fusion and mitochondria transfer," *Stem Cells*, vol. 29, no. 5, pp. 812–824, 2011.

[39] B. E. Strauer, M. Brehm, T. Zeus et al., "Intracoronary, human autologous stem cell transplantation for myocardial regeneration following myocardial infarction," *Deutsche Medizinische Wochenschrift*, vol. 126, pp. 932–938, 2001.

[40] K. C. Wollert, G. P. Meyer, J. Lotz et al., "Intracoronary autologous bone-marrow cell transfer after myocardial infarction: the boost randomised controlled clinical trial," *The Lancet*, vol. 364, no. 9429, pp. 141–148, 2004.

[41] K. S. Telukuntla, V. Y. Suncion, I. H. Schulman, and J. M. Hare, "The advancing field of cell-based therapy: insights and lessons from clinical trials," *Journal of the American Heart Association*, vol. 2, no. 5, Article ID e000338, 2013.

[42] J. M. Hare, J. E. Fishman, G. Gerstenblith et al., "Comparison of allogeneic vs autologous bone marrow-derived mesenchymal stem cells delivered by transendocardial injection in patients with ischemic cardiomyopathy: the POSEIDON randomized trial," *The Journal of the American Medical Association*, vol. 308, no. 22, pp. 2369–2379, 2012.

[43] J. Bartunek, A. Behfar, D. Dolatabadi et al., "Cardiopoietic stem cell therapy in heart failure: the c-cure (cardiopoietic stem cell therapy in heart failure) multicenter randomized trial with lineage-specified biologics," *Journal of the American College of Cardiology*, vol. 61, no. 23, pp. 2329–2338, 2013.

[44] A. W. Heldman, D. L. DiFede, J. E. Fishman et al., "Transendocardial mesenchymal stem cells and mononuclear bone marrow cells for ischemic cardiomyopathy: the TAC-HFT randomized trial," *Journal of the American Medical Association*, vol. 311, no. 1, pp. 62–73, 2014.

[45] A. B. Mathiasen, A. A. Qayyum, E. Jorgensen et al., "Bone marrow-derived mesenchymal stromal cell treatment in patients with severe ischaemic heart failure: a randomized placebo-controlled trial (MSC-HF trial)," *European Heart Journal*, 2015.

[46] S.-L. Chen, W.-W. Fang, F. Ye et al., "Effect on left ventricular function of intracoronary transplantation of autologous bone marrow mesenchymal stem cell in patients with acute myocardial infarction," *The American Journal of Cardiology*, vol. 94, no. 1, pp. 92–95, 2004.

[47] A. E. Ting and W. Sherman, "Allogeneic stem cell transplantation for ischemic myocardial dysfunction," *Current Opinion in Organ Transplantation*, vol. 17, no. 6, pp. 675–680, 2012.

[48] E. Martin-Rendon, S. J. Brunskill, C. J. Hyde, S. J. Stanworth, A. Mathur, and S. M. Watt, "Autologous bone marrow stem cells to treat acute myocardial infarction: a systematic review," *European Heart Journal*, vol. 29, no. 15, pp. 1807–1818, 2008.

[49] K. Lunde, S. Solheim, S. Aakhus et al., "Intracoronary injection of mononuclear bone marrow cells in acute myocardial infarction," *The New England Journal of Medicine*, vol. 355, no. 12, pp. 1199–1209, 2006.

[50] M. Gyöngyösi, J. Blanco, T. Marian et al., "Serial noninvasive in vivo positron emission tomographic tracking of percutaneously intramyocardially injected autologous porcine mesenchymal stem cells modified for transgene reporter gene expression," *Circulation: Cardiovascular Imaging*, vol. 1, no. 2, pp. 94–103, 2008.

[51] L. M. McGinley, J. McMahon, A. Stocca et al., "Mesenchymal stem cell survival in the infarcted heart is enhanced by lentivirus vector-mediated heat shock protein 27 expression," *Human Gene Therapy*, vol. 24, no. 10, pp. 840–851, 2013.

[52] M. Hofmann, K. C. Wollert, G. P. Meyer et al., "Monitoring of bone marrow cell homing into the infarcted human myocardium," *Circulation*, vol. 111, no. 17, pp. 2198–2202, 2005.

[53] A. Facciabene, X. Peng, I. S. Hagemann et al., "Tumour hypoxia promotes tolerance and angiogenesis via CCL28 and T_{reg} cells," *Nature*, vol. 475, no. 7355, pp. 226–230, 2011.

[54] V. Schächinger, A. Aicher, N. Döbert et al., "Pilot trial on determinants of progenitor cell recruitment to the infarcted human myocardium," *Circulation*, vol. 118, no. 14, pp. 1425–1432, 2008.

[55] H. Hamdi, A. Furuta, V. Bellamy et al., "Cell delivery: intramyocardial injections or epicardial deposition? A head-to-head comparison," *Annals of Thoracic Surgery*, vol. 87, no. 4, pp. 1196–1203, 2009.

[56] A. Elsässer, K. Suzuki, S. Lorenz-Meyer, C. Bode, and J. Schaper, "The role of apoptosis in myocardial ischemia: a critical appraisal," *Basic Research in Cardiology*, vol. 96, no. 3, pp. 219–226, 2001.

[57] C. A. Thompson, B. A. Nasseri, J. Makower et al., "Percutaneous transvenous cellular cardiomyoplasty: a novel nonsurgical approach for myocardial cell transplantation," *Journal of the American College of Cardiology*, vol. 41, no. 11, pp. 1964–1971, 2003.

[58] D. Hou, E. A.-S. Youssef, T. J. Brinton et al., "Radiolabeled cell distribution after intramyocardial, intracoronary, and interstitial retrograde coronary venous delivery: implications for current clinical trials," *Circulation*, vol. 112, no. 9, pp. I150–I156, 2005.

[59] S. Fukushima, A. Varela-Carver, S. R. Coppen et al., "Direct intramyocardial but not intracoronary injection of bone marrow cells induces ventricular arrhythmias in a rat chronic ischemic heart failure model," *Circulation*, vol. 115, no. 17, pp. 2254–2261, 2007.

[60] H. Hamdi, V. Planat-Benard, A. Bel et al., "Epicardial adipose stem cell sheets results in greater post-infarction survival than intramyocardial injections," *Cardiovascular Research*, vol. 91, no. 3, pp. 483–491, 2011.

[61] J. Leor, S. Aboulafia-Etzion, A. Dar et al., "Bioengineered cardiac grafts: a new approach to repair the infarcted myocardium?" *Circulation*, vol. 102, no. 19, pp. III56–III61, 2000.

[62] W. H. Zimmermann, C. Fink, D. Kralisch, U. Remmers, J. Weil, and T. Eschenhagen, "Three-dimensional engineered heart tissue from neonatal rat cardiac myocytes," *Biotechnology and Bioengineering*, vol. 68, no. 1, pp. 106–114, 2000.

[63] W.-H. Zimmermann, I. Melnychenko, and T. Eschenhagen, "Engineered heart tissue for regeneration of diseased hearts," *Biomaterials*, vol. 25, no. 9, pp. 1639–1647, 2004.

[64] J. Jin, S. I. Jeong, Y. M. Shin et al., "Transplantation of mesenchymal stem cells within a poly(lactide-co-epsilon-caprolactone) scaffold improves cardiac function in a rat myocardial infarction model," *European Journal of Heart Failure*, vol. 11, no. 2, pp. 147–153, 2009.

[65] K. L. Christman, A. J. Vardanian, Q. Fang, R. E. Sievers, H. H. Fok, and R. J. Lee, "Injectable fibrin scaffold improves cell transplant survival, reduces infarct expansion, and induces neovasculature formation in ischemic myocardium," *Journal of the American College of Cardiology*, vol. 44, no. 3, pp. 654–660, 2004.

[66] P. Maureira, P.-Y. Marie, F. Yu et al., "Repairing chronic myocardial infarction with autologous mesenchymal stem cells engineered tissue in rat promotes angiogenesis and limits ventricular remodeling," *Journal of Biomedical Science*, vol. 19, no. 1, article 93, 2012.

[67] J. Leor, S. Tuvia, V. Guetta et al., "Intracoronary injection of in situ forming alginate hydrogel reverses left ventricular remodeling after myocardial infarction in swine," *Journal of the American College of Cardiology*, vol. 54, no. 11, pp. 1014–1023, 2009.

[68] P. Sreejit and R. S. Verma, "Cardiogel supports adhesion, proliferation and differentiation of stem cells with increased oxidative stress protection," *European Cells & Materials*, vol. 21, pp. 107–121, 2011.

[69] X. Bourges, P. Weiss, G. Daculsi, and G. Legeay, "Synthesis and general properties of silated-hydroxypropyl methylcellulose in prospect of biomedical use," *Advances in Colloid and Interface Science*, vol. 99, no. 3, pp. 215–228, 2002.

[70] X. Li, J. Zhou, Z. Liu et al., "A PNIPAAm-based thermosensitive hydrogel containing SWCNTs for stem cell transplantation in myocardial repair," *Biomaterials*, vol. 35, no. 22, pp. 5679–5688, 2014.

[71] C. Ceccaldi, R. Bushkalova, C. Alfarano et al., "Evaluation of polyelectrolyte complex-based scaffolds for mesenchymal stem cell therapy in cardiac ischemia treatment," *Acta Biomaterialia*, vol. 10, no. 2, pp. 901–911, 2014.

[72] R. Ravichandran, J. R. Venugopal, S. Sundarrajan, S. Mukherjee, and S. Ramakrishna, "Cardiogenic differentiation of mesenchymal stem cells on elastomeric poly (glycerol sebacate)/collagen core/shell fibers," *World Journal of Cardiology*, vol. 5, no. 3, pp. 28–41, 2013.

[73] X.-Y. Li, T. Wang, X.-J. Jiang et al., "Injectable hydrogel helps bone marrow-derived mononuclear cells restore infarcted myocardium," *Cardiology*, vol. 115, no. 3, pp. 194–199, 2010.

[74] X. Bourges, P. Weiss, A. Coudreuse, G. Daculsi, and G. Legeay, "General properties of silated hydroxyethylcellulose for potential biomedical applications," *Biopolymers*, vol. 63, no. 4, pp. 232–238, 2002.

[75] C. A. Holladay, A. M. Duffy, X. Chen, M. V. Sefton, T. D. O'Brien, and A. S. Pandit, "Recovery of cardiac function mediated by MSC and interleukin-10 plasmid functionalised scaffold," *Biomaterials*, vol. 33, no. 5, pp. 1303–1314, 2012.

[76] E. Mathieu, G. Lamirault, C. Toquet et al., "Intramyocardial delivery of mesenchymal stem cell-seeded hydrogel preserves cardiac function and attenuates ventricular remodeling after myocardial infarction," *PLoS ONE*, vol. 7, no. 12, Article ID e51991, 2012.

[77] N. C. Panda, S. T. Zuckerman, O. O. Mesubi et al., "Improved conduction and increased cell retention in healed MI using mesenchymal stem cells suspended in alginate hydrogel," *Journal of Interventional Cardiac Electrophysiology*, vol. 41, no. 2, pp. 117–127, 2014.

[78] X. Zhang, H. Wang, X. Ma et al., "Preservation of the cardiac function in infarcted rat hearts by the transplantation of adipose-derived stem cells with injectable fibrin scaffolds," *Experimental Biology and Medicine*, vol. 235, no. 12, pp. 1505–1515, 2010.

[79] N. Frey, A. Linke, T. Suselbeck et al., "Intracoronary delivery of injectable bioabsorbable scaffold (ik-5001) to treat left ventricular remodeling after st-elevation myocardial infarction: a first-in-man study," *Circulation: Cardiovascular Interventions*, vol. 7, no. 6, pp. 806–812, 2014.

[80] M. Araña, J. J. Gavira, E. Peña et al., "Epicardial delivery of collagen patches with adipose-derived stem cells in rat and minipig models of chronic myocardial infarction," *Biomaterials*, vol. 35, no. 1, pp. 143–151, 2014.

[81] J. H. Li, N. Zhang, and J. A. Wangi, "Improved anti-apoptotic and anti-remodeling potency of bone marrow mesenchymal

stem cells by anoxic pre-conditioning in diabetic cardiomyopathy," *Journal of Endocrinological Investigation*, vol. 31, no. 2, pp. 103–110, 2008.

[82] X. Hu, S. P. Yu, J. L. Fraser et al., "Transplantation of hypoxia-preconditioned mesenchymal stem cells improves infarcted heart function via enhanced survival of implanted cells and angiogenesis," *Journal of Thoracic and Cardiovascular Surgery*, vol. 135, no. 4, pp. 799–808, 2008.

[83] L. Wang, X. Hu, W. Zhu et al., "Increased leptin by hypoxic-preconditioning promotes autophagy of mesenchymal stem cells and protects them from apoptosis," *Science China Life Sciences*, vol. 57, no. 2, pp. 171–180, 2014.

[84] U. Saini, R. J. Gumina, B. Wolfe, M. L. Kuppusamy, P. Kuppusamy, and K. D. Boudoulas, "Preconditioning mesenchymal stem cells with caspase inhibition and hyperoxia prior to hypoxia exposure increases cell proliferation," *Journal of Cellular Biochemistry*, vol. 114, no. 11, pp. 2612–2623, 2013.

[85] F. Figeac, P.-F. Lesault, O. Le Coz et al., "Nanotubular crosstalk with distressed cardiomyocytes stimulates the paracrine repair function of mesenchymal stem cells," *Stem Cells*, vol. 32, no. 1, pp. 216–230, 2014.

[86] J. L. Herrmann, Y. Wang, A. M. Abarbanell, B. R. Weil, J. Tan, and D. R. Meldrum, "Preconditioning mesenchymal stem cells with transforming growth factor-alpha improves mesenchymal stem cell-mediated cardioprotection," *Shock*, vol. 33, no. 1, pp. 24–30, 2010.

[87] B. Xu, Y. Luo, Y. Liu, B. Y. Li, and Y. Wang, "Platelet-derived growth factor-BB enhances MSC-mediated cardioprotection via suppression of miR-320 expression," *The American Journal of Physiology—Heart and Circulatory Physiology*, vol. 308, no. 9, pp. H980–H989, 2015.

[88] S. Filip, J. Mokry, J. Horacek, and D. English, "Stem cells and the phenomena of plasticity and diversity: a limiting property of carcinogenesis," *Stem Cells and Development*, vol. 17, no. 6, pp. 1031–1038, 2008.

[89] Q. Mao, C. Lin, J. Gao et al., "Mesenchymal stem cells overexpressing integrin-linked kinase attenuate left ventricular remodeling and improve cardiac function after myocardial infarction," *Molecular and Cellular Biochemistry*, vol. 397, no. 1-2, pp. 203–214, 2014.

[90] W. Li, N. Ma, L.-L. Ong et al., "Bcl-2 engineered MSCs inhibited apoptosis and improved heart function," *Stem Cells*, vol. 25, no. 8, pp. 2118–2127, 2007.

[91] S. Y. Lim, Y. S. Kim, Y. Ahn et al., "The effects of mesenchymal stem cells transduced with Akt in a porcine myocardial infarction model," *Cardiovascular Research*, vol. 70, no. 3, pp. 530–542, 2006.

[92] M. Gnecchi, H. He, N. Noiseux et al., "Evidence supporting paracrine hypothesis for Akt-modified mesenchymal stem cell-mediated cardiac protection and functional improvement," *The FASEB Journal*, vol. 20, no. 6, pp. 661–669, 2006.

[93] S. Jiang, H. K. Haider, N. M. Idris, A. Salim, and M. Ashraf, "Supportive interaction between cell survival signaling and angiocompetent factors enhances donor cell survival and promotes angiomyogenesis for cardiac repair," *Circulation Research*, vol. 99, no. 7, pp. 776–784, 2006.

[94] X. Wang, T. Zhao, W. Huang et al., "Hsp20-engineered mesenchymal stem cells are resistant to oxidative stress via enhanced activation of Akt and increased secretion of growth factors," *Stem Cells*, vol. 27, no. 12, pp. 3021–3031, 2009.

[95] M. Mirotsou, Z. Zhang, A. Deb et al., "Secreted frizzled related protein 2 (Sfrp2) is the key Akt-mesenchymal stem cell-released paracrine factor mediating myocardial survival and repair," *Proceedings of the National Academy of Sciences of the United States of America*, vol. 104, no. 5, pp. 1643–1648, 2007.

[96] L. Fan, C. Lin, S. Zhuo et al., "Transplantation with survivin-engineered mesenchymal stem cells results in better prognosis in a rat model of myocardial infarction," *European Journal of Heart Failure*, vol. 11, no. 11, pp. 1023–1030, 2009.

[97] Y. L. Tang, Y. Tang, Y. C. Zhang, K. Qian, L. Shen, and M. I. Phillips, "Improved graft mesenchymal stem cell survival in ischemic heart with a hypoxia-regulated heme oxygenase-1 vector," *Journal of the American College of Cardiology*, vol. 46, no. 7, pp. 1339–1350, 2005.

[98] J. Cho, P. Zhai, Y. Maejima, and J. Sadoshima, "Myocardial injection with GSK-3β-overexpressing bone marrow-derived mesenchymal stem cells attenuates cardiac dysfunction after myocardial infarction," *Circulation Research*, vol. 108, no. 4, pp. 478–489, 2011.

[99] S. H. Ranganath, O. Levy, M. S. Inamdar, and J. M. Karp, "Harnessing the mesenchymal stem cell secretome for the treatment of cardiovascular disease," *Cell Stem Cell*, vol. 10, no. 3, pp. 244–258, 2012.

[100] J. Huang, Z. Zhang, J. Guo et al., "Genetic modification of mesenchymal stem cells overexpressing CCR1 increases cell viability, migration, engraftment, and capillary density in the injured myocardium," *Circulation Research*, vol. 106, no. 11, pp. 1753–1762, 2010.

[101] J. Tang, J. Wang, L. Guo et al., "Mesenchymal stem cells modified with stromal cell-derived factor 1α improve cardiac remodeling via paracrine activation of hepatocyte growth factor in a rat model of myocardial infarction," *Molecules and Cells*, vol. 29, no. 1, pp. 9–19, 2010.

[102] W. E. Wang, D. Yang, L. Li et al., "Prolyl hydroxylase domain protein 2 silencing enhances the survival and paracrine function of transplanted adipose-derived stem cells in infarcted myocardium," *Circulation Research*, vol. 113, no. 3, pp. 288–300, 2013.

[103] H. Li, S. Zuo, Z. He et al., "Paracrine factors released by GATA-4 overexpressed mesenchymal stem cells increase angiogenesis and cell survival," *The American Journal of Physiology—Heart and Circulatory Physiology*, vol. 299, no. 6, pp. H1772–H1781, 2010.

[104] F. Huang, M.-L. Li, Z.-F. Fang et al., "Overexpression of MicroRNA-1 improves the efficacy of mesenchymal stem cell transplantation after myocardial infarction," *Cardiology*, vol. 125, no. 1, pp. 18–30, 2013.

[105] J. Xu, Z. Huang, L. Lin et al., "miR-210 over-expression enhances mesenchymal stem cell survival in an oxidative stress environment through antioxidation and c-Met pathway activation," *Science China. Life Sciences*, vol. 57, no. 10, pp. 989–997, 2014.

[106] A. P. Beltrami, L. Barlucchi, D. Torella et al., "Adult cardiac stem cells are multipotent and support myocardial regeneration," *Cell*, vol. 114, no. 6, pp. 763–776, 2003.

[107] R. Bolli, A. R. Chugh, D. D'Amario et al., "Cardiac stem cells in patients with ischaemic cardiomyopathy (SCIPIO): initial results of a randomised phase 1 trial," *The Lancet*, vol. 378, no. 9806, pp. 1847–1857, 2011.

[108] R. Mazhari and J. M. Hare, "Mechanisms of action of mesenchymal stem cells in cardiac repair: potential influences on the

cardiac stem cell niche," *Nature Clinical Practice Cardiovascular Medicine*, vol. 4, supplement 1, pp. S21–S26, 2007.

[109] B. N. Oskouei, G. Lamirault, C. Joseph et al., "Increased potency of cardiac stem cells compared with bone marrow mesenchymal stem cells in cardiac repair," *Stem Cells Translational Medicine*, vol. 1, no. 2, pp. 116–124, 2012.

[110] A. R. Williams, K. E. Hatzistergos, B. Addicott et al., "Enhanced effect of combining human cardiac stem cells and bone marrow mesenchymal stem cells to reduce infarct size and to restore cardiac function after myocardial infarction," *Circulation*, vol. 127, no. 2, pp. 213–223, 2013.

[111] A. Facciabene, G. T. Motz, and G. Coukos, "T-regulatory cells: key players in tumor immune escape and angiogenesis," *Cancer Research*, vol. 72, no. 9, pp. 2162–2171, 2012.

[112] Y. Zhou, A. K. Singh, R. F. Hoyt Jr. et al., "Regulatory T cells enhance mesenchymal stem cell survival and proliferation following autologous cotransplantation in ischemic myocardium," *The Journal of Thoracic and Cardiovascular Surgery*, vol. 148, no. 3, pp. 1131–1137, 2014.

[113] Y.-J. Yang, J.-L. Zhao, S.-J. You et al., "Post-infarction treatment with simvastatin reduces myocardial no-reflow by opening of the KATP channel," *European Journal of Heart Failure*, vol. 9, no. 1, pp. 30–36, 2007.

[114] C. P. Sparrow, C. A. Burton, M. Hernandez et al., "Simvastatin has anti-inflammatory and antiatherosclerotic activities independent of plasma cholesterol lowering," *Arteriosclerosis, Thrombosis, and Vascular Biology*, vol. 21, no. 1, pp. 115–121, 2001.

[115] B. Assmus, C. Urbich, A. Aicher et al., "HMG-CoA reductase inhibitors reduce senescence and increase proliferation of endothelial progenitor cells via regulation of cell cycle regulatory genes," *Circulation Research*, vol. 92, no. 9, pp. 1049–1055, 2003.

[116] B. Kwak, F. Mulhaupt, S. Myit, and F. Mach, "Statins as a newly recognized type of immunomodulator," *Nature Medicine*, vol. 6, no. 12, pp. 1399–1402, 2000.

[117] J.-D. Luo, F. Xie, W.-W. Zhang, X.-D. Ma, J.-X. Guan, and X. Chen, "Simvastatin inhibits noradrenaline-induced hypertrophy of cultured neonatal rat cardiomyocytes," *British Journal of Pharmacology*, vol. 132, no. 1, pp. 159–164, 2001.

[118] Y.-J. Yang, H.-Y. Qian, J. Huang et al., "Combined therapy with simvastatin and bone marrow-derived mesenchymal stem cells increases benefits in infarcted swine hearts," *Arteriosclerosis, Thrombosis, and Vascular Biology*, vol. 29, no. 12, pp. 2076–2082, 2009.

[119] Z. Zhang, S. Li, M. Cui et al., "Rosuvastatin enhances the therapeutic efficacy of adipose-derived mesenchymal stem cells for myocardial infarction via PI3K/Akt and MEK/ERK pathways," *Basic Research in Cardiology*, vol. 108, no. 2, article 333, 2013.

[120] X. Hu, J. Wang, J. Chen et al., "Optimal temporal delivery of bone marrow mesenchymal stem cells in rats with myocardial infarction," *European Journal of Cardio-Thoracic Surgery*, vol. 31, no. 3, pp. 438–443, 2007.

[121] S. Zhang, A. Sun, D. Xu et al., "Impact of timing on efficacy and safety of intracoronary autologous bone marrow stem cells transplantation in acute myocardial infarction: a pooled subgroup analysis of randomized controlled trials," *Clinical Cardiology*, vol. 32, no. 8, pp. 458–466, 2009.

[122] Y. Yang, F. M. V. Rossi, and E. E. Putnins, "Ex vivo expansion of rat bone marrow mesenchymal stromal cells on microcarrier beads in spin culture," *Biomaterials*, vol. 28, no. 20, pp. 3110–3120, 2007.

[123] R. Sarugaser, L. Hanoun, A. Keating, W. L. Stanford, and J. E. Davies, "Human mesenchymal stem cells self-renew and differentiate according to a deterministic hierarchy," *PLoS ONE*, vol. 4, no. 8, Article ID e6498, 2009.

[124] A. Aicher, C. Heeschen, K.-I. Sasaki, C. Urbich, A. M. Zeiher, and S. Dimmeler, "Low-energy shock wave for enhancing recruitment of endothelial progenitor cells: a new modality to increase efficacy of cell therapy in chronic hind limb ischemia," *Circulation*, vol. 114, no. 25, pp. 2823–2830, 2006.

[125] B. Assmus, D. H. Walter, F. H. Seeger et al., "Effect of shock wave-facilitated intracoronary cell therapy on LVEF in patients with chronic heart failure: the CELLWAVE randomized clinical trial," *Journal of the American Medical Association*, vol. 309, no. 15, pp. 1622–1631, 2013.

[126] X. Liang, Y. Ding, Y. Zhang, H.-F. Tse, and Q. Lian, "Paracrine mechanisms of mesenchymal stem cell-based therapy: current status and perspectives," *Cell Transplantation*, vol. 23, no. 9, pp. 1045–1059, 2014.

[127] T. Wang, X.-J. Jiang, Q.-Z. Tang et al., "Bone marrow stem cells implantation with α-cyclodextrin/MPEG-PCL-MPEG hydrogel improves cardiac function after myocardial infarction," *Acta Biomaterialia*, vol. 5, no. 8, pp. 2939–2944, 2009.

[128] N. Tano, T. Narita, M. Kaneko et al., "Epicardial placement of mesenchymal stromal cell-sheets for the treatment of ischemic cardiomyopathy; *in vivo* proof-of-concept study," *Molecular Therapy*, vol. 22, pp. 1864–1871, 2014.

[129] Q. Zhang, H. Wang, Y.-J. Yang et al., "Atorvastatin treatment improves the effects of mesenchymal stem cell transplantation on acute myocardial infarction: the role of the RhoA/ROCK/ERK pathway," *International Journal of Cardiology*, vol. 176, no. 3, pp. 670–679, 2014.

[130] Y. Wang, C. Li, K. Cheng et al., "Activation of liver X receptor improves viability of adipose-derived mesenchymal stem cells to attenuate myocardial ischemia injury through TLR4/NF-kappaB and Keap-1/Nrf-2 signaling pathways," *Antioxidants & Redox Signaling*, vol. 21, no. 18, pp. 2543–2557, 2014.

[131] Z. Zhang, D. Liang, X. Gao et al., "Selective inhibition of inositol hexakisphosphate kinases (IP6Ks) enhances mesenchymal stem cell engraftment and improves therapeutic efficacy for myocardial infarction," *Basic Research in Cardiology*, vol. 109, article 417, 2014.

[132] D. Han, W. Huang, S. Ma et al., "Ghrelin improves functional survival of engrafted adipose-derived mesenchymal stem cells in ischemic heart through pi3k/akt signaling pathway," *BioMed Research International*, vol. 2015, Article ID 858349, 12 pages, 2015.

[133] B. Huang, J. Qian, J. Ma et al., "Myocardial transfection of hypoxia-inducible factor-1α and co-transplantation of mesenchymal stem cells enhance cardiac repair in rats with experimental myocardial infarction," *Stem Cell Research & Therapy*, vol. 5, article 22, 2014.

[134] T. Deuse, C. Peter, P. W. M. Fedak et al., "Hepatocyte growth factor or vascular endothelial growth factor gene transfer maximizes mesenchymal stem cell-based myocardial salvage after acute myocardial infarction," *Circulation*, vol. 120, no. 1, pp. S247–S254, 2009.

Hindawi Publishing Corporation
Stem Cells International
Volume 2016, Article ID 8197325, 11 pages
http://dx.doi.org/10.1155/2016/8197325

Research Article

Uric Acid-Induced Adipocyte Dysfunction Is Attenuated by HO-1 Upregulation: Potential Role of Antioxidant Therapy to Target Obesity

Komal Sodhi,[1] Jordan Hilgefort,[1] George Banks,[1] Chelsea Gilliam,[1] Sarah Stevens,[1] Hayden A. Ansinelli,[1] Morghan Getty,[1] Nader G. Abraham,[2] Joseph I. Shapiro,[1] and Zeid Khitan[1]

[1]*Departments of Internal Medicine and Surgery, Marshall University Joan C. Edwards School of Medicine, Huntington, WV 25701, USA*
[2]*Departments of Pharmacology and Medicine, New York Medical College, Valhalla, NY 10595, USA*

Correspondence should be addressed to Zeid Khitan; zkhitan@marshall.edu

Received 23 April 2015; Accepted 11 June 2015

Academic Editor: Luca Vanella

Increased uric acid levels have been implicated in the pathogenesis of metabolic syndrome. To examine the mechanisms by which this occurs, we hypothesized that an increase in heme oxygenase 1, a potent antioxidant gene, will decrease uric acid levels and adipocyte dysfunction via suppression of ROS and xanthine oxidase (XO) levels. We examined the effect of uric acid on adipogenesis in human mesenchymal stem cells (MSCs) in the presence and absence of cobalt protoporphyrin (CoPP), an HO-1 inducer, and tin mesoporphyrin (SnMP), an HO activity inhibitor. Uric acid increased adipogenesis by increasing NADPH oxidase expression and elevation in the adipogenesis markers C/EBPα, PPARγ, and Mest, while decreasing small lipid droplets and Wnt10b levels. We treated MSCs with fructose, a fuel source that increases uric acid levels. Our results showed that fructose increased XO expression as compared to the control and concomitant treatment with CoPP significantly decreased XO expression and uric acid levels. These beneficial effects of CoPP were reversed by SnMP, supporting a role for HO activity in mediating these effects. These findings demonstrate that increased levels of HO-1 appear crucial in modulating the phenotype of adipocytes exposed to uric acid and in downregulating XO and NADPH oxidase levels.

1. Introduction

Obesity is an epidemic that is becoming increasingly more prevalent, particularly in Western societies. Fructose, a dietary component, is often implicated in the development and exacerbation of obesity [1–6]. Much like glucose, fructose is a monosaccharide that is metabolized through the glycolytic pathway [7, 8]. However, unlike glucose, fructose is not primarily phosphorylated by hexokinase/glucokinase in the liver, but rather fructokinase, also known as ketohexokinase (KHK). KHK utilizes ATP to phosphorylate fructose to fructose-1-phosphate [2, 3]. This step is not regulated by insulin or fasting; furthermore, it bypasses the regulatory step in glycolysis catalyzed by phosphofructokinase. Therefore, unregulated fructose metabolism produces uric acid as a byproduct through the induction of XO, thereby contributing to obesity and the potential for metabolic syndrome by increasing reactive oxygen species (ROS).

We hypothesized, as have others, that one mediator of fructose-induced symptoms of metabolic syndrome is uric acid [9–12]. Hyperuricemia is a well-known prelude to the development of many conditions, including gout and kidney disease [13]. Uric acid levels, highly predictive of body mass index (BMI) in humans, are elevated by many factors, including high purine diets and high fructose diets [10, 14]. While uric acid is a potent antioxidant, it can be highly damaging at elevated levels as seen in gout [15]. Ironically, its intracellular effect is to stimulate the production

of reactive oxygen species [16]. Intracellular uric acid has multiple origins, one of which is urate transport into cells through various transporters including URAT1, OAT, and SLC2A9 [13]. However, another origin of a more problematic nature is the KHK-dependent ATP depletion during fructose metabolism, which leads to a dramatic intracellular increase in purine degradation and uric acid. This pathway accelerates production of uric acid, as evidenced by diseases that inhibit purine recovery, such as Lesch-Nyhan syndrome. Uric acid induces oxidative stress via activation of NADPH oxidase [16]. NADPH oxidase increases production of O_2^-, resulting in increases in ROS, adipogenesis, insulin resistance, and inflammation [15, 17]. In addition, uric acid stimulates fructokinase and increases fructose breakdown [18]. This suggests that hyperuricemia is an indicator of adipocyte dysfunction in metabolic syndrome, and inducers of uric acid, especially fructose, may pose a serious threat to adipocyte function.

Imbalances in cellular redox status have been linked to adipose tissue dysfunction [4, 16]. It has been demonstrated that an NADPH oxidase inhibitor abolished the augmented ROS production accompanying adipogenesis in adipocytes [16, 19]. On the other hand, there is evidence that oxidative stress may promote adipogenesis via an upregulation of C/EBPα and PPARγ in human bone marrow MSC [2, 20, 21]. The ROS produced by NADPH oxidase go on to activate the transcriptional factor Peg-1/Mest and induce adipocyte enlargement [22]. Induction of HO-1 decreases endogenous ROS and the protective effect of increased HO-1 expression is ascribed to several factors that include a reduction in cellular heme, the induction of the iron binding protein ferritin, and the increased formation of bilirubin, which efficiently scavenges toxic oxygen species [23]. Induction of HO-1 expression *in vivo* and *in vitro* is associated with an increase in preadipocytes, a reduction in the number of enlarged adipocytes, elevated adiponectin secretion, and an increase in the number of small adipocytes, which are regarded as "healthy" adipocytes [24]. HO-1 upregulates the transcriptional proteins β-catenin and Wnt10b that induce production of adiponectin, a hormone that keeps adipocytes small and healthy, and inhibits the activity of PPARγ, a transcriptional factor that induces adipogenesis [25, 26].

The goal of this study was to determine whether fructose- and uric acid-induced adipocyte dysfunction in MSC-derived adipocytes could be ameliorated by suppression of XO and NADPH oxidase by upregulation of HO-1. Our results showed that induction of HO-1 gene expression decreased lipid deposition and positive regulators of adipogenic markers and downregulated the expression of XO and NADPH oxidase. These findings demonstrate that increased levels of HO-1 appear crucial in modulating the phenotype of adipocytes exposed to uric acid and in suppressing markers of adipocyte hyperplasia and inflammation.

2. Material and Methods

2.1. Human Bone-Marrow-Derived MSC Culture. Frozen bone marrow mononuclear cells were purchased from All Cells (Emeryville, CA). After thawing, mononuclear cells (MSCs) were resuspended in α-minimal essential medium (α-MEM, Invitrogen, Carlsbad, CA) that was supplemented with 20% FBS and 1% A/A. The cells were transferred into a 75-cm^2 flask, cultured in α-MEM with 20% FBS and 1% A/A, and maintained at 37°C in a 5% CO_2 incubator. The medium was changed after 24 hours and every 2 days thereafter. Once being 80% confluent, the MSCs were recovered by the addition of 0.25% trypsin/EDTA, split, and partitioned into additional 75 cm^2 flasks.

2.2. Human Bone-Marrow-Derived MSC Adipocyte Differentiation. MSCs (passages 2-3) were plated in 75 cm^2 flasks and 24-well plates at a density of 1-2 $\times$ 10^4 cells per cm^2 and were again cultured in their respective maintenance media until cells were 80% confluent. The maintenance medium was then replaced with adipogenic medium and the cells were cultured for an additional 14 days. The adipogenic medium consisted of complete culture medium supplemented with DMEM-high glucose (Invitrogen, Carlsbad, CA), 10% FBS, 1% A/A, 10 μg/mL insulin, 1 μM dexamethasone (Sigma-Aldrich, St. Louis, MO), and 0.1 mM Indomethacin (Sigma-Aldrich, St. Louis, MO). Human MSCs were cultured in this adipogenic differentiation medium along with fructose and uric acid in the presence and absence of the HO-1 inducer cobalt protoporphyrin (CoPP) (5 μM), HO activity inhibitor tin-mesoporphyrin (SnMP) (5 μM), xanthine oxidase inhibitor allopurinol (50 μM) (Sigma-Aldrich, St. Louis, MO), and NADPH oxidase inhibitor apocynin (100 μM) (Sigma-Aldrich, St. Louis, MO). The medium and treatments were renewed daily.

2.3. Fructose and Uric Acid Concentrations on Adipogenesis. To determine the optimal effect of fructose and uric acid on MSC-derived adipocyte differentiation, cells were treated with fructose at concentrations of 500 and 1000 μM/L and uric acid at concentrations of 5 and 10 mg/dL, respectively. After 14 days, cells were stained with Oil Red O solution. Optimum concentrations for fructose and uric acid were found to be 500 μM/L and 5 mg/dL, respectively. These concentrations were utilized during treatment of cells throughout experimentation.

2.4. Oil Red O Staining. 0.21% Oil Red O in 100% isopropanol (Sigma-Aldrich, St. Louis, MO) was used for staining. Briefly, adipocytes were fixed in 4% formaldehyde, stained with Oil Red O for 10 min, and rinsed with pH 7.2 PBS (1x) (Invitrogen, Carlsbad, CA). Pictures were captured using an Olympus IX81 Motorized Inverted Microscope. Oil Red O was eluted by adding 100% isopropanol for 10 min and OD was measured at 490 nm 24 hours later.

2.5. Measurement of Lipid Droplet Size. Cell size was measured using *ImagePro* Analyzer (Media Cybernetics, Inc., MD). The classification of the size of lipid droplets was based on size by area (pixels).

2.6. Measurement of MSC-Derived Adipocyte Signaling Molecules. Cells were maintained at −80°C until required for assay. Frozen cells were pulverized and placed in a homogenization buffer (10 mM phosphate buffer, 250 mM sucrose,

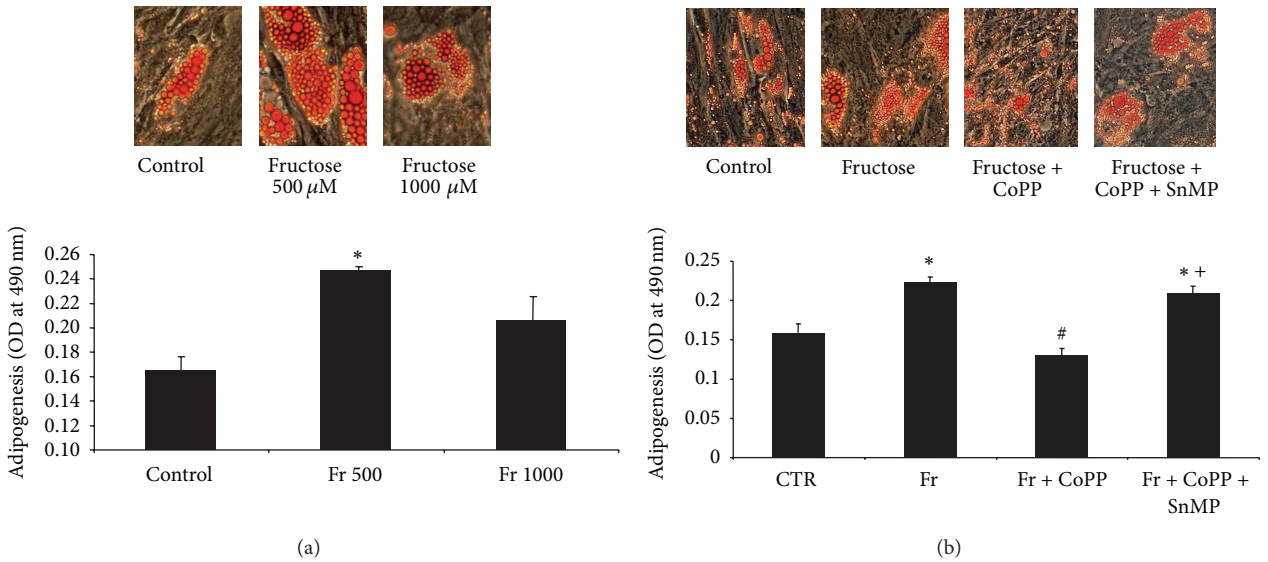

FIGURE 1: (a) Adipogenesis as shown by Oil Red O staining in MSCs treated with 500 μM and 1000 μM fructose. A representative section for each group is shown. (b) Adipogenesis as shown by Oil Red O staining in MSCs treated with 500 μM fructose with or without CoPP, in the presence or absence of SnMP, magnifications: 40x ($n = 5$). A representative section for each group is shown. Values represent means ± SEM of five independent treatments. $^{*}p < 0.05$ versus CTR; $^{\#}p < 0.05$ versus Fr; and $^{+}p < 0.05$ versus Fr + CoPP.

1 mM EDTA, 0.1 mM PMSF, and 0.1% Tergitol, pH 7.5). Homogenates were centrifuged at 10,000 rpm for 10 minutes at 4°C. The supernatant was isolated and protein levels were assayed (Bradford method). The supernatant was used for measurement of XO, NADPH oxidase, and β-actin levels. β-actin was used to ensure adequate sample loading for all western blots.

2.7. Measurement of Superoxide Levels. MSC-derived adipocytes were cultured on 96-well plates until they achieved approximately 70% confluence. After treatment with or without uric acid (5 mg/dL) in the absence and presence of CoPP (5 μM) and SnMP (5 μM) for 2 days, the cells were incubated with 10 μM dihydroethidium (DHE) for 30 min at 37°C. Fluorescence intensity was measured using a Perkin-Elmer Luminescence Spectrometer at excitation/emission filters of 530/620 nm.

2.8. RNA Extraction and Real-Time PCR Experiments. Total RNA was extracted from MSC-derived adipocytes using RNeasy Protect Mini kit (QIAGEN, MD, USA) according to the manufacturer's instructions. Total RNA (1 μg) was transcribed into cDNA using GeneAmp kit (Applied Biosystems, Branchburg, NJ, USA) reverse transcription reagents. Total RNA was analyzed by a quantitative real-time polymerase chain reaction (qRT-PCR). Real-time PCR was performed using SYBR Green PCR Master Mix (Applied Biosystems) on a 7500 HT Fast Real-Time PCR System (Applied Biosystems). Specific primers used were HO-1, PPARγ, FAS, C/EBPα, Wnt10b, Mest, and actin. Each reaction was performed in triplicate. The comparative threshold cycle (Ct) method was used to calculate the fold amplification as specified by the manufacturer. All experimental samples were normalized using GAPDH as an internal control and normalization was performed in separate reactions.

2.9. Statistical Analyses. Statistical significance was determined using one-way analysis of variance followed by Tukey-Kramer post hoc test. $p < 0.05$ was considered to be significant. Data are expressed as means ± standard error of the mean (SEM).

3. Results

3.1. Effect of Fructose on Adipogenesis in MSC-Derived Adipocytes. We measured adipogenesis in MSC-derived adipocytes after treatment with increasing concentrations of fructose. Fructose at a concentration of 500 μM/L was determined to be the optimal concentration for stimulating adipogenesis in MSC-derived adipocytes as compared to the control (Figure 1(a); $p < 0.05$) as shown by us previously [27]. The same instrumental analysis was applied to MSC-derived adipocytes being treated with CoPP, an HO-1 agonist, which showed a reduction in adipogenesis to levels similar to the control group. When SnMP, an HO-1 activity inhibitor, was added to cells treated with both fructose and CoPP, adipogenesis increased to levels seen with only fructose treatment (Figure 1(b); $p < 0.05$).

3.2. Effect of HO-1 Induction on XO and Uric Acids Levels in MSC-Derived Adipocytes. Fructose metabolism invokes the consumption of ATP and thereby increases intracellular activity of XO and its product, uric acid. In concordance with our hypothesis, our results showed that fructose treatment of MSC-derived adipocytes significantly increased XO expression and uric acid to levels higher than the control

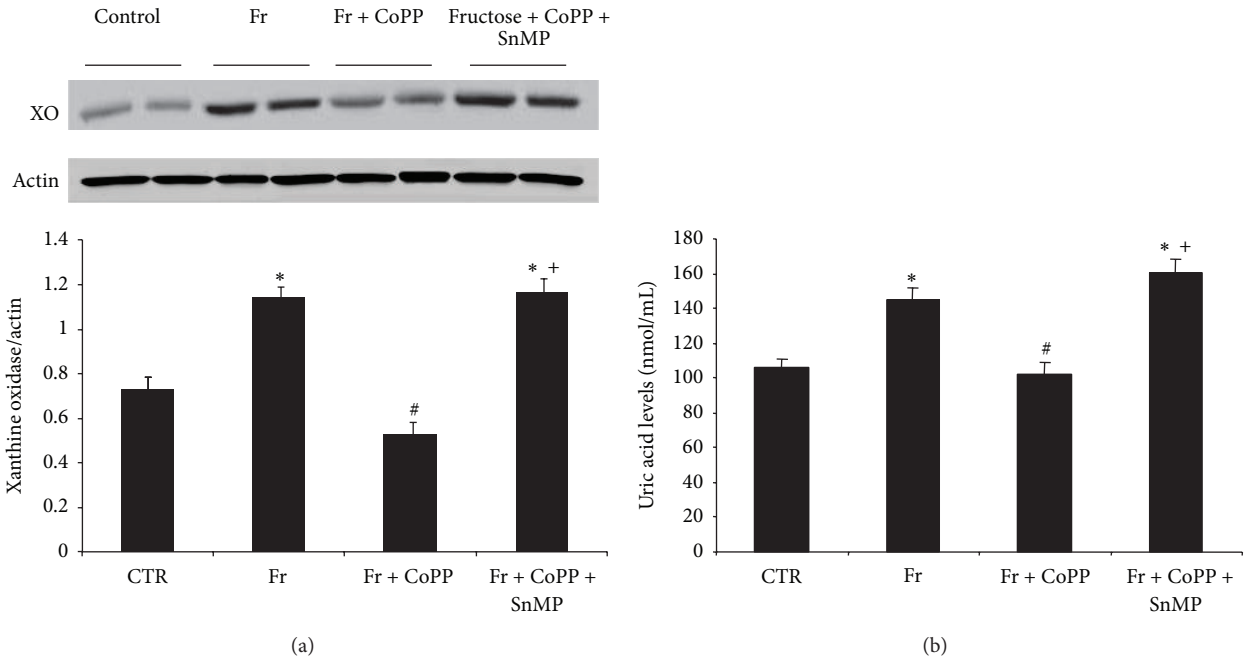

Figure 2: (a) XO expression by western blot analysis. Data are shown as mean band density normalized to β-actin. Results are means ± SE, $n = 4$/group. $^{*}p < 0.05$ versus CTR; $^{\#}p < 0.05$ versus Fr; and $^{+}p < 0.05$ versus Fr + CoPP. (b) Measurement of uric acid levels in pelleted cells at day 14 of adipogenesis in human MSCs treated with 500 μM fructose with or without CoPP, in the presence or absence of SnMP. Values represent means ± SEM of five independent treatments. $^{*}p < 0.05$ versus CTR; $^{\#}p < 0.05$ versus Fr; and $^{+}p < 0.05$ versus Fr + CoPP.

(Figures 2(a) and 2(b), resp.; $p < 0.05$). Concurrent treatment with fructose and CoPP effectively reversed both XO and uric acid levels to that of the control ($p < 0.05$). The addition of SnMP negated the beneficial effects of CoPP and increased XO and uric acid levels.

3.3. Effect of Uric Acid on Adipogenesis in MSC-Derived Adipocytes. We studied whether uric acid might be mediating fructose-induced adipogenesis. A concentration curve was obtained by treating cultured MSCs with uric acid concentrations of 5 mg/dL and 10 mg/dL. We demonstrated that cells treated with uric acid at a concentration of 5 mg/dL showed the maximum adipogenesis as compared to the control (Figure 3(a); $p < 0.05$). After observing an increase in adipogenesis in cells treated with uric acid, we then treated MSCs concurrently with uric acid and CoPP to confirm that HO-1 decreased uric acid-mediated adipogenesis. CoPP administration was shown to negate the adipogenic effect of uric acid and reduce adipogenesis to that of the control (Figure 3(b); $p < 0.05$). Our results further showed that SnMP, an HO activity inhibitor, reversed the beneficial effect of CoPP, resulting in increased adipogenesis (Figure 3(b); $p < 0.05$).

3.4. Effect of Uric Acid on Lipid Droplet Size and Mest and FAS Levels in MSC-Derived Adipocytes. The number of large, inflamed lipid droplets and small, healthy lipid droplets were measured in cells treated with uric acid (Figure 4(a)). Uric acid was shown to increase the number of large lipid droplets (Figure 4(b)) and decrease the number of small droplets as compared to the control (Figure 4(c); $p < 0.05$). However, the concurrent administration of CoPP completely reversed this effect and decreased large droplets and increased small droplets when compared to control ($p < 0.05$). Concurrent treatment with SnMP reversed the beneficial effects of CoPP and the number of large lipid droplets was measured to be higher than that of the control (Figure 4(a); $p < 0.05$). Furthermore, our results showed that uric acid increased Mest and FAS expression levels compared to the control (Figures 4(d) and 4(e), resp.; $p < 0.05$). CoPP reversed the effects of uric acid and decreased Mest and FAS expression as compared to the cells treated with uric acid alone.

3.5. Effect of Uric Acid on HO-1 and Adipogenic Markers in MSC-Derived Adipocytes. Uric acid reduced expression of Wnt10b but had no effect on HO-1 expression. The effects of uric acid were reversed upon addition of CoPP, which increased HO-1 and Wnt10b expression to levels above the control (Figures 5(a) and 5(b), resp.; $p < 0.05$). When these MSCs were treated with the combination of uric acid, CoPP, and SnMP, the expression of Wnt10b was reduced to that of control. HO-1 expression remained unchanged as expected, given that SnMP modifies HO-1 activity and not its expression.

The expression of C/EBPα and PPARγ, known mediators of adipocyte hypertrophy, were also measured by RT-PCR. Treatment of MSCs with uric acid increased expression of both C/EBPα and PPARγ (Figures 5(c) and 5(d), resp.; $p < 0.05$), and the levels of these proadipogenic mediators were reduced with addition of CoPP. When SnMP was added to

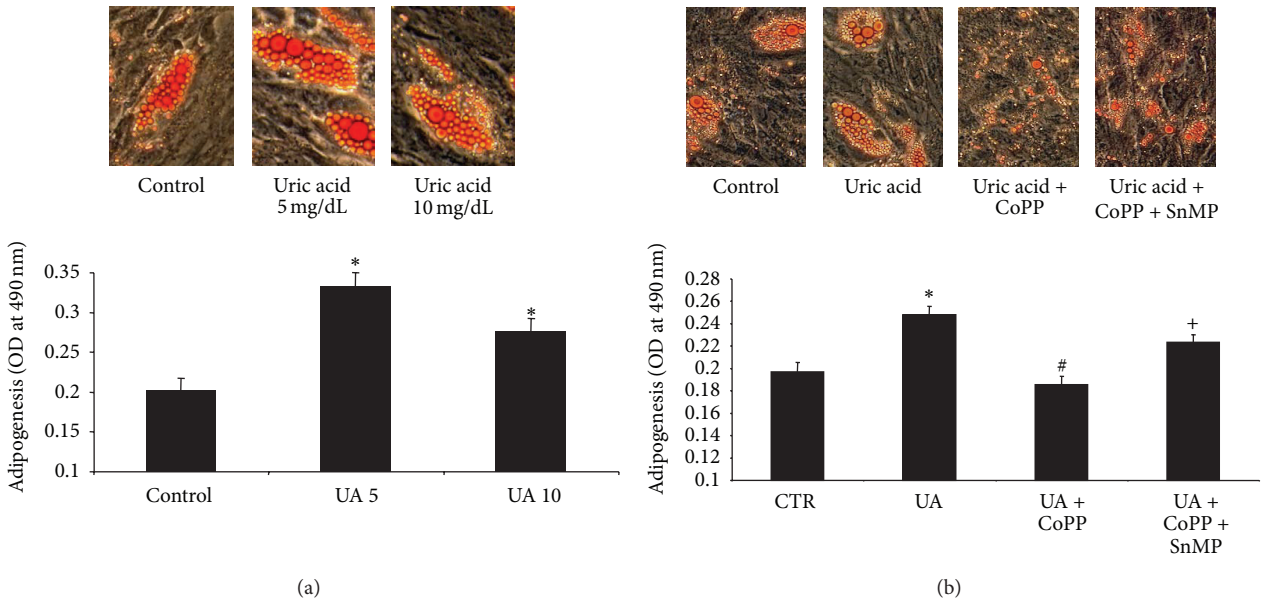

Figure 3: (a) Adipogenesis as shown by Oil Red O staining in MSCs treated with 5 mg/dL and 10 mg/dL uric acid. A representative section for each group is shown. (b) Adipogenesis as shown by Oil Red O staining in MSCs treated with 5 mg/dL uric acid with or without CoPP, in the presence or absence of SnMP, magnifications: 40x ($n = 5$). A representative section for each group is shown. Values represent means ± SEM of five independent treatments. $^{*}p < 0.05$ versus CTR; $^{\#}p < 0.05$ versus UA; and $^{+}p < 0.05$ versus UA + CoPP.

MSCs treated with uric acid and CoPP, the protective factor of HO-1 was eliminated and the expression levels of PPARγ and C/EBPα significantly increased as compared to the cells treated with uric acid and CoPP alone.

3.6. Effect of Uric Acid on Oxidative Stress in MSC-Derived Adipocytes. In order to better understand the mechanism by which uric acid was inducing adipogenesis and whether HO-1 induction plays an important role in attenuating uric acid-induced adipogenesis, NADPH oxidase expression and superoxide levels were measured. In MSC-derived adipocytes treated with uric acid, NADPH oxidase significantly increased compared to the control (Figure 6(a); $p < 0.05$). Similarly, superoxide levels were elevated in MSC-derived adipocytes treated with uric acid (Figure 6(b); $p < 0.05$). This oxidative stress was predicted to be an important cause of adipocyte dysfunction, so we treated cells with both uric acid and CoPP to see if HO-1 could decrease adipogenesis. Our results showed that CoPP significantly suppressed NADPH oxidase expression and superoxide levels as compared to cells treated with uric acid alone ($p < 0.05$). This positive outcome was effectively reversed by the addition of SnMP.

3.7. Inhibition of Fructose-Mediated Adipogenesis with Allopurinol and Uric Acid-Mediated Adipogenesis with Apocynin. First we sought to compare the effects on adipogenesis of CoPP and allopurinol, a known antagonist of XO. MSC-derived adipocytes were exposed to either fructose and allopurinol (100 mM) or fructose and CoPP, and adipogenesis was measured. Our results showed that allopurinol and CoPP attenuated adipogenesis at similar levels (Figure 7(a)). Then we sought to compare the effects on adipogenesis of CoPP and apocynin (500 mM), a known inhibitor of NADPH oxidase. In a similar fashion, MSC-derived adipocytes were treated with the combination of uric acid and apocynin or uric acid and CoPP. Adipogenesis was inhibited in both treatment groups when compared to control ($p < 0.05$), and the magnitude of inhibition was relatively equal (Figure 7(b)).

4. Discussion

This study demonstrates the stimulatory effect of exogenous uric acid on adipogenesis in MSC-derived adipocytes, confirming their proadipogenic effects and the positive link between uric acid and the occurrence of obesity. This uric acid-mediated adipogenesis is attenuated by the induction of HO-1, suggesting its beneficial role in improving adipocyte function and decreasing XO and NADPH oxidase levels, thereby decreasing oxidative stress. The effects of uric acid were accompanied by increases in the proadipogenic factors Mest, FAS, C/EBPα, and PPARγ, as well as decreases in the antiadipogenic factor Wnt10b; these findings are significantly reversed by treatment with CoPP. Thus, hyperuricemia stands as a potential contributing agent to obesity, and augmentation of HO-1 offers a promising avenue in attenuating adipocyte dysfunction.

Using MSCs as our study vehicle, we demonstrated that administration of either fructose or uric acid induced an increase in the amount of adipogenesis as compared to the control. These results verify that fructose and uric acid both have proadipogenic effects. Further our data demonstrated that MSC-derived adipocytes treated with uric acid produced a decreased expression of Wnt10b, which is essential in

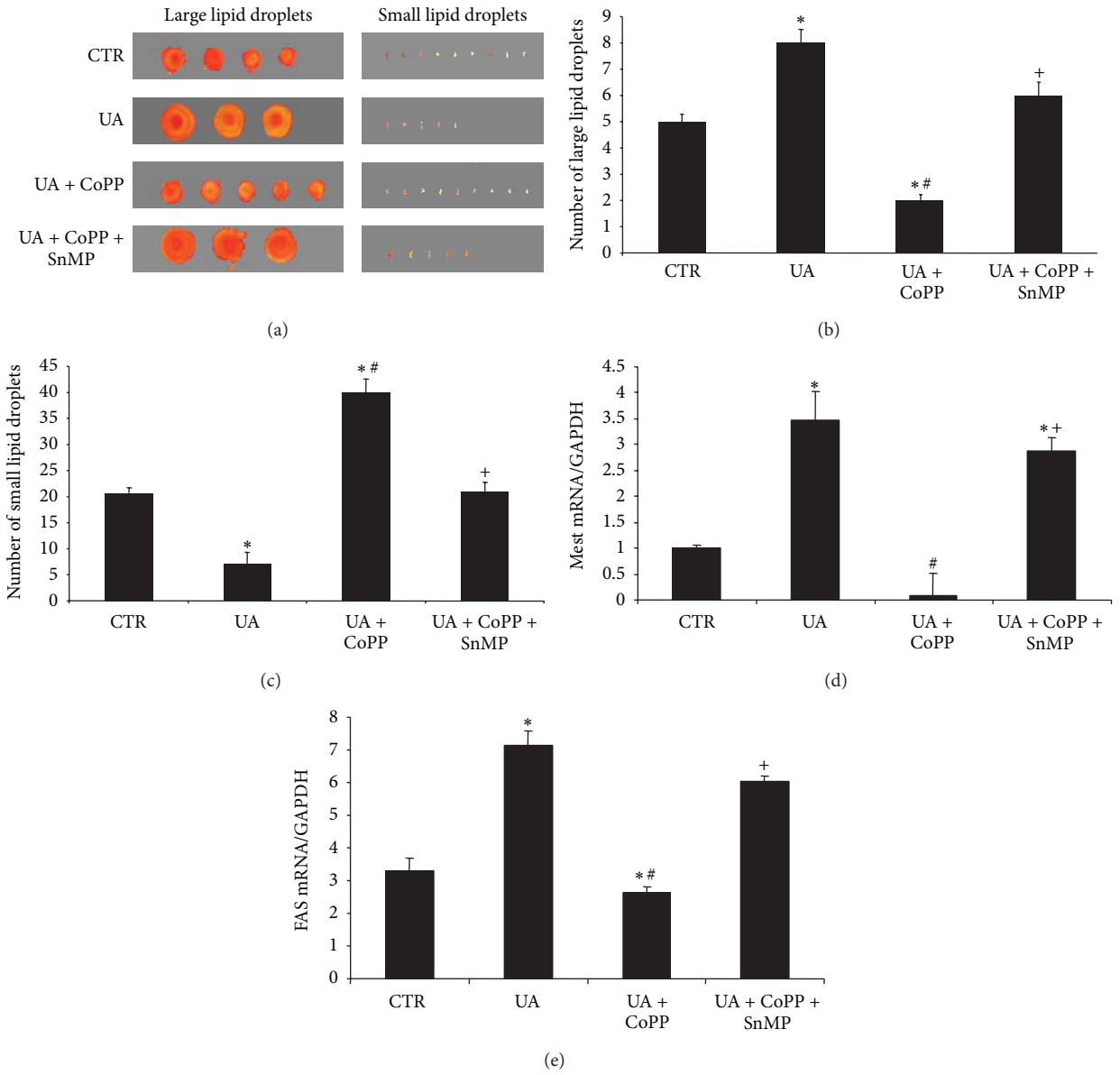

FIGURE 4: (a–c) Number of large and small lipid droplets from Oil Red O stained MSCs with 5 mg/dL uric acid with or without CoPP, in the presence or absence of SnMP; magnifications: 40x ($n = 3$). A representative section for each group is shown. Values represent means ± SEM of five independent treatments. $^{*}p < 0.05$ versus CTR; $^{\#}p < 0.05$ versus UA; and $^{+}p < 0.05$ versus UA + CoPP. (d) Real-time PCR of Mest. (e) and (d) Real-time PCR of FAS expression in MSCs treated with uric acid with or without CoPP, in the presence or absence of SnMP. Values represent means ± SEM of five independent treatments. $^{*}p < 0.05$ versus CTR; $^{\#}p < 0.05$ versus UA; and $^{+}p < 0.05$ versus UA + CoPP.

the activation of the canonical pathway and inhibition of adipogenesis [28, 29]. We also showed increased expression of C/EBP-α and PPARγ, which has a crucial role in the transcriptional regulation of the adipocyte gene [21]. Moreover, our results showed that uric acid increased Mest expression, which is an important marker for enlargement of adipocytes during adipose tissue expansion [30]. Adipocyte enlargement is associated with an increase in the levels of inflammatory cytokines and oxidative stress [20, 24]. The morphologic changes induced by fructose and uric acid to the MSC-derived adipocytes support the link between excessive fructose intake and obesity.

Our results demonstrated that HO-1 induction attenuated adipogenesis induced by uric acid and fructose in MSC-derived adipocytes. One process by which fructose has been postulated to fuel such an increase in adipogenesis is the aforementioned unregulated ATP-dependent phosphorylation of fructose and subsequent buildup of uric acid via the purine degradation pathway [30]. Support for this theory stems from the result that uric acid, like fructose, is also proadipogenic. Since uric acid exerts its effects through ROS, HO-1, a potent antioxidant, was explored as a method of treatment. Induction of HO-1 decreases adipogenesis via suppression of transcription factors, including PPARγ, aP2,

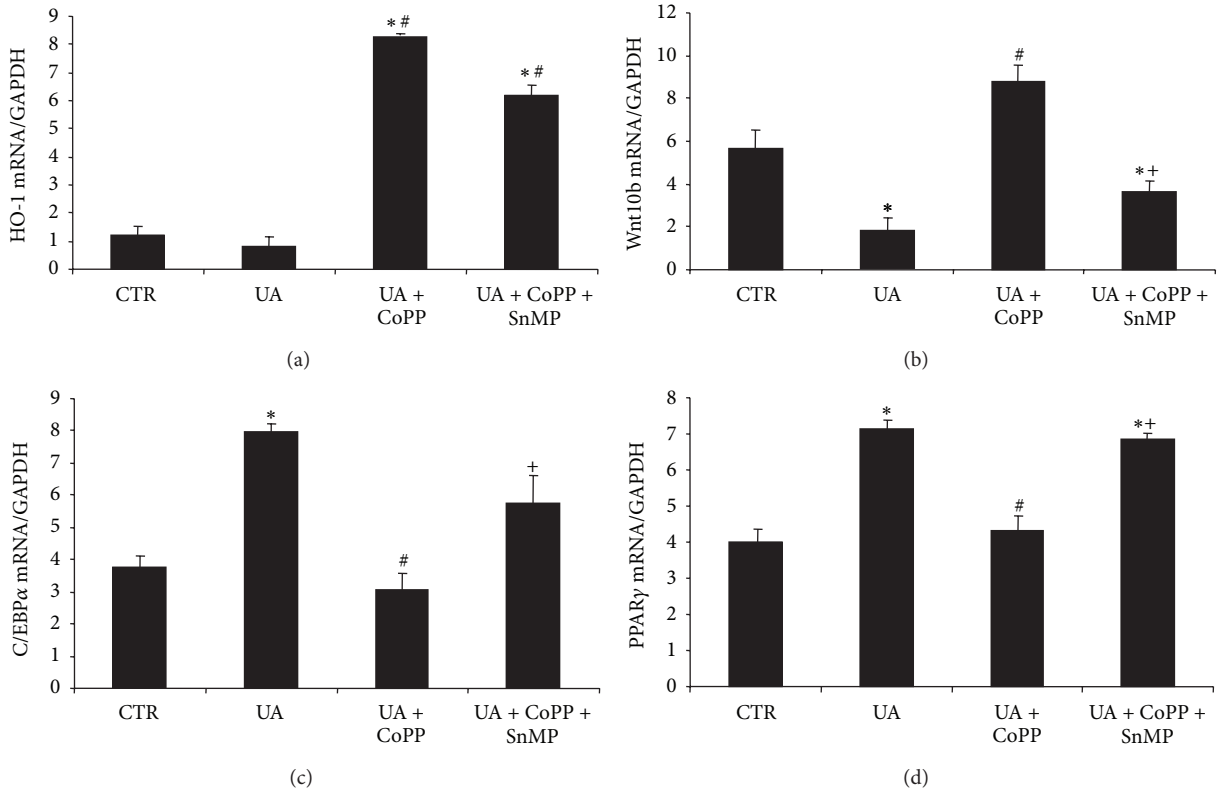

Figure 5: Real-time PCR of (a) HO-1; (b) Wnt10b; (c) C/EBPα; and (d) PPARγ expression in MSCs treated with uric acid with or without CoPP, in the presence or absence of SnMP. Values represent means ± SEM of five independent treatments. $^{*}p < 0.05$ versus CTR; $^{\#}p < 0.05$ versus UA; and $^{+}p < 0.05$ versus UA + CoPP.

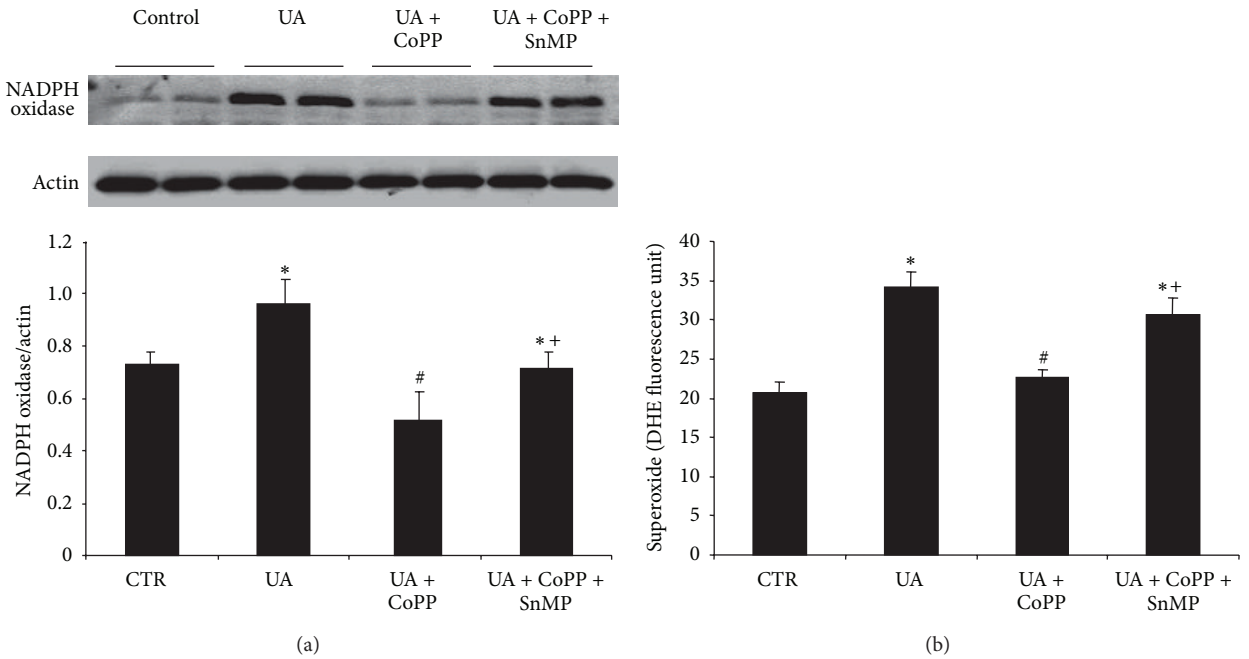

Figure 6: (a) NADPH oxidase expression by western blot analysis. Data are shown as mean band density normalized to β-actin. Results are means ± SE, $n = 4$/group. $^{*}p < 0.05$ versus CTR; $^{\#}p < 0.05$ versus UA; and $^{+}p < 0.05$ versus UA + CoPP. (b) Measurement of superoxide levels in pelleted cells at day 14 of adipogenesis in human MSCs treated with 5 mg/dL uric acid with or without CoPP, in the presence or absence of SnMP. Values represent means ± SEM of five independent treatments. $^{*}p < 0.05$ versus CTR; $^{\#}p < 0.05$ versus UA; and $^{+}p < 0.05$ versus UA + CoPP.

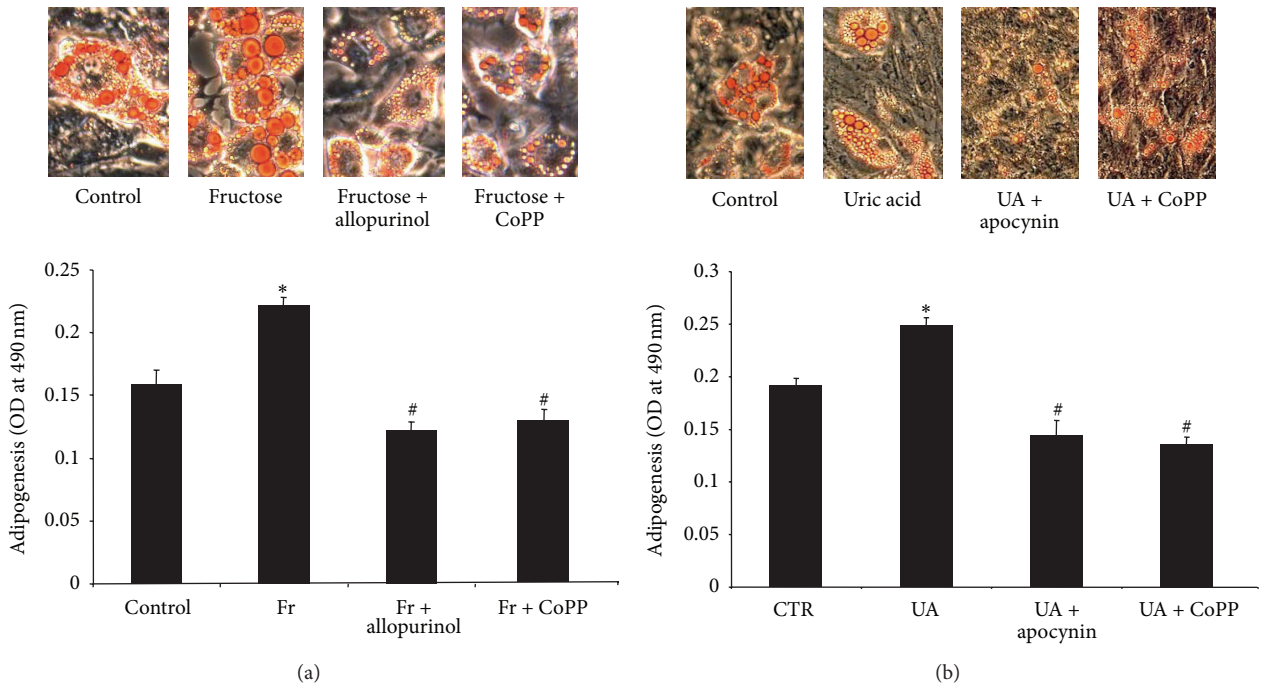

FIGURE 7: (a) Adipogenesis as shown by Oil Red O staining in MSCs treated with 500 μM fructose with or without CoPP and with or without allopurinol, a known inhibitor of XO. A representative section for each group is shown; $^{*}p < 0.05$ versus CTR; $^{\#}p < 0.05$ versus Fr. (b) Adipogenesis as shown by Oil Red O staining in MSCs treated with 5 mg/dL uric acid with or without CoPP and with or without apocynin, a known inhibitor of NADPH oxidase, magnifications: 40x ($n = 5$). A representative section for each group is shown. Values represent means ± SEM of five independent treatments. $^{*}p < 0.05$ versus CTR; $^{\#}p < 0.05$ versus UA.

and Mest proteins, while concomitantly increasing Wnt10b and adiponectin levels [25, 26, 28, 29, 31, 32]. We demonstrated in our study that upregulation of HO-1 counteracts the increase in adipogenesis resulting from treatment with fructose or uric acid in MSCs-derived adipocytes and also decreased adipocyte size, whereas inhibition of HO activity by SnMP increased adipocyte dysfunction. Our data further showed that the induction of HO-1 suppressed adipocyte differentiation, as evidenced by an increase in the canonical Wnt cascade and a decrease in Peg-1/Mest, FAS, and PPARγ in uric acid-treated cells.

This study showed that induction of HO-1 via CoPP reduced expression of XO and NADPH oxidase and decreased oxidative stress-mediated adipogenesis in MSC-derived adipocytes. Uric acid produced in the presence of fructose via the upregulation of xanthine oxidase leads to an increase in oxidative stress. Our results showed for the first time that the MSC-derived adipocytes treated with fructose and CoPP downregulated XO expression. HO-1 induction also decreased uric acid levels, the final product of XO, further suggesting the beneficial role of HO-1 in attenuating XO-mediated oxidative stress and adipogenesis. Another potential mechanism by which HO-1 upregulation decreases adipogenesis in MSC-derived adipocytes may be related to suppression of NADPH oxidase, which contributes to oxidative stress. Bilirubin, a product of HO-1 catabolism, has been shown to scavenge ROS and play a role in the inhibition of NADPH oxidase [27]. Our results showed that uric acid increased expression of NADPH oxidase in MSC-derived adipocytes, and concurrent administration of CoPP decreased its expression, suggesting that upregulation of HO-1 attenuates NADPH oxidase-mediated adipogenesis. NADPH oxidase also had the effect of upregulating the transcriptional factor Peg-1/Mest through the generation of the superoxide ion [33]. In concordance with these reports, our results showed that uric acid treatment in MSCs increased expression of Peg-1/Mest, and upregulation of HO-1 negated this increase in Peg-1/Mest expression. To further confirm our hypothesis that HO-1 upregulation plays an important role in attenuating XO- and NADPH oxidase-mediated adipogenesis, the efficacy of HO-1 was established by comparing its effect on adipogenesis to known antagonists of XO and NADPH oxidase, allopurinol and apocynin, respectively. Our results demonstrated that HO-1 induction displayed similar efficacy to that of both allopurinol and apocynin in terms of suppressing adipogenesis. These observations indicate that induction of HO-1 plays an important role in the prevention of adipocyte hypertrophy and the promotion of smaller healthier adipocytes in MSCs, in large part, through reduced expression of XO and NADPH oxidase. Our data underscores the importance of oxidative stress-induced adipocyte dysfunction as a result of uncontrolled fructose metabolism and offers new insights into potential therapies by which targeting fructose metabolism and/or downstream signaling of uric acid can curtail adipogenesis.

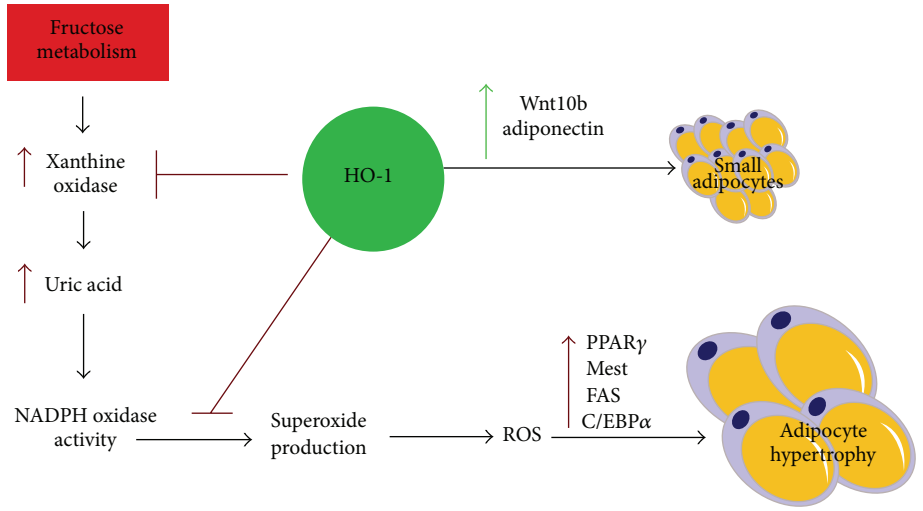

Figure 8: Proposed mechanism demonstrating the beneficial role of heme oxygenase 1 (HO-1) in the attenuation of adipocyte dysfunction in mesenchymal stem cell- (MSC-) derived adipocytes. Excessive fructose consumption is accompanied by an increase in xanthine oxidase and uric acid and a concurrent increase in cellular ROS levels. HO-1 suppresses adipocyte differentiation by increasing expression of key regulators including Wnt10b and adiponectin and decreasing expression of adipogenic transcription factors CCAAT/enhancer binding protein α (C/EBPα), peroxisome proliferator-activated receptor γ (PPARγ), Mest, and FAS. These effects led to decrease in lipid accumulation and increase of preadipocytes and healthy adipocytes that improve adipocyte function.

5. Conclusion

In conclusion (Figure 8), we demonstrate that fructose increases adipogenesis in MSC-derived adipocytes. This effect is mediated through uric acid resulting from uncontrolled fructose metabolism, leading to upregulation of XO and NADPH oxidase. Given that obesity is correlated with increased blood levels of uric acid, this provides a potentially highly effective pharmacological intervention for overweight and obese individuals. It also highlights the crucial role of antioxidant therapy represented by HO-1 induction in targeting metabolic syndrome and obesity resulting from excessive fructose intake. Future research should seek to explore how treatment with HO-1 agonists may alter body mass index in patients suffering from obesity comorbid with increased plasma concentrations of uric acid. Investigation into this topic may prove to be extremely helpful in improving the health of Western society.

Abbreviations

XO: Xanthine oxidase
C/EBPα: CCAAT/enhancer binding protein alpha
CoPP: Cobalt protoporphyrin IX dichloride
FAS: Fatty acid synthase
HO: Heme oxygenase
HO-1: Heme oxygenase isozyme 1, inducible form
HO-2: Heme oxygenase isozyme 2, constitutive form
MSC: Mesenchymal stem cell
NADPH: Nicotinamide adenine dinucleotide phosphate (reduced form)
Peg-1/Mest: Paternally expressed gene 1/mesoderm-specific transcript
PPARγ: Peroxisome proliferator activated receptor gamma
ROS: Reactive oxygen species
SnMP: Tin mesoporphyrin IX dichloride
Wnt10b: Wingless-type MMTV integration site family, member 10b.

Disclaimer

The content of this paper is solely the responsibility of the authors and does not necessarily represent the official views of the National Institutes of Health.

Conflict of Interests

The authors declare that there is no conflict of interests regarding the publication of this paper.

Authors' Contribution

Jordan Hilgefort and George Banks contributed to work equally.

Acknowledgments

This work was supported by National Institutes of Health Grants to Joseph I. Shapiro (HL109015, HL105649, and HL071556) and by the BrickStreet Foundation (Joseph I. Shapiro, Nader G. Abraham).

References

[1] M. I. Goran, S. J. Ulijaszek, and E. E. Ventura, "High fructose corn syrup and diabetes prevalence: a global perspective," *Global Public Health*, vol. 8, no. 1, pp. 55–64, 2013.

[2] Z. Khitan and D. H. Kim, "Fructose: a key factor in the development of metabolic syndrome and hypertension," *Journal of Nutrition and Metabolism*, vol. 2013, Article ID 682673, 12 pages, 2013.

[3] R. J. Johnson, M. S. Segal, Y. Sautin et al., "Potential role of sugar (fructose) in the epidemic of hypertension, obesity and the metabolic syndrome, diabetes, kidney disease, and cardiovascular disease," *The American Journal of Clinical Nutrition*, vol. 86, no. 4, pp. 899–906, 2007.

[4] K. L. Stanhope and P. J. Havel, "Fructose consumption: potential mechanisms for its effects to increase visceral adiposity and induce dyslipidemia and insulin resistance," *Current Opinion in Lipidology*, vol. 19, no. 1, pp. 16–24, 2008.

[5] T. Ishimoto, M. A. Lanaspa, M. T. Le et al., "Opposing effects of fructokinase C and A isoforms on fructose-induced metabolic syndrome in mice," *Proceedings of the National Academy of Sciences of the United States of America*, vol. 109, no. 11, pp. 4320–4325, 2012.

[6] R. J. Johnson, S. E. Perez-Pozo, Y. Y. Sautin et al., "Hypothesis: could excessive fructose intake and uric acid cause type 2 diabetes?" *Endocrine Reviews*, vol. 30, no. 1, pp. 96–116, 2009.

[7] F.-Q. Zhao and A. F. Keating, "Functional properties and genomics of glucose transporters," *Current Genomics*, vol. 8, no. 2, pp. 113–128, 2007.

[8] J. J. Rumessen and E. Gudmand-Hoyer, "Absorption capacity of fructose in healthy adults. Comparison with sucrose and its constituent monosaccharides," *Gut*, vol. 27, no. 10, pp. 1161–1168, 1986.

[9] I. H. Fox and W. N. Kelley, "Studies on the mechanism of fructose-induced hyperuricemia in man," *Metabolism*, vol. 21, no. 8, pp. 713–721, 1972.

[10] D. Gustafsson and R. Unwin, "The pathophysiology of hyperuricaemia and its possible relationship to cardiovascular disease, morbidity and mortality," *BMC Nephrology*, vol. 14, no. 1, article 164, 2013.

[11] A. S. Cardoso, N. C. Gonzaga, C. C. M. Medeiros, and D. F. De Carvalho, "Association of uric acid levels with components of metabolic syndrome and non-alcoholic fatty liver disease in overweight or obese children and adolescents," *Jornal de Pediatria*, vol. 89, no. 4, pp. 412–418, 2013.

[12] R. Salehidoost, A. Aminorroaya, M. Zare, and M. Amini, "Is uric acid an indicator of metabolic syndrome in the first-degree relatives of patients with type 2 diabetes?" *Journal of Research in Medical Sciences*, vol. 17, no. 11, pp. 1005–1010, 2012.

[13] P. L. Riches, A. F. Wright, and S. H. Ralston, "Recent insights into the pathogenesis of hyperuricaemia and gout," *Human Molecular Genetics*, vol. 18, no. 2, pp. R177–R184, 2009.

[14] F. Stirpe, E. D. Corte, E. Bonetti, A. Abbondanza, A. Abbati, and F. de Stefano, "Fructose-induced hyperuricaemia," *The Lancet*, vol. 2, no. 7686, pp. 1310–1311, 1970.

[15] Y. Y. Sautin and R. J. Johnson, "Uric acid: the oxidant-antioxidant paradox," *Nucleosides, Nucleotides and Nucleic Acids*, vol. 27, no. 6-7, pp. 608–619, 2008.

[16] Y. Y. Sautin, T. Nakagawa, S. Zharikov, and R. J. Johnson, "Adverse effects of the classic antioxidant uric acid in adipocytes: NADPH oxidase-mediated oxidative/nitrosative stress," *The American Journal of Physiology—Cell Physiology*, vol. 293, no. 2, pp. C584–C596, 2007.

[17] G. X. Shen, "Oxidative stress and diabetic cardiovascular disorders: roles of mitochondria and NADPH oxidase," *Canadian Journal of Physiology and Pharmacology*, vol. 88, no. 3, pp. 241–248, 2010.

[18] M. A. Lanaspa, L. G. Sanchez-Lozada, C. Cicerchi et al., "Uric acid stimulates fructokinase and accelerates fructose metabolism in the development of fatty liver," *PLoS ONE*, vol. 7, no. 10, Article ID e47948, 2012.

[19] K. Sodhi, N. Puri, D. H. Kim et al., "PPARδ binding to heme oxygenase 1 promoter prevents angiotensin II-induced adipocyte dysfunction in Goldblatt hypertensive rats," *International Journal of Obesity*, vol. 38, no. 3, pp. 456–465, 2014.

[20] L. Vanella, K. Sodhi, D. H. Kim et al., "Increased heme-oxygenase 1 expression in mesenchymal stem cell-derived adipocytes decreases differentiation and lipid accumulation via upregulation of the canonical Wnt signaling cascade," *Stem Cell Research & Therapy*, vol. 4, no. 2, article 28, 2013.

[21] R. M. Evans, G. D. Barish, and Y.-X. Wang, "PPARs and the complex journey to obesity," *Nature Medicine*, vol. 10, no. 4, pp. 355–361, 2004.

[22] L. Vanella, D. H. Kim, K. Sodhi et al., "Crosstalk between EET and HO-1 downregulates Bach1 and adipogenic marker expression in mesenchymal stem cell derived adipocytes," *Prostaglandins and Other Lipid Mediators*, vol. 96, no. 1–4, pp. 54–62, 2011.

[23] M. Li, S. Peterson, D. Husney et al., "Interdiction of the diabetic state in NOD mice by sustained induction of heme oxygenase: possible role of carbon monoxide and bilirubin," *Antioxidants and Redox Signaling*, vol. 9, no. 7, pp. 855–863, 2007.

[24] A. Nicolai, M. Li, D. H. Kim et al., "Heme oxygenase-1 induction remodels adipose tissue and improves insulin sensitivity in obesity-induced diabetic rats," *Hypertension*, vol. 53, no. 3, pp. 508–515, 2009.

[25] S. J. Peterson, G. Drummond, D. H. Kim et al., "L-4F treatment reduces adiposity, increases adiponectin levels, and improves insulin sensitivity in obese mice," *Journal of Lipid Research*, vol. 49, no. 8, pp. 1658–1669, 2008.

[26] M. Li, D. H. Kim, P. L. Tsenovoy et al., "Treatment of obese diabetic mice with a heme oxygenase inducer reduces visceral and subcutaneous adiposity, increases adiponectin levels, and improves insulin sensitivity and glucose tolerance," *Diabetes*, vol. 57, no. 6, pp. 1526–1535, 2008.

[27] Z. Khitan, M. Harsh, K. Sodhi, J. I. Shapiro, and N. G. Abraham, "HO-1 upregulation attenuates adipocyte dysfunction, obesity, and isoprostane levels in mice fed high fructose diets," *Journal of Nutrition and Metabolism*, vol. 2014, Article ID 980547, 13 pages, 2014.

[28] C. N. Bennett, S. E. Ross, K. A. Longo et al., "Regulation of Wnt signaling during adipogenesis," *The Journal of Biological Chemistry*, vol. 277, no. 34, pp. 30998–31004, 2002.

[29] B. T. MacDonald, K. Tamai, and X. He, "Wnt/beta-catenin signaling: components, mechanisms, and diseases," *Developmental Cell*, vol. 17, no. 1, pp. 9–26, 2009.

[30] M. Chhikara, S. Wang, S. J. Kern et al., "Carbon monoxide blocks lipopolysaccharide-induced gene expression by interfering with proximal TLR4 to NF-κB signal transduction in human monocytes," *PLoS ONE*, vol. 4, no. 12, Article ID e8139, 2009.

[31] S. J. Peterson, D. H. K. Kim, M. Li et al., "The L-4F mimetic peptide prevents insulin resistance through increased levels of

HO-1, pAMPK, and pAKT in obese mice," *Journal of Lipid Research*, vol. 50, no. 7, pp. 1293–1304, 2009.

[32] L. Vanella, D. H. Kim, D. Asprinio et al., "HO-1 expression increases mesenchymal stem cell-derived osteoblasts but decreases adipocyte lineage," *Bone*, vol. 46, no. 1, pp. 236–243, 2010.

[33] M. Takahashi, Y. Kamei, and O. Ezaki, "Mest/Peg1 imprinted gene enlarges adipocytes and is a marker of adipocyte size," *The American Journal of Physiology—Endocrinology and Metabolism*, vol. 288, no. 1, pp. E117–E124, 2005.

Hindawi Publishing Corporation
Stem Cells International
Volume 2016, Article ID 1801340, 11 pages
http://dx.doi.org/10.1155/2016/1801340

Research Article

Effects on Proliferation and Differentiation of Human Umbilical Cord-Derived Mesenchymal Stem Cells Engineered to Express Neurotrophic Factors

Yi Wang,[1] Youguo Ying,[2] and Xiaoyan Cui[3]

[1]*Department of Orthopaedics, Tongren Hospital, Shanghai Jiao Tong University School of Medicine, Shanghai 200336, China*
[2]*Department of Intensive Care Unit, Shanghai 9th People's Hospital, Shanghai Jiao Tong University School of Medicine, Shanghai 201999, China*
[3]*Stem Cell Research Center, Tongji University School of Medicine, Shanghai 200092, China*

Correspondence should be addressed to Youguo Ying; yingyouguo@sina.com and Xiaoyan Cui; xiaoy5671312@163.com

Received 20 January 2015; Revised 29 March 2015; Accepted 6 April 2015

Academic Editor: Ming Li

Mesenchymal stem cells (MSCs) are multipotential cells with capability to form colonies *in vitro* and differentiate into distinctive end-stage cell types. Although MSCs secrete many cytokines, the efficacy can be improved through combination with neurotrophic factors (NTFs). Moreover, MSCs are excellent opportunities for local delivery of NTFs into injured tissues. The aim of this present study is to evaluate the effects of overexpressing NTFs on proliferation and differentiation of human umbilical cord-derived mesenchymal stem cells (HUMSCs). Overexpressing NTFs had no effect on cell proliferation. Overexpressing NT-3, BDNF, and NGF also had no significant effect on the differentiation of HUMSCs. Overexpressing NTFs all promoted the neurite outgrowth of embryonic chick E9 dorsal root ganglion (DRG). The gene expression profiles of the control and NT-3- and BDNF-modified HUMSCs were compared using RNA sequencing and biological processes and activities were revealed. This study provides novel information about the effects of overexpressing NTFs on HUMSCs and insight into the choice of optimal NTFs for combined cell and gene therapy.

1. Introduction

Mesenchymal stem cells (MSCs) are multipotential cells with capability to form colonies *in vitro* and differentiate into distinctive end-stage cell types, such as adipocytes, osteoblasts, and chondrocytes, as well as other connective tissues and neuronal cells [1–4]. They are also a heterogeneous population and can be isolated from several tissues, including bone marrow, adipose, umbilical cord blood, umbilical cord, and amnion. Human umbilical cord-derived mesenchymal stem cells (HUMSCs) have no ethical concerns and are capable of being isolated and expanded easily *in vitro*; therefore, they are a promising source of MSCs.

MSCs have been used to animal models and clinical trials for treatment of many diseases, such as myocardial infarcts, graft-versus-host disease, stroke, and spinal cord injury [5]. MSCs possess many properties directed to the hurdle for disease treatment, such as paracrine effect, immunomodulatory effect, anti-inflammatory effect, antiapoptotic effect [6, 7]. They can migrate and secrete a variety of cytokines in an injury environment, including insulin-like growth factor (IGF), brain-derived neurotrophic factor (BDNF), vascular endothelial growth factor (VEGF), granulocyte-macrophage colony stimulating factor (GM-CSF), fibroblast growth factor- (FGF-) 2, and transforming growth factor (TGF) [8].

Although MSCs secrete many cytokines, the efficacy can be improved through combination with neurotrophic factors (NTFs) [9]. NTF alone does not cross the blood-brain barrier and is difficultly delivered to the central nervous system [10]. Moreover, MSCs are excellent opportunities for local delivery of NTFs into injured tissues. Multifunctional therapies seem to be extremely promising because they counteract multiple disease mechanisms and combine both neuroprotective and

Table 1: Primers used for real-time polymerase chain reaction.

Gene	Forward primer	Reverse primer
GAPDH	GCACCGTCAAGGCTGAGAAC	TGGTGAAGACGCCAGTGGA
NT-3	CATTCGGGGACACCAGGTC	TTTGCACTGAGAGTTCCAGTGTTT
BDNF	GAACTCCCAGTGCCGAACTACC	TTATGAATCGCCAGCCAATTCTC
GDNF	TGCAGTCTTTGCCTAACAGCAAT	GCCACGACATCCCATAACTTCAT
NGF	ATGCTGGACCCAAGCTCA	TGATCAGAGTGTAGAACAACATGGA

neuroregenerative agents [11]. Genetic modification of MSCs with neurotrophic factors can not only increase secretion of peptide or total length of protein with potential to repair injury of central nervous system, but also promote the survival of themselves and the survival or regeneration of neurons [12]. In this context, it is essential to evaluate the effects of overexpressing NTFs on MSCs, including neurotrophin 3 (NT-3), BDNF, glial cell line-derived neurotrophic factor (GDNF), and nerve growth factor (NGF).

2. Materials and Methods

2.1. Cell Isolation, Culture, and Phenotype Identification. HUMSCs were isolated as previously described [13]. Ten human umbilical cords were obtained after the delivery of normal-term babies with institutional review board approval. A portion of the umbilical cord was cut into approximately a 7 cm long segment. The segment was then placed immediately into 25 mL of DMEM/F12 (Gibco) supplemented with 10% fetal bovine serum (FBS; Gibco) and antibiotics (100 U/mL penicillin, 100 μg/mL streptomycin). The tubes were brought to the laboratory on the ice for dissection within 4 hours. Umbilical cord segment was washed three times with phosphate-buffered saline without calcium and magnesium (PBS; Gibco) and dissected longitudinally utilizing aseptic technique. The umbilical vein and both umbilical arteries were removed. The umbilical cord segment was cut into 0.5–1 mm^3 tissue block and incubated in 3 mL of 0.2% Collagenase Type II at 37°C for 1 hour. Fivefold volume of complete medium was added and the supernatant was filtered with 70 μm filter after free settling for 20 minutes. Cells were collected with centrifugation at 1500 rpm for 5 minutes and finally plated in plastic culture flasks at a concentration of $5 \times 10^3/cm^2$. After 3 days, nonadherent cells were removed by washing three times with PBS. Medium was changed every 2-3 days. HUMSCs were identified antigen expression using flow cytometry with human MSC analysis kit (BD Biosciences) containing CD90 FITC/CD105 PerCP-Cy5.5/CD73 APC.

2.2. Lentiviral Vectors and MSC Transduction. MSCs were, respectively, transduced with pLVX-IRES-ZsGreen1 Vector with the insertion of the full length cDNA of NT-3, BDNF, GDNF, and NGF, or without insertion (as control). MSCs at a concentration of $1 \times 10^4/cm^2$ were infected with lentivirus for 72 hours. The volume of lentivirus used for each transduction was determined by titration as the required volume to generate 90%–95% ZsGreen1 positive MSCs after 3 days.

2.3. RNA Extraction and Real-Time Polymerase Chain Reaction. Total RNA was extracted with TRIzol (Invitrogen), following the manufacturer's instructions. Genomic DNA contamination in RNA samples was removed and reverse transcription using 1 μg of RNA was performed using QuantiTect Reverse Transcription Kit (Qiagen). For all mRNAs detected, SYBR *Premix Ex Taq* II (Perfect Real Time) (Takara) was used for real-time polymerase chain reaction, using primers listed in Table 1.

2.4. Measurement of NTF Levels in Cell Culture Supernatant. Transduced MSCs were plated in six-well plates (5,000 cells per square centimeter). After overnight, medium was changed to 2 mL per well of DMEM/F12 and incubated for 48 hours. Then, supernatants were collected to confirm overexpression and secretion of each factor using human enzyme-linked immunosorbent assay (ELISA) kit following the manufacturer's instructions (Abcam). Cell number was determined for normalization.

2.5. Western Blots. For detection of overexpressing NT-3, BDNF, GDNF, and NGF in HUMSCs, proteins in transduced cells were extracted using RIPA (radio immunoprecipitation assay) Lysis Buffer supplemented with 1 mM of PMSF (Beyotime Institute of Biotechnology). Proteins were loaded in 12% SDS-PAGE gels and transferred to PVDF membranes (Millipore). After blocking for 1 hour, membranes were incubated with primary antibodies (diluted at 1 : 200) overnight at 4°C. Antibodies against NT-3, BDNF, GDNF, and NGF were purchased from Santa Cruz Biotechnology.

2.6. Cell Proliferation Assay. Transduced MSCs were plated in triplicate in 96-well plates at a density of 2,000 per well and then the live cell count was assayed using the Cell Counting Kit-8 (CCK-8) (Dojindo, Kumamoto, Japan) according to the manufacturer's protocol. In brief, 10 μL of CCK-8 solution was added to each well and the samples were incubated for 3 h. The absorbance was measured at 450 nm.

2.7. Differentiation Procedures. The adipogenic, osteogenic, and chondrogenic differentiation potentials of HUMSCs were determined by incubating them in differentiation media from the Human Mesenchymal Stem Cell Functional Identification Kit (SC006; R&D Systems, UK).

2.7.1. Adipogenic Differentiation Protocol. HUMSCs were seeded onto 12 mm coverslips at a density of 3.7×10^4 cells per well in α-MEM basal medium supplemented with 10%

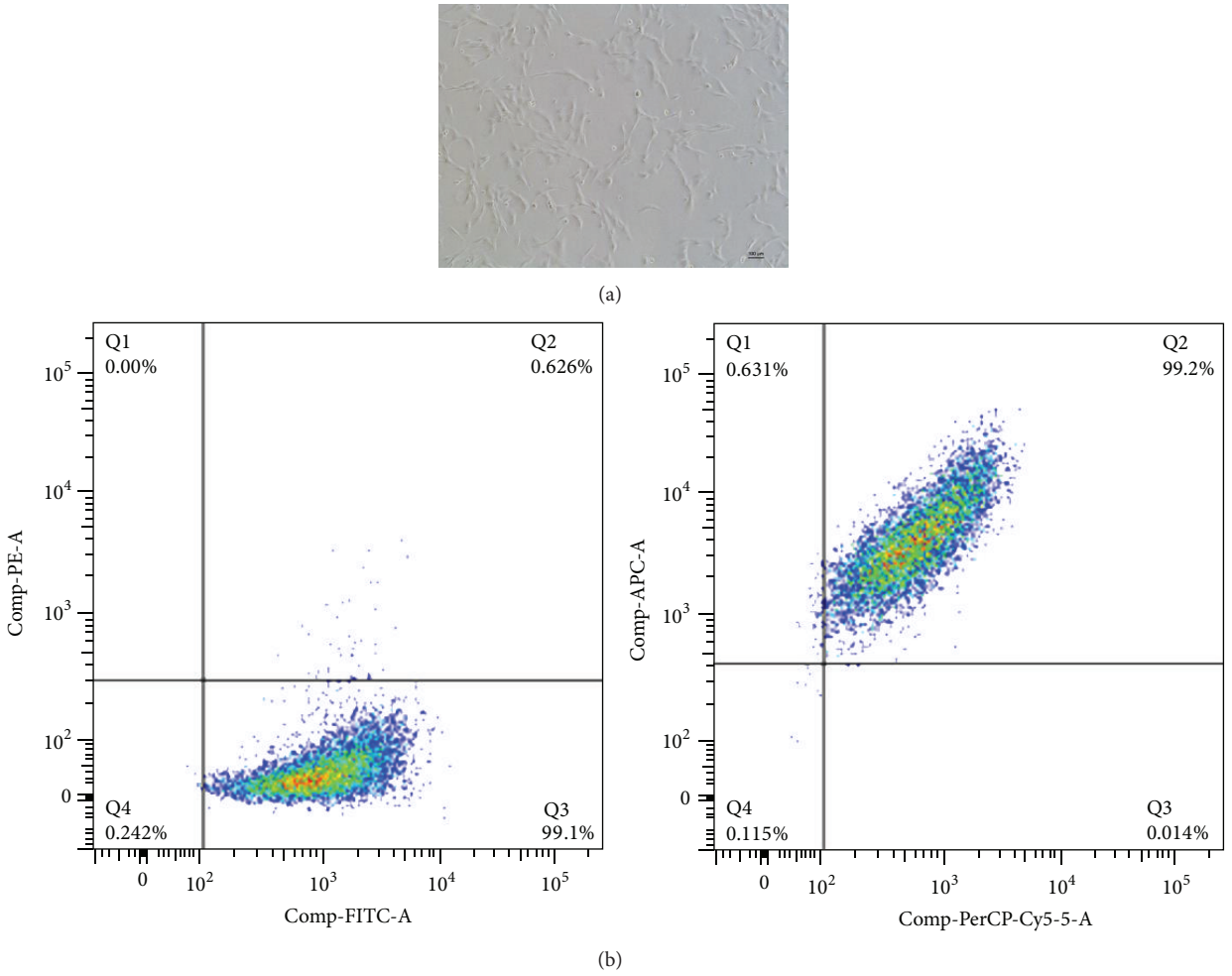

Figure 1: Phenotype identification of HUMSCs using flow cytometry. (a) Morphology of HUMSCs. Scale bar = 100 μm. (b) There are 98.3% of HUMSCs, positive for CD90 FITC/CD105 PerCP-Cy5.5/CD73 APC but negative for CD34, CD45, CD11b or CD14, CD19 or CD79α, and HLA-DR.

FBS + 100 U/mL penicillin, 100 μg/mL streptomycin, and 2 mM L-glutamine. Cells were cultured in a 37°C and 5% CO_2 incubator. When 100% confluence was reached, the medium was replaced with the Adipogenic Differentiation Medium (R&D Systems). The medium was replaced every 3 days. After 2 weeks, cells seeded on coverslips were washed with PBS twice and fixed with 4% formaldehyde (Beijing Solarbio Science & Technology) for 20 min at room temperature. For Oil Red O staining, cells were washed once with PBS and stained for 30 minutes with Oil Red O (Sigma) and for 5 minutes with DAPI (4′, 6-diamidino-2-phenylindole; 1 : 1,000, Sigma). After washing twice with PBS, cells were photographed under a microscope (Nikon).

2.7.2. Osteogenic Differentiation. For osteogenic induction, 7.4 × 10^3 HUMSCs per well were cultured in α-MEM basal medium supplemented with 10% FBS + 100 U/mL penicillin, 100 μg/mL streptomycin, and 2 mM L-glutamine. After 50–70% confluency, the medium was replaced with the Osteogenic Differentiation Medium (R&D Systems), with a medium change every 3 days. After culture for 21 days, cells were fixed with 4% paraformaldehyde for 20 minutes, washed three times with PBS, and stained with mouse anti-human osteocalcin antibody and NorthernLights 557 Fluorochrome-conjugated donkey anti-mouse secondary antibody (R&D Systems). Cells from 3 wells of each cell line were photographed with a fluorescence microscope. All images of osteogenic and chondrogenic differentiation were analyzed using ImageJ (NIH; Bethesda, MD, USA).

2.7.3. Chondrogenic Differentiation. For chondrogenic differentiation, 2.5 × 10^5 cells were centrifuged at 200 ×g for 5 minutes at room temperature and resuspended with DMEM/F-12 basal medium supplemented with ITS Supplement (R&D Systems) and 100 U/mL penicillin, 100 μg/mL streptomycin, and 2 mM L-glutamine. The cells were centrifuged again at 200 ×g for 5 minutes, resuspended in Chondrogenic Differentiation Medium (R&D Systems), and

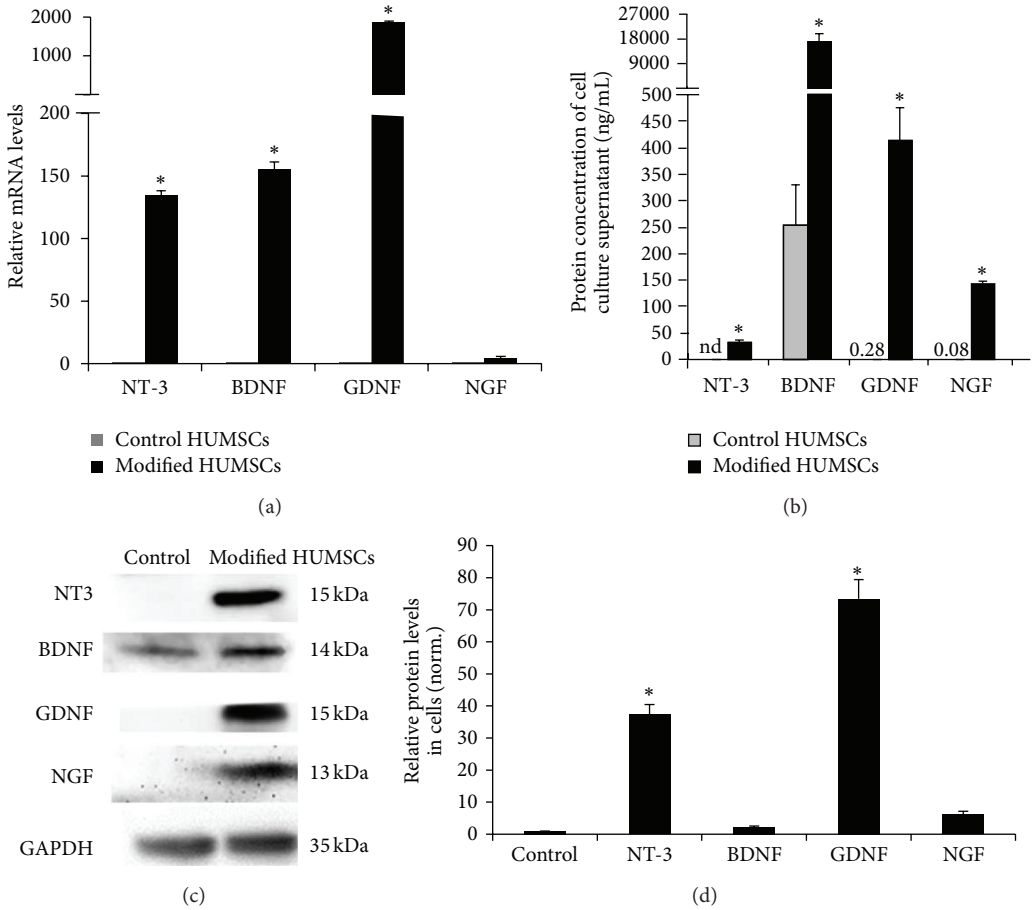

Figure 2: HUMSCs were transduced with control lentiviral vectors or those designed to overexpress NTFs. Overexpression of NTFs was then confirmed at both mRNA and protein levels. (a) mRNA was extracted from HUMSCs 3 days after transduction and measured by real-time reverse transcription polymerase chain reaction ($n = 3$). (b) Protein levels of NTF were measured in supernatant of HUMSCs using enzyme-linked immunosorbent assay ($n = 3$). (c) Protein levels of NTF measured in HUMSCs using western blot. (d) Semiquantitative analysis of results of western blot. $^*P < 0.05$ versus control ($n = 3$).

centrifuged. Pellets were incubated at 37°C and 5% CO_2 for 21 days, with medium change every 3 days. The pellets were fixed with 4% paraformaldehyde in PBS for 20 minutes at room temperature and frozen and sectioned using standard cryosectioning methods. The sections were stained with the goat anti-human aggrecan antibody and NorthernLights 557 Fluorochrome-conjugated donkey anti-goat secondary antibody (R&D Systems). Cells from triplicate of each cell line were photographed with a fluorescence microscope.

2.8. Neurite Outgrowth of Embryonic Chick Dorsal Root Ganglion (DRG). Fertilized eggs were purchased from the stock farm of Shanghai Academy of Agricultural Sciences. The eggs were incubated under 37.6°C, 60% humidity for 9 days. DRG was dissected cleanly from E9 chick embryos and cultured in six-well tissue culture plates (2 wells for each testing sample) with five DRGs in each well. Excess media were drained off and 920 μL of ice-cold fresh-made BME-collagen mixture was added into each well to cover entire surface. One mL of each testing sample (1 : 1 diluted with 10% FBS-DMEM/F12) was added into the wells, respectively, on the top of collagen. Serum-free DMEM/F12 (1 : 1 diluted with 10% FBS-DMEM/F12) was used as blank and NT-3 (final concentration: 3.5 ng/mL) and NGF (final concentration: 10 ng/mL) were used as positive controls. The plates were incubated at 37°C with 5% CO_2 for 24 hours and the ganglions were examined using an Olympus inverted microscope. The photo of each ganglion was divided into 8 sectors and the longest neurites in each sector were joined to form an octagon. The area of this octagon (A_{tot}) and the area of the DRG (A_{DRG}) were obtained using ImageJ software (v 1.4.3.). The neurite outgrowth index (OI) was calculated by the formulation $\text{OI} = (A_{\text{tot}}/\pi)^{1/2} - (A_{\text{DRG}}/\pi)^{1/2}$.

2.9. RNA Sequencing and Analysis. To compare gene expression profiles among control and NT-3- and BDNF-overexpressing HUMSCs, these cells were submitted to RNA isolation using TRIzol Reagent (Invitrogen), and then total RNA

was digested with DNase I (Invitrogen) to ensure that samples were not contaminated with genomic DNA. Six samples derived from 2 allogeneic cell lines with three different modifications of control, NT-3, and BDNF were performed. Library preparation and paired end sequencing (length of 101 bp) were done using Illumina HiSeq 2500 sequencer. Short reads were aligned to the reference human genome (Homo_sapiens GRCh37) using TopHat. Gene annotations were from Ensembl packaged into iGenome (Illumina). The sequence reads were used to calculate overall gene expression in terms of RPKM (reads per kilobase of exon per million mapped reads). The differentially expressed transcripts were screened using the cufflinks procedure. Genes with gene expression greater than or equal to 2-fold ($P \leq 0.01$ compared with other groups) were identified in control and NT-3- and BDNF-overexpressing HUMSCs, respectively. Functional enrichment analyses were performed.

Genes related to cytokine-cytokine receptor interactions, which had RPKM values of more than 5 in control and NT-3- and BDNF-modified HUMSCs, were selected based on the KEGG PATHWAY Database (http://www.genome.jp/kegg/pathway.html).

2.10. Data Presentation and Statistical Analysis. All values in figures represent averages with the standard error of mean as error bars. All significant differences were evaluated using ANOVA or repeated measures of general linear model, comparing raw data (not normalized) of conditions with control. Significance level was set at $P < 0.05$.

3. Results

3.1. Overexpression of NT-3, BDNF, GDNF, and NGF in HUMSCs. HUMSCs were similar to fibroblasts (Figure 1(a)). There were 98.3% of HUMSCs positive for CD90 FITC, CD105 PerCP-Cy5.5, and CD73 APC but negative for CD34, CD45, CD11b or CD14, CD19 or CD79α, and HLA-DR (Figure 1(b)). After transduction of HUMSCs with NT-3, BDNF, GDNF, and NGF lentivirus, we confirmed that production and secretion of these NTFs were increased in HUMSCs. As shown in Figure 2(a), the mRNA of each of NT-3, BDNF, and GDNF was significantly increased and the mRNA of NGF was slightly increased in HUMSCs transduced with the respective NTFs using real-time polymerase chain reaction. Each NTF was also found to be significantly increased in HUMSC culture supernatant upon overexpression using ELISA (Figure 2(b)). In HUMSCs transduced with the respective NTFs using western blots, the protein of each of NT-3 and GDNF was significantly increased and the protein of each of BDNF and NGF was slightly increased (Figures 2(c) and 2(d)).

3.2. Overexpressing NTFs Had No Effect on Cell Proliferation. Viable cell count assay was performed for cell proliferation of transduced HUMSCs. As shown in Figure 3, overexpression of NTFs did not significantly affect HUMSC growth compared with control HUMSCs.

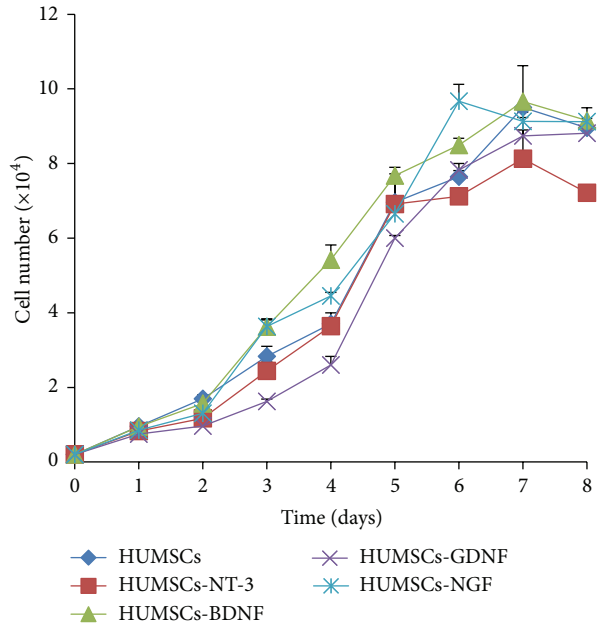

Figure 3: Cell growth curve of control and modified HUMSCs (P_5, $n = 3$).

3.3. Overexpressing NTFs Had No Effect on the Adipogenic Differentiation of HUMSCs. The adipogenic differentiation potential from each NTF-overexpressing HUMSC population was determined using microscopic count of adipocyte-like cells based on oil droplet accumulation. After culturing MSCs with adipogenic induction medium for 14 days, cells with large lipid droplets were observed (Figure 4(a)). Overexpression of BDNF and GDNF led to only a minor, but nonsignificant, reduction in the adipogenic differentiation (Figure 4(b)).

3.4. Osteogenic Differentiation of HUMSCs Is Inhibited by Overexpression of GDNF. The effects of overexpressing NTFs on the osteogenic differentiation potential of HUMSCs were evaluated by culturing transduced cells for 21 days in Osteogenic Differentiation Medium and then staining cells with anti-human osteocalcin antibody (Figure 5(a)). Osteocalcin level in HUMSCs engineered to overexpress GDNF was significantly lower under standard culture conditions (Figure 5(b)).

3.5. Overexpressing NTFs Had No Effect on the Chondrogenic Differentiation of HUMSCs. The effects of overexpressing NTFs on the chondrogenic differentiation potential of HUMSCs were evaluated by culturing transduced cells for 21 days in Chondrogenic Differentiation Medium and then staining cells with anti-human aggrecan antibody (Figure 6(a)). Aggrecan level in HUMSCs engineered to overexpress GDNF was slightly higher and aggrecan level in HUMSCs engineered to overexpress BDNF and NGF was slightly lower under standard culture conditions (Figure 6(b)).

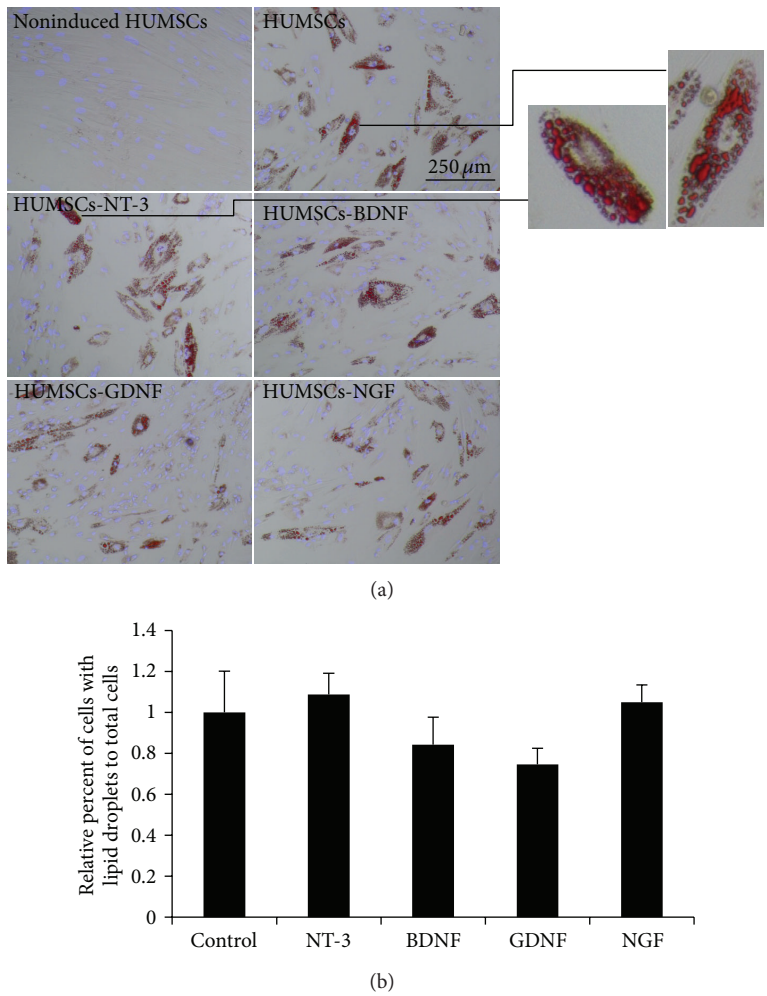

Figure 4: The effect of overexpression of NTFs on the adipogenic differentiation of HUMSCs. Transduced MSCs were cultured in adipogenic induction medium for 14 days. (a) Cells stained with Oil Red O and pictured in representative areas. Scale bar = 250 μm. (b) Relative percentage of adipocytes to total cells stained with DAPI ($n = 6$).

3.6. Overexpression of NTFs from HUMSCs Promoted the Neurite Outgrowth of Embryonic Chick E9 DRG. Short neurite extension was observed in DRG cultured in DMEM-F12 (blank, 1 : 1 diluted with 10% FBS-DMEM), while obvious neurite outgrowth was noted in DRG cultured with overexpression of NTFs from HUMSCs (1 : 1 diluted with 10% FBS-DMEM), 3.5 ng/mL NT-3 or 10 ng/mL NGF (Figure 7(a)). Neurite outgrowth was assessed in at least ten E9 chick DRGs for each sample. The outgrowth index of overexpression of NTFs from HUMSCs, 3.5 ng/mL NT-3 or 10 ng/mL NGF treated groups, was significantly increased compared with blank group (Figure 7(b), $^*P < 0.05$), while the cell culture supernatant of control HUMSCs did not exhibit any promotive effect.

3.7. Gene Expression Data Analysis. Six samples derived from 2 allogeneic cell lines (−1 and −2) with three different modifications of control, NT-3, and BDNF were performed. The heat map of the differentially expressed gene set is shown in Figure 8 between the different genetic modifications. There were 317 and 144 genes differentially expressed (greater than or equal to 2-fold) between NT-3-modified and control HUMSCs and between BDNF-modified and control HUMSCs, respectively (Figures 8(a) and 8(b)). The most significant biological processes were "circulatory system development" and "locomotion" for NT-3- and BDNF-modified HUMSCs compared with control, respectively. There were 63 genes differentially expressed (greater than or equal to 2-fold) between NT-3- and BDNF-modified HUMSCs (Figure 8(c)), and the most significant biological processes were "circulatory system development."

Gene expression related to cytokine-cytokine receptor interactions among groups was analyzed to clarify the molecular basis of the heterogeneity. HUMSCs have been shown to display anti-inflammatory and immunomodulatory properties, and we also focused on comparative analysis of genes related to cytokine-cytokine receptor interactions in control and NT-3- and BDNF-modified HUMSCs. There were 6 genes with RPKM values of more than 5

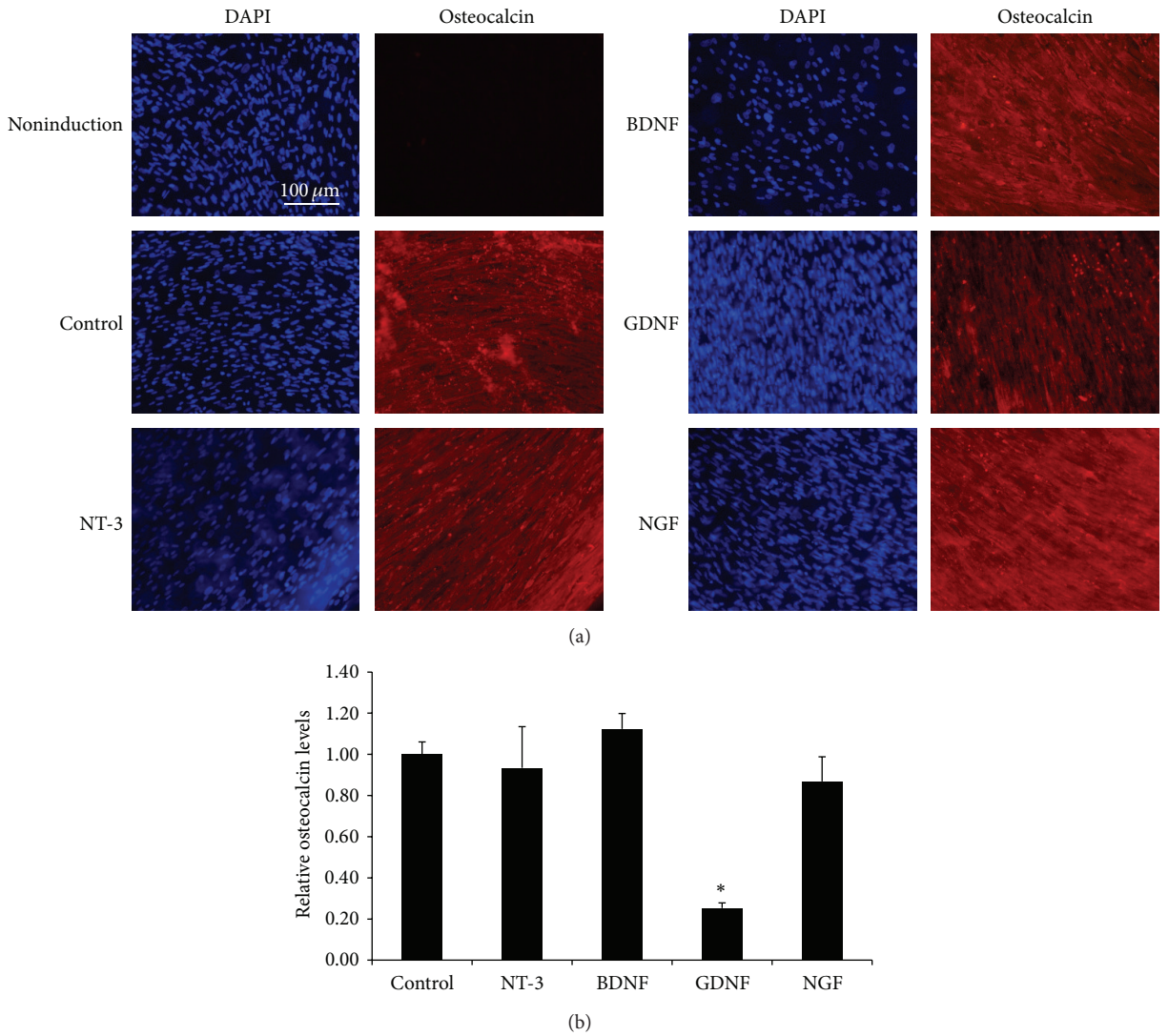

Figure 5: The effect of overexpression of NTFs on the osteogenic differentiation of MSCs. Transduced MSCs were cultured in osteogenic induction medium for 21 days. (a) Cells were stained with anti-human osteocalcin antibody and pictured in representative areas. Scale bar = 100 μm. (b) Relative osteocalcin levels. $^*P < 0.05$ versus control ($n = 6$).

related to cytokine-cytokine receptor interactions. Clustering highlighted two inflammatory related genes VEGFC and PLEKHO2 with higher expression in NT-3-modified HUMSCs. Clustering also highlighted three genes LIF, PLEKHO2, and TNFRSF10D with higher expression in BDNF-modified HUMSCs, respectively (Figure 9).

4. Discussion

MSCs can secrete a variety of NTFs and exert their functions partly through paracrine effect. Human MSCs derived from dental pulp (hDPSCs), bone marrow (hBMSCs), and adipose (hAMSCs) secreted multiple neuroprotective NTFs that promoted the growth of neurites [14]. To further enhance the efficacy of HUMSCs, we conducted genetic modification of HUMSCs. The effects of various NTFs' overexpression on MSCs *in vitro* are rarely studied in a comparative manner. First, we examined the levels of NTF overexpression in HUMSCs after transduction with the respective lentiviral vectors. The mRNA levels and protein secretion of NT-3, BDNF, and GDNF were significantly increased compared with those of the control. Although the mRNA level of overexpressing NGF was slightly increased compared with the control, the protein level of NGF overexpressed in HUMSCs culture supernatant was significantly increased. Therefore, all four overexpressed mature NTFs can be released from cells and perform their functions. The protein level of BDNF in modified HUMSCs measured using western blot was rather low compared with NT-3 and GDNF. This protein reduction of BDNF in cells may be due to excess release into cell culture supernatant. We also noted significant effects on the neurite outgrowth of the MSCs engineered to express NT-3, BDNF, GDNF, and NGF, indicating that these NTFs were biologically active.

Overexpression of NTFs did not significantly affect HUMSC growth compared with control HUMSCs. In our

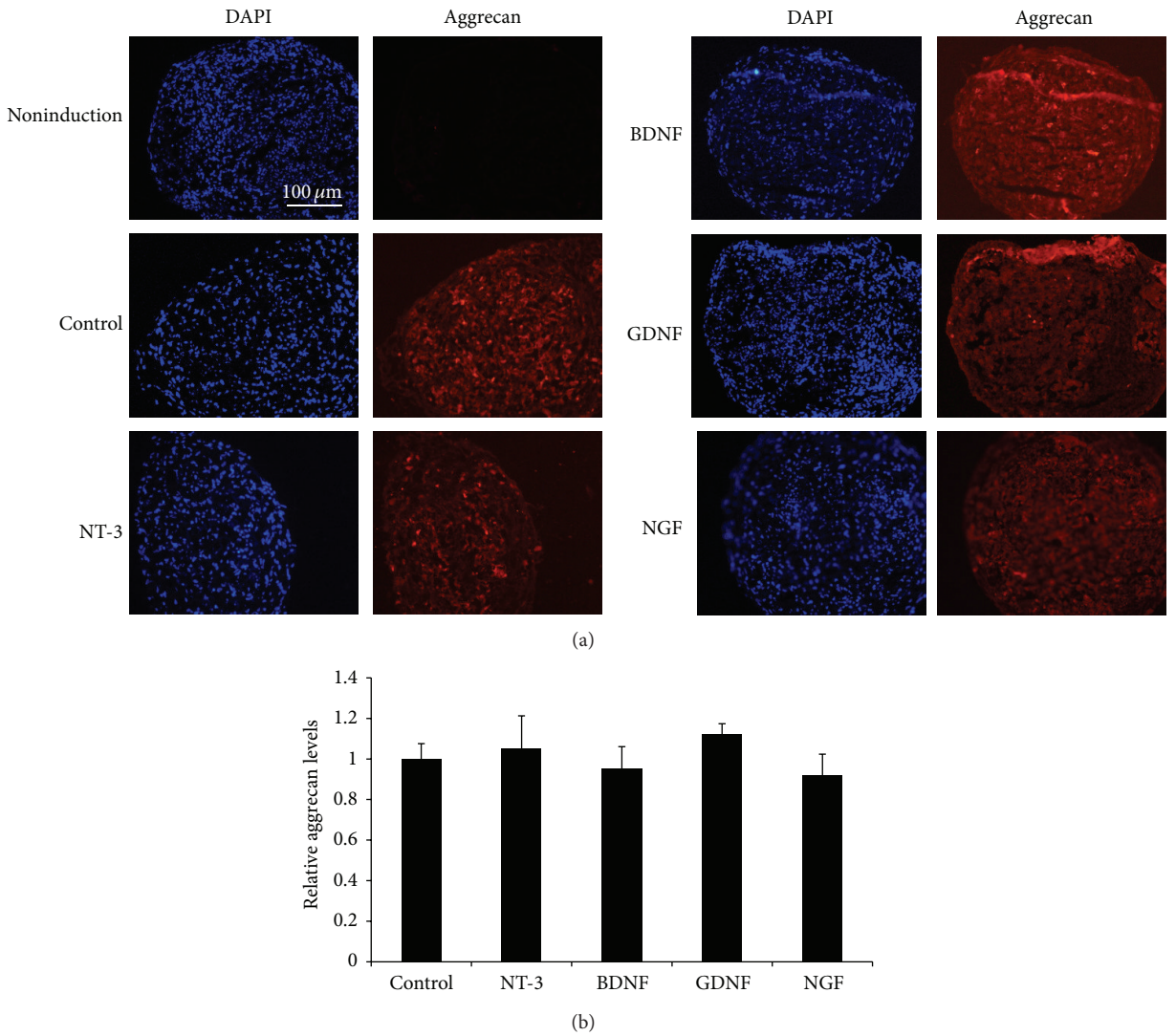

Figure 6: The effect of the overexpression of NTFs on the chondrogenic differentiation of MSCs. Transduced MSCs were cultured in chondrogenic induction medium for 21 days. (a) Cells were stained with anti-human aggrecan antibody and pictured in representative areas. Scale bar = 100 μm. (b) Relative aggrecan levels (n = 6).

experimental setting, overexpression of GDNF inhibited the osteogenic differentiation of HUMSCs. GDNF might induce the downregulation of gene specific for osteogenic differentiation and more work is needed to study the mechanism of reduced osteogenic differentiation. GDNF is necessary for normal neuromuscular development and exists in embryonic limb and muscle at high levels at the time of innervation [15]. GDNF can increase neural sprouting and prevent cell death [16–18]. Overexpression of NT-3, BDNF, and NGF had no significant effects on adipogenic, osteogenic, and chondrogenic differentiation of HUMSCs. These data suggest that MSCs engineered to overexpress NT-3, BDNF, and NGF in a controlled manner might be a better candidate for alleviating nervous system disease. Other investigators demonstrated that BDNF overexpressing human umbilical cord blood-MSCs (MSCs-BDNF) yielded an increased number of neuron-like cells and MSCs-BDNF exhibited decreased labeling for MSCs-related antigens such as CD73 and CD90 and decreased potential to differentiate into mesodermal lineages [19]. The differences between our experimental results and their results may be due to the different cell lines used and different experimental setting. We used umbilical cord jelly-derived MSCs and they used umbilical cord blood-derived MSCs.

RNA sequencing analyses can provide new insight into the variable biological properties among control and modified HUMSCs. We performed RNA sequencing analyses for control and NT-3- and BDNF-modified HUMSCs because we are more interested in NT-3 and BDNF. Compared with control HUMSCs, the most significant biological processes were "circulatory system development" and "locomotion" for NT-3- and BDNF-modified HUMSCs, respectively. Gene analyses provide some cues for MSC-mediated anti-inflammatory and immunomodulatory properties of different groups.

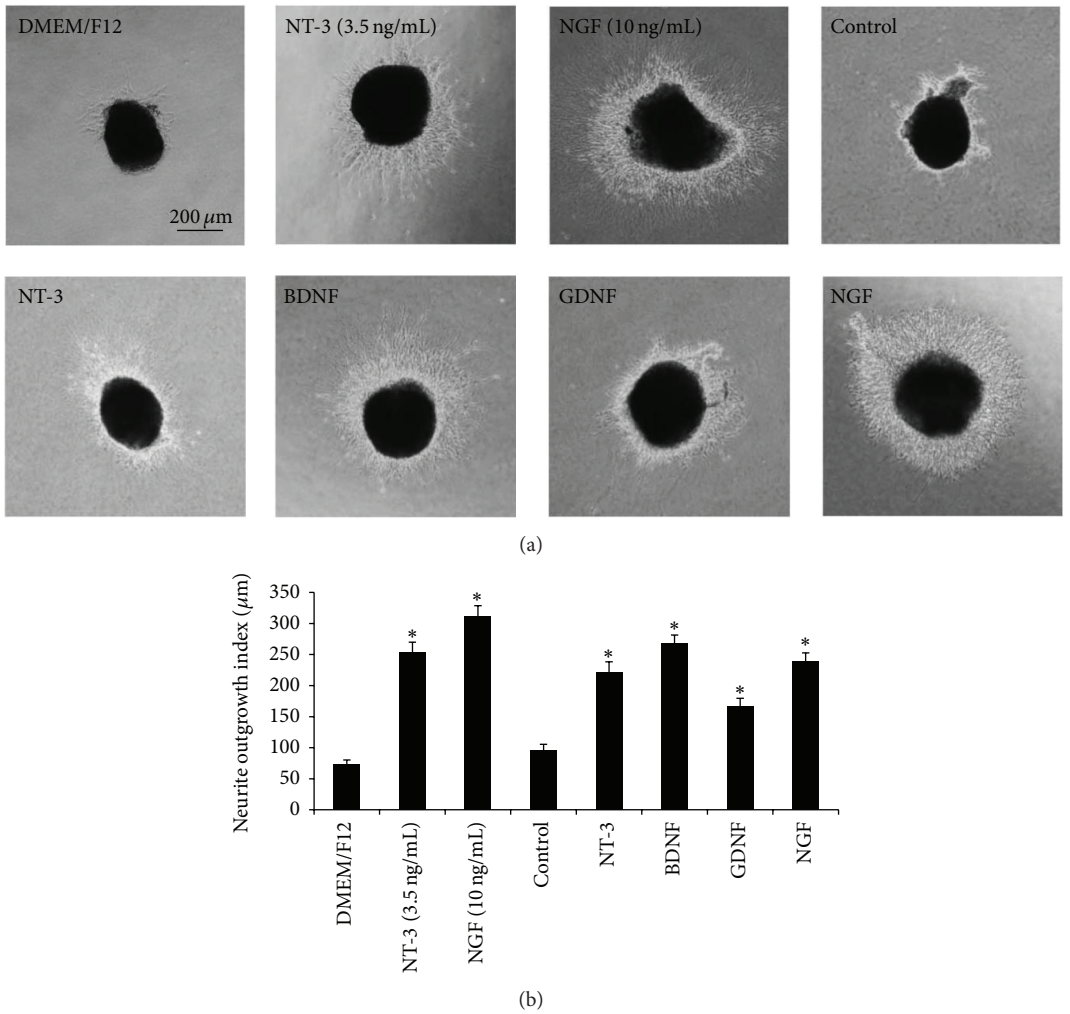

Figure 7: Effects of overexpression of NTFs from HUMSCs on the neurite outgrowth of embryonic chick DRG. (a) Representative images of E9 DRG culture for 24 hours (scale bar = 200 μm). (b) DRG cultured in blank culture medium extended short neurites. NT-3 (3.5 ng/mL), NGF (10 ng/mL), and overexpression of NTFs from HUMSCs treatment effectively promoted neurite outgrowth. Neurite extension of DRG treated with cell culture supernatant of HUMSCs (control) was similar to that of blank group. $^*P < 0.05$ versus blank or control ($n = 10$).

The anti-inflammatory and immunoregulation-related gene VEGFC (vasculogenesis and angiogenesis) and PLEKHO2 (involved STAT3 pathway) were expressed highly in NT-3-modified HUMSCs. Three genes PLEKHO2, leukemia inhibitory factor (LIF, cytokine activity and receptor binding, induction of neuronal cell differentiation, and immune tolerance at the maternal-fetal interface) [20, 21], and TNFRSF10D (playing an inhibitory role in TRAIL-induced cell apoptosis) [22] were expressed highly in BDNF-modified HUMSCs. VEGFC activated lymphatic vessels in the skin lead not only to an expanded lymphatic network with enhanced fluid drainage, but also to a potent inhibition of acute and chronic skin inflammation [23]. In a model of chronic inflammatory arthritis, VEGFC increased lymphangiogenesis and lymphatic flow and also reduced the severity of joint lesions [24]. The antagonist of the LIF receptor increased gene transcripts for the proinflammatory cytokines tumor necrosis factor, interleukin-1β, and interleukin-6 during the inflammatory phase [25]. Hence, LIF can regulate the inflammatory response. Moreover, LIF regulated nonclassical *MHC* class I gene expression and has been suggested to contribute to the localized immunosuppressive environment in endometrium [26]. Therefore, genetic modification with NT-3 and BDNF can also upregulate anti-inflammatory and immunoregulation-related genes in HUMSCs.

In conclusion, NT-3 and BDNF modifications had no effect on proliferation and differentiation of HUMSCs and may be excellent opportunities for combined cell and gene therapy. However, extensive efficacy (including neuronal differentiation) and safety experiments need to be done before MSCs/NTFs therapy could ever be considered.

Conflict of Interests

The authors declare that there is no conflict of interests regarding the publication of this paper.

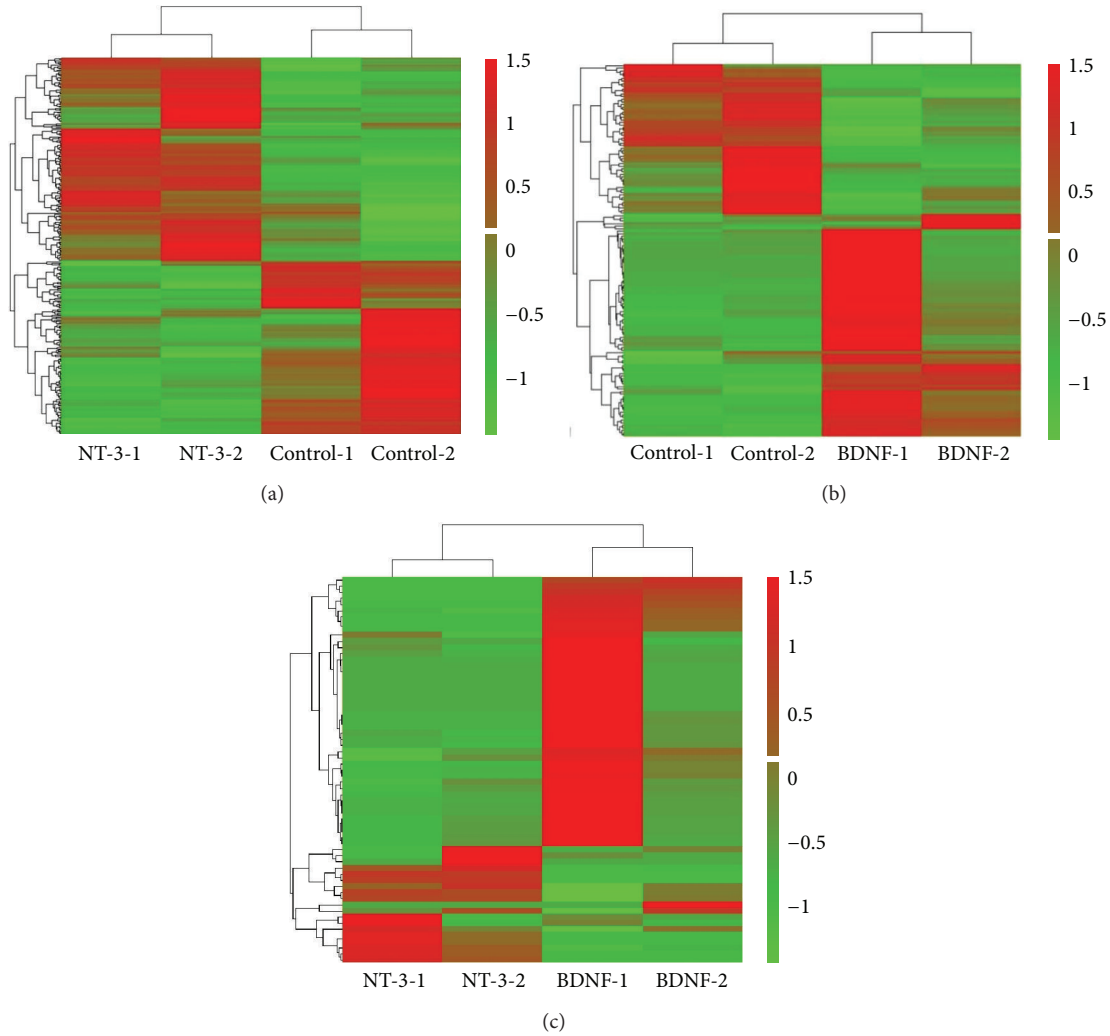

Figure 8: Heat map of the differentially expressed gene set between the different genetic modifications. (a) NT-3 modification and control. (b) BDNF modification and control. (c) NT-3 and BDNF modification.

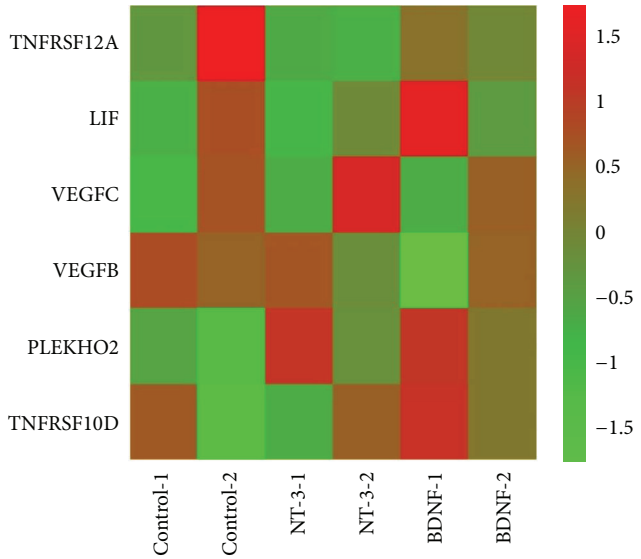

Figure 9: Heat map showing genes related to cytokine-cytokine receptor interaction with RPKM values of more than 5 in three groups.

Acknowledgments

This project was supported by a grant (2012M520933) from the National Science Foundation for Post-Doctoral Scientists of China, a grant (20124y147) from the Shanghai Municipal Health Bureau Youth Projects, and a grant (2012KJ016) from the Fundamental Research Funds for the Central Universities.

References

[1] A. M. Dimarino, A. I. Caplan, and T. L. Bonfield, "Mesenchymal stem cells in tissue repair," *Frontiers in Immunology*, vol. 4, article 201, 2013.

[2] P.-F. Choong, P.-L. Mok, S.-K. Cheong, C.-F. Leong, and K.-Y. Then, "Generating neuron-like cells from BM-derived mesenchymal stromal cells in vitro," *Cytotherapy*, vol. 9, no. 2, pp. 170–183, 2007.

[3] M. F. Pittenger, A. M. Mackay, S. C. Beck et al., "Multilineage potential of adult human mesenchymal stem cells," *Science*, vol. 284, no. 5411, pp. 143–147, 1999.

[4] R. Xu, X. Jiang, Z. Guo et al., "Functional analysis of neuron-like cells differentiated from neural stem cells derived from bone marrow stroma cells in vitro," *Cellular and Molecular Neurobiology*, vol. 28, no. 4, pp. 545–558, 2008.

[5] A. I. Caplan, "Adult mesenchymal stem cells for tissue engineering versus regenerative medicine," *Journal of Cellular Physiology*, vol. 213, no. 2, pp. 341–347, 2007.

[6] J. A. Kode, S. Mukherjee, M. V. Joglekar, and A. A. Hardikar, "Mesenchymal stem cells: immunobiology and role in immunomodulation and tissue regeneration," *Cytotherapy*, vol. 11, no. 4, pp. 377–391, 2009.

[7] L. da Silva Meirelles, A. M. Fontes, D. T. Covas, and A. I. Caplan, "Mechanisms involved in the therapeutic properties of mesenchymal stem cells," *Cytokine and Growth Factor Reviews*, vol. 20, no. 5-6, pp. 419–427, 2009.

[8] M. F. Azari, L. Mathias, E. Ozturk, D. S. Cram, R. L. Boyd, and S. Petratos, "Mesenchymal stem cells for treatment of CNS injury," *Current Neuropharmacology*, vol. 8, no. 4, pp. 316–323, 2010.

[9] M. Sasaki, C. Radtke, A. M. Tan et al., "BDNF-hypersecreting human mesenchymal stem cells promote functional recovery, axonal sprouting, and protection of corticospinal neurons after spinal cord injury," *Journal of Neuroscience*, vol. 29, no. 47, pp. 14932–14941, 2009.

[10] R. K. Sumbria, R. J. Boado, and W. M. Pardridge, "Combination stroke therapy in the mouse with blood-brain barrier penetrating IgG-GDNF and IgG-TNF decoy receptor fusion proteins," *Brain Research*, vol. 1507, pp. 91–96, 2013.

[11] F. Rossi, R. Ferrari, S. Papa et al., "Tunable hydrogel-nanoparticles release system for sustained combination therapies in the spinal cord," *Colloids and Surfaces B: Biointerfaces*, vol. 108, pp. 169–177, 2013.

[12] X. Y. Cui, L. Chen, Y. Ren et al., "Genetic modification of mesenchymal stem cells in spinal cord injury repair strategies," *BioScience Trends*, vol. 7, no. 5, pp. 202–208, 2013.

[13] A. Kikuchi-Taura, A. Taguchi, T. Kanda et al., "Human umbilical cord provides a significant source of unexpanded mesenchymal stromal cells," *Cytotherapy*, vol. 14, no. 4, pp. 441–450, 2012.

[14] B. Mead, A. Logan, M. Berry, W. Leadbeater, B. A. Scheven, and E. Mezey, "Paracrine-mediated neuroprotection and neuritogenesis of axotomised retinal ganglion cells by human dental pulp stem cells: comparison with human bone marrow and adipose-derived mesenchymal stem cells," *PLoS ONE*, vol. 9, no. 10, Article ID e109305, 2014.

[15] C.-Y. Wang, F. Yang, X.-P. He et al., "Regulation of neuromuscular synapse development by glial cell line-derived neurotrophic factor and neurturin," *The Journal of Biological Chemistry*, vol. 277, no. 12, pp. 10614–10625, 2002.

[16] D. M. Deshpande, Y.-S. Kim, T. Martinez et al., "Recovery from paralysis in adult rats using embryonic stem cells," *Annals of Neurology*, vol. 60, no. 1, pp. 32–44, 2006.

[17] C. E. Henderson, W. Camu, C. Mettling et al., "Neurotrophins promote motor neuron survival and are present in embryonic limb bud," *Nature*, vol. 363, no. 6426, pp. 266–270, 1993.

[18] X. Deng, Y. Liang, H. Lu et al., "Co-transplantation of GDNF-overexpressing neural stem cells and fetal dopaminergic neurons mitigates motor symptoms in a rat model of parkinson's disease," *PLoS ONE*, vol. 8, no. 12, Article ID e80880, 2013.

[19] J. Y. Lim, S. I. Park, S. M. Kim et al., "Neural differentiation of brain-derived neurotrophic factor-expressing human umbilical cord blood-derived mesenchymal stem cells in culture via TrkB-mediated ERK and β-catenin phosphorylation and following transplantation into the developing brain," *Cell Transplantation*, vol. 20, no. 11-12, pp. 1855–1866, 2011.

[20] S.-C. Liu, N.-M. Tsang, W.-C. Chiang et al., "Leukemia inhibitory factor promotes nasopharyngeal carcinoma progression and radioresistance," *The Journal of Clinical Investigation*, vol. 123, no. 12, pp. 5269–5283, 2013.

[21] K. Imaizumi, S.-I. Nishikawa, H. Tarui, and T. Akuta, "High-level expression and efficient one-step chromatographic purification of a soluble human leukemia inhibitory factor (LIF) in *Escherichia coli*," *Protein Expression and Purification*, vol. 90, no. 1, pp. 20–26, 2013.

[22] V. F. Bonazzi, D. J. Nancarrow, M. S. Stark et al., "Cross-platform array screening identifies *COL1A2*, *THBS1*, *TNFRSF10D* and *UCHL1* as genes frequently silenced by methylation in melanoma," *PLoS ONE*, vol. 6, no. 10, Article ID e26121, 2011.

[23] R. Huggenberger, S. S. Siddiqui, D. Brander et al., "An important role of lymphatic vessel activation in limiting acute inflammation," *Blood*, vol. 117, no. 17, pp. 4667–4678, 2011.

[24] Q. Zhou, R. Guo, R. Wood et al., "Vascular endothelial growth factor C attenuates joint damage in chronic inflammatory arthritis by accelerating local lymphatic drainage in mice," *Arthritis & Rheumatism*, vol. 63, no. 8, pp. 2318–2328, 2011.

[25] L. C. Hunt, A. Upadhyay, J. A. Jazayeri, E. M. Tudor, and J. D. White, "An anti-inflammatory role for leukemia inhibitory factor receptor signaling in regenerating skeletal muscle," *Histochemistry and Cell Biology*, vol. 139, no. 1, pp. 13–34, 2013.

[26] A. Al Naib, S. Mamo, G. M. O'Gorman, P. Lonergan, A. Swales, and T. Fair, "Regulation of non-classical major histocompatability complex class I mRNA expression in bovine embryos," *Journal of Reproductive Immunology*, vol. 91, no. 1-2, pp. 31–40, 2011.